# Generation and Reactivity of Transient Aminoboranes and Phosphinoboranes: Intermediates in the Formation of Inorganic Polymers

by

Matthew A. Wiebe

B.Sc., University of Winnipeg, 2017
M.Sc., York University, 2019

A Dissertation Submitted in Partial Fulfillment

of the Requirements for the Degree of

DOCTOR OF PHILOSOPHY

in the Department of Chemistry



University of Victoria



We acknowledge and respect the Lək̓ʷəŋən (Songhees and Esquimalt) Peoples on whose territory the university stands, and the Lək̓ʷəŋən and W̱SÁNEĆ Peoples whose historical relationships with the land continue to this day.

# Generation and Reactivity of Transient Aminoboranes and Phosphinoboranes: Intermediates in the Formation of Inorganic Polymers

by

Matthew A. Wiebe

B.Sc. (Hons.), University of Winnipeg, 2017
M.Sc., York University, 2019

**Supervisory Committee**

Prof. Dr. Ian Manners (Supervisor), Deceased
Department of Chemistry, University of Victoria

Prof. Dr. Jeremy Wulff (Supervisor)
Department of Chemistry, University of Victoria

Prof. Dr. Lisa Rosenberg
Department of Chemistry, University of Victoria

Prof. Dr. Chris Bose
Department of Mathematics, University of Victoria

**Abstract**

Polymers are ubiquitous. From the infamous plastic water bottle, typically made of polyethylene terephthalate, to chitin, a polysaccharide, polymeric materials are produced on massive scales in both industry and the biosphere. Most known polymers consist of long chains containing C–C, C–O, or C–N bonds. However, inclusion of elements other than carbon, oxygen, or nitrogen, can introduce valuable properties into the resulting bulk material. For example, the first boot to make contact with the moon had a sole comprised of silicone rubber, a material that can remain rubbery at even lunar temperatures. The ability of this material to remain pliable at such low temperatures is largely due to the inorganic Si–O bonds in its main-chain, which allow for greater conformational flexibility compared to polymers comprised primarily of C–C bonds.

The work described in this thesis focuses on a different class of inorganic polymers, polyaminoboranes and polyphosphinoboranes. These polymers feature main-chains of alternating nitrogen and boron or phosphorus and boron atoms.

- **Chapter 1** provides a general introduction to inorganic polymers as well as a more detailed survey of polyaminoboranes and polyphosphinoboranes.
- **Chapter 2** explores the synthesis of polyphosphinoboranes *via* the generation of transient phosphinoboranes ($PhRP–BH_2$; R = H, Ph, Et) through the deprotonation of $PhRPH•BH_2(NTf_2)$. These transient phosphinoboranes then undergo an addition polymerization.
- **Chapter 3** describes the solution generation, observation, and subsequent reactivity of primary aminoboranes ($RNH=BH_2$; R = *t*Bu, Me, $CPh_3$), a class of species that has only otherwise been isolated on solid argon matrices or observed as a complex

mixture of products by $^{11}B$ NMR spectroscopy. These aminoboranes were generated *via* the deprotonation of $RNH_2•BH_2(NTf_2)$ and observed at –78 °C as the sole $^{11}B$ containing species, allowing for subsequent reactivity studies.

- **Chapter 4** explores the role of catalysts in the catalytic dehydropolymerization of phosphine-borane adducts, where it is discovered that high molar mass, low dispersity polymers can be accessed using commercially available salts such as LiOTf or by adding catalytic amounts of $BH_3•SMe_2$. Further, a new potential mechanism for phosphine-borane dehydropolymerization is discussed.
- **Chapter 5** ties together the themes of phosphinoboranes and aminoboranes, revealing that sterically unencumbered aminoboranes can accept hydrogen from phosphine-borane adducts, producing amine-borane adducts and phosphinoboranes. These transient phosphinoboranes then undergo subsequent reactivity to form dehydrocoupled products.
- **Chapter 6** summarizes the findings of the research, discusses future research directions, and provides an overall outlook.

**Table of Contents**

**List of Figures**

**List of Schemes**

**List of Tables**

**Acknowledgements**

As I come to the end of this Ph.D. I am filled with joy as I reflect back on the people who have made this achievement possible.

First, I want to thank Ian Manners for taking a chance on me and teaching me so much about chemistry and life. From the first interaction I had with Ian, he has treated me with respect and as a colleague, and I am forever grateful for the time I got to be in his group. I also want to thank Deborah O'Hanlon Manners, as because of her assistance and presence, this journey has been made much more enjoyable.

Next, I want to thank Jeremy Wulff for stepping in after Ian's passing. Jeremy, your guidance and support throughout the final stages of my degree has been invaluable and I look forward to continuing to lean on your wisdom. I would also like to thank Lisa Rosenberg for being a part of my committee. Your rigor has helped me build confidence as a scientist. Thank you also to Chris Bose, whose insightful comments were greatly appreciated throughout this process. I am incredibly grateful to Doug Stephen, my external examiner, whose innovative work inspired me as an undergraduate and led me to pursue graduate school in chemistry. Finally, I want to thank Anne Staubitz and Erin Leitao for their thoughtful feedback on my research and writing in this final year.

I am also grateful to the members of the Manners lab, past and present. Special thanks to the members of the main-group chemistry lab, including Nicola Oldroyd, Alastair Knights, Etienne Lapierre, Mitchell Nascimento, Casper Macaulay, Harvey McKenzie, Harrison Young, Florian Schön, Deborah Hartmann, James Race, Martin Trapero, Jade Watson, and Helen Leslie. I am also grateful to the people in the self-assembly lab, in particular: Liam Macfarlane, Steven Street, Huda Shaikh, Charlotte Ellis, Hayley Parkin,

Hannah Schnicke, Chen Li, Jiangdong Cai, Marcus Vespa, Matt Brumwell, Ayesha Nadeem, Shixing Lei, Diego Garcia Hernandez, Yifan Zhang, and Chuanqi Zhao. Special thanks to the broader chemistry community at UVic including J. Scott McIndoe, Chris Barr, Ori Granot, Adriaan Frencken, Charles Kileen, Gil Thomas, Greg Gaube, Peter Williams, Nick Dyck, Ian Chagunda, Lea Gozdzialski, and Derek Blevins.

Outside of chemistry, I want to express my appreciate for the people I lived with in Victoria: Cindy, Tory, Natalie, Mitch, Huda, Steffie, JP, Tory 2, Marissa, Laura, Sophia, Ava, and Claire. I found you all quite pleasant to live with and be friends with – I hope you'd say the same about me! I also want to thank Lydia Toorenburgh and Jordin Fletcher, my fellow Indigenous scholars for whose friendship I truly cherish. I am also thankful for the friendships I've built with Mari, Jayden, Jake, Nate, and Sean, as well as sustained support from friends in Toronto: Anmol, Brandon, Juan, Jordan, Jeanette, Selvyn, and Francis. Also those from my University of Winnipeg days, who I lovingly call the fantastic four (myself included, obviously): Kevin, Megan, and Jake.

I also want to thank Christopher Graham. You have been my closest friend throughout this Ph.D., and your unwavering support, communication, and companionship have been incredibly valuable.

Lastly, I want to thank the folks back home. Mom, Dad, Nan, Colin, Mike, and the extended community, I'm here because of you and your efforts. From the merchandise bingo that helped fund my move to Toronto for my masters to the endless words of advice that I've received during my Ph.D., I have always felt so supported in pursuing my dreams, even if they take me far away from home. I hope to pay it back, and I hope to share my success however I can.

*I dedicate this thesis to my uncle, Reginald Thomas,*

*who passed December of 2022.*

## Chapter 1

# Introduction

## 1.1 Research Objectives

Within this thesis, the generation and reactivity of transient aminoboranes and phosphinoboranes is explored. The main target of this research is to learn more about the details of phosphine-borane dehydropolymerization *via* discovery of new routes to access polyphosphinoboranes. Further, I explore the generation and reactivity of transient primary aminoboranes.

This first chapter serves as a general introduction to the relevant known chemistry of transient aminoboranes and phosphinoboranes and their polymers. However, as this is not a comprehensive review of the field, each subsequent chapter begins with an introduction that is more specific to the research that is discussed within that chapter.

## 1.2 Formation of Main Group Element Bonds

Connecting molecular building blocks to access valuable products accounts for a large proportion of chemical research. From macromolecular polymers to small molecules, these products rely on transformations such as olefin polymerization,[1,2] olefin metathesis,[3–5] and cross coupling (**Figure 1.1**).[6,7] Accordingly, key discoverers and researchers of each aforementioned reaction were awarded with a Nobel Prize in 1963, 2005, and 2010, respectively. However, these reactions largely focus on the formation of C–C bonds. The formation of C–E bonds, where E represents an element from the p-block, is also well studied. One example is the hydroelementation reaction (**Figure 1.1**) where there is the delivery of an E–H bond across an unsaturated C–C bond. The most

common examples are hydroboration, hydrosilation, and hydrophosphination reactions.[8–10] Research within this field of chemistry is still active with a recent example being the delivery of a Bi–H bond, or hydrobismuthation, that was reported in a collaborative project by the Power and Heikke groups.[11] Compared to C–C or C–E bond forming reactions, the formation of E–E and E–E' bonds are studied significantly less. Often, this is due to the greater challenges associated with forming bonds between heavier elements that have inherently weaker bonds.[12]

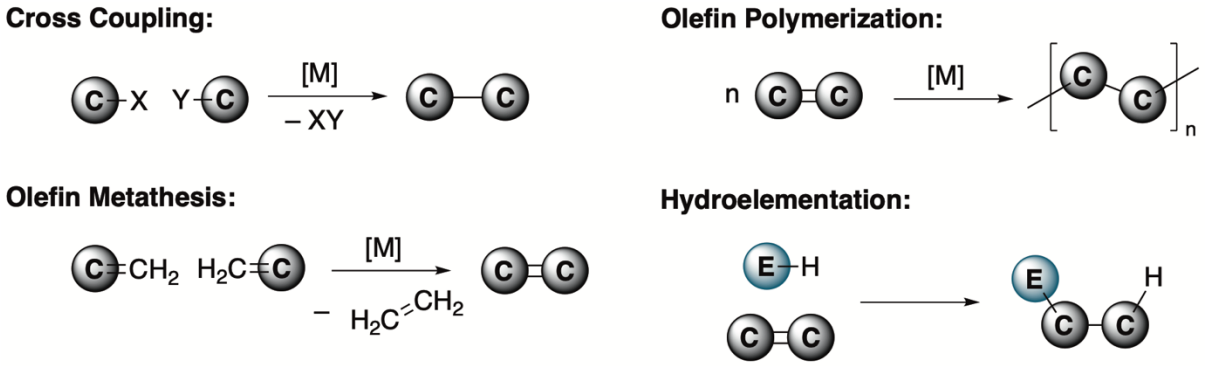


**Figure 1.1:** Simplified representations of cross coupling, olefin metathesis, olefin polymerization, and hydroelementation reactions.

### 1.2.1 Synthesis of E–E and E–E' bonds

Historically, the formation of main-group element-element bonds has relied on salt elimination and reductive coupling reactions. For example, the reaction of silyl chlorides with sodium metal can result in Si–Si bond formation with loss of sodium chloride, known as Wurtz coupling (**Figure 1.2**).[13] However, these reaction conditions are rather harsh, have a limited substrate scope, and often result in undesired by-products.

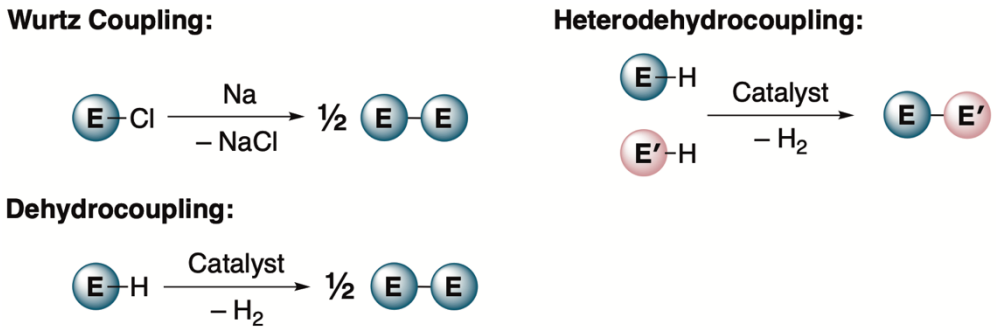


**Figure 1.2**: Simplified representations of E–E and E–E' coupling reactions.

Alternatively, synthesis of E–E and E–E' bonds can be achieved *via* dehydrocoupling reactions where two molecules containing an element-hydrogen bond are reacted to result in bond formation paired with hydrogen loss (**Figure 1.2**).[14] The earliest example of catalytic dehydrocoupling of main-group substrates was reported by Sneddon *et al*. where two polyhedral boron clusters containing B–H bonds were reacted with catalytic platinum (II) bromide to result in B–B coupling.[15] Since then, dehydrocoupling has been a commonly employed strategy to access E–E bonds, often under mild conditions when compared to Wurtz coupling.[12,14,16] Further, the development of catalysts based on main-group element centres has been of recent interest.[17–21]

### 1.2.2 Synthesis of Polymers with E–E and E–E' bonds

Polymers contain long chains of repeating monomer units that are generally linked by covalent bonds. Materials comprised of polymers have found a plethora of uses from simple containers to conductive plastics resulting in over 300 million tonnes of polymers being produced globally per year. [22,23] However, most linkages in polymers are C–C bonds. The synthesis of polymers with a backbone comprised of E–E or E–E' bonds, otherwise known as main-group or inorganic polymers, are generally much less explored.

The main reason for this is the preparation of suitable precursors or polymerization methodologies often presents considerable challenges.[24] However, the inclusion of inorganic elements into the main-chain of polymers is of interest as unique properties can be introduced into the bulk material (conductivity, inherent flame-retardancy, pre-ceramics, hydrogen storage capability) while maintaining the attractive properties of other polymers as a result of chain-entanglement.[12,25–32] Success in the synthesis of inorganic polymers has been found with catalytic dehydrocoupling reactions, polycondensations, or ring-opening polymerization (ROP) of main group heterocycles (**Figure 1.3**).

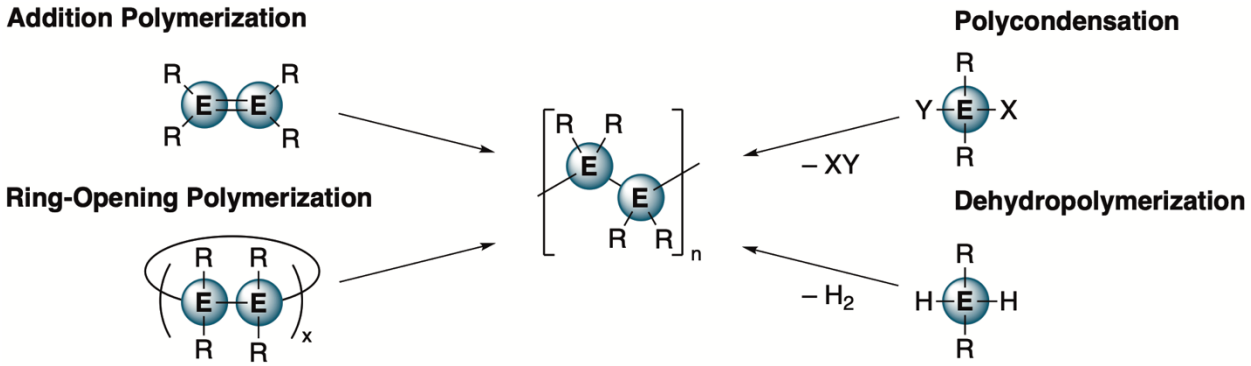


**Figure 1.3**: Simplified representations of E–E and E–E' coupling reactions.

Polysiloxanes, $[RR'SiO]_n$, and polyphosphazenes, $[RR'P{=}N]_n$, represent two of the earliest examples of inorganic polymers (**Figure 1.4**). Polysiloxanes are well-developed, chemically inert, and have found numerous applications as thermally stable elastomers, sealants, biocompatible implants, and as adhesives.[33,34] Alternatively, polyphosphazenes are another inorganic polymer that feature a main chain of repeating phosphorus and nitrogen atoms connected by alternating double and single bonds.[35,36] These polymers have attracted interest as biocompatible materials for drug-delivery micelles and hydrogels. Further, our group has recently reported on the synthesis of a new class of

inorganic polymers featuring alternating P–O bonds, polyphosphonates $[RPO_2]_n$, through the ROP of cyclic phosphonates (**Figure 1.4**).[37]

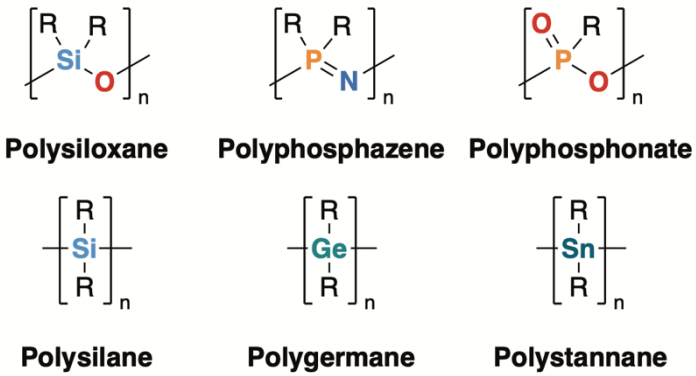


**Figure 1.4:** Examples of main-group polymers.

Polymers comprised of a main chain with repeating group 14 atoms other than carbon have also been explored. Namely, polysilanes, $[R_2Si]_n$, polygermanes $[R_2Ge]_n$, and polystannanes $[R_2Sn]_n$ (**Figure 1.4**).[38–40] Polysilanes were the first to be discovered from this group of main group polymers, where they were found to be semi-conductive as a result of delocalization of core-electrons along the main chain. In pursuit of more conductive polymers, research was then directed to polygermanes and polystannanes. However, inclusion of the heavier tin atoms into a polymer main chain presented significant challenges in producing stable polymers. One way to overcome these issues was recently reported by Foucher *et al* where they discovered that the inclusion of ether functional groups within the substituents that can bind to the Sn atoms of the main chain could reduce the polymers' susceptibility to nucleophilic attack and subsequent depolymerization.[41]

The work within this thesis focuses on another class of main-group polymers, polyaminoboranes, which feature alternating N and B atoms, and polyphosphinoboranes,

which feature alternating P and B atoms (**Figure 1.5**). These polymers are of interest as they are isoelectronic to polyolefins, but due to their polarized monomer unit have markedly different properties than their olefinic analogues.[12,42] The synthesis and properties of these polymers will be discussed in detail in the following sections.

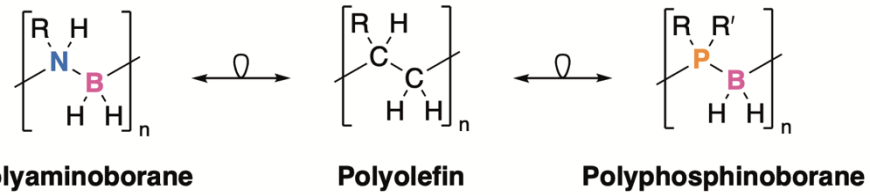


**Figure 1.5**: Structure of polyaminoboranes and polyphosphinoboranes and their isolobal analogy to polyolefins.

## 1.3 Polyaminoboranes

Polyaminoboranes are polymers that have alternating N and B atoms connected by single bonds. The first report of a polyaminoborane came from studies using $NH_3$•$BH_3$ as hydrogen storage materials, but more recently, soluble polyaminoboranes have been explored as precursors to boron nitride ceramics and piezoelectric materials.[43–45] Generally, polyaminoboranes are accessed *via* the dehydropolymerization of amine-borane adducts.[46]

### 1.3.1. Synthesis and Structure of Amine-Borane Adducts and Aminoboranes

Amine-borane adducts are molecules that contain a dative bond between a Lewis basic amine and a Lewis acidic borane. The first report of an amine-borane adduct came from Gay-Lussac and Thenard in 1809 where they had discovered $NH_3$•$BF_3$.[47] More than a century later, the parent amine-borane, $NH_3$•$BH_3$, was reported by Shore and Parry in

1955.[48] Since then, many amine-borane adducts have been synthesized and reported with substituents at either the nitrogen or boron centres, or both.

Several synthetic strategies have been described for amine-borane adducts. The most common route to access amine-borane adducts is through a direct reaction between the amine and a ligand-stabilized borane. For example, the reaction between RR'R"N (R,R', and R" = alkyl, aryl, H) and $BH_3$•L where L is a Lewis basic donor such as tetrahydrofuran (THF) or dimethylsulfide ($SMe_2$) will result in the displacement of the weaker Lewis base and formation of an amine-borane adduct (**Scheme 1.1**). However, these reactions have disadvantages as the former requires large volumes of solvent considering solutions of $BH_3$•THF are only available in low concentrations and the second reagent, $BH_3$•$SMe_2$, is malodourous due to the $SMe_2$ Lewis base donor.[42]

Amine-boranes and their unsaturated analogues are polarized due to the different Pauling electronegativity values each atom have ($\chi_N$ = 3.04; $\chi_B$ = 2.04).[49] This polarization extends to the behavior of any N–H and B–H bonds present in the amine-borane adduct, where any hydrogen atoms bound to the amine moiety will be polarized positively and behave as a Brønsted acid while any hydrogen atoms bound to boron will be polarized negatively and be of hydridic nature.[50] The dehydrogenation of amine-borane adducts results in the formation of an aminoborane, RR'N=$BH_2$, a class of compounds with a formal double bond (**Scheme 1.1**). Accordingly, both the boron and nitrogen centres have planar geometries, and large nitrogen substituents are required to yield stable aminoboranes as they will otherwise readily undergo catenation, hydrogen transfer, or other reactions.[51]

As alluded to above, the dehydrogenation of ammonia-borane ($H_3N{\bullet}BH_3$) has been of much interest to the research community as it has a high gravimetric hydrogen content (19.6%) making it a molecule of interest for hydrogen storage.[52–55] However, regenerating ammonia borane from its dehydrogenation products has proven to be a significant challenge.[43] The work in this thesis focusses on transient primary aminoboranes ($RNH{=}BH_2$), as they are precursor to polyaminoboranes. Thus, the generation of transient aminoboranes and polyaminoboranes will be the focus of the next sections.

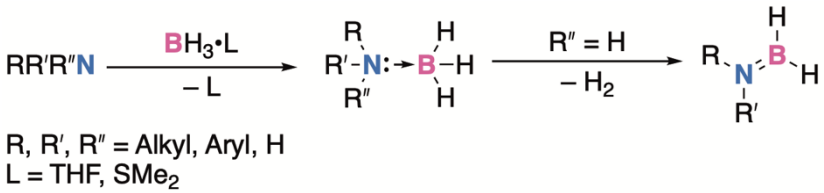


**Scheme 1.1:** Synthesis of amine-borane adducts and aminoboranes.

### 1.3.2 Properties and Applications of Polyaminoboranes

Polyaminoboranes are significantly different than polyolefins. For example, poly(*N*-methylaminoborane) is soluble in a range of solvents (e.g., tetrahydrofuran (THF), dichloromethane (DCM), and chloroform) whereas polypropylene, the analogous polymer with main chain comprised of carbon atoms, is insoluble in these solvents, and is only soluble in hot xylenes. This difference in solubilities is partially attributed to the inherent polarity of the main chain of polyaminoboranes. Further, thermal decomposition of these polymers occurs at different temperatures. Poly(*N*-methylaminoborane) decomposes at 160 °C where polypropylene decomposes at 400 °C.[28] This could be due to the formally dative N→B bonds within the polyaminoborane main chain that are weaker than the covalent C–C bonds within polypropylene, and thus release B–N fragments at lower

temperatures. Moreover, the presence of alternating protic and hydridic hydrogen atoms in polyaminoboranes may allow for the release of $H_2$ from the polymer and allow for the formation of products such as borazine $[MeN–BH]_3$.[56]

Polyaminoboranes have been sought as materials for several uses. One such use is as pre-ceramic polymers for hexagonal boron-nitride (h-BN), the B–N analogue of graphite.[57–59] In h-BN, the individual layers are bonded by weak van der Waals interactions. Accordingly, the layers are able to slide over each other giving h-BN lubricant properties. Further, h-BN has been sought for its useful properties such as thermal stability and conductivity, poor wettability, chemical inertness, and non-toxicity.[44,60] Moreover, a review on the application of h-BN in photonic devices has been recently published.[61] Accordingly, this material is of high interest to the scientific community. Preceramic polymers are attractive for the generation of ceramics as they often can be moulded into a desired shape prior to heating to yield the final ceramic material.[28]

Polyaminoboranes have also been sought as hydrogen storage materials as they are capable of releasing an equivalent of hydrogen.[54] However, considering they have lost one equivalent of hydrogen in the dehydropolymerization process, they are less attractive for hydrogen storage than their parent amine-borane adducts. More recently, polyaminoboranes have been shown to undergo catalytic depolymerization in the presence of strong bases.[62] Polyaminoboranes have also been explored computationally as piezoelectric materials. They were found to have up to double the spontaneous polarizability compared to polyvinylidene fluoride, $[H_2CCF_2]$, and thus would likely have enhanced piezoelectric responses.[45] Further, polyaminoboranes have been sought as

precursors for aluminum borate nanowires[63] or as delivery agents for boron neutron capture therapy.[64]

### 1.3.3 Synthesis of Polyaminoboranes

Accessing well-defined polyaminoboranes from their precursor amine-borane adducts involves two fundamental transformations: dehydrogenation and polymerization (**Scheme 1.2**).[65] The control over the dehydrogenation of amine-borane adducts is of particular importance as over dehydrogenation can lead to ill-defined cross-linked materials.[28] However, once generated, transient aminoboranes without significant steric encumbrance of the nitrogen centre can undergo addition polymerization.[65]

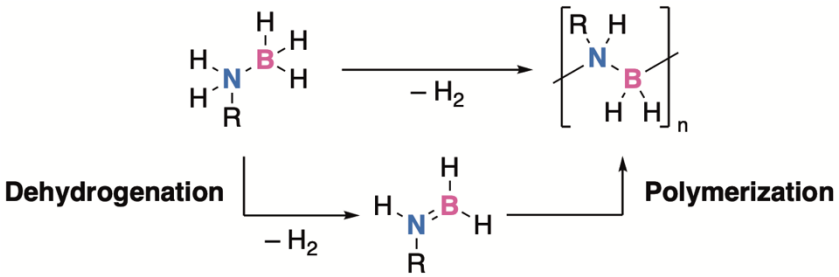


**Scheme 1.2**: General scheme for the dehydropolymerization of amine-borane adducts.

Attempted thermal dehydropolymerization of ammonia borane ($H_3N{\bullet}BH_3$) or cyclotriborazane ($H_2N–BH_2$) yields insoluble materials that are not well characterized.[66,67] Thermal dehydrogenation of primary and secondary amine-borane adducts yields cyclic oligomers, or, if the *N*-substituents are sufficiently sterically encumbering, stable aminoborane monomers.[65,68–70]

### 1.3.3.1 Metal Catalyzed Dehydropolymerization of Amine-Borane Adducts

Catalytic ambient condition dehydrocoupling of amine-borane adducts was first reported in 2001 using a rhodium precatalyst, $[Rh(COD)(\mu\text{-}Cl)]_2$ (COD = 1,5-cyclooctadiene) (**Scheme 1.3**).[71] Dehydrocoupling of *N*,*N*-dimethylamine-borane adduct ($Me_2NH{\bullet}BH_3$) resulted in the quantitative formation of the cyclic dimethylaminoborane (DMAB) dimer, $(Me_2N{-}BH_2)_2$. However, this precatalyst was shown to result in exhaustive dehydrogenation of *N*-methylamine borane adduct ($MeNH_2{\bullet}BH_3$), resulting in the formation of *N*-methyl borazine $(MeN{-}BH)_3$. Further, dehydrocoupling of ammonia borane ($NH_3{\bullet}BH_3$) results in the formation of borazine and other insoluble materials that are presumably a mix of oligomeric and polymeric materials. Mechanistic studies on the dehydrocoupling of amine borane adducts using $[Rh(COD)(\mu\text{-}Cl)]_2$ have concluded that the active species is of a heterogeneous nature.[72]

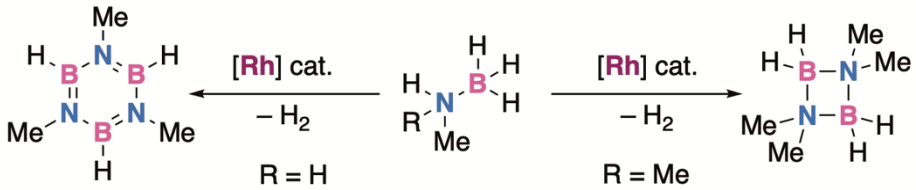


**Scheme 1.3**: Dehydrogenation of amine-borane adducts using a rhodium catalyst.

Dehydrocoupling of amine-borane adducts has since been a field of interest and a variety of transition metal catalysts for this transformation have been reported based on titanium,[73,74] manganese,[75] iron,[76–79] cobalt,[80–82] nickel,[83–85] rhodium,[86–91] ruthenium,[92–94] rhenium,[95] and iridium.[96,97] Beyond transition metal catalysts, several metal-free amine-borane dehydrocoupling catalysts have also been explored.[98–102]

Homogenous dehydropolymerization of ammonia-borane was first realized in 2006, where Goldberg *et. al.* used $IrH_2$(POCOP) (POCOP = $\eta^3$-1,3-$(OPtBu_2)_2C_6H_3$) to access a product assigned to be a cyclic pentameric product, $(H_2N–BH_2)_5$.[96] This same catalyst, $IrH_2$(POCOP), was later shown in 2008 to be proficient in the dehydropolymerization of $MeNH_2•BH_3$, accessing high molar mass material ($M_w$ = 160 000, $Đ$ = 2.9) (**Scheme 1.4**).[57,103] The ability of the iridium catalyst to access poly(*N*-methylaminoborane) and not undergo exhaustive dehydrogenation to *N*-methyl borazine has been attributed to the sterically encumbering *P*-substituents of the POCOP ligand, slowing down the second dehydrogenation step and allowing for formation of polymer. Since this seminal discovery, many homogenous (pre)catalysts have been reported for titanium,[104,105] iron,[106–108] cobalt,[109] zirconium,[110] ruthenium,[94] rhodium,[111–114] and iridium[115] centres.

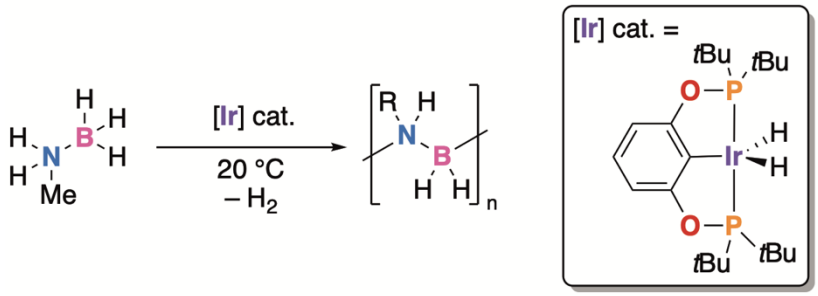


**Scheme 1.4**: Iridium catalyzed dehydropolymerization of $MeNH_2•BH_3$.

### 1.3.3.2 Metal-Free Synthesis of Polyaminoboranes

Metal-free synthesis of polyaminoboranes was first reported in 1970, where subjugation of borazine vapour to a radio frequency discharge followed by immediate quenching in liquid nitrogen (−196 °C) lead to the formation of $[H_2N–BH_2]$.[66] They reported

that $H_2N{=}BH_2$ was formed and would spontaneously polymerize between −196 °C and −155 °C. However, only the infrared spectrum of the resulting material was reported.

Later, in 2014, the generation of aminoborane monomers *in situ* through elimination reactions was explored (**Scheme 1.5**).[116] Here, initial reaction of amine-borane adducts ($MeRNH{\bullet}BH_3$; R = H, Me) with an acid (HCl, HOTf, $[H{\bullet}(OEt_2)_2][B(Ar^F)_4]$; OTf = triflate; $Ar^F$ = 1,3-bis-trifluoromethylphenyl) would result in liberation of hydrogen gas and formation of a new B functionalized amine-borane adduct ($MeRNH{\bullet}BH_2X$ (R = H, Me; X = Cl, OTf) or $[MeRNH{\bullet}BH_2(OEt_2)][B(Ar^F)_4]$ (R = H, Me). Subsequent deprotonation results in an elimination reaction producing aminoborane ($MeRN{=}BH_2$) and the corresponding conjugate acid. Monitoring these reactions by $^{11}B$ NMR spectroscopy confirmed that aminoboranes were accessed, but the products would quickly undergo cyclooligomerization to yield $[Me_2N{-}BH_2]_2$ or, in the case of $MeNH{=}BH_2$, addition polymerization to polyaminoborane.

Recent work from Alcaraz *et. al.* has shown an alternate route to access polyaminoboranes through reactions of primary amines ($RNH_2$) with diisopropylaminoborane (DIAB; $i Pr_2N{=}BH_2$) (**Scheme 1.5**).[117] Here, DIAB acts as a $BH_2$ transfer agent, where reaction with the primary amine results in the formation of the transient aminoborane ($RNH{=}BH_2$) and diisopropylamine ($iPr_2NH$). The resulting aminoborane can undergo head-to-tail catenation to access high molar mass materials. However, maintaining temperatures at or below –40 °C is essential as otherwise other reactions become thermodynamically viable, producing other non-polymeric products.

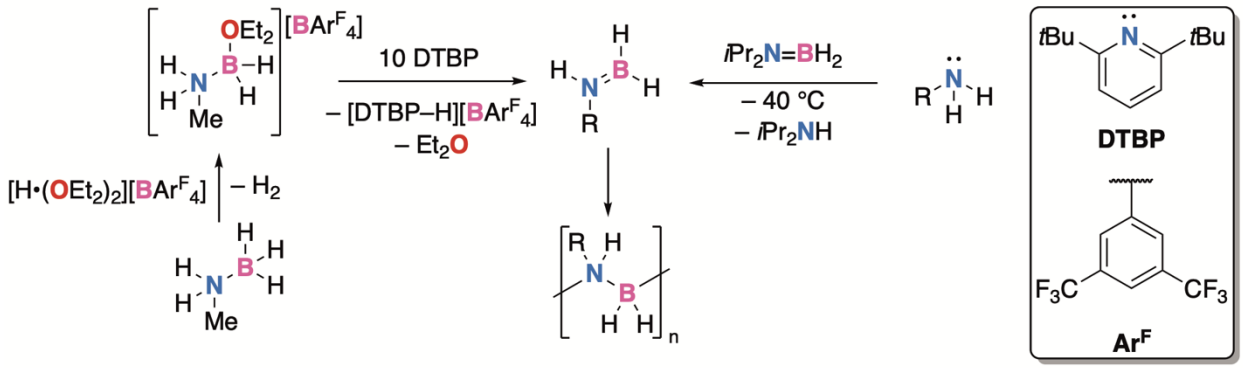


**Scheme 1.5**: Overview of metal-free synthesis of polyaminoboranes *via* the generation of aminoboranes *in situ*.

### 1.3.3.3 Substrate Scope for Amine-Borane Dehydropolymerization

The synthesis of polyaminoboranes from dehydropolymerization of amine-borane adducts has focussed on primarily *N*-monosubstituted amine-borane adducts (i.e., $RNH_2•BH_3$) (**Figure 1.6**).[57,104,105,117,118] To date, there are no reported polyaminoboranes bearing two non-hydrogen *N*-substituents nor are there polymers bearing both one *N*-substituent and one *B*-substituent. Further, no *N*-aryl substituted polyaminoboranes have been reported as their precursor adducts undergo spontaneous dehydrogenation and further reactivity to yield non-polymeric products.[119]

There are limited examples of B-substituted polyaminoboranes $[H_2N–BHR]_n$ (R = Ph, *p*-$(CF_3)C_6H_4$) (**Figure 1.6**).[120] However, the synthesis of these polymers is low yielding as a significant amount of borazine is formed and poly(*B*-phenylaminoborane) is thermally unstable. Attempts to prepare the *B*-methylated polyaminoborane from $H_3N•BH_2Me$ have been unsuccessful where thermal dehydrogenation has resulted in scrambling of B–Me and B–H bonds to yield mixed $H_3N•BH_xMe_{3-x}$ (x = 0, 1, 2, 3) adducts and catalytic dehydrogenation instead yields borazine $(HN–BMe)_3$ and bisamidoborane, $MeB(NH_2)_2$.[121]

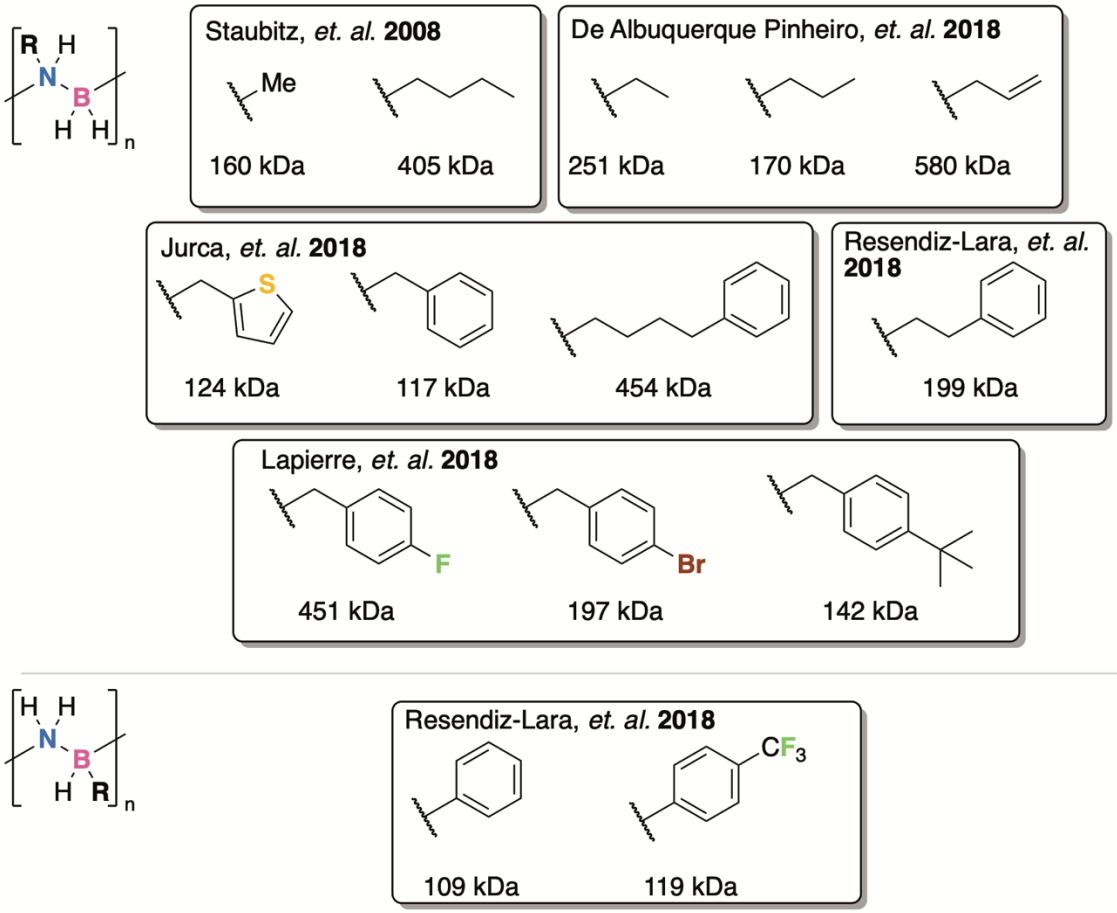


**Figure 1.6:** Overview of well characterized polyaminoboranes with organic substituents at nitrogen or boron, with $M_w$ values of the first characterized polymer of each type under each substituent.

## 1.4 Polyphosphinoboranes

Polyphosphinoboranes are a heavier congener of polyaminoboranes, where the nitrogen atoms are replaced with phosphorus atoms. Likewise, they are isoelectronic to polyolefins. These materials were first sought in the 1950's as they were predicted to have desirable traits such as high thermal stability.[122] Typically, they are synthesized from the dehydropolymerization of phosphine-borane adducts ($RR'PH{\bullet}BH_3$).

### 1.4.1 Synthesis and Structure of Phosphine-Borane Adducts and Phosphinoboranes

Phosphine-boranes adducts are comprised of a Lewis basic phosphine datively bound to a Lewis acidic borane. The first phosphine-borane adduct, $PH_3$•$BCl_3$, was reported in 1890.[123] The simplest phosphine-borane adduct, $PH_3$•$BH_3$ was first reported in 1940.[124] However, at the time it was misidentified as diborane diphosphine ($B_2H_6$•2($PH_3$)). It was not until 1966 where its correct structure was reported.[125] Since then, a large library of phosphine-borane adducts with one, two, and three *P*-substituents have been reported.

Phosphine-borane adducts are typically accessed in one of two ways (**Scheme 1.6**). They can be synthesized through the direct reaction between a phosphine (RR'R"P; R, R', R" = H, alkyl, aryl) and $BH_3$•L (L = THF, $SMe_2$) through a ligand displacement reaction.[126] Alternatively, phosphine-borane adducts can be accessed through the reduction of a chlorophosphine (RR'PCl) with two equivalents of $LiBH_4$.[127,128]

In contrast to amine-boranes which have a strong polarization of the N–B unit because of a great difference in their respective Pauling electronegativities, phosphine-borane adducts are less strongly polarized as they have similar Pauling electronegativity values ($\chi_P$ = 2.19, $\chi_B$ = 2.04, $\chi_H$ = 2.20).[49] This results in a reduced favourability in the dehydrogenation of phosphine-borane adducts into phosphinoboranes when compared to the dehydrogenation of amine-borane adducts into aminoboranes. Further, this is reflected in the general conditions required for catalytic dehydrogenation of either adduct (i.e., 20 °C to 60 °C for amine-borane adducts and 90 to 130 °C for phosphine-borane adducts).[46]

Dehydrogenation of phosphine-borane adducts ($RR'PH{\bullet}BH_3$) results in the formation of phosphinoboranes ($RR'P–BH_2$) (**Scheme 1.6**). Unlike aminoboranes, phosphinoboranes lack a P–B double bond and do not exhibit planar geometries at both phosphorus and boron centres. This is partly due to the high energy barrier for pyramidal inversion, which involves a change in phosphorus hybridization from $sp^3$ to $sp^2$, and the greater orbital size mismatch between boron and phosphorus.[51]

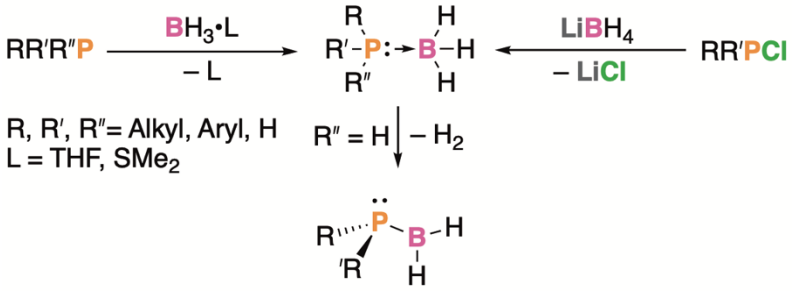


**Scheme 1.6**: Synthesis and structure of phosphine-borane adducts and phosphinoboranes.

### 1.4.2 Properties and Applications of Polyphosphinoboranes

Polyphosphinoboranes are air- and moisture-stable, making them ideal candidates for materials with real life applications. These materials are generally soft and malleable, with glass transition temperatures ($T_g$) that depend on the *P*-substituents.[28] Further, the $T_g$ of polyphosphinoboranes are generally lower than that of their analogous polyolefins likely because of longer P–B bonds in polyphosphinoboranes (*ca.* 1.90 – 2.0 Å) than C–C bonds (1.54 Å) in polyolefins.[129,130] For example, $[PhHP–BH_2]_n$, has a $T_g$ of 38 °C, while its carbon-based analogue, $[PhHC–CH_2]_n$ has a $T_g$ of 107 °C.

Application of polyphosphinoboranes has remained in its infancy as they are relatively unexplored polymers when compared to other classes polymeric materials. However, thin films of polyphosphinoboranes have demonstrated effectiveness as negative-tone resists in electron beam lithography and as tunable hydrophobic surfaces, where the water droplet contact angle can be adjusted by modifying the *P*-substituent.[129,131,132] Further, polyphosphinoboranes have recently been explored as self-extinguishing polymers[133] and as high-yielding precursors to boron phosphide-ceramics.[134] Polyphosphinoboranes have also been proposed to be candidates for non-linear optic materials,[135] but this has yet to be experimentally explored.

Polyphosphinoboranes can also be cross-linked into solvent swellable gels. These gels can be accessed through interchain dihydrogen loss which is reported to be controlled both by the *P*-substituents and the reaction conditions.[129] However, more recently Manners *et. al.* have explored the cross-linking of $[PhPH{\bullet}BH_2]_n$ through post-polymerization hydrophosphination reactions with 1,5-hexadiene.[136] This route has allowed for more control over the degree of cross-linking, and the resulting materials have shown to exhibit reversibly swellable organogel behaviour.

### 1.4.3 Synthesis of Polyphosphinoboranes

Polyphosphinoboranes were first targeted in the 1950's through the thermal dehydrogenation of *P*-methylated phosphine borane adducts ($MeRPH{\bullet}BH_3$; R = H, Me) at temperatures up to 200 °C in the presence of amines.[137–139] However, this resulted in low yields of low molecular weight materials that were poorly soluble and thus not well-characterized. Later, the thermal dehydrogenation of $PhPH_2{\bullet}BH_3$ at 100 – 150 °C was reported to yield a benzene soluble material that was assigned to be $[PhPH–BH_2]_n$.[140]

However, the material was determined to be of low molar mass and is poorly characterized by modern standards.

#### 1.4.3.1 Metal-Catalyzed Dehydropolymerization of Phosphine-Borane Adducts

Catalytic dehydropolymerization of phosphine-borane adducts was not reported until 1999, where it was discovered that $[Rh(COD)(\mu\text{-}Cl)]_2$ could dehydropolymerize $PhPH_2{\bullet}BH_3$ to $[PhPH–BH_2]_n$ in the melt phase (90 °C – 130 °C).[141,142] The material accessed was the first high molecular weight, definitively characterized polyphosphinoborane ($M_w$ = 31 kDa). However, the polymer displayed a large degree of chain branching and crosslinking due to the forcing conditions.

Later, $Cp(CO)_2Fe(OTf)$ was shown to be an effective catalyst.[131] This polymerization occurs in toluene, rather than in the melt, and at 100 °C, yielding material of relatively low dispersity and high molecular weight ($M_n$ = 40 000, $Đ$ = 1.70). Further, it was shown that the molecular weight of the resulting polymer could be controlled by the loading of the iron catalyst and a chain-growth polymerization mechanism for $PhPH_2{\bullet}BH_3$ was proposed.

Other transition metal catalysts have been discovered for the dehydropolymerization of various phosphine-borane adducts based on iron,[108,143] iridium,[144] and rhodium (**Scheme 1.7**).[145,145] However, these catalysts also generally operate under similar conditions (≥24 h, *ca.* 100 °C). The titanium catalyzed polymerization of trimethylamine-stabilized phosphinoboranes has also been recently explored.[146]

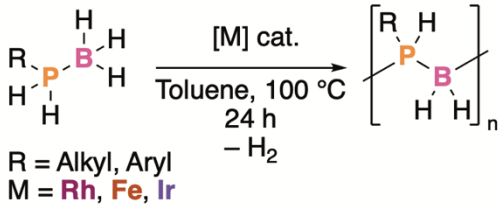


**Scheme 1.7:** Metal-catalyzed dehydropolymerization of phosphine-borane adducts.

### 1.4.3.2 Metal-Free Synthesis of Polyphosphinoboranes

Metal-free catalytic dehydropolymerization of phosphine-boranes was first explored in 2003, using tris(pentafluorophenylborane) (BCF) as a catalyst (**Scheme 1.8**).[147] Here, analysis of the reaction mixture by $^{31}$P NMR spectroscopy revealed that oligomeric and cyclic structures were accessed, which was confirmed by GPC ($M_n$ = 800 – 3 900 Da).

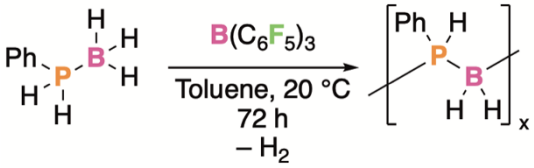


**Scheme 1.8:** BCF catalyzed dehydropolymerization of phosphine-borane adducts.

The metal-free synthesis of high molar mass polyphosphinoboranes was not achieved until 2015, through a collaborative effort between the Scheer and Manners groups.[148] The trimethylamine-stabilized phosphinoborane was first reported in 2006.[149] However to access polymeric materials, a trimethylamine stabilized phosphinoborane monomer, *t*BuPH–$BH_2$($NMe_3$) was synthesized. Subsequently, thermally driven (22 – 40 °C) dissociation of the trimethylamine ligand would yield phosphinoborane monomers *in situ* which would undergo head to tail addition polymerization to yield [*t*BuPH–$BH_2$]$_n$ ($M_n$ = 27 800 – 35 000 Da) (**Scheme 1.9**).

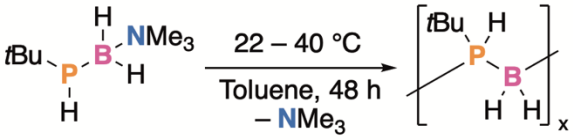


**Scheme 1.9**: Synthesis of polyphosphinoboranes *via* thermolysis of *t*BuPH–$BH_2(NMe_3)$.

Later, in 2019, cyclic alkyl(amino)carbenes (CAACs) were shown to accept $H_2$ from phosphine-borane adducts ($PhRPH{\bullet}BH_3$; R = H, Ph, Et) at 60 °C allowing for the synthesis of polyphosphinoboranes (**Scheme 1.10**).[150] Significantly, *P*-disubstituted polymeric material is accessed directly from phosphinoborane monomers, a transformation unrealized by metal-mediated catalytic dehydropolymerization.

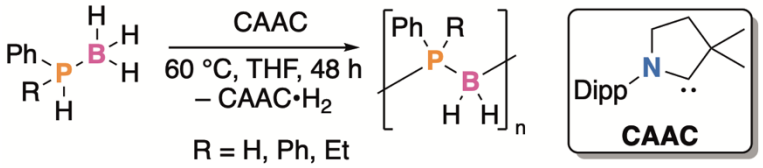


**Scheme 1.10:** Synthesis of polyphosphinoboranes using CAAC as a dihydrogen acceptor.

### 1.4.3.3 Substrate Scope for Phosphine-Borane Dehydropolymerization

The vast majority of polyphosphinoboranes are *P*-monosubstituted polymers. In most cases, attempted dehydropolymerization of *P*-disubstituted phosphine-borane adducts results in the formation of linear dimers, or other non-polymeric compounds. Using the transformations mentioned above polymers bearing several different substituents have been accessed including alkyl, aryl, and ferrocenyl subunits (**Figure 1.7**).[142,144,151,148,129,143,145,152,153]

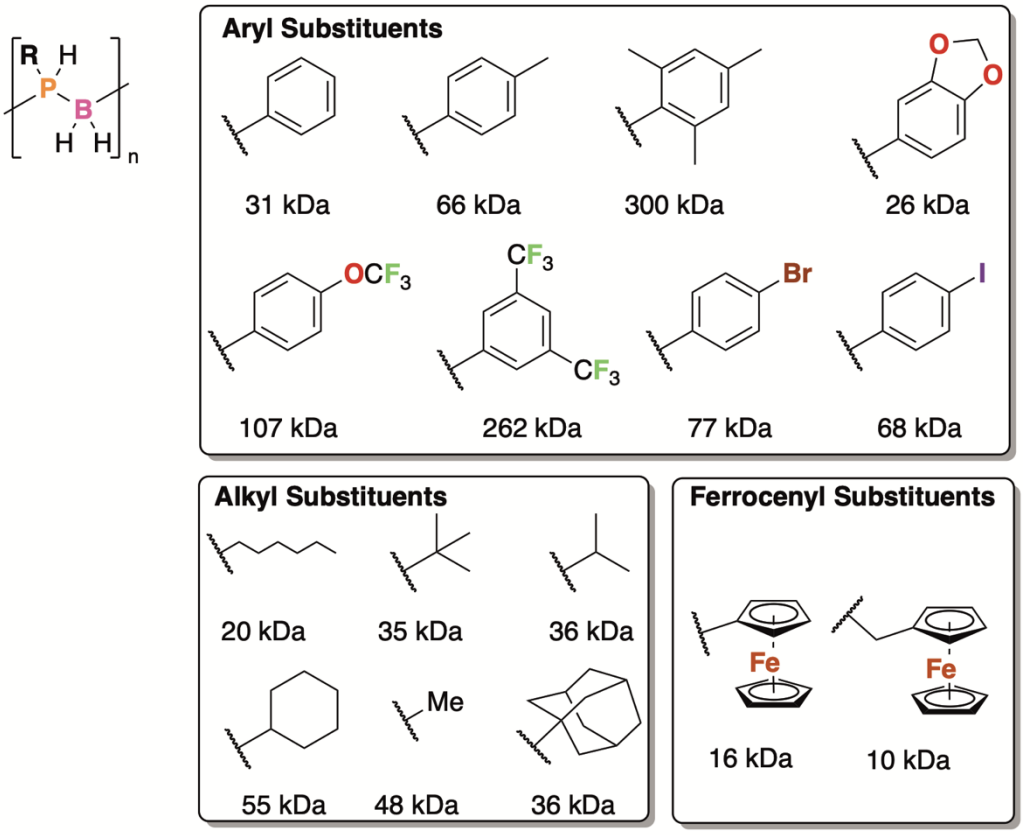


**Figure 1.7:** Polyphosphinoboranes accessed *via* metal-catalyzed dehydropolymerization with $M_w$ values (kDa) given for the first polymer accessed of each type below each substituent.

### 1.4.3.4 *P*-Disubstituted Polyphosphinoboranes

Accessing *P*-disubstituted polymers has been possible through two strategies. These polymers are sought after as the lack of a P–H bond in their resulting materials is predicted to result in a more robust material that is more suitable for large-scale use. Post-polymerization functionalization is one way to access these materials (**Scheme 1.11**). Here, hydrophosphination reactions between $[PhPH–BH_2]_n$ and olefinic substrates can result in materials that are either fully *P*-disubstituted or random copolymers of *P*-mono-

and disubstituted monomers.[136] However, this route results in a chain scission and generation of materials with lower molar mass, especially at high degrees of insertion. Alternatively, *P*-disubstituted polymers can be accessed from the reaction of phosphine-borane adducts ($PhRPH{\bullet}BH_3$; R = Ph, Et) with CAAC.[150] However, the materials produced have bimodal mass distributions where the high molar mass fraction of material is significantly lower than the fraction of low molar mass materials.

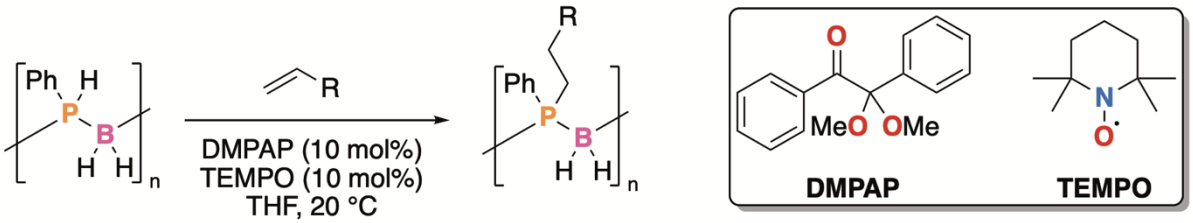


**Scheme 1.11**: Post-polymerization functionalization of polyphosphinoboranes to access *P*-disubstituted materials.

## 1.5 Mechanistic Insights into Amine- and Phosphine-Borane Dehydropolymerization

Intimately understanding the mechanism of transformations allows for the hypothesis-driven design of better catalysts and may allow for access to new materials. Most experimental mechanistic studies in the dehydropolymerization of amine- and phosphine-borane adducts have been on transition-metal mediated transformations. Accordingly, much of the following section will summarize this topic. However, with increasing examples of transition-metal-free syntheses of polyamino- and phosphinoboranes more mechanistic work has been done and will be discussed.

### 1.5.1 Amine-Borane Dehydropolymerization

Dehydropolymerization of amine-borane adducts $RNH_2•BH_3$; R = H, Alkyl, Aryl) is a challenge as often the formation of oligomeric species and other small molecule products is thermodynamically favoured. Further, a second dehydrogenation can occur, yielding borazine or other poorly soluble materials (**Scheme 1.12**).[46] As mentioned above, many catalysts have been discovered for the dehydrogenation and dehydropolymerization of amine-borane adducts, but few have been studied in detail.

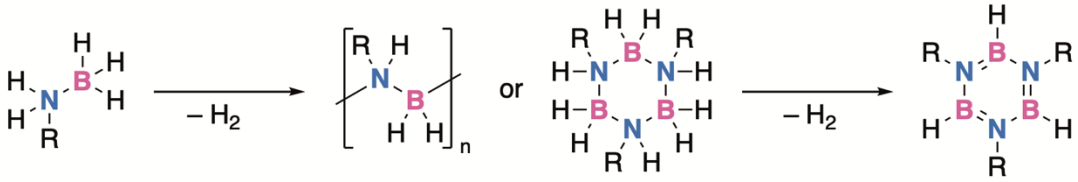


**Scheme 1.12**: Dehydrogenation of amine-borane adducts into polymers and cyclotriborazane and further dehydrogenation into borazine.

Dehydropolymerization of amine-boranes involves two fundamental transformations: the initial dehydrogenation of the amine-borane adducts and subsequent polymerization of the generated monomers.[65] Normally, mechanistic evidence is obtained through monitoring the rate of dehydrogenation by measuring the pressure or volume of hydrogen gas produced over the course of the reaction. The amount of hydrogen produced can also give information on how many dehydrogenation events have occurred. Further, kinetic isotope effects can be determined using deuterated amine-boranes and supported computationally.[154] For determining the rate of dehydrogenation, *N,N*-dimethylamine borane ($Me_2NH•BH_3$) is commonly used as its product of dehydrogenation

is the well characterized and easily identified dimethylaminoborane cyclic dimer, $(Me_2N–BH_2)_2$ (DMAB).

The metal-catalyzed dehydrogenation of amine-borane adducts has been reported to operate *via* three different routes. Amine-boranes can either interact with metal centres through an inner-sphere N–H/B–H interaction (**Scheme 1.13**, **a**) or a metal-ligand cooperative mechanism (**Scheme 1.13**, **b**). Alternatively, initial hydride abstraction by a metal centre can result in formation of a boronium species that can subsequently release an aminoborane with an equivalent of dihydrogen (**Scheme 1.13**, **c**). Each case involves the formation of a σ-bond interaction between the metal and the amine-borane.[65] The study of the aminoborane monomers that are formed, especially those that polymerize, is especially challenging as they readily catenate or undergo other reactivity. There are examples of aminoboranes interacting with metal centres where the primary coordination mode is *via* two bridging B–H hydrides.[97,155–157] However, there has been a recent report in which incorporation of an aminoborane into a pincer ligand allowed for the study of $\eta^2$-N,B coordination mode.[158] Further, aminoboranes can be trapped using cyclohexene through hydroboration reactions to yield $RHN=BCy_2$.[159] However, this depends on the relative rate of hydroboration or coordination vs. catenation.

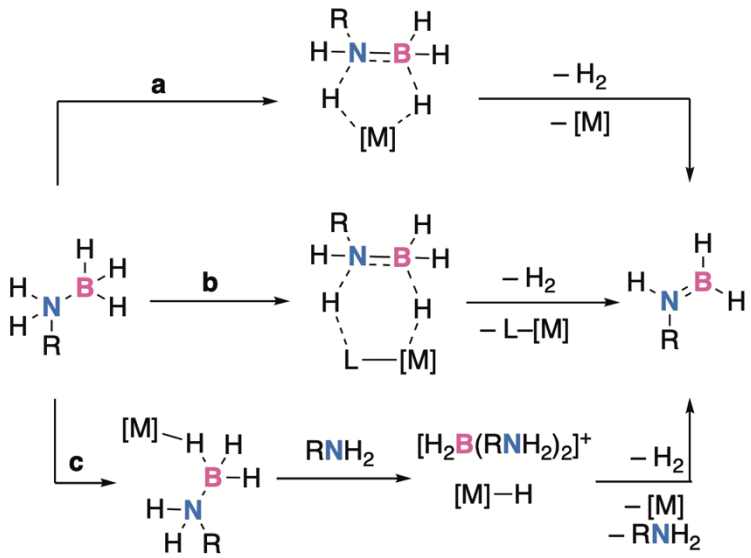


**Scheme 1.13**: Overview of metal-mediated amine-borane dehydrogenation.

After dehydrogenation, polymerization occurs. Typically, polymerizations are broadly categorized as chain-growth or step growth. Chain growth polymerizations are generally identified by the presence of high molecular weight materials at low conversions of monomer or through the presence of higher molecular weight materials when a lower polymerization catalyst loading is used. Step growth polymerization is typically identified *via* the presence of high molecular weight materials at only high rates of conversion.[160]

Coordination–insertion mechanisms evocative of single-site olefin polymerization catalysts benefit from the ability to intimately control the way in which individual monomers are incorporated into the polymer chain.[161–163] An analogous coordination, dehydrogenation, polymerization mechanism has been reported for dehydropolymerization of amine-borane adducts using [Rh(Xantphos){$H_2B(NMe_3)((CH_2)_2tBu)$}][$BAr^F_4$] (**Figure 1.8**).[164] When the reaction is monitored, this catalyst displays an induction period, indicative that the added catalyst undergoes an initial transformation into an active species, proposed to be a rhodium-

amidoborane complex. Next, an equivalent of amine-borane is coordinated to the Rh-centre and subsequently dehydrogenated yielding $MeNH{=}BH_2$ which can insert into the growing polyaminoborane chain. For this catalyst, a chain-growth polymerization mechanism was proposed as high molar mass material would be accessed at low conversions of $MeNH_2{\bullet}BH_3$ and using high loadings of catalyst would result in lower molar mass materials being formed. Further, it was shown that hydrogen has a deleterious effect on polymer molecular weights and was proposed to be a chain transfer agent. Chain transfer reactions were shown to be disfavoured in a polar coordinating solvent, THF, as higher molar mass materials were accessed in THF than in the non-coordinating solvent, fluorobenzene.

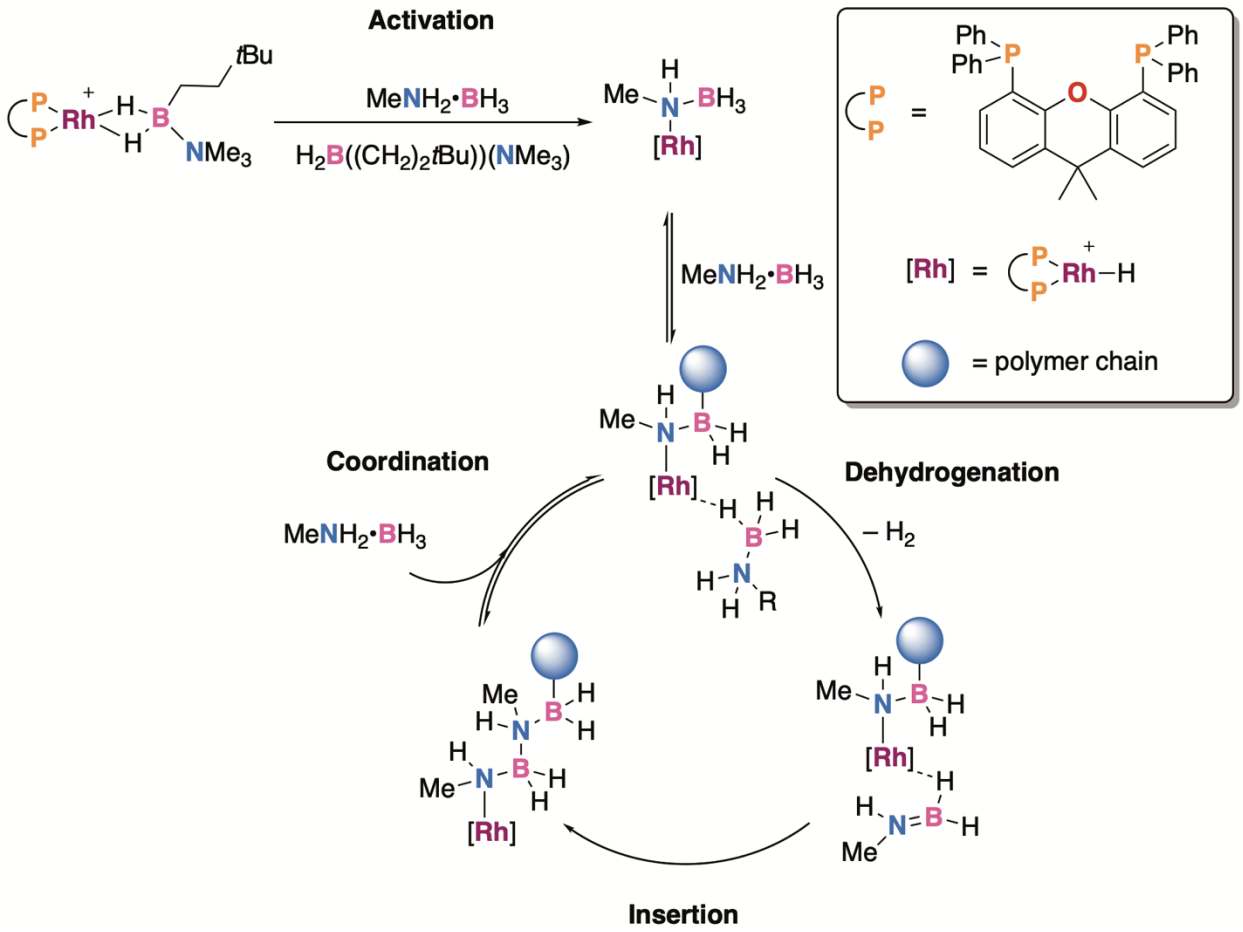


**Figure 1.8:** Proposed mechanism for the dehydropolymerization of $MeNH_2•BH_3$ using a rhodium catalyst.

The dehydropolymerization of $NH_3•BH_3$ has been proposed to also undergo a coordination/insertion mechanism using $[IrH_2(H_2)_2(PCy_3)_2][BAr^F{}_4]$ as the catalyst (**Figure 1.9**).[165] However, in addition to dehydrogenation and insertion events, this catalyst was also proposed to undergo key reversible chain transfer events. These key chain transfer events were evidenced by the reaction of $[Ir(PCy_3)_2(H)_2\{\eta^2\text{-}H_3B•NH_3\}][BAr^F{}_4]$ with further equivalents of $NH_3•BH_3$, which would result in the formation of a mixture of Ir-bound oligomers, $[Ir(PCy_3)_2(H)_2\{\eta^2\text{-}H_3B•(H_2N–BH_2)_n•NH_3\}][BAr^F{}_4]$ (n = 1 – 3), and free oligomers, $H_3B•(NH_2–BH_2)•NH_3$. The presence of free oligomers suggests that the Ir-bound

oligomers are weakly coordinated and can be displaced by free $H_3N{\bullet}BH_3$. Computational studies into the polymerization mechanism favour an entirely on-metal dehydropolymerization. This catalyst is capable of dehydrogenating bulkier amine-borane adducts, $MeRNH{\bullet}BH_3$ (R = H, Me), but is unable to accommodate their oligomers bound to the metal centre.[97,115] Chain transfer reactions have later shown to be effective ways of controlling polymer molecular weights in the $[Rh\{\kappa^3\text{-}(i\text{Pr}_2PCH_2CH_2)_2NH\}(\eta^2,\eta^2\text{-NBD})]Cl$ (NBD = norbanadiene) mediated dehydropolymerizations of $MeNH_2{\bullet}BH_3$.[114]

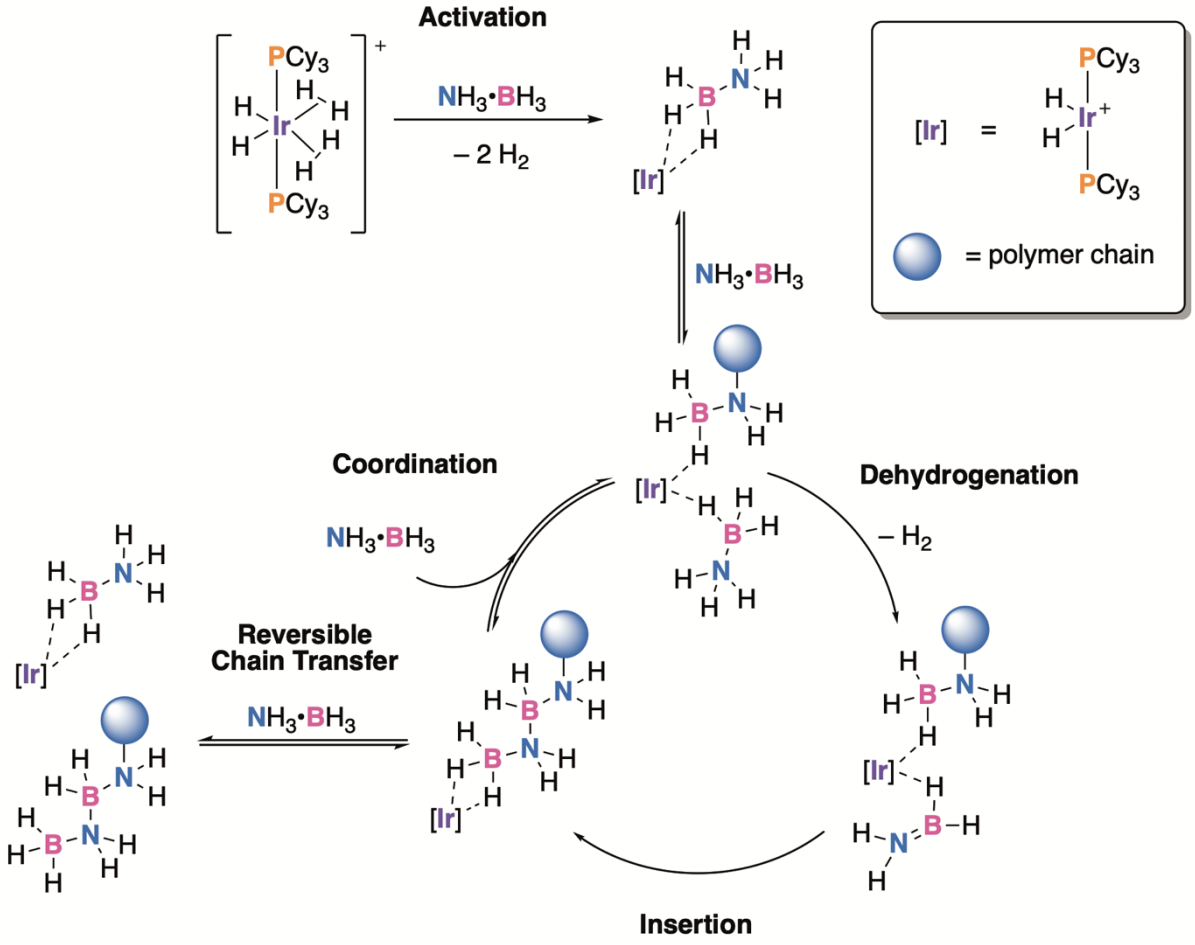


**Figure 1.9:** Proposed mechanism for the dehydropolymerization of $NH_3{\bullet}BH_3$ using $[IrH_2(H_2)_2(PCy_3)_2][BAr^F{}_4]$ as the catalyst.

Alternatively, a mechanism for amine-borane dehydropolymerization in which separate metal centres are involved in the dehydrogenation and polymerization events has been reported. Polymerizations that operate *via* this mechanism show no clear correlation between molecular weight and catalyst loading. Individual studies by the Manners and Paul groups suggest that dehydropolymerization of $NH_3$•$BH_3$ using $IrH_2$POCOP follows this mechanism.[103,166] Here, an iridium centre first dehydrogenates an equivalent of $NH_3$•$BH_3$, and a separate iridium centre binds an aminoborane monomer, initiating the polymerization. The polymerization is proposed to occur from an [Ir(POCOP)$(H)_2(\eta^2$-$H_2B$–$NH_2)$] complex, with a terminal amine unit that can undergo successive nucleophilic attack reactions upon aminoboranes formed *in situ* to access polyaminoborane chains (**Figure 1.10**). These addition events were shown to be strongly exergonic computationally, resulting in a facile oligomerization pathway. Nucleophilic chain growth has also been proposed for the {Rh(Xantphos)} and [Rh{$\kappa^3$-($i$Pr$_2$P$CH_2CH_2)_2$NH}$(\eta^2,\eta^2$-NBD)]Cl (NBD = norbanadiene) mediated dehydropolymerizations of $MeNH_2$•$BH_3$.[113,114]

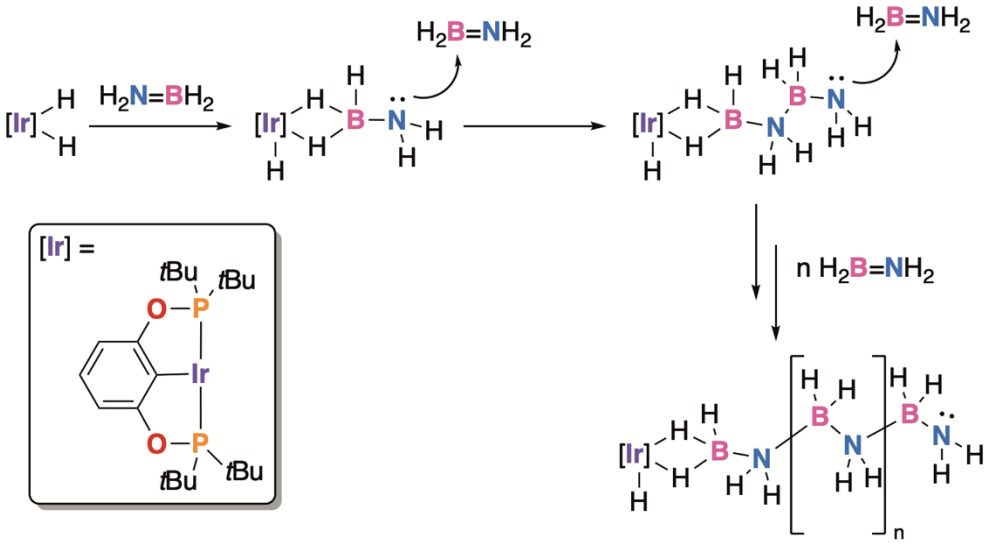


**Figure 1.10**: Proposed mechanism for the Ir-initiated head-to-tail addition polymerization of $H_2N{=}BH_2$ formed *in situ*.

The dehydropolymerization of amine-boranes using early transition metals has been less explored. However, in 2018 the Manners group reported a titanium catalyst formed from the *in situ* reaction of $Cp^*_2TiCl_2$ with 2 equivalents of *n*BuLi for the dehydropolymerization of $MeNH_2{\bullet}BH_3$.[104] This catalyst was hypothesized to have a step-growth polymerization mechanism as high molar mass polyaminoborane was only accessed at high conversion of amine-borane. Further, treating low molar mass material with catalyst would result in the formation of higher molecular weight material and higher molar mass material was accessed with higher catalyst loadings. Later, $Cp^*_2TiMe$ was reported to be an active catalyst in the dehydropolymerization of amine-boranes ($RNH_2{\bullet}BH_3$) where preliminary mechanistic studies evoke a redox neutral mechanism with a Ti(III)–H resting state.[105]

### 1.5.2 Phosphine-Borane Dehydropolymerization

The dehydropolymerization of phosphine-boranes has been studied far less than their lighter congeners, amine-boranes.[46] In contrast to amine-borane dehydropolymerization that normally occurs under ambient conditions, catalytic phosphine-borane dehydropolymerization occurs only at elevated temperatures, complicating the observation of reactive intermediates as they readily undergo further reactivity.

The first catalyst reported for phosphine-borane dehydropolymerization, $[Rh(COD)(\mu\text{-}Cl)_2]_2$, has been shown to likely operate *via* a homogenous step-growth mechanism.[72,134,167] The homogenous nature of the catalyst was evidenced through mechanistic studies on the dehydrocoupling of $Ph_2PH{\bullet}BH_3$. Here, it was shown that addition of excess mercury or substoichiometric $Ph_3P$ had no effect on the activity of the catalyst. The addition of mercury to heterogenous catalysts often poisons the catalyst by adsorbing or forming an amalgam on the catalyst surface. Further, if the catalyst was heterogeneous in nature, the addition of substoichiometric phosphine would poison the catalyst as only a fraction of the metal centres are present on the surface of the particles. Moreover, no effect was observed in the rate of dehydrocoupling after filtering the reaction mixture through a 0.5 μm filter and no induction period or black precipitate was observed. The step-growth nature of the dehydropolymerization was determined from the observation that high molar mass polymeric material would only be accessed at high conversions of $PhPH_2{\bullet}BH_3$. However, these reactions are performed at elevated temperatures in the melt phase impeding the observation of reaction intermediates and further mechanistic studies.

The first detailed study of a phosphine-borane dehydrocoupling catalyst was performed by the Weller group in 2012.[168] Here, they explored the ability of $[Rh(COD)_2][BAr^F_4]$ to dehydrocouple $t$Bu$_2$PH•BH$_3$ to $t$Bu$_2$PH•BH$_2$–$t$Bu$_2$P•BH$_3$ under melt conditions. Dissolution of the reaction mixture in 1,2-$F_2C_6H_4$ and analysis by ESI-MS revealed the formation of $[Rh(t\text{Bu}_2\text{PH})_2(\eta^6\text{-}F_2C_6H_4)]^+$ and $[Rh(t\text{Bu}_2\text{PH})_2(\eta^2\text{-}H_3B\bullet t\text{Bu}_2\text{P–BH}_2\bullet t\text{Bu}_2)]^+$. It was proposed that $[Rh(t\text{Bu}_2\text{PH})_2(\eta^6\text{-}F_2C_6H_4)]^+$ was accessed through the substitution of the COD ligands of $[Rh(COD)_2][BAr^F_4]$ with $t$Bu$_2$PH formed *in situ*. Subsequently, it was revealed that $[Rh(t\text{Bu}_2\text{PH})_2(\eta^6\text{-}F_2C_6H_4)]^+$ was also a competent catalyst in the dehydrocoupling of $t$Bu$_2$PH•BH$_3$ and had comparable activity to $[Rh(COD)_2][BAr^F_4]$. Therefore, it was hypothesized that $[Rh(t\text{Bu}_2\text{PH})_2(\eta^6\text{-}F_2C_6H_4)]^+$ was the active catalyst.

Later, the Weller group explored the dehydrocoupling of phosphine-borane adducts using a Rh catalyst bearing a chelating diphosphine ligand, $[Rh(dppp)(\eta^6\text{-}C_6H_5F)][BAr^F_4]$ (dppp = $Ph_2P(CH_2)_3PPh_2$) (**Figure 1.11**).[169] Reaction of this complex with two equivalents of $Ph_2PH•BH_3$ gave displacement of $C_6H_5F$, and formation of $[Rh(dppp)(\sigma,\kappa^2\text{-}PPh_2BH_3)(\kappa^1\text{-}H_3B•PPh_2H)][BAr^F_4]$. The phosphidoborane is a result of an initial P–H activation event resulting in a P–Rh(III) bond, and the unit is further tethered *via* a B–H agostic interaction. The unreacted phosphine-borane is bound *via* a B–H σ-bond to the metal centre. However, confirmation of these binding modes could not be obtained as this complex will readily undergo a dehydrocoupling event to give $[Rh(dppp)(\sigma,\eta^1\text{-}PPh_2•BH_2–Ph_2•PBH_3)][BAr^F_4]$. The electronic nature of the organic phosphorus substituents were shown to have an effect on the rate of this P–B dehydrocoupling event, where a higher rate is observed for phosphine-borane adducts

with electron withdrawing groups and a slower one is observed for electron donating groups.[170] [Rh(dppp)(η$^6$-$C_6H_5F$)][$BAr^F_4$] was also shown to be an effective catalyst for the dehydropolymerization of $CyPH_2$•$BH_3$ where analogous intermediates to $Ph_2PH$•$BH_3$ were observed.

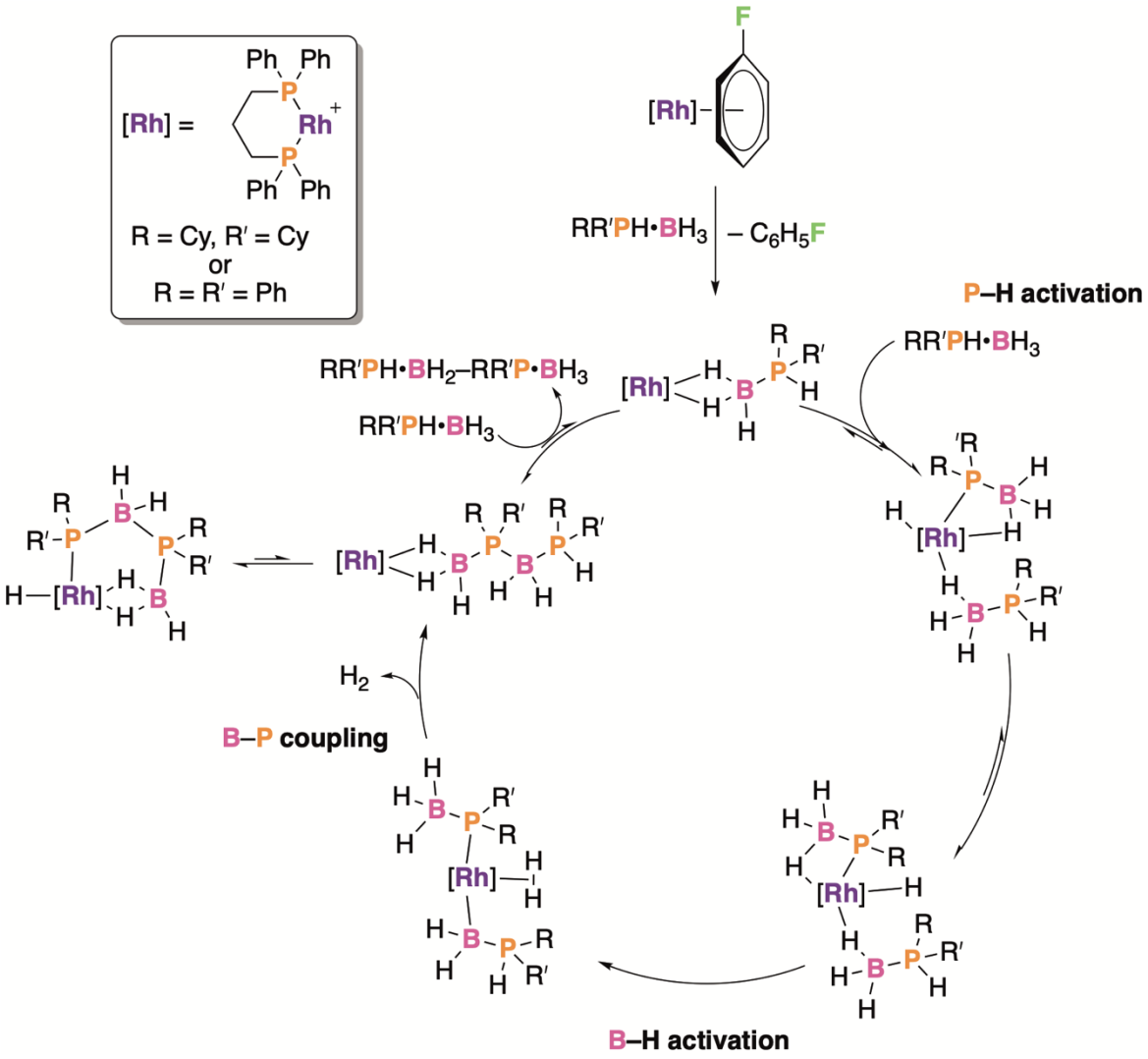


**Figure 1.11**: Proposed mechanism for the dehydrocoupling of $Ph_2PH$•$BH_3$ or $CyPH_2$•$BH_3$ using [Rh(dppp)(η$^6$-$C_6H_5F$)][$BAr^F_4$].

In 2016, the Weller group turned their attention to [RhCp*Me($PMe_3$)($CH_2Cl_2$)][$BAr^F_4$] as a phosphine-borane dehydrocoupling catalyst (**Figure 1.12**).[145] The authors targeted this catalyst as it should be able to readily access a vacant coordination site *via* dissociation of $CH_2Cl_2$ which may allow for the monitoring of P/B–H activation events. Similar to analogous amine-borane chemistry, the authors used *P*-disubstituted phosphine-borane adducts to model the E–H (E = P, B) activation events, and complementary computational studies suggested that B–H activation occurs first followed by P–H activation to yield the active catalyst, [RhCp*(Cp)($PhPH–BH_2$)]. Following the formation of this phosphidoborane complex, a step growth dehydropolymerization of phosphineborane units is proposed to occur *via* reversible chain transfer. This is proposed as $PhPH_2•BH_3$ is rapidly consumed and a significant portion of linear dimer, $PhPH_2•BH_2–PhPH•BH_3$, is observed early in the reaction.

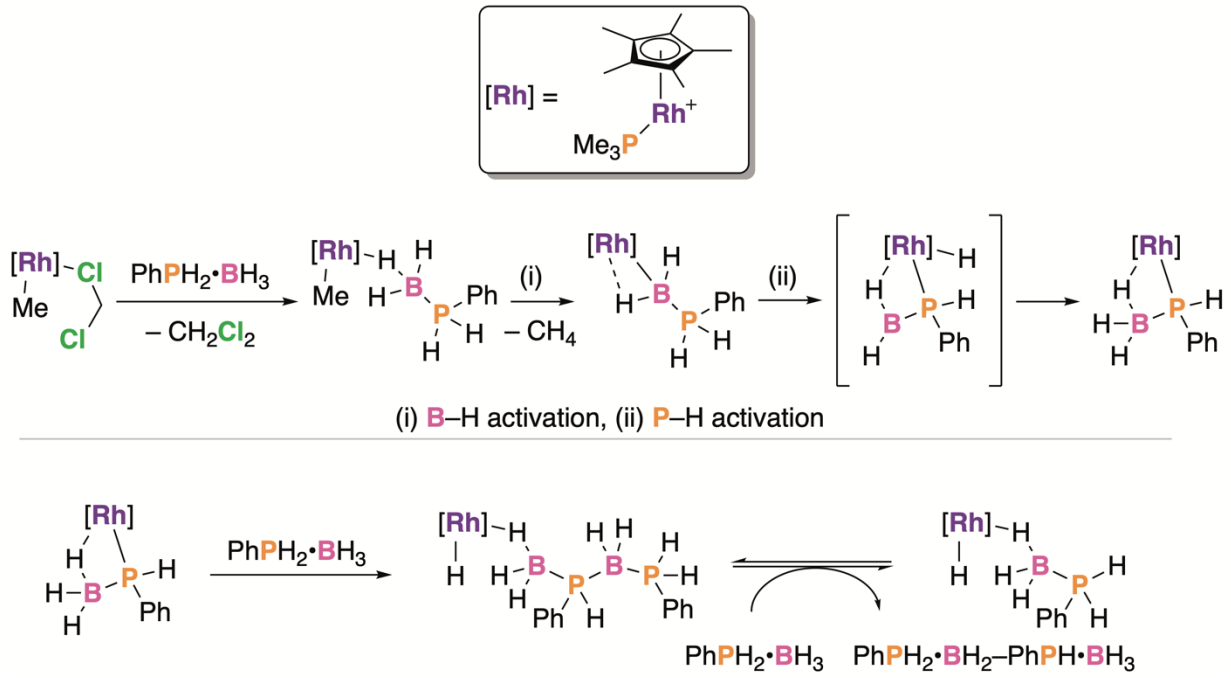


**Figure 1.12**: Dehydrocoupling of $PhPH_2•BH_3$ using $[Rh(Cl_2CH_2)(PMe_3)Cp^*][BAr^F{}_4]$ *via* generation of the active species (top) and subsequent reversible chain transfer (bottom).

The use of more abundant metals in the dehydropolymerization of phosphine-boranes is also of interest. In 2015, our group explored the ability of $CpFe(CO)_2OTf$ to catalyze the dehydropolymerization of $PhPH_2•BH_3$.[131] This catalyst operates in the solution phase and was determined to be homogenous through a $PMe_3$ poisoning experiment. Further, previously synthesized iron nanoparticles were shown to be incapable of catalyzing the dehydropolymerization of $PhPH_2•BH_3$. $CpFe(CO)_2OTf$ has been proposed to operate *via* a chain growth coordination/insertion mechanism. It is suggested to undergo a chain growth mechanism as at low conversion of $PhPH_2•BH_3$, high molar mass $[PhPH–BH_2]_n$ is observed. Further, polymer molar mass was found to have an inverse relationship with catalyst loading, where at low [Fe] loadings, higher

molar mass material was obtained and lower molar mass material was obtained at high [Fe] loadings. The stoichiometric reaction between $CpFe(CO)_2OTf$ and $PhPH_2•BH_3$ would result in P–H activation and yield the phosphidoborane complex, $CpFe(CO)_2(PPhHBH_3)$. Further, this phosphidoborane complex was shown to be equally active in the dehydropolymerization of $PhPH_2•BH_3$. Photolysis of $CpFe(CO)_2(PPhHBH_3)$ would result in the loss of an equivalent of CO and formation of a B–H agostic interaction yielding $CpFe(CO)(\kappa^2\text{-}PPhHBH_3)$. However no comment on its ability to catalyze the dehydropolymerization of $PhPH_2•BH_3$ was made. Reaction of $CpFe(CO)_2(PPhHBH_3)$ with a further equivalent of $PhH_2•BH_3$ resulted in the formation of an iron-bound P–B dimeric species, $CpFe(CO)_x(\kappa^1\text{-}PPhH•BH_2–PhPH•BH_3)$, as suggested by ESI-MS. Based on their findings, the authors proposed the following chain growth polymerization mechanism (**Figure 1.13**). First, an iron phosphide borane species formed *in situ* coordinates another equivalent of phosphine-borane adduct, and subsequently activates the B–H bond of the P–B adduct and inserts the phosphine-borane into the growing polymer chain. This polymer is tethered *via* a terminal B–H σ-complex. Subsequent P–H activation results in a species in which a new iron phosphide bond from the recently inserted P–B unit is formed. Next, $H_2$ elimination and coordination of another equivalent of $PhPH_2•BH_3$ allows for the turnover of the catalytic cycle for further chain propagation.

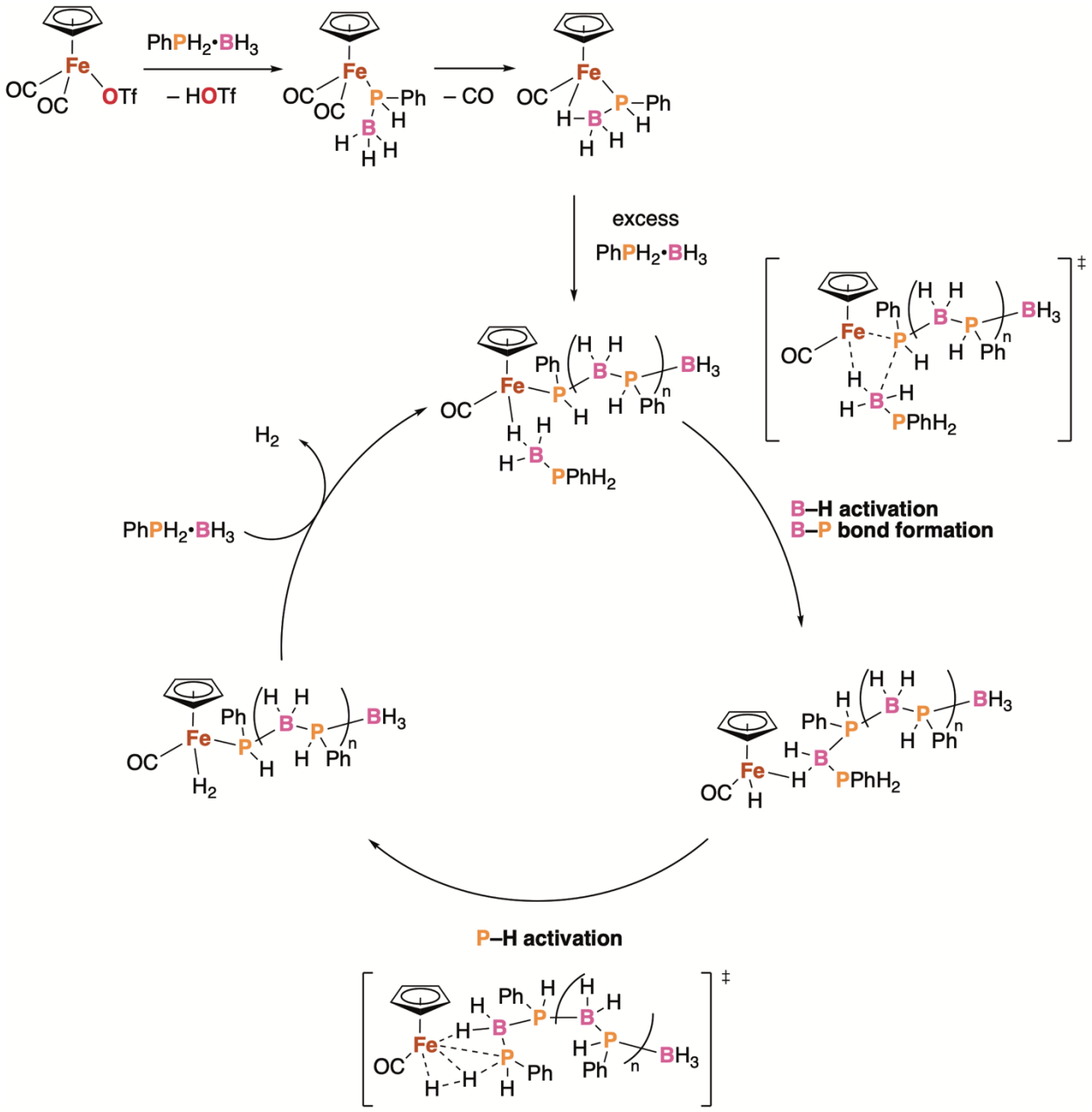


**Figure 1.13:** Proposed mechanism for the dehydropolymerization of $PhPH_2{\bullet}BH_3$ using $CpFe(CO)_2(OTf)$ as the catalyst.

### 1.5.3 Transition-Metal-Free Synthesis of Polyaminoboranes and Polyphosphinoboranes

The synthesis of polyaminoboranes and polyphosphinoboranes without metal-catalyzed dehydrocoupling targets the generation of reactive aminoboranes or phosphinoboranes *in situ*. These reactive species can self-initiate and undergo head-to-tail addition polymerization (**Figure 1.14**).

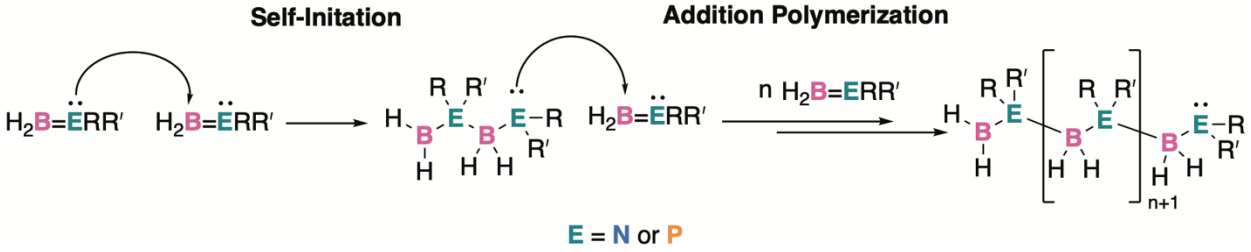


**Figure 1.14:** Self-initiated polymerization of transient aminoboranes and phosphinoboranes.

In 2018, the Alcaraz group reported the metal-free-synthesis of polyaminoboranes through the reaction of primary aminoboranes $RNH_2$ with $iPr_2N{=}BH_2$.[117] Here, DIAB acts as a "$BH_2$" transfer unit, producing the more reactive aminoborane, $RNH{=}BH_2$, and $iPr_2NH$. If the reaction is performed at –40 °C, the reactive aminoborane then undergoes uncontrolled polymerization to access high molar mass materials. However, if the reaction is performed under ambient conditions, many other reactions occur to give small molecule products. The authors later reported a more detailed study in which they explained that the polymerization is kinetically controlled, where at higher temperatures the formation of cyclotriborazane is the thermodynamically favoured process.[171] The other products

observed are a result of bimolecular N–H proton and B–H hydride transfer reactions through 6-membered transition states.

In 2006, Gaumont *et*. al. explored $B(C_6F_5)_3$ (BCF) as a catalyst for phosphine-borane dehydropolymerization where only oligomeric material was obtained ($M_n$ *ca.* 3000 Da).[147] Later in 2015, in a collaboration the Scheer and Manners groups, the synthesis of trimethylamine stabilized phosphinoboranes, $RPH–BH_2(NMe_3)$, as polymer precursors was reported.[148] Here, thermolysis of the B–N bond would result in the release of transient phosphinoboranes *in situ* that could undergo head-to-tail addition polymerization to yield polymeric materials.

Metal-free dehydropolymerization of phosphine-borane adducts has allowed access to materials that are so far inaccessible *via* metal-based catalysis. In 2019, the Manners group reported on the ability to use CAACs to accept $H_2$ from phosphine-borane adducts.[150] Here, initial deprotonation of $Ph_2PH•BH_3$ with CAAC results in the formation of the $[PhPH(BH_3)][CAAC–H]$ ion pair. Under ambient conditions, the phosphorus centre can undergo a nucleophilic attack of iminium carbon of $[CAAC–H]^+$ resulting in the formation of $PhPH(CAAC–H)•BH_3$. However, at 60 °C, it is possible for the $[CAAC–H]^+$ ion to accept a hydride from the $BH_3$ unit, resulting in the formation of $CAAC•H_2$ and $PhHP–BH_2$. It is then proposed that as the phosphinoborane is ambipolar, it can self-initiate and begin polymerization. However, linear oligomers can undergo cyclization reactions, as observed for $PhRPH•BH_3$ (R = Ph, Et). However, if the rate of oligomer cyclization is less than the rate of continued linear growth, high molar mass polymeric materials can be obtained, as observed for $PhPH_2•BH_3$. The authors also proposed a second mechanism, in which trace Lewis acids or bases can initiate a polymerization,

allowing for chain growth from either boron or phosphorus termini (**Figure 1.15**). This chain-capping would prevent cyclization of linear oligomers and allow for the formation of only linear polymers, allowing for the formation of $[PhRP–BH_2]_n$ (R = Ph, Et). They supported this hypothesis with ESI-MS data, where oligomers capped with CAAC were observed. Later, in a separate report by Pomogaeva and Timoshkin exploring phosphinoborane tetramers and decamers, $[PH_2–BH_2]_{4,10}$, they found that capping a phosphinoborane oligomer with either a strong Lewis base (i.e. CAAC) or both a weak Lewis acid and base could disfavour cyclization reactions.[172]

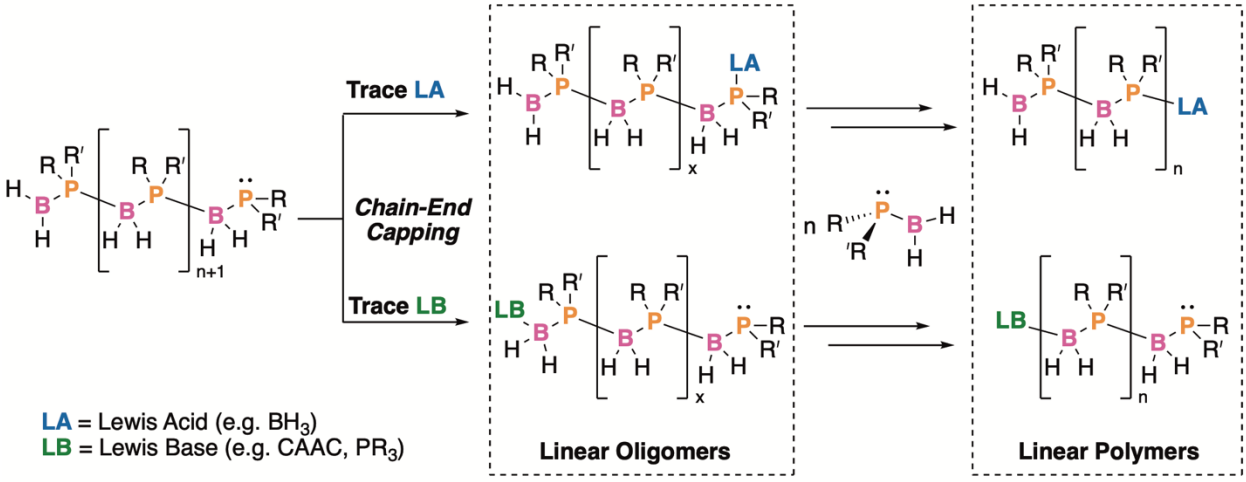


**Figure 1.15**: Proposed chain-growth mechanism for the head-to-tail addition polymerization of phosphinoborane monomers made *in situ*.

## 1.6 Thesis Summary and Acknowledgement of Collaborators

This thesis describes four research projects related to the generation and reactivity of transient aminoboranes and phosphinoboranes as polymer precursors. The following five chapters are:

- Chapter 2. Transition-Metal-Free Dehydropolymerization of Phosphine-Borane Adducts at Ambient Temperature
- Chapter 3. Generation and Reactivity of Transient Primary Aminoboranes
- Chapter 4. Chain-Stabilization Yields High Molecular Weight Polyphosphinoboranes and Molecular Weight Control in the Thermal Dehydropolymerization of $PhPH_2 \bullet BH_3$
- Chapter 5. Ambient Condition Dehydrocoupling of Phosphine-Borane Adducts using Aminoboranes as Hydrogen Acceptors
- Chapter 6. Conclusions and Future Work

In line with Prof. Ian Manners' research group policy, this thesis is comprised of self-contained chapters, each intended for publication. Most research projects involved collaboration, with contributions outlined below, as well as expanded upon at the beginning of each chapter.

Chapter 2. This chapter was reproduced from *Chem. Eur. J.* **2022**, *29* (2), e202202897. Dr Subrata Kundu performed exploratory reactions to access polyphosphinoboranes. Dr. Etienne A. LaPierre had input on experimental design and assisted with solving single crystal X-ray diffraction data. Dr. Patrick O. Brian acquired single crystal X-ray diffraction data.

Chapter 3. This chapter contains as of yet unpublished work. Dr. Owen J. Metters performed exploratory reactions in trapping reactive aminoboranes formed *in situ*. Dr. Patrick O. Brian acquired single crystal X-ray diffraction data.

Chapter 4. This chapter contains as of yet unpublished work. Jade E. T. Watson assisted with the synthesis of polyphosphinoboranes. Charles Kileen and Dr. J. Scott McIndoe assisted with acquisition and analysis of mass spectrometry data.

Chapter 5. This chapter contains as of yet unpublished work. This chapter had no significant collaborations.

In addition to the work included in this thesis, I was also involved in research projects related to polyphosphinoboranes that resulted in two other publications (*Angew. Chem. Int. Ed.* **2022**, *61* (22), e202202176 and *Angew. Chem. Int. Ed.* **2023***, 62* (3), e202216106). However, as this thesis is a single author document, only the projects in which I was responsible for the majority of experiment design, data acquisition, data interpretation, and communication are presented.

## 1.7 References

(1) Natta, G.; Pino, P.; Mazzanti, G.; Giannini, U. A Crystallizable Organometallic Complex Containing Titanium and Aluminum. *Journal of the American Chemical Society* **1957**, *79* (11), 2975–2976. https://doi.org/10.1021/ja01568a083.

(2) Eisch, J. J. Fifty Years of Ziegler–Natta Polymerization: From Serendipity to Science. A Personal Account. *Organometallics* **2012**, *31* (14), 4917–4932. https://doi.org/10.1021/om300349x.

(3) Chauvin, Y. Olefin Metathesis: The Early Days (Nobel Lecture). *Angewandte Chemie International Edition* **2006**, *45* (23), 3740–3747. https://doi.org/10.1002/anie.200601234.

(4) Schrock, R. R. Multiple Metal–Carbon Bonds for Catalytic Metathesis Reactions (Nobel Lecture). *Angewandte Chemie International Edition* **2006**, *45* (23), 3748–3759. https://doi.org/10.1002/anie.200600085.

(5) Grubbs, R. H. Olefin-Metathesis Catalysts for the Preparation of Molecules and Materials (Nobel Lecture). *Angewandte Chemie International Edition* **2006**, *45* (23), 3760–3765. https://doi.org/10.1002/anie.200600680.

(6) Miyaura, N.; Suzuki, A. Palladium-Catalyzed Cross-Coupling Reactions of Organoboron Compounds. *Chemical Reviews* **1995**, *95* (7), 2457–2483. https://doi.org/10.1021/cr00039a007.

(7) Beletskaya, I. P.; Cheprakov, A. V. The Heck Reaction as a Sharpening Stone of Palladium Catalysis. *Chemistry Reviews.* **2000**, *100* (8), 3009–3066. https://doi.org/10.1021/cr9903048.

(8) Rosenberg, L. Mechanisms of Metal-Catalyzed Hydrophosphination of Alkenes and Alkynes. *ACS Catalysis* **2013**, *3* (12), 2845–2855. https://doi.org/10.1021/cs400685c.

(9) Obligacion, J. V.; Chirik, P. J. Earth-Abundant Transition Metal Catalysts for Alkene Hydrosilylation and Hydroboration. *Nature Reviews Chemistry* **2018**, *2* (5), 15–34. https://doi.org/10.1038/s41570-018-0001-2.

(10) Nakajima, Y.; Shimada, S. Hydrosilylation Reaction of Olefins: Recent Advances and Perspectives. *RSC Advances* **2015**, *5* (26), 20603–20616. https://doi.org/10.1039/C4RA17281G.

(11) Mears, K. L.; Nguyen, G.-A.; Ruiz, B.; Lehmann, A.; Nelson, J.; Fettinger, J. C.; Tuononen, H. M.; Power, P. P. Hydrobismuthation: Insertion of Unsaturated Hydrocarbons into the Heaviest Main Group Element Bond to Hydrogen. *Journal of the American Chemical Society* **2024**, *146* (1), 19–23. https://doi.org/10.1021/jacs.3c06535.

(12) Leitao, E. M.; Jurca, T.; Manners, I. Catalysis in Service of Main Group Chemistry Offers a Versatile Approach to P-Block Molecules and Materials. *Nature Chem*istry **2013**, *5* (10), 817–829. https://doi.org/10.1038/nchem.1749.

(13) Jones, R. G.; Holder, S. J. High-Yield Controlled Syntheses of Polysilanes by the Wurtz-Type Reductive Coupling Reaction. *Polymer International* **2006**, *55* (7), 711–718. https://doi.org/10.1002/pi.1945.

(14) Clark, T. J.; Lee, K.; Manners, I. Transition-Metal-Catalyzed Dehydrocoupling: A Convenient Route to Bonds between Main-Group Elements. *Chemistry – A European Journal* **2006**, *12* (34), 8634–8648. https://doi.org/10.1002/chem.200600981.

(15) Corcoran, E. W.; Sneddon, L. G. Transition-Metal-Promoted Reactions of Boron Hydrides. 6. Platinum(II) Bromide Catalyzed Borane and Carborane

Dehydrodimerization Reactions: A New Synthetic Route to Boron-Boron Linked Multicage Boranes and Carboranes. *Journal of the American Chemical Society* **1984**, *106* (25), 7793–7800. https://doi.org/10.1021/ja00337a024

(16) Waterman, R. Mechanisms of Metal-Catalyzed Dehydrocoupling Reactions. *Chemical Society Reviews* **2013**, *42* (13), 5629–5641. https://doi.org/10.1039/C3CS60082C.

(17) Less, R. J.; Melen, R. L.; Wright, D. S. Catalytic versus Stoichiometric Dehydrocoupling Using Main Group Metals. *RSC Advances* **2012**, *2* (6), 2191–2199. https://doi.org/10.1039/c2ra00882c.

(18) Melen, R. L. Dehydrocoupling Routes to Element–Element Bonds Catalysed by Main Group Compounds. *Chemical Society Reviews* **2016**, *45* (4), 775–788. https://doi.org/10.1039/C5CS00521C.

(19) S. Hill, M.; J. Liptrot, D.; Weetman, C. Alkaline Earths as Main Group Reagents in Molecular Catalysis. *Chemical Society Reviews* **2016**, *45* (4), 972–988. https://doi.org/10.1039/C5CS00880H.

(20) Weetman, C.; Inoue, S. The Road Travelled : After Main-group Elements as Transition Metals. *ChemCatChem* **2018**, *10* (19), 4213–4228. https://doi.org/10.1002/cctc.201800963.

(21) Melen, R. L. Frontiers in Molecular P-Block Chemistry: From Structure to Reactivity. *Science* **2019**, *363* (6426), 479–484. https://doi.org/10.1126/science.aau5105.

(22) Feldman, D. Polymer History. *Designed Monomers and Polymers* **2008**, *11* (1), 1–15. https://doi.org/10.1163/156855508X292383.

(23) Walsh, D. J.; Hyatt, M. G.; Miller, S. A.; Guironnet, D. Recent Trends in Catalytic Polymerizations. *ACS Catalysis* **2019**, *9* (12), 11153–11188. https://doi.org/10.1021/acscatal.9b03226.

(24) Manners, I. Polymer Science with Transition Metals and Main Group Elements: Towards Functional, Supramolecular Inorganic Polymeric Materials. *Journal of Polymer Science Part A: Polymer Chemistry* **2002**, *40* (2), 179–191. https://doi.org/10.1002/pola.10069.

(25) Vidal, F.; Jäkle, F. Functional Polymeric Materials Based on Main-Group Elements. *Angewandte Chemie International Edition* **2019**, *58* (18), 5846–5870. https://doi.org/10.1002/anie.201810611.

(26) Baumgartner, T.; Jaekle, F. *Main Group Strategies Towards Functional Hybrid Materials*; John Wiley & Sons, Incorporated: Newark, 2018.

(27) Dück, K.; Gates, D. P. Main-Chain, Phosphorus-Based Polymers. In *Main Group Strategies towards Functional Hybrid Materials*; John Wiley & Sons, Ltd, 2018; pp 329–355. https://doi.org/10.1002/9781119235941.ch13.

(28) Staubitz, A.; Hoffmann, J.; Gliese, P. Group 13–Group 15 Element Bonds Replacing Carbon–Carbon Bonds in Main Group Polyolefin Analogs. *Smart Inorganic Polymers* **2019**, 17–39. https://doi.org/10.1002/9783527819140.ch2_1.

(29) He, X.; Baumgartner, T. Conjugated Main-Group Polymers for Optoelectronics. *RSC Advances* **2013**, *3* (29), 11334–11350. https://doi.org/10.1039/c3ra40286j.

(30) Caminade, A.-M.; Hey-Hawkins, E.; Manners, I. Smart Inorganic Polymers. *Chemical Society Reviews* **2016**, *45* (19), 5144–5146. https://doi.org/10.1039/c6cs90086k.

(31) Manners, I. Polymers and the Periodic Table: Recent Developments in Inorganic Polymer Science. *Angewandte Chemie International Edition in English* **1996**, *35* (15), 1602–1621. https://doi.org/10.1002/anie.199616021.

(32) Chivers, T.; Manners, I. *Inorganic Rings and Polymers of the P-Block Elements*. RSC publishing, 2009.

(33) Mark, J. E. Some Interesting Things about Polysiloxanes. *Accounts of Chemical Research* **2004**, *37* (12), 946–953. https://doi.org/10.1021/ar030279z.

(34) Shit, S. C.; Shah, P. A Review on Silicone Rubber. *National Academy Science Letters.* **2013**, *36* (4), 355–365. https://doi.org/10.1007/s40009-013-0150-2.

(35) Rothemund, S.; Teasdale, I. Preparation of Polyphosphazenes: A Tutorial Review. *Chemical Society Reviews* **2016**, *45* (19), 5200–5215. https://doi.org/10.1039/c6cs00340k.

(36) Allcock, H. R. The Expanding Field of Polyphosphazene High Polymers. *Dalton Transactions* **2016**, *45* (5), 1856–1862. https://doi.org/10.1039/c5dt03887a.

(37) Arz, M. I.; Annibale, V. T.; Kelly, N. L.; Hanna, J. V.; Manners, I. Ring-Opening Polymerization of Cyclic Phosphonates: Access to Inorganic Polymers with a P(V)–O Main Chain. *Journal of the American Chemical Society* **2019**, *141* (7), 2894–2899. https://doi.org/10.1021/jacs.8b13435.

(38) West, R. The Polysilane High Polymers. *Journal of Organometallic Chemistry* **1986**, *300* (1), 327–346. https://doi.org/10.1016/0022-328X(86)84068-2.

(39) Adachi, Y.; Ohshita, J. Germanium and Tin in Conjugated Organic Materials. In *Main Group Strategies towards Functional Hybrid Materials*; John Wiley & Sons, Ltd, 2018; pp 237–264. https://doi.org/10.1002/9781119235941.ch10.

(40) Foucher, D. Catenated Germanium and Tin Oligomers and Polymers. In *Main Group Strategies towards Functional Hybrid Materials*; John Wiley & Sons, Ltd, 2018; pp 209–236. https://doi.org/10.1002/9781119235941.ch9.

(41) Pau, J.; Lough, A. J.; Wylie, R. S.; Gossage, R. A.; Foucher, D. A. Proof of Concept Studies Directed Towards Designed Molecular Wires: Property-Driven Synthesis of Air and Moisture-Stable Polystannanes. *Chemistry – A European Journal* **2017**, *23* (57), 14367–14374. https://doi.org/10.1002/chem.201703453.

(42) Staubitz, A.; Robertson, A. P. M.; Sloan, M. E.; Manners, I. Amine− and Phosphine−Borane Adducts: New Interest in Old Molecules. *Chemical Reviews.* **2010**, *110* (7), 4023–4078. https://doi.org/10.1021/cr100105a.

(43) Staubitz, A.; Robertson, A. P. M.; Manners, I. Ammonia-Borane and Related Compounds as Dihydrogen Sources. *Chemical Reviews* **2010**, *110* (7), 4079–4124. https://doi.org/10.1021/cr100088b.

(44) Bernard, S.; Miele, P. Polymer-Derived Boron Nitride: A Review on the Chemistry, Shaping and Ceramic Conversion of Borazine Derivatives. *Materials* **2014**, *7* (11), 7436–7459. https://doi.org/10.3390/ma7117436.

(45) Nakhmanson, S. M.; Nardelli, M. B.; Bernholc, J. Ab Initio Studies of Polarization and Piezoelectricity in Vinylidene Fluoride and BN-Based Polymers. *Physical Review Letters* **2004**, *92* (11). https://doi.org/10.1103/PhysRevLett.92.115504.

(46) Han, D.; Anke, F.; Trose, M.; Beweries, T. Recent Advances in Transition Metal Catalysed Dehydropolymerisation of Amine Boranes and Phosphine Boranes. *Coordination Chemistry Reviews* **2019**, *380*, 260–286. https://doi.org/10.1016/j.ccr.2018.09.016.

(47) Gay-Lussac, J. L.; Thenard, J. L. $NH_3BF_3$. *Mémoires de Physique et de Chimie de la Société d'Arcueil* **1809**, *2*, 207–234.

(48) Shore, S. G.; Parry, R. W. The Crystalline Compound Ammonia-Borane $H_3N{\bullet}BH_3$ *Journal of the American Chemical Society* **1955**, *77* (22), 6084–6085. https://doi.org/10.1021/ja01627a103.

(49) Atkins, P.; Robertson, A. P. M.; Rourke, J.; Weller, M.; Armstrong, F. *Inorganic Chemistry*; Oxford University Press: New York, USA, 2014; Vol. 6.

(50) Liu, Z.; Marder, T. B. B-N versus C-C: How Similar Are They? *Angewandte Chemie International Edition* **2008**, *47* (2), 242–244. https://doi.org/10.1002/anie.200703535.

(51) Power, P. P. π-Bonding and the Lone Pair Effect in Multiple Bonds between Heavier Main Group Elements. *Chemical Reviews* **1999**, *99* (12), 3463–3504. https://doi.org/10.1021/cr9408989.

(52) Stephens, F. H.; Pons, V.; Tom Baker, R. Ammonia-Borane: The Hydrogen Source Par Excellence? *Dalton Transactions* **2007**, No. 25, 2613–2626. https://doi.org/10.1039/B703053C.

(53) Marder, T. B. Will We Soon Be Fueling Our Automobiles with Ammonia–Borane? *Angewandte Chemie International Edition* **2007**, *46* (43), 8116–8118. https://doi.org/10.1002/anie.200703150.

(54) W. Hamilton, C.; Tom Baker, R.; Staubitz, A.; Manners, I. B–N Compounds for Chemical Hydrogen Storage. *Chemical Society Reviews* **2009**, *38* (1), 279–293. https://doi.org/10.1039/B800312M.

(55) Bhunya, S.; Malakar, T.; Ganguly, G.; Paul, A. Combining Protons and Hydrides by Homogeneous Catalysis for Controlling the Release of Hydrogen from Ammonia-Borane: Present Status and Challenges. *ACS Catalysis* **2016**, *6* (11), 7907–7934. https://doi.org/10.1021/acscatal.6b01704.

(56) Wideman, T.; Sneddon, L. G. Dipentylamine-Modified Polyborazylene: A New, Melt-Spinnable Polymeric Precursor to Boron Nitride Ceramic Fibers. *Chemistry of Materials* **1996**, *8* (1), 3–5. https://doi.org/10.1021/cm950398b.

(57) Staubitz, A.; Presa Soto, A.; Manners, I. Iridium-Catalyzed Dehydrocoupling of Primary Amine–Borane Adducts: A Route to High Molecular Weight Polyaminoboranes, Boron–Nitrogen Analogues of Polyolefins. *Angewandte Chemie* **2008**, *120* (33), 6308–6311. https://doi.org/10.1002/ange.200801197.

(58) Kim, D. P.; Moon, K. T.; Kho, J. G.; Economy, J.; Gervais, C.; Babonneau, F. Synthesis and Characterization of Poly-(Aminoborane) as a New Boron Nitride Precursor. *Polymers for Advanced Technologies* **1999**, *10* (12), 702–712. https://doi.org/10.1002/(sici)1099-1581(199912)10:12<702::aid-pat931>3.0.co;2-q.

(59) Wang, X.; Hooper, T. N.; Kumar, A.; Priest, I. K.; Sheng, Y.; Samuels, T. O. M.; Wang, S.; Robertson, A. W.; Pacios, M.; Bhaskaran, H.; Weller, A. S.; Warner, J. H. Oligomeric Aminoborane Precursors for the Chemical Vapour Deposition Growth of Few-Layer Hexagonal Boron Nitride. *Crystal Engineering Communication* **2017**, *19* (2), 285–294. https://doi.org/10.1039/c6ce02006b.

(60) Eichler, J.; Lesniak, C. Boron Nitride (BN) and BN Composites for High-Temperature Applications. *Journal of the European Ceramic Society* **2008**, *28* (5), 1105–1109. https://doi.org/10.1016/j.jeurceramsoc.2007.09.005.

(61) Caldwell, J. D.; Aharonovich, I.; Cassabois, G.; Edgar, J. H.; Gil, B.; Basov, D. N. Photonics with Hexagonal Boron Nitride. *Nature Reviews Materials* **2019**, *4* (8), 552–567. https://doi.org/10.1038/s41578-019-0124-1.

(62) Oldroyd, N. L.; Chitnis, S. S.; LaPierre, E. A.; Annibale, V. T.; Walsgrove, H. T. G.; Gates, D. P.; Manners, I. Ambient Temperature Carbene-Mediated Depolymerization: Stoichiometric and Catalytic Reactions of *N* -Heterocyclic- and Cyclic(Alkyl)Amino Carbenes with Poly( *N* -Methylaminoborane) $[MeNH–BH_2]_n$. *Journal of the American Chemical Society.* **2022**, *144* (50), 23179–23190. https://doi.org/10.1021/jacs.2c10931.

(63) An Du, V.; Jurca, T.; R. Whittell, G.; Manners, I. Aluminum Borate Nanowires from the Pyrolysis of Polyaminoborane Precursors. *Dalton Transactions* **2016**, *45* (3), 1055–1062. https://doi.org/10.1039/C5DT03324A.

(64) Barth, R. F.; Coderre, J. A.; Vicente, M. G. H.; Blue, T. E. Boron Neutron Capture Therapy of Cancer: Current Status and Future Prospects. *Clinical Cancer Research* **2005**, *11* (11), 3987–4002. https://doi.org/10.1158/1078-0432.CCR-05-0035.

(65) Colebatch, A. L.; Weller, A. S. Amine-Borane Dehydropolymerization: Challenges and Opportunities. *Chemistry* **2019**, *25* (6), 1379–1390. https://doi.org/10.1002/chem.201804592.

(66) McGee, H. A.; Kwon, C. T. Cryochemical Preparation of Monomeric Aminoborane. *Inorganic Chemistry* **1970**, *9* (11), 2458–2461. https://doi.org/10.1021/ic50093a015.

(67) Baumann, J.; Baitalow, F.; Wolf, G. Thermal Decomposition of Polymeric Aminoborane $(H_2BNH_2)_x$ under Hydrogen Release. *Thermochimica Acta* **2005**, *430* (1), 9–14. https://doi.org/10.1016/j.tca.2004.12.002.

(68) Chopard, P. A.; Hudson, R. F. Some Adducts of Phosphines and Amines with Borane. *Journal of Inorganic and Nuclear Chemistry* **1963**, *25* (7), 801–805. https://doi.org/10.1016/0022-1902(63)80365-6.

(69) Beachley, O. T. Intermediates in the Formation of N-Methylaminoborane Trimer and N,N-Dimethylaminoborane Dimer. *Inorganic Chemistry* **1967**, *6* (5), 870–874. https://doi.org/10.1021/ic50051a004.

(70) Ryschkewitsch, G. E.; Wiggins, J. W. Hydrogen Elimination in Dimethylamine-Borane. *Inorganic Chemistry* **1970**, *9* (2), 314–317. https://doi.org/10.1021/ic50084a028.

(71) Jaska, C. A.; Temple, K.; Lough, A. J.; Manners, I. Rhodium-Catalyzed Formation of Boron-Nitrogen Bonds: A Mild Route to Cyclic Aminoboranes and Borazines. *Chemical Communications* **2001**, No. 11, 962–963. https://doi.org/10.1039/B102361F.

(72) Jaska, C. A.; Manners, I. Heterogeneous or Homogeneous Catalysis? Mechanistic Studies of the Rhodium-Catalyzed Dehydrocoupling of Amine-Borane and Phosphine-Borane Adducts. *Journal of the American Chemical Society* **2004** *126* (31), 9776–9785. https://doi.org/10.1021/ja0478431.

(73) Sloan, M. E.; Staubitz, A.; Clark, T. J.; Russell, C. A.; Lloyd-Jones, G. C.; Manners, I. Homogeneous Catalytic Dehydrocoupling/Dehydrogenation of Amine−Borane Adducts by Early Transition Metal, Group 4 Metallocene Complexes. *Journal of the American Chemical Society* **2010**, *132* (11), 3831–3841. https://doi.org/10.1021/ja909535a.

(74) Helten, H.; Dutta, B.; Vance, J. R.; Sloan, M. E.; Haddow, M. F.; Sproules, S.; Collison, D.; Whittell, G. R.; Lloyd-Jones, G. C.; Manners, I. Paramagnetic Titanium(III) and Zirconium(III) Metallocene Complexes as Precatalysts for the Dehydrocoupling/Dehydrogenation of Amine–Boranes. *Angewandte Chemie International Edition* **2013**, *52* (1), 437–440. https://doi.org/10.1002/anie.201207903.

(75) Sharpe, H. R.; Geer, A. M.; Blundell, T. J.; Hastings, F. R.; Fay, M. W.; Rance, G. A.; Lewis, W.; Blake, A. J.; Kays, D. L. Dehydrocoupling of Dimethylamine-Borane Promoted by Manganese(II) m-Terphenyl Complexes. *Catalysis Science & Technology* **2018**, *8* (1), 229–235. https://doi.org/10.1039/c7cy02086d.

(76) Vance, J. R.; Schäfer, A.; Robertson, A. P. M.; Lee, K.; Turner, J.; Whittell, G. R.; Manners, I. Iron-Catalyzed Dehydrocoupling/Dehydrogenation of Amine–Boranes. *Journal of the American Chemical Society* **2014**, *136* (8), 3048–3064. https://doi.org/10.1021/ja410129j.

(77) Baker, R. T.; Gordon, J. C.; Hamilton, C. W.; Henson, N. J.; Lin, P.-H.; Maguire, S.; Murugesu, M.; Scott, B. L.; Smythe, N. C. Iron Complex-Catalyzed Ammonia–Borane Dehydrogenation. A Potential Route toward B–N-Containing Polymer

Motifs Using Earth-Abundant Metal Catalysts. *Journal of the American Chemical Society* **2012**, *134* (12), 5598–5609. https://doi.org/10.1021/ja210542r.

(78) Bhattacharya, P.; Krause, J. A.; Guan, H. Mechanistic Studies of Ammonia Borane Dehydrogenation Catalyzed by Iron Pincer Complexes. *Journal of the American Chemical Society* **2014**, *136* (31), 11153–11161. https://doi.org/10.1021/ja5058423.

(79) Luo, W.; Campbell, P. G.; Zakharov, L. N.; Liu, S.-Y. A Single-Component Liquid-Phase Hydrogen Storage Material. *Journal of the American Chemical Society* **2011**, *133* (48), 19326–19329. https://doi.org/10.1021/ja208834v.

(80) Maier, T. M.; Sandl, S.; Shenderovich, I. G.; Jacobi von Wangelin, A.; Weigand, J. J.; Wolf, R. Amine-Borane Dehydrogenation and Transfer Hydrogenation Catalyzed by Alpha-Diimine Cobaltates. *Chemistry – A European Journal* **2019**, *25* (1), 238–245. https://doi.org/10.1002/chem.201804811.

(81) Todisco, S.; Luconi, L.; Giambastiani, G.; Rossin, A.; Peruzzini, M.; Golub, I. E.; Filippov, O. A.; Belkova, N. V.; Shubina, E. S. Ammonia Borane Dehydrogenation Catalyzed by (K4-$EP_3$)Co(H) [$EP_3$ = $E(CH_2CH_2PPh_2)_3$; E = N, P] and H2 Evolution from Their Interaction with NH Acids. *Inorganic Chemistry* **2017**, *56* (8), 4296–4307. https://doi.org/10.1021/acs.inorgchem.6b02673.

(82) K. Pagano, J.; W. Stelmach, J. P.; Waterman, R. Cobalt-Catalyzed Ammonia Borane Dehydrocoupling and Transfer Hydrogenation under Aerobic Conditions. *Dalton Transactions* **2015**, *44* (27), 12074–12077. https://doi.org/10.1039/C5DT00108K.

(83) Keaton, R. J.; Blacquiere, J. M.; Baker, R. T. Base Metal Catalyzed Dehydrogenation of Ammonia−Borane for Chemical Hydrogen Storage. *Journal of the American Chemical Society* **2007**, *129* (7), 1844–1845. https://doi.org/10.1021/ja066860i.

(84) Vogt, M.; de Bruin, B.; Berke, H.; Trincado, M.; Grützmacher, H. Amino Olefin Nickel(I) and Nickel(0) Complexes as Dehydrogenation Catalysts for Amine Boranes. *Chemical Science* **2011**, *2* (4), 723–727. https://doi.org/10.1039/C0SC00483A.

(85) Robertson, A. P. M.; Suter, R.; Chabanne, L.; Whittell, G. R.; Manners, I. Heterogeneous Dehydrocoupling of Amine-Borane Adducts by Skeletal Nickel Catalysts. *Inorganic Chemistry* **2011**, *50* (24), 12680–12691. https://doi.org/10.1021/ic201809g.

(86) Jaska, C. A.; Temple, K.; Lough, A. J.; Manners, I. Transition Metal-Catalyzed Formation of Boron−Nitrogen Bonds: Catalytic Dehydrocoupling of Amine-Borane Adducts to Form Aminoboranes and Borazines. *Journal of the American Chemical Society* **2003**, *125* (31), 9424–9434. https://doi.org/10.1021/ja030160l.

(87) Douglas, T. M.; Chaplin, A. B.; Weller, A. S. Amine-Borane σ-Complexes of Rhodium. Relevance to the Catalytic Dehydrogenation of Amine-Boranes. *Journal of the American Chemical Society* **2008**, *130* (44), 14432–14433. https://doi.org/10.1021/ja806582n.

(88) Dallanegra, R.; B. Chaplin, A.; Tsim, J.; S. Weller, A. Amino-Borane Oligomers Bound to a Rh(I) Metal Fragment. *Chemical Communications* **2010**, *46* (18), 3092–3094. https://doi.org/10.1039/C003055D.

(89) Sewell, L. J.; Lloyd-Jones, G. C.; Weller, A. S. Development of a Generic Mechanism for the Dehydrocoupling of Amine-Boranes: A Stoichiometric, Catalytic, and Kinetic Study of $H_3B{\cdot}NMe_2H$ Using the $[Rh(PCy_3)_2]$+ Fragment. *Journal of the American Chemical Society* **2012**, *134* (7), 3598–3610. https://doi.org/10.1021/ja2112965.

(90) Zahmakiran, M.; Özkar, S. Dimethylammonium Hexanoate Stabilized Rhodium(0) Nanoclusters Identified as True Heterogeneous Catalysts with the Highest Observed Activity in the Dehydrogenation of Dimethylamine−Borane. *Inorganic Chemistry* **2009**, *48* (18), 8955–8964. https://doi.org/10.1021/ic9014306.

(91) Chen, Y.; Fulton, J. L.; Linehan, J. C.; Autrey, T. In *Situ* XAFS and NMR Study of Rhodium-Catalyzed Dehydrogenation of Dimethylamine Borane. *Journal of the American Chemical Society.* **2005**, *127* (10), 3254–3255. https://doi.org/10.1021/ja0437050.

(92) Friedrich, A.; Drees, M.; Schneider, S. Ruthenium-Catalyzed Dimethylamineborane Dehydrogenation: Stepwise Metal-Centered Dehydrocyclization. *Chemistry – A European Journal* **2009**, *15* (40), 10339–10342. https://doi.org/10.1002/chem.200901372.

(93) Käß, M.; Friedrich, A.; Drees, M.; Schneider, S. Ruthenium Complexes with Cooperative PNP Ligands: Bifunctional Catalysts for the Dehydrogenation of Ammonia–Borane. *Angewandte Chemie International Edition* **2009**, *48* (5), 905–907. https://doi.org/10.1002/anie.200805108.

(94) Marziale, A. N.; Friedrich, A.; Klopsch, I.; Drees, M.; Celinski, V. R.; Schmedt auf der Günne, J.; Schneider, S. The Mechanism of Borane–Amine Dehydrocoupling

with Bifunctional Ruthenium Catalysts. *Journal of the American Chemical Society* **2013**, *135* (36), 13342–13355. https://doi.org/10.1021/ja311092c.

(95) Jiang, Y.; Berke, H. Dehydrocoupling of Dimethylamine-Borane Catalysed by Rhenium Complexes and Its Application in Olefin Transfer-Hydrogenations. *Chemical Communications* **2007**, No. 34, 3571–3573. https://doi.org/10.1039/B708913A.

(96) Denney, M. C.; Pons, V.; Hebden, T. J.; Heinekey, D. M.; Goldberg, K. I. Efficient Catalysis of Ammonia Borane Dehydrogenation. *Journal of the American Chemical Society* **2006**, *128* (37), 12048–12049. https://doi.org/10.1021/ja062419g.

(97) Stevens, C. J.; Dallanegra, R.; Chaplin, A. B.; Weller, A. S.; Macgregor, S. A.; Ward, B.; McKay, D.; Alcaraz, G.; Sabo-Etienne, S. $[Ir(PCy_3)_2(H)_2(H_2B\text{-}NMe_2)]+$ as a Latent Source of Aminoborane: Probing the Role of Metal in the Dehydrocoupling of $H_3B\text{-}NMe_2H$ and Retrodimerisation of $[H_2BNMe_2]_2$. *Chemistry - A European Journal* **2011**, *17* (10), 3011–3020. https://doi.org/10.1002/chem.201002517.

(98) Harder, S.; Spielmann, J. Unprecedented Reactivity of an Aluminium Hydride Complex with $ArNH_2BH_3$: Nucleophilic Substitution versus Deprotonation. *Chemical Communications* **2011**, *47* (43), 11945–11947. https://doi.org/10.1039/C1CC14689K.

(99) Erickson, K. A.; Wright, D. S.; Waterman, R. Dehydrocoupling of Amine Boranes *via* Tin(IV) and Tin(II) Catalysts. *Journal of Organometallic Chemistry* **2014**, *751*, 541–545. https://doi.org/10.1016/j.jorganchem.2013.11.012.

(100) Bellham, P.; Hill, M. S.; Kociok-Köhn, G. Stoichiometric and Catalytic Reactivity of Tert-Butylamine–Borane with Calcium Silylamides. *Organometallics* **2014**, *33* (20), 5716–5721. https://doi.org/10.1021/om500467b.

(101) Stephens, F. H.; Baker, R. T.; Matus, M. H.; Grant, D. J.; Dixon, D. A. Acid Initiation of Ammonia–Borane Dehydrogenation for Hydrogen Storage. *Angewandte Chemie International Edition* **2007**, *46* (5), 746–749. https://doi.org/10.1002/anie.200603285.

(102) Boom, D. H. A.; Jupp, A. R.; Slootweg, J. C. Dehydrogenation of Amine-Boranes Using p-Block Compounds. *Chemistry – A European Journal* **2019**, *25* (39), 9133–9152. https://doi.org/10.1002/chem.201900679.

(103) Staubitz, A.; Sloan, M. E.; Robertson, A. P. M.; Friedrich, A.; Schneider, S.; Gates, P. J.; Schmedt auf der Günne, J.; Manners, I. Catalytic Dehydrocoupling/Dehydrogenation of N-Methylamine-Borane and Ammonia-Borane: Synthesis and Characterization of High Molecular Weight Polyaminoboranes. *Journal of the American Chemical Society* **2010**, *132* (38), 13332–13345. https://doi.org/10.1021/ja104607y.

(104) Jurca, T.; Dellermann, T.; Stubbs, N. E.; Resendiz-Lara, D. A.; Whittell, G. R.; Manners, I. Step-Growth Titanium-Catalysed Dehydropolymerisation of Amine-Boranes. *Chemical Science* **2018**, *9* (13), 3360–3366. https://doi.org/10.1039/c7sc05395a.

(105) LaPierre, E. A.; Patrick, B. O.; Manners, I. Trivalent Titanocene Alkyls and Hydrides as Well-Defined, Highly Active, and Broad Scope Precatalysts for

Dehydropolymerization of Amine-Boranes. *Journal of the American Chemical Society* **2019**, *141* (51), 20009–20015. https://doi.org/10.1021/jacs.9b11112.

(106) Vance, J. R.; Robertson, A. P. M.; Lee, K.; Manners, I. Photoactivated, Iron-Catalyzed Dehydrocoupling of Amine–Borane Adducts: Formation of Boron–Nitrogen Oligomers and Polymers. *Chemistry – A European Journal.* **2011**, *17* (15), 4099–4103. https://doi.org/10.1002/chem.201003397.

(107) Anke, F.; Han, D.; Klahn, M.; Spannenberg, A.; Beweries, T. Formation of High-Molecular Weight Polyaminoborane by Fe Hydride Catalysed Dehydrocoupling of Methylamine Borane. *Dalton Transactions* **2017**, *46* (21), 6843–6847. https://doi.org/10.1039/C7DT01487B.

(108) Coles, N. T.; Webster, R. L. Iron Catalyzed Dehydrocoupling of Amine- and Phosphine-Boranes. *Israel Journal of Chemistry* **2017**, *57* (12), 1070–1081. https://doi.org/10.1002/ijch.201700018.

(109) Boyd, T. M.; Andrea, K. A.; Baston, K.; Johnson, A.; Ryan, D. E.; Weller, A. S. A Simple Cobalt-Based Catalyst System for the Controlled Dehydropolymerisation of $H_3B{\cdot}NMeH_2$ on the Gram-Scale. *Chemical Communications* **2020**, *56* (3), 482–485. https://doi.org/10.1039/C9CC08864D.

(110) Trose, M.; Reiß, M.; Reiß, F.; Anke, F.; Spannenberg, A.; Boye, S.; Lederer, A.; Arndt, P.; Beweries, T. Dehydropolymerisation of Methylamine Borane Using a Dinuclear 1,3-Allenediyl Bridged Zirconocene Complex. *Dalton Transactions* **2018**, *47* (37), 12858–12862. https://doi.org/10.1039/C8DT03311K.

(111) Dallanegra, R.; Robertson, A. P. M.; Chaplin, A. B.; Manners, I.; Weller, A. S. Tuning the $[L_2Rh{\cdot}\cdot\cdot{\cdot}H_3B{\cdot}NR_3]$+ Interaction Using Phosphine Bite Angle. Demonstration by

the Catalytic Formation of Polyaminoboranes. *Chemical Communications* **2011**, *47* (13), 3763–3765. https://doi.org/10.1039/C0CC05460G.

(112) Adams, G. M.; Ryan, D. E.; Beattie, N. A.; McKay, A. I.; Lloyd-Jones, G. C.; Weller, A. S. Dehydropolymerization of $H_3B{\bullet}NMeH_2$ Using a Rh(DPEphos) (+) Catalyst: The Promoting Effect of $NMeH_2$. *ACS Catalysis* **2019**, *9* (4), 3657–3666. https://doi.org/10.1021/acscatal.9b00081.

(113) Adams, G. M.; Colebatch, A. L.; Skornia, J. T.; McKay, A. I.; Johnson, H. C.; Lloyd−Jones, G. C.; Macgregor, S. A.; Beattie, N. A.; Weller, A. S. Dehydropolymerization of $H_3B{\cdot}NMeH_2$ To Form Polyaminoboranes Using [Rh(Xantphos-Alkyl)] Catalysts. *Journal of the American Chemical Society* **2018**, *140* (4), 1481–1495. https://doi.org/10.1021/jacs.7b11975.

(114) Brodie, C. N.; Boyd, T. M.; Sotorríos, L.; Ryan, D. E.; Magee, E.; Huband, S.; Town, J. S.; Lloyd-Jones, G. C.; Haddleton, D. M.; Macgregor, S. A.; Weller, A. S. Controlled Synthesis of Well-Defined Polyaminoboranes on Scale Using a Robust and Efficient Catalyst. *Journal of the American Chemical Society* **2021**, *143* (49), 21010–21023. https://doi.org/10.1021/jacs.1c10888.

(115) Johnson, H. C.; Robertson, A. P. M.; Chaplin, A. B.; Sewell, L. J.; Thompson, A. L.; Haddow, M. F.; Manners, I.; Weller, A. S. Catching the First Oligomerization Event in the Catalytic Formation of Polyaminoboranes: $H_3B{\bullet}NMeHBH_2{\bullet}NMeH_2$ Bound to Iridium. *Journal of the American Chemical Society* **2011**, *133* (29), 11076–11079. https://doi.org/10.1021/ja2040738.

(116) Metters, O. J.; Chapman, A. M.; Robertson, A. P. M.; Woodall, C. H.; Gates, P. J.; Wass, D. F.; Manners, I. Generation of Aminoborane Monomers $RR'NBH_2$ from

Amine–Boronium Cations [RR′NH–$BH_2$L]+: Metal Catalyst-Free Formation of Polyaminoboranes at Ambient Temperature. *Chemical Communications* **2014**, *50* (81), 12146–12149. https://doi.org/10.1039/C4CC05145A.

(117) De Albuquerque Pinheiro, C. A.; Roiland, C.; Jehan, P.; Alcaraz, G. Solventless and Metal-Free Synthesis of High-Molecular-Mass Polyaminoboranes from Diisopropylaminoborane and Primary Amines. *Angewandte Chemie International Edition* **2018**, *57* (6), 1519–1522. https://doi.org/10.1002/anie.201710293.

(118) Resendiz-Lara, D. A.; Whittell, G. R.; Leitao, E. M.; Manners, I. Catalytic Synthesis, Characterization, and Properties of Polyaminoborane Homopolymers and Random Copolymers. *Macromolecules* **2019**, *52* (18), 7052–7064. https://doi.org/10.1021/acs.macromol.9b01139.

(119) Helten, H.; Robertson, A. P. M.; Staubitz, A.; Vance, J. R.; Haddow, M. F.; Manners, I. “Spontaneous” Ambient Temperature Dehydrocoupling of Aromatic Amine–Boranes. *Chemistry – A European Journal* **2012**, *18* (15), 4665–4680. https://doi.org/10.1002/chem.201103241.

(120) Resendiz-Lara, D. A.; Stubbs, N. E.; Arz, M. I.; Pridmore, N. E.; Sparkes, H. A.; Manners, I. Boron-Nitrogen Main Chain Analogues of Polystyrene: Poly(B-Aryl)Aminoboranes *via* Catalytic Dehydrocoupling. *Chemical Communications* **2017**, *53*, 11701–11704. https://doi.org/10.1039/C7CC07331C.

(121) Stubbs, N. E.; Schafer, A.; Robertson, A. P. M.; Leitao, E. M.; Jurca, T.; Sparkes, H. A.; Woodall, C. H.; Haddow, M. F.; Manners, I. B-Methylated Amine-Boranes: Substituent Redistribution, Catalytic Dehydrogenation, and Facile Metal-Free

Hydrogen Transfer Reactions. *Inorganic Chemistry* **2015** *54* (22), 10878–10889. https://doi.org/10.1021/acs.inorgchem.5b01946.

(122) Parshall, G. W. Boron--Phosphorus Compounds; 1967; pp 617–646.

(123) Besson, A. Sur Les Combinaisons Du Gaz Hydrogène Phosphoré et Du Gaz Ammoniac Avec Le Chlorure de Bore et Le Sesquichlorure de Silicium. *Comptes Rendus Hebdomadaires des Séances de L'Académie des Sciences* **1890**, *710*, 516.

(124) Gamble, E. L.; Gilmont, P. Preparation and Properties of Diborane Diphosphine. *Journal of the American Chemical Society* **1940**, *62*, 717–721. https://doi.org/10.1021/ja01861a007.

(125) Rudolph, R. W.; Parry, R. W.; Farran, C. F. The Structure of Phosphine Borane. *Inorganic Chemistry* **1966**, *5* (5), 723-. https://doi.org/10.1021/ic50039a005.

(126) Hurtado, M.; Yanez, M.; Herrero, R.; Guerrero, A.; Davalos, J. Z.; Abboud, J. L. M.; Khater, B.; Guillemin, J.-C. The Ever-Surprising Chemistry of Boron: Enhanced Acidity of Phosphine•Boranes. *Chemistry – A European Journal* **2009**, *15* (18), 4622–4629. https://doi.org/10.1002/chem.200802307.

(127) Burg, A. B.; Slota, P. J. New Approaches to the Phosphinoborine Polymers[1]. *Journal of the American Chemical Society* **1960**, *82* (9), 2145–2148. https://doi.org/10.1021/ja01494a014.

(128) Jong, G. B. de; Ortega, N.; Lutz, M.; Lammertsma, K.; Slootweg, J. C. Easy Access to Phosphine-Borane Building Blocks. *Chemistry – A European Journal* **2020**, *26* (68), 15944–15952. https://doi.org/10.1002/chem.202002367.

(129) Turner, J. R.; Resendiz-Lara, D. A.; Jurca, T.; Schäfer, A.; Vance, J. R.; Beckett, L.; Whittell, G. R.; Musgrave, R. A.; Sparkes, H. A.; Manners, I. Synthesis, Characterization, and Properties of Poly(Aryl)Phosphinoboranes Formed *via* Iron-Catalyzed Dehydropolymerization. *Macromolecular Chemistry and Physics* **2017**, *218* (19), 1700120. https://doi.org/10.1002/macp.201700120.

(130) Rieger, J. The Glass Transition Temperature of Polystyrene - Results of a Round Robin Test. *Journal of Thermal Analysis* **1996**, *46* (3–4), 965–972. https://doi.org/10.1007/bf01983614.

(131) Schäfer, A.; Jurca, T.; Turner, J.; Vance, J. R.; Lee, K.; Du, V. A.; Haddow, M. F.; Whittell, G. R.; Manners, I. Iron-Catalyzed Dehydropolymerization: A Convenient Route to Poly(Phosphinoboranes) with Molecular-Weight Control. *Angewandte Chemie International Edition* **2015**, *54* (16), 4836–4841. https://doi.org/10.1002/anie.201411957.

(132) Clark, T. J.; Rodezno, J. M.; Clendenning, S. B.; Aouba, S.; Brodersen, P. M.; Lough, A. J.; Ruda, H. E.; Manners, I. Rhodium-Catalyzed Dehydrocoupling of Fluorinated Phosphine–Borane Adducts: Synthesis, Characterization, and Properties of Cyclic and Polymeric Phosphinoboranes with Electron-Withdrawing Substituents at Phosphorus. *Chemistry – A European Journal* **2005**, *11* (15), 4526–4534. https://doi.org/10.1002/chem.200401296.

(133) Knights, A. W.; Nascimento, M. A.; Manners, I. An Investigation of Polyphosphinoboranes as Flame-Retardant Materials. *Polymer* **2022**, *247*, 124795. https://doi.org/10.1016/j.polymer.2022.124795.

(134) Dorn, H.; Rodezno, J. M.; Brunnhofer, B.; Rivard, E.; Massey, J. A.; Manners, I. Synthesis, Characterization, and Properties of the Polyphosphinoboranes [RPH-$BH_2$]$_n$ (R=Ph, iBu, p-n$BuC_6H_4$, p-dodecyl$C_6H_4$): Inorganic Polymers with a Phosphorus-Boron Backbone. *Macromolecules* **2003**, *36* (2), 291–297. https://doi.org/10.1021/ma021447q.

(135) Jacquemin, D. Theoretical Study of Dehydrogenation Effects upon the First Hyperpolarizability of Polyphosphinoborane. *Journal of Physical Chemistry A* **2004**, *108* (3), 500–506. https://doi.org/10.1021/jp0364755.

(136) Knights, A. W.; Chitnis, S. S.; Manners, I. Photolytic, Radical-Mediated Hydrophosphination: A Convenient Post-Polymerisation Modification Route to P-Di(Organosubstituted) Polyphosphinoboranes [RR′$PBH_2$]n. *Chemical Science* **2019**, *10*, 7281–7289. https://doi.org/10.1039/C9SC01428D.

(137) Burg, A. B.; Wagner, R. I. Chemistry of P–B bonding – the Phosphinoborines and their Polymers. *Journal of the American Chemical Society* **1953**, *75* (16), 3872–3877. https://doi.org/10.1021/ja01112a002.

(138) Burg, A. B. Phosphinoborine Polymer Rings and Chains from Tetramethylbiphosphine. *Journal of Inorganic and Nuclear Chemistry* **1959**, *11* (3), 258. https://doi.org/10.1016/0022-1902(59)80257-8.

(139) Wagner, R. I.; Caserio, F. F. Linear Phosphinoborine Polymers. *Journal of Inorganic and Nuclear Chemistry* **1959**, *11* (3), 259. https://doi.org/10.1016/0022-1902(59)80258-X.

(140) Korshak, V. V.; Zamyatina, V. A.; Solomatina, A. I.; Fedin, E. I.; Petrovskii, P. V. Synthesis of Polyphosphinoboranes by the Reaction of Secondary Bisphosphines

with Triethylamineborane. *Journal of Organometallic Chemistry* **1969** *17* (2), 201–212. https://doi.org/10.1016/S0022-328X(00)88608-8.

(141) Dorn, H.; Singh, R. A.; Massey, J. A.; Lough, A. J.; Manners, I. Rhodium-Catalyzed Formation of Phosphorus–Boron Bonds: Synthesis of the First High Molecular Weight Poly(Phosphinoborane). *Angewandte Chemie International Edition* **1999**, *38* (22), 3321–3323. https://doi.org/10.1002/(SICI)1521-3773(19991115)38:22<3321::AID-ANIE3321>3.0.CO;2-0.

(142) Dorn, H.; Singh, R. A.; Massey, J. A.; Nelson, J. M.; Jaska, C. A.; Lough, A. J.; Manners, I. Transition Metal-Catalyzed Formation of Phosphorus−Boron Bonds: A New Route to Phosphinoborane Rings, Chains, and Macromolecules. *Journal of the American Chemical Society* **2000**, *122* (28), 6669–6678. https://doi.org/10.1021/ja000732r.

(143) Coles, N. T.; Mahon, M. F.; Webster, R. L. Phosphine- and Amine-Borane Dehydrocoupling Using a Three-Coordinate Iron(II) β-Diketiminate Precatalyst. *Organometallics* **2017**, *36* (11), 2262–2268. https://doi.org/10.1021/acs.organomet.7b00326.

(144) D. Paul, U. S.; Braunschweig, H.; Radius, U. Iridium-Catalysed Dehydrocoupling of Aryl Phosphine–Borane Adducts: Synthesis and Characterisation of High Molecular Weight Poly(Phosphinoboranes). *Chemical Communications* **2016**, *52* (55), 8573–8576. https://doi.org/10.1039/C6CC04363A.

(145) Hooper, T. N.; Weller, A. S.; Beattie, N. A.; Macgregor, S. A. Dehydrocoupling of Phosphine-Boranes Using the [RhCp*Me($PMe_3$)($CH_2Cl_2$)][$BArF_4$] Precatalyst:

Stoichiometric and Catalytic Studies. *Chemical Science* **2016**, *7* (3), 2414–2426. https://doi.org/10.1039/c5sc04150c.

(146) Braese, J.; Lehnfeld, F.; Annibale, V. T.; Oswald, T.; Beckhaus, R.; Manners, I.; Scheer, M. Titanium-Catalyzed Polymerization of a Lewis Base-Stabilized Phosphinoborane. *Chemistry – A European Journal* **2023**, *29* (58), e202301741. https://doi.org/10.1002/chem.202301741.

(147) Denis, J.-M.; Forintos, H.; Szelke, H.; Toupet, L.; Pham, T.-N.; Madec, P.-J.; Gaumont, A.-C. $B(C_6F_5)_3$-Catalyzed Formation of B-P Bonds by Dehydrocoupling of Phosphine-Boranes. *Chemical Communications* ***2003*** 54–55. https://doi.org/10.1039/B206559B.

(148) Marquardt, C.; Jurca, T.; Schwan, K. C.; Stauber, A.; Virovets, A. V.; Whittell, G. R.; Manners, I.; Scheer, M. Metal-Free Addition/Head-to-Tail Polymerization of Transient Phosphinoboranes, $RPH\text{-}BH_2$: A Route to Poly(Alkylphosphinoboranes). *Angewandte Chemie-International Edition* **2015**, *54* (46), 13782–13786. https://doi.org/10.1002/anie.201507084.

(149) Schwan, K.-C.; Timoskin, A. Y.; Zabel, M.; Scheer, M. Lewis Base Stabilized Phosphanylborane. *Chemistry – A European Journal* **2006**, *12* (18), 4900–4908. https://doi.org/10.1002/chem.200600185.

(150) Oldroyd, N. L.; Chitnis, S. S.; Annibale, V. T.; Arz, M. I.; Sparkes, H. A.; Manners, I. Metal-Free Dehydropolymerisation of Phosphine-Boranes Using Cyclic (Alkyl)(Amino)Carbenes as Hydrogen Acceptors. *Nature Communications* **2019**, *10* (1), 1–9. https://doi.org/10.1038/s41467-019-08967-8.

(151) Pandey, S.; Lönnecke, P.; Hey-Hawkins, E. Phosphorus-Boron-Based Polymers Obtained by Dehydrocoupling of Ferrocenylphosphine-Borane Adducts. *European Journal of Inorganic Chemistry* **2014**, *2014* (14), 2456–2465. https://doi.org/10.1002/ejic.201402021.

(152) Arz, M. I.; Knights, A. W.; Manners, I. Synthesis and Post-Polymerization Functionalization of Halogen-Substituted Polyphosphinoboranes to Access Alkyne-Functionalized Derivatives. *Macromolecular Rapid Communications* **2020**, *41* (4), 1900468. https://doi.org/10.1002/marc.201900468.

(153) Resendiz-Lara, D. A.; Annibale, V. T.; Knights, A. W.; Chitnis, S. S.; Manners, I. High Molar Mass Poly(Alkylphosphinoboranes) *via* Iron-Catalyzed Dehydropolymerization. *Macromolecules* **2021**, *54* (1), 71–82. https://doi.org/10.1021/acs.macromol.0c02082.

(154) Colebatch, A. L.; Hawkey Gilder, B. W.; Whittell, G. R.; Oldroyd, N. L.; Manners, I.; Weller, A. S. A General, Rhodium-Catalyzed, Synthesis of Deuterated Boranes and N-Methyl Polyaminoboranes. *Chemistry – A European Journal* **2018**, *24* (21), 5450–5455. https://doi.org/10.1002/chem.201800737.

(155) Kumar, A.; Beattie, N. A.; Pike, S. D.; Macgregor, S. A.; Weller, A. S. The Simplest Amino-Borane $H_2B{=}NH_2$ Trapped on a Rhodium Dimer: Pre-Catalysts for Amine–Borane Dehydropolymerization. *Angewandte Chemie* **2016**, *128* (23), 6763–6768. https://doi.org/10.1002/ange.201600898.

(156) Drover, M. W.; Bowes, E. G.; Schafer, L. L.; Love, J. A.; Weller, A. S. Phosphoramidate-Supported $Cp^*Ir^{III}$ Aminoborane $H_2B{=}NR_2$ Complexes:

Synthesis, Structure, and Solution Dynamics. *Chemistry – A European Journal* **2016**, *22* (20), 6793–6797. https://doi.org/10.1002/chem.201600951.

(157) Addy, D. A.; Bates, J. I.; Kelly, M. J.; Riddlestone, I. M.; Aldridge, S. Aminoborane σ Complexes: Significance of Hydride Co-Ligands in Dynamic Processes and Dehydrogenative Borylene Formation. *Organometallics* **2013**, *32* (6), 1583–1586. https://doi.org/10.1021/om400040q.

(158) Tiddens, M. R.; Kappé, B. T.; Smak, T. J.; Lutz, M.; Moret, M.-E. Coordination of a Phosphine-Tethered Aminoborane to Group 10 Metals. *Chemistry – A European Journal* **2024**, *30* (32), e202400666. https://doi.org/10.1002/chem.202400666.

(159) Pons, V.; Baker, R. T.; Szymczak, N. K.; Heldebrant, D. J.; Linehan, J. C.; Matus, M. H.; Grant, D. J.; Dixon, D. A. Coordination of Aminoborane, $NH_2BH_2$, Dictates Selectivity and Extent of $H_2$ Release in Metal-Catalysed Ammonia Borane Dehydrogenation. *Chemical Communications* **2008**, No. 48, 6597–6599. https://doi.org/10.1039/b809190k.

(160) Odian, G. *Principles of Polymerization*, Fourth.; John Wiley & Sons, Inc.: Hoboken, New Jersey, 2004.

(161) Chum, P. S.; Swogger, K. W. Olefin Polymer Technologies—History and Recent Progress at The Dow Chemical Company. *Progress in Polymer Science* **2008**, *33* (8), 797–819. https://doi.org/10.1016/j.progpolymsci.2008.05.003.

(162) Collins, R. A.; Russell, A. F.; Mountford, P. Group 4 Metal Complexes for Homogeneous Olefin Polymerisation: A Short Tutorial Review. *Applied Petrochemical Research* **2015**, *5* (3), 153–171. https://doi.org/10.1007/s13203-015-0105-2.

(163) Cossee, P. Ziegler-Natta Catalysis I. Mechanism of Polymerization of α-Olefins with Ziegler-Natta Catalysts. *Journal of Catalysis* **1964**, *3* (1), 80–88. https://doi.org/10.1016/0021-9517(64)90095-8.

(164) Johnson, H. C.; Leitao, E. M.; Whittell, G. R.; Manners, I.; Lloyd-Jones, G. C.; Weller, A. S. Mechanistic Studies of the Dehydrocoupling and Dehydropolymerization of Amine–Boranes Using a [Rh(Xantphos)]+ Catalyst. *Journal of the American Chemical Society* **2014**, *136* (25), 9078–9093. https://doi.org/10.1021/ja503335g.

(165) Kumar, A.; Johnson, H. C.; Hooper, T. N.; Weller, A. S.; Algarra, A. G.; Macgregor, S. A. Multiple Metal-Bound Oligomers from Ir-Catalysed Dehydropolymerisation of $H_3B{\bullet}NH_3$ as Probed by Experiment and Computation. *Chemical Science* **2014**, *5* (6), 2546–2553. https://doi.org/10.1039/c4sc00735b.

(166) Bhunya, S.; Malakar, T.; Paul, A. Unfolding the Crucial Role of a Nucleophile in Ziegler–Natta Type Ir Catalyzed Polyaminoborane Formation. *Chemical Communications* **2014**, *50* (44), 5919–5922. https://doi.org/10.1039/C4CC01337A.

(167) Jaska, C. A.; Manners, I. Catalytic Dehydrocoupling of Amine-Borane and Phosphine-Borane Adducts: The Mechanism Is Heterogeneous in One Case and Homogeneous in the Other. *Journal of the American Chemical Society* **2004**, *126* (5), 1334–1335. https://doi.org/10.1021/ja039162w.

(168) Huertos, M. A.; Weller, A. S. Intermediates in the Rh-Catalysed Dehydrocoupling of Phosphine–Borane. *Chemical Communications* **2012**, *48* (57), 7185–7187. https://doi.org/10.1039/c2cc32696e.

(169) Huertos, M. A.; Weller, A. S. Revealing the P-B Coupling Event in the Rhodium Catalysed Dehydrocoupling of Phosphine-Boranes $H_3B$•PRH (R = Bu-t, Ph). *Chemical Science* **2013**, *4* (4), 1881–1888. https://doi.org/10.1039/c3sc50122a.

(170) Hooper, T. N.; Huertos, M. A.; Jurca, T.; Pike, S. D.; Weller, A. S.; Manners, I. Effect of the Phosphine Steric and Electronic Profile on the Rh-Promoted Dehydrocoupling of Phosphine–Boranes. *Inorganic Chemistry* **2014**, *53* (7), 3716–3729. https://doi.org/10.1021/ic500032f.

(171) Devillard, M.; Pinheiro, C. A. D. A.; Caytan, E.; Roiland, C.; Dinoi, C.; Rosal, I. D.; Alcaraz, G. Uncatalyzed Formation of Polyaminoboranes from Diisopropylaminoborane and Primary Amines: A Kinetically Controlled Polymerization Reaction. *Advanced Synthesis & Catalysis* **2021**, *363* (9), 2417–2426. https://doi.org/10.1002/adsc.202001458.

(172) Pomogaeva, A. V.; Timoshkin, A. Y. Stability and Electronic Structure of Donor–Acceptor Stabilized Group 13/15 Oligomers. *Journal of Physical Chemistry A* **2021**, *125* (16), 3415–3424. https://doi.org/10.1021/acs.jpca.1c02258.

**Chapter 2**

# Transition Metal-Free Dehydropolymerization of Phosphine-Boranes at Ambient Temperature

*This chapter has been adapted from:*

Matthew A. Wiebe, Subrata Kundu, Etienne LaPierre, Brian O. Patrick, and Ian Manners. *Chem. Eur. J.* **2023**, *29* (2), e202202897

*Contributions: M. A. W., S. K. and I. M. conceived the project. S. K. performed exploratory reactions to access P-disubstituted polymeric materials. E. L. contributed to useful conversations regarding the project and in the solving of single crystal data. B. O. P. obtained single crystal X-ray data. M. A. W. performed all other synthesis and characterization. M. A. W. interpreted the data and wrote the manuscript which was subsequently edited with I. M. and the other authors.*

## 2.1 Abstract

Stoichiometric reaction of phosphine-borane adducts RR'PH•$BH_3$ (R = Ph, R' = H, Ph, Et, and R = R' = *t*Bu) with the strong acid, $HNTf_2$ (Tf = $SO_2CF_3$) leads to $H_2$ elimination and the formation of the triflimido derivatives, RR'PH•$BH_2(NTf_2)$. Subsequent deprotonation using bases such as diisopropylethylamine or the carbene IPr (IPr = *N,N'*-bis(2,6-diisopropylphenyl)imidazol-2-ylidene) results in the formation *P*-mono- or *P*-disubstituted polyphosphinoboranes, $[RR'P–BH_2]_n$. End-group analysis by electrospray ionization reveals the presence of IPr or *i*$Pr_2$EtN end groups, implicating their involvement in both deprotonation and polymerization. Evidence for the intermediacy of transient phosphinoborane monomers, RR'$PBH_2$, was provided by trapping reactions.

## 2.2 Introduction

Main group polymers featuring boron or phosphorus atoms in the main chain have attracted interest with respect to their valuable physical and chemical properties and for applications in optoelectronics, sensing, catalysis, and biomedicine.[1–12] High molar mass polyphosphinoboranes, $[RR'P–BH_2]_n$, have recently been explored for potential uses as thermally-stable and flame retardant materials, electron beam resists, and as precursors to boron phosphide ceramics or hydrogels.[13–19] A wide range of transition metal catalysts for the dehydropolymerization of phosphine-borane adducts has been explored;[20–27] however, all require temperatures at or above 100 °C and fail to polymerize (*P*-disubstituted)phosphine-boranes (**Scheme 2.1**). In addition, the polymer produced is generally discoloured due to the presence of catalyst-derived impurities. Recently, transition metal-free routes have been developed which offer potential with respect to overcoming these limitations. For example, in collaboration with Greb we have reported on the catalytic performance of an aluminate species bearing a calix[4]pyrrolato ligand in the dehydropolymerization of phosphine-boranes at forcing conditions (105 °C, 24 h), the first reported transition metal-free catalyst capable of producing high molar mass polyphosphinoboranes.[28] In an early study, tris(pentafluorophenyl)borane was briefly reported to dehydrocouple phosphine-boranes to access oligomeric material ($M_n$ < 2000 Da).[29] More recently, stoichiometric generation of phosphinoborane monomers, RR'P–$BH_2$ (R, R' = alkyl, aryl, H), in *situ* has yielded polyphosphinoboranes (**Scheme 2.1**). This was first demonstrated for the thermally-induced (22 – 40 °C) polymerization of a trimethylamine-stabilized phosphinoborane precursor (*t*BuHP$BH_2$•$NMe_3$), to give the transient phosphinoborane monomer, [*t*BuPH-$BH_2$], which undergoes spontaneous head-

to-tail catenation to high molar mass [*t*BuPH-$BH_2$]$_n$ (27,800-35,000 Da).[30] Reactive phosphinoborane monomers can also be generated by dehydrogenation of phosphine-borane adducts with cyclic alkyl amino carbene (CAAC), yielding polymer and CAAC•$H_2$, allowing access to both *P*-mono and, in low-yield, *P*-disubstituted polyphosphinoboranes.[31] Unfortunately, these routes require relatively laborious synthesis of reagents, and in order to access *P*-disubstituted polymers using the CAAC-mediated route, elevated temperature (60 °C). The development of new direct routes to polyphosphinoboranes that proceed in high yield under mild conditions are therefore of key importance, especially those that provide direct access to materials with two organic substituents at phosphorus, [RR'P–$BH_2$]$_n$, which are likely to be the most diverse, stable, and useful for applications.

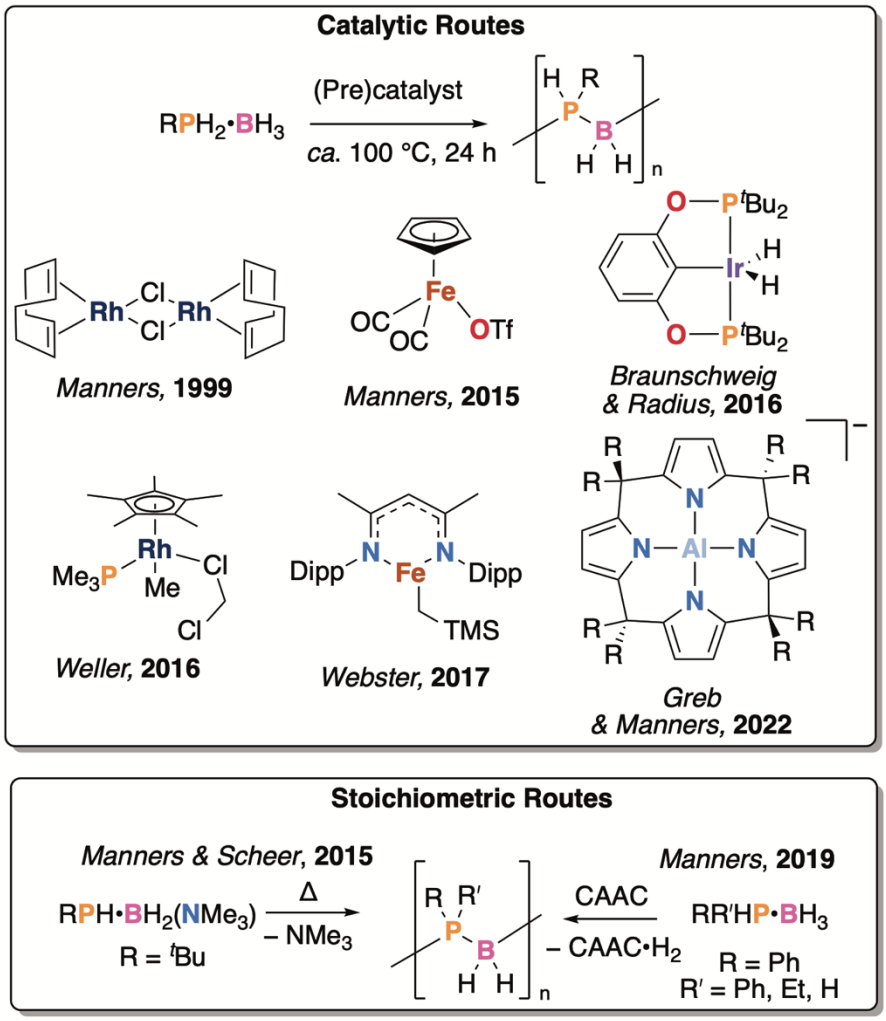


**Scheme 2.1:** Overview of the synthesis of polyphosphinoboranes. Selected catalysts are shown in the top box, while stoichiometric routes are shown in bottom box. TMS = trimethylsilyl, Tf = trifluoromethylsulfonyl, CAAC = cyclic(alkyl)amino carbene.

Recently, we reported the synthesis of isoelectronic polyaminoboranes [MeNH-$BH_2$]$_n$ by generation of transient amino-boranes [MeNH=$BH_2$], through deprotonation of readily accessible acidic amine-boronium complexes with simple amine bases (**Scheme 2.2**, top).[32,33] Hypothesizing that analogous reactivity may provide a facile route to polyphosphinoboranes (**Scheme 2.2**, bottom) we set out to synthesize analogous phosphine-boranes with acidic P–H bonds and to explore their potential as polymer

precursors. Herein, we report a new and convenient ambient temperature protocol for the synthesis of polyphosphinoboranes *via* the facile generation of transient phosphinoborane monomers as intermediates.

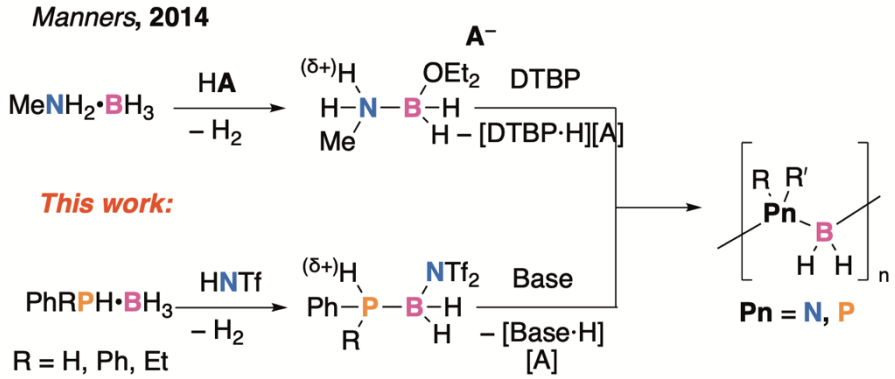


**Scheme 2.2:** Overview of the reported polyaminoborane and proposed polyphosphinoborane synthesis from deprotonation of amine-borane and phosphine-borane derivatives. HA = $[H(OEt_2)_2][BAr^F{}_4]$ ($Ar^F$ = tetrakis(3,5-bis(trifluoromethyl0phenyl)borate), DTBP = di(tertbutyl)pyridine, Tf = trifluoromethylsulfonyl.

## 2.3 Results and Discussion

The synthesis of phenylphosphine-(triflimido)borane complex (**2.2a**) from the respective phosphine-borane adduct (**2.1a**) was readily accomplished by the treatment of the latter in toluene at 20 °C over 30 min with bis(trifluoromethane)sulfonimide ($HNTf_2$), where the reaction was made evident by the liberation of $H_2$ gas (**Figure 2.1a**). Once the reaction was complete the volatiles were removed *in vacuo* to yield a colourless oil which was characterized by multinuclear nuclear magnetic resonance (NMR) spectroscopy and electrospray ionization mass spectrometry (ESI-MS). $^{11}B$ NMR revealed consumption of **2.1a** ($\delta(^{11}B)$ = −41.1 ppm, quartet of doublets, $^1J_{BP}$ = 33.6 Hz and $^1J_{BH}$ = 102 Hz) and

generation of a new species with a broad signal at −18.3 ppm, consistent with the formation of **2.2a**. Further characterization by $^{31}$P NMR revealed a new triplet at –56.0 ppm ($^{1}J_{PH}$ = 405 Hz) which was also assigned to **2a**. Positive-mode ESI-MS revealed mass peaks corresponding to the M–H cation for **2.2a**, corresponding to $[PhPH_2BH(NTf_2)]^+$.

The scope of this reaction was then explored with *P*-disubstituted phosphine-borane adducts **2.1b-d**. Addition of $HNTf_2$ to toluene solutions of **2.1b-d** at 20 °C similarly resulted in the formation of phosphine-(triflimido)borane adducts, **2.2b-d** as the sole products. Broad signals were observed by $^{11}$B NMR spectroscopy for these species in a narrow range of −17.1 to −18.6 ppm, downfield from those of their respective adducts (−41.1 to −42.2 ppm), while $^{31}$P NMR spectroscopy revealed doublets with chemical shifts that varied with the *P*-substituents (**2.2b:** −9.5 ppm $^{1}J_{PH}$ = 415 Hz, **2.2c:** –5.4 ppm $^{1}J_{PH}$ = 400 Hz, and **2.2d:** 26.0 ppm, $^{1}J_{PH}$ = 385 Hz). Furthermore, positive mode ESI-MS gave mass peaks corresponding to the $[M - H]^+$ molecular ions, $[RR'PH{\bullet}BH(NTf_2)]^+$, in each case.

Compounds **2.2a-2.2c** were isolated in very high yields (> 90%) as colorless oils whereas **2.2d** was a crystalline solid at room temperature, which permitted further characterization by single-crystal X-ray diffraction. Suitable single crystals of **2.2d** were grown from a toluene solution by slow diffusion of *n*-hexane at –40 °C and analyzed by single-crystal X-ray diffraction (SC-XRD). Interrogation of the molecular structure revealed κ-N coordination of the bistriflimide anion to the boron atom in the solid state (**Figure 2.1b**). P1–B1 and B1–N1 bond lengths are 1.974(2) and 1.616(2) Å respectively, both of which are typical B–Pn (Pn = P, N) single bonds.[34,35] Furthermore, the P1–B1–N1

bond angle of 114.1(1)°, which is slightly larger than that expected for a tetrahedral boron atom (109.5°), and reflects steric repulsion between bulky *tert*-butyl and trifluoromethylsulfonyl groups. This data supports the presence of a B–$N_{triflimide}$ single bond, resulting in a structure similar to the polar-covalent species $MeNH_2$•$BH_2(Cl)$ with a B–Cl single bond and in contrast to the donor-stabilized amine-boronium cation salts $[MeNH_2$•$BH_2(OEt_2)][BAr^F{}_4]$; $Ar^F$ = 3,5-bis(trifluoromethyl)phenyl) reported previously.[33]

a)

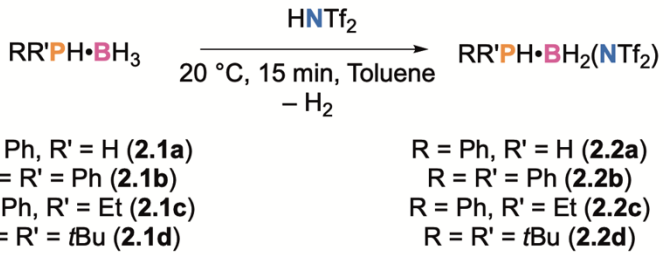


b)

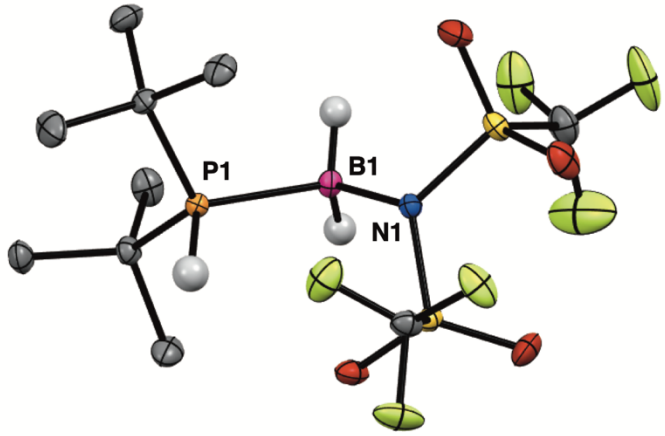


**Figure 2.1:** a) Synthesis of phosphine-(triflimido)boranes from phosphine-borane adducts. b) Molecular structure of *t*$Bu_2HPBH_2(NTf_2)$, **3.2d**, with thermal ellipsoids displayed at the 50% probability level. H-atoms belonging to the *t*Bu groups omitted for clarity. The colour scheme is as follows: phosphorus (orange), boron (pink), carbon (grey), nitrogen (blue), oxygen (red), sulfur (yellow), fluorine (lime green).

Next, the deprotonation of **2.2a-c** was explored. In order to generate transient phosphinoborane monomers, **2.2a** was reacted with the sterically hindered amine base, *i*$Pr_2$EtN, as a 2M toluene solution over 4 h at 20 °C (**Scheme 2.3**, top).[11]B and [31]P NMR spectroscopic analysis of the reaction mixture showed complete consumption of **2.2a** and new peaks at δ([11]B) = −32.9 ppm and δ([31]P) = −48.2 ppm ($^1J_{PH}$ = 350 Hz) in approximately 80% yield by [31]P NMR spectroscopy, consistent with formation of poly(phenylphosphinoborane), **2.3a**, as the major reaction product with formation of oligomers and free phosphine, $PhPH_2$, as minor species.[23–25,31,35] Furthermore, an immiscible oil was also isolated from the reaction, presumably the ionic liquid, [*i*$Pr_2$EtNH][$NTf_2$].[36] In order to remove this oil and other impurities observed by NMR spectroscopy, **2.3a** was purified by repeated precipitation of the toluene soluble fraction into *i*PrOH twice and then once into *n*-hexane, yielding **2.3a** as a white powder. During this process significant material loss occurred and **2.3a** was isolated in 29% yield. Analysis by gel permeation chromatography (GPC) showed the presence of polymeric material with a bimodal mass distribution ($M_n$ = 46 470 Da, $Đ$ = 1.54, $M_n$ = 2 960 Da, $Đ$ = 1.51) with a percentage of high molar mass material to low molar mass material ($\%_{HMM}$) of 30% based on peak area (Figure 2.3). Considering the high yield obtained for **2.2a**, we then explored the ability to access polyphosphinoborane **2.3a** from **2.1a** without the isolation of the phosphine-(triflimido)borane intermediate, **2.2a** (**Scheme 2.3,** bottom). Preparation of **2.2a** *in situ* from the reaction of $HNTf_2$ with a 2 M toluene solution of **2.1a** at 20 °C over 1 h followed by the addition of *i*$Pr_2$EtN revealed consumption of **2.2a** with formation of **2.3a** after 4 h at 20 °C with [11]B and [31]P NMR spectra matching those from deprotonation of isolated **2.2a** (δ([11]B): −32.9 ppm, and δ([31]P): −48.2 ppm; *ca*. 80% **2.3a**

by $^{31}$P NMR spectroscopy). GPC analysis of material purified by repeated precipitations revealed polymer with a bimodal mass distribution (isolated yield of **2.3a** after precipitations = 42%, $M_n$ = 54 590 Da, $Đ$ = 1.27; $M_n$ = 2 980 Da, $Đ$ = 2.33; $\%_{HMM}$: 29%). The high-molar mass fraction is of comparable molecular weight to that of **2.3a** produced by the most commonly used catalyst, $Cp(CO)_2FeOTf$.[23] However, in contrast to polyphosphinoboranes produced by transition metal-catalyzed polymerization, which are generally yellow due to the presence of metal-contaminants, **2.3a** made by deprotonation of **2a** is pure-white (**Figure 2.4**).

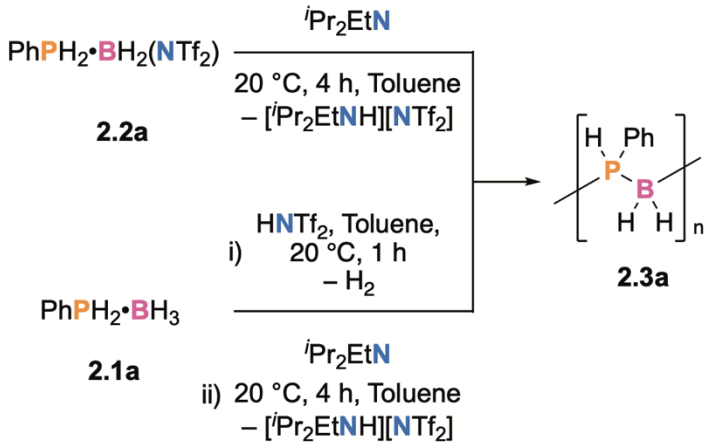


**Scheme 2.3:** Generation of polyphosphinoborane, **2.3a**, from **2.2a** (top) and **2.1a** (bottom).

As the synthesis of *P*-disubstituted polyphosphinoboranes directly from their respective phosphine-borane adduct precursors is a challenge, having only been reported at elevated temperature in low yields using a CAAC-mediated route,[31] the deprotonation of *P*-disubstituted phosphine-(triflimido)boranes **2.2b** and **2.2c** was then explored at ambient temperature. While the deprotonation of a primary phosphine-(triflimido)borane (**2.2a**) yielded the desired polyphosphinoborane (**2.3a**), deprotonation of secondary phosphine-(triflimido)borane **2.2b** using *i*Pr$_2$EtN (toluene, 2M, 4 h) did not result in the

formation of polymeric material as determined by GPC. Instead, the NMR and ESI-MS data were consistent with the formation of an inseparable mixture of oligomers tentatively assigned as $[Ph_2PH\text{-}(BH_2\text{–}PPh_2)_x\text{-}BH_2(i Pr_2EtN)]^+$ and $Ph_2PH\text{-}(BH_2\text{–}PPh_2)_x\text{-}BH_2X$ (**2.4X**: X = H or $NTf_2$) (Figure 2.7).

As an alternative base, we explored the addition of the readily accessible N-heterocyclic carbene IPr (IPr = *N,N′*-bis(2,6-diisopropylphenyl)imidazol-2-ylidene) to 2 M toluene solutions of **2.2b** or **2.2c** at 20 °C. This resulted in the formation of polyphosphinoboranes **2.3b** and **2.3c** within 4 h (**Scheme 2.4**) as determined by NMR spectroscopy and GPC. Filtering the reaction mixtures, followed by repeated precipitations of the toluene soluble fractions into cold *i*PrOH yields white powders in *ca.* 30% isolated yield. Investigating the $^{11}B$ NMR spectra of the purified samples revealed broad signals at −30.4 ppm for **2.3b** and −32.8 ppm for **2.3c** while $^{31}P$ NMR spectra gave broad signals at −15.2 ppm for **2.3b** and at –21.5 ppm for **2.3c**, matching assignments for **3a** and **3c** made *via* the CAAC-mediated route (Figure 2.9 and Figure 2.12).[31] In contrast to **3b** produced by the previously reported CAAC-mediated route, only a small amount of $Ph_2PH\text{–}BH_2\text{–}PPh_2\text{–}BH_3$ was formed (Figure 2.9).[31] GPC analysis of the products obtained revealed the formation of polymeric materials with bimodal mass distributions (**2.3b**: $M_n$ = 24 250 Da, $Đ$ = 1.31; $M_n$ = 1 500 Da, $Đ$ = 1.42; $\%_{HMM}$: 67%; **2.3c**: $M_n$ = 19 100 Da, $Đ$ = 1.41; $M_n$ = 880 Da, $Đ$ = 1.85; $\%_{HMM}$: 50%) (**Figure 2.10** and **Figure 2.13**). Significantly, polymers made by the deprotonation of **2.2b** and **2.2c** using IPr possessed a much higher percent of high molar mass material (50% – 67%) than those produced by the previously reported CAAC-mediated dehydropolymerization (12 – 18%).[31] Deprotonation of **2.2a** as a 2 M toluene solution using IPr at 20 °C also yielded polymeric material within 4 h in 34%

yield, evidenced by NMR spectra of purified product matching that for the deprotonation of **2.2a** using *i*Pr$_2$EtN and GPC analysis revealing material with a bimodal mass distribution ($M_n$ = 28 210 Da, $Đ$ = 1.59; $M_n$ = 2 630 Da, $Đ$ = 1.36; %$_{HMM}$: 70%). Moreover, imidazolium triflimide by-product, [IPr–H][NTf$_2$], can be recovered from the reaction and then readily deprotonated by KO*t*Bu to regenerate free carbene in 89% isolated yield (**Scheme 2.5**).

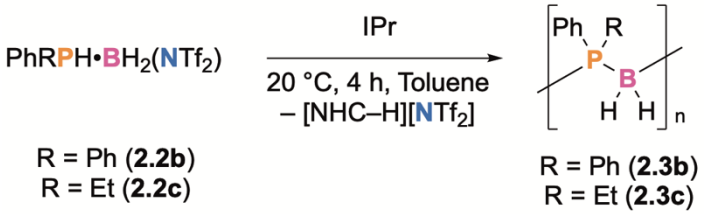


**Scheme 2.4:** Deprotonation of phosphine-(triflimido)boranes **2.2b** and **2.2c** to yield polymeric material (**2.3b** or **2.3c**).

The mechanism for the polymerization of **2.2a** – **2.2c** probably operates through formation of a phosphinoborane monomer from the triflimide salt, which then undergoes head-to-tail catenation to produce polymeric and oligomeric materials. The formation of two separate fractions may arise from the ability of the growing chain to either undergo linear growth to form polymeric chains of high molar mass, or cyclization or termination at lower degrees of polymerization to form oligomeric materials. Head-to-tail catenation of phosphinoborane monomers has been suggested as a mechanism for the polymerization observed on mild heating of the trimethylamine adduct *t*BuHP–BH$_2$•NMe$_3$, as well as the CAAC-mediated polymerization of phosphine-boranes.[30,31] Furthermore, monomeric aminoboranes have been evidenced as intermediates in the formation of polyaminoboranes.[33,37,38] As phosphinoborane monomers without significant kinetic stabilization from bulky organic substituents are highly reactive, transient species which

defy isolation, indirect evidence for their formation was targeted using ESI-MS and trapping reactions.[39]

Analysis using ESI-MS of **2.3a, 2.3b,** and **2.3c** accessed from deprotonation of **2.2a** using *i*Pr$_2$EtN or deprotonation of **2.2a-c** using IPr revealed the presence of Lewis base-capped oligomers with up to 9 repeat R$_2$P–BH$_2$ units (**Figure 2.15** to **Figure 2.18**). This data suggests that as phosphinoborane chain grows, residual unreacted base can coordinate at the Lewis acidic boron terminus. The ability of Lewis bases to coordinate to oligomers formed *in situ* is consistent with recent computational studies by Pomogaeva, Timoshkin, and Scheer on phosphinoborane linear oligomers, [PH$_2$–BH$_2$]$_7$, where it was shown that the lowest unoccupied molecular orbital is localized at the boron terminus.[40] A further report on the stability of Lewis acid- and Lewis base adducts of analogous phosphinoborane decamers, [PH$_2$–BH$_2$]$_{10}$, showed that tethering of N-heterocyclic carbenes (NHCs) to boron favours the formation of linear over cyclic species.[41] In contrast, the work also indicated that coordination of weaker Lewis bases (such as NH$_3$) at the boron terminus did not result in linear chains that were more stable than cyclic analogues. This may explain the successful access to *P*-disubstituted polymers and the greater percentages of high molar mass material in the isolated products when IPr is used as the base, as residual unreacted IPr can coordinate to the *B*-termini of growing chains and thereby prevent cyclization to form cyclic oligomers. On the other hand, analogous coordination of the weaker Lewis base, *i*Pr$_2$EtN, would not favour continued growth of linear high molar mass polymer.

Further evidence for the intermediacy of monomeric phosphinoboranes was performed by trapping an example with two kinetically stabilizing *tert*-butyl phosphorus

substituents. This was achieved by dropwise addition of a toluene solution of *t*$Bu_2PH•BH_2(NTf_2)$ (**2.2d**), to a toluene solution of two equivalents of IPr at 20 °C over 30 min (**Figure 2.2**, a), which afforded *t*$Bu_2P–BH_2$(IPr), **2.5**, in near-quantitative yield (96%), together with [IPr–H][$NTf_2$] as by-product. Adduct **2.5** was characterized by multinuclear NMR spectroscopy, ESI-MS, and SC-XRD. $^{31}P$ and $^{11}B$ NMR spectra of **2.5** showed that the phosphorus and boron centers possessed chemical shifts of δ($^{31}P$) = 4.96 ppm and δ($^{11}B$) = −29.8 ppm, which are comparable to those of the $CAAC^{Me}$ analog, *t*$Bu_2P–BH_2(CAAC^{Me})$, (δ($^{31}P$) = 13.2 ppm and δ($^{11}B$) = −24.6 ppm).[31] These differences could possibly be due to the differences in σ-donating and π-accepting properties between IPr and $CAAC^{Me}$.[42] The structure of **5** was confirmed by SC-XRD (**Figure 2.2**, b). The P–B and B–C(carbene) bond lengths (1.980(1) and 1.599(2) Å, respectively), are similar to the those reported for other phosphinoborane-NHC and -CAAC adducts reported recently.[31,43] Stoichiometric reaction of **2.2d** with IPr does not yield isolable free phosphinoborane, but instead results in unreacted **2.2d** and **2.5** as the major products.

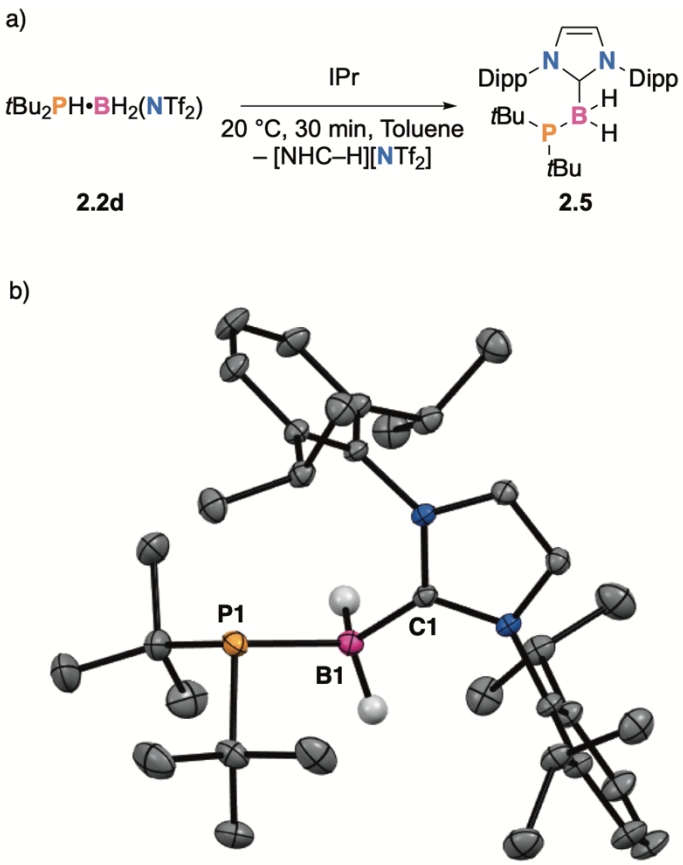


**Figure 2.2:** a) Trapping of phosphinoborane monomer, *t*Bu$_2$P–BH$_2$, generated in *situ* with an additional equivalent of IPr as **2.5**. b) ORTEP diagram of *t*Bu$_2$PBH$_2$(IPr), **2.5**, with the non-BH$_2$ hydrogen atoms and a molecule of toluene omitted for clarity and ellipsoids at the 50% probability level. The colour scheme is as follows: phosphorus (orange), boron (pink), carbon (grey), nitrogen (blue).

## 2.4 Conclusion

In summary, we report a convenient synthesis of polyphosphinoboranes, [PhRP–$BH_2$]$_n$ (**2.3a**: R = H; **2.3b**: R = Ph; **2.3c**: R = Et), using commercially available reagents and readily accessed phosphine-borane adducts that operates under ambient conditions and produces material that is not contaminated with metal-derived impurities. Significantly, *P*-disubstituted materials accessed by deprotonation of phosphine-(triflimido)boranes **2.2b** and **2.2c** with IPr exhibited a much greater percentage of high molar mass material than *P*-disubstituted polymers made from the reported CAAC-mediated route.[31] The IPr can be readily regenerated by treatment of the hydrogenated by-product with KO*t*Bu. The polymerization is proposed to occur by head-to-tail catenation of phosphinoborane monomers, RR'P–$BH_2$, which was supported by the trapping of reactive phosphinoboranes generated *in situ* as an IPr adduct (**2.5**). Exploration of the chemistry of hitherto elusive reactive phosphinoborane monomers generated using this method as well as scale-up and studies of polymer properties will be the focus of future studies.

## 2.5 Experimental Section

### General Considerations

Storage and manipulation of all compounds were performed under an inert atmosphere either in a dinitrogen-filled MBraun 200B glovebox equipped with a cold-well and regulated to 20 °C with a Polyscience 6000 portable chiller or using a dinitrogen Schlenk

line using standard techniques. Hexanes and toluene were dried and purified using an MBraun Grubbs/Dow solvent purification system[44] and stored over activated 4Å molecular sieves. $C_6D_6$ was dried over sodium/benzophenone ketyl, de-gassed and vacuum distilled prior to use. N-heterocyclic carbenes[45] and phosphine-borane adducts (**2.1a-2.1c**),[26,46–48] were synthesized according to literature procedures, while **2.1d** was purchased from Sigma-Aldrich and used as received. Diisopropylethylamine was dried over $CaH_2$ then vacuum distilled before use. All other reagents were purchased from Sigma-Aldrich and used as received. $^{1}H$ and $^{13}C$ NMR spectrometry chemical shifts were referenced to residual proteo-solvent resonances and naturally abundant $^{13}C$ resonances for all deuterated solvents. All heteronuclear NMR spectra were referenced externally to IUPAC standards. Chemical shift assignments are based on NMR experiments performed on Bruker Avance NEO 500 MHz or AV III 300 MHz spectrometers. Gel-permeation chromatography was performed on a Malvern RI max Gel Permeation Chromatograph, equipped with an automatic sampler, a pump, an injector, and inline degasser. The columns (styrene/divinyl benzene gel, 1xT5000 and 1xT3000) were maintained at 35 °C. Sample elution was detected by means of a differential refractometer. THF (VWR), containing 0.1 wt% [*n*-$Bu_4N$]Br, was used as the eluent at a flow rate of 1 mL $min^{-1}$. Samples were dissolved in THF (2 mg/mL) and filtered through a 0.2 μm PTFE syringe filter before analysis. Calibration was conducted using commercially available monodisperse polystyrene standards (Aldrich, 1,200 - 4,200,000 Da). Mass spectra were obtained using a 3D ion trap Thermo LCQ Classic mass spectrometer from ions produced from electrospray ionization. Samples for mass spectrometry were prepared by dissolving

approximately 1 mg of solid in a minimal amount of dichloromethane which was then diluted to 1 mL using acetonitrile.

**General procedure for the preparation of phosphine-(triflimido)boranes (2.2a-d)**

A 2 M solution of the corresponding phosphine-borane adduct (**2.1a-d**, 1.0 mmol) was prepared in toluene (500 µL) in a 20 mL vial charged with a stirring bar. To the rapidly stirred solution was carefully added 1.0 mmol of solid bis(trifluoromethanesulfonyl)amine resulting in the immediate evolution of a gas. The solution was allowed to stir for 30 min further followed by removal of volatiles *in vacuo* which yielded a colourless oil apart from **2.2d**, which is a white crystalline solid, in very high yields. Products were used without further purification.

**$PhPH_2$•$BH_2(NTf_2)$ (2.2a):**

Prepared from phenylphosphine-borane adduct, **2.1a**. Yield: 386 mg, 96%.

$^1$H NMR ($C_6D_6$, 500 MHz, 298 K) δ: 6.91 (m, 3 H, Ph-**H**), 6.82 (m, 2 H, Ph-**H**), 4.54 (d m, 2 H, PhP**H$_2$**, $^2J_{HP}$ = 405 Hz), 3.18 (br d, B**H$_2$**($NTf_2$)) ppm.

$^{11}$B NMR ($C_6D_6$, 160 MHz, 298 K) δ: −18.2 ppm (br).

$^{13}$C{$^1$H} NMR ($C_6D_6$, 126 MHz, 298 K) δ: 133.6 (d, Ph-**C**$_{meta}$, $^3J_{CP}$ = 8.8 Hz), 132.6 (d, Ph-**C**$_{para}$, $^4J_{CP}$ = 3.7 Hz), 129.4 (d, Ph-**C**$_{ortho}$, $^2J_{CP}$ = 11.3 Hz), 120.0 (q, **C**$F_3$, $^1J_{CF}$ = 327 Hz), 114.8 (d, Ph-C$_{ipso}$, $^1J_{CP}$ = 64.2 Hz) ppm.

$^{19}$F{$^1$H} NMR ($C_6D_6$, 471 MHz, 298 K) δ: –72.4 ppm (s).

$^{31}$P NMR ($C_6D_6$, 202 MHz, 298 K) δ: –56.0 ppm (t, $^1J_{PH}$ = 405 Hz).

ESI-MS (+ve mode): Calculated for $C_8H_8BF_6NO_4PS_2^+$, [M – H]: 401.96 m/z, found: 401.96 m/z.

**$Ph_2PH•BH_2(NTf_2)$ (2.2b):**

Prepared from Diphenylphosphine-borane adduct, **2.1b**. Yield: 454 mg, 95 %.

$^1$H NMR ($C_6D_6$, 500 MHz, 298 K) δ: 7.27 (dd, 4 H, Ph-**H**$_{ortho}$, $^3J_{HH}$ = 10.0 Hz, $^3J_{HP}$ = 12.5 Hz), 7.09 (t, 2 H, Ph-**H**$_{para}$, $^3J_{HH}$ = 10.0 Hz), 7.00 (t, 4 H, Ph-**H**$_{meta}$, $^3J_{HH}$ = 10.0 Hz), 6.14 (d m, 1 H, $Ph_2$**H**P, $^1J_{HP}$ = 415 Hz), 3.48 (br, 2 H, B**H**$_2$($NTf_2$)) ppm.

$^{11}$B NMR ($C_6D_6$, 160 MHz, 298 K) δ: –17.1 ppm (br).

$^{13}$C{$^1$H} NMR ($C_6D_6$, 126 MHz, 298 K) δ: 133.4 (d, Ph-**C**$_{meta}$, $^3J_{CP}$ = 8.8 Hz), 132.7 (d, Ph-**C**$_{para}$, $^4J_{CP}$ = 2.5 Hz), 129.6 (d, Ph-**C**$_{ortho}$, $^2J_{CP}$ = 11.3 Hz), 120.9 (d, Ph-**C**$_{ipso}$, $^1J_{CP}$ = 61.6), 120.0 (q, **C**$F_3$, $^1J_{CF}$ = 326 Hz) ppm.

$^{19}$F{$^1$H} NMR ($C_6D_6$, 471 MHz, 298 K) δ: –71.8 ppm (s).

$^{31}$P NMR ($C_6D_6$, 202 MHz, 298 K) δ: –9.5 ppm (d, $^1J_{PH}$ = 415 Hz).

ESI-MS (+ve mode): Calculated for $C_{14}H_{12}BF_6NO_4PS_2^+$, [M – H]: 477.99 m/z, found: 477.99 m/z.

**PhEtPH•$BH_2(NTf_2)$ (2.2c):**

Prepared from Phenylethylphosphine-borane adduct, **2.1c**. Yield: 415 mg, 96%.

$^1$H NMR ($C_6D_6$, 500 MHz, 298 K) δ: 7.01 (m, 3 H, Ph-**H**), 6.91 (t, 2 H, Ph-**H**, $^3J_{HH}$ = 10.0 Hz), 4.85 (d m, 1 H, PhEtP**H**, $^1J_{HP}$ = 400 Hz), 3.08 (br, 2 H, B**H$_2$**($NTf_2$)), 2.60 (d m, 2 H, P(C**H$_2$**$CH_3$), $^2J_{HP}$ = 60.0 Hz), 0.44 (d t, 3 H, P($CH_2$C**H$_3$**), $^3J_{HP}$ = 15.0 Hz, $^3J_{HH}$ = 10.0 Hz) ppm.

$^{11}$B NMR ($C_6D_6$, 160 MHz, 298 K) δ: –17.4 ppm (br s).

$^{13}C\{^1H\}$ NMR ($C_6D_6$, 126 MHz, 298 K) δ: 133.0 (d, Ph-**C*meta***, $^3J_{CP}$ = 8.8 Hz), 132.4 (d, Ph-**C*para***, $^4J_{CP}$ = 2.52 Hz), 129.4 (d, Ph-**C$_{ortho}$**, $^2J_{CP}$ = =10.1 Hz), 119.7 (d, Ph-**C*ipso***, $^1J_{CP}$ = 60.4), 119.0 (q, **C**$F_3$, $^1J_{CF}$ = 323 Hz), 13.4 (d, P(**C**$H_2CH_3$), $^1J_{CP}$ = 36.5 Hz), 8.2 (d, P($CH_2$**C**$H_3$), $^2J_{CP}$ = 6.3 Hz) ppm.

$^{19}F\{^1H\}$ NMR ($C_6D_6$, 471 MHz, 298 K) δ: –71.9 ppm (s).

$^{31}$P NMR ($C_6D_6$, 202 MHz, 298 K) δ: –5.4 ppm (d, $^1J_{PH}$ = 400 Hz).

ESI-MS (+ve mode): Calculated for $C_{14}H_{12}BF_6NO_4PS_2^+$, [M – H]: 429.99 m/z, found: 430.0 m/z.

**$t$Bu$_2$PH•BH$_2$(NTf$_2$) (2.2d):**

Prepared from Di-*tert*-butylphosphine-borane adduct, **2.1d**. Yield: 419 mg, 96%.

$^1$H NMR ($C_6D_6$, 500 MHz, 298 K) δ: 4.09 (dt, 1 H, $t$Bu$_2$P**H**, $^1J_{HP}$ = 385 Hz, $^2J_{HP}$ = 5.0 Hz), 2.97 (br d, 2H, B**H$_2$**), 0.87 (d, 18 H, C**H$_3$,** $^3J_{HP}$ = 15.0 Hz) ppm.

$^{11}$B NMR ($C_6D_6$, 160 MHz, 298 K) δ: –18.8 ppm (br).

$^{13}C\{^1H\}$ NMR ($C_6D_6$, 126 MHz, 298 K) δ: 120.2 (q, **C**$F_3$, $^1J_{CF}$ = 325 Hz), 31.6 (d, **C**$(CH_3)_3$, $^1J_{CP}$ = 28.9 Hz), 28.3 (s, C(**C**$H_3)_3$)

$^{19}F\{^1H\}$ NMR ($C_6D_6$, 471 MHz, 298 K) δ: 70.9 ppm (s).

$^{31}$P NMR ($C_6D_6$, 202 MHz, 298 K) δ: 26.0 ppm (br d, $^1J_{PH}$ = 385 Hz)

ESI-MS (+ve mode): Calculated for $C_{10}H_{20}BF_6NO_4PS_2^+$, [M – H]: 438.06 m/z, found: 438.04 m/z.

**Synthesis of Polyphosphinoborane 2.3a from 2.2a**

A 2 M solution of **2.2a** (403 mg, 1.0 mmol) was prepared in toluene (500 µL) in a 20 mL vial equipped with a stirbar. To the rapidly stirring colourless solution, *i*Pr$_2$EtN (174 µL, 1.0 mmol) was added, resulting in the formation of an immiscible oil evident by a murky solution. The reaction was then allowed to stir for 4 additional hours, removed from the glovebox, then filtered through a 0.45 µm PTFE syringe filter in open air. Subsequently, the filtrate was concentrated, and the polymer was precipitated from toluene into rapidly stirring *i*PrOH that was cooled to –20 °C, followed by decanting the supernatant. The precipitation was then performed twice more by redissolving the polymer in a minimal amount of toluene (*c.a.* 1 mL) and adding the solution dropwise to rapidly stirring cooled (–5 °C) hexanes. Volatiles were then removed from the precipitate *in vacuo* overnight to yield a white solid (36 mg, 29%). The low yield is attributed to loss of material from the repeated precipitations that are necessary to remove [*i*Pr$_2$EtNH][NTf$_2$]. GPC analysis of this material revealed a bimodal mass distribution ($M_n$ = 46 470, D = 1.54, $M_n$ = 2 960, D = 1.51, $\%_{HMM}$ = 30%) with NMR spectra matching previously reported data.[20,23]

**"One-pot" synthesis of 2.3a from 2.1a**

A 2 M solution of **2.1a** (124 mg, 1.0 mmol) was prepared in toluene (500 µL) in a 20 mL vial charged with a stirbar. To this solution, HNTf$_2$ (281 mg, 1.0 mmol) was added, resulting in the evolution of a gas. To ensure completion of the initial reaction, the mixture was stirred for 30 min longer. Afterwards, *i*Pr$_2$EtN (174 µL, 1.0 mmol) was added, resulting in the formation of an immiscible oil. The reaction mixture was then left to stir for 4 h after which a work-up identical to that described for the reaction of **2.2a** with *i*Pr$_2$EtN above.

From this, a white powder with $^{31}P$ and $^{11}B$ and $^{1}H$ NMR spectra matching that from the reaction of isolated **2a** with *i*$Pr_2$EtN was obtained in an isolated yield of 51 mg or 42%. GPC analysis of the material revealed polymeric material with a bimodal mass distribution.

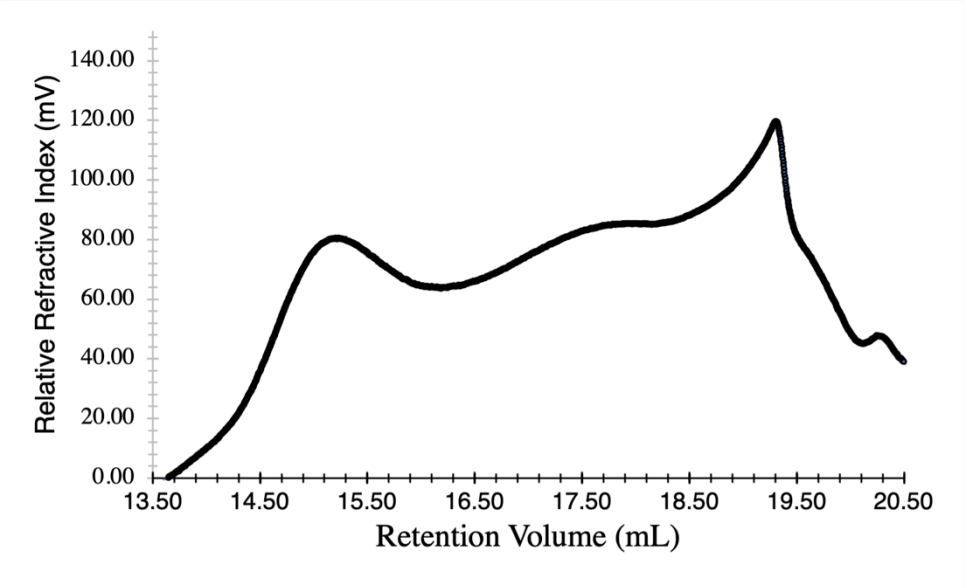


**Figure 2.3:** GPC trace (RI) of purified **2.3a** obtained from deprotonation of **2.2a** using *i*$Pr_2$EtN. The sharp peak at *ca*. 19 mL may arise from a preponderance of a specific oligomer.

**Figure 2.4:** Photographs of polyphosphinoborane **2.3a** made by deprotonation of **2.1a** (left) and polyphosphinoborane **2.3a** made by $Cp(CO)_2FeOTf$-catalyzed dehydropolymerization of **2.1a** (1 mol%, toluene, 100 °C, 24 h)[11] and discoloured by residual iron species (right). Photographs taken by Matthew A. Wiebe.

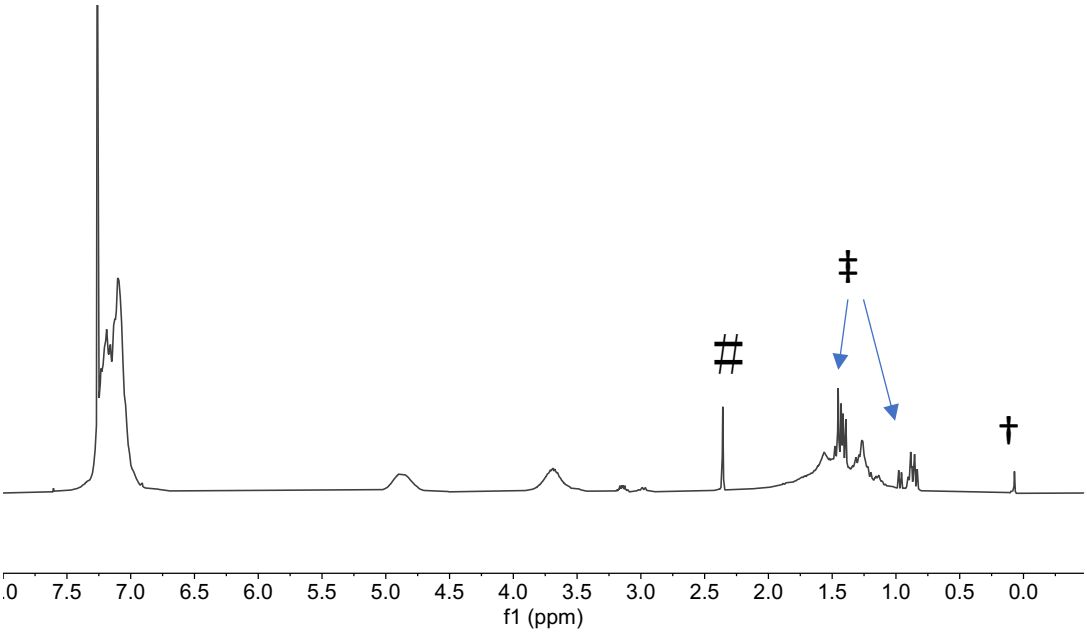


**Figure 2.5:** $^1H$ NMR (300 MHz, $CDCl_3$, 298 K) of **2.3a** purified by precipitation into *i*PrOH and hexanes then dried under high vacuum for 16 h. † Silicone grease impurity. ‡ Hexanes impurity. # Toluene impurity.

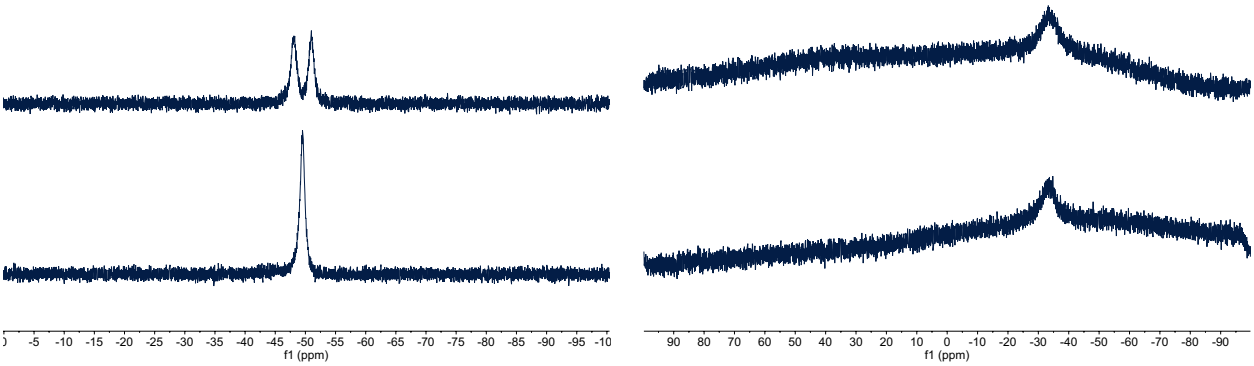


**Figure 2.6:** Left: $^{31}P$ (top) and $^{31}P\{^{1}H\}$ (bottom) NMR spectra (202 MHZ, $CDCl_3$, 298 K) of purified **2.3a**. Right: $^{11}B$ (top) and $^{11}B\{^{1}H\}$ (bottom) NMR spectra (160 MHZ, $CDCl_3$, 298 K) of **2.3a**.

**Deprotonation of 2.2b using $iPr_2EtN$ to yield 2.4X**

To a rapidly stirred 2 M toluene solution at 20 °C of **2.2b** in a 4-dram vial was added *i*$Pr_2EtN$ (174 µL, 1.0 mmol), resulting in the production of an immiscible liquid. NMR analysis of the reaction mixture after 1 h had revealed the consumption of **2.2b** to give a mixture of products as observed in Figure 2.7, consistent with the formation of linear dimers of type $Ph_2PHBH_2PPh_2BH_2$(X), **2.4X**. This assignment is supported by analysis of the reaction product by ESI-MS which revealed a mass peak at 398.13 m/z, which corresponds to $[Ph_2PH–BH_2–PPh_2–BH_2]^+$. Another peak at 526.07 m/z was observed, which corresponds to $[Ph_2PH–BH_2–PPh_2–BH_2(iPr_2EtN)]^+$. Attempts to purify a single species from this mixture by crystallization from toluene and hexanes were unsuccessful.

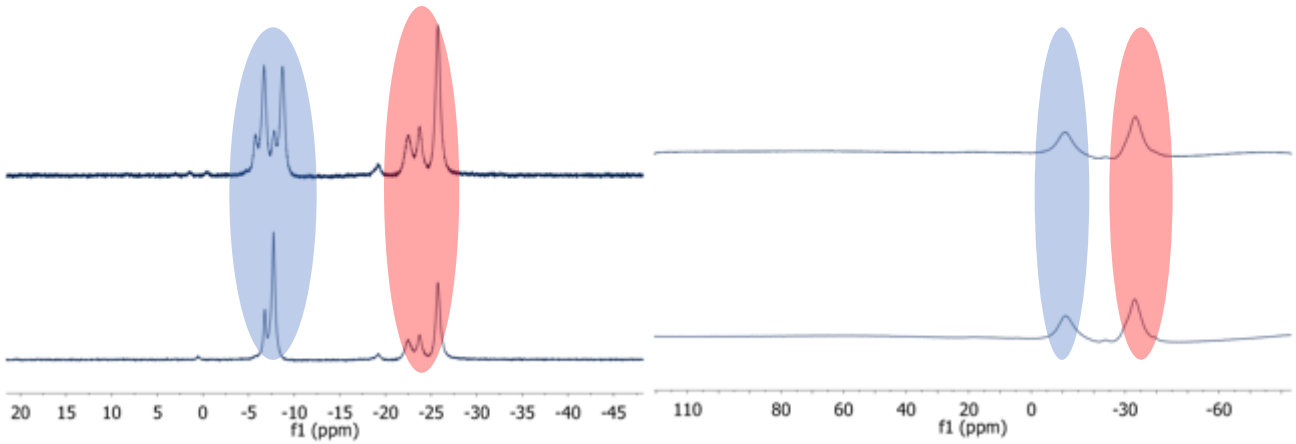


**Figure 2.7:** Left: $^{31}P$ (top) and $^{31}P\{^{1}H\}$ (bottom) NMR spectra (202 MHZ, $C_6D_6$, 298 K) of the product of reaction between **2.2b** and *i*$Pr_2EtN$. Right: $^{11}B$ (top) and $^{11}B\{^{1}H\}$ (bottom) NMR spectra (160 MHZ, $C_6D_6$, 298 K) of the product of reaction between **2.2b** and *i*$Pr_2EtN$. Peaks for $Ph_2\underline{P}H$– and –$Ph_2\underline{P}$– for $Ph_2PH–BH_2–PPh_2–BH_2X$ are highlighted in blue (*ca.* –7 ppm) and red (*ca.* –25 ppm) respectively in the $^{31}P$ NMR spectra. Peaks for –$\underline{B}H_2X$ and –$\underline{B}H_2$– and are highlighted in blue (*ca.*–10 ppm) and red (*ca* –35 ppm) respectively.

**Deprotonation of 2.2b and 2.2c using IPr to yield Polyphosphinoboranes 2.3b and 2.3c:**

A 2 M solution of **2.2b** or **2.2c** (1.0 mmol) was prepared in toluene (500 µL) in a 20 mL vial charged with a stir bar. To this stirring solution was added *N,N*-bis(2,6-diisopropylphenyl)imidazole-2-ylidene (IPr) (388 mg, 1.0 mmol), which was immediately followed by precipitation of a white solid, presumably the imidazolium triflimide [IPr–H][$NTf_2$]. The vial was then removed from the glovebox and polymeric material was then extracted with toluene (*ca*. 2 mL) and filtered using a 0.45 µm syringe filter in air. The filtrate was then concentrated under vacuum to *ca* 0.5 mL. The concentrated solution was

then added dropwise to cooled *i*PrOH (–10 °C), resulting in the precipitation of a white solid. The supernatant was decanted, and the precipitation was repeated twice more giving white powders in approximately 30% yield (**2.3b**: 61 mg, 31% yield, **2.3c**: 42 mg, 28% yield). Loss of material and reduced yield are presumably a consequence of repeated precipitations necessary to purify polymers. NMR and GPC analysis for **2.3b** and **2.3c** are given below with NMR assignments matching those from our previous report.[31]

**2.3b**:

**NMR:**

$^{11}$B NMR ($CDCl_3$, 160 MHz, 298 K) δ: −30.4 ppm (br).

$^{31}$P NMR ($CDCl_3$, 202 MHz, 298 K) δ: –15.2 ppm (br).

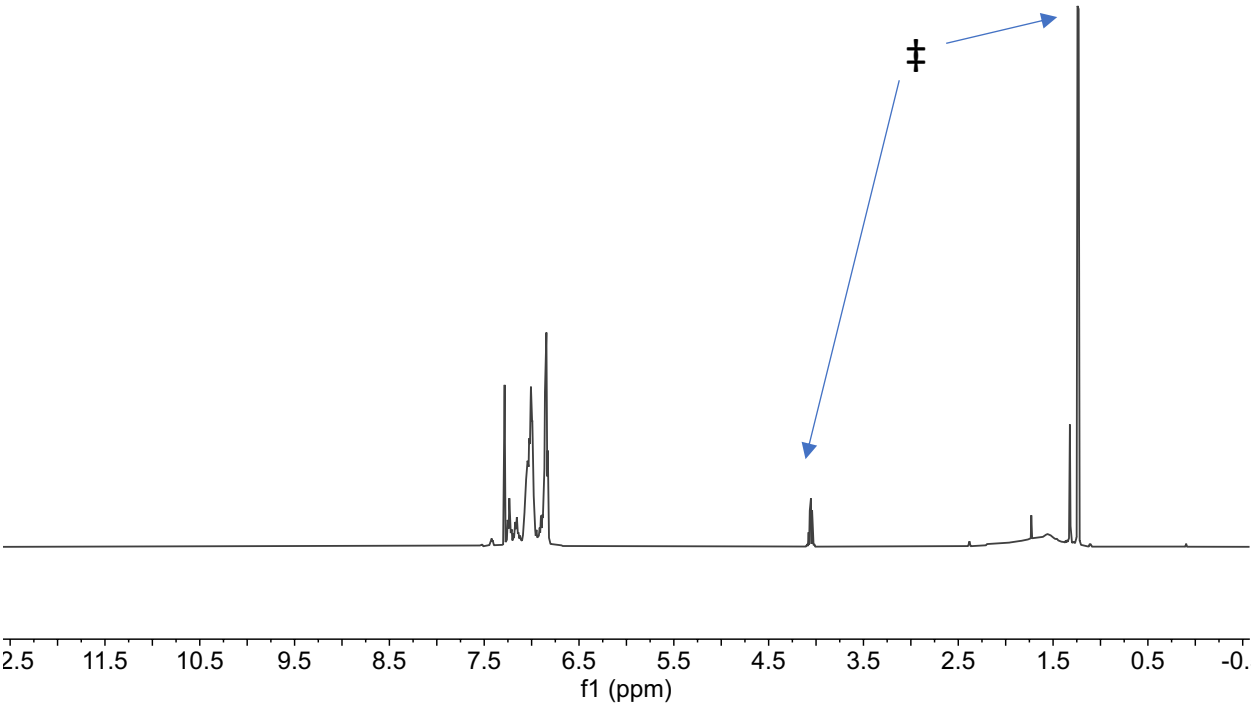


**Figure 2.8:** $^{1}$H NMR (300 MHz, $CDCl_3$, 298 K) of **2.3b** purified by precipitation into *i*PrOH and hexanes. ‡ *i*PrOH impurity.

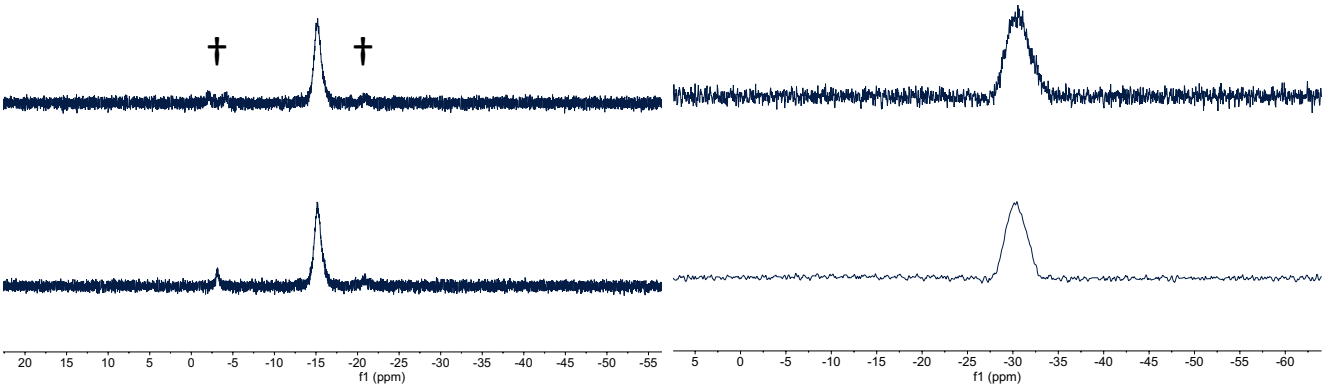


**Figure 2.9:** Left: $^{31}$P NMR (top) (202 MHz, $CDCl_3$, 298 K) and $^{31}P\{^{1}H\}$ NMR (bottom) (202 MHz, $CDCl_3$, 298 K) of **2.3b**, where † denotes peaks for linear dimer $Ph_2PH{\bullet}BH_2PPh_2{\bullet}BH_3$. Right: $^{11}$B NMR (top) (160 MHz, $CDCl_3$, 298 K) and $^{11}B\{^{1}H\}$ NMR (bottom) (160 MHz, $CDCl_3$, 298 K) of 2.3b, where peaks for linear dimer $Ph_2PH{\bullet}BH_2PPh_2{\bullet}BH_3$ are obscured by the peaks for 2.3b.

**GPC:**

Material was found to polymeric with a bimodal mass distribution with: $M_n$ = 24 250 Da, $Đ$ = 1.31; $M_n$ = 1 500 Da, $Đ$ = 1.42; $\%_{HMM}$: 67%.

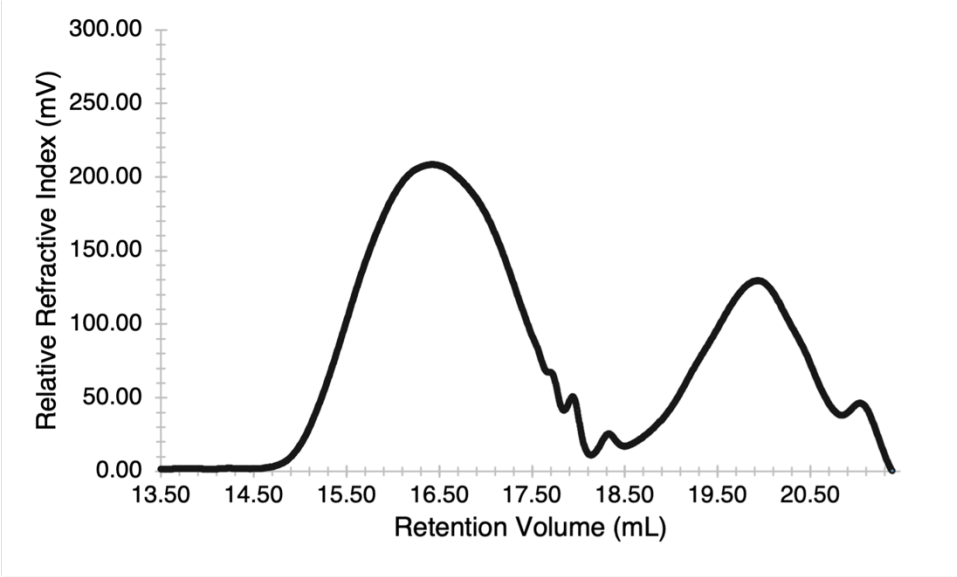


**Figure 2.10** GPC trace of purified **2.3b** obtained from the deprotonation of **2.2b** using IPr.

**2.3c:**

**NMR:**

$^{11}$B NMR ($CDCl_3$, 160 MHz, 298 K) δ: −32.8 ppm (br).

$^{31}$P NMR ($CDCl_3$, 202 MHz, 298 K) δ: –21.5 ppm (br).

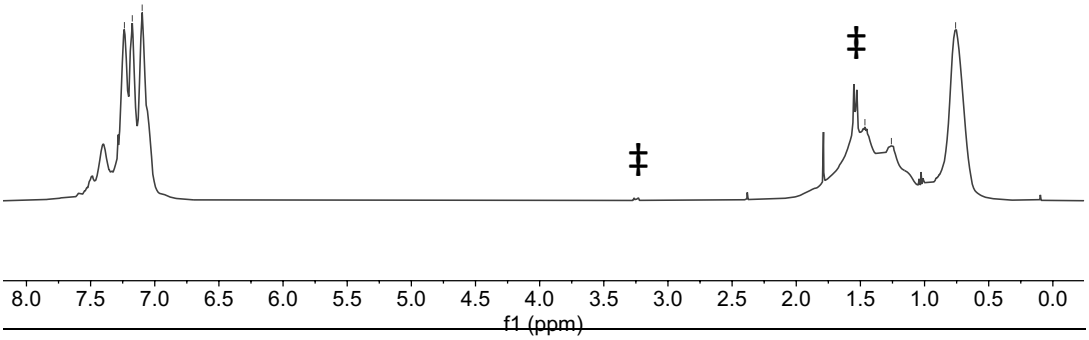


**Figure 2.11:** $^{1}H$ NMR (300 MHz, $CDCl_3$, 298 K) of **2.3c** purified by precipitation into *i*PrOH and hexanes. ‡ *i*PrOH impurity.

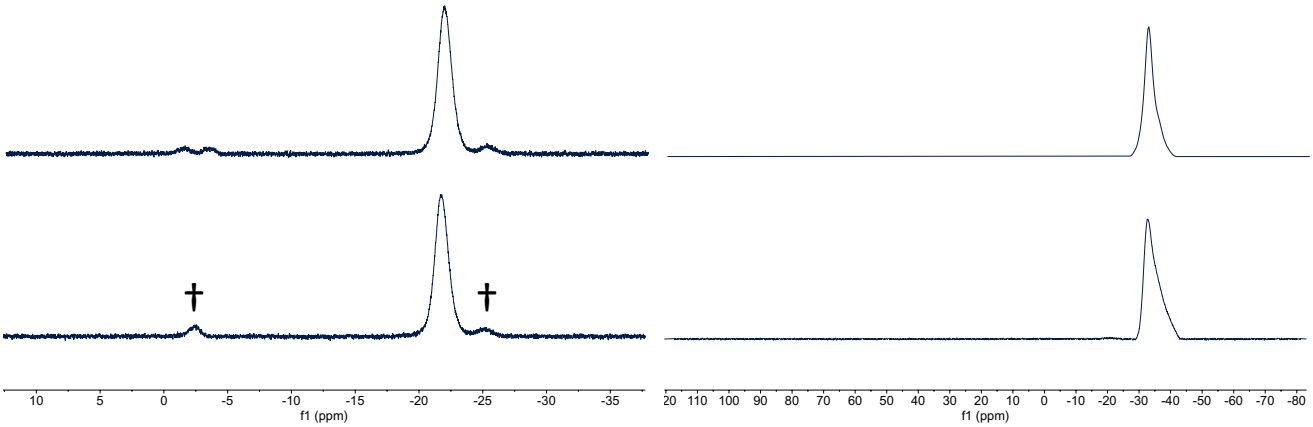


**Figure 2.12:** Left: $^{31}P$ NMR (top) (202 MHz, $CDCl_3$, 298 K) and $^{31}P\{^{1}H\}$ NMR (bottom) (202 MHz, $CDCl_3$, 298 K) of **2.3c**, where † denotes peaks for linear dimer PhEtPH•$BH_2$PPhEt•$BH_3$. Right: $^{11}B$ NMR (top) (160 MHz, $CDCl_3$, 298 K) and $^{11}B\{^{1}H\}$ NMR (bottom) (160 MHz, $CDCl_3$, 298 K) of **2.3c**, where peaks for linear dimer PhEtPH•$BH_2$PPhEt•$BH_3$ are obscured by the peaks for **2.3c**.

**GPC:**

Material was found to polymeric with a bimodal mass distribution with: $M_n$ = 19 100 Da, $Đ$ = 1.41; $M_n$ = 880 Da, $Đ$ = 1.85; $\%_{HMM}$: 50%.

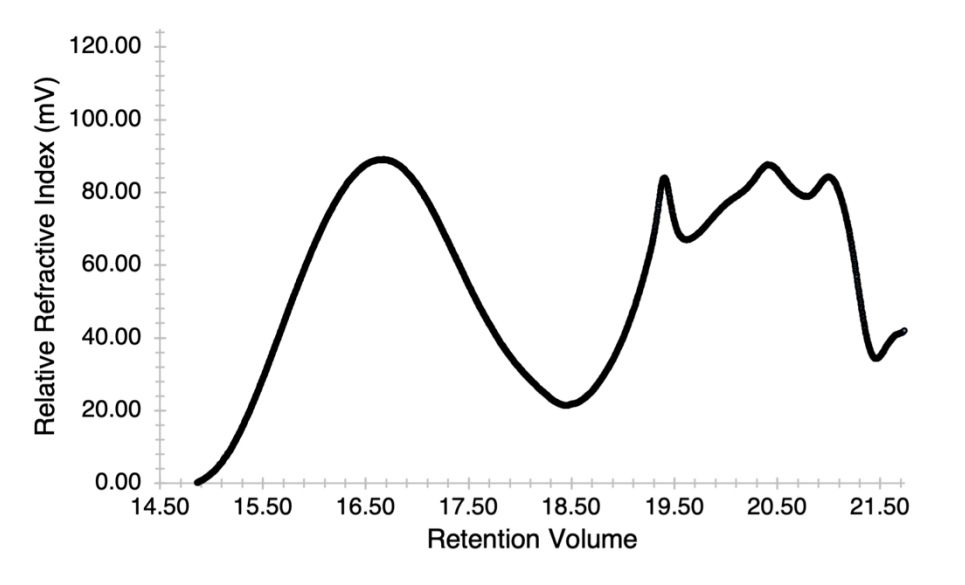


**Figure 2.13:** GPC trace of purified **2.3c** obtained by deprotonation of **2.2c** using IPr. The sharp peaks within the low molar mass fractions may be due to the preponderance of oligomers of a specific length.

**"One-pot" Dehydropolymerization of 2.1a using IPr as the base**

To a stirring 2 M toluene solution of phosphine-borane adduct, **2.1a** (124 mg, 1.0 mmol) in a 20 mL vial was added $HNTf_2$ (281 mg, 1.0 mmol), resulting in immediate formation of a gas. To ensure full conversion of **2.1a** to **2.2a**, the reaction was stirred for 1 h longer, during which bubbling from gas evolution ceased. Afterwards, solid IPr (388 mg, 1.0 mmol) was added to the rapidly stirring solution, which resulted in the immediate precipitation of the imidazolium salt, [IPr–H][$NTf_2$]. This solution was left to stir for 4 hours longer, after which the reaction product, **2.3a**, was extracted with toluene (*ca*. 2 mL) and filtered through a 0.45 μm syringe filter. The filtrate was then concentrated to approximately 0.5 mL, and then added dropwise to 40 mL of *i*PrOH cooled to –10 °C, resulting in the precipitation of a white solid. The solid was collected then dissolved in a minimal amount of toluene (*ca.* 0.5 mL) and precipitated from a cooled solution of *i*PrOH once more. This process was repeated a third time, however from dropwise addition of the concentrated toluene solution of **2.3a** to 40 mL of hexanes cooled to –10 °C. The resulting white solids were collected, and volatiles were removed under vacuum for a minimum of 16 h before analysis, resulting in 41 mg of a white powder which corresponds to a 34% isolated yield. Analysis of this material by NMR spectroscopy resulted in spectra that matched that for polymer produced by deprotonation of **2.2a** using *i*$Pr_2$EtN. However, GPC analysis revealed the formation of material with a much higher fraction of high-molar mass material to low molar mass material ($M_n$ = 28 210 Da*,* $Đ$ = 1.59; $M_n$ = 2 630 Da, $Đ$ = 1.36; $\%_{HMM}$: 70%) as seen in **Figure 2.14.**

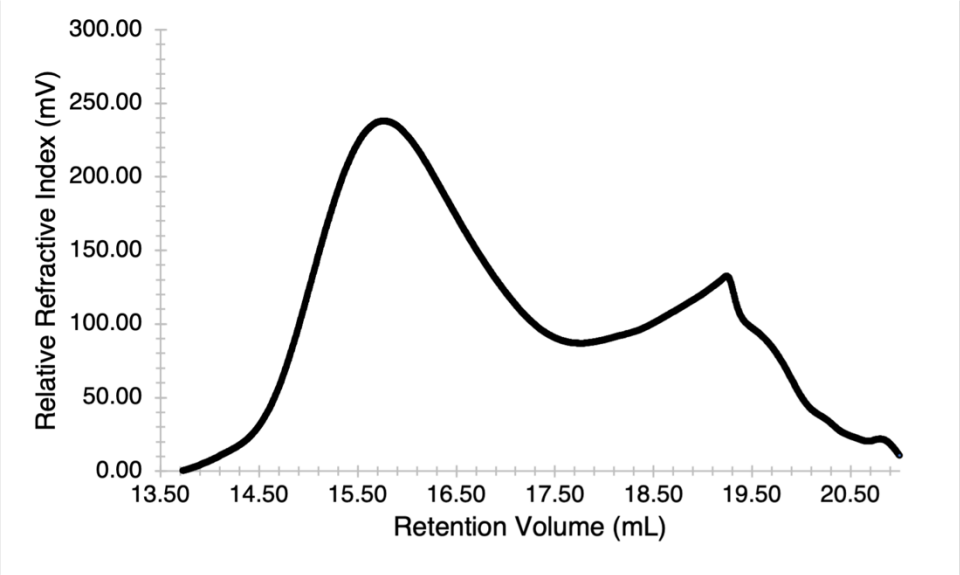


**Figure 2.14:** GPC trace of purified **2.3a** obtained by the "one-pot" dehydropolymerization of **2.1a** using IPr as the base. The sharp peak at *ca*. 19 mL may be due the preponderance of a discrete oligomer.

**Regeneration of free carbene, IPr, from [IPr-H][NTf$_2$]**

To a stirring THF solution of [IPr–H][NTf$_2$] (100 mg, 0.15 mmol) in a 20 mL vial was added *t*BuOK (17 mg, 0.15 mmol) at 20 °C. The resulting solution was then left to stir for 30 min at 20 °C, after which volatiles were removed *in vacuo*. The product of the reaction, IPr, was extracted with toluene and filtered through a 0.45 μm syringe filter. Subsequent removal of volatiles gave a white solid in 89% yield (49 mg, 0.13 mmol). Analysis of the product by $^1$H NMR revealed the free carbene, IPr, as the sole the product.[45]

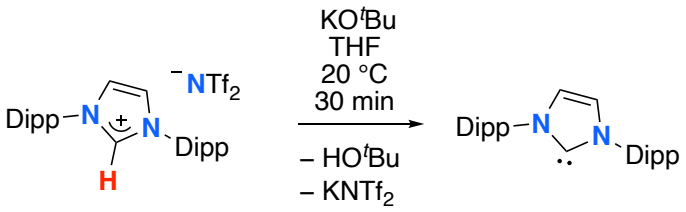


**Scheme 2.5:** Deprotonation of Imidazolium salt, [IPr–H][$NTf_2$] using KO*t*Bu as the base, regenerating free carbene.

**End Group Analysis of 2.3a, 2.3b, and 2.3c:**

End group analysis was determined using ESI-MS.

**2.3a from deprotonation of 2.2a with *i*Pr$_2$EtN:**

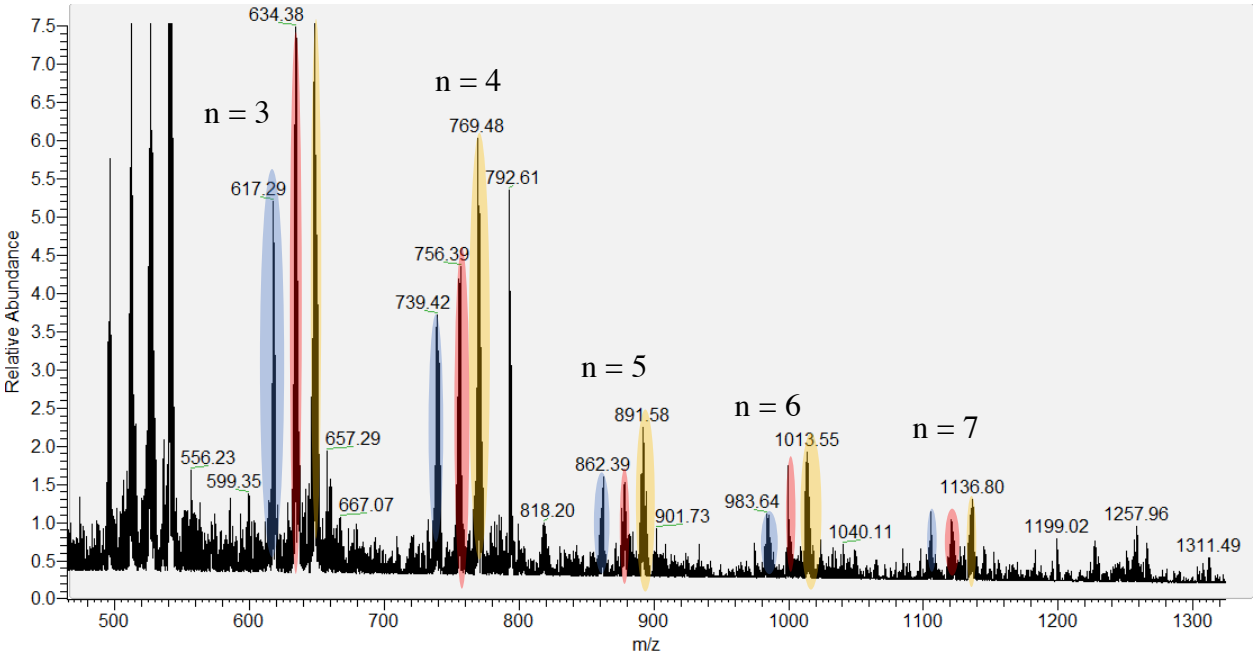


**Figure 2.15:** ESI(+)-MS spectrum (DCM/MeCN) of **2.3a** obtained using *i*Pr$_2$EtN as the base. The peaks highlighted in blue are those of linear [PhHP–BH$_2$]$_n$ chains (n = 2 to 7) with *i*Pr$_2$EtN end groups. Highlighted in red and yellow are linear chains with unknown end groups with a m/z of 147 and 160, respectively.

**2.3a from deprotonation of 2.2a with IPr:**

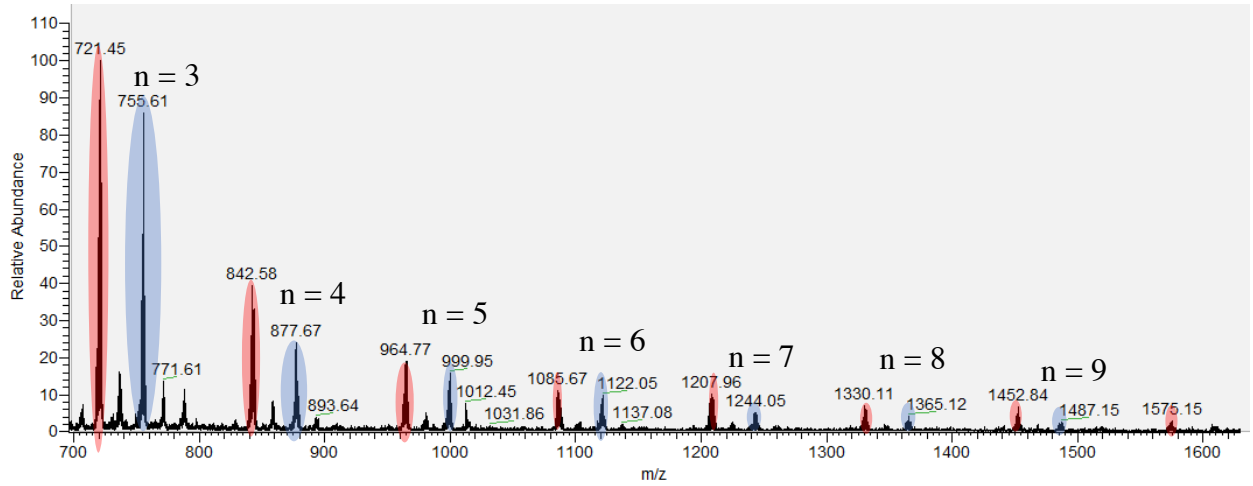


**Figure 2.16:** ESI(+)-MS spectrum (DCM/MeCN) of **2.3a** obtained using IPr as the base. The peaks highlighted in blue are those of linear $[PhHP–BH_2]_n$ chains (n = 2 to 9) with IPr end groups. Highlighted in red are linear chains with $PhPH_2$ end groups (n = 5 to 11).

**2.3b from deprotonation of 2.2b with IPr:**

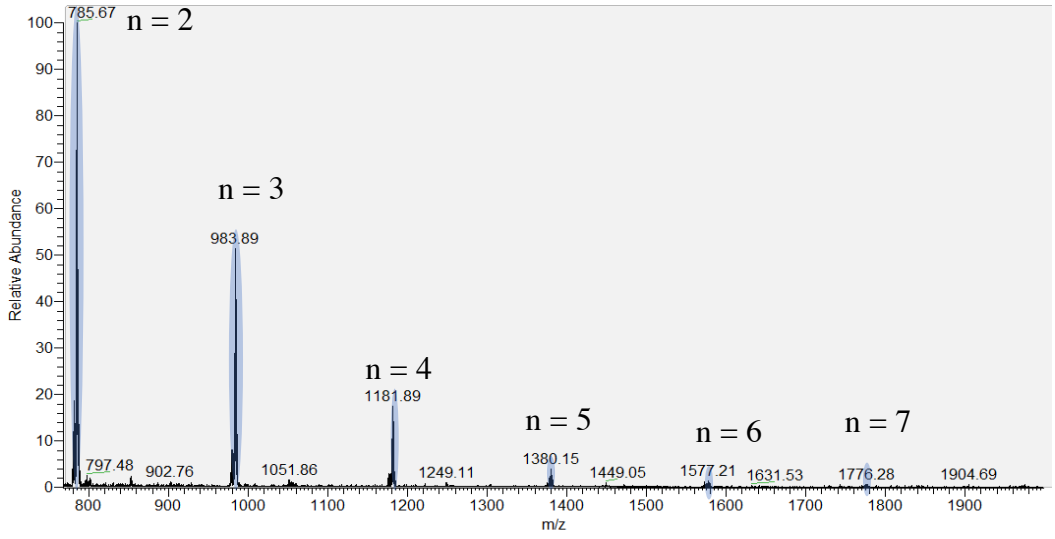


**Figure 2.17**: ESI(+)-MS spectra (DCM/MeCN) of **2.3b** obtained using IPr to deprotonate 2.3b. Peaks corresponding to oligomer with IPr terminal groups highlighted in blue (n = 2 to 7).

**2.3c from deprotonation of 2.2c with IPr:**

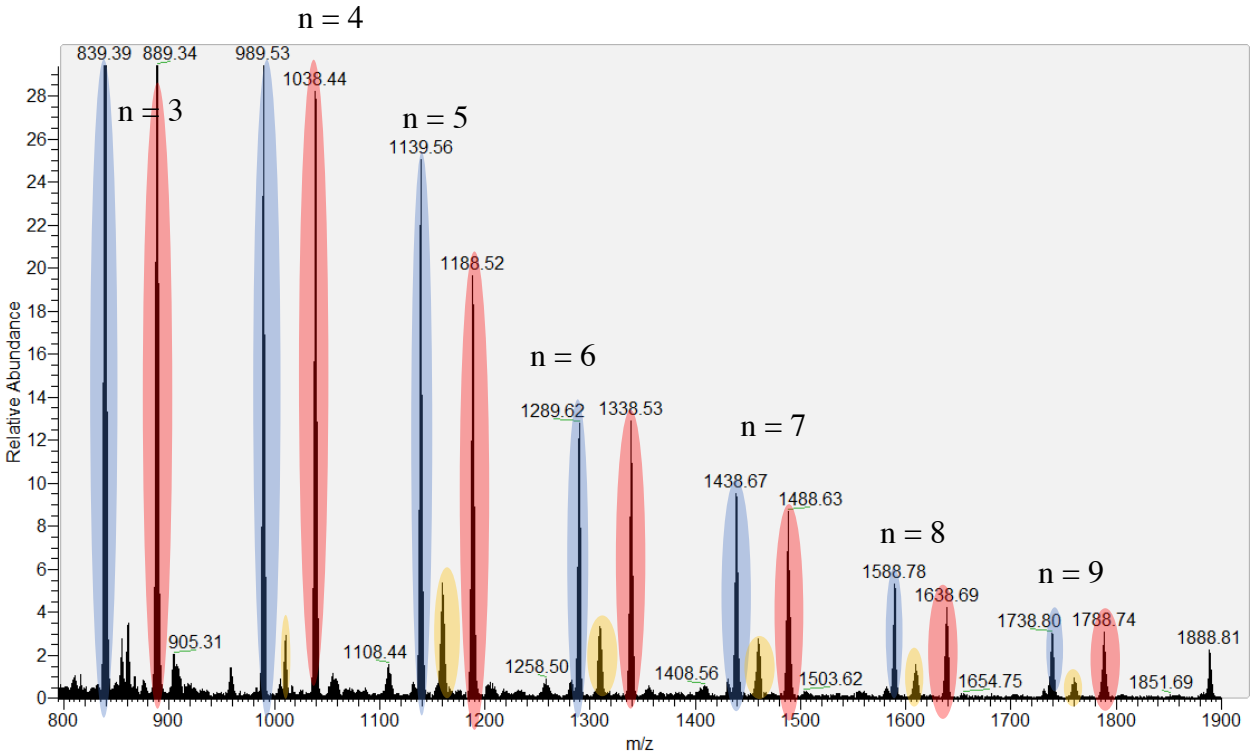


**Figure 2.18:** ESI(+)-MS spectra (DCM/MeCN) of **2.3c** obtained using IPr to deprotonate **2.3c**. Peaks corresponding to oligomeric chains terminated with IPr groups (blue, n = 3 to 9) and PhEtPH groups (red, n = 5 to 11) and unknown end groups (yellow) are highlighted.

**Deprotonation of 2.2d with excess IPr to yield 2.5**

***t*Bu$_2$PBH$_2$(IPr), 2.5:**

Separate solutions of **2.2d** (439 mg, 1.0 mmol) and IPr (776 mg, 2.0 mmol) were prepared in toluene in 4-dram vials, with the vial containing the IPr solution being charged with a stirbar. Then, to the rapidly stirring carbene solution, the solution of **2.2d** was added dropwise resulting in an immediate precipitation of [IPr–H][NTf$_2$]. The reaction is left to stir for 30 minutes longer, after which it is filtered using a 0.45 μm syringe filter and volatiles are removed *in vacuo* which yielded the carbene-phosphinoborane adduct as an off-white crystalline solid (523 mg, 96% yield). Single crystals of *t*Bu$_2$PBH$_2$(IPr) were grown by slow diffusion of hexanes into a toluene solution of **2.2d** at –40 °C with the ORTEP diagram shown in Figure 2.2

$^1$H NMR (C$_6$D$_6$, 500 MHz, 298 K) δ: 7.23 (t, 2 H, Dipp-H$_{para}$, $^3J_{HH}$ = 7.6 Hz, Dipp = 2,6-diisopropylphenyl), 7.12 (d, 4 H, Dipp-H$_{meta}$, $^3J_{HH}$ = 7.7 Hz), 6.44 (s, 2 H, NC**H**C**H**N), 2.86 (sept, 4 H, C**H**(CH$_2$), $^3J_{HH}$ = 7.3 Hz), 1.50 (d, 12 H, CH(C**H$_3$**)$_2$, $^3J_{HH}$ = 7.3 Hz), 1.19 (d, 18 H, C(C**H$_3$**)$_3$, $^3J_{HP}$ = 9.9 Hz) ppm. *Note, B**H$_2$** resonance not observed, however coupling to two hydrogen atoms is clearly observed in $^{11}$B spectrum.*

$^{11}$B NMR (C$_6$D$_6$, 160 MHz, 298 K) δ: −29.7 ppm (t, $^1J_{BH}$ = 84.9 Hz)

$^{13}$C{$^1$H} NMR (C$_6$D$_6$, 126 MHz, 298 K) δ: 146.1 (s, Dipp-**C$_{ortho}$**), 134.9 (s, Dipp-**C$_{ipso}$**), 130.3 ppm (s, Dipp-**C$_{meta}$**), 124.2 (s, Dipp-**C$_{para}$**), 122.6 (s, N**C**H$_2$**C**H$_2$N), 31.9 (d; C(**C**H$_3$)$_3$, $^2J_{CP}$

= 13.9 Hz), 30.2 (d, **C**$(CH_3)_3$, $^1J_{CP}$ = 23.9 Hz), 29.2 ppm (s, **C**H$(CH_3)_2$), 26.2 (s, CH(**C**$H_3)_2$), 22.54 (s, CH(**C**$H_3)_2$), 22.52 (s, CH(**C**$H_3)_2$) ppm. *Note, carbene carbon of IPr is not observed, likely due to coupling to nearby $^{11}B$ and $^{31}P$ nuclei.*

$^{31}$P NMR ($C_6D_6$, 202 MHz, 298 K) δ: 4.89 ppm (br).

ESI-MS (+ve mode): Calculated for $C_{35}H_{56}BN_2P^+$, [M – H]: 546.43 m/z, found: 546.48 m/z.

## X-Ray Diffraction Data

X-ray data for **2.2d** and **2.5** were carried out on a Bruker Apex II diffractometer using MoKα radiation (λ = 0.71073) Å at 100 K. The data collections were performed using a CCD area detector from a single crystal mounted on a glass fibre. Intensities were integrated[49] and absorption corrections based on equivalent reflections using SADABS[50] were applied. The structures were solved by the dual-space algorithm SHELXT[51] and refined against all $F^2$ in ShelXL[52] using Olex2.[53] All the non-hydrogen atoms were refined anisotropically. Hydrogen atoms bound to P1 and B1 in **2.2d** and B1 in **2.5** were located directly from the electron density map, while all other hydrogen atoms were calculated geometrically and refined using a riding model. Hydrogen atom positions were calculated geometrically and refined using the riding model. Most hydrogen atom positions were calculated geometrically and refined using the riding model, but some hydrogen atoms were refined freely.

**Table 2.1:** Selected crystallographic data for **2.2d** and **2.5.**

| **Identification** | **2.2d** | **2.5** |
|---|---|---|
| **chemical formula** | $C_{10}H_{21}BF_6NO_4PS_2$ | $C_{35}H_{56}BN_2P$, $C_7H_8$ |
| **crystal colour** | Colourless | Colourless |
| ***Fw*; *F*(000)** | 439.18; 904 | 638.73; 1400 |
| ***T* (K)** | 100(2) | 100(2) |
| **wavelength (Å)** | 0.71073 | 0.71073 |
| **space group** | $P2_12_12_1$ | $P2_1/n$ |
| ***a* (Å)** | 9.9439(3) | 19.5015(6) |
| ***b* (Å)** | 12.3958(3) | 10.1767(3) |
| ***c* (Å)** | 15.4671(4) | 21.5050(7) |
| **α (deg)** | 90 | 90 |
| **β (deg)** | 90 | 111.190(2) |
| **γ (deg)** | 90 | 90 |
| ***Z*** | 4 | 4 |
| ***V* (Å$^3$)** | 1906.52(9) | 3979.3(2) |
| **$\varrho_{calcd}$ (g·cm$^{-3}$)** | 1.530 | 1.066 |
| **μ (mm$^{-1}$)** | 0.434 | 0.098 |
| **θ range (deg); completeness** | 2.105 − 30.537; 1.000 | 1.210 − 30.645; 0.999 |
| **collected reflections; $R_\sigma$** | 22733; 0.0237 | 75893; 0.0325 |
| **unique reflections; $R_{int}$** | 22733; 0.0252 | 75893; 0.0436 |
| **R1[a]; wR2[b] [I > 2σ(I)]** | 0.0234; 0.0560 | 0.0467; 0.1162 |
| **R1; wR2 [all data]** | 0.0258; 0.0571 | 0.0669; 0.1283 |
| **GOF** | 1.034 | 1.020 |
| **largest diff peak and hole** | 0.278 and -0.226 | 0.693 and -0.321 |

**[a] $R_1=\Sigma(||F_o|-|F_c||)/\Sigma|F_o|$**

**[b] $wR_2=\{\Sigma[w(F_o^2-F_c^2)^2]/\Sigma[w(F_o^2)^2]\}^{½}$**

## 2.6 References


(1) Manners, I. Polymer Science with Transition Metals and Main Group Elements: Towards Functional, Supramolecular Inorganic Polymeric Materials. *Journal of Polymer Science Part A: Polymer Chemistry* **2002**, *40* (2), 179–191. https://doi.org/10.1002/pola.10069.

(2) Allcock, H. R. Recent Developments in Polyphosphazene Materials Science. *Current Opinion in Solid State and Materials Science* **2006**, *10* (5), 231–240. https://doi.org/10.1016/j.cossms.2007.06.001.

(3) Baumgartner, T.; Réau, R. Organophosphorus π-Conjugated Materials. *Chemical Reviews* **2006**, *106* (11), 4681–4727. https://doi.org/10.1021/cr040179m.

(4) M. Priegert, A.; W. Rawe, B.; C. Serin, S.; P. Gates, D. Polymers and the P-Block Elements. *Chemical Society Reviews* **2016**, *45* (4), 922–953. https://doi.org/10.1039/C5CS00725A.

(5) Rothemund, S.; Teasdale, I. Preparation of Polyphosphazenes: A Tutorial Review. *Chemical Society Reviews* **2016**, *45* (19), 5200–5215. https://doi.org/10.1039/c6cs00340k.

(6) Dück, K.; Gates, D. P. Main-Chain, Phosphorus-Based Polymers. In *Main Group Strategies towards Functional Hybrid Materials*; John Wiley & Sons, Ltd, 2018; pp 329–355. https://doi.org/10.1002/9781119235941.ch13.

(7) Ayhan, O.; Riensch, N. A.; Glasmacher, C.; Helten, H. Cyclolinear Oligo- and Poly(Iminoborane)s: The Missing Link in Inorganic Main-Group Macromolecular Chemistry. *Chemistry – A European Journal* **2018**, *24* (22), 5883–5894. https://doi.org/10.1002/chem.201705913.

(8) Vidal, F.; Jäkle, F. Functional Polymeric Materials Based on Main-Group Elements. *Angewandte Chemie International Edition* **2019**, *58* (18), 5846–5870. https://doi.org/10.1002/anie.201810611.

(9) Arz, M. I.; Annibale, V. T.; Kelly, N. L.; Hanna, J. V.; Manners, I. Ring-Opening Polymerization of Cyclic Phosphonates: Access to Inorganic Polymers with a P(V)–

O Main Chain. *Journal of the American Chemical Society* **2019**, *141* (7), 2894–2899. https://doi.org/10.1021/jacs.8b13435.

(10) Colebatch, A. L.; Weller, A. S. Amine-Borane Dehydropolymerization: Challenges and Opportunities. *Chemistry – A European Journal* **2019**, *25* (6), 1379–1390. https://doi.org/10.1002/chem.201804592.

(11) Allcock, H. R.; Chen, C. Polyphosphazenes: Phosphorus in Inorganic–Organic Polymers. *Journal of Organic Chemistry* **2020**, *85* (22), 14286–14297. https://doi.org/10.1021/acs.joc.0c01710.

(12) Devillard, M.; Pinheiro, C. A. D. A.; Caytan, E.; Roiland, C.; Dinoi, C.; Rosal, I. D.; Alcaraz, G. Uncatalyzed Formation of Polyaminoboranes from Diisopropylaminoborane and Primary Amines: A Kinetically Controlled Polymerization Reaction. *Advanced Synthesis & Catalysis* **2021**, *363* (9), 2417–2426. https://doi.org/10.1002/adsc.202001458.

(13) Burg, A. B.; Wagner, R. I. Chemistry of P–B Bonding — the Phosphinoborines and Their Polymers. *Journal of the American Chemical Society* **1953**, *75* (16), 3872–3877. https://doi.org/10.1021/ja01112a002.

(14) Burg, A. B. Phosphinoborine Polymer Rings and Chains from Tetramethylbiphosphine. *Journal of Inorganic and Nuclear Chemistry* **1959**, *11*, 258. https://doi.org/10.1016/0022-1902(59)80257-8.

(15) Wagner, R. I.; Caserio, F. F., Jr. Linear Phosphinoborine Polymers. *Journal of Inorganic and Nuclear Chemistry* **1959** *11*, 259. https://doi.org/10.1016/0022-1902(59)80258-X.

(16) Clark, T. J.; Rodezno, J. M.; Clendenning, S. B.; Aouba, S.; Brodersen, P. M.; Lough, A. J.; Ruda, H. E.; Manners, I. Rhodium-Catalyzed Dehydrocoupling of Fluorinated Phosphine–Borane Adducts: Synthesis, Characterization, and Properties of Cyclic and Polymeric Phosphinoboranes with Electron-Withdrawing Substituents at Phosphorus. *Chemistry – A European Journal* **2005**, *11* (15), 4526–4534. https://doi.org/10.1002/chem.200401296.

(17) Priegert, A. M.; Siu, P. W.; Hu, T. Q.; Gates, D. P. Flammability Properties of Paper Coated with Poly (Methylenephosphine), an Organophosphorus Polymer. *Fire and Materials* **2015**, *39* (7), 647–657. https://doi.org/10.1002/fam.2264.

(18) Knights, A. W.; Chitnis, S. S.; Manners, I. Photolytic, Radical-Mediated Hydrophosphination: A Convenient Post-Polymerisation Modification Route to P-Di(Organosubstituted) Polyphosphinoboranes $[RR'PBH_2]_n$. *Chemical Science* **2019**, *10*, 7281–7289. https://doi.org/10.1039/C9SC01428D.

(19) Knights, A. W.; Nascimento, M. A.; Manners, I. An Investigation of Polyphosphinoboranes as Flame-Retardant Materials. *Polymer* **2022**, *247*, 124795. https://doi.org/10.1016/j.polymer.2022.124795.

(20) Dorn, H.; Singh, R. A.; Massey, J. A.; Lough, A. J.; Manners, I. Rhodium-Catalyzed Formation of Phosphorus–Boron Bonds: Synthesis of the First High Molecular Weight Poly(Phosphinoborane). *Angewandte Chemie International Edition* **1999**, *38* (22), 3321–3323. https://doi.org/10.1002/(SICI)1521-3773(19991115)38:22<3321::AID-ANIE3321>3.0.CO;2-0.

(21) Pandey, S.; Lönnecke, P.; Hey-Hawkins, E. Phosphorus-Boron-Based Polymers Obtained by Dehydrocoupling of Ferrocenylphosphine- Borane Adducts. *European*

*Journal of Inorganic Chemistry* **2014**, *2014* (14), 2456–2465. https://doi.org/10.1002/ejic.201402021.

(22) Cavaye, H.; Clegg, F.; Gould, P. J.; Ladyman, M. K.; Temple, T.; Dossi, E. Primary Alkylphosphine–Borane Polymers: Synthesis, Low Glass Transition Temperature, and a Predictive Capability Thereof. *Macromolecules* **2017**, *50* (23), 9239–9248. https://doi.org/10.1021/acs.macromol.7b02030.

(23) Schäfer, A.; Jurca, T.; Turner, J.; Vance, J. R.; Lee, K.; Du, V. A.; Haddow, M. F.; Whittell, G. R.; Manners, I. Iron-Catalyzed Dehydropolymerization: A Convenient Route to Poly(Phosphinoboranes) with Molecular-Weight Control. *Angewandte Chemie International Edition* **2015**, *54* (16), 4836–4841. https://doi.org/10.1002/anie.201411957.

(24) Paul, U. S. D.; Braunschweig, H.; Radius, U. Iridium-Catalysed Dehydrocoupling of Aryl Phosphine-Borane Adducts: Synthesis and Characterisation of High Molecular Weight Poly(Phosphinoboranes). *Chemical Communications* **2016**, *52* (55), 8573–8576. https://doi.org/10.1039/c6cc04363a.

(25) Hooper, T. N.; Weller, A. S.; Beattie, N. A.; Macgregor, S. A. Dehydrocoupling of Phosphine-Boranes Using the [RhCp*Me($PMe_3$)($CH_2Cl2$)][$BAr^F{}_4$] Precatalyst: Stoichiometric and Catalytic Studies. *Chemical Science* **2016**, *7* (3), 2414–2426. https://doi.org/10.1039/c5sc04150c.

(26) Coles, N. T.; Mahon, M. F.; Webster, R. L. Phosphine- and Amine-Borane Dehydrocoupling Using a Three-Coordinate Iron(II) b-Diketiminate Precatalyst. *Organometallics* **2017**, *36* (11), 2262–2268. https://doi.org/10.1021/acs.organomet.7b00326.

(27) Han, D.; Anke, F.; Trose, M.; Beweries, T. Recent Advances in Transition Metal Catalysed Dehydropolymerisation of Amine Boranes and Phosphine Boranes. *Coordination Chemistry Reviews* **2019**, *380*, 260–286. https://doi.org/10.1016/j.ccr.2018.09.016.

(28) Schön, F.; Sigmund, L. M.; Schneider, F.; Hartmann, D.; Wiebe, M. A.; Manners, I.; Greb, L. Calix[4]Pyrrolato Aluminate Catalyzes the Dehydrocoupling of Phenylphosphine Borane to High Molar Weight Polymers. *Angewandte Chemie International Edition* **2022**, *61* (22), e202202176. https://doi.org/10.1002/anie.202202176.

(29) Denis, J.-M.; Forintos, H.; Szelke, H.; Toupet, L.; Pham, T.-N.; Madec, P.-J.; Gaumont, A.-C. $B(C_6F_5)_3$-Catalyzed Formation of B–P Bonds by Dehydrocoupling of Phosphine–Boranes. *Chemical Communications* **2003**, No. 1, 54–55. https://doi.org/10.1039/B206559B.

(30) Marquardt, C.; Jurca, T.; Schwan, K.-C.; Stauber, A.; Virovets, A. V.; Whittell, G. R.; Manners, I.; Scheer, M. Metal-Free Addition/Head-to-Tail Polymerization of Transient Phosphinoboranes, $RPH\text{-}BH_2$: A Route to Poly(Alkylphosphinoboranes). *Angewandte Chemie International Edition* **2015**, *54* (46), 13782–13786. https://doi.org/10.1002/anie.201507084.

(31) Oldroyd, N. L.; Chitnis, S. S.; Annibale, V. T.; Arz, M. I.; Sparkes, H. A.; Manners, I. Metal-Free Dehydropolymerisation of Phosphine-Boranes Using Cyclic (Alkyl)(Amino)Carbenes as Hydrogen Acceptors. *Nature Communications* **2019**, *10* (1), 1–9. https://doi.org/10.1038/s41467-019-08967-8.

(32) Stephens, F. H.; Baker, R. T.; Matus, M. H.; Grant, D. J.; Dixon, D. A. Acid Initiation of Ammonia–Borane Dehydrogenation for Hydrogen Storage. *Angewandte Chemie International Edition* **2007**, *46* (5), 746–749. https://doi.org/10.1002/anie.200603285.

(33) Metters, O. J.; Chapman, A. M.; Robertson, A. P. M.; Woodall, C. H.; Gates, P. J.; Wass, D. F.; Manners, I. Generation of Aminoborane Monomers RR′NBH2 from Amine–Boronium Cations $[RR'NH–BH_2L]^+$: Metal Catalyst-Free Formation of Polyaminoboranes at Ambient Temperature. *Chemical Communications.* **2014**, *50* (81), 12146–12149. https://doi.org/10.1039/C4CC05145A.

(34) Aldridge, S.; Downs, A. J.; Tang, C. Y.; Parsons, S.; Clarke, M. C.; Johnstone, R. D. L.; Robertson, H. E.; Rankin, D. W. H.; Wann, D. A. Structures and Aggregation of the Methylamine−Borane Molecules, $Me_nH_{3-n}N·BH3$ (n = 1−3), Studied by X-Ray Diffraction, Gas-Phase Electron Diffraction, and Quantum Chemical Calculations. *Journal of the American Chemical Society* **2009**, *131* (6), 2231–2243. https://doi.org/10.1021/ja807545p.

(35) Dorn, H.; Singh, R. A.; Massey, J. A.; Nelson, J. M.; Jaska, C. A.; Lough, A. J.; Manners, I. Transition Metal-Catalyzed Formation of Phosphorus−Boron Bonds: A New Route to Phosphinoborane Rings, Chains, and Macromolecules. *Journal of the American Chemical Society* **2000**, *122* (28), 6669–6678. https://doi.org/10.1021/ja000732r.

(36) Timperman, L.; Béguin, F.; Frackowiak, E.; Anouti, M. Comparative Study of Two Protic Ionic Liquids as Electrolyte for Electrical Double-Layer Capacitors. *Journal of*

*the Electrochemical Society.* **2013**, *161* (3), A228. https://doi.org/10.1149/2.016403jes.

(37) Johnson, H. C.; Robertson, A. P. M.; Chaplin, A. B.; Sewell, L. J.; Thompson, A. L.; Haddow, M. F.; Manners, I.; Weller, A. S. Catching the First Oligomerization Event in the Catalytic Formation of Polyaminoboranes: $H_3B{\bullet}NMeHBH_2{\bullet}NMeH_2$ Bound to Iridium. *Journal of the American Chemical Society* **2011**, *133* (29), 11076–11079. https://doi.org/10.1021/ja2040738.

(38) Brodie, C. N.; Boyd, T. M.; Sotorríos, L.; Ryan, D. E.; Magee, E.; Huband, S.; Town, J. S.; Lloyd-Jones, G. C.; Haddleton, D. M.; Macgregor, S. A.; Weller, A. S. Controlled Synthesis of Well-Defined Polyaminoboranes on Scale Using a Robust and Efficient Catalyst. *Journal of the American Chemical Society* **2021**, *143* (49), 21010–21023. https://doi.org/10.1021/jacs.1c10888.

(39) Adolf, A.; Vogel, U.; Zabel, M.; Timoshkin, A. Y.; Scheer, M. N-Heterocyclic Carbenes in Lewis Acid/Base Stabilised Phosphanylboranes. *European Journal of Inorganic Chemistry* **2008**, No. 22, 3482–3492. https://doi.org/10.1002/ejic.200800305.

(40) Pomogaeva, A. V.; Scheer, M.; Timoshkin, A. Y. Why Do B-P and Al-P Polymers Differ? Structures, Stability, and Electronic Properties of Chain and Ring $[H_2PEH_2]_{(n)}$ Oligomers (E=B, Al; N=1-15). *Chemistry – A European Journal* **2018**, *24* (64), 17046–17054. https://doi.org/10.1002/chem.201803008.

(41) Pomogaeva, A. V.; Timoshkin, A. Y. Stability and Electronic Structure of Donor–Acceptor Stabilized Group 13/15 Oligomers. *The Journal of Physical Chemistry A* **2021**, *125* (16), 3415–3424. https://doi.org/10.1021/acs.jpca.1c02258.

(42) Back, O.; Henry-Ellinger, M.; Martin, C. D.; Martin, D.; Bertrand, G. $^{31}$P NMR Chemical Shifts of Carbene–Phosphinidene Adducts as an Indicator of the π-Accepting Properties of Carbenes. *Angewandte Chemie International Edition* **2013**, *52* (10), 2939–2943. https://doi.org/10.1002/anie.201209109.

(43) Marquardt, C.; Hegen, O.; Vogel, A.; Stauber, A.; Bodensteiner, M.; Timoshkin, A. Y.; Scheer, M. Depolymerization of Poly(Phosphinoboranes): From Polymers to Lewis Base Stabilized Monomers. *Chemistry – A European Journal* **2018**, *24* (2), 360–363. https://doi.org/10.1002/chem.201705510.

(44) Pangborn, A. B.; Giardello, M. A.; Grubbs, R. H.; Rosen, R. K.; Timmers, F. J. Safe and Convenient Procedure for Solvent Purification. *Organometallics* **1996**, *15* (5), 1518–1520. https://doi.org/10.1021/om9503712.

(45) Bantreil, X.; Nolan, S. P. Synthesis of N -Heterocyclic Carbene Ligands and Derived Ruthenium Olefin Metathesis Catalysts. *Nature Protocols* **2011**, *6* (1), 69–77. https://doi.org/10.1038/nprot.2010.177.

(46) Turner, J. R.; Resendiz-Lara, D. A.; Jurca, T.; Schäfer, A.; Vance, J. R.; Beckett, L.; Whittell, G. R.; Musgrave, R. A.; Sparkes, H. A.; Manners, I. Synthesis, Characterization, and Properties of Poly(Aryl)Phosphinoboranes Formed *via* Iron-Catalyzed Dehydropolymerization. *Macromolecular Chemistry and Physics* **2017**, *218* (19), 1700120. https://doi.org/10.1002/macp.201700120.

(47) Resendiz-Lara, D. A.; Annibale, V. T.; Knights, A. W.; Chitnis, S. S.; Manners, I. High Molar Mass Poly(Alkylphosphinoboranes) *via* Iron-Catalyzed Dehydropolymerization. *Macromolecules* **2021**, *54* (1), 71–82. https://doi.org/10.1021/acs.macromol.0c02082.

(48) Lebel, H.; Morin, S.; Paquet, V. Alkylation of Phosphine Boranes by Phase-Transfer Catalysis. *Organic Letters* **2003**, *5* (13), 2347–2349. https://doi.org/10.1021/ol0347139.

(49) Bruker, SAINT+ v8.38A Integration Engine, Data Reduction Software, Bruker Analytical X-Ray Instruments Inc., Madison, WI, USA, 2015.

(50) Bruker, SADABS 2014/5, Bruker AXS Area Detector Scaling and Absorption Correction, Bruker Analytical X-Ray Instruments Inc., Madison, Wisconsin, USA, 2014/5.

(51) Sheldrick, G. M. SHELXT - Integrated Space-Group and Crystal-Structure Determination. *Acta Crystallographica Section A: Foundations of Crystallography* **2015**, *71* (1), 3–8. https://doi.org/10.1107/S2053273314026370.

(52) Sheldrick, G. M. Crystal Structure Refinement with SHELXL. *Acta Crystallographica Section C: Structural Chemistry* **2015**, *71* (Md), 3–8. https://doi.org/10.1107/S2053229614024218.

(53) Dolomanov, O. V.; Bourhis, L. J.; Gildea, R. J.; Howard, J. A. K.; Puschmann, H. OLEX2: A Complete Structure Solution, Refinement and Analysis Program. *Journal of Applied Crystallography* **2009**, *42* (2), 339–341. https://doi.org/10.1107/S0021889808042726.

**Chapter 3**

# Synthesis and Reactivity of Transient Primary Aminoboranes

*This chapter has been adapted from the as of yet unpublished work:*

Matthew A. Wiebe, Owen J. Metters, Duncan Wass, Erin. M. Leitao, and Ian Manners. *Manuscript in preparation.*

*Contributions: M. A. W., O. M., D. W. and I. M. conceived the project. O. M. performed exploratory reactions and obtained single crystals of **3.4**. M. A. W. performed all other synthesis and characterization. M. A. W. interpreted the data and wrote the first draft manuscript which was subsequently edited with I. M., E. M. L., and the other authors.*

## 3.1 Abstract

The transient nature of primary aminoboranes, $RNH–BH_2$, has precluded their detailed study. These difficult-to-handle species are often accessed as intermediates *via* thermally, catalytically, or chemically induced dehydrogenation of their amine-borane adduct precursors, or by a substitution reaction between diisopropylaminoborane, $iPr_2N–BH_2$, and the requisite primary amine, $RNH_2$. Transient aminoboranes can also be accessed *via* HX elimination from corresponding amine-borane adducts, ($RR'NH•BH_2X$; X = halide or pseudohalide, R and R' = alkyl substituent or H). Primary aminoboranes have only been observed as part of a mixture of products in solution by NMR spectroscopy, or in solid Ar matrices by IR spectroscopy at 14 K. Herein we describe the synthesis of primary aminoboranes *in situ* by deprotonation of $RNH_2•BH_2(NTf_2)$ (R = *t*Bu, Me, and $CPh_3$) and their observation by low temperature NMR spectroscopy. We then trap transient aminoboranes using an N-heterocyclic carbene to unequivocally prove that they are accessed *in situ*. Subsequently, we exemplify the ability to stoichiometrically deliver aminoborane to a metal substrate, rather than relying on on-metal dehydrogenation, by accessing a ruthenium complex of $tBuNH=BH_2$. Lastly, we explore the reactivity of $tBuNH=BH_2$ in detail, first showing its reactivity with itself as it warms to ambient temperature to participate in versatile chemistry producing several products with N–B linkages.

## 3.2 Introduction

Polyaminoboranes are isoelectronic to polyolefins, featuring a main chain with alternating quaternary nitrogen and boron atoms.[1–6] However, in contrast to polyolefins, polyaminoboranes have a polarized repeat monomer unit, resulting in remarkably different properties in both the bulk materials and the polymer precursors. Particularly, polyaminoboranes have been sought as piezoelectric materials,[7] processable precursors to BN ceramics,[8] recyclable polymers,[9] and as polymers of fundamental interest as a relatively new class of inorganic materials. However, in contrast to polyolefin precursor olefins ($RCH{=}CH_2$), whose reactivity is well known, there is no existing method to perform analogous studies on the reactivity of transient aminoboranes ($RNH{=}BH_2$), as they are known to readily catenate and undergo other reactions without significant kinetic hindrance.[10–12]

Generating reactive aminoboranes ($RNH{=}BH_2$) normally involves thermal or catalytic dehydrogenation of their precursor amine-borane adducts (**Scheme 3.1**).[3] However, alternative strategies for the generation of aminoboranes that readily catenate *in situ* have been of recent interest. For example, Alcaraz *et al*. have reported on the generation of aminoboranes through the reaction of diisopropylaminoborane ($i\text{Pr}_2\text{N}{=}BH_2$) with primary amines ($RNH_2$), generating diisopropylamine as a side-product.[13,14] Alternatively, initial reaction of amine-borane adducts, $RR'NH{\bullet}BH_3$, with an acid results in a net hydrogen loss and formation of a functionalized amine-borane adduct that can be deprotonated to generate reactive aminoboranes in solution.[15,16] However, these studies have focussed on accessing amine-borane dehydrogenation products (i.e. polymers, cyclic oligomers) or on acid-induced dehydrogenation of ammonia-borane for hydrogen

storage applications. Notably, in 2014, we were able to observe $MeNH{=}BH_2$ *in situ* by $^{11}B$ NMR spectroscopy at –10 °C, although only as a small fraction of the products in solution.[15] To date, the only studies that have explicitly targeted the characterization of transient aminoboranes have been by Carpenter and Ault where thermally generated $MeNH{=}BH_2$ was trapped in solid argon matrices (–260 °C) and characterized by IR spectroscopy.[17]

There are some studies on the reactivity of a primary aminoborane featuring the more sterically encumbering *tert*-butyl substituent, $t$BuNH=$BH_2$. Weller *et al.* have reported an iridium complex bearing $t$BuNH=$BH_2$ coordinated *via* two hydridic hydrogen atoms bridging the boron and iridium centres accessed from the on-metal dehydrogenation of $t$BuNH$_2$•$BH_3$.[18] Further, reaction of this complex with an excess of acetonitrile resulted in the slow release of $t$BuNH=$BH_2$ which generates the corresponding borazine and amine-borane adduct evidenced by $^{11}B$ NMR spectroscopy. Other complexes of $t$BuNH=$BH_2$ have been accessed on ruthenium,[19] osmium,[20] and rhodium centres.[21] The reactivity of $t$BuNH=$BH_2$ has also been studied *via* the thermal, stoichiometric, and catalytic dehydrocoupling of $t$BuNH$_2$•$BH_3$. Thermal dehydrogenation of neat $t$BuNH$_2$•$BH_3$ at temperatures up to 200 °C resulted in the initial evolution of an equivalent of $H_2$ and formation of cyclotriborazane which then releases a second equivalent of $H_2$ to yield borazine.[22] Other routes to stoichiometrically and catalytically dehydrogenate $t$BuNH$_2$•$BH_3$ results in the formation additional reaction products including diamidoborane, borylamine-borane, and in the case of Ca-mediated dehydrocoupling, cyclic aminoborane dimer.[23–30] However, as all reports rely on the generation of $t$BuNH=$BH_2$ by using an active catalytic species, or at elevated temperatures, no reactivity

studies on primary aminoboranes in the absence of other reactive species have been performed.

In this report, we study the generation of transient aminoboranes from their corresponding amine-(triflimido)borane adducts, ($RNH_2$•$BH_2(NTf_2)$) and observe the exclusive formation of aminoboranes *in situ* at −78 °C by $^{11}B$ NMR spectroscopy ($RNH{=}BH_2$, R = *t*Bu, Me, $CPh_3$). To ensure we are actually accessing transient aminoboranes *in situ* we trapped the aminoborane using an N-heterocyclic carbene (NHC) to access an aminoborane-NHC adduct. Next, we explore the ability to stoichiometrically deliver *t*BuNH=$BH_2$ to a metal centre accessing and obtaining a molecular structure of a ruthenium complex bearing a primary aminoborane as a ligand. We then explore the reactivity of *t*BuNH=$BH_2$ in detail, showcasing its ability to participate in many different modes of reactivity in reactions with itself.

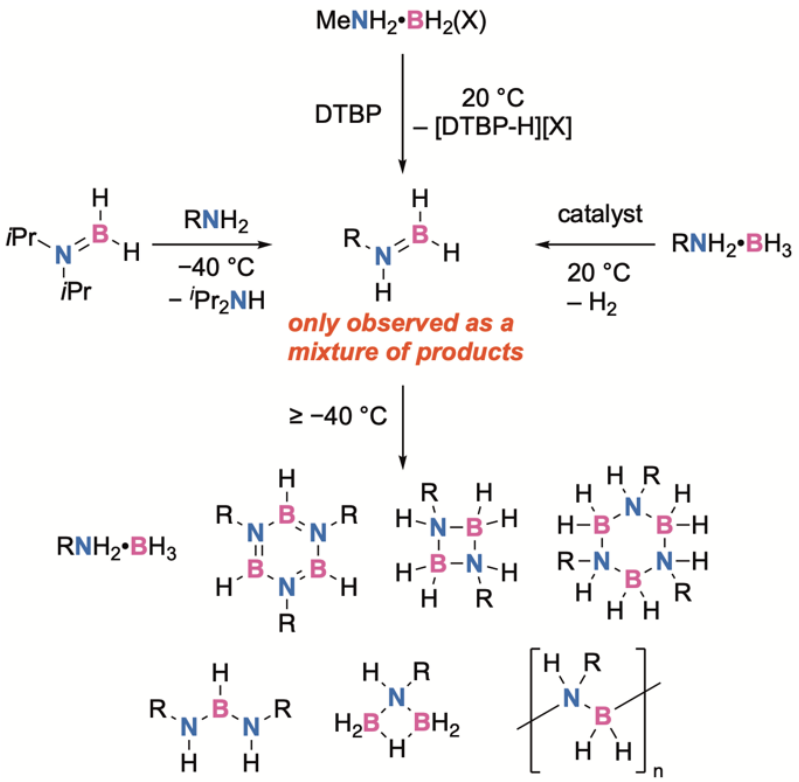


**Scheme 3.1:** Synthesis of transient primary aminoboranes, $RNH{=}BH_2$, and the different types of products observed from the generation of aminoboranes *in situ*.

## 3.3 Results and Discussion

### 3.3.1 Synthesis of Amine-(triflimido)boranes

Aminoborane precursors, amine-(triflimido)boranes (**3.2**$_{a–c}$) were prepared by the addition of triflimidic acid ($HNTf_2$) to DCM solutions of amine-borane adducts (**3.1**$_{a–c}$) at 20 °C (Figure 3.1 a). The generation of **3.1**$_{a–c}$ was inferred by the observation of $H_2$ gas evolution, which ceased within an hour. Subsequent removal of volatiles *in vacuo* yielded white powders, apart from $CPh_3NH_2{\bullet}BH_2(NTf_2)$, which was yellowish, presumably due to small amounts of trityl radical impurities.[31,32] Analysis of these products by $^{11}B$ NMR spectroscopy revealed consumption of their precursor amine-borane adducts to produce

new signals downfield, with chemical shift values in the range of −7.7 to −9.7 ppm, which indicated that the reaction had proceeded. These values are similar to the $^{11}$B NMR chemical shift values reported for amine-(chloro)boranes and amine-(triflate)boranes ($\delta(^{11}B)$ = −0.4 to −6.8 ppm).[15] Moreover, electrospray ionization mass spectrometry (ESI-MS) molecular ion peaks corresponding to $[M–H]^+$ cations were observed, which further supports the generation of these amine-(triflimido)boranes.

Single crystals of the reaction product between *t*BuNH$_2$•BH$_3$ and HNTf$_2$ were grown from the slow diffusion of hexane into a saturated DCM solution of **3.1$_c$** at −40 °C. Analysis of the colourless crystals by X-ray diffraction (XRD) revealed a molecular structure corresponding to *t*BuNH$_2$•BH$_2$(NTf$_2$), **3.1$_c$** (**Figure 3.1** b). The N1–B1 bond (1.597(1) Å) is shorter than the N2–B1 bond (1.611(1) Å), however both bonds are within the range of a N–B single bond. Further, the N1–B1–N2 bond angle is 106.9°, indicative of a tetrahedral coordination environment around boron. These parameters are similar to those in phosphine-(triflimide)boranes, where the triflimide substituent is bound to boron centre *via* the nitrogen atom (i.e., *κ*-N). Moreover, this structure is similar to the closely related adducts, MeRNH•BH$_2$(X) (X = Cl, OTf; R = H, Me), where there is coordination of

the chloride or triflate moiety to the boron centre.[15] Together, the data unequivocally supports the formation of this series of new amine-(triflimido)borane adducts.

a)

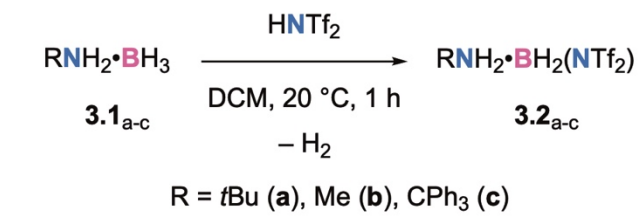


b)

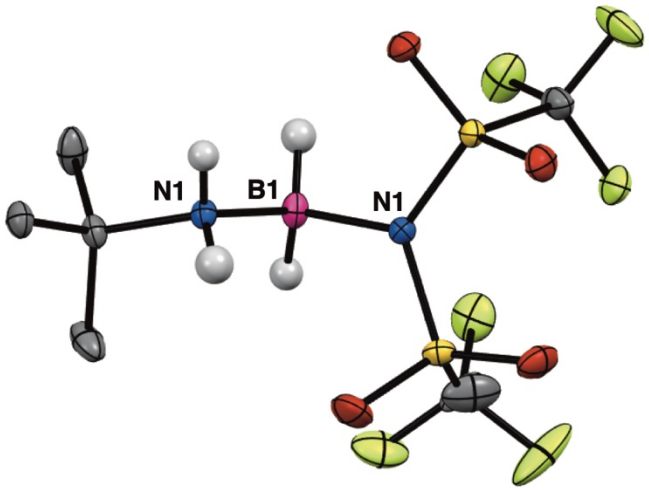


**Figure 3.1:** a) Synthesis of triflimidoboranes, **3.2$_{a–c}$** *via* the reaction between amine-borane adducts, **3.1$_{a–c}$,** and $HNTf_2$, and b) the molecular structure of *t*$BuNH_2$•$BH_2(NTf_2)$ (**3.2$_a$**) obtained from single crystal XRD. Thermal ellipsoids are shown at the 50% probability level, and B- and N-bound hydrogen atoms are arbitrarily assigned based on the obtained structure. Further, only one component of a disordered $CF_3$ fragment is shown. Colour scheme is as follows; carbon (grey), nitrogen (blue), boron (pink), sulfur (yellow), oxygen (red), fluorine (lime green).

### 3.3.2 Generation and Observation of Transient Aminoboranes

With the requisite amine-(triflimido)borane adducts accessed, generation and observation of their corresponding transient aminoboranes was then targeted. Generation of the aminoborane was achieved through the addition of *i*$Pr_2$EtN to a frozen $Et_2O$ solution of **3.1$_{a–c}$** in a J-Young NMR tube in the glovebox (**Figure 3.2** a). Afterwards the tube was sealed, removed from the glovebox, and submerged in a dry ice and acetone cooling bath (–78 °C). The cooling bath with the J–Young NMR tube containing the reaction mixture was then taken to the NMR spectrometer, in which the probe had been previously cooled to –78 °C, for analysis. The resulting $^{11}$B NMR spectra revealed the presence of the free aminoboranes as the only boron containing species in solution, **3.3$_{a–c}$**, evident by signals at 34.2 ($^1J_{BH}$ = 126 Hz), 37.4 ($^1J_{BH}$ = 120 Hz), and 34.0 (br, width at ½ height: 475 Hz) ppm for **3.3$_a$**, **3.3$_b$**, and **3.3$_c$** respectively (**Figure 3.2** b). Notably, MeNH=$BH_2$ has only been observed as a mixture of products in solution by NMR spectroscopy,[15] or in an argon matrix (–260 °C).[17] The $^{11}$B chemical shifts of these species fall within a range expected for aminoboranes, between 37.4 and 34.0 ppm. Apart from **3.2$_c$**, which shows a broad singlet, all aminoboranes are observed to be triplets with coupling constants near 120 Hz. With the ability to cleanly generate primary aminoboranes, we then aimed to explore the ability to trap and transform **3.3$_a$**.

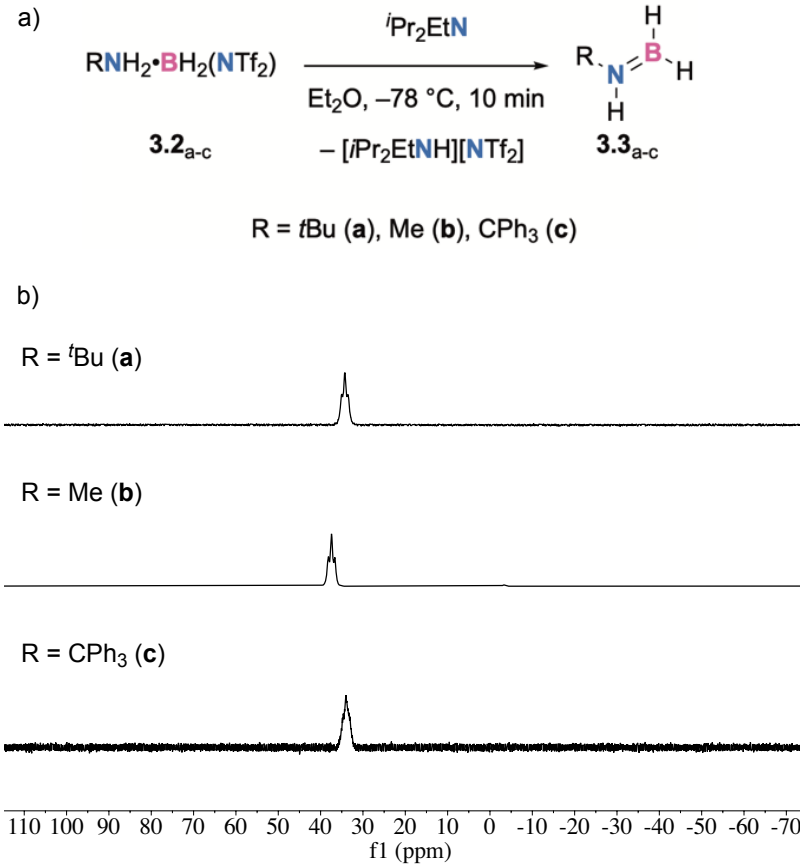


**Figure 3.2:** a) Deprotonation of adducts **3.2$_{a–c}$** using *i*Pr$_2$EtN to produce free transient aminoboranes, RNH=BH$_2$ (**3.3$_{a–c}$**), *in situ* at –78 °C and b) the $^{11}$B NMR spectra of the free aminoboranes, **3.3$_{a–c}$**, taken at –78 °C in Et$_2$O at 160 MHz.

### 3.3.3 Trapping Aminoboranes as NHC Adducts

N-heterocyclic carbene (NHC) adducts of aminoboranes have been accessed in a variety of ways.[9,33,34] Here, in order to unequivocally prove that we are accessing aminoboranes *in situ,* we aimed to first generate the aminoborane and subsequently trap it by adding NHC to the solution of aminoborane, forming the more thermally stable aminoborane-NHC adduct. This was achieved by first generating the aminoborane **3.3$_a$**

using the method described above, but then the conjugate acid by-product, [*i*Pr$_2$EtN–H][NTf$_2$], was removed by performing a distillation at –78 °C on the reaction mixture (**Figure 3.3** a). The resulting distillate was kept at or below –78 °C while an aliquot was taken, and it was verified to be a solution of **3.3$_a$** in Et$_2$O by low temperature $^{11}$B NMR spectroscopy. Subsequently, an Et$_2$O solution of *N,N*-bis(2,6-diisopropylphenyl)imidazol-2-ylidene (IPr) was added dropwise to the cooled stirring solution of **3.3$_a$** in Et$_2$O and the reaction was left to stir for 30 minutes longer. Removing volatiles from the solution yielded a colourless powder believed to be **3.4$_a$**. Single crystals were grown from this powder from Et$_2$O and hexane in 47% yield. Analysis of crystals of **3.4$_a$** by $^{11}$B NMR spectroscopy revealed a triplet at –19.7 ppm ($^1J_{BH}$ = 87 ppm), similar to what is observed for the already reported *N*-methyl analogue (δ($^{11}$B) = –17.2 ppm, t, $^1J_{BH}$ = 90 Hz).[33] Further, single-crystal XRD confirmed that **3.4$_a$** had been accessed (**Figure 3.3** b). Analysis of the resulting structure reveals a tetrahedral boron centre, a C1-B1 bond length of 1.632(2) and a N1–B1 bond length of 1.536(2), both of which are values that are close to those reported for other IPr adducts of borane and other aminoboranes.[9,33,35–37]

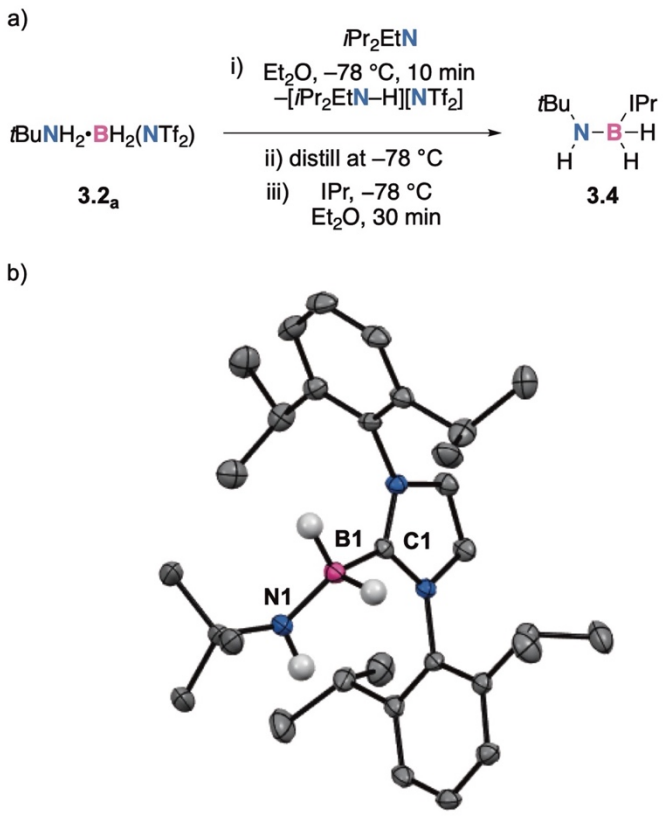


**Figure 3.3**: a) Synthesis of the aminoborane NHC-adduct, **3.4** from the aminoborane precursor, **3.2$_a$** and b) the molecular structure of **3.4** obtained from single-crystal XRD. Thermal ellipsoids shown at the 50% probability level, and B- and N-bound hydrogen atoms are arbitrarily assigned based on the obtained structure. Colour scheme is follows; carbon (grey), nitrogen (blue), boron (pink).

### 3.3.4 Coordination Chemistry of a Transient Aminoborane

Coordination compounds of transient aminoboranes are normally accessed through the initial formation of the corresponding amine-borane complex, which then undergoes metal-mediated dehydrogenation to access the aminoborane.[19,38–49] For

example, Aldrich *et al* reported the reaction of $[(IMes)_2RhH_2Cl(Na)][BAr^F{}_4]$ (IMes = *N,N*-bis(2,4,6-trimethylphenyl)imidazol-2-ylide; $Ar^F$ =3,5-bis(trifluoromethyl)phenyl) with 20 equivalents of **3.1$_a$**.[21] After 6 hours the authors observed the formation of the Rh complex of the amine-borane adduct, $[(IMes)_2RhH_2((\mu\text{–}H)_2HB\text{–}NH_2tBu)][BAr^F{}_4]$, which, if reacted for a further 42 hours (for a total of 48 h) yields the complex of the aminoborane, $[(IMes)_2RhH_2((\mu\text{–}H)_2B\text{–}NHtBu)][BAr^F{}_4]$. They were able to isolate both species as single-crystals and obtain molecular structures from XRD, unambiguously confirming the structure and binding modes of the amine-borane and aminoborane in each compound. Other complexes of **3.3$_a$** have been accessed, but in these cases there are no reports on the molecular structures of the complexes.[18–20] Generally, the coordination chemistry of aminoboranes has focussed on late transition metals[19,38–49] such as the readily accessed ruthenium complex, $(PCy_3)_2(H_2)_2RuH_2$.

Thus, using the ability to generate aminoboranes as the sole product *in situ* we targeted the formation of $(PCy_3)_2(\eta^2\text{-}t\text{BuNH=BH}_2)RuH_2$ by reacting **3.3$_a$** made *in situ* directly with $(PCy_3)_2(H_2)_2RuH_2$. Accordingly, a toluene solution of $(PCy_3)_2(H_2)_2RuH_2$ in a J-Young NMR tube was placed in the glovebox cold well that was submerged in liquid nitrogen. Once frozen, a layer of **3.2$_a$** in toluene was deposited on top and cooled before $i\text{Pr}_2\text{EtN}$ was added. The reaction was then sealed, removed from the glovebox, and placed in a dry ice and acetone cooling bath to warm to –78 °C (**Figure 3.4** a). Once both layers were thawed, the tube was briefly removed from the bath, inverted twice to ensure homogeneity, and placed back in the cooling bath for 30 minutes. Letting the reaction mixture warm to 20 °C and monitoring by $^1$H and $^{11}$B NMR spectroscopy gives two key indications that the reactions have occurred and complex **3.5** was accessed. Firstly, the

hydridic region of the $^{1}H$ NMR spectra reveals two environments, one for the metal hydrides at –7.02 ppm and one for the bridging hydrides at –12.53 ppm that bind the aminoborane to the metal centre, similar to those reported for $(PCy_3)_2(\eta^2$-$NH2{=}BH_2)RuH_2$.[38] Secondly, neither **3.3$_a$** nor its decomposition products were observable by $^{11}B$ NMR spectroscopy, instead a broad peak at 44.3 ppm was observed. These values are all similar to those reported for the analogous complexes bearing *t*BuNH=$BH_2$ previously reported.[18,19,21] Single-crystals of **3.5** suitable for x-ray crystallography were grown from a concentrated solution in pentane held at –40 °C over several days and XRD unambiguously determined the structure of **3.5** (**Figure 3.5** b). Close examination of the structure reveals a pseudo-octahedral Ru environment with phosphines coordinated in the axial positions. The aminoborane ligand is bound *via* the hydride atoms of boron, with a Ru–B bond length of 1.978(4) Å. The N–B bond is 1.396(5) Å and the Ru–B–N bond angle is nearly linear at 176.6°, values that are similar to other Ru-bound aminoboranes.[19,38,39,41,41,42,46,48,49] Notably, the P1–Ru1–P2 angle of **3.5** is 154.5°, which is significantly distorted from the expected angle of 180° for two equivalent ligands bound in the axial positions of an octahedral complex likely a result of the sterically demanding ligands.

a)

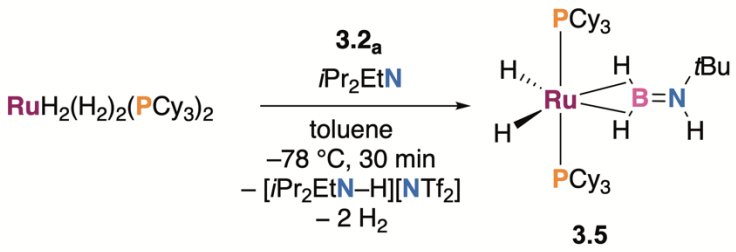


b)

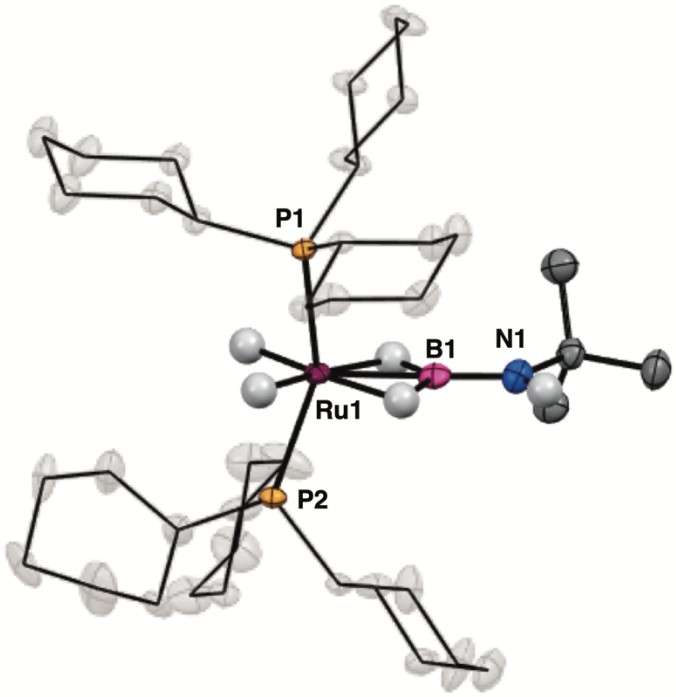


**Figure 3.4**: a) Synthesis of a ruthenium complex (**3.5**) bearing **3.3$_a$** as a ligand, and b) molecular structure of **3.5**. Thermal ellipsoids shown at a 50% probability level. Ruthenium-, boron- and nitrogen-bound hydrogen atoms were assigned directly from the electron density map, while all others were assigned arbitrarily. Colour scheme is follows; carbon (grey), nitrogen (blue), boron (pink), ruthenium (burgundy), phosphorus (orange).

### 3.3.5 Reactivity of Free Transient Aminoboranes

Reactivity studies on transient primary aminoboranes such as **3.3$_a$** performed so far were done either through solvent induced liberation from metal centres,[18] or by thermal (T = 200 °C) or catalytic dehydrogenation of amine-borane adducts ($RNH_2$•$BH_3$).[22–30] Each of these studies do not allow for reaction monitoring while starting from **3.3$_a$** as the sole species in solution. Therefore, we sought to observe the reactivity of this transient aminoborane starting from only **3.3$_a$** in solution.

Accordingly, a 0.1 M sample of **3.3$_a$** in $Et_2O$ was prepared as described above in a J-Young NMR tube and warmed to 20 °C (**Scheme 3.2**). Monitoring the reaction by $^{11}$B NMR spectroscopy after 2 h reveals consumption of the aminoborane **3.3$_a$** begins, producing *t*$BuNH_2$•$BH_3$ (**3.1$_a$**, 11%), [*t*BuN=BH]$_3$ (**3.6$_a$**, 21%), *t*BuNH–BH–NH*t*Bu (**3.7$_a$**, 15%), and $BH_2$–NH*t*Bu–$BH_2$(*B*,*B*-μ-H) (**3.8$_a$**, 29%) with a small amount of **3.3$_a$** observed (Figure 3.5). After a total of 24 h $^{11}$B NMR spectroscopy reveals full consumption of **3.3$_a$** and formation of *t*$BuNH_2$•$BH_3$ (**3.1$_a$**, 17%), [*t*BuN=BH]$_3$ (**3.6$_a$**, 19%), and $BH_2$–NH*t*Bu–$BH_2$(*B*,*B*-μ-H) (**3.8$_a$**, 23%) (Figure 3.6). There are also unidentified products that are observed at *ca.* –10 ppm (*ca*. 40%) in the $^{11}$B NMR spectra obtained. This is in opposition to what was observed by Weller *et. al*. where they had observed **3.3**$_a$ produced from the chemically induced release from its iridium precursor to slowly convert into approximately equimolar amounts of **3.6$_a$** and **3.1$_a$** over 14 h, and fully convert to **3.6$_a$** within 36 h.[18] It is also different from what was observed from the $Ca^{II}$ catalyzed dehydrocoupling of *t*$BuNH_2$•$BH_3$ where the cyclic dimer borazane, [*t*BuNH–$BH_2$]$_2$, was one of the main products.[28] Further, in the $Al(NMe_2)_3$ mediated catalytic dehydrocoupling of **3.1$_a$**, the cyclic trimerization product of **3.3$_a$** was observed and isolated.[23] Otherwise, there are shared

products between the dehydrocoupling studies of primary aminoboranes,[26,27,30] but the distribution and products obtained differ in each case, highlighting the importance of producing free aminoboranes *in situ* to better understand their reactivity.

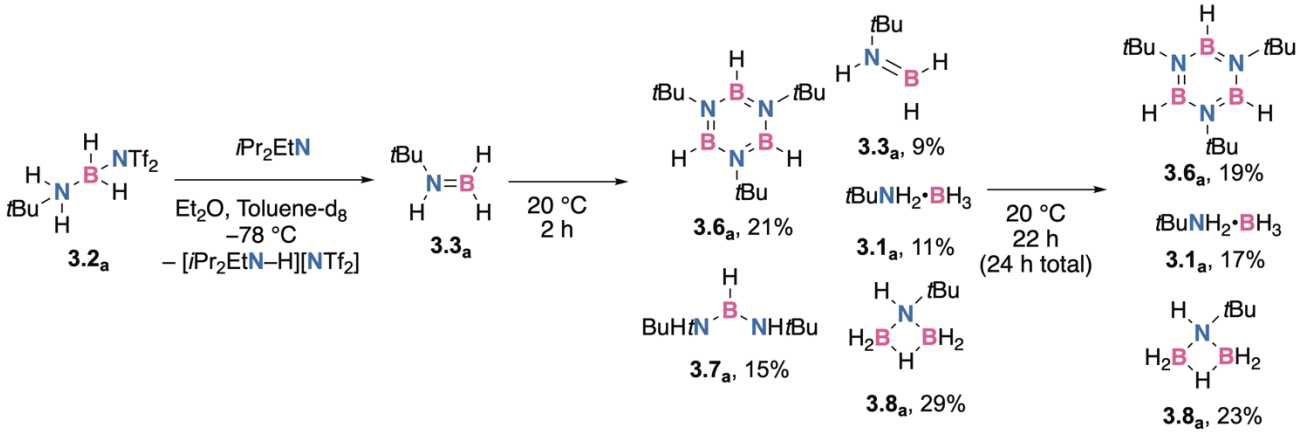


**Scheme 3.2:** Product mixture of the reaction of **3.3$_a$** with itself as the reaction solution warmed to ambient temperature. Proportions of products within the reaction mixture were determined by their relative $^{11}$B NMR integration values. After 2 h there is an unidentified product that represents *ca*. 24% of the boron content in solution, which increases to *ca*. 40% after 24 h.

### 3.3.6 Mechanism of Reactivity

The generation of *t*BuNH$_2$•BH$_3$ (**3.1$_a$**) suggests that at least some of the free aminoborane made in *situ* is acting as a H$_2$ acceptor. The ability of aminoboranes to accept H$_2$ from amine-borane adducts has been reported in detail by our group.[50,51] However, the mechanism in which **3.1$_a$** and **3.6$_a$** are formed is not immediately clear. We envision two possibilities (**Scheme 3.3**), the first (route A) involves a disproportionation reaction where free aminoborane is acting as both a H$_2$ acceptor and donor, generating the amine-borane adduct and iminoborane (*t*BuN≡BH, i). It is expected that the iminoborane can rapidly cyclotrimerize into borazine, **3.6$_a$**. The second proposed

mechanism (route B), involves an initial cyclotrimerization of aminoborane, yielding cyclotriborazane ([*t*BuNH–$BH_2$]$_3$, ii). Then, subsequent dehydrogenation by three equivalents of **3.3$_a$** would yield **3.6$_a$** and 3 equivalents of **3.1$_a$**. In the first case, it is reasonable to assume that any iminoborane formed *in situ* would readily cyclotrimerize.[52,53] However, in the second case, it is expected the cyclic borazane ([*t*BuNH–$BH_2$]$_3$) would be more stable, considering the stability of the closely related *N*-methyl cyclotriborazane.[54] Further, *N*-*tert*-butylcyclotriborazane is the intermediate in the thermal dehydrogenation at 120 °C of **3.1$_a$**,[22] and is one of the reaction products in the catalytic dehydrocoupling of **3.1$_a$** at 20 °C over using an Al(III) catalyst, identified by $^{11}$B NMR spectroscopy as a triplet with a chemical shift of –5.1 ppm.[23] Thus, it would be expected that the iminoborane intermediate may not be observable by NMR spectroscopy, but the cyclotriborazane intermediate should be, unless the rate of dehydrogenation is very high.

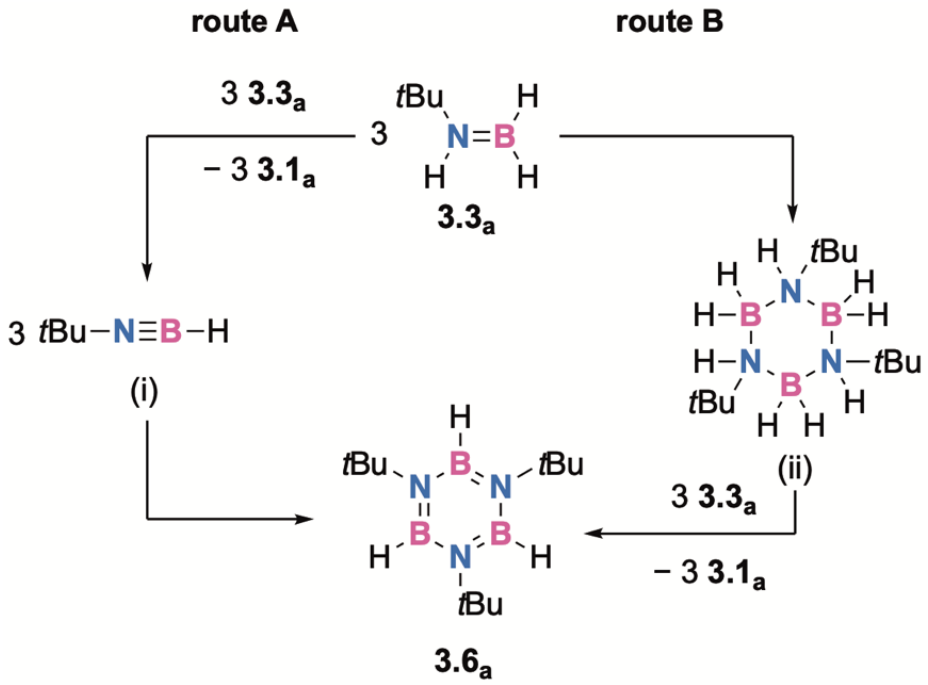


**Scheme 3.3:** Two possible routes to form borazine, **3.6**$_a$, from its corresponding aminoborane, **3.3**$_a$.

We aimed to observe potential intermediates that could lead to **3.6**$_a$ by monitoring the decomposition of **3.3**$_a$ by $^{11}$B NMR spectroscopy. Accordingly, a 0.1 M solution of **3.2**$_a$ in $Et_2O$ was prepared in a J–Young NMR tube cooled to −78 °C and *i*$Pr_2$EtN was added. Immediately after, the sample was transferred to the NMR spectrometer with the probe cooled to –30 °C, as this temperature would allow for reactions to occur at a considerable rate, and $^{11}$B spectra were obtained every 5 minutes over the next two hours. Monitoring this reaction at –30 °C reveals the main product of the reaction is **3.1**$_a$, but **3.6**$_a$, **3.7**$_a$, and **3.8**$_a$ can also be observed. The four products are generated simultaneously at similar rates (**Figure 3.7**, in the experimental), resulting in a complex reaction mixture as soon as the temperature is high enough for the reaction to proceed. However, what is more informative is what is not observed by $^{11}$B NMR spectroscopy at this temperature, namely

peaks consistent with oligomerization of **3$_a$** into linear or cyclic products or iminoborane (**Scheme 3.3**).

As we could not observe *tert*-butyl cyclotriborazane (ii) as a reaction product by $^{11}$B NMR spectroscopy, we aimed to assess the ability of **3.3$_a$** to dehydrogenate *N*-methyl cyclotriborazane (**Scheme 3.4**). Considering the reduced steric crowding of the nitrogen centres in *N*-methyl cyclotriborazane compared to *N*-*tert*-butyl cyclotriborazane, the reaction between **3.3$_a$** and *N*-methyl cyclotriborazane should proceed at a significantly higher rate than the analogous reaction between **3.3$_a$** and *N*-*tert*-butyl cyclotriborazane (ii), producing a significant amount of *N*-methyl borazine. Thus, to a solution of *N*-methylborazane and **3.2$_a$** in $Et_2O$ that was cooled to –78 °C was added *i*$Pr_2$EtN. The solution was then left to warm to –35 °C and held at this temperature over 16 h, as **3.3$_a$** is unreactive in hydrogen transfer chemistry at –78 °C. Subsequently, this reaction was monitored by $^{11}$B NMR spectroscopy and no significant evidence for a reaction to generate *N*-methylborazine was observed (**Figure 3.8**, in the experimental). This is similar to what was observed by Weller *et. al.* in their studies on the reactivity of slowly liberated **3.3$_a$** with methyl cyclotriborazane.[45] Thus, based on the fact that methyl cyclotriborazane is not observed in solution by NMR spectroscopy, and the lack of reactivity between **3.3$_a$** and methyl cyclotriborazane, it is unlikely that borazine, **3.6$_a$**, is formed *via* a *tert*-butyl cyclotriborazane intermediate. Therefore, we considered the alternative route where two equivalents of aminoborane react to transfer one equivalent of hydrogen to yield iminoborane and amine-borane adduct (**Scheme 3.3**, route A).

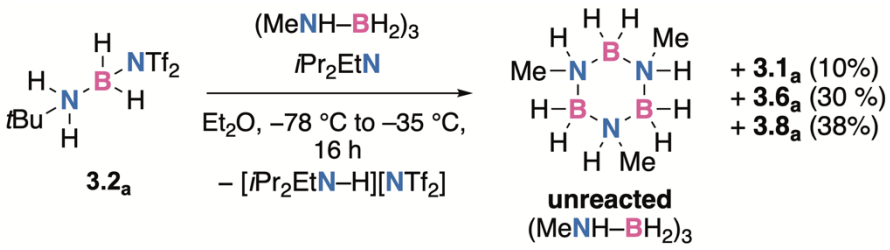


**Scheme 3.4:** Reaction of **3.3$_a$** generated *in situ* with *N*-methylcyclotriborazane.

Braunschweig and coworkers have studied the spontaneous reaction of an iminoborane, *t*BuN≡B*t*Bu, with amine-borane ($H_3N$•$BH_3$) to produce aminoboranes,[55] the reverse of what is the first step for the proposed mechanism in route A to access **3.1$_a$** and **3.6$_a$** from **3.3$_a$**. They determined that the reaction proceeds through a concerted mechanism where an initial hydrogen bonding interaction leads to a transition state (**Scheme 3.5**) where transfer hydrogenation occurs in a B-to-B' and N-to-N' fashion,[55] similar to what our group reported for reactions between *i*$Pr_2N$=$BH_2$ and $Me_2NH$•$BH_3$.[50,51] Moreover, the reaction between *t*BuN≡B*t*Bu and $H_3N$•$BH_3$ is driven by the highly exothermic nature of cyclooligomerization of the produced aminoborane, $H_2N$=$BH_2$. We envision a similar pathway is possible for the generation of **3.6$_a$** and **3.1$_a$** from **3.3$_a$**, where an initial hydrogen bonding N–H interaction between two aminoboranes leads to a 6-membered intermediate, allowing for hydrogen transfer between the two aminoboranes to produce amine-borane adduct **3.1$_a$** and the iminoborane, *t*BuN≡BH. However, in this case, the reaction would be driven by the highly exothermic cyclization of the iminoborane intermediate.[52,53] Computations on this pathway (PBE1PBE/def2SVP) indicate that the initial hydrogen transfer between two aminoboranes to produce amine-borane and iminoborane are thermodynamically uphill ($\Delta H°$ = +3.9 kcal•mol$^{-1}$), but confirm that the

subsequent cyclotrimerization is highly exothermic ($\Delta H° = -61$ kcal•mol$^{-1}$). Thus, this overall transformation of **3.3$_a$** to **3.6$_a$** and **3.1$_a$** through route A of Scheme 3.3 should be possible provided there is an accessible kinetic pathway. Together these data suggest that **3.6$_a$** and **3.1$_a$** are formed as a result of the formation of an iminoborane intermediate (i), a species that appears to be even more transient than **3.3$_a$** as it is not observed in this reaction mixture.

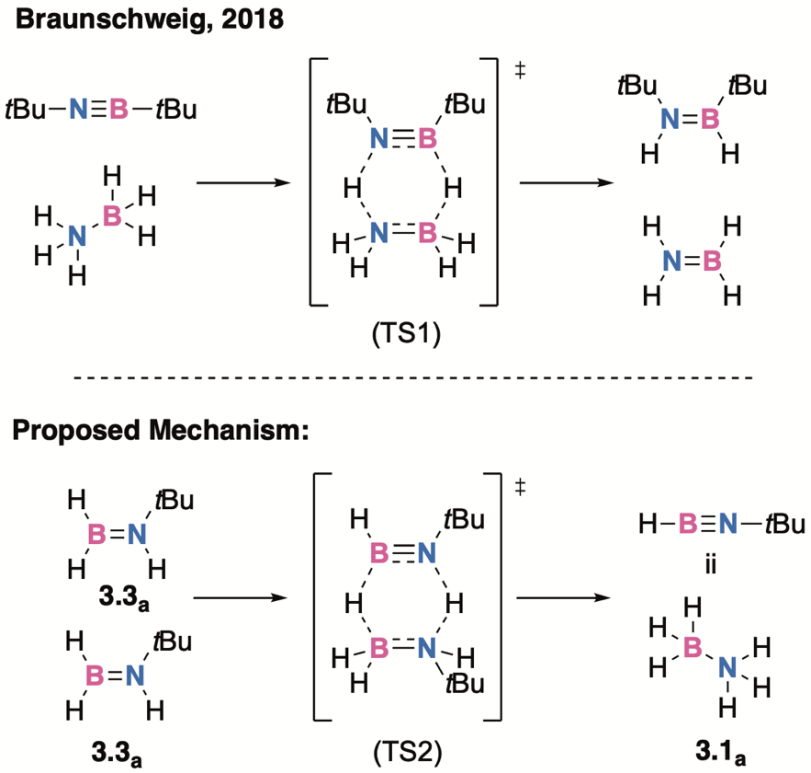


**Scheme 3.5:** Hydrogen transfer between and an iminoborane and an amine-borane adduct *via* transition state, **TS1** (top), and proposed mechanism for accessing iminoboranes from two aminoboranes *via* **TS2** (bottom).

The other products that were observed from the reactivity of **3.3a** include the diamidoborane (**3.7$_a$**) and borylamine-borane (**3.8$_a$**) species (**Scheme 3.2**). Boryl-amine boranes have been previously synthesized from the reaction of amine-borane adducts

(RR'NH•$BH_3$; R,R' = Me, H) with excess borane.[50,56] We predict that the diamidoborane species is a result of a hydroboration reaction between two aminoborane molecules in solution to yield a dimeric chain, which then loses an equivalent of $BH_3$ (**Scheme 3.6** a). This would provide an equivalent of $BH_3$ to react with aminoborane **3.3$_a$** *in situ* to yield borylamine-borane (**3.8$_a$**) (**Scheme 3.6** b). The hydroboration chemistry of primary aminoboranes has been explored, mainly with alkene substrates.[15,56] Similarly, addition of 2.5 equivalents of cyclohexene to an ether solution of **3.2$_a$** before the addition of *i*$Pr_2$EtN also results in a $^{11}$B NMR peak at 45.1 ppm, consistent with *t*BuNH=$BCy_2$ (**Figure 3.9**). Further, the insertion of aminoborane ($H_2N{=}BH_2$) into the B–H bond of another equivalent of aminoborane has been previously studied computationally, where it was found the enthalpic barrier to insertion was relatively low.[57] Thus, based on the ability of **3.3$_a$** to undergo insertion chemistry with cyclohexene and the previous related computational studies, we believe that the dimeric chain is a plausible intermediate that accounts for the resulting reaction products. Computations (PBE1PBE/def2SVP) on this reaction reveal that the formation of the linear dimer intermediate is thermodynamically downhill ($\Delta H° = -10$ kcal•mol$^{-1}$). However, the dissociation of borane from the dimer is uphill ($\Delta H° = +30$ kcal•mol$^{-1}$). But the subsequent sequestration of $BH_3$ by **3.3$_a$** is favourable ($\Delta H° = -39$ kcal•mol$^{-1}$), resulting in an overall thermodynamically favourable process.

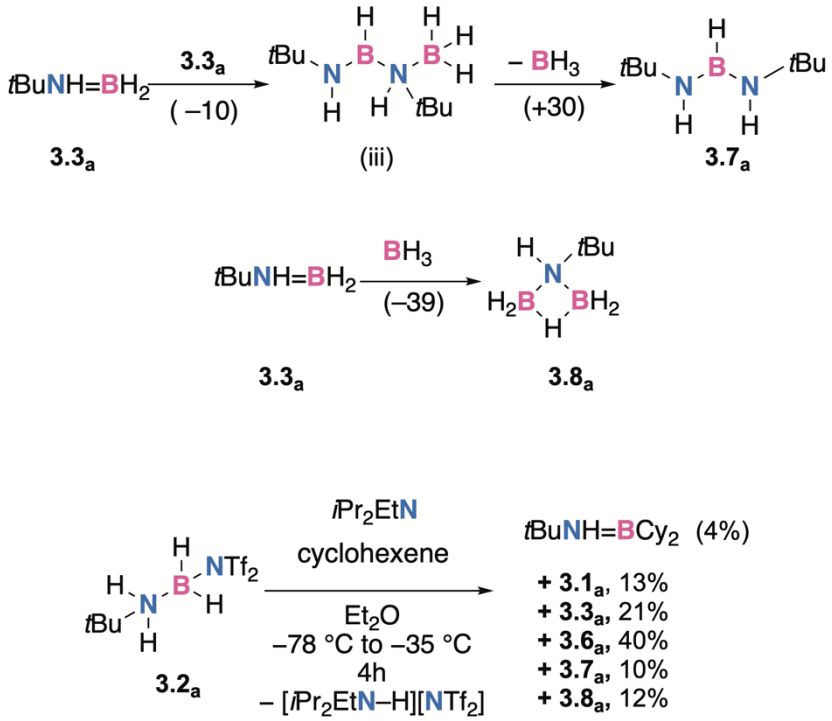


**Scheme 3.6:** a) Proposed mechanism for formation of **3.7**$_a$ from **3.1**$_a$, b) proposed mechanism for formation of **3.8**$_a$ from **3.3**$_a$, and c) reaction of **3.3**$_a$ generated *in situ* with cyclohexene to access *t*BuNH=BCy$_2$. For proposed reactions to access **3.7**$_a$ and **3.8**$_a$, ΔH° values in kcal•mol$^{-1}$ are given for each reaction calculated at the PBE1PBE/def2SVP level of theory.

The reaction pathways to **3.1**$_a$, **3.6**$_a$, **3.7**$_a$, and **3.8**$_a$ from **3.3**$_a$ are inaccessible at –78 °C, evidenced by the remarkable stability of **3.3**$_a$ at this temperature. However, warming the reaction to temperatures between –30 and 20 °C allow for diverse reactivity to occur. We have identified the likely pathways to these products, where an initial hydrogen transfer between two equivalents of **3.3**$_a$ and subsequent cyclotrimerization of iminoborane made *in situ* results in the formation of **3.1**$_a$ and **3.6**$_a$, while **3.7**$_a$ and **3.8**$_a$ are accessed *via* an initial hydroboration between two equivalents of **3.3**$_a$ to yield a BN dimer

intermediate which releases $BH_3$ producing **3.7$_a$**, and the free borane is trapped by a third equivalent of **3.3$_a$** to yield **3.8$_a$**.

### 3.3.7 Reactivity of a Transient Primary Aminoborane at 60 °C

The generation of catenated products, either linear or cyclic, is a common outcome for aminoboranes. Cyclic oligomers of **3.3$_a$** have been reported and discussed in this report, namely the cyclic dimer,[28] and the cyclotriborazane,[23] ($t$BuNH=$BH_2$)$_x$ (x = 2,3). However, in our studies on the reactivity of **3.3$_a$** at or below 20 °C, we had no evidence of either of these products being formed. While ($t$BuNH=$BH_2$)$_3$ was accessed in low concentrations at 20 °C by the dehydrogenation of **3.1$_a$** using $Al(NMe_2)_3$ as a catalyst, ($t$BuNH=$BH_2$)$_2$ was accessed by the $Ca^{II}$-mediated catalytic dehydrogenation of **3.1$_a$** at 60 °C. Thus, we were interested in the chemistry of **3.3$_a$** at elevated temperatures and to determine if cyclic species could be produced at 60 °C at these elevated temperatures in absence of a catalyst.

To monitor the reactivity of **3.3$_a$** at elevated temperature, a THF solution of **3.2$_a$** was prepared in a J-Young NMR tube, and $i$Pr$_2$EtN was added. This tube was sealed, and placed in a heating block at 60 °C. After 24 h, the reaction was monitored by $^{11}$B NMR spectrometry (**Figure 3.10**), revealing the generation of cyclic species, evidenced by a triplet at −6.1 ppm, consistent with the dimer, ($t$BuNH–$BH_2$)$_2$, observed by Hill *et. al*.[28] Exploring this reaction computationally (PBE1PBE/def2SVP) reveals that the overall cyclodimerization is exothermic ($\Delta H°$ = –20 kcal•mol$^{-1}$). However, this reaction product is only observed at elevated temperature indicating that there is a high activation barrier that must be overcome which is likely due to the presence of the sterically bulky *tert*-butyl group on nitrogen.

## 3.4 Conclusion

Herein we report the first detailed study on the reactivity of a transient primary aminoborane. By deprotonating amine-(triflimido)boranes (**3.2$_{a–c}$**) we have demonstrated that reactive aminoboranes can be generated and are stable enough at −78 °C to be observed as the sole product of the reaction by $^{11}$B NMR spectroscopy. We were able to trap the transient aminoborane using IPr or a Ru centre. We then explored the reactivity of the aminoborane, **3.3$_a$**, at elevated temperatures, identifying the likely routes to the main reaction products. Together these reactions show the breadth of transformations a relatively simple molecule, a primary aminoborane, can undergo, which may inform other studies on reactions that evoke transient aminoboranes as intermediates. Moreover, this study further demonstrates the drastic change in reactivity introduction of inorganic elements into an organic molecule can induce. For example, **3.3a** is the isoelectronic, inorganic B–N analogue of 3,3-dimethyl-1-butene; the former undergoes exhaustive reactions above –40 °C within hours and the latter is a liquid that can be stored in a chemical fridge and purchased from a common chemical supplier. Future directions will focus on leveraging the ability to synthesize reactive aminoboranes and developing greater control over their reactivity including the polymerization of *N*-methylaminoborane as the sole species *in situ*.

## 3.5 Experimental

### General Considerations

Unless otherwise noted, storage and manipulation of chemicals were performed under an inert atmosphere of either $N_2$ or Ar gas using standard Schlenk techniques, or, carried out in an MBraun 200B glovebox equipped with a cold well partially filled with stainless steel beads, a freezer set to −40 °C, and a Polyscience chiller set to regulate the internal temperature to 20 °C. Further, any glassware used was dried overnight in a 200 °C oven. Hexanes, diethyl ether, toluene, and dichloromethane were dried using an MBraun Grubbs/Dow solvent purification system[58] and stored over activated 4 Å molecular sieves. Pentane was degassed and stored over 4 Å molecular sieves. Amine borane adducts, $RNH_2{\bullet}BH_3$ (R = Me, $CPh_3$) were synthesized using standard procedures.[54] *N,N*-bis(2,6-diisopropylphenyl)imidazol-2-ylide,[59] methyl cyclotriborazane $(MeNH–BH_2)_3$,[54] and $(PCy_3)_2(H_2)_2RuH_2$[60] were prepared according to literature procedures. Diisopropylethylamine was purchased from Sigma Aldrich then dried over $CaH_2$ and distilled prior to use. Cyclohexene was purchased from Sigma Aldrich, distilled and stored over sieves prior to use. *N,N*-dimethylamine-borane adduct was purchased from Sigma Aldrich and purified by sublimation. *t*$BuNH_2{\bullet}BH_3$, 9-BBN, $BPh_3$, and imine X were purchased from Sigma Aldrich and used as received. $HNTf_2$ was purchased from TCI chemicals and used as received. Solvents for NMR were purchased from Sigma Aldrich and $CDCl_3$ was dried over $CaH_2$, then distilled prior to use, and toluene-d8 was dried over sodium/benzophenone ketyl and distilled before use.

Nuclear Magnetic Resonance (NMR) spectroscopy was performed on a Bruker Avance NEO 500 MHz spectrometer or AV360 with $^{1}H$ NMR spectra being referenced to residual proteo solvents and $^{13}C$ spectra being referenced against the $^{13}C$ signal of the deuterated solvent used. Otherwise, heteronuclear spectra were referenced using the recommended IUPAC reference compounds. Electrospray Ionization Mass Spectrometry (ESI-MS) was performed on a 3D ion trap Thermo LCQ Classic mass spectrometer. Samples were prepared by dissolving a small amount (*ca*. 0.1 – 1 mg) of sample in 1 mL of acetonitrile.

**Synthetic Procedures**

**Synthesis of Amine-(triflimido)boranes**

Amine-(triflimido)borane adducts, $RNH_2{\bullet}BH_2(NTf_2)$ (R = *t*Bu (**3.1$_a$**), Me (**3.2$_a$**), and $CPh_3$ (**3.3$_a$**)) were all prepared in an identical manner and prepared in the glove box. To a 4-dram vial charged with a stirring bar was added the requisite amine-borane adduct (1 mmol: **3.1$_a$** = 87 mg, **3.1$_b$** = 45 mg, **3.1$_c$** = 271 mg) and 5 mL of DCM resulting in a 0.2 M solution of the amine-borane adduct. To this solution was added $HNTf_2$ (1 mmol, 281 mg) in 3 to 5 separate portions as addition induced vigorous bubbling of $H_2$ gas. After all of the solid $HNTf_2$ was added, the reaction was left to stir for an additional 30 minutes at ambient temperature (20 °C). Afterwards, removal of volatiles *in vacuo* results in the formation of crystalline powders in near-quantitative yields (≥ 95%) and were of sufficient purity to be used without further purification. All products are colourless, apart from $CPh_3NH_2{\bullet}BH_2(NTf_2)$, which has some yellow discolouration which presumably originates from the generation of $[CPh_3]^{\bullet+}$ containing species in solution. These solids can be recrystallized from slow diffusion of hexane into saturated DCM solutions of **3.2$_{a–d}$**.

**$tBuNH_2•BH_2(NTf_2)$, $3.2_a$**

Prepared from **$3.1_a$** adduct. Yield: 349 mg, 96%.

$^1$H NMR ($CDCl_3$, 500 MHz, 298 K): 3.94 ppm (RN**$H_2$**•$BH_3$, 2 H, s), 2.63 (RN$H_2$•B**H**$_2(NTf_2)$, 2 H, br s), 1.37 ppm (C**$H_3$**, 9 H, s).

$^{11}$B NMR ($CDCl_3$, 160 MHz, 298 K): −9.7 ppm (br).

$^{13}$C NMR{$^1$H} ($CDCl_3$, 126 MHz, 298 K): 119.8 ppm ($SO_2$(**C**$F_3)_2$, q, $^1J_{CF}$ = 325 Hz), 55.9 ppm (**C**$(CH_3)_3$, s), 28.8 ppm (C(**C**$H_3)_3$, s).

$^{19}$F NMR ($CDCl_3$, 471 MHz, 298 K): −71.9 ppm (s).

ESI-MS(+): Expected for $[M–H]^+$: 366.0 *m/z*, observed: 366.3 *m/z*.

**$MeNH_2•BH_2(NTf_2)$, $3.2_b$**

Prepared from **$3.1_b$**. Yield: 312 mg, 97%.

$^1$H NMR ($CDCl_3$, 500 MHz, 298 K): 4.16 ppm (RN**$H_2$**•$BH_2(NTf_2)$, 2 H, br s), 2.60 ppm (C**$H_3$**, 3 H, t, $^3J_{HH}$ = 6.23 Hz), 2.54 (RN$H_2$•B**H**$_2(NTf_2)$, 2 H, br s).

$^{11}$B NMR ($CDCl_3$, 160 MHz, 298 K): −7.7 ppm (br).

$^{13}$C{$^1$H} NMR ($CDCl_3$, 126 MHz, 298 K): 119.8 ppm ($SO_2$(**C**$F_3)_2$, q, $^1J_{CF}$ = 323 Hz), 30.7 ppm (**C**$H_3$, s).

$^{19}$F NMR ($CDCl_3$, 471 MHz, 298 K): −72.1 ppm (s).

ESI-MS(+): Expected for $[M–H]^+$: 323.0 *m/z*, observed: 323.2 *m/z*.

**$CPh_3NH_2•BH_2(NTf_2)$, $3.2_c$**

Prepared from **$3.1_c$**. Yield: 523 mg, 95%.

$^{1}$H NMR ($CDCl_3$, 500 MHz, 298 K): 7.38 ppm (Ph-H, 9 H, m), 7.26 ppm (Ph-H, 6 H, m), 5.51 ppm (RN**H$_2$**•$BH_2(NTf_2)$, 2 H, br s), 2.40 (RN**H$_2$**•B**H**$_2(NTf_2)$, 2 H, br s).

$^{11}$B NMR ($CDCl_3$, 160 MHz, 298 K): −8.85 ppm (br).

$^{13}$C{$^{1}$H} NMR ($CDCl_3$, 126 MHz, 298 K): 140.1 ppm (Ph-C), 128.6 ppm (Ph-C), 128.5 ppm (Ph-C), 128.4 (Ph-C), 119.3 ppm ($SO_2$(**C**$F_3)_2$, q, $^{1}J_{CF}$ = 324 Hz), 72.5 ppm (**C**$(Ph)_3$).

$^{19}$F NMR ($CDCl_3$, 471 MHz, 298 K): –71.6 ppm (s).

ESI-MS(+): Expected for $[M–H]^+$: 551.1 *m/z*, observed: 551.3 *m/z.*

**Generation and Observation of Transient Aminoboranes by 11B NMR Spectroscopy**

Each aminoborane was prepared in a similar manner, using the appropriate amine-(triflimido)borane adduct (**3.2$_{a–c}$**). Firstly, the glove box cold well was cooled by submerging it in a bath of liquid nitrogen. Then, in the glovebox, the requisite amine-(triflimido)borane (1 mmol; **3.2$_a$** = 37 mg, **3.2$_b$** = 32 mg, **3.2$_c$** = 55 mg) and 600 µL of $Et_2O$ was added to a J-Young NMR tube. The J-Young NMR tube with the resulting solution was placed upright in the cooled cold well, allowing for the solution to freeze. Meanwhile, the NMR probe was cooled to –70 °C, and a dry ice/acetone cold bath was prepared in a thermos with a handle for sample transport. Once the NMR spectrometer was prepared, *i*$Pr_2$EtN (0.1 mmol, 17.5 µL) was added using a micropipette to the frozen $Et_2O$ solution of **3.2$_{a–c}$** in the glovebox cold well. Afterwards, the samples were sealed and removed from the glovebox and immediately placed in the thermos containing the dry ice/acetone cold bath. Once the samples were warmed to a temperature closer to –78 °C, made evident by no longer being frozen, they were inverted and then put back upright in the

cold bath to ensure sample homogeneity. The samples were then transported to the NMR spectrometer and inserted into the cooled probe, allowing for the $^{11}$B NMR spectra of each transient aminoborane (**3.3$_{a–c}$**) to be obtained. Generated aminoboranes should remain at temperatures below –60 °C, otherwise extensive reactivity occurs.

**tBuNH=BH$_2$, 3.3a**

Prepared from **3.2a**.

$^{11}$B NMR ($Et_2O$, 160 MHz, 203 K): 34.2 ppm (t, $^1J_{BH}$ = 126 Hz).

**MeNH=BH$_2$, 3.3b**

Prepared from **3.2b**.

$^{11}$B NMR ($Et_2O$, 160 MHz, 203 K): 37.4 ppm (t, $^1J_{BH}$ = 120 Hz).

**CPh$_3$NH=BH$_2$, 3.3c**

Prepared from **3.2c**.

$^{11}$B NMR ($Et_2O$, 160 MHz, 203 K): 3.9 ppm (br, width at ½ height: 475 Hz).

**Distillation of 3.3a and subsequent trapping with IPr**

In the glove box, **3.2$_a$** (1 mmol, 366 mg) and 50 mL of $Et_2O$ was added to a 100 mL round-bottom flask fitted with a Schlenk tap and charged with a stir bar. The flask was then sealed and transferred to the Schlenk line and put under an inert argon atmosphere. Then, the flask was submerged in a dry ice/acetone bath atop a stirring plate set to 600 rpm to cool the solution to −78 °C, followed by the addition of *i*Pr$_2$EtN (1 mmol, 0.17 mL)

to the rapidly stirring, cooled solution using a 1 mL syringe. After 30 minutes, the reaction was assumed to be complete, and the round bottom flask was fitted with a short path column and another 100 mL round-bottom flask fitted with a Schlenk tap and charged with a stirring bar to act as the receiving flask. The reaction vessel was submerged in liquid nitrogen, allowing for the solution to freeze, then the distillation apparatus was evacuated under vacuum for approximately 10 minutes. The distillation apparatus was then sealed, and the reaction vessel was warmed to –78 °C to allow for the $Et_2O$ solution to thaw. This modified freeze-pump-thaw was repeated two more times where upon the last thawing step, the reaction vessel was submerged in the dry ice/acetone bath (−78 °C), while the receiving flask was submerged in liquid nitrogen. After about 1.5–2 hours, the majority of the solution had transferred to the receiving flask and a residue had remained in the reaction vessel, which is primarily the by-product, [*i*$Pr_2$EtNH][$NTf_2$]. The receiving flask can then be removed from the distillation apparatus, warmed to –78 °C, and used immediately afterwards as an approximately 0.02 M solution of **3.3$_a$** in $Et_2O$. Afterwards, to the flask of approximately 1 mmol of **3.3$_a$** in $Et_2O$, 1 mmol of *N,N*-bis(2,6-diisopropylphenyl)imidazol-2-ylide (IPr) dissolved in 15 mL of $Et_2O$ (388 mg) was added dropwise. The solution was then subsequently left to stir for 30 minutes. Afterwards, volatiles were removed and the flask was brought into the glovebox *via* the antechamber.. Recrystallization of the beige solid from a saturated solution of **3.4** in hexanes held overnight at –40 °C gave colourless crystals of **3.4** in 47% yield (222 mg). Growing a second batch of crystals from this supernatant resulted in an addition 198 mg of colourless crystals, for a total yield of 89%.

$^{1}$H NMR (Toluene-$d_8$, 500 MHz, 298 K) δ: $^{1}$δ 7.19 ppm (Ar-H, t, $^{3}J_{HH}$ = 7.7 Hz, 2H), 7.06 ppm (Ar-H, d, $^{3}J_{HH}$ = 7.7 Hz, 4H), 6.33 ppm ((Dipp)N–C**H**=C**H**–N(Dipp), s, 2H), 2.73 ppm (C**H**$(CH_3)_2$, sept, $^{3}J_{HH}$ = 6.9 Hz, 5H), 2.46 ppm (*t*BuNH•B**H$_2$**(IPr), 1.40 ppm (CH(C**H$_3$**)$_2$, d, $^{3}J_{HH}$ = 6.8 Hz, 12H), 1.07 ppm (CH(C**H$_3$**)$_2$, d, $^{3}J_{HH}$ = 6.9 Hz, 12H), 1.00 ppm (C(C**H$_3$**)$_3$, s, 9H).

$^{11}$B NMR (Toluene-$d_8$, 160 MHz, 298 K) δ: −19.7 ppm (t, $^{1}J_{BH}$ = 87.8 Hz).

$^{13}$C{$^{1}$H} NMR (Toluene-$d_8$, 126 MHz, 298 K) δ: 145.7 ppm (Dipp-**C$_{ortho}$**), 135.1 ppm (Dipp-**C$_{ipso}$**),130.1 ppm (Dipp-**C$_{meta}$**), 123.7 ppm (Dipp-**C$_{para}$**), 121.8 ppm ((Dipp)N–**C**H=**C**H–N(Dipp)), 49.3 ppm (**C**$(CH_3)_3$), 32.1 ppm (**C**H$(CH_3)_2$), 29.0 ppm (C(**C**$H_3)_3$), 24.9 (CH(**C**$H_3)_2$), 23.3 (CH(**C**$H_3)_2$). *Note, the carbenoid carbon of IPr is not observed, likely due to coupling to $^{11}$B.*

ESI-MS(+): Expected for $[M+H]^+$: 474.4 *m/z*, observed: 474.3 *m/z*.

**Coordination Chemistry of a Transient Aminoborane**

In the glovebox, $(PCy_3)_2(H_2)_2RuH_2$ (0.05 mmol, 33.4 mg) was dissolved in 500 µL of toluene and added into a J-Young NMR tube. This solution was then placed in the glovebox cold well that was submerged in liquid nitrogen and cooled until a thermometer placed in it gave temperatures below −100 °C, resulting in the solution to freeze in the flask. Then solution of *t*BuNH$_2$•B$H_2$($NTf_2$) (0.05 mmol, 18 mg) in 1 mL of toluene was added on top of this frozen solution of the ruthenium precursor and also allowed to freeze, after which *i*$Pr_2$EtN (0.05 mmol, 9 µL) was added to the reaction mixture. The J-Young NMR tube was then sealed, removed from the glovebox, and submerged in a dry ice and acetone cooling bath (–78 °C). The solution was then left to stir over the next hour as it

warmed to −78 °C. Afterwards, the solution was warmed to room temperature, brought back inside the glovebox, and transferred to a 4-dram vial. Volatiles were removed *in vacuo*, and then **3.5** was extracted with pentane (3 x 1 mL). The resulting solution was then placed into the glovebox freezer in a 1-dram vial (−35 °C), where pale yellow crystals had been grown over several days, removal of the supernatant and subsequent drying *in vacuo* gave the complex in modest yield (23 mg, 61% yield).

$^{1}$H NMR (Toluene-$d_8$, 500 MHz, 298 K): 3.02 ppm (s, 1H, N**H**), 2.26 ppm (br m, 12 H, Cy-**H**), 1.90 ppm (br s, 20 H, Cy-**H**), 1.76 ppm (br s, 9 H, Cy-**H**), 1.67 ppm (br m, 14 H, Cy-**H**), 1.35 ppm (br m, 21 H, Cy-**H**), 1.21 ppm (s, 9 H, *t*Bu-**H**), −6.97 ppm (br s, 2 H, B**H$_2$**), −12.25 ppm (br s, 2 H, Ru-**H$_2$**).

$^{11}$B NMR (Toluene-$d_8$, 160MHz, 298 K): 44.3 ppm (br).

$^{31}$P NMR (Toluene-$d_8$, 202 MHz, 298 K): −77.19 ppm (s).

**Deprotonation of 3.2$_a$ at ambient temperature**

A solution of **3.2$_a$** (0.1 mmol, 37 mg) in 1.5 mL of $Et_2O$ was prepared in a J-Young NMR tube in a glovebox maintained at 20 °C. To this tube was added an equimolar amount of *i*$Pr_2$EtN (17 µL). The tube was sealed, and the tube was inverted several times to ensure complete incorporation of the base into the reaction mixture. At 2 h, the reaction had separated into two phases, one smaller, presumably [*i*$Pr_2$EtN–H][$NTf_2$], and another $Et_2O$ layer on top. Obtaining a $^{11}$B NMR spectra of the $Et_2O$ layer within the tube revealed that **3.3$_a$** was mostly consumed by $^{11}$B NMR spectroscopy, producing several species including **3.1$_a$**, a diamidoborane ((*t*BuNH)$_2$BH, **3.7$_a$**), boryl-amineborane ($BH_2$–NH*t*Bu–

$BH_2$(*B*,*B*-μ-H), **3.8$_a$**), borazine ([*t*BuN–BH]$_3$, **3.6$_a$**), and other unidentified species (Figure 3.5After 24 h, **3.3$_a$** and **3.7$_a$** were consumed, leaving **3.6$_a$**, **3.1$_a$**, and **3.5$_a$** as the main products of the reaction (Figure 3.6).

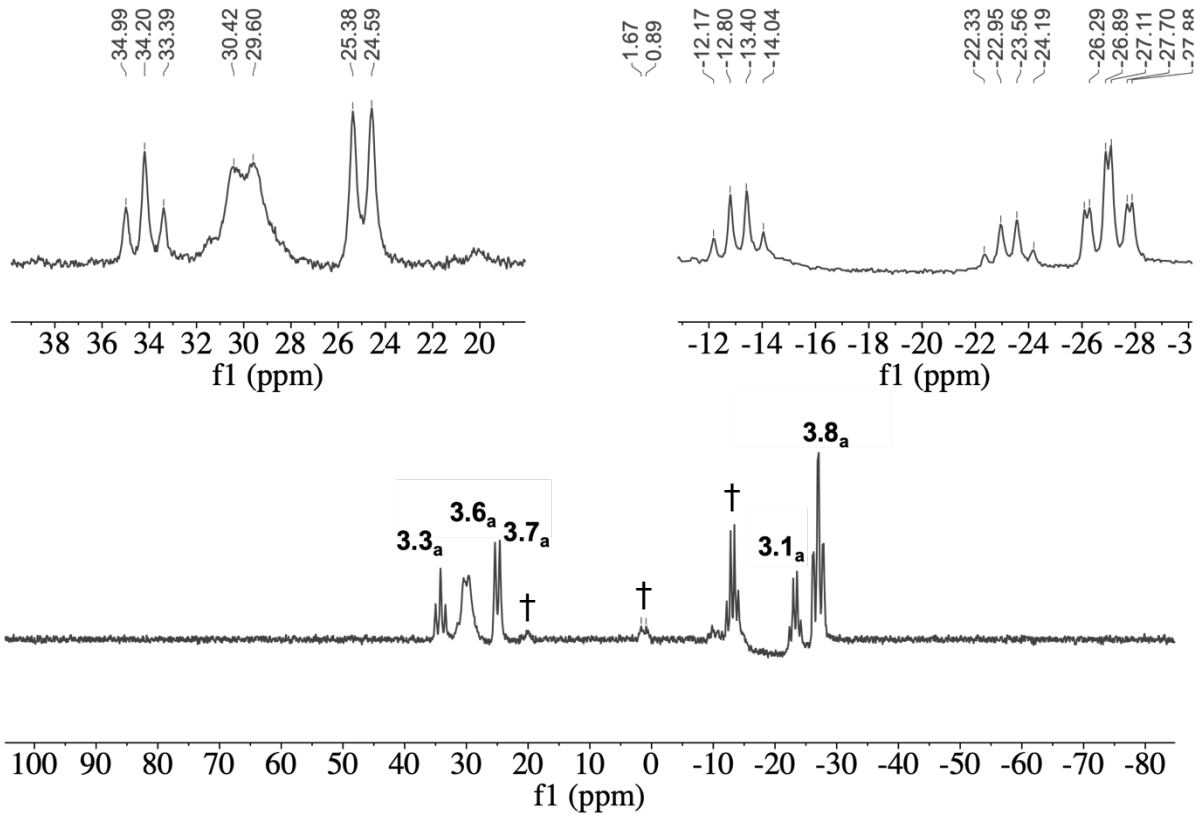


**Figure 3.5:** $^{11}$B NMR spectrum taken 2 h after an aliquot of **3.3$_a$** had been warmed to ambient temperature. Unknown $^{11}$B-containing species are labelled with a "†". Inset $^{11}$B NMR spectra showcase the coupling patterns of the various species produced.

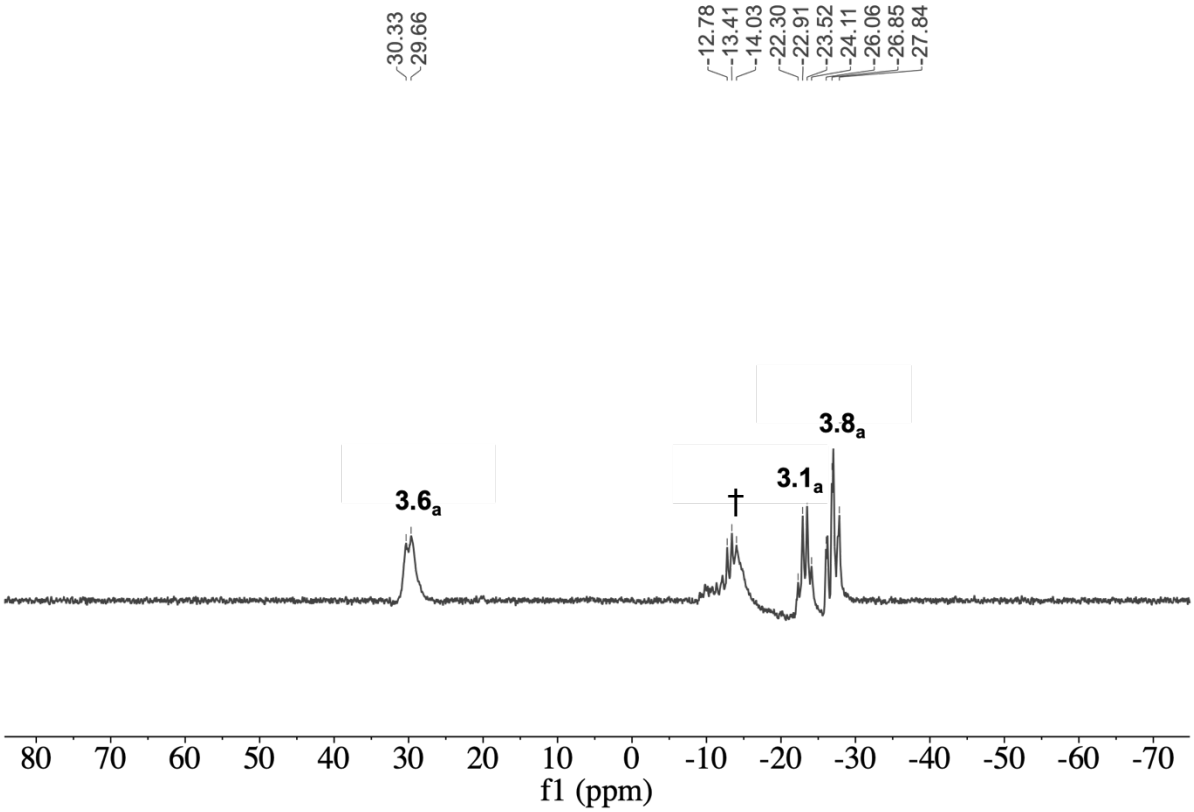


**Figure 3.6:** $^{11}$B NMR spectrum taken 16 h after an aliquot of **3.3$_a$** in $Et_2O$ had been warmed to ambient temperature. Unknown $^{11}$B-containing species are labelled with a "†".

**Monitoring the Reactivity of 3.3$_a$ at –30 °C**

In the glovebox a solution of **3.2$_a$** (37 mg, 0.1 mmol) in a J-Young NMR tube was prepared in $Et_2O$. Subsequently, the solution was placed in the cold well of the glovebox that was submerged in liquid nitrogen until it was frozen. Then, *i*$Pr_2EtN$ (0.1 mmol, 17 µL) was added to the J-Young NMR tube, sealed, and removed from the glovebox and placed immediately in a dry-ice and acetone bath. Meanwhile, the NMR probe was cooled to –30 °C. Then, the J-Young NMR tube was brought down to the spectrometer, and before inserting the sample, the tube was inverted twice to ensure sample homogeneity.

Afterwards, NMR spectra were recorded regularly over two hours, resulting in the spectra in Figure 3.7**.**

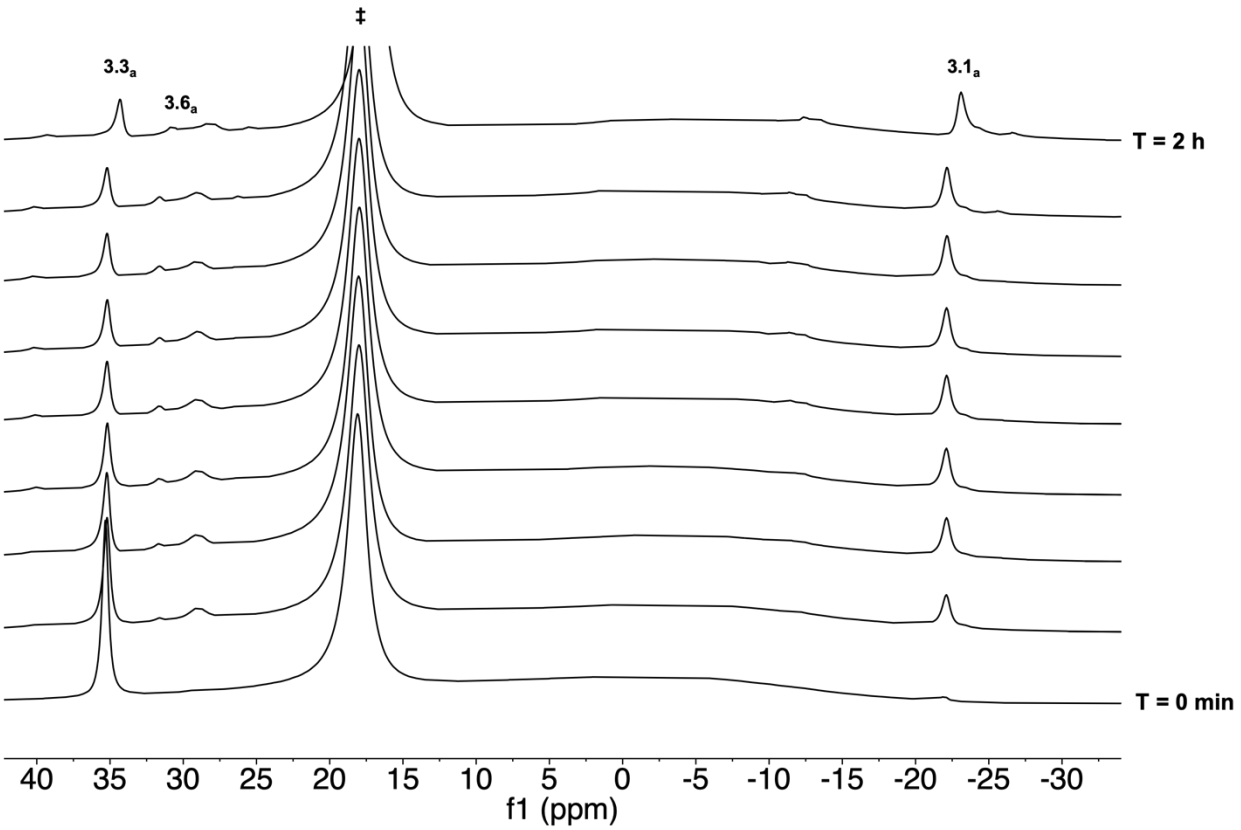


**Figure 3.7:** $^{11}$B NMR spectra of the reactivity of **3.3$_a$** at –30 °C over two hours. Mainly the depletion of the peak for **3.3$_a$** and the formation of the peak for **3.1$_a$** is observed. Signal for B(O*i*Pr)$_3$ is marked by a ‡.

**Reaction of 3.3$_a$ with *N*-methyl Cyclotriborazane**

In the glovebox a solution of **3.2$_a$** (37 mg, 0.1 mmol) in 4 mL of $Et_2O$ was prepared in a 20 mL vial charged with a stirring bar. Meanwhile, the glovebox cold well was submerged in liquid nitrogen. Once the cold well was below –80 °C, the vial with the reaction mixture was placed in the well, cooled, and then *i*Pr$_2$EtN (17 µL) was added to produce **3.3$_a$** *in situ*. After 30 minutes *N*,*N*,*N*-trimethylcyclotriborazane (0.07 mmol, 8 mg) was added to

the reaction mixture. The reaction mixture was then transferred to the glovebox freezer which was set at –35 °C and left to react overnight. Afterwards monitoring the reaction by $^{11}$B NMR spectroscopy revealed that *N*,*N*,*N*-trimethylcyclotriborazane did not react with **3.3$_a$**. Instead, the decomposition products of **3.3$_a$** were observed (Figure 3.8).

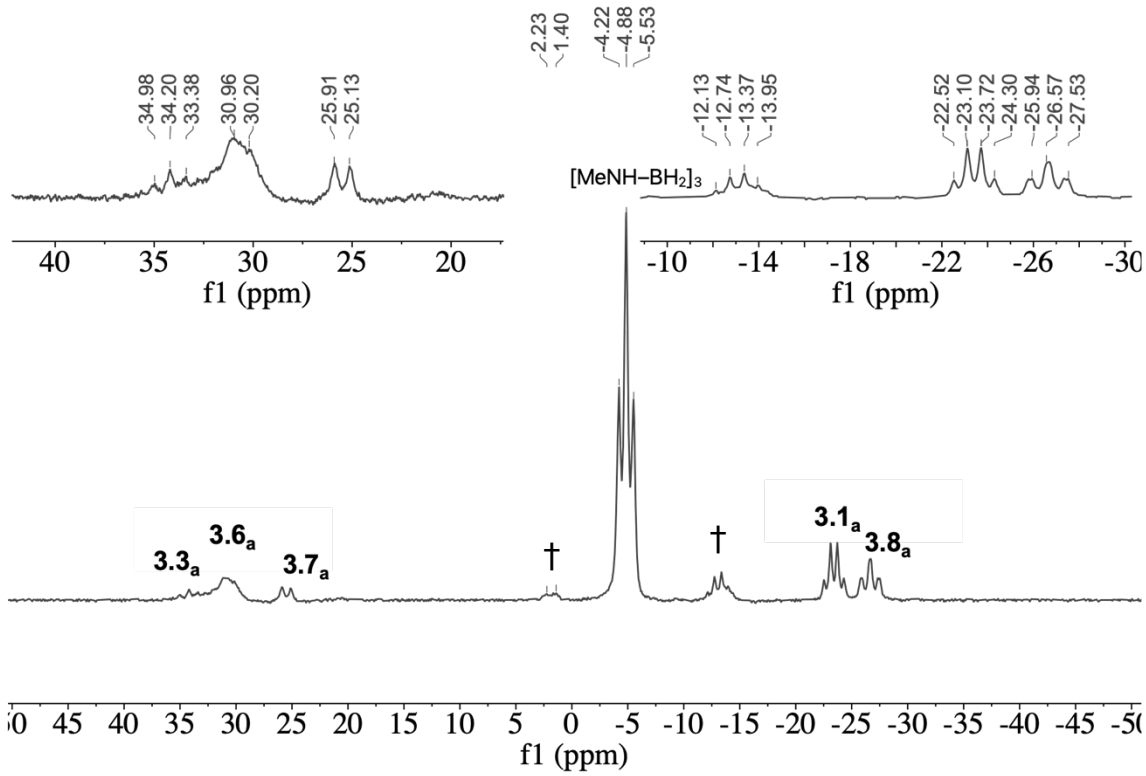


**Figure 3.8:** $^{11}$B NMR spectrum of the reaction between **3.3$_a$** and *N*-methyl cyclotriborazane taken after 16 h at –35 °C. Unknown $^{11}$B-containing species are labelled with a "†". Inset spectra show coupling patterns of compounds produced.

**Reaction of 3.3a with cyclohexene to generate tBuNH=BCy$_2$**

In the glovebox a solution of **3.2$_a$** (37 mg, 0.1 mmol) in 4 mL of $Et_2O$ was prepared in a 20 mL vial charged with a stirring bar. Meanwhile, the glovebox cold well was submerged in liquid nitrogen. Once the cold well was below –80 °C, the vial with the reaction mixture was placed in the well, cooled, and then *i*Pr$_2$EtN (17 µL) was added to produce **3.3$_a$** *in situ*. After 30 minutes a small excess of cyclohexene (0.25 mmol, 25 µL) was added to the reaction mixture. The reaction mixture was then transferred to the glovebox freezer which was set at –35 °C and left to react overnight. Afterwards monitoring the reaction by $^{11}$B NMR spectroscopy revealed a singlet at 46.1 ppm, indicative of *t*BuNH=BCy$_2$ being formed (**Figure 3.9**).

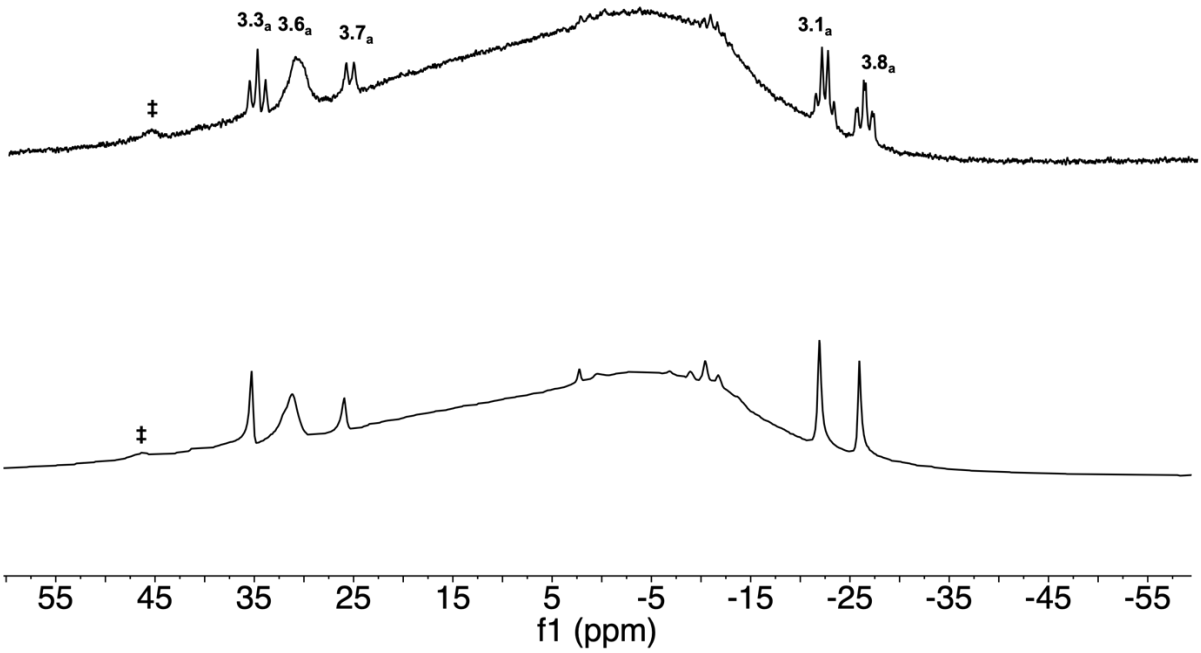


**Figure 3.9:** $^{11}B$ NMR (top) and $^{11}B\{^1H\}$ NMR (bottom) spectra of the reaction between 3.3a and cyclohexene *in situ*. Peak proposed to be *t*BuNH=$BCy_2$ is marked by ‡.

**Reactivity of 3.3a at Elevated Temperature**

In the glovebox a solution of **3.2a** (37 mg, 0.1 mmol) in 1000 µL of THF was prepared in a J-young NMR tube. Afterwards 0.1 mmol of *i*$Pr_2$EtN (17 µL) was added, the tube was sealed and inverted several times to ensure homogeneity. Then the tube was removed from the glovebox and placed in a heating block set to 60 °C. After 4 days, the reaction was monitored by $^{11}B$ NMR spectroscopy revealing the formation of cyclic species by a triplet at –6.1 ppm (**Figure 3.10**).

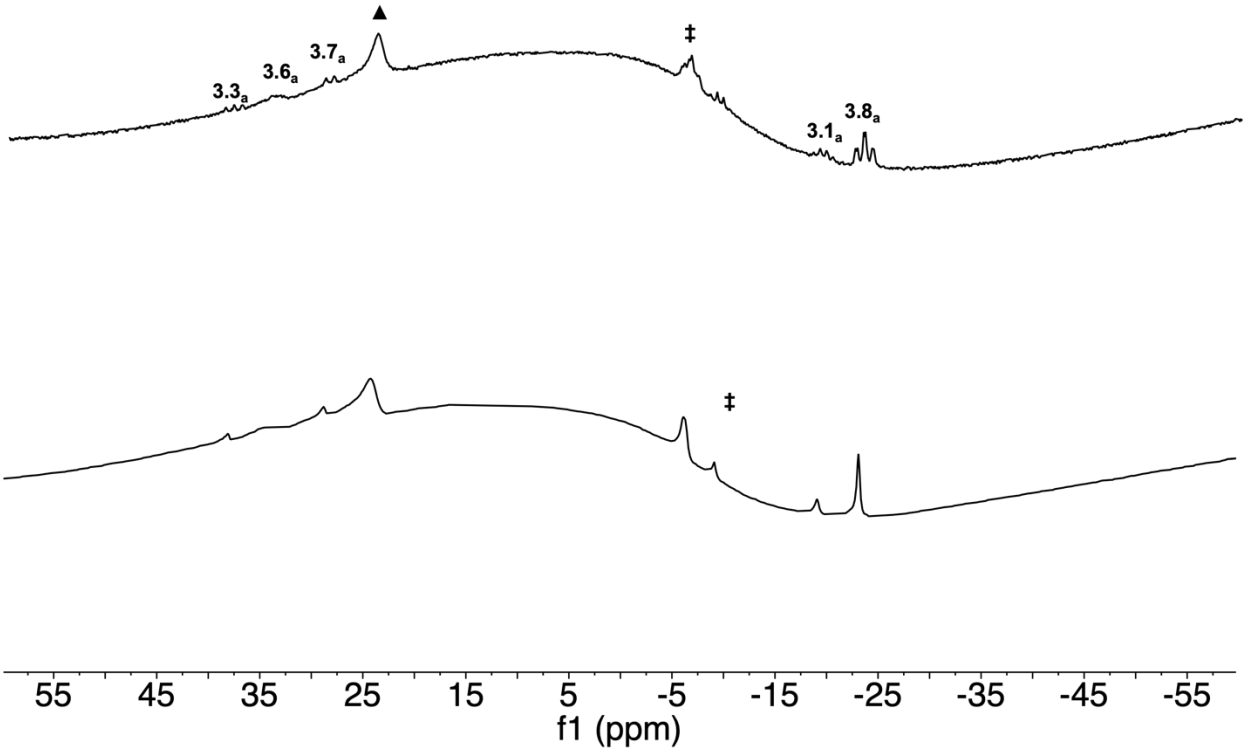


**Figure 3.10:** Reaction products from heating a sample of **3.3a** to 60 °C over 4 days. Unknown dehydrogenated product observed at *ca.* 20 pp, marked by a ▲. Peak for cyclic aminoborane species at –6.1 ppm, marked by a ‡.

**Computations**

All the computations were performed using the Gaussian16.C01 program suite.[61] In each case, the PBE0 hybrid functional[62] was used with the def2-SVP basis set.[63] Computations were performed using the SCRF solvent model set to $Et_2O$. Stationary points were confirmed as local minima by the lack of imaginary frequencies.

## X-Ray Diffraction Data

X-ray data for **3.2$_a$**, **3.4** and **3.5** were carried out on a Bruker Apex II diffractometer using MoKα radiation (λ = 0.71073) Å at 100 K. The data collections were performed using a CCD area detector from a single crystal mounted on a glass fibre. Intensities were integrated[49] and absorption corrections based on equivalent reflections using SADABS[50] were applied. The structures were solved by the dual-space algorithm SHELXT[51] and refined against all $F^2$ in ShelXL[52] using Olex2.[53] All the non-hydrogen atoms were refined anisotropically. Hydrogen atoms bound to N1 and B1 in **3.2a** and N1, B1, and Ru1 in **3.5** were located directly from the electron density map, while all other hydrogen atoms were calculated geometrically and refined using a riding model. Hydrogen atom positions were calculated geometrically and refined using the riding model. Most hydrogen atom positions were calculated geometrically and refined using the riding model, but some hydrogen atoms were refined freely.

**Table 3.1:** Selected crystallographic data for **3.2a**, **3.4**, and **3.5.**

| Identification | 3.2a | 3.4 | 3.5 |
|---|---|---|---|
| chemical formula | $C_6H_{13}BF_6N_2O_4S_2$ | $C_{31}H_{48}BN_3$ | $C_{40}H_{80}BNP_2Ru$ |
| crystal colour | Colourless | Colourless | Pale Yellow |
| *Fw*; *F*(000) | 366.11; 372.0 | 473.53; 1040.0 | 748.87; 812.0 |
| *T* (K) | 100(2) | 100(2) | 100(2) |
| wavelength (Å) | 0.71073 | 0.71073 | 0.71073 |
| space group | P-1 | $P2_1/n$ | P-1 |
| *a* (Å) | 7.1264(12) | 12.1391(3) | 9.7888(19) |
| *b* (Å) | 10.4767(17) | 19.3257(5) | 10.243(2) |
| *c* (Å) | 10.9091(18) | 12.6049(3) | 21.124(4) |
| α (deg) | 68.718(3) | 90 | 96.333(3) |
| β (deg) | 77.003(3) | 94.4863(14) | 91.127(2) |
| γ (deg) | 70.331(3) | 77.003(3) | 102.878(2) |
| *Z* | 2 | 4 | 2 |
| *V* (Å$^3$) | 709.7(2) | 2948.01(13) | 2049.9(7) |
| $\rho_{calcd}$ (g·cm$^{-3}$) | 1.713 | 1.067 | 1.213 |
| μ (mm$^{-1}$) | 0.458 | 0.061 | 0.487 |
| θ range (deg); completeness | 4.034 to 61.328; 0.988 | 3.866 to 55.89; 1.000 | 1.942 to 50.736; 0.999 |
| collected reflections; $R_\sigma$ | 42357; 0.0094 | 40202; 0.0359 | 7510; 0.0371 |
| unique reflections; $R_{int}$ | 22733; 0.0194 | 7056; 0.0503 | 7510; 0.0000 |
| R1[a]; wR2[b] [I > 2σ(I)] | 0.0248; 0.0635 | 0.0475; 0.1126 | 0.0399; 0.0850 |
| R1; wR2 [all data] | . 0.0275; 0.0655 | 0.0701; 0.1260 | 0.0542; 0.0897 |
| GOOF | 1.056 | 1.024 | 1.039 |
| largest diff peak and hole | 0.57 and -0.36 | 0.28 and -0.26 | 0.87 and -0.43 |

[a] $R_1=\Sigma(||F_o|-|F_c||)/\Sigma|F_o|$

[b] $wR_2=\{\Sigma[w(F_o^2-F_c^2)^2]/\Sigma[w(F_o^2)^2]\}^{1/2}$

## 3.6 References


(1) Staubitz, A.; Robertson, A. P. M.; Sloan, M. E.; Manners, I. Amine− and Phosphine−Borane Adducts: New Interest in Old Molecules. *Chemical Reviews* **2010**, *110* (7), 4023–4078. https://doi.org/10.1021/cr100105a.

(2) Leitao, E. M.; Jurca, T.; Manners, I. Catalysis in Service of Main Group Chemistry Offers a Versatile Approach to P-Block Molecules and Materials. *Nature Chemistry* **2013**, *5*, 817. https://doi.org/10.1038/nchem.1749.

(3) Han, D.; Anke, F.; Trose, M.; Beweries, T. Recent Advances in Transition Metal Catalysed Dehydropolymerisation of Amine Boranes and Phosphine Boranes. *Coordination Chemistry Reviews* **2019**, *380*, 260–286. https://doi.org/10.1016/j.ccr.2018.09.016.

(4) Dück, K.; Gates, D. P. Main-Chain, Phosphorus-Based Polymers. In *Main Group Strategies towards Functional Hybrid Materials*; John Wiley & Sons, Ltd, 2018; pp 329–355. https://doi.org/10.1002/9781119235941.ch13.

(5) Vidal, F.; Jäkle, F. Functional Polymeric Materials Based on Main-Group Elements. *Angewandte Chemie International Edition* **2019**, *58* (18), 5846–5870. https://doi.org/10.1002/anie.201810611.

(6) Colebatch, A. L.; Weller, A. S. Amine-Borane Dehydropolymerization: Challenges and Opportunities. *Chemistry – A European Journal* **2019**, *25* (6), 1379–1390. https://doi.org/10.1002/chem.201804592.

(7) Nakhmanson, S. M.; Nardelli, M. B.; Bernholc, J. Ab Initio Studies of Polarization and Piezoelectricity in Vinylidene Fluoride and BN-Based Polymers. *Physical Review Letters* **2004**, *92* (11). https://doi.org/10.1103/PhysRevLett.92.115504.

(8) Bernard, S.; Miele, P. Polymer-Derived Boron Nitride: A Review on the Chemistry, Shaping and Ceramic Conversion of Borazine Derivatives. *Materials* **2014**, *7* (11), 7436–7459. https://doi.org/10.3390/ma7117436.

(9) Oldroyd, N. L.; Chitnis, S. S.; LaPierre, E. A.; Annibale, V. T.; Walsgrove, H. T. G.; Gates, D. P.; Manners, I. Ambient Temperature Carbene-Mediated Depolymerization: Stoichiometric and Catalytic Reactions of *N* -Heterocyclic- and Cyclic(Alkyl)Amino Carbenes with Poly( *N* -Methylaminoborane) $[MeNH–BH_2]_n$. *Journal of the American Chemical Society* **2022**, *144* (50), 23179–23190. https://doi.org/10.1021/jacs.2c10931.

(10) Sailors, H. R.; Hogan, J. P. History of Polyolefins. *Journal of Macromolecular Science: Part A - Chemistry* **1981**, *15* (7), 1377–1402. https://doi.org/10.1080/00222338108056789.

(11) Galli, P.; Vecellio, G. Technology: Driving Force behind Innovation and Growth of Polyolefins. *Progress in Polymer Science* **2001**, *26* (8), 1287–1336. https://doi.org/10.1016/S0079-6700(01)00029-6.

(12) Sauter, D. W.; Taoufik, M.; Boisson, C. Polyolefins, a Success Story. *Polymers* **2017**, *9* (6), 185. https://doi.org/10.3390/polym9060185.

(13) De Albuquerque Pinheiro, C. A.; Roiland, C.; Jehan, P.; Alcaraz, G. Solventless and Metal-Free Synthesis of High-Molecular-Mass Polyaminoboranes from Diisopropylaminoborane and Primary Amines. *Angewandte Chemie International Edition* **2018**, *57* (6), 1519–1522. https://doi.org/10.1002/anie.201710293.

(14) Devillard, M.; Pinheiro, C. A. D. A.; Caytan, E.; Roiland, C.; Dinoi, C.; Rosal, I. D.; Alcaraz, G. Uncatalyzed Formation of Polyaminoboranes from

Diisopropylaminoborane and Primary Amines: A Kinetically Controlled Polymerization Reaction. *Advanced Synthesis & Catalysis* **2021**, *363* (9), 2417–2426. https://doi.org/10.1002/adsc.202001458.

(15) Metters, O. J.; Chapman, A. M.; Robertson, A. P. M.; Woodall, C. H.; Gates, P. J.; Wass, D. F.; Manners, I. Generation of Aminoborane Monomers RR′$NBH_2$ from Amine–Boronium Cations [RR′NH–$BH_2$L]+: Metal Catalyst-Free Formation of Polyaminoboranes at Ambient Temperature. *Chemical Communications* **2014**, *50* (81), 12146–12149. https://doi.org/10.1039/C4CC05145A.

(16) Stephens, F. H.; Baker, R. T.; Matus, M. H.; Grant, D. J.; Dixon, D. A. Acid Initiation of Ammonia–Borane Dehydrogenation for Hydrogen Storage. *Angewandte Chemie International Edition* **2007**, *46* (5), 746–749. https://doi.org/10.1002/anie.200603285.

(17) Carpenter, J. D.; Ault, B. S. Infrared Matrix Isolation Study of the Reaction of Diborane with the Methylamines. *Journal of Physical Chemistry* **1991**, *95* (9), 3507–3511. https://doi.org/10.1021/j100162a014.

(18) Johnson, H. C.; Weller, A. S. A Tert-Butyl-Substituted Amino-Borane Bound to an Iridium Fragment: A Latent Source of Free $H_2BN$*t*BuH. *Journal of Organometallic Chemistry* **2012**, *721–722*, 17–22. https://doi.org/10.1016/j.jorganchem.2012.07.018.

(19) MacInnis, M. C.; McDonald, R.; Ferguson, M. J.; Tobisch, S.; Turculet, L. Four-Coordinate, 14-Electron $Ru^{II}$ Complexes: Unusual Trigonal Pyramidal Geometry Enforced by Bis(Phosphino)Silyl Ligation. *Journal of the American Chemical Society* **2011**, *133* (34), 13622–13633. https://doi.org/10.1021/ja204935x.

(20) Babón, J. C.; Esteruelas, M. A.; Fernández, I.; López, A. M.; Oñate, E. Evidence for a Bis(Elongated σ)-Dihydrideborate Coordinated to Osmium. *Inorganic Chemistry* **2018**, *57* (8), 4482–4491. https://doi.org/10.1021/acs.inorgchem.8b00155.

(21) Tang, C. Y.; Thompson, A. L.; Aldridge, S. Dehydrogenation of Saturated CC and BN Bonds at Cationic N-Heterocyclic Carbene Stabilized M(III) Centers (M = Rh, Ir). *Journal of the American Chemical Society* **2010**, *132* (30), 10578–10591. https://doi.org/10.1021/ja1043787.

(22) Yamamoto, Y.; Miyamoto, K.; Umeda, J.; Nakatani, Y.; Yamamoto, T.; Miyaura, N. Synthesis of B-Trisubstituted Borazines *via* the Rhodium-Catalyzed Hydroboration of Alkenes with N,N′,N″-Trimethyl or N,N′,N″-Triethylborazine. *Journal of Organometallic Chemistry* **2006**, *691* (23), 4909–4917. https://doi.org/10.1016/j.jorganchem.2006.08.024.

(23) M. Hansmann, M.; L. Melen, R.; S. Wright, D. Group 13 BN Dehydrocoupling Reagents, Similar to Transition Metal Catalysts but with Unique Reactivity. *Chemical Science* **2011**, *2* (8), 1554–1559. https://doi.org/10.1039/C1SC00154J.

(24) Ledger, A. E. W.; Ellul, C. E.; Mahon, M. F.; Williams, J. M. J.; Whittlesey, M. K. Ruthenium Bidentate Phosphine Complexes for the Coordination and Catalytic Dehydrogenation of Amine– and Phosphine–Boranes. *Chemistry – A European Journal* **2011**, *17* (31), 8704–8713. https://doi.org/10.1002/chem.201100101.

(25) Malcolm, A. C.; Sabourin, K. J.; McDonald, R.; Ferguson, M. J.; Rivard, E. Donor–Acceptor Complexation and Dehydrogenation Chemistry of Aminoboranes. *Inorganic Chemistry* **2012**, *51* (23), 12905–12916. https://doi.org/10.1021/ic3018997.

(26) García-Vivó, D.; Huergo, E.; Ruiz, M. A.; Travieso-Puente, R. Thermally Induced Dehydrogenation of Amine–Borane Adducts and Ammonia–Borane by Group 6 Cyclopentadienyl Complexes Having Single and Triple-Metal–Metal Bonds. *European Journal of Inorganic Chemistry* **2013**, *2013* (28), 4998–5008. https://doi.org/10.1002/ejic.201300629.

(27) Erickson, K. A.; Wright, D. S.; Waterman, R. Dehydrocoupling of Amine Boranes *via* Tin(IV) and Tin(II) Catalysts. *Journal of Organometallic Chemistry* **2014**, *751*, 541–545. https://doi.org/10.1016/j.jorganchem.2013.11.012.

(28) Bellham, P.; Hill, M. S.; Kociok-Köhn, G. Stoichiometric and Catalytic Reactivity of Tert-Butylamine–Borane with Calcium Silylamides. *Organometallics* **2014**, *33* (20), 5716–5721. https://doi.org/10.1021/om500467b.

(29) Esteruelas, M. A.; Fernández, I.; López, A. M.; Mora, M.; Oñate, E. Osmium-Promoted Dehydrogenation of Amine–Boranes and B–H Bond Activation of the Resulting Amino–Boranes. *Organometallics* **2014**, *33* (5), 1104–1107. https://doi.org/10.1021/om500027p.

(30) Erickson, K. A.; Stelmach, J. P. W.; Mucha, N. T.; Waterman, R. Zirconium-Catalyzed Amine Borane Dehydrocoupling and Transfer Hydrogenation. *Organometallics* **2015**, *34* (19), 4693–4699. https://doi.org/10.1021/acs.organomet.5b00415.

(31) Gomberg, M. An instance of trivalent carbon, triphenylmethyl. *Journal of the American Chemical Society* **1900**, *22* (11), 757–771. https://doi.org/10.1021/ja02049a006.

(32) Hicks, R. G. What's New in Stable Radical Chemistry? *Organic & Biomolecular Chemistry* **2007**, *5* (9), 1321. https://doi.org/10.1039/b617142g.

(33) E. Stubbs, N.; Jurca, T.; M. Leitao, E.; H. Woodall, C.; Manners, I. Polyaminoborane Main Chain Scission Using N-Heterocyclic Carbenes ; Formation of Donor-Stabilised Monomeric Aminoboranes. *Chemical Communications* **2013**, *49* (80), 9098–9100. https://doi.org/10.1039/C3CC44373F.

(34) Sabourin, K. J.; Malcolm, A. C.; McDonald, R.; Ferguson, M. J.; Rivard, E. Metal-Free Dehydrogenation of Amine–Boranes by an N-Heterocyclic Carbene. *Dalton Transactions* **2013**, *42* (13), 4625. https://doi.org/10.1039/c3dt32988g.

(35) Wang, Y.; Quillian, B.; Wei, P.; Wannere, C. S.; Xie, Y.; King, R. B.; Schaefer, H. F.; Schleyer, P. v. R.; Robinson, G. H. A Stable Neutral Diborene Containing a BB Double Bond. *Journal of the American Chemical Society* **2007**, *129* (41), 12412–12413. https://doi.org/10.1021/ja075932i.

(36) Al-Rafia, S. M. I.; McDonald, R.; Ferguson, M. J.; Rivard, E. Preparation of Stable Low-Oxidation-State Group 14 Element Amidohydrides and Hydride-Mediated Ring-Expansion Chemistry of N-Heterocyclic Carbenes. *Chemistry – A European Journal* **2012**, *18* (43), 13810–13820. https://doi.org/10.1002/chem.201202195.

(37) Paetzold, P. New Perspectives in Boron-Nitrogen Chemistry - I. *Pure and Applied Chemistry* **1991**, *63* (3), 345–350. https://doi.org/10.1351/pac199163030345.

(38) Alcaraz, G.; Vendier, L.; Clot, E.; Sabo-Etienne, S. Ruthenium Bis(σ-B–H) Aminoborane Complexes from Dehydrogenation of Amine–Boranes: Trapping of $H_2B{=}NH_2$. *Angewandte Chemie* **2010**, *122* (5), 930–932. https://doi.org/10.1002/ange.200905970.

(39) Addy, D. A.; Bates, J. I.; Kelly, M. J.; Riddlestone, I. M.; Aldridge, S. Aminoborane σ Complexes: Significance of Hydride Co-Ligands in Dynamic Processes and Dehydrogenative Borylene Formation. *Organometallics* **2013**, *32* (6), 1583–1586. https://doi.org/10.1021/om400040q.

(40) Vidovic, D.; Addy, D. A.; Krämer, T.; McGrady, J.; Aldridge, S. Probing the Intrinisic Structure and Dynamics of Aminoborane Coordination at Late Transition Metal Centers: Mono(σ-BH) Binding in $[CpRu(PR_3)_2(H_2BNCy_2)]^+$. *Journal of the American Chemical Society* **2011**, *133* (22), 8494–8497. https://doi.org/10.1021/ja203051d.

(41) Joost, M.; Alcaraz, G.; Vendier, L.; Poblador-Bahamonde, A.; Clot, E.; Sabo-Etienne, S. Synthesis of a Ruthenium Bis(Diisopropylamino(Isocyano)Borane) Complex from the Activation of an Amino(Cyano)Borane. *Dalton Transactions* **2013**, *42* (3), 776–781. https://doi.org/10.1039/C2DT32274A.

(42) Bénac-Lestrille, G.; Helmstedt, U.; Vendier, L.; Alcaraz, G.; Clot, E.; Sabo-Etienne, S. Dimethylaminoborane ($H_2BNMe_2$) Coordination to Late Transition Metal Centers: Snapshots of the B–H Oxidative Addition Process. *Inorganic Chemistry* **2011**, *50* (21), 11039–11045. https://doi.org/10.1021/ic201573q.

(43) Tang, C. Y.; Thompson, A. L.; Aldridge, S. Rhodium and Iridium Aminoborane Complexes: Coordination Chemistry of BN Alkene Analogues. *Angewandte Chemie International Edition* **2010**, *49* (5), 921–925. https://doi.org/10.1002/anie.200906171.

(44) Y. Tang, C.; Phillips, N.; I. Bates, J.; L. Thompson, A.; J. Gutmann, M.; Aldridge, S. Dimethylamine Borane Dehydrogenation Chemistry: Syntheses, X-Ray and Neutron Diffraction Studies of 18-Electron Aminoborane and 14-Electron

Aminoboryl Complexes. *Chemical Communications* **2012**, *48* (65), 8096–8098. https://doi.org/10.1039/C2CC33361A.

(45) Stevens, C. J.; Dallanegra, R.; Chaplin, A. B.; Weller, A. S.; Macgregor, S. A.; Ward, B.; McKay, D.; Alcaraz, G.; Sabo-Etienne, S. $[Ir(PCy_3)_2(H)_2(H_2B\text{-}NMe_2)]^+$ as a Latent Source of Aminoborane: Probing the Role of Metal in the Dehydrocoupling of $H_3B\text{-}NMe_2H$ and Retrodimerisation of $[H_2BNMe_2]_2$. *Chemistry – A European Journal* **2011**, *17* (10), 3011–3020. https://doi.org/10.1002/chem.201002517.

(46) Cassen, A.; Vendier, L.; Daran, J.-C.; Poblador-Bahamonde, A. I.; Clot, E.; Alcaraz, G.; Sabo-Etienne, S. B–C Bond Cleavage and Ru–C Bond Formation from a Phosphinoborane: Synthesis of a Bis-σ Borane Aryl-Ruthenium Complex. *Organometallics* **2014**, *33* (24), 7157–7163. https://doi.org/10.1021/om500972f.

(47) Gorgas, N.; Stöger, B.; Veiros, L. F.; Kirchner, K. Access to FeII Bis(σ-B−H) Aminoborane Complexes through Protonation of a Borohydride Complex and Dehydrogenation of Amine-Boranes. *Angewandte Chemie* **2019**, *131* (39), 14012–14017. https://doi.org/10.1002/ange.201906971.

(48) Wallis, C. J.; Alcaraz, G.; Petit, A. S.; Poblador-Bahamonde, A. I.; Clot, E.; Bijani, C.; Vendier, L.; Sabo-Etienne, S. A Highly Effective Ruthenium System for the Catalyzed Dehydrogenative Cyclization of Amine–Boranes to Cyclic Boranes under Mild Conditions. *Chemistry – A European Journal* **2015**, *21* (37), 13080–13090. https://doi.org/10.1002/chem.201501569.

(49) Wallis, C. J.; Dyer, H.; Vendier, L.; Alcaraz, G.; Sabo-Etienne, S. Dehydrogenation of Diamine–Monoboranes to Cyclic Diaminoboranes: Efficient Ruthenium-

Catalyzed Dehydrogenative Cyclization. *Angewandte Chemie International Edition* **2012**, *51* (15), 3646–3648. https://doi.org/10.1002/anie.201108874.

(50) Robertson, A. P. M.; Leitao, E. M.; Manners, I. Catalytic Redistribution and Polymerization of Diborazanes: Unexpected Observation of Metal-Free Hydrogen Transfer between Aminoboranes and Amine-Boranes. *Journal of the American Chemical Society* **2011**, *133* (48), 19322–19325. https://doi.org/10.1021/ja208752w.

(51) Leitao, E. M.; Stubbs, N. E.; Robertson, A. P. M.; Helten, H.; Cox, R. J.; Lloyd-Jones, G. C.; Manners, I. Mechanism of Metal-Free Hydrogen Transfer between Amine–Boranes and Aminoboranes. *Journal of the American Chemical Society* **2012**, *134* (40), 16805–16816. https://doi.org/10.1021/ja307247g.

(52) Paetzold, P.; Plotho, C. V.; Schmid, G.; Boese, R.; Schrader, B.; Bougeard, D.; Pfeiffer, U.; Gleiter, R.; Schüfer, W. Darstellung, Reaktionen und Struktur von tert-Butyl(tert-butylimino)boran. *Chemische Berichte* **1984**, *117* (3), 1089–1102. https://doi.org/10.1002/cber.19841170324.

(53) Bulak, E.; Herberich, G. E.; Manners, I.; Mayer, H.; Paetzold, P. Synthesis and Structure of [$Cp_2$NbH(tBuB≡NtBu)], a Compound with Side-on Coordinated Iminoborane. *Angewandte Chemie International Edition in English* **1988**, *27* (7), 958–959. https://doi.org/10.1002/anie.198809581.

(54) Jaska, C. A.; Temple, K.; Lough, A. J.; Manners, I. Transition Metal-Catalyzed Formation of Boron−Nitrogen Bonds: Catalytic Dehydrocoupling of Amine-Borane Adducts to Form Aminoboranes and Borazines. *Journal of the American Chemical Society* **2003**, *125* (31), 9424–9434. https://doi.org/10.1021/ja030160l.

(55) Winner, L.; Ewing, W. C.; Geetharani, K.; Dellermann, T.; Jouppi, B.; Kupfer, T.; Schäfer, M.; Braunschweig, H. Spontaneous Metal-Free Transfer Hydrogenation of Iminoboranes with Ammonia Borane and Amine Boranes. *Angewandte Chemie International Edition* **2018**, *57* (38), 12275–12279. https://doi.org/10.1002/anie.201807435.

(56) Robertson, A. P. M.; Leitao, E. M.; Jurca, T.; Haddow, M. F.; Helten, H.; Lloyd-Jones, G. C.; Manners, I. Mechanisms of the Thermal and Catalytic Redistributions, Oligomerizations, and Polymerizations of Linear Diborazanes. *Journal of the American Chemical Society* **2013**, *135* (34), 12670–12683. https://doi.org/10.1021/ja404247r.

(57) Nutt, W. R.; McKee, M. L. Theoretical Study of Reaction Pathways to Borazine. *Inorganic Chemistry* **2007**, *46* (18), 7633–7645. https://doi.org/10.1021/ic070193s.

(58) Pangborn, A. B.; Giardello, M. A.; Grubbs, R. H.; Rosen, R. K.; Timmers, F. J. Safe and Convenient Procedure for Solvent Purification. *Organometallics* **1996**, *15* (5), 1518–1520. https://doi.org/10.1021/om9503712.

(59) Bantreil, X.; Nolan, S. P. Synthesis of N -Heterocyclic Carbene Ligands and Derived Ruthenium Olefin Metathesis Catalysts. *Nature Protocols* **2011**, *6* (1), 69–77. https://doi.org/10.1038/nprot.2010.177.

(60) Borowski, A. F.; Sabo-Etienne, S.; Christ, M. L.; Donnadieu, B.; Chaudret, B. Versatile Reactivity of the Bis(Dihydrogen) Complex $RuH_2(H_2)_2(PCy_3)_2$ toward Functionalized Olefins: Olefin Coordination versus Hydrogen Transfer *via* the Stepwise Dehydrogenation of the Phosphine Ligand. *Organometallics* **1996**, *15* (5), 1427–1434. https://doi.org/10.1021/om950888d.

(61) Gaussian 16, Revision C.01, Frisch, M. J.; Trucks, G. W.; Schlegel, H. B.; Scuseria, G. E.; Robb, M. A.; Cheeseman, J. R.; Scalmani, G.; Barone, V.; Petersson, G. A.; Nakatsuji, H.; Li, X.; Caricato, M.; Marenich, A. V.; Bloino, J.; Janesko, B. G.; Gomperts, R.; Mennucci, B.; Hratchian, H. P.; Ortiz, J. V.; Izmaylov, A. F.; Sonnenberg, J. L.; Williams-Young, D.; Ding, F.; Lipparini, F.; Egidi, F.; Goings, J.; Peng, B.; Petrone, A.; Henderson, T.; Ranasinghe, D.; Zakrzewski, V. G.; Gao, J.; Rega, N.; Zheng, G.; Liang, W.; Hada, M.; Ehara, M.; Toyota, K.; Fukuda, R.; Hasegawa, J.; Ishida, M.; Nakajima, T.; Honda, Y.; Kitao, O.; Nakai, H.; Vreven, T.; Throssell, K.; Montgomery, J. A., Jr.; Peralta, J. E.; Ogliaro, F.; Bearpark, M. J.; Heyd, J. J.; Brothers, E. N.; Kudin, K. N.; Staroverov, V. N.; Keith, T. A.; Kobayashi, R.; Normand, J.; Raghavachari, K.; Rendell, A. P.; Burant, J. C.; Iyengar, S. S.; Tomasi, J.; Cossi, M.; Millam, J. M.; Klene, M.; Adamo, C.; Cammi, R.; Ochterski, J. W.; Martin, R. L.; Morokuma, K.; Farkas, O.; Foresman, J. B.; Fox, D. J. Gaussian, Inc., Wallingford CT, 2016.

(62) Adamo, C.; Barone, V. Toward Reliable Density Functional Methods without Adjustable Parameters: The PBE0 Model. *The Journal of Chemical Physics* **1999**, *110* (13), 6158–6170. https://doi.org/10.1063/1.478522.

(63) Weigend, F.; Ahlrichs, R. Balanced Basis Sets of Split Valence, Triple Zeta Valence and Quadruple Zeta Valence Quality for H to Rn: Design and Assessment of Accuracy. *Physical Chemistry Chemical Physics* **2005**, *7* (18), 3297–3305. https://doi.org/10.1039/B508541A.

**Chapter 4**

# Chain Stabilization Yields High Molar Mass Polymers and Molecular Weight Control in the Thermal Dehydropolymerization of *P*-Phenyl Phosphine-Borane

*This chapter has been adapted from the as of yet unpublished work:*

Matthew A. Wiebe, J. E. T. Watson, Charles Killeen, J. Scott McIndoe, Anne Staubitz, and Ian Manners. *Manuscript in preparation.*

*Contributions: M. A. W. and I. M. conceived the project. J. E. T. W. performed dehydropolymerizations of $PhPH_2$•$BH_3$ using commercially available salts ($Sc(OTf_3)$, $[NBu_4][OTf]$, $LiNTf_2$, and MgOTf) in 2-MeTHF. C. K. obtained ESI-MS data on polymeric materials. C. K. and J. S. M. assisted in ESI-MS data interpretation. M. A. W. performed all other synthesis and characterization. M. A. W. interpreted the data and wrote the first draft manuscript which was subsequently edited with A. S. and the other authors.*

## 4.1 Abstract

We report the synthesis of high molar mass polyphosphinoboranes using commercially available reagents through thermal dehydropolymerization in the presence of Lewis acids and bases. The dehydropolymerizations described here produce material of higher molecular weight than the state-of-the-art catalyst, $Cp(CO)_2FeOTf$, ([PhPH–$BH_2$]$_n$ (**4.2**), 5 mol% LiOTf, 2 M in 2-MeTHF, 100 °C, 24 h; $M_n$ = 80 kDa, $Đ$= 1.64). We also propose a three-part mechanism for the high temperature thermal dehydropolymerization of $PhPH_2$•$BH_3$ (**4.1**), which occurs in three distinctive steps. Initially the phosphine-borane adduct dissociates yielding borane *in situ*. This then catalyzes the dehydrogenation of **4.1**. Subsequent addition polymerization occurs as described previously, but the addition of Lewis acids and Lewis bases allow for reversible complexation of both termini. Thus, a competition of temporary chain capping and termination events is generated, ultimately resulting in fewer termination events, leading to high molar mass material. With this mechanism in mind, we are able to show that added $BH_3$•$SMe_2$ allows for control over the molar mass of the resulting materials.

## 4.2 Introduction

Polymers incorporating main-group elements into their main chain are of interest as inclusion of these elements can lead to desirable properties and useful materials, such as polysiloxanes which exhibit tunable glass transition temperatures.[1–9] Another class of polymers that feature a main chain comprised of main group elements are polyphosphinoboranes which feature alternating phosphorus and boron atoms along their main-chain.[1,5,10–13] Polyphosphinoboranes are of interest for materials that exhibit self-extinguishing behaviour,[14] materials for soft lithography,[15] and precursors to solvogels.[16] Further, poly(*P*-phenyl)phosphinoborane is of fundamental interest as an inorganic P–B analogue of polystyrene. These materials were first sought in the 1950's.[17,18] However, well characterized polyphosphinoboranes were not accessed until the turn of the 21st century where the Manners group reported on phosphine-borane adduct dehydropolymerization using Rh catalysts.[19,20] Since this seminal discovery, catalysts have been explored by our and other groups based on Fe,[21,22] Ir,[23] and Rh (**Scheme 4.1**).[24–26] More recently, we have worked in collaboration with the Greb group to showcase the ability of a geometrically constrained aluminate species to act as a dehydropolymerization catalyst[27] and with the Weller group to characterize the first well-defined block copolymer that is comprised of two distinct polyphosphinoborane blocks.[28]

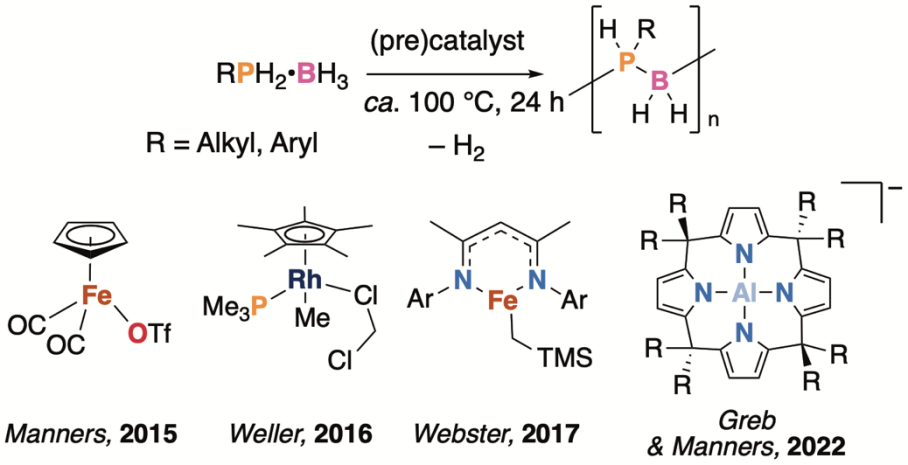


**Scheme 4.1:** Overview of catalytic phosphine-borane dehydropolymerization.

Polyphosphinoboranes can also be accessed through direct generation of transient phosphinoborane monomers *in situ.* This was first demonstrated through the synthesis of *t*BuPH–$BH_2(NMe_3)$ adducts that would lose $NMe_3$ under gentle heating to generate phosphinoborane monomers in solution.[29] Later, we have reported on the synthesis of *P*-disubstituted polyphosphinoborane polymers (i.e. $[PhRP–BH_2]_n$; R = Ph, Et) through the cyclic(alkyl)amino carbene (cAAC) mediated dehydrogenation of requisite phosphine-borane adducts[30] or through the deprotonation of phosphine-(triflimido)borane adducts (**Scheme 4.2**).[31]

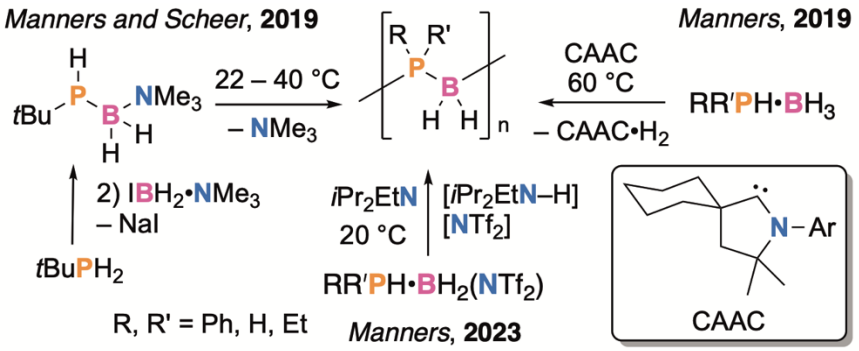


**Scheme 4.2:** Metal-free routes to polyphosphinoboranes *via* the generation of phosphinoboranes *in situ*.

The mechanism of phosphine-borane dehydropolymerization is of interest as mechanism led design of catalysts can result in greater efficiency in accessing materials as well as greater control over the polymer microstructure and degree of polymerization.[32] However, despite mechanistic studies performed thus far,[21,24,25,33,34] the norm for phosphine-borane dehydropolymerization requires the use of a catalyst that normally takes several steps to synthesize, and forcing reaction conditions (≥ 16 h, ≥ 100 °C).[13] Some work has been done computationally, where Pomogaeva and Timoshkin have explored the chemistry of PB decamers *in silico*.[35] They found that end-group complexation of phosphine-borane oligomers can prevent back-biting/cyclization of oligomers (and thus terminating the reactive growing chain). End-group capping by either just a relatively weak Lewis acid or a relatively weak Lewis base is insufficient to prevent this cyclization event to occur, but capping at both ends can disfavor back biting. Further, computational studies have suggested that $BH_3$ can act as a catalyst for the dehydrogenation of phosphine-boranes.[36] Thus, in attempts to better understand the mechanism of dehydropolymerization using the state-of-the-art $CpFe(CO)_2OTf$ catalyst, we explored the ability of LiOTf to catalyze the dehydropolymerization of $PhPH_2{\bullet}BH_3$, **4.1**.

## 4.3 Results and Discussion

First, thermal dehydropolymerization in the absence of additives was explored to generate a benchmark for the reaction. This was achieved by preparing 250 µL of a 2 M solution of $PhPH_2{\bullet}BH_3$ (**4.1**) in toluene in a J Young NMR tube. This tube was then placed in a heating block set to 100 °C for 24 h. Afterwards, the reaction was analyzed by $^{31}P\{^1H\}$

and $^{11}B\{^1H\}$ NMR spectroscopy revealing broad peaks at −48.9 ppm and −34.7 ppm, respectively, indicating that $[PhPH–BH_2]_n$ (**4.2**) had been accessed. Subsequently, the polymeric material was isolated *via* repeated precipitations, first in cold *i*PrOH, and then twice more in cold hexanes resulting in a 35% yield of colourless material. Analysis of the material by gel permeation chromatography (GPC) confirmed that polymer was present, albeit polydisperse material of low molar mass ($M_n$ = 12 680; $Đ$= 2.00) (**Figure 4.1**, left) was detected.

Repeating the above procedure, however with added 5 mol% LiOTf to the reaction mixture, resulted in the formation of higher molecular weight **4.2** ($M_n$ = 42 200; $Đ$= 1.69) in 62% yield. These mass values nearly match the polymer produced when this reaction is performed with 5 mol% of $CpFe(CO)_2OTf$ ($M_n$ = 40 000 $Đ$= 1.70).[21] We were surprised by these results as our initial mechanistic studies suggested that the iron centre was involved in the dehydrogenation and chain growth steps in dehydropolymerization. However, the resulting polymer from LiOTf catalyzed dehydropolymerization is distinct from polymer made from the [Fe] catalyst in that it has no iron-derived impurities. Instead, any LiOTf derived impurities are colourless, and do not discolour the resulting material. Intrigued by this result, we continued to explore the ability of commercially available salts to dehydropolymerize phosphine borane adducts.

To determine the role of trifluoromethanesulfonate (OTf) moiety within LiOTf we explored the ability of other OTf and bis(trifluoromethanesulfonyl)imide ($NTf_2$) salts to catalyze the dehydropolymerization of **4.1**. Accordingly, performing the polymerization described above using $Mg(OTf)_2$ as an additive worked well as a catalyst for the dehydropolymerization of **4.1** to **4.2** ($M_n$ = 32 020; $Đ$ = 1.70, 67% yield). However, using

$Sc(OTf)_3$ resulted in polymer that resembled that of thermal dehydropolymerization ($M_n$ = 12 370; $Đ$= 2.26, 42% yield). Thus, the ability to access high molar mass **4.2** is not general across all OTf species. We then explored dehydropolymerization using the closely related salt, $LiNTf_2$. Similar to LiOTf and $Mg(OTf)_2$, the addition of $LiNTf_2$ also resulted in the formation of high, albeit slightly less high, molar mass **2** ($M_n$ = 29 260; $Đ$= 1.73; 58% yield).

We continued to explore the effect of choice of anionic and cationic components of the additive salts by exploring the effect of using salts with non-coordinating cation in one case and a non-coordinating anion in the other. Here we found that using either $[Bu_4N][OTf]$ or $[Li][B(C_6F_5)_4]•Et_2O$ resulted in polymer that resembled that of thermal dehydropolymerizations with no additives ($[Bu_4N][OTf]$: $M_n$ = 13 110; $Đ$= 1.68; 30% yield; $[Li][B(C_6F_5)_4]•Et_2O$: $M_n$ = 10 980; $Đ$= 2.29; 36% yield) similar to what was observed for $Sc(OTf)_3$. This suggests that being able to access a coordinatively unsaturated anion and cation is key to accessing high molar mass **4.2** as $Sc(OTf)_3$ is a well-established Lewis acid.[37]

We were curious if it was possible to access high molar mass material in the thermal dehydropolymerization of **4.1a** using a more traditional Lewis acid and Lewis base adduct, $BH_3•SMe_2$. Accordingly, performing the polymerization as described above with the addition of 5 mol% of $BH_3•SMe_2$ resulted in the formation of polymeric material as confirmed by GPC ($M_n$ = 27 990; $Đ$= 1.70).

As the presence of Lewis acids and bases *in situ* appeared to assist in the formation of high molar mass **4.2** we targeted the thermal dehydropolymerization of **4.1** in a coordinating solvent rather than an arene solvent, which is more typical for this transformation. Further, in the dehydropolymerizations of closely related amine-borane

adducts, performing reactions in coordinating solvents can result in the formation of higher molar mass material as chain transfer reactions are disfavoured.[38] Accordingly, we performed the dehydropolymerization of **4.1** in 2-MeTHF as this is a solvent has a higher boiling point than THF and is derived from sustainable sources.[39]

Performing the dehydropolymerization of **4.1** as a 2 M solution in 2-MeTHF without any other additives also resulted in the formation of **4.2** after 24 h at 100 °C as determined by $^{31}$P and $^{11}$B NMR spectroscopy. Subsequent isolation was performed in the same manner as described above resulting in a good yield of 70%. Analysis of the polymeric material by GPC revealed that it was of very high molar mass ($M_n$ = 80,680 Da; $Đ$ = 1.66). Notably, this mass is double that from thermal dehydropolymerizations performed under comparable reaction conditions using a 5 mol% loading of $CpFe(CO)_2OTf$ in toluene. Moreover, in our initial study on the dehydropolymerization of $PhPH_2•BH_3$ using $CpFe(CO)_2OTf$ we found that performing the dehydropolymerization in 1,4-dioxane resulted in the formation of higher molar mass material ($M_n$ = 67,000; $Đ$ = 1.35).[21] Further, we assessed the ability of salts to catalyze the formation of high molar mass material and found similar results to those obtained in toluene, where LiOTf, $Mg(OTf)_2$, $LiNTf_2$, and $BH_3•SMe_2$ would produce high molar mass material and $Sc(OTf)_3$, $[Bu_4N][OTf]$, and $[Li][B(C_6F_5)_4]•Et_2O$ produced material of lower molecular weights (**Figure 4.1**, right).

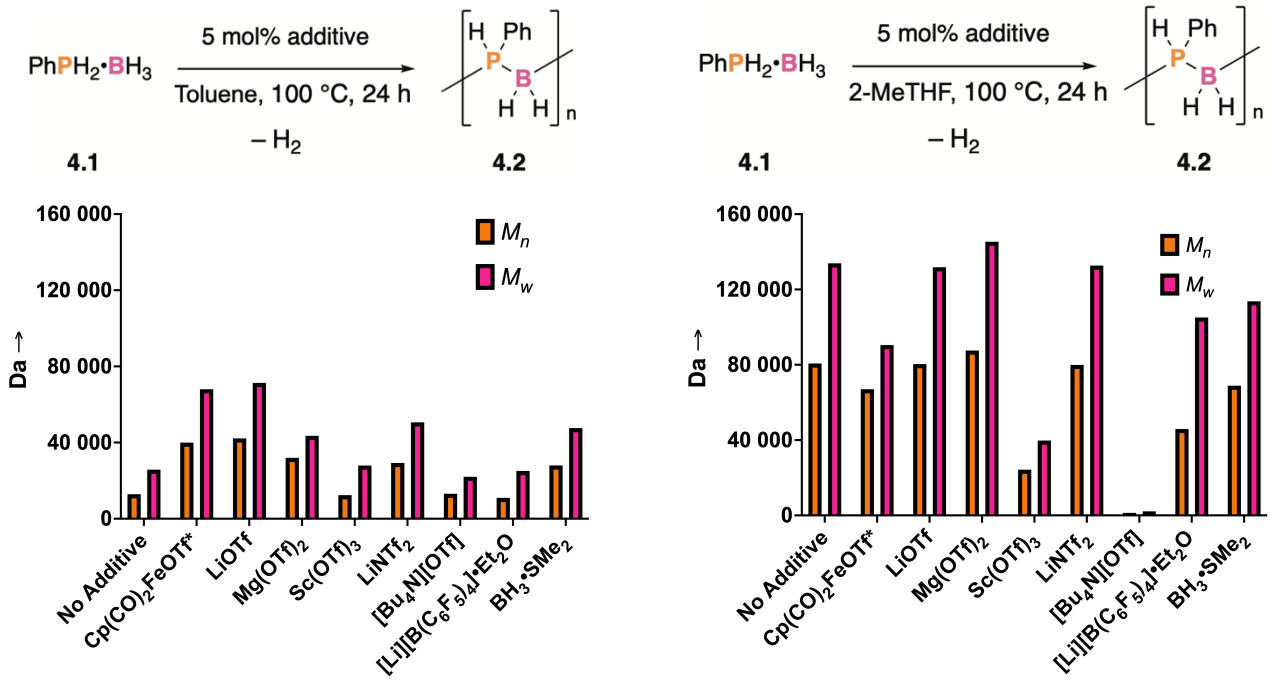


**Figure 4.1:** Left: Dehydropolymerization of **4.1** in toluene with a bar chart depicting the $M_n$ and $M_w$ values obtained from the resulting isolated materials. The value for $Cp(CO)_2FeOTf$ is taken from our previous study on its ability to dehydropolymerize **4.1**.[21] Right: Dehydropolymerization of **4.1** in 2-MeTHF with a bar chart depicting the $M_n$ and $M_w$ values obtained from the resulting isolated materials. *Data for $Cp(CO)_2FeOTf$ is from our initial study on $Cp(CO)_2FeOTf$, where a dehydropolymerization of **4.1** was performed in 1,4-dioxane.[21]

The thermal dehydropolymerization of **4.1** without any additives in 2-MeTHF might appear counterintuitive at first, as the studies in toluene suggest both a Lewis acid and Lewis base must be present *in situ* for high molar mass material to be accessed. However, it may be possible that under the reaction conditions, a small fraction of **4.1** can undergo

adduct dissociation into phenylphosphine ($PhPH_2$) and borane ($BH_3$). Computational studies into the bonding of phosphine-borane adducts estimates that the bond dissociation is unfavourable ($\Delta G° = 13.8$ kcal•mol$^{-1}$),[40] but only a small amount of catalyst is needed in solution. Further, if this dissociation were to occur, both Lewis base (2-MeTHF, $PhPH_2$) and Lewis acid ($BH_3$) would be present *in situ* and would satisfy the conditions established for dehydropolymerizations in toluene.

Having identified LiOTf and $BH_3$•$SMe_2$ as good catalysts in the dehydropolymerization of **4.1**, we aimed establish a relationship between polymer molecular weight and conversion of **4.1** (**Figure 4.2**). Accordingly, separate 2 M solutions of **4.1** with either 5 mol% of $BH_3$•$SMe_2$ or LiOTf in 2-MeTHF were prepared. Each solution was separated equally between eight J Young NMR tubes which were then sealed and placed in a heating block set to 100 °C. Afterwards, the J Young NMR tubes were removed at 15 min, 30 min, 1 h, 2 h, 3, 6 h, 16 h and 24 h. Once cooled to ambient temperature, the solutions were diluted with $CDCl_3$ and analyzed by $^{11}B\{^1H\}$ and $^{31}P\{^1H\}$ NMR spectroscopy (**Figure 4.2**, top). Performing the dehydropolymerization in 2-MeTHF with 5 mol% of LiOTf gave results similar to those observed for the dehydropolymerization with $Cp(CO)_2FeOTf$ performed in toluene, where at 6 h there was *ca.* 35% conversion of **4.1**. Further, analysis of each reaction using LiOTf over the 24 hour period revealed that high molar mass material is obtained within 6 h (**Figure 4.2**, bottom) at this low conversion, similar to what was observed for dehydropolymerizations performed with $CpFe(CO)_2OTf$.[21] However, dehydropolymerizations performed with 5 mol% $BH_3$•$SMe_2$ in 2-MeTHF appeared to occur at a significantly higher rate than LiOTf as significant conversion (> 80%) of **4.1** had occurred within 6 h. Further, analysis of the reaction

products by GPC revealed that a significant portion of high molar mass material was obtained as early as within 3 h. Moreover, two clear polymerization phases can be observed where GPC traces of materials obtained in the dehydropolymerization of **4.1** with 5 mol% of $BH_3$•$SMe_2$. First, GPC traces obtained at or before 6 hours show the progression into a lower molecular weight material as **4.1** approaches *ca.* 90% conversion by NMR spectroscopy with high molar mass material obtained at low conversion (< 25%). However, GPC traces obtained after 6 h reveal the formation of a higher molar mass material, indicative of a step growth mechanism.

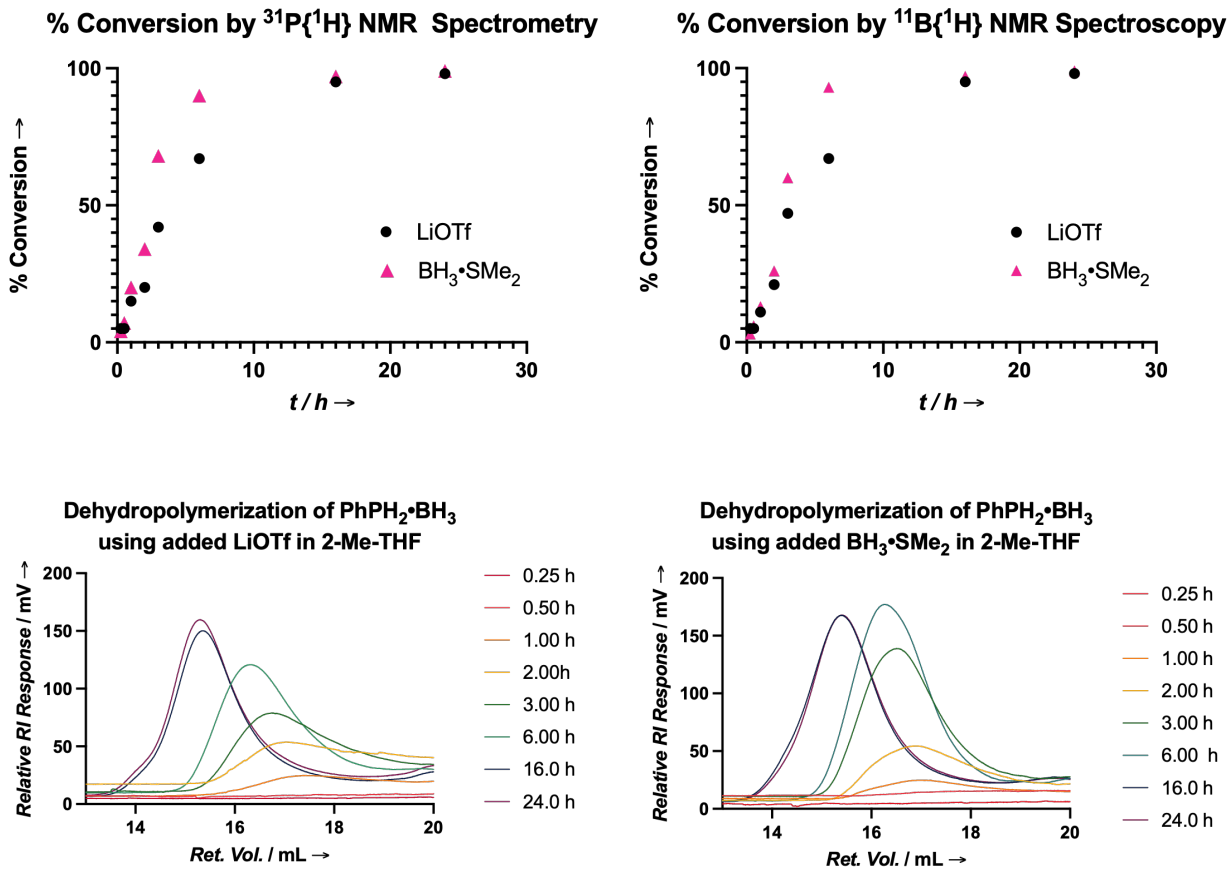


**Figure 4.2**: Conversion of **4.1** to dehydrogenated products over 24 h using either $BH_3$•$SMe_2$ or LiOTf as the catalyst (top) and GPC traces of dehydropolymerizations performed over 24 h. Conversion values were obtained by the relative integrations of **4.1** to **4.2** in $^{31}P\{^1H\}$ or $^{11}B\{^1H\}$ NMR spectra (bottom).

To explore whether parts of the additives could be observed as end-groups in **4.2**, we conducted end-group analysis using electrospray ionization mass spectrometry (ESI-MS). This technique was chosen for its ability to identify oligomeric chains with specific end-groups. Samples of **4.2** were prepared in DCM, and both positive and negative mode

spectra were recorded. For polymerizations performed with either LiOTf or $BH_3$•$SMe_2$, series of peaks separated by 122 m/z, the mass of the [PhPH–$BH_2$] monomer, were observed and signals corresponding to oligomers with up to 23 repeat units could be identified (**Figure 4.8**, in the experimental). Closer inspection of the positive mode spectra with peaks in the 1 300 – 1 500 m/z range indicated that polymerizations carried out with 5 mol% of LiOTf predominantly featured decamers and undecamers with H and $PhPH_2$ end-groups (**Figure 4.9**, in the experimental). In contrast, for polymerizations performed with 5 mol% of $BH_3$•$SMe_2$, positive mode spectra within the same range reveal signals corresponding to oligomers with $BH_2(SMe_2)$ and H end groups, in addition to those with H and $PhPH_2$ end-groups. In negative mode ESI-MS spectra for polymerizations performed with either LiOTf or $BH_3$•$SMe_2$, a series of peaks corresponding to *P*-phenylphosphinoborane decamers and undecamers with $BH_3$ and H end groups are consistently observed. Thus, for polymerizations performed in LiOTf, end-groups incorporating either component of LiOTf could not be observed by ESI-MS. However, as both components of LiOTf are weakly coordinating, it is possible that these potential end groups are displaced in the work up, sample preparation, or in the ESI-MS instrument itself. In contrast, for polymerizations performed with $BH_3$•$SMe_2$, both $BH_3$ and $SMe_2$ were observed as chain caps. The source of $BH_3$ end groups could either be from **4.1** or $BH_3$•$SMe_2$, but the presence of the $BH_2(SMe_2)$ chain-ends implicates that $BH_3$•$SMe_2$ has a role in chain propagation of the growing polymer.

Based on the results from dehydropolymerizations of **4.1** performed in toluene and 2-MeTHF, as well as the studies on the dehydropolymerizations performed over 24 hours, and the end-group analysis of samples of **4.2**, I believe the following mechanism may be

occurring (**Scheme 4.3**). First, at elevated temperatures cleavage of phosphine-borane at elevated temperature yields a small portion of free borane ($BH_3$) *in situ* (**Scheme 4.3** a). Then, free borane acts as the true dehydrogenation catalyst, enabling the formation of phosphinoborane monomers (**M**), which undergo subsequent addition polymerization to produce polymeric material (**P**) (**Scheme 4.3** b). This hypothesis is supported by the observation that polymerizations performed with added $BH_3$ exhibit significantly higher rates of conversion (> 80% conversion of **4.1** within 6 h, **Figure 4.2**) and yield high molar mass, low dispersity materials more rapidly (within 3 h, **Figure 4.2**) than polymerizations performed without. For example, for the polymerization performed with LiOTf (i.e. no added borane), greater than 80% conversion of **4.1** occurs after 6 h, and a significant portion of high molar mass, low dispersity material is also only obtained after 6 h.

Thus, the role of the additive is likely in the stabilization of the growing chain (**P**). From the polymerizations performed in toluene and 2-MeTHF, it was revealed that additives that had both Lewis acidic and basic components were required to access high molar mass materials (**Figure 4.1**). Further, ESI-MS of polymeric materials obtained using added $BH_3$•$SMe_2$ revealed the presence of oligomers with end groups corresponding to both $BH_3$ and $SMe_2$ (**Figure 4.10**, in the experimental). Furthermore, polymerizations performed in coordinating solvents accessed material of higher molar mass than those performed in non-coordinating solvents (**Figure 4.1**). Moreover, performing polymerizations in the presence of a strong Lewis acid ($Sc(OTf)_3$)[41] consistently results in materials of relatively low molecular weight (**Figure 4.1**). Therefore, we propose that the stabilization may be occurring through the reversible coordination of weak Lewis acids and weak Lewis bases to chain termini (**Scheme 4.3** c). This would allow for the

attenuation of the reactivity of the growing oligomer chain, through accessing a chain-capped dormant species, **LB-P-LA**, allowing for reactions that compete with chain termination including cyclization reactions.[35] The dormant species, **LB-P-LA**, could release either **LB** or **LA** to access **P-LA** or **LB-P**. Either dissociation would result in the formation of an active species which can continue growth *via* addition polymerization through reactions with **M**. Further, either **LB-P** or **P-LA** can readily recombine with either **LA** or **LB** to access the dormant species. However, reactions between **LB-P** and **P-LA** would also allow for reformation of the dormant species coupled with an increase in the chain length. Moreover, the ability to favour the formation of the dormant species either through choice of Lewis acid and Lewis base, or the loading of the chosen Lewis acid and Lewis base may allow for greater control over the polymerization of phosphinoboranes produced *in situ*.

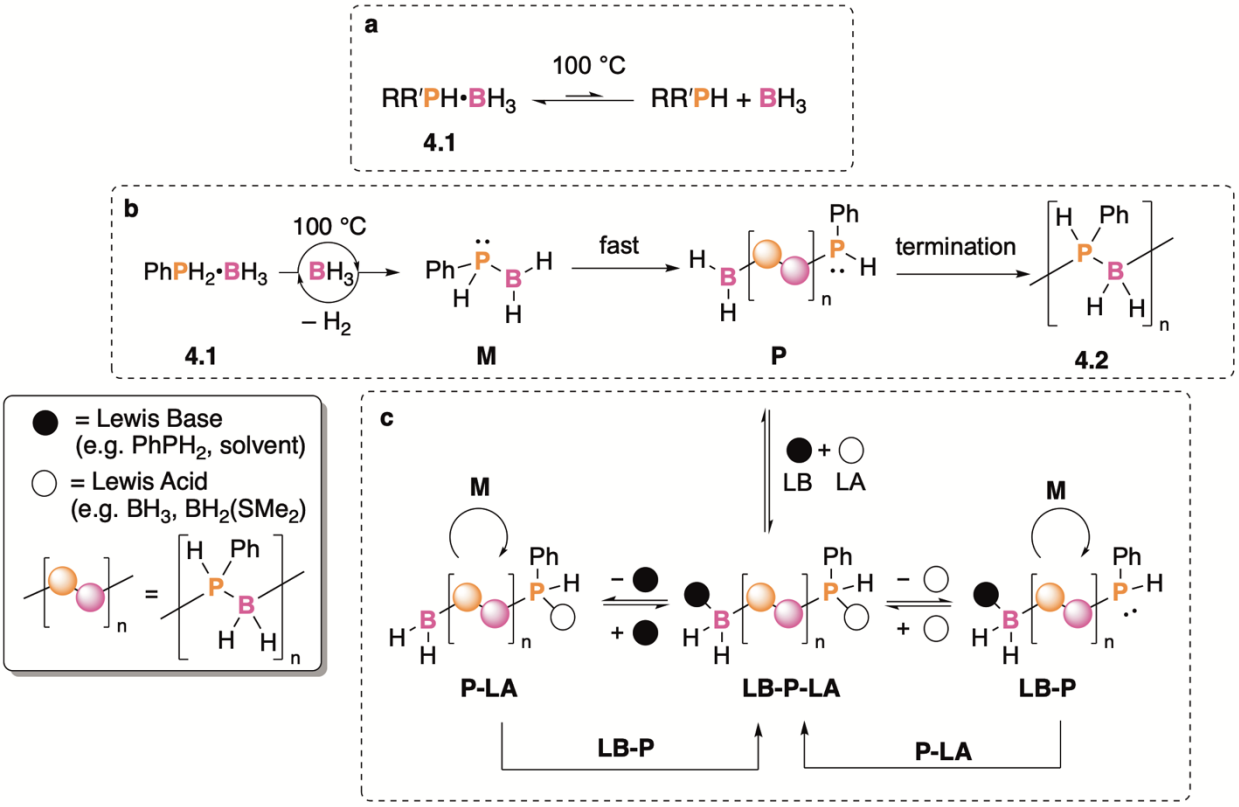


**Scheme 4.3:** Proposed mechanism for the dehydropolymerization of **4.1** at elevated temperatures.

If the above mechanism were in operation, it may be possible to control the degree of polymerization as a greater concentration of Lewis Base and Lewis Acid *in situ* would potentially favour the dormant species (**LB-P-LA**) and result in material of lower molecular weight. Accordingly, 5 different loadings were explored (1 mol%, 2.5 mol%, 5 mol%, 7.5 mol%, and 10 mol%) of either LiOTf or $BH_3$•$SMe_2$ while maintaining a concentration of 2 M of **4.1** in 2-MeTHF (**Figure 4.3**). The dehydropolymerization reactions were performed at 100 °C and the reactions occurred over the course of 24 hours. Dehydrocoupling was determined to have occurred in each case and subsequent isolation of the materials resulted in moderate to good yields (50% to 74%). Analysis of the polymers produced

with 1 – 10 mol% of LiOTf added revealed that while low loadings of LiOTf resulted in material of higher molar mass, no real correlation between LiOTf loading and the obtained polymer molar mass could be observed at loadings at or greater than 5 mol%. However, polymerizations performed with added $BH_3$•$SMe_2$ revealed a clear relationship between loading and degree of polymerization across conditions attempted (1 – 10 mol% of $BH_3$•$SMe_2$), obtaining materials over a wide mase range with similar dispersity (83,120 – 57,740 Da; *Đ ca*. 1.66). This control over the resulting material further supports the mechanism proposed in **Scheme 4.3.**

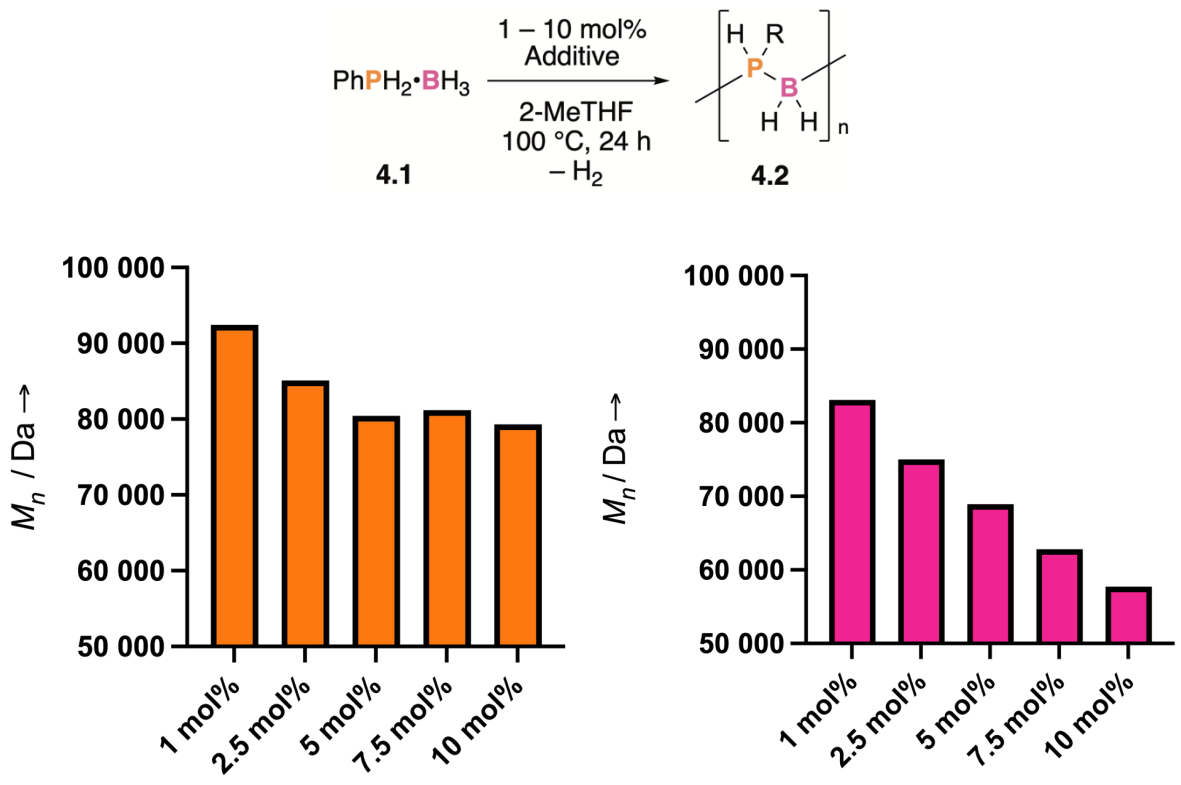


**Figure 4.3**: Effect of additive loading on the dehydropolymerization of **4.1** with a bar chart showing the $M_n$ values obtained for reactions performed using LiOTf on the left and reactions performed using $BH_3$•$SMe_2$ on the right.

## 4.4 Conclusion

In summary, we report the synthesis of high molar mass polyphosphinoboranes using commercially available reagents. We propose that thermal dehydropolymerization occurs in three major steps: adduct dissociation to give free borane, allowing for the second step where free borane catalytically dehydrogenates **4.1**. The third phase is the polymerization step where reactive phosphinoboranes *in situ* catenate to yield linear chains that can then undergo termination events to yield polymeric materials. However, in the presence of additives, such as LiOTf or $BH_3$•$SMe_2$, phosphinoboranes and their chains can participate in Lewis acid base chemistry at either terminus, competing with termination events and allowing for further chain growth to access polymers. This approach has allowed for the synthesis of high molar mass **4.2** from the dehydropolymerization of **4.1** in 2-MeTHF, where the presence of additives can afford control over the resulting materials, with $BH_3$•$SMe_2$ having a clear relationship to $M_n$ of the resulting material over a wide mass range ($M_n$ = 57,740 – 83,120 Da). Overall this work has implications for the field of phosphine-borane dehydropolymerization in that high molar mass material can be accessed using sustainable and readily available reagents. Moreover, this work provides evidence for an alternative mechanism that may allow for greater control over the addition polymerization of phosphinoborane monomers produced *in situ*. Further work is underway in supporting this mechanism, exploring scope, and ability to synthesize block-copolymers.

## 4.5 Experimental

Unless otherwise noted, storage and manipulation of chemicals were performed under an inert atmosphere of either $N_2$ or Ar gas using standard Schlenk techniques, or, carried out in an MBraun 200B glovebox. Further, any glassware used was dried overnight in a 200 °C oven. Toluene was dried using an MBraun Grubbs/Dow solvent purification system[42] and stored over activated 4 Å molecular sieves. 2-Methyl tetrahydrofuran was purchased from Sigma Aldrich and was dried *via* distillation off sodium metal and degassed *via* freeze-pump-thaw cycles. The phosphine-borane adduct, $PhPH_2{\bullet}BH_3$ (**4.1**), was prepared using standard literature procedures.[19] LiOTf, $Mg(OTf)_2$, $Sc(OTf)_3$, $LiNTf_2$, $[Bu_4N][OTf]$, $[Li][B(C_6F_5)_4]{\bullet}Et_2O$, $BH_3{\bullet}SMe_2$, and $CDCl_3$ were all purchased from Sigma Aldrich and used as received. Solvents used in the isolation of polymeric material were purchased from Sigma Aldrich and used as received.

Nuclear Magnetic Resonance (NMR) spectroscopy was performed on a Bruker Avance NEO 500 MHz spectrometer. $^1H$ NMR spectra were referenced to protons in the solvents and heteronuclear spectra were referenced using the recommended IUPAC reference compounds.

Mass spectrometry experiments were performed with a Waters Synapt G2-Si in positive and negative modes with a capillary voltage of 3.00 kV, a cone voltage of 60 V, and a source offset voltage of 80 V. All samples were prepared in HPLC grade dichloromethane (Supelco, EMD Millipore). An optimal response was obtained using a desolvation gas flow of 100 L $h^{-1}$, cone gas flow of 100 L $h^{-1}$, source temperature of 50 °C, and desolvation gas

temperature of 150 °C. The scan time was set to 2 s with an inter-scan time of 0.1 seconds, over a mass range of *m/z* 50-3000 Da.

Gel-permeation chromatography (GPC) was performed on a Malvern RI max Gel Permeation Chromatograph, equipped with an automatic sampler, a pump, an injector, and inline degasser. The columns (styrene/divinyl benzene gel, 1xT5000 and 1xT3000) were maintained at 35 °C. Sample elution was detected by means of a differential refractometer. THF (VWR), containing 0.1 wt% [*n*-$Bu_4N$]Br to reduce polymer adsorption[15] was used as the eluent at a flow rate of 1 mL $min^{-1}$. Samples were dissolved in THF (2 mg/mL) and filtered through a 0.2 µm PTFE syringe filter before analysis. Calibration was conducted using commercially available monodisperse polystyrene standards (Aldrich, 1 200 – 4 200 000 Da).

**Thermal Dehydrogenation of 1 in Toluene**

To a 1 dram vial was added 0.5 mmol (62 mg) of phosphine-orane adduct, **4.1**, and toluene (250 µL). Then, this solution was transferred to a J Young NMR tube. The J Young NMR tube containing **4.1** was then sealed and removed from the glovebox and placed in a heating block set to 100 °C. The reaction was heated at this temperature over the course of 24 h, after which the heating plate was turned off, and the reaction was left to cool. Once the thermometer indicated the heating block was at or below 30 °C, the tubes were removed from the heating block and carefully unsealed to allow the built-up pressure to release. Afterwards, $CDCl_3$ was added to the tube in open air, and the reactions were

assessed by $^{31}$P NMR to confirm the reaction was complete and that polyphosphinoborane, **4.2**, was accessed. In order to isolate the polymeric material (**4.2**), the resulting solution of **4.2** was added dropwise to a rapidly stirring solution of *i*PrOH that was previously chilled to –20 °C, resulting in the precipitation of colourless polymeric material. The vial containing the precipitate and supernatant was then centrifugated at 4 000 revolutions per minute (RPM) for 1 h, before decanting the supernatant and collecting the white precipitate. The precipitate was briefly dried in air and redissolved in THF before the precipitation was repeated in rapidly stirring hexanes that was cooled to –20 °C. Subsequently the precipitation was centrifugated at 4000 RPM for 5 minutes, then the precipitate was collected by removal of the supernatant. This precipitate was then dried *in vacuo* for 16 h, resulting in a white powder in 35% yield (22 mg). Analysis by $^{1}$H, $^{11}$B, and $^{31}$P NMR spectra that match what is previously reported. Analysis by GPC resulted in the trace in **Figure 4.4** with tabulated data ($M_n$, $Đ$) given in **Table 4.1**.

.

**Polymerizations Performed in Toluene with Additives**

To a 1 dram vial was added Phosphine-Borane adduct (**4.1**) (0.50 mmol, 62 mg) and toluene (250 µL). Then, in a J Young NMR tube 5 mol% (0.025 mmol) of the additive was weighed out and the solution of **4.1** in toluene was transferred to the tube. The J-Young NMR tube containing **4.1** and the additive was then sealed and removed from the glovebox and placed in a heating block set to 100 °C. The reaction was heated at this temperature over the course of 24 h, after which the heating plate was turned off, and the reaction was left to cool. Once the temperature gauge gave a value below 30 °C, the

tubes were removed from the heating block and carefully unsealed to allow the built-up pressure to release. Afterwards, $CDCl_3$ was added to the tube in open air, and the reactions were assessed by $^{31}P$ NMR to confirm the reaction was complete and polyphosphinoborane (**4.2**) was accessed. Polymer samples were isolated as described above in 30–64% yield. Gel permeation chromatography was used to determine the molar mass of materials accessed with the resulting traces in **Figure 4.4** and tabulated data given in **Table 4.1**.

**$^{1}$H NMR (500 MHz, 298 K, $CDCl_3$)**: δ = 6.85 – 7.52 ppm (5 H, br m, Ar-H), 4.29 ppm (1 H, br d, $^{1}J_{HP}$ = 349 Hz, PH), 1.53 ppm (2 H, br, $BH_2$). **$^{11}$B{$^{1}$H} NMR (160 MHz, 298 K, $CDCl_3$)**: δ = −34.7 ppm (br); **$^{31}$P NMR (200 MHz, 298 K, $CDCl_3$)**: δ = −48.9 ppm (d, $^{1}J_{PH}$ = 349 Hz).

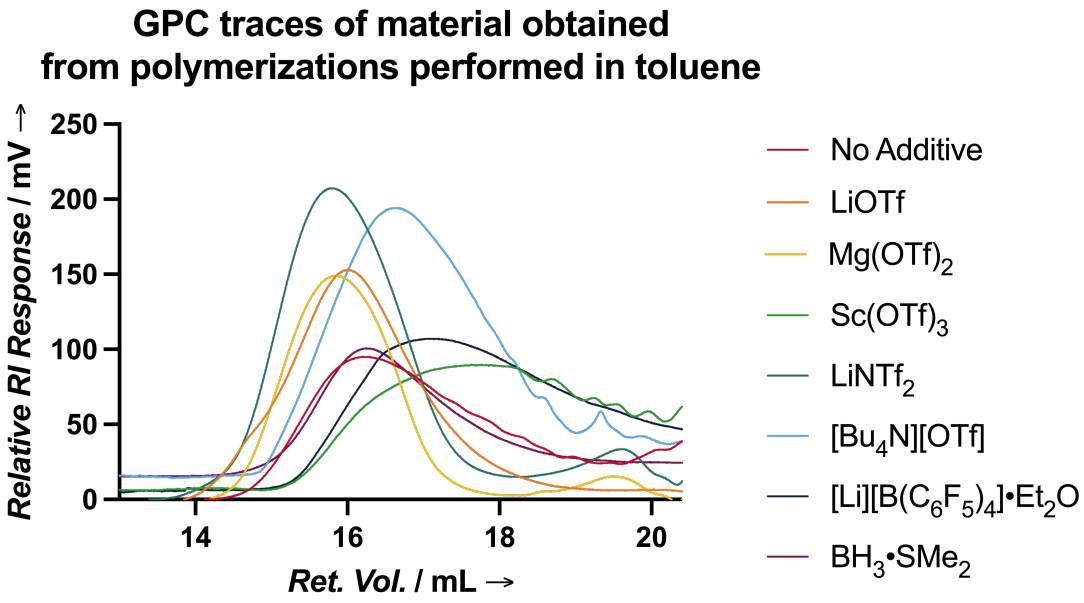


**Figure 4.4:** GPC traces of materials obtained from dehydropolymerizations of **4.1** performed in toluene.

**Thermal Dehydropolymerization in 2-MeTHF**

To a 1-dram vial was added phosphine-borane adduct, (**4.1**) (0.50 mmol, 62 mg) and 2-methyl tetrahydrofuran (250 µL). Then, this solution was transferred to a J Young NMR tube. The J Young NMR tube was then sealed and removed from the glovebox and placed in a heating block set to 100 °C. The reaction was heated at this temperature over the course of 24 h, after which the heating plate was turned off, and the reaction was left to cool. Once the temperature gauge gave a value below 30 °C, the tubes were removed from the heating block and carefully unsealed to allow the built-up pressure to release. Afterwards, $CDCl_3$ was added to the tube in open air, and the reactions were assessed by $^{31}P$ NMR to determine the reaction was complete and confirm that

polyphosphinoborane (**4.2**) was accessed. Afterwards, the polymer was isolated as described above in 70% yield (43 mg). GPC was used to determine the molar mass of materials accessed with the resulting trace in **Figure 4.5** and tabulated data available in **Table 4.1**.

**Polymerizations Performed in 2-MeTHF with Additives**

To a 1 dram vial, **4.1** (0.50 mmol, 62 mg) was added. Then, 5 mol% of the additive and 2-MeTHF was added to this vial. Subsequently, the reaction mixtures were transferred to J Young NMR tubes. The J Young NMR tubes were then sealed, removed from the glovebox, and placed in a heating block set to 100 °C. The reaction was then heated at this temperature for 24 h, after which it was allowed to cool and carefully depressurized. Subsequently, samples of **4.2** were isolated as described for reactions performed in toluene in 24 – 71% yield. GPC was used to determine the molar mass of materials accessed with the resulting trace in **Figure 4.6** and tabulated data available in **Table 4.1**.

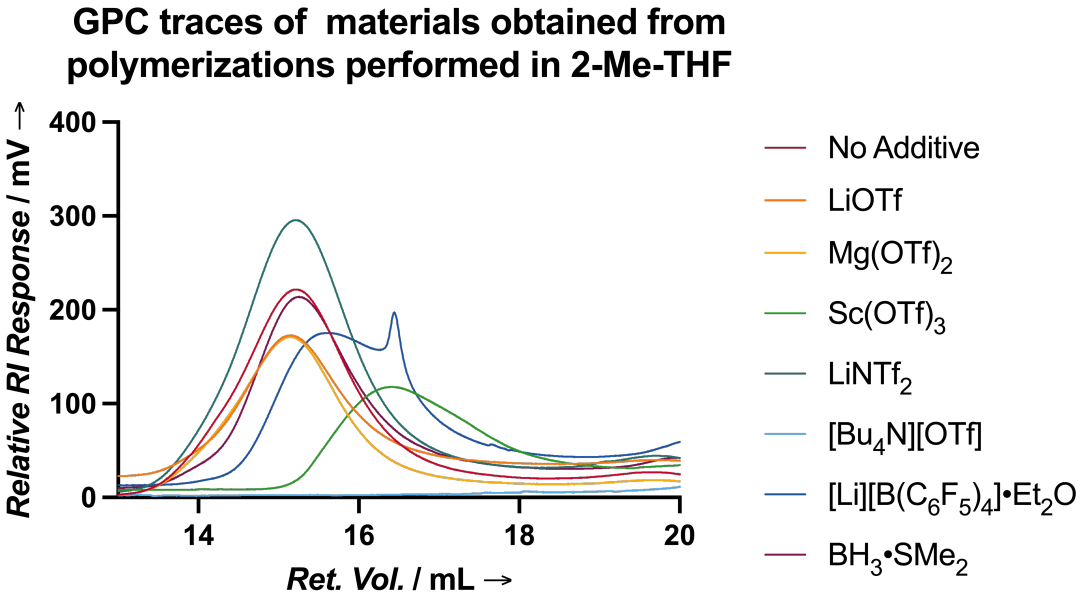


**Figure 4.5:** GPC traces of materials obtained from dehydropolymerizations of 1 performed in 2-MeTHF.

**Determination of Conversion and Molar Mass of 2 at 0.25 to 24 h**

To determine the approximate rate of dehydropolymerization of **4.1** to **4.2** in 2-MeTHF solutions with LiOTf or $BH_3$•$SMe_2$ added reactions were set up in J Young NMR tubes with **4.1** (0.025 mmol, 31 mg), either 5 mol% of LiOTf or $BH_3$•$SMe_2$ and total reaction volumes of 125 µL of 2-MeTHF. The J Young NMR tubes were sealed, removed from the glove box, and heated for either 0.25, 0.5, 1, 2, 3, 6, 16, or 24 h. Afterwards, the tubes were removed from heating and cooled to 20 °C, diluted with $CDCl_3$ (750 µL), and monitored by $^{11}B\{^1H\}$ and $^{31}P\{^1H\}$ NMR spectroscopy yielding the spectra in **Figure 4.15** to **Figure 4.18** and represented graphically in **Figure 4.2**. Afterwards, the polymers were isolated as described above as white powders in 49–72% yields and monitored by GPC

to determine the molar mass of isolated materials as shown in **Figure 4.6** and with tabulated data available in **Table 4.1**.

**Polymerizations Performed in 2-MeTHF using LiOTf (1–10 mol%)**

First, a solution of LiOTf (1 M) in 2-MeTHF was prepared. Afterwards, in a 1 dram vial, phosphine-borane adduct (**4.1**) (0.50 mmol, 62 mg) was added. Then, the required amount of the solution of LiOTf (1 M) was added to the vial (5 – 50 µL), and the reaction was topped off to have a total volume of 250 µL (i.e., 2 M of **4.1** in 2-MeTHF). The reaction mixture was transferred to a J Young NMR tube and placed in a heating block set to 100 °C. The reactions were heated for 20 h, after which it was allowed to cool and carefully depressurized. Then, $CDCl_3$ was added and the reactions were analyzed by $^{31}P$ NMR spectroscopy to ensure that the reaction had reached completion and that **4.2** was produced. Polymer samples were isolated as described for reactions performed in toluene in 50 – 74% yield. Similarly, GPC was used to assess the materials produced with GPC traces available in **Figure 4.6** and tabulated data available in **Table 4.1**.

.

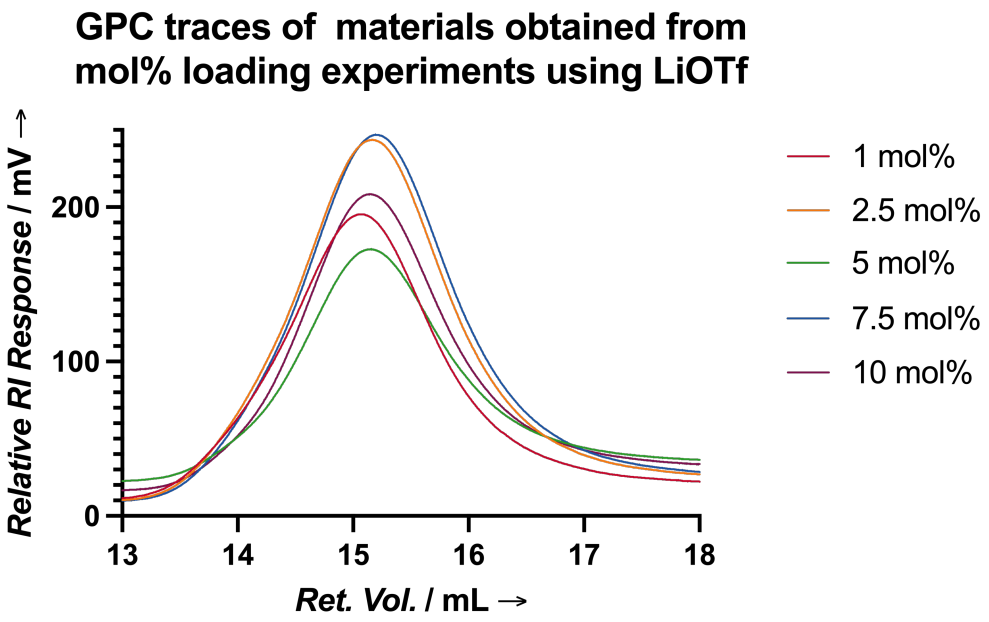


**Figure 4.6:** GPC traces of materials obtained from the dehydropolymerization of 1 in 2-MeTHF with 1 – 10 mol% of LiOTf added.

**Polymerizations Performed in 2-MeTHF using $BH_3$•$SMe_2$ (1–10 mol%)**

To a 1 dram vial, phosphine-borane adduct was added (**4.1**) (0.50 mmol, 62 mg). Then, the required amount of $BH_3$•$SMe_2$ in THF (2 M, 2.5 – 25 µL) was added to this vial. Afterwards 2-MeTHF (250 µL) was added resulting in an approximately 2 M solution of **4.1**, with $BH_3$•$SMe_2$. The reaction mixture was transferred to a J Young NMR tube, sealed, removed from the glovebox and placed in a heating block set to 100 °C. The reaction was then heated at this temperature for 24 h, after which it was allowed to cool and carefully depressurized. Then, $CDCl_3$ was added and the reactions were monitored by $^{31}P$ NMR spectroscopy to ensure that the reaction had reached completion and that **4.2** was produced. Polymer samples were isolated as described for reactions performed in toluene

in 63 – 79% yield. Similarly, GPC was used to assess the materials produced with GPC traces available in **Figure 4.7** and tabulated data available in **Table 4.1**.

.

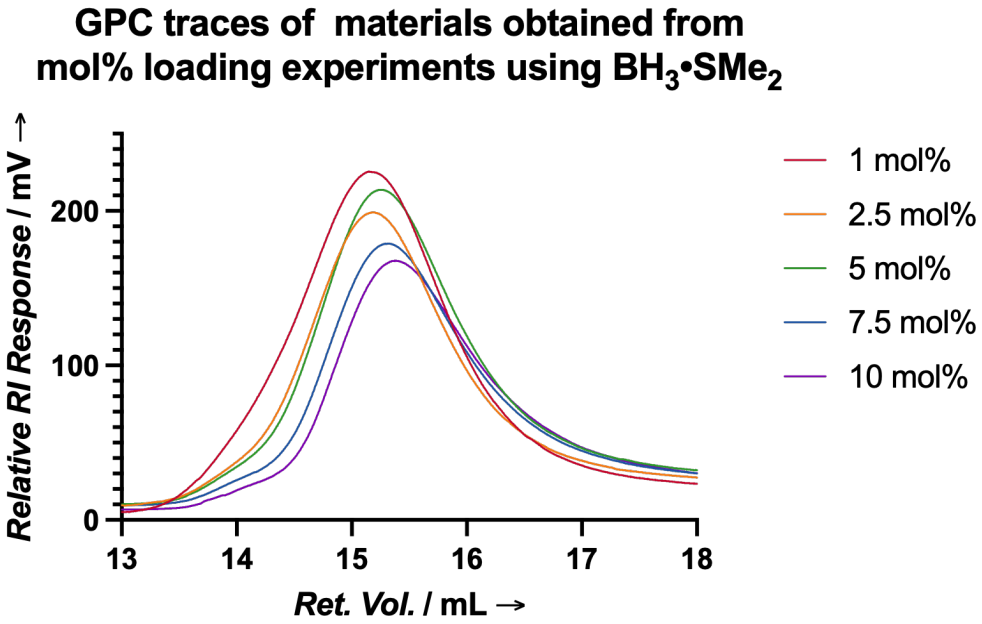


**Figure 4.7**: GPC traces of materials obtained from the dehydropolymerization of 1 in 2-MeTHF with 1 – 10 mol% of $BH_3$•$SMe_2$ added.

**Mass Spectra Obtained for End Group Analysis**

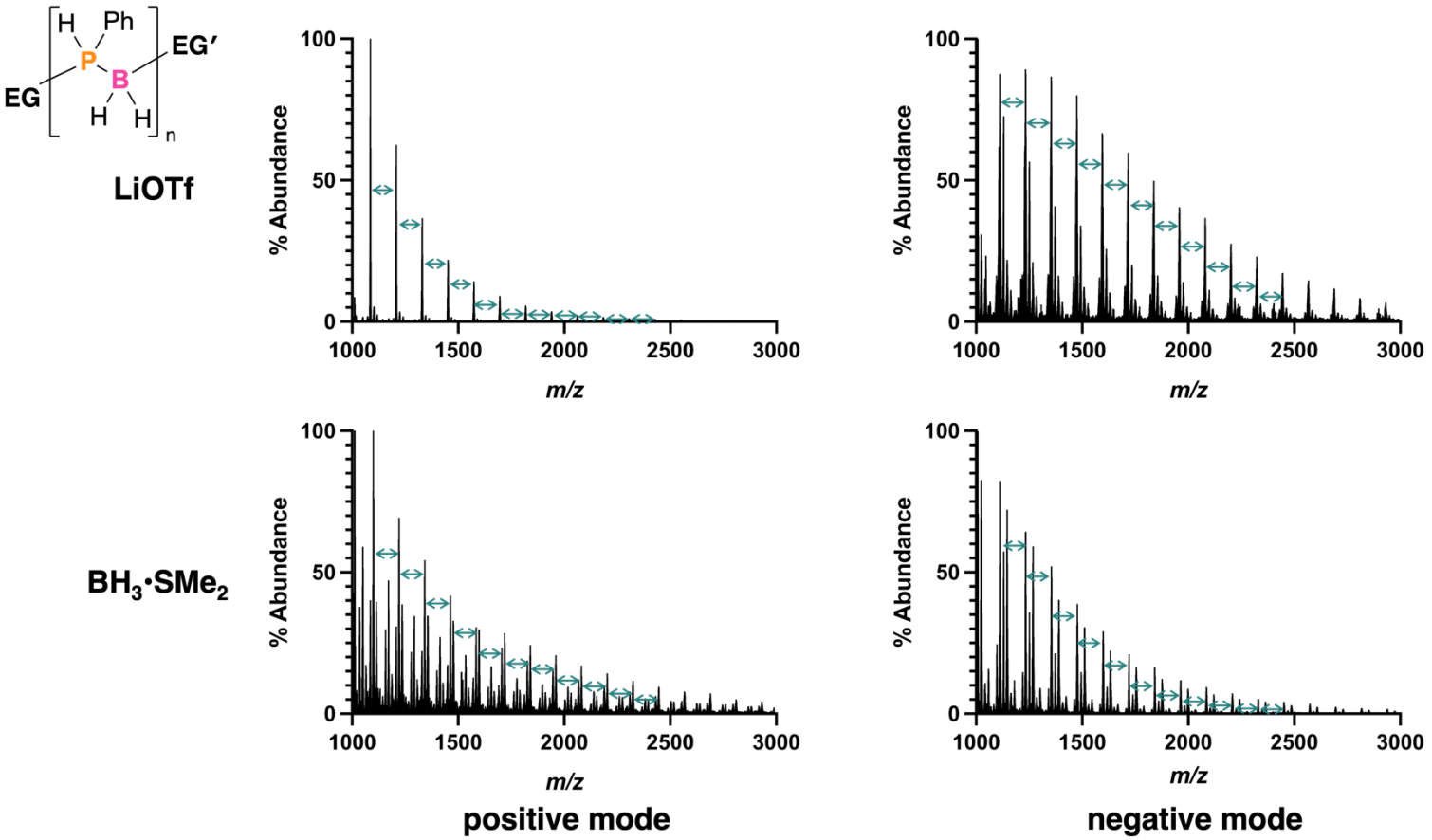


**Figure 4.8:** ESI-MS spectra (1 000 – 3 000 *m/z*) of residual oligomers present in the materials obtained from the dehydropolymerization of 4.1 in the presence of added LiOTf or $BH_3$•$SMe_2$. The turquoise double-headed arrows indicate a spacing of 122 *m/z*.

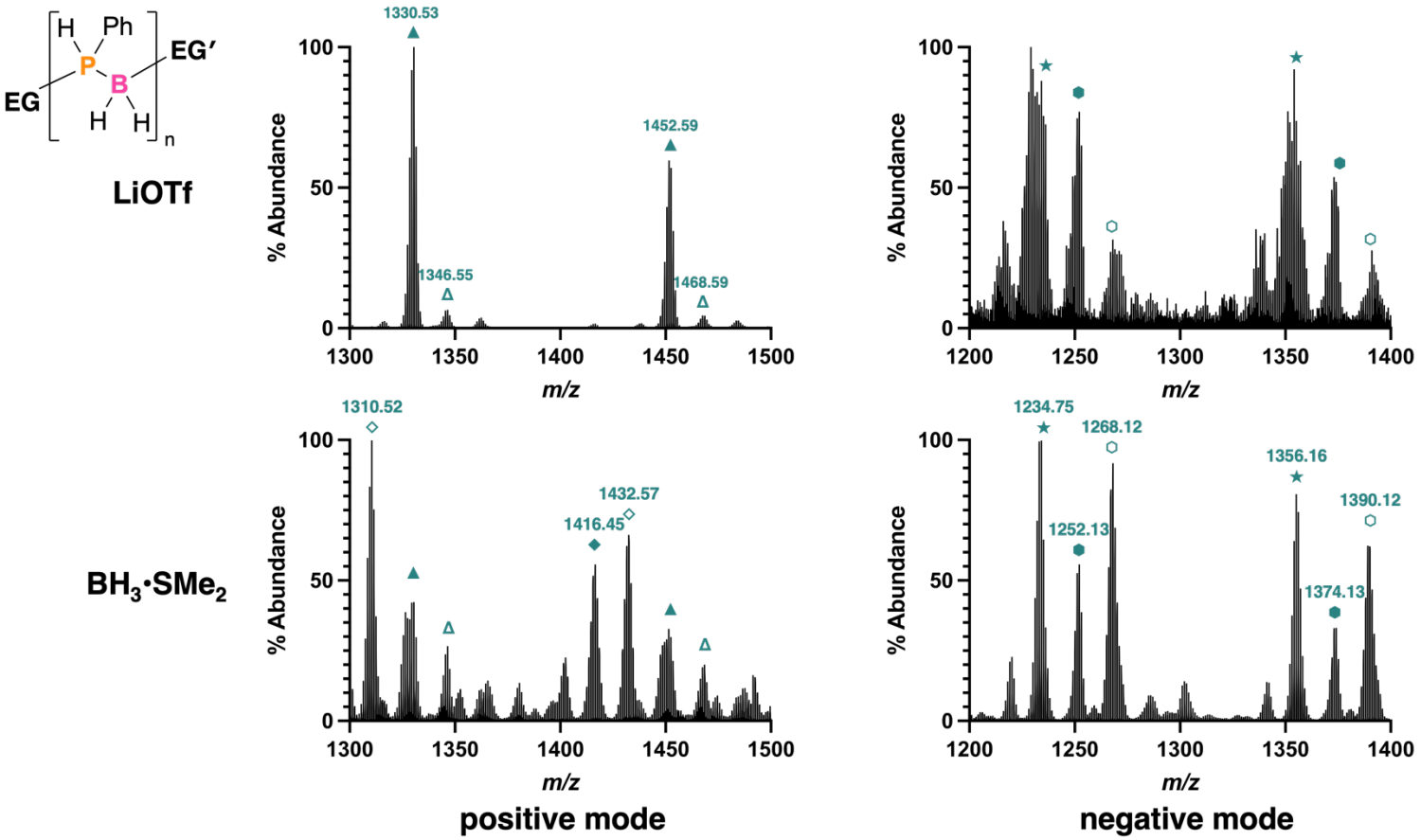


**Figure 4.9:** ESI-MS spectra of residual oligomers present in materials obtained from the dehydropolymerization of 4.1 in the presence of either LiOTf or $BH_3$•$SMe_2$. Selected peaks are labelled with a mass and corresponding symbol for the type of oligomer (▲, EG = H, EG′ = $PhPH_2$; Δ, ▲-oxide; ◆, EG = $BH_2(SMe_2)$, EG′ = H; ◇, ◆-oxide; ★, EG = $BH_3$; EG′ = H; ⬢, EG, EG' = unknown end groups with *m/z* corresponding to either 32 or 154; ⬡, tentatively assigned as ⬢-oxide).

**GPC Data**

**Table 4.1**: Data obtained from the dehydropolymerizations of **4.1** performed within this study as described in the synthetic procedures. (n/a = not applicable).

| Entry | Solvent | ***1*** */ mmol* | *Additive* | *mol%* | *Time* / h | $M_n$ / Da | *Đ* |
|---|---|---|---|---|---|---|---|
| ***1*** | toluene | 0.5 | none | n/a | 24 | 12,680 | 2.00 |
| ***2*** | toluene | 0.5 | LiOTf | 5 | 24 | 42,200 | 1.69 |
| ***3*** | toluene | 0.5 | $Mg(OTf)_2$ | 5 | 24 | 32,020 | 1.36 |
| ***4*** | toluene | 0.5 | $Sc(OTf)_3$ | 5 | 24 | 12,370 | 2.26 |
| ***5*** | toluene | 0.5 | $LiNTf_2$ | 5 | 24 | 29,260 | 1.73 |
| ***6*** | toluene | 0.5 | [*n*$Bu_4$N][OTf] | 5 | 24 | 13,110 | 1.68 |
| ***7*** | toluene | 0.5 | $[Li][B(C_6F_5)_4]•Et_2O$ | 5 | 24 | 10,980 | 2.29 |
| ***8*** | toluene | 0.5 | $BH_3•SMe_2$[a] | 5 | 24 | 27,990 | 1.70 |
| ***9*** | 2-MeTHF | 0.5 | none | n/a | 24 | 80,680 | 1.66 |
| ***10*** | 2-MeTHF | 0.5 | LiOTf | 5 | 24 | 80,403 | 1.64 |
| ***11*** | 2-MeTHF | 0.5 | $Mg(OTf)_2$ | 5 | 24 | 87,570 | 1.66 |
| ***12*** | 2-MeTHF | 0.5 | $Sc(OTf)_3$ | 5 | 24 | 24,260 | 1.64 |
| ***13*** | 2-MeTHF | 0.5 | $LiNTf_2$ | 5 | 24 | 79,690 | 1.66 |

| | | | | | | | |
|---|---|---|---|---|---|---|---|
| ***14*** | 2-MeTHF | 0.5 | [*n*$Bu_4$N][OTf] | 5 | 24 | 1,320 | 1.62 |
| ***15*** | 2-MeTHF | 0.5 | [Li][$B(C_6F_5)_4$]•$Et_2O$ | 5 | 24 | 45,900 | 2.29 |
| ***16*** | 2-MeTHF | 0.5 | $BH_3$•$SMe_2$[a] | 5 | 24 | 68,930 | 1.65 |
| ***17*** | 2-MeTHF | 0.5 | LiOTf | 1 | 24 | 92,240 | 1.64 |
| ***18*** | 2-MeTHF | 0.5 | LiOTf | 2.5 | 24 | 85,120 | 1.64 |
| ***19*** | 2-MeTHF | 0.5 | LiOTf | 7.5 | 24 | 81,170 | 1.62 |
| ***20*** | 2-MeTHF | 0.5 | LiOTf | 10 | 24 | 79,330 | 1.67 |
| ***21*** | 2-MeTHF | 0.5 | $BH_3$•$SMe_2$[a] | 1 | 24 | 83,120 | 1.65 |
| ***22*** | 2-MeTHF | 0.5 | $BH_3$•$SMe_2$[a] | 2.5 | 24 | 75,000 | 1.66 |
| ***23*** | 2-MeTHF | 0.5 | $BH_3$•$SMe_2$[a] | 7.5 | 24 | 62,820 | 1.66 |
| ***24*** | 2-MeTHF | 0.5 | $BH_3$•$SMe_2$[a] | 10 | 24 | 57,740 | 1.66 |

[a] Used as a 2 M solution in THF. [b] Approximate mass of the higher molar mass fraction of material.

**NMR Spectra**

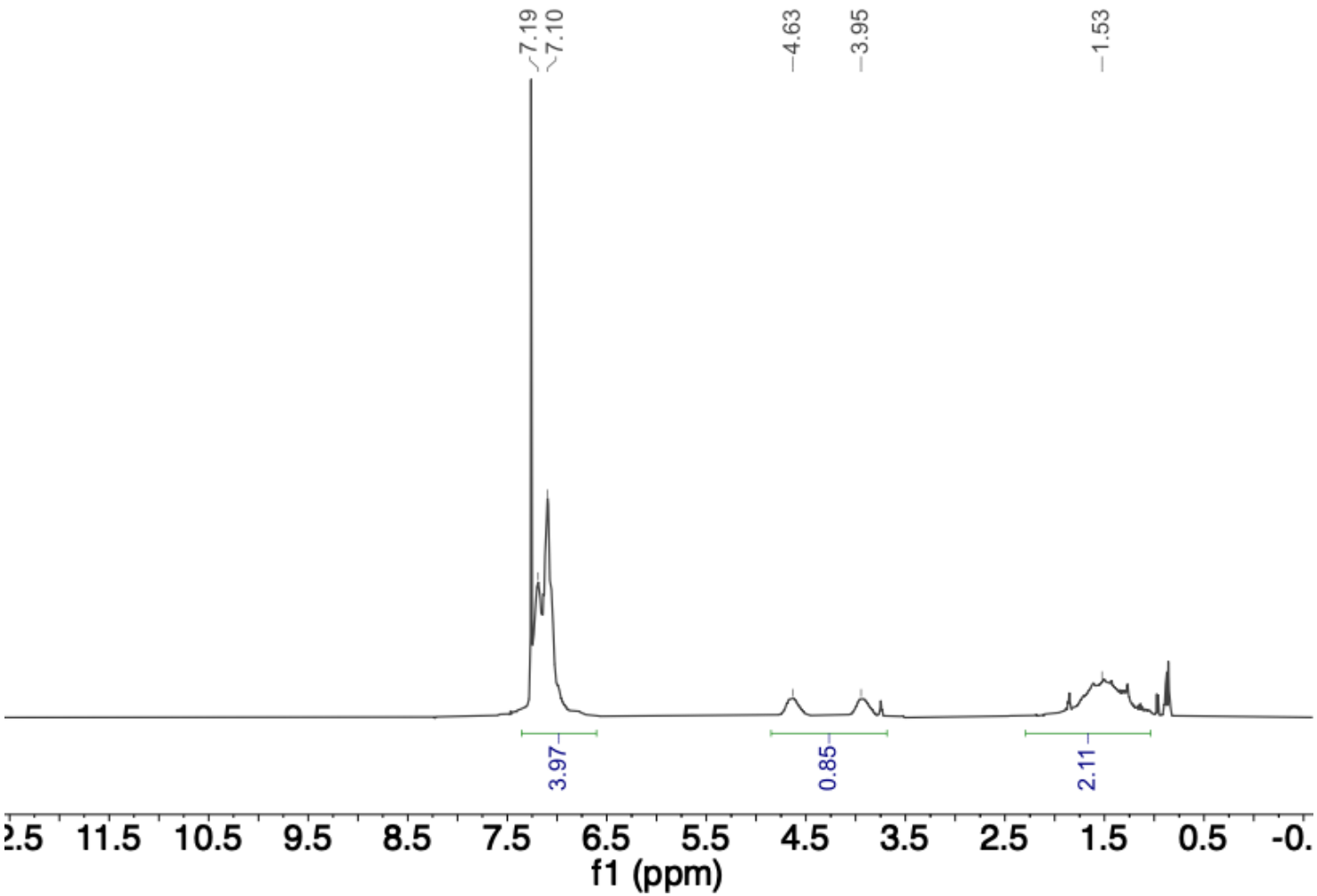


**Figure 4.10:** $^{1}$H NMR (500 MHz, $CDCl_3$, 298 K) of **4.2** from dehydropolymerization of **4.1** in 2-MeTHF with added LiOTf.

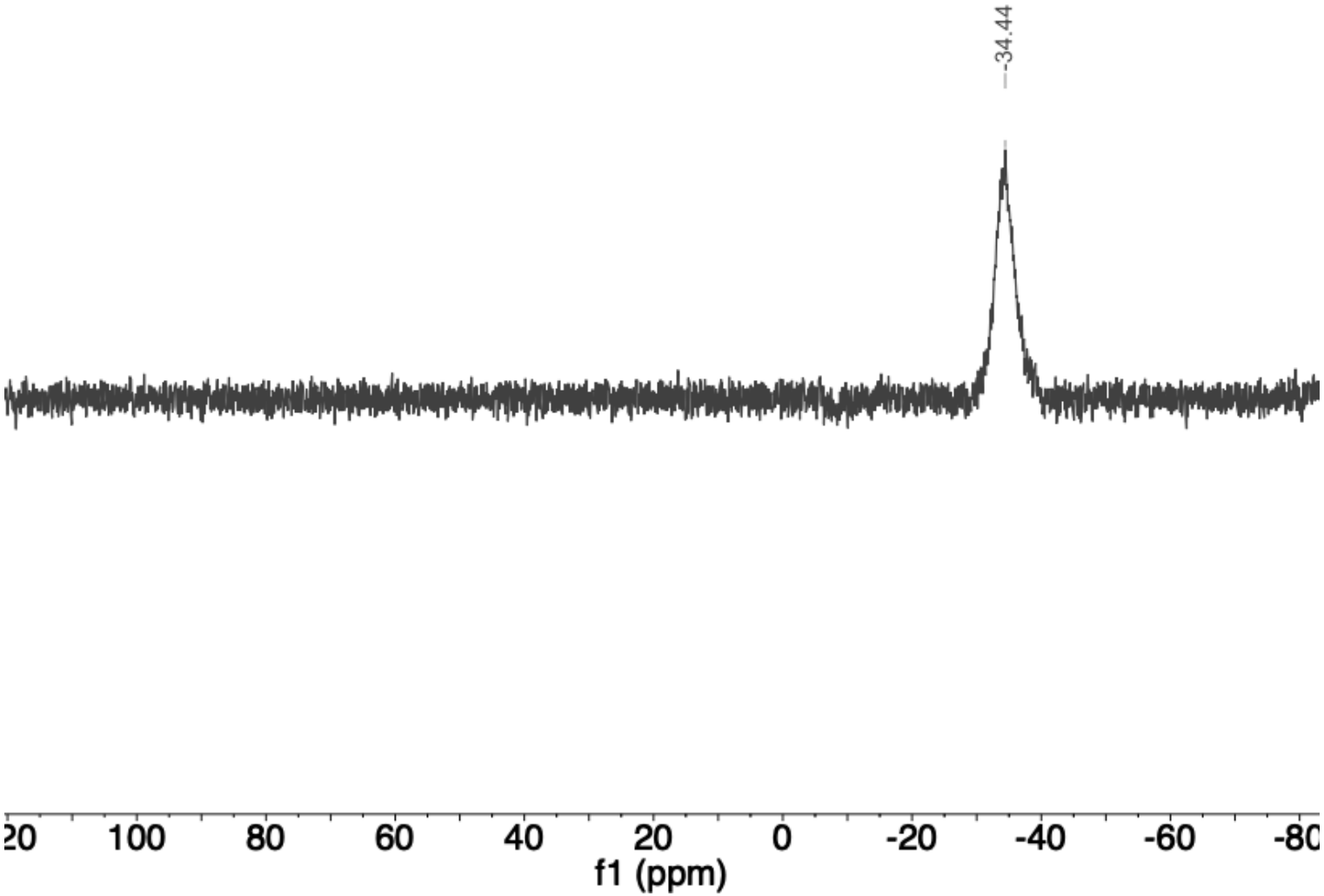


**Figure 4.11:** $^{11}B$ NMR spectrum (161 MHz, $CDCl_3$, 298 K) of **4.2** obtained from the dehydropolymerization of **4.1** in 2-MeTHF with 5 mol% of LiOTf added.

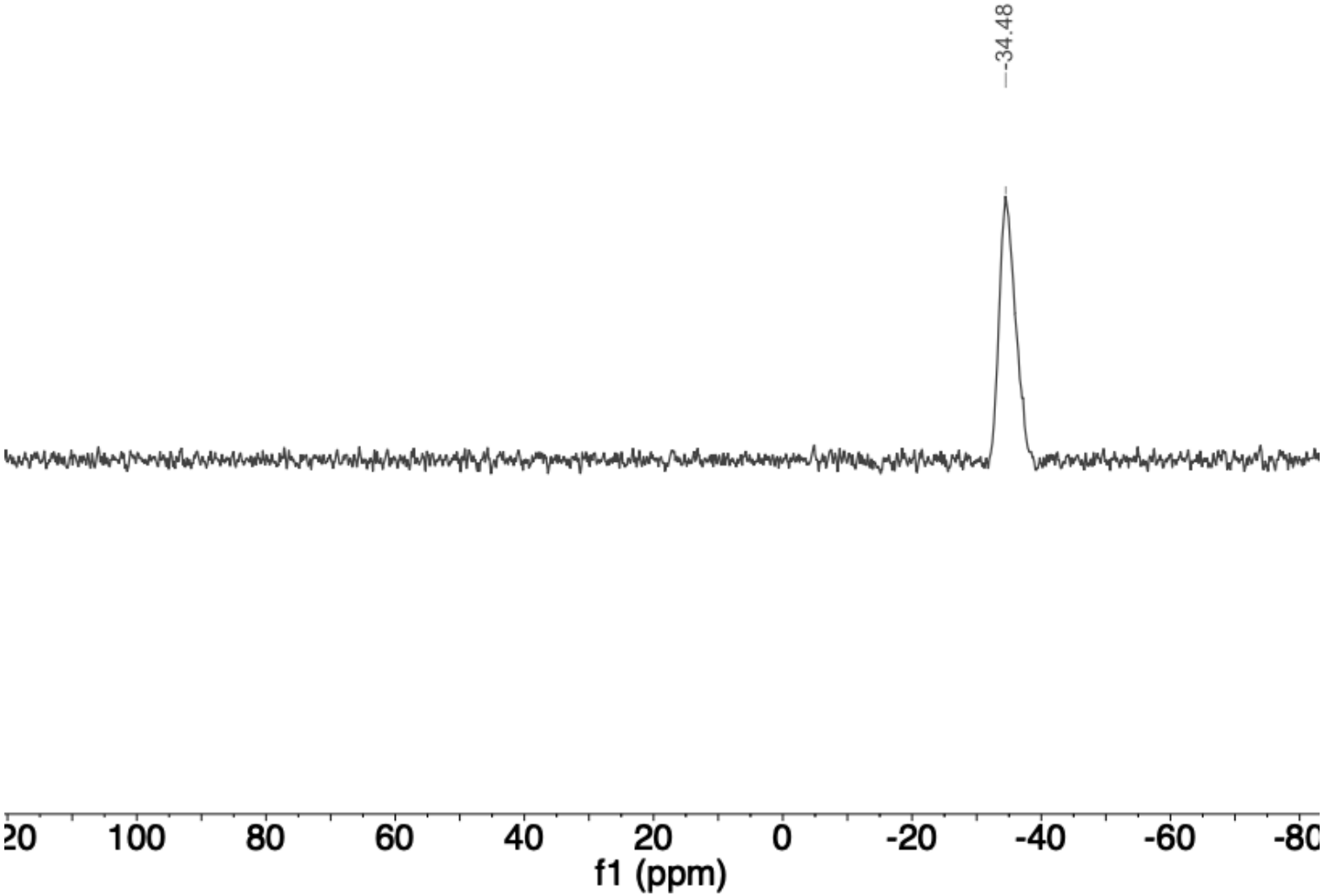


**Figure 4.12:** $^{11}B\{^{1}H\}$NMR spectrum (161 MHz, $CDCl_3$, 298 K) of **4.2** obtained from the dehydropolymerization of **4.1** in 2-MeTHF with 5 mol% of LiOTf added.

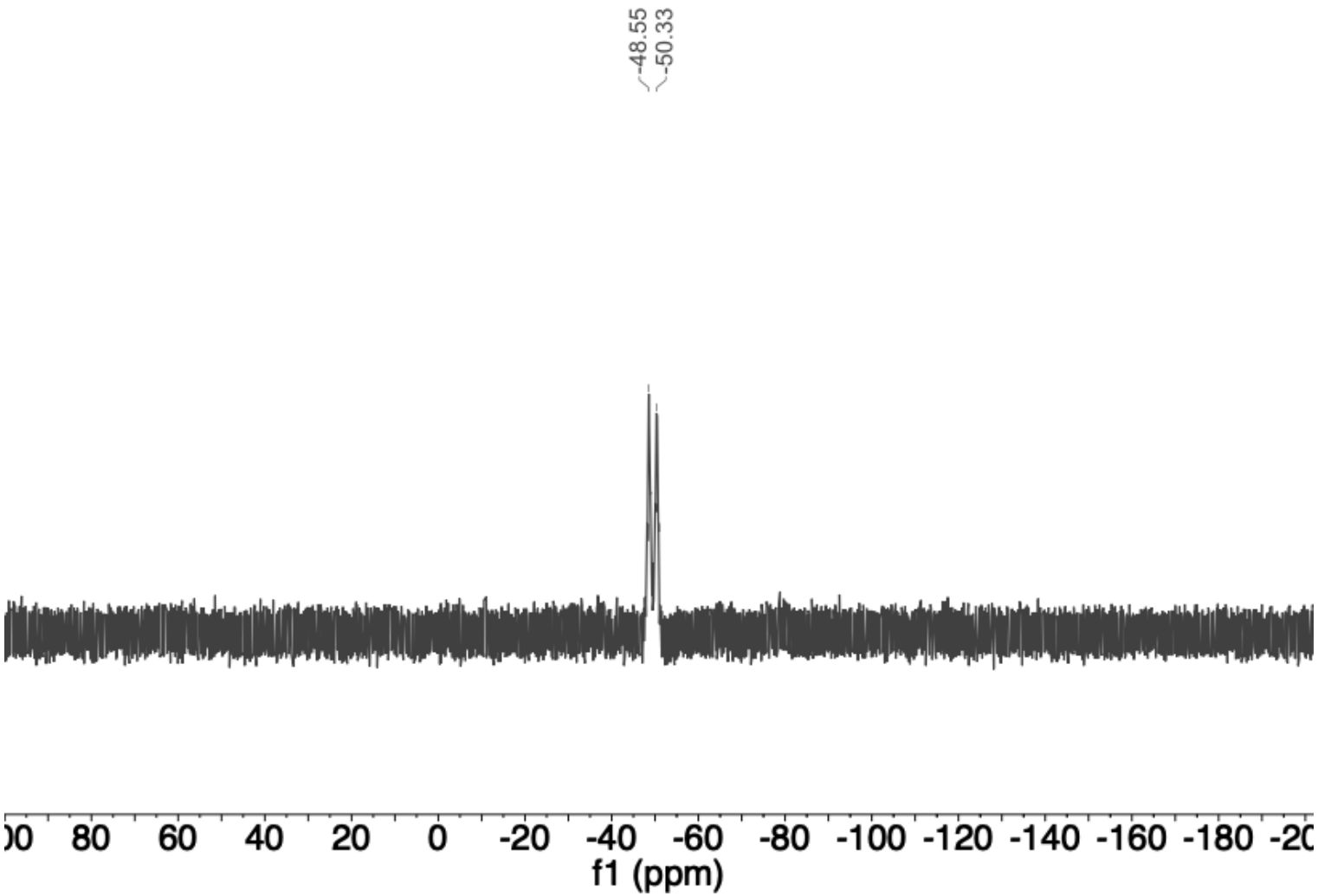


**Figure 4.13:** $^{31}P$ NMR spectrum (201 MHz, $CDCl_3$, 298 K) of **4.2** obtained from the dehydropolymerization of **4.1** in 2-MeTHF with 5 mol% of LiOTf added.

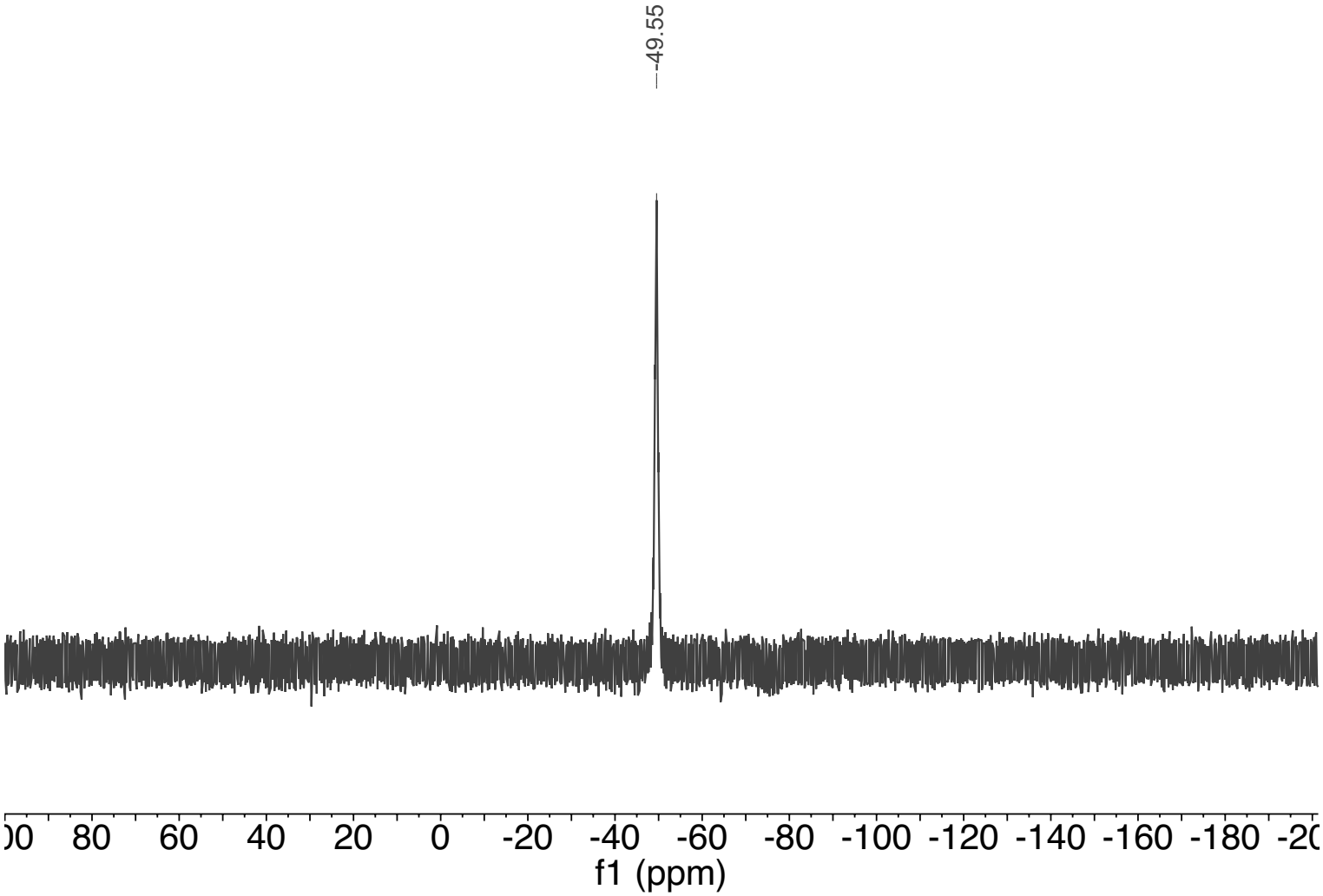


**Figure 4.14:** $^{31}P\{^{1}H\}$ NMR spectrum (201 MHz, $CDCl_3$, 298 K) of **4.2** obtained from the dehydropolymerization of **4.1** in 2-MeTHF with 5 mol% of LiOTf added.

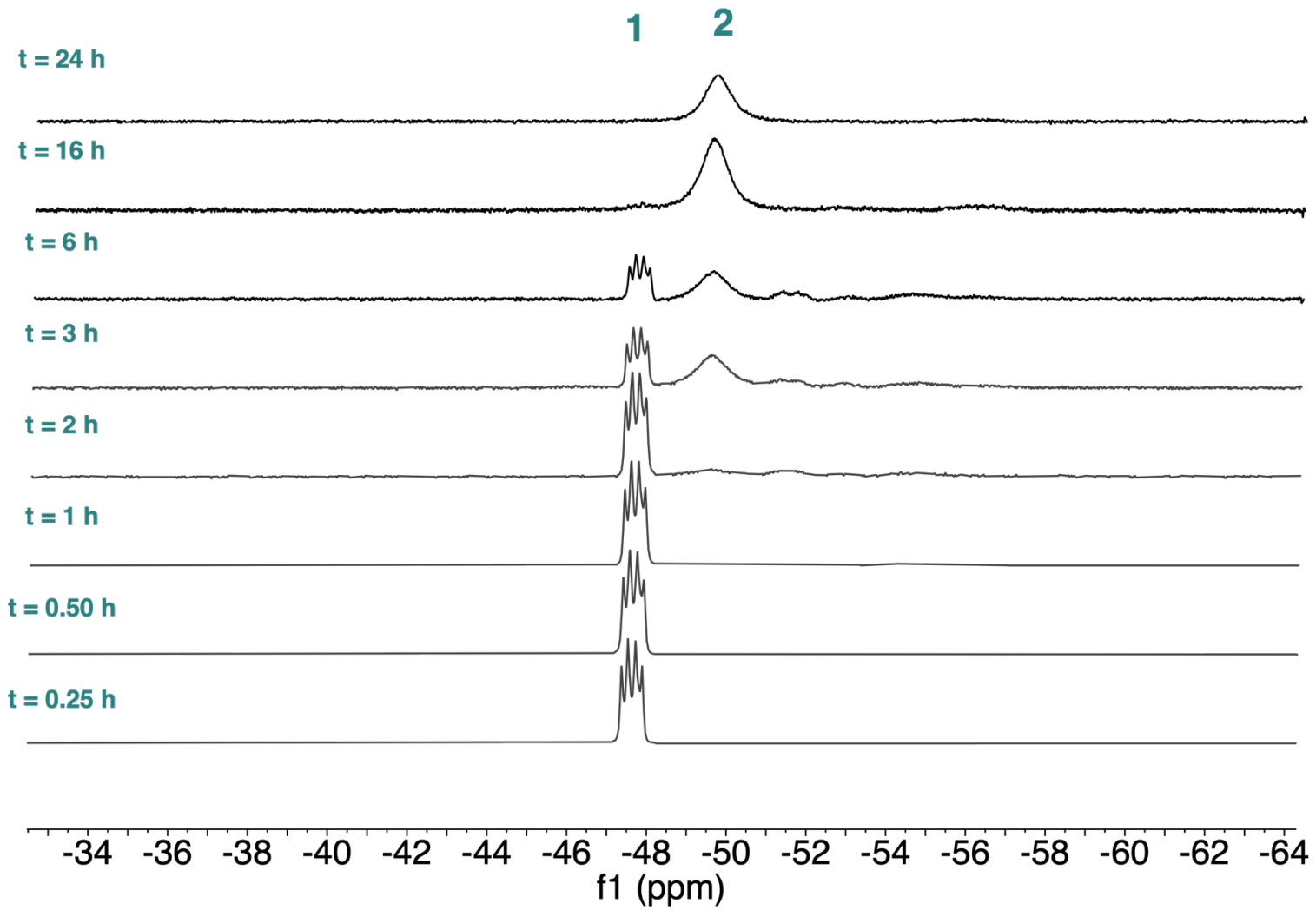


**Figure 4.15:** $^{31}P\{^{1}H\}$ NMR spectra (201 MHz, 2-MeTHF and $CDCl_3$ (1:6 ratio), 298 K) of **4.2** obtained from the dehydropolymerization of **4.1** in 2-MeTHF with 5 mol% of LiOTf over 24 h.

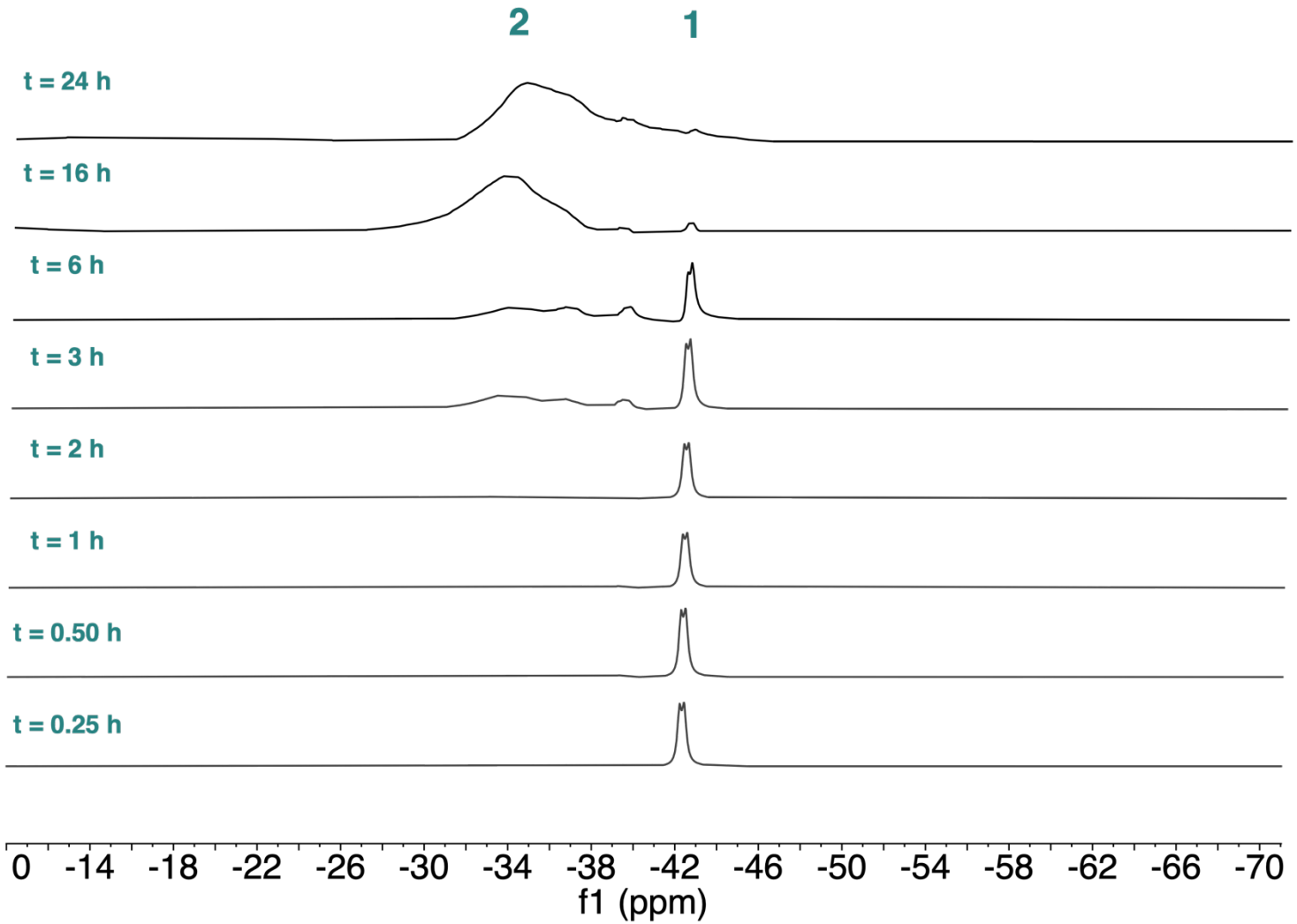


**Figure 4.16**: $^{11}B\{^{1}H\}$ NMR spectra (201 MHz, 2-MeTHF and $CDCl_3$ (1:6 ratio), 298 K) of **4.2** obtained from the dehydropolymerization of **4.1** in 2-MeTHF with 5 mol% of LiOTf added over 6 (bottom), 16 (middle), and 24 (top) h.

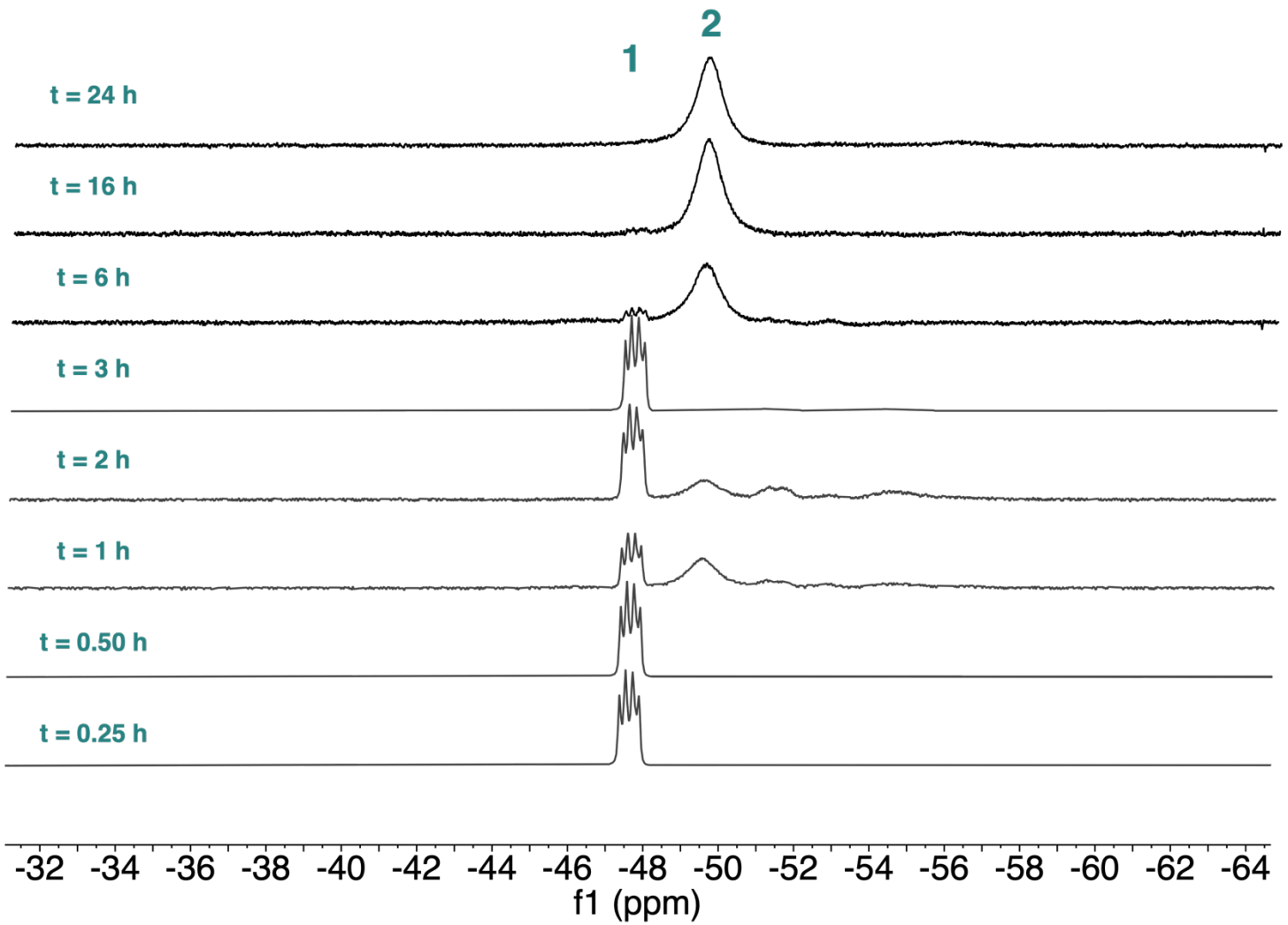


**Figure 4.17:** $^{31}P\{^{1}H\}$ NMR spectra (201 MHz, 2-MeTHF and $CDCl_3$ (1:6 ratio), 298 K) of **4.2** obtained from the dehydropolymerization of **4.1** in 2-MeTHF with 5 mol% of $BH_3$•$SMe_2$ over 24 h.

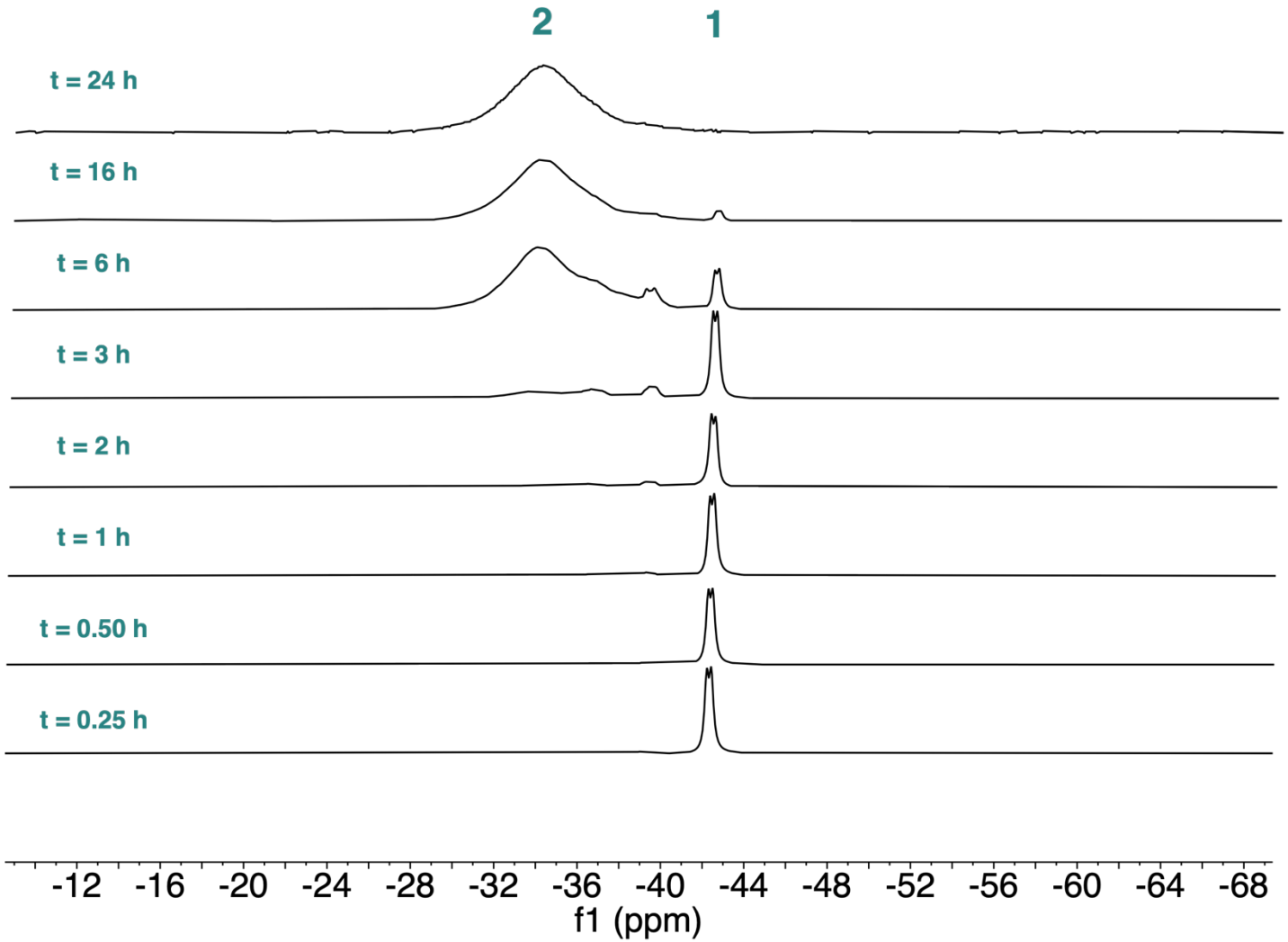


**Figure 4.18:** $^{11}B\{^{1}H\}$ NMR spectra (161 MHz, 2-MeTHF and $CDCl_3$ (1:6 ratio),, 298 K) of **4.2** obtained from the dehydropolymerization of **4.1** in 2-MeTHF with 5 mol% of LiOTf over 24 h**.**

## 4.6 References


(1) Baumgartner, T.; Jaekle, F. *Main Group Strategies Towards Functional Hybrid Materials*; John Wiley & Sons, Incorporated: Newark, 2018.

(2) Jaekle, F. Advances in the Synthesis of Organoborane Polymers for Optical, Electronic, and Sensory Applications. *Chemical Reviews* **2010**, *110* (7), 3985–4022. https://doi.org/10.1021/cr100026f.

(3) Chung, W. J.; Griebel, J. J.; Kim, E. T.; Yoon, H.; Simmonds, A. G.; Ji, H. J.; Dirlam, P. T.; Glass, R. S.; Wie, J. J.; Nguyen, N. A.; Guralnick, B. W.; Park, J.; Somogyi, A.; Theato, P.; Mackay, M. E.; Sung, Y.-E.; Char, K.; Pyun, J. The Use of Elemental Sulfur as an Alternative Feedstock for Polymeric Materials. *Nature Chemistry* **2013**, *5* (6), 518–524. https://doi.org/10.1038/nchem.1624.

(4) De Jaeger, R.; Gleria, M. Poly(Organophosphazene)s and Related Compounds: Synthesis, Properties and Applications. *Progress in Polymer Science* **1998**, *23* (2), 179–276. https://doi.org/10.1016/s0079-6700(97)00027-0.

(5) M. Priegert, A.; W. Rawe, B.; C. Serin, S.; P. Gates, D. Polymers and the P-Block Elements. *Chemical Society Reviews* **2016**, *45* (4), 922–953. https://doi.org/10.1039/C5CS00725A.

(6) Chivers, T.; Manners, I. *Inorganic Rings and Polymers of the P-Block Elements*; RSC Publishing, 2009.

(7) Caminade, A.-M.; Hey-Hawkins, E.; Manners, I. Smart Inorganic Polymers. *Chemical Society Reviews* **2016**, *45* (19), 5144–5146. https://doi.org/10.1039/c6cs90086k.

(8) Mark, J. E. Some Interesting Things about Polysiloxanes. *Accounts of Chemical Research* **2004**, *37* (12), 946–953. https://doi.org/10.1021/ar030279z.

(9) Colebatch, A. L.; Weller, A. S. Amine-Borane Dehydropolymerization: Challenges and Opportunities. *Chemistry – A European Journal* **2019**, *25* (6), 1379–1390. https://doi.org/10.1002/chem.201804592.

(10) Staubitz, A.; Robertson, A. P. M.; Sloan, M. E.; Manners, I. Amine− and Phosphine−Borane Adducts: New Interest in Old Molecules. *Chemical Reviews* **2010**, *110* (7), 4023–4078. https://doi.org/10.1021/cr100105a.

(11) Leitao, E. M.; Jurca, T.; Manners, I. Catalysis in Service of Main Group Chemistry Offers a Versatile Approach to P-Block Molecules and Materials. *Nature Chemistry* **2013**, *5* (10), 817–829. https://doi.org/10.1038/nchem.1749.

(12) Vidal, F.; Jäkle, F. Functional Polymeric Materials Based on Main-Group Elements. *Angewandte Chemie International Edition* **2019**, *58* (18), 5846–5870. https://doi.org/10.1002/anie.201810611.

(13) Han, D.; Anke, F.; Trose, M.; Beweries, T. Recent Advances in Transition Metal Catalysed Dehydropolymerisation of Amine Boranes and Phosphine Boranes. *Coordination Chemistry Reviews* **2019**, *380*, 260–286. https://doi.org/10.1016/j.ccr.2018.09.016.

(14) Knights, A. W.; Nascimento, M. A.; Manners, I. An Investigation of Polyphosphinoboranes as Flame-Retardant Materials. *Polymer* **2022**, *247*, 124795. https://doi.org/10.1016/j.polymer.2022.124795.

(15) Clark, T. J.; Rodezno, J. M.; Clendenning, S. B.; Aouba, S.; Brodersen, P. M.; Lough, A. J.; Ruda, H. E.; Manners, I. Rhodium-Catalyzed Dehydrocoupling of

Fluorinated Phosphine–Borane Adducts: Synthesis, Characterization, and Properties of Cyclic and Polymeric Phosphinoboranes with Electron-Withdrawing Substituents at Phosphorus. *Chemistry – A European Journal* **2005**, *11* (15), 4526–4534. https://doi.org/10.1002/chem.200401296.

(16) Knights, A. W.; Chitnis, S. S.; Manners, I. Photolytic, Radical-Mediated Hydrophosphination: A Convenient Post-Polymerisation Modification Route to P-Di(Organosubstituted) Polyphosphinoboranes $[RR'PBH_2]_n$. *Chemical Science* **2019**, *10*, 7281–7289. https://doi.org/10.1039/C9SC01428D.

(17) Burg, A. B.; Wagner, R. I. Chemistry of P–B Bonding — the Phosphinoborines and Their Polymers. *Journal of the American Chemical Society* **1953**, *75* (16), 3872–3877. https://doi.org/10.1021/ja01112a002.

(18) Burg, A. B. Phosphinoborine Polymer Rings and Chains from Tetramethylbiphosphine. *Journal of Inorganic and Nuclear Chemistry* **1959**, *11* (3), 258. https://doi.org/10.1016/0022-1902(59)80257-8.

(19) Dorn, H.; Singh, R. A.; Massey, J. A.; Lough, A. J.; Manners, I. Rhodium-Catalyzed Formation of Phosphorus–Boron Bonds: Synthesis of the First High Molecular Weight Poly(Phosphinoborane). *Angewandte Chemie International Edition* **1999**, *38* (22), 3321–3323. https://doi.org/10.1002/(SICI)1521-3773(19991115)38:22<3321::AID-ANIE3321>3.0.CO;2-0.

(20) Dorn, H.; Singh, R. A.; Massey, J. A.; Nelson, J. M.; Jaska, C. A.; Lough, A. J.; Manners, I. Transition Metal-Catalyzed Formation of Phosphorus−Boron Bonds: A New Route to Phosphinoborane Rings, Chains, and Macromolecules. *Journal of*

*the American Chemical Society* **2000**, *122* (28), 6669–6678. https://doi.org/10.1021/ja000732r.

(21) Schäfer, A.; Jurca, T.; Turner, J.; Vance, J. R.; Lee, K.; Du, V. A.; Haddow, M. F.; Whittell, G. R.; Manners, I. Iron-Catalyzed Dehydropolymerization: A Convenient Route to Poly(Phosphinoboranes) with Molecular-Weight Control. *Angewandte Chemie International Edition* **2015**, *54* (16), 4836–4841. https://doi.org/10.1002/anie.201411957.

(22) Coles, N. T.; Mahon, M. F.; Webster, R. L. Phosphine- and Amine-Borane Dehydrocoupling Using a Three-Coordinate Iron(II) β-Diketiminate Precatalyst. *Organometallics* **2017**, *36* (11), 2262–2268. https://doi.org/10.1021/acs.organomet.7b00326.

(23) D. Paul, U. S.; Braunschweig, H.; Radius, U. Iridium-Catalysed Dehydrocoupling of Aryl Phosphine–Borane Adducts: Synthesis and Characterisation of High Molecular Weight Poly(Phosphinoboranes). *Chemical Communications* **2016**, *52* (55), 8573–8576. https://doi.org/10.1039/C6CC04363A.

(24) Huertos, M. A.; Weller, A. S. Revealing the P-B Coupling Event in the Rhodium Catalysed Dehydrocoupling of Phosphine-Boranes $H_3B{\bullet}PR_2H$ (R = Bu-t, Ph). *Chemical Science* **2013**, *4* (4), 1881–1888. https://doi.org/10.1039/c3sc50122a.

(25) Hooper, T. N.; Weller, A. S.; Beattie, N. A.; Macgregor, S. A. Dehydrocoupling of Phosphine-Boranes Using the $[RhCp^*Me(PMe_3)(CH_2Cl_2)][BAr^F{}_4]$ Precatalyst: Stoichiometric and Catalytic Studies. *Chemical Science* **2016**, *7* (3), 2414–2426. https://doi.org/10.1039/c5sc04150c.

(26) Hooper, T. N.; Huertos, M. A.; Jurca, T.; Pike, S. D.; Weller, A. S.; Manners, I. Effect of the Phosphine Steric and Electronic Profile on the Rh-Promoted Dehydrocoupling of Phosphine–Boranes. *Inorganic Chemistry* **2014**, *53* (7), 3716–3729. https://doi.org/10.1021/ic500032f.

(27) Schön, F.; Sigmund, L. M.; Schneider, F.; Hartmann, D.; Wiebe, M. A.; Manners, I.; Greb, L. Calix[4]Pyrrolato Aluminate Catalyzes the Dehydrocoupling of Phenylphosphine Borane to High Molar Weight Polymers. *Angewandte Chemie International Edition* **2022**, *61* (22), e202202176. https://doi.org/10.1002/anie.202202176.

(28) Race, J. J.; Heyam, A.; Wiebe, M. A.; Diego-Garcia Hernandez, J.; Ellis, C. E.; Lei, S.; Manners, I.; Weller, A. S. Polyphosphinoborane Block Copolymer Synthesis Using Catalytic Reversible Chain-Transfer Dehydropolymerization. *Angewandte Chemie International Edition* **2023**, *62* (3), e202216106. https://doi.org/10.1002/anie.202216106.

(29) Marquardt, C.; Jurca, T.; Schwan, K. C.; Stauber, A.; Virovets, A. V.; Whittell, G. R.; Manners, I.; Scheer, M. Metal-Free Addition/Head-to-Tail Polymerization of Transient Phosphinoboranes, RPH-$BH_2$: A Route to Poly(Alkylphosphinoboranes). *Angewandte Chemie International Edition* **2015**, *54* (46), 13782–13786. https://doi.org/10.1002/anie.201507084.

(30) Oldroyd, N. L.; Chitnis, S. S.; Annibale, V. T.; Arz, M. I.; Sparkes, H. A.; Manners, I. Metal-Free Dehydropolymerisation of Phosphine-Boranes Using Cyclic (Alkyl)(Amino)Carbenes as Hydrogen Acceptors. *Nature Communications* **2019**, *10* (1), 1–9. https://doi.org/10.1038/s41467-019-08967-8.

(31) Wiebe, M. A.; Kundu, S.; LaPierre, E. A.; Patrick, B. O.; Manners, I. Transition-Metal-Free Dehydropolymerization of Phosphine–Boranes at Ambient Temperature. *Chemistry – A European Journal* **2023**, *29* (2), e202202897. https://doi.org/10.1002/chem.202202897.

(32) Chum, P. S.; Swogger, K. W. Olefin Polymer Technologies—History and Recent Progress at The Dow Chemical Company. *Progress in Polymer Science* **2008**, *33* (8), 797–819. https://doi.org/10.1016/j.progpolymsci.2008.05.003.

(33) Jaska, C. A.; Manners, I. Heterogeneous or Homogeneous Catalysis? Mechanistic Studies of the Rhodium-Catalyzed Dehydrocoupling of Amine-Borane and Phosphine-Borane Adducts. *Journal of the American Chemical Society* **2004**, *126* (31), 9776–9785. https://doi.org/10.1021/ja0478431.

(34) Hooper, T. N.; Huertos, M. A.; Jurca, T.; Pike, S. D.; Weller, A. S.; Manners, I. Effect of the Phosphine Steric and Electronic Profile on the Rh-Promoted Dehydrocoupling of Phosphine–Boranes. *Inorganic Chemistry* **2014**, *53* (7), 3716–3729. https://doi.org/10.1021/ic500032f.

(35) Pomogaeva, A. V.; Timoshkin, A. Y. Stability and Electronic Structure of Donor–Acceptor Stabilized Group 13/15 Oligomers. *The Journal of Physical Chemistry A* **2021**, *125* (16), 3415–3424. https://doi.org/10.1021/acs.jpca.1c02258.

(36) Wang, L.; Zhang, T.; He, H.; Zhang, J. Mechanism for H2 Release from Potential Hydrogen Storage Materials of Phosphine Alane and Phosphine Borane in the Presence or Absence of Alane or Borane: A Theoretical Study. *RSC Advances* **2013**, *3* (44), 21949–21958. https://doi.org/10.1039/C3RA43859G.

(37) Kobayashi, S. Scandium Triflate in Organic Synthesis. *European Journal of Organic Chemistry* **1999**, *1999* (1), 15–27. https://doi.org/10.1002/(SICI)1099-0690(199901)1999:1<15::AID-EJOC15>3.0.CO;2-B.

(38) Johnson, H. C.; Leitao, E. M.; Whittell, G. R.; Manners, I.; Lloyd-Jones, G. C.; Weller, A. S. Mechanistic Studies of the Dehydrocoupling and Dehydropolymerization of Amine–Boranes Using a $[Rh(Xantphos)]^+$ Catalyst. *Journal of the American Chemical Society* **2014**, *136* (25), 9078–9093. https://doi.org/10.1021/ja503335g.

(39) Slater, C. S.; Savelski, M. J.; Hitchcock, D.; Cavanagh, E. J. Environmental Analysis of the Life Cycle Emissions of 2-Methyl Tetrahydrofuran Solvent Manufactured from Renewable Resources. *Journal of Environmental Science and Health, Part A* **2016**, *51* (6), 487–494. https://doi.org/10.1080/10934529.2015.1128719.

(40) Adamson, A.; Burk, P. P-Substituted Phosphine-Boranes: Gas Phase Acidities, Basicities and Dihydrogen Release. A Comparison to Amine-Boranes. *Computational and Theoretical Chemistry* **2014**, *1032*, 12–19. https://doi.org/10.1016/j.comptc.2014.01.008.

(41) Bentley, J. N.; Elgadi, S. A.; Gaffen, J. R.; Demay-Drouhard, P.; Baumgartner, T.; Caputo, C. B. Fluorescent Lewis Adducts: A Practical Guide to Relative Lewis Acidity. *Organometallics* **2020**, *39* (20), 3645–3655. https://doi.org/10.1021/acs.organomet.0c00389.

(42) Pangborn, A. B.; Giardello, M. A.; Grubbs, R. H.; Rosen, R. K.; Timmers, F. J. Safe and Convenient Procedure for Solvent Purification. *Organometallics* **1996**, *15* (5), 1518–1520. https://doi.org/10.1021/om9503712.

**Chapter 5**

# Dehydrocoupling of Phosphine-Borane Adducts Under Ambient Conditions Using Aminoboranes as Hydrogen Acceptors

*This chapter has been adapted from the as of yet unpublished work:*

Matthew A. Wiebe, Anne Staubitz, and Ian Manners. *Manuscript in preparation.*

*Contributions: M. A. W. and I. M. conceived the project. M. A. W. performed all synthesis, characterization and computations. M. A. W. interpreted the data and wrote the first draft manuscript which was subsequently edited with A. S. Dr. Etienne A. LaPierre prepared the titanium catalyst used in the ambient condition catalytic dehydropolymerization study.*

## 5.1 Abstract

Herein we report on the reactivity of aminoboranes ($R_2N{=}BH_2$; R = *i*Pr, Et, Me) with phosphine-borane adducts ($PhR'PH{\bullet}BH_3$; R' = H, Ph). We discovered that when sufficiently sterically unencumbered, aminoboranes can accept hydrogen from phosphine-borane adducts. The hydrogen transfer results in the formation of amine-borane adducts ($R_2NH{\bullet}BH_3$) and transient phosphinoboranes ($PhR'P{-}BH_2$) *in situ*. These phosphinoboranes undergo subsequent reactivity to access either polyphosphinoborane, $[PhPH{-}BH_2]_n$, or linear dimer, $Ph_2PH{\bullet}BH_2{-}Ph_2P{\bullet}BH_3$. Unlike metal catalyzed phosphine-borane dehydrocoupling, which occurs at elevated temperatures (2 M, toluene, ≥ 100 °C, ≥ 24 h), these dehydrocoupling reactions occur under ambient conditions (2 M, toluene or $C_6D_6$, 20 °C, ≤ 24 h). We performed a computational and experimental mechanistic study in which we have identified that this transformation likely occurs *via* a P-to-N and B-to-B hydrogen transfer *via* a 6-membered transition state. Lastly we explore the ambient condition catalytic dehydrocoupling of phosphine-borane adducts, where we are able to obtain 16% conversion of $Ph_2PH{\bullet}BH_3$.

## 5.2 Introduction

The dehydropolymerization of phosphine-borane adducts leads to polyphosphinoboranes, $[R_2P\text{-}BR_2]_n$, which are main-chain, main-group inorganic polymers.[1–9] Main chain main group inorganic polymers are much less explored than organic polymers, but certain classes, such as polyphosphazenes[10–12] or polysiloxanes[13,14] have found useful applications due to their complementary properties compared to organic polymers. Polyphosphinoboranes are another class of main-chain main-group polymers that are much less explored because the synthetic access to them is still very limited. However, it has been shown that they can be of high interest for example for self-extinguishing materials,[15] thin films for lithography,[16] or solution-processable ceramic precursors.[17]

The first attempted synthesis of polyphosphinoboranes was through the thermal dehydrogenation of phosphine-borane adducts in the 1950's, but the resulting materials were poorly characterized by modern standards.[18–20] Since then, several advances have been made: The first major advancement was the first metal catalyzed dehydrocoupling of phosphine-borane adducts using $[Rh(COD)Cl]_2$ in 1999 by Manners and co-workers.[21,22] This was followed by the discovery that $CpFe(CO)_2OTf$ can dehydropolymerize phosphine-borane adducts to yield high molar mass, low dispersity polyphosphinoboranes.[23] Other catalysts have reported based on Ru,[24–29] Ir,[30] or Fe[31,32], or Al[33] centers that are capable of the dehydropolymerization phosphine-borane adducts (**Scheme 5.1**). In one case, a block copolymer comprised of two distinct polyphosphinoborane blocks was accessed.[29] Generally, these catalysts require forcing

conditions (*ca.* 100 °C, 24 h) and the mechanisms that occur at each catalyst appear to differ,[4,23,24,28,29,34] and often are unknown.

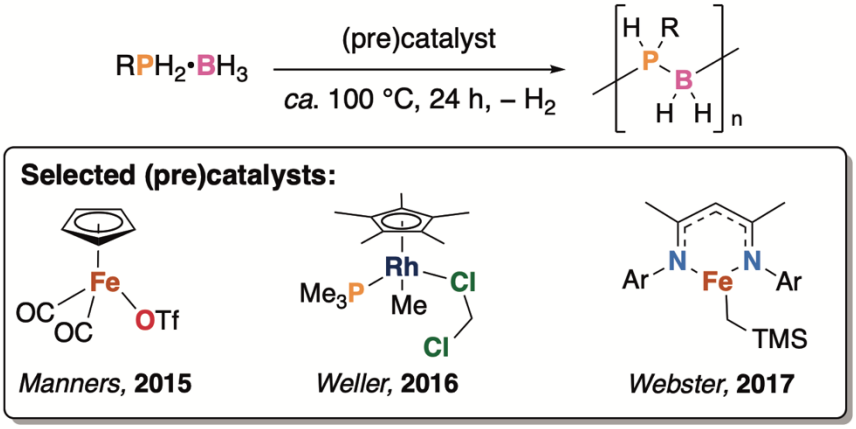


**Scheme 5.1:** Overview of catalytic *P*-phenylphosphine-borane dehydropolymerization.

To overcome these barriers, other strategies for the dehydropolymerization of phosphine-boranes *via* the targeted generation of transient phosphinoboranes ($R_2P–BH_2$) have been explored (**Scheme 5.2**). In a collaborative endeavor with the Scheer group, the Manners group reported on phosphinoborane-trimethylamine adducts ($RPH–BH_2(NMe_3)$; R = *t*Bu, Me), which upon gentle heating (22–50 °C) release phosphinoborane *in situ* that can then catenate to yield polymeric materials.[35,36] It was then discovered that cyclic alkylamino carbenes (CAAC) accept $H_2$ from phosphine-borane adducts ($PhRPH•BH_3$; R = H, Ph, Et) leading to polyphosphinoboranes $[RR'P–BH_2]_n$ in a transition metal free dehydrocoupling reaction.[37] Most recently, the ability access transient phosphinoboranes through the deprotonation of phosphine-(bis(trifluoromethanesulfonyl)imide)borane adducts ($PhRPH•BH_2(NTf_2)$; R = H, Ph, Et) to yield polymeric materials was realized.[38] Thus, it is well established that the generation of transient phosphinoboranes *in situ* can yield these coveted inorganic polymers. However, *catalytic* routes to generate phosphinoboranes *in situ* as precursors for

polymers, and that operate at mild conditions, and with a well-defined catalytic cycle are not yet known.

In this article, we explore the ability of aminoboranes (*i*$Pr_2N{=}BH_2$ (**5.2a**), $Et_2N{=}BH_2$ (**5.2b**), and $Me_2N{=}BH_2$ (**5.2c**)) to accept $H_2$ from phosphine-borane adducts under ambient conditions. We find that both **5.2b** and **5.2c** are capable of phosphine-borane dehydrocoupling and then explore the mechanism of how this transformation occurs.

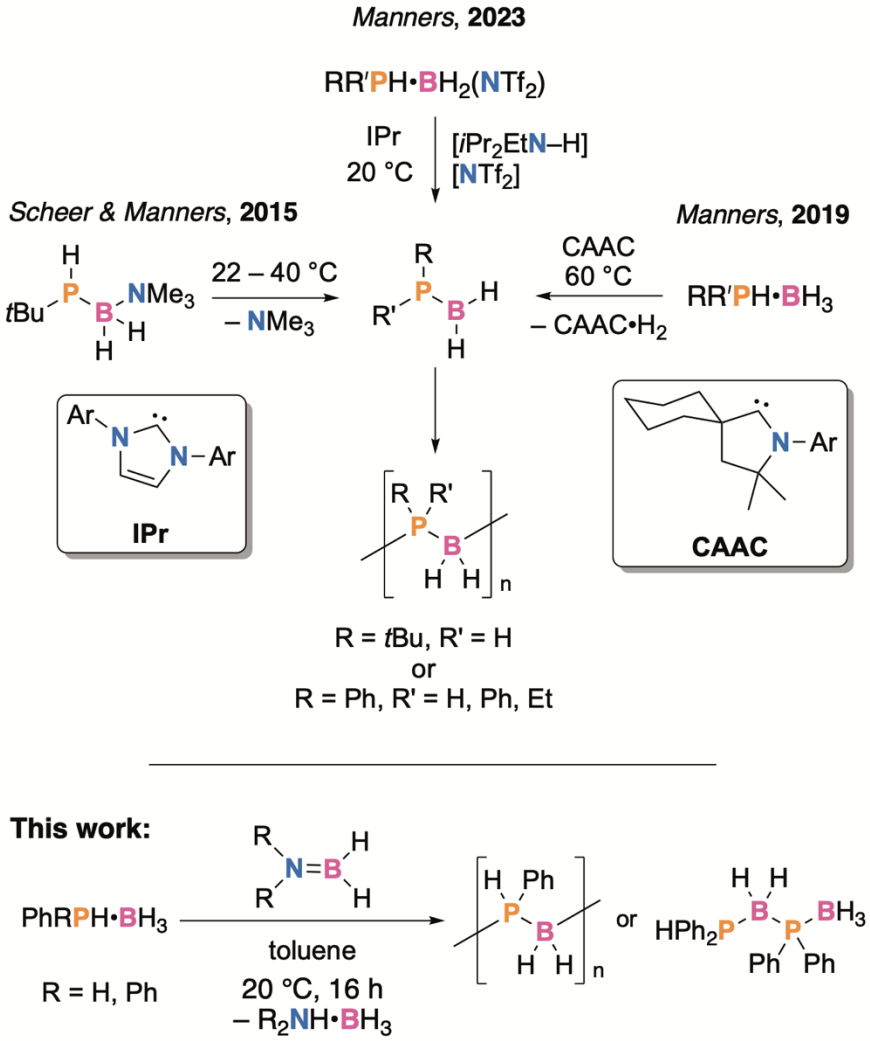


**Scheme 5.2**: Overview of synthesis of phosphinoboranes *in situ* as polymer precursors (top) and the focus of this study, the ability of aminoboranes to act as dehydrocoupling agents for phosphine-borane adducts (bottom).

## 5.3 Results and Discussion

The dehydrogenation of amine-boranes has been explored in greater detail than the dehydrogenation of phosphine-boranes.[39] What is striking about the chemistry of amine-boranes is that hydrogen can be transferred easily and spontaneously between amine-boranes and aminoboranes.[40] The mechanism of this transformation has been researched in great detail: An initial hydrogen bonding interaction between an amine-borane and an aminoborane leads to a 6-membered intermediate (**TS1**) which then undergoes an asynchronous concerted N-to-N' and B-to-B' hydrogen transfer (**Scheme 5.3**).[41] This reaction is driven forward by the cyclodimerization of **5.2c** to ***cyclo*-5.2c$_2$**. Therefore, we hypothesized that phosphine-boranes could undergo a similar transformation with an aminoborane where a 6-membered cyclic intermediate leads to a P-to-N and B-to-B' hydrogen transfer. This would yield transient phosphinoboranes (PhRP–BH$_2$) that are known to readily catenate into polymeric materials and amine-borane adducts (RRNH•BH$_3$).

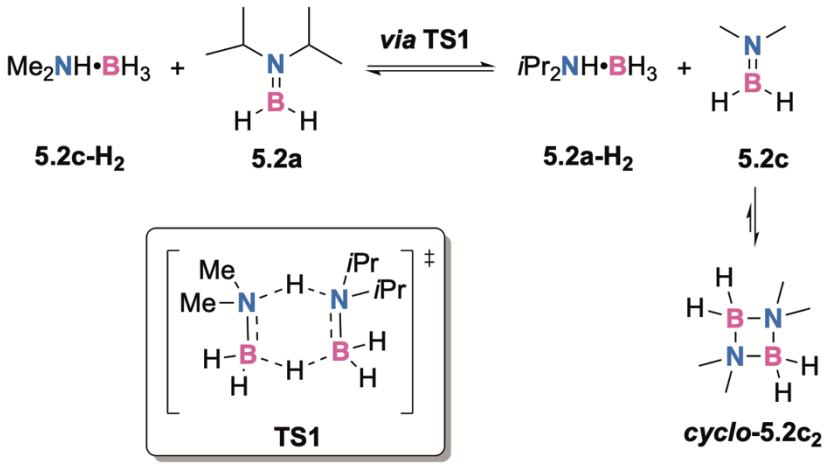


**Scheme 5.3:** Metal-free hydrogen transfer between aminoboranes and amine-borane adducts.

For this study, we chose to explore the reactivity of phosphine-borane adducts ($PhRPH{\bullet}BH_3$; R = H (**5.1a)** and Ph (**5.1b**)) with three different aminoboranes ($R_2N{=}BH_2$; R = *i*Pr (**5.2a**), Me (**5.2b**), and Et (**5.2c**)) (**Figure 5.1**). Each aminoborane **5.2a-c** has a different steric environment at the nitrogen centre, with *i*Pr being the most sterically demanding organic *N*-substituent, and Me being the least. In the case of **5.2a**, the free aminoborane has been detected *in situ*, indicated by its $^{11}B$ NMR spectrum with a single signal at *ca.* 34 ppm.[42]

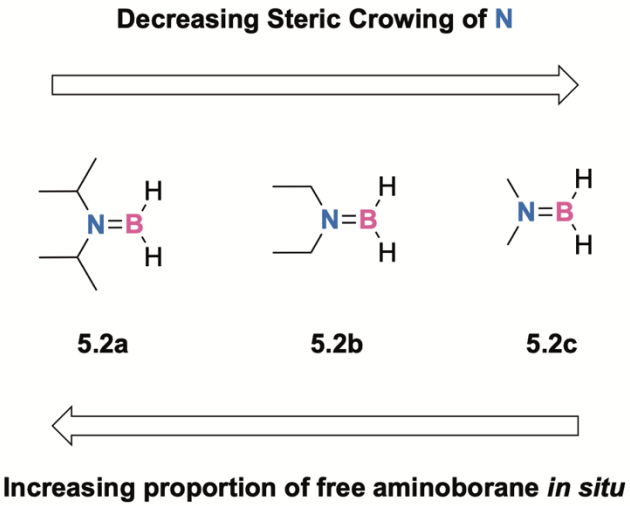


**Figure 5.1**: Overview of aminoboranes used in this study.

Di-isopropylaminoborane, **5.2a**, is readily accessed *via* the thermal dehydrogenation of its precursor amine-borane adduct ($iPr_2NH{\bullet}BH_3$) and can be stored indefinitely. However, aminoboranes **5.2b** and **5.2c** are known to readily cyclodimerize and exist in equilibria between free aminoborane and cyclic dimer, which is evidenced by $^{11}B$ NMR peaks at 36.5 ppm for **5.2b**[43] and 36.6 ppm for **5.2c**,[44,45] and 1.5 ppm for the cyclodimer of **5.2b** (***cyclo*-5.2b$_2$**)[43] and 4.5 ppm for that of **5.2c**, (**cyclo-5.2c$_2$**).[43] Thus, in

order to obtain high concentrations of an amino borane in solution for **5.2b** and **5.2c**, we targeted the synthesis of amine-(bis(trifluoromethanesulfonyl)imide)boranes ($R_2NH{\bullet}BH_2(NTf_2)$; R = Me (**5.3b**) and Et (**5.3c**); Tf = $SO_2CF_3$) as the deprotonation of these adducts should yield the respective aminoboranes (**Scheme 5.4**). Accordingly, to rapidly stirring DCM solutions of either $Et_2NH{\bullet}BH_3$ (**5.2b-$H_2$**) or $Me_2NH{\bullet}BH_2$ (**5.2c-$H_2$**) solid $HNTf_2$ was added at 20 °C, resulting in the formation of bubbles. After 1 h the formation of bubbles had ceased, and the reaction was determined to be complete by $^{11}B$ NMR spectroscopy as the precursor amine-borane adducts were consumed (with a peak at −17.9 ppm for **5.2b-$H_2$**[43] and −14.3 ppm for **5.2c-$H_2$**[46]) and that the new amine-(triflimido)boranes **5.3b** and **5.3c** were accessed indicated by new signals at –6.7 ppm and –5.2 ppm respectively. These are similar $^{11}B$ NMR chemical shifts reported for other closely related species.[38,47] Removing volatiles from these reactions, and recrystallizing **5.3b** and **5.3c** from DCM and hexanes allowed for the isolation of both as colorless crystals in high yields (87% for **5.3b** and 89% for **5.3c**). With **5.2a**, **5.3b**, and **5.3c** in hand, we sought to explore the reactivity of aminoboranes with phosphine-borane adducts.

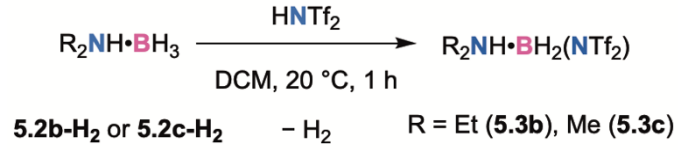


**Scheme 5.4:** Synthesis of aminoborane precursors **5.3b** and **5.3c**.

Initially, we explored the reactivity between the phosphine-borane adducts ($PhRPH{\bullet}BH_3$) (**5.1a** and **5.1b**) and **5.2a**. Accordingly, **5.2a** was added to toluene solutions of $PhRPH{\bullet}BH_3$ (**5.1a** and **5.1b**) and these solutions were left at 20 °C. After 24, the solutions were examined by $^{11}B$ and $^{31}P$ NMR spectroscopy revealed that no reaction had

occurred in either case. Thus, the solutions were transferred to J-Young tubes and placed in a heating block set to 60 °C. After another 24 hours, $^{11}$B and $^{31}$P NMR spectroscopy revealed that still no dehydrocoupling had occurred, and efforts were turned to other aminoboranes.

Our hypothesis was that *i*Pr$_2$N=BH$_2$ has a nitrogen centre that was too sterically encumbered and prohibited any hydrogen transfer chemistry. Thus, we explored the ability of the less sterically encumbered *N,N*-diethylaminoborane (**5.2b**) and *N,N*-dimethylaminoborane (**5.2c**) to accept H$_2$ from **5.1a** or **5.1b**. Accordingly, 2 M toluene solutions of equimolar amounts of either **5.3b** or **5.3c** and either **5.1a** or **5.1b** were prepared in 4 dram vials charged with stirring bars and to each one equivalent of *i*Pr$_2$EtN was added. After 24 hours at 20 °C, the reactions were investigated by $^{11}$B and $^{31}$P NMR spectroscopy after which revealed that both adducts had undergone dehydrocoupling, to access polyphosphinoborane, **5.4a** (δ($^{11}$B{$^1$H}): −34.7 ppm; δ($^{31}$P{$^1$H}): −48.9 ppm), from **5.1a**, and the dimeric species, **5.4b** (δ($^{11}$B{$^1$H}): −33.2 ppm, –37.3 ppm; $^{31}$P{$^1$H} −3.3 ppm, −17.7 ppm), from **5.1b** (**Figure 5.2**). While conversion of **5.1a** to **5.4a** was high when either aminoborane was used (100% from generating **5.2b** and 91% for **5.2c**), the conversion of **5.1b** to **5.4b** was low when using **5.2b** (44%) but significantly higher when using **5.2c** (71% conversion). Further, by $^{11}$B NMR spectroscopy, it was revealed that the corresponding amine-borane adduct (**5.2b-H$_2$** or **5.2c-H$_2$**) was formed in each reaction, and unreacted ***cyclo*-5.2b$_2$** and ***cyclo*-5.2c$_2$** was also observed. Gel-permeation chromatography of isolated **5.4a** accessed using **5.3c** confirmed the material was polymeric, albeit of low molecular weight ($M_n$ = 10 280, $Đ$ = 1.84). This is notable, as typically to access dehydrocoupled materials directly from phosphine-borane adducts

such as **5.1a** or **5.1b** significant heating is required for long periods of time.[4] Alternatively, cAAC-mediated dehydrocoupling of **5.1a** or **5.1b** requires temperatures at or above 60 °C for 4 hours.[37]

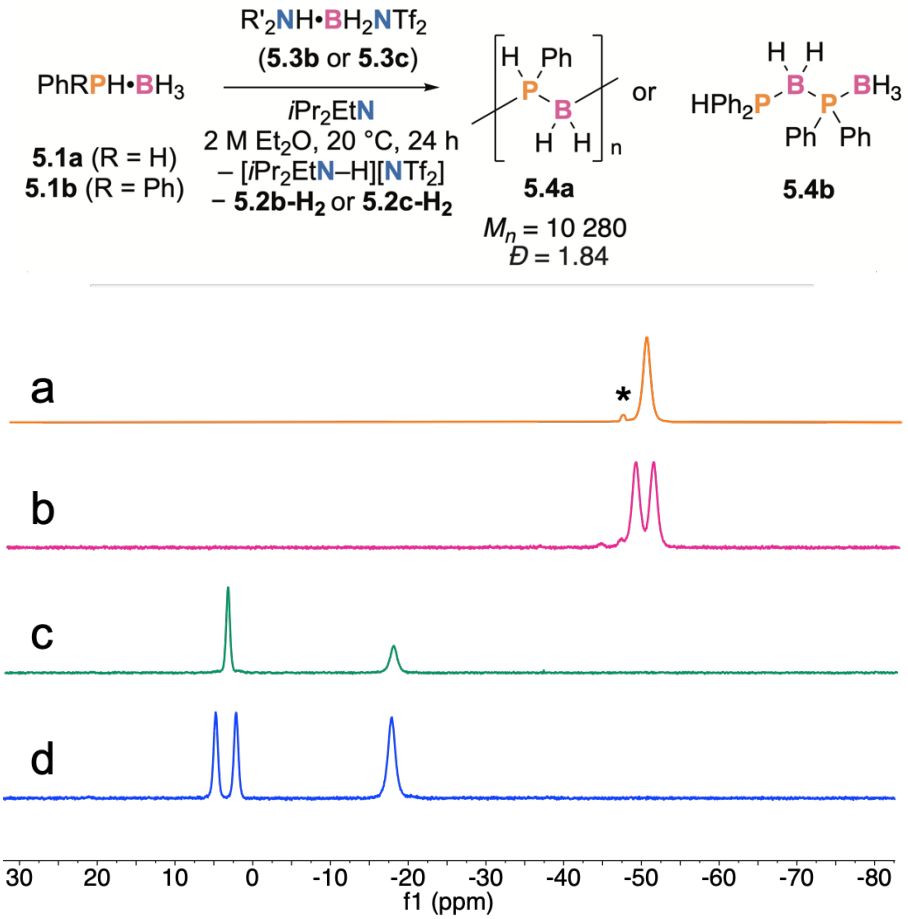


**Figure 5.2**: Dehydrocoupling of **5.1a** or **5.1b** using aminoboranes generated *in situ* under ambient conditions (top) and $^{31}P$ (a and c) and $^{31}P\{^{1}H\}$ (b and d) NMR spectra of crude reaction mixture containing dehydrocoupled products from **5.1a** (a and b) and **5.1b** (c and d) (bottom). Signal for residual unreacted **5.1a** marked with a "*". P–P coupling is not observed in the $^{31}P$ and $^{31}P\{^{1}H\}$ NMR spectra of **5.4b** likely due to the influence of adjacent $^{11}B$ nuclei.

After the discovery of this transformation, we aimed to monitor the reactivity more closely by following the depletion and generation of boron containing species by $^{11}B\{^1H\}$ NMR spectroscopy. Accordingly, 0.17 M $C_6D_6$ solutions of equimolar amounts of **5.1a** or **5.1b** with **5.3a** or **5.3b** were prepared in J-Young NMR tubes, and *i*$Pr_2$EtN was added subsequently. Then, within 5 minutes of base addition, $^{11}B\{^1H\}$ NMR spectra were obtained every minute over the course of one hour, of which relative concentrations are plotted below (**Figure 5.3**). In dehydrocoupling reactions between either **5.2b** or **5.2c** with **5.1a**, by the time the first spectrum was obtained, nearly all of the aminoborane had already converted into amine-borane adduct, and a significant portion of phosphine-borane had undergone dehydrogenation. Conversely, in dehydrocoupling reactions with **5.2b** or **5.2c** with **5.1b**, very little conversion of aminoborane to amine-borane adduct occurs. This suggests that the reaction between aminoboranes and *P*-disubstituted phosphine-borane adducts occur at a slower rate, likely due to the greater steric crowding of the phosphorus centre. However, in the dehydrocoupling reaction between **5.2b** and **5.1b**, the conversion of **5.2b** to ***cyclo*-5.2b$_2$** can be clearly observed. However, when using **5.2c** to dehydrocouple **5.1b**, only very small amounts of **5.2c** was observed *in situ* for the first few spectra, after which only ***cyclo*-5.2c$_2$** was observed.

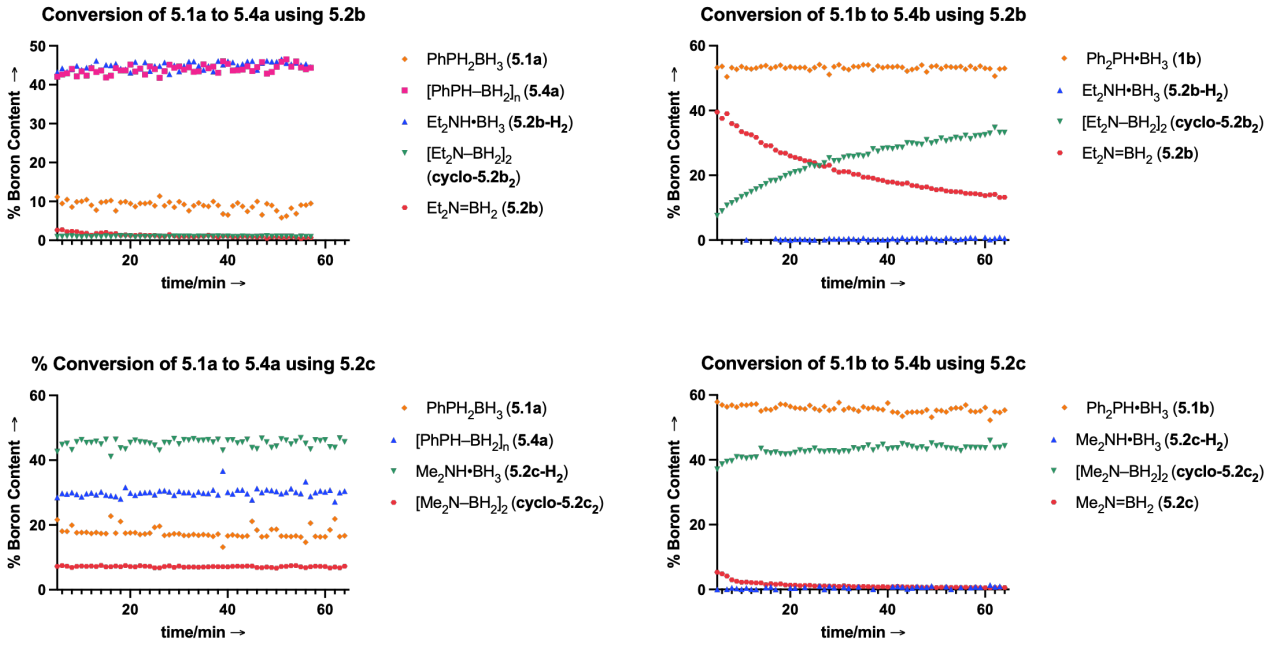


**Figure 5.3**: Conversion plots of **5.1a** to **5.4a** (left) and **5.1b** to **5.2b** (right) using **5.2b** (top_ and **5.2c** (bottom) generated *in situ*. Values were determined by $^{11}$B NMR spectroscopy.

The mechanism of this reaction was further investigated by a DFT study. This endeavor was aided by the fact that the hydrogen transfer chemistry between **5.2a** and $Me_2NH•BH_3$ has already been reported.[41] In this study it was revealed that the dehydropolymerization operates through a concerted N-to-N and B-to-B hydrogen transfer *via* a 6-membered transition state (**Scheme 5.3**, **TS1**).[41] The computations were performed at the PBE0 level of theory with 6-31G(d,p) basis set, which revealed an transition state energetic barrier of 91 kJ•mol$^{-1}$ (22 kcal•mol$^{-1}$). Furthermore, the overall hydrogen transfer was endergonic with a ΔG° value of 11 kJ•mol$^{-1}$ (2.6 kcal•mol$^{-1}$). However, as DMAB readily dimerizes, the overall transformation was exergonic, with a ΔG° of –18 kJ•mol$^{-1}$ (−4.3 kcal•mol$^{-1}$).

For exploring the reaction between **5.1a** and **5.2b** we chose to use the PBE0-D3BJ level of theory and the def2-TZVP basis set. The 6-membered transition state (**Figure 5.3**, **TS2**) was located computationally with a barrier of 84 kJ•mol$^{-1}$ (20 kcal•mol$^{-1}$), comparable to the barrier determined for the hydrogen transfer between $Me_2NH•BH_3$ and **5.2a**. Further, similar to the reactions between **5.2a** and $Me_2NH•BH_3$, the overall dehydrogenation of $PhPH_2•BH_3$ with **5.2b** is endergonic (49 kJ•mol$^{-1}$ or 12 kcal•mol$^{-1}$). However, as phosphinoboranes without significant steric protection defy isolation and readily undergo subsequent reactivity,[48,49] it is reasonable that this reaction is driven forward by subsequent head-to-tail addition polymerization. The values were also calculated for the reaction between **5.1b** and **5.2b** where the transition state was located with a barrier of 82 kJ•mol$^{-1}$ (20 kcal•mol$^{-1}$) and the overall hydrogen transfer was also endergonic (61 kJ•mol$^{-1}$ or 15 kcal•mol$^{-1}$).

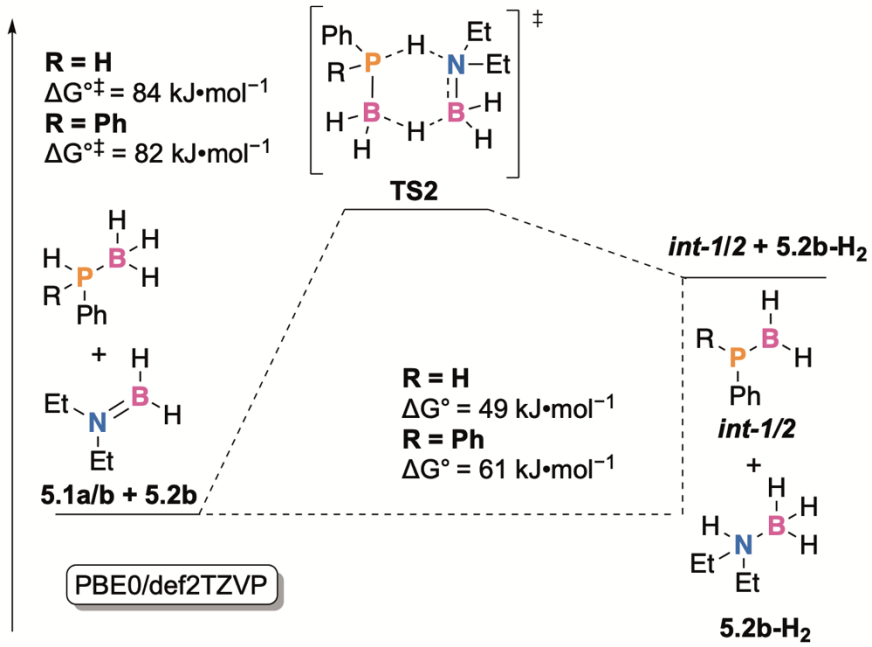


**Figure 5.4:** Gibbs free energy reaction profile for the dehydrogenation of **5.1a** and **5.1b** using **5.2b** to access *int-1* (R = H) and *int-2* (R = Ph) and **5.2b-H$_2$** *via* **TS2**.

If the computed mechanism were to operate, one would expect a kinetic isotope effect to occur. Accordingly, for the dehydrogenation of **5.1a** using **5.2b** as a hydrogen acceptor we explored the effect of replacing P- and B-bound hydrogen atoms with deuterium atoms. Firstly, a kinetic isotope effect ($k_H/k_D$) of 1.64 was determined from computed structures (PBE0/def2TZVP) using conventional transition state theory including Wigner's tunnelling correction.[50] Further, reaction of **5.1a-*d*$_5$** ($PhPD_2{\bullet}BD_3$) with **5.2b** generated *in situ* resulted in what appears to be a slower rate of dehydrogenation. When dehydrocoupling **5.1a**, the reaction reaches nearly full completion by the time the first $^{11}B\{^1H\}$ NMR spectrum is obtained, while in the case of **5.1a-*d*$_5$** only about half of the phosphine-borane adduct has undergone dehydrogenation within the same time.

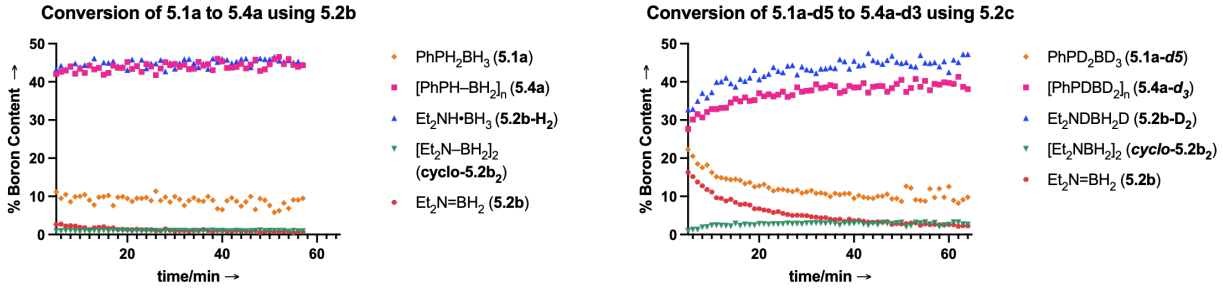


**Figure 5.5:** Comparison of the rates of reaction between **5.2b** generated *in situ* with **5.1a** and **5.1a-*d*$_5$**.

Thus, based on our studies we currently believe that this reaction operates under the following mechanism (**Scheme 5.5**). Free aminoborane (**5.2b** or **5.2c**) formed *in situ* can react with itself to generate the corresponding cyclic dimer species (***cyclo*-5.2b$_2$** or ***cyclo*-5.2c$_2$**), which is a well-studied phenomenon.[41] However, it can also react with phosphine borane adduct (**5.1a** or **5.1b**), possibly *via* a 6-membered transition state to access phosphinoboranes (***int-1*** or ***int-2***) and amine-borane adducts (**5.2b-H$_2$** or **5.2c-**

$H_2$) *in situ*. These reactive phosphinoboranes undergo subsequent chemistry, depending on the steric environment of the phosphorus centre. The less sterically encumbered ***int-1*** ($PhPH–BH_2$), can undergo subsequent addition polymerization to yield **5.4a**, and the more sterically encumbered ***int-2*** ($Ph_2P–BH_2$) undergoes P–B bond forming reactions to access the linear dimer, **5.4b**.

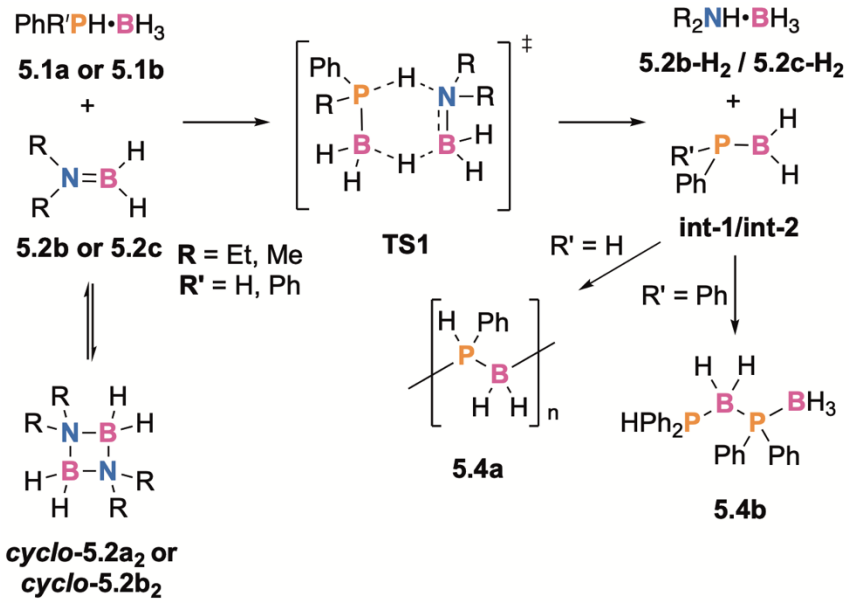


**Scheme 5.5**: Proposed mechanism of aminoborane-mediated dehydrocoupling of phosphine-borane adducts.

The catalytic dehydrocoupling of phosphine-borane adducts under ambient conditions was also targeted. We envisioned this would be possible through the generation and regeneration of reactive aminoboranes *in situ* as they are much less challenging to dehydrogenate than phosphine-boranes.[4] In this survey $Cp^*_2TiMe$ (**5**, $Cp^*$ = pentamethylcyclopentadienyl), a potent single-site, early transition metal-based amine-

borane dehydrogenation catalyst,[51] was used to dehydrogenate either **5.2b-H$_2$** or **5.2c-H$_2$** in the presence of phosphine-borane adducts (**5.1a** or **5.1b**). Here, 1.33 M solutions containing **5.2b-H$_2$** or **5.2c-H$_2$**, **5.1a** or **5.1b**, and 2.5 mol% (relative to amine-borane and phosphine-borane) of **5.5** were prepared in $C_6D_6$ at 20 °C. Upon addition of **5.5**, the solution went from a dark blue color to green, indicating that a transformation had occurred. However, the solutions were left to stir for 24 hours longer, after which they were monitored by $^{11}$B and $^{31}$P NMR spectroscopy. Investigation of the heteronuclear spectra revealed that some conversion (*ca.* 16%) of **5.1b** to **5.4b** had occurred when **5.2c-H$_2$** was used as the aminoborane source (**Figure 5.5**). In each other case, very little to no conversion of **5.1a** or **5.1b** to **5.4a** or **5.4b** was observed. Further in a control reaction under the same conditions without the presence of **5.2c**, no conversion of **5.1b** to **5.4b** was observed. It is possible that the conversion of 16% of **5.1b** to **5.4b** in the presence of **5.5** was due to the higher rate of dehydrogenation of **5.2c-H$_2$** to **5.2c**, compared to the slightly bulkier **5.2b-H$_2$**. The limited success may be due to the fact that phosphine-borane adducts are known to undergo reactions with Ti$^{III}$ species.[52] Accordingly, **5.1b** likely reacts with **5.5** slower than **5.1a** would as it is more sterically encumbered, potentially explaining why dehydrocoupling with a *P*-disubstituted phosphine-borane has occurred while dehydrocoupling with the *P*-monosubstituted phosphine-borane has not.

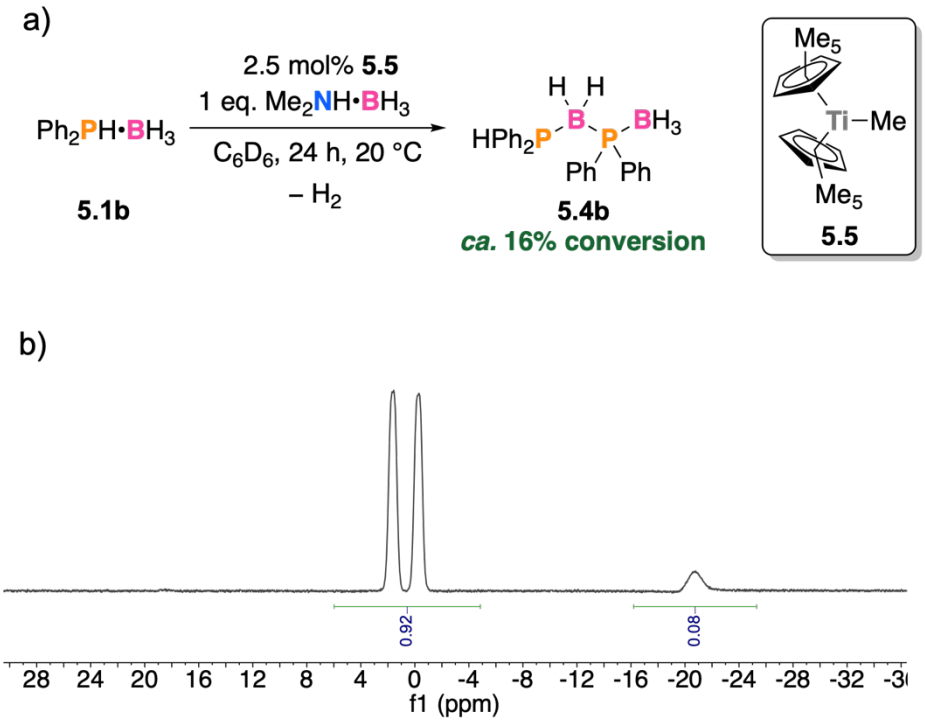


**Figure 5.6:** Reaction conditions for the ambient condition catalytic dehydrocoupling of **5.1b** using a Ti catalyst to generate aminoboranes *in situ* (a), and the $^{31}P\{^{1}H\}$ NMR spectrum of the reaction mixture, revealing 16% conversion of **5.1b** to **5.4b**.

## 5.4 Conclusion

In this study, we have unlocked the ambient condition dehydrocoupling of phosphine-borane adducts using simple reagents. This was made possible through using aminoboranes as hydrogen acceptors. It was found that the steric environment of the nitrogen centre was an important factor in whether or not this reaction could occur. Here, a too sterically encumbered nitrogen centre of the aminoborane would prevent the dehydrogenation reaction from occurring, but if the nitrogen centre is not sufficiently kinetically protected, the aminoborane will dimerize and compete with the dehydrogenation reaction. We propose that this reaction occurs *via* the 6-membered transition state where hydrogen transfer occurs in a concerted P-to-N and B-to-B fashion, similar to what has been observed for $H_2$ transfer between amine-borane adducts and aminoboranes. Lastly, through metal-catalyzed regeneration of reactive aminoboranes, we have been able to catalytically dehydrocouple phosphine-boranes under ambient conditions using an early transition metal through a transfer dehydrogenation mechanism. Further studies will aim to explore other catalysts to access the ambient condition catalytic dehydropolymerization of phosphine-borane adducts *via* the proposed transfer dehydrogenation mechanism. Also, a more in-depth study of the reaction mechanism for the dehydrogenation of phosphine-boranes by aminoboranes is underway.

## 5.5 Experimental

Unless otherwise noted, storage and manipulation of chemicals were performed under an inert atmosphere of either $N_2$ or Ar gas using standard Schlenk techniques or carried out in an MBraun 200B glovebox. Further, any glassware used was dried overnight in an oven at 200 °C. Toluene was dried using an MBraun Grubbs/Dow solvent purification system[53] and stored over activated 4 Å molecular sieves. Benzene-$d_6$ was purchased from Sigma Aldrich and was dried *via* distillation off sodium metal and degassed *via* freeze-pump-thaw cycles, chlorodorm-$d_1$ *was purchased from Sigma Aldrich and used as received*. The phosphine-borane adducts, $PhPH_2{\bullet}BH_3$ (**5.1a**) and $Ph_2PH{\bullet}BH_3$ (**5.1b**),[21,22] amine-borane adducts $Et_2NH{\bullet}BH_3$ (**5.2b-$H_2$**) and $Me_2NH{\bullet}BH_3$ (**5.2c-$H_2$B**),[54–56] and $i$$Pr_2N{=}BH_2$ (DIAB)[42] were prepared using standard literature procedures. Solvents used in the isolation of polymeric material were purchased from Sigma Aldrich and used as received. Nuclear Magnetic Resonance (NMR) spectroscopy was performed on a Bruker Avance NEO 500 MHz spectrometer. $^1$H NMR spectra were referenced to the residual protons in the deuterated solvents and heteronuclear spectra were referenced using the recommended IUPAC reference compounds. $^{13}$C were referenced to their corresponding solvent peaks. Mass Spectrometry was performed on a Thermo brand Ultimate 3000 ESI-MS, equipped with an orbitrap mass selector with a resolution of 140,000. Samples were prepared by dissolving *ca*. 0.1 mg of product in 3 mL of HPLC grade acetonitrile and the resulting solution passed through a 0.2 μm PTFE syringe filter prior to analysis. IR spectroscopy was performed using an Agilent Cary 630 FTIR spectrometer fitted with an ATR diamond sampling module with a resolution of 4 $cm^{-1}$. For each IR experiment, 32 background scans were performed, and spectra were obtained from 4000–650 $cm^{-1}$. Gel-

permeation chromatography (GPC) was performed on a Malvern RI max Gel Permeation Chromatograph, equipped with an automatic sampler, a pump, an injector, and inline degasser. The columns (styrene/divinyl benzene gel, 1xT5000 and 1xT3000) were maintained at 35 °C. Sample elution was detected by means of a differential refractometer. THF (VWR), containing 0.1 wt% [*n*-$Bu_4N$]Br to prevent adsorption,[57] was used as the eluent at a flow rate of 1 mL•$min^{-1}$. Samples were dissolved in THF (2 mg/mL) and filtered through a 0.2 µm PTFE syringe filter before analysis. Calibration was conducted using commercially available monodisperse polystyrene standards (Aldrich, 1 200 – 4 200 000 Da).

**General Procedure for the synthesis of Amine-(Triflimido)Borane Adducts**

A solution of the corresponding amine-borane adduct (1.0 mmol, **5.2b-**$H_2$: 86 mg, **5.2c-$H_2$**: 58 mg) was prepared in dichloromethane (1 mL) in a 20 mL vial charged with a stirring bar. To the rapidly stirred solution was carefully added solid bis(trifluoromethanesulfonyl)amine (1.0 mmol, 281 mg) resulting in the immediate evolution of a gas. The solution was allowed to stir for 30 min further followed by removal of volatiles *in vacuo* which yielded colourless solids. The solids were then recrystallized from a mixture of dichloromethane and hexanes resulting in high yields of the colourless product.

**$Et_2NH•BH_2(NTf_2)$ 5.3b:** 87% yield (318 mg). $^1$H NMR ($CDCl_3$, 298 K, 500 MHz): 3.90 ppm (1H, br s, N–H), 3.05 ppm (2 H, m, $N(C\underline{H_2}CH_3)_2$), 2.87 ppm (2 H, m, $N(C\underline{CH_2}CH_3)$, 2.50 (2 H, br m, $B\underline{H_2}NTf_2$), 1.29 ppm (6 H, t, $^3J_{HH}$ = 6.5 Hz, $N(CH_2C\underline{H_3})$. ; $^{11}$B NMR ($CDCl_3$, 295 K, 161 MHz): –6.7 ppm; $^{13}C\{^1H\}$ NMR ($CDCl_3$, 298 K, 126 MHz): 119.6 ppm (q, $\underline{C}F_3$), 45.4

ppm (s, N($\underline{C}H_2CH_3)_2$), 11.18 (s, N($CH_2\underline{C}H_3$) . ESI-MS: (*note, cleavage of B–$NTf_2$ was observed in an acetonitrile solution, and instead the accurate mass values for [$Et_2NH$–$BH_2(MeCN)]^+$ and [$NTf_2]^-$ are reported)* Positive mode calculated for $C_6H_{16}BN_2$: 127.14065 m/z, Found: 127.14098 m/z; Negative mode calculated for $C_2F_6NO_4S_2$: 279.91729 m/z, Found: 279.91756. FTIR-ATR (neat): $\nu_{N–H}$: 3255 $cm^{-1}$, $\nu_{B–H}$: 2486 $cm^{-1}$.

**$Me_2NH•BH_2(NTf_2)$ 5.3c:** 89% yield (300 mg). $^1H$ NMR ($CDCl_3$, 298 K, 500 MHz): 4.51 ppm (1 H, br s, N–H), 2.62 (6 H, d, N($C\underline{C}H_3)_2$), (2 H, br m, $B\underline{H}_2NTf_2$); $^{11}B$ NMR ($CDCl_3$, 295 K, 161 MHz): –5.21 ppm (br); $^{13}C\{^1H\}$ NMR ($CDCl_3$, 298 K, 126 MHz): 119.6 ppm (q, $\underline{C}F_3$), 40.5 ppm (s, N($\underline{C}H_3)_2$). ESI-MS: (*note, cleavage of B–$NTf_2$ was observed in an acetonitrile solution, thus the accurate mass values for [$Me_2NH$–$BH_2(MeCN)]^+$ and [$NTf_2]^-$ are reported)* Positive mode calculated for $C_6H_{16}BN_2$: 99.10935 m/z, Found: 99.10912 m/z; Negative mode calculated for $C_2F_6NO_4S_2$: 279.91729 m/z, Found: 279.91798. FTIR-ATR (neat): $\nu_{N–H}$: 3263 $cm^{-1}$, $\nu_{B–H}$: 2475 $cm^{-1}$.

**Reaction of Phosphine-Borane Adducts (5.1a and 5.1b) with *i*$Pr_2N=BH_2$ (5.2a)**

To an 8-dram vial charged with a stirring bar was added phosphine-borane adduct (1 mmol; **5.1a**: 124 mg, **5.1b**: 200 mg), *N,N*-diisopropylaminoborane (0.5 mmol, **5.2a**: 113 mg) and 250 µL of toluene. The solution was then left to stir at room temperature for 24 h, after which it was transferred to a J-Young NMR tube and diluted to 750 µL. Monitoring the reaction by $^{11}B$ and $^{31}P$ NMR spectroscopy revealed no conversion of either phosphine-borane adduct occurred. Thus, the sealed NMR tubes were transferred to a heating block set to 60 °C and left to react for another 24 h. Subsequently, the reactions

were monitored once more by $^{11}B$ and $^{31}P$ NMR spectroscopy. In both reactions, no dehydrocoupling was observed.

**General Procedure for Ambient Condition Dehydrocoupling of Phosphine-Borane Adducts using Aminoboranes generated *in situ* as Hydrogen Acceptors**

To an 8-dram vial charged with a stirring bar was added phosphine-borane adduct (0.5 mmol; **5.1a**: 62 mg, **5.1b**: 100 mg), amine-triflimidoborane adduct (0.5 mmol; **5.3a**: 183 mg, **5.3b**: 169 mg) and 250 µL of toluene. Then, to this stirring solution was added *i*$Pr_2$EtN (0.5 mmol, 87 µL). The solution was allowed to stir for 24 h. For reactions involving **5.1a**, after 24 h the reaction mixture was poured into stirring cold hexanes, resulting in the formation of a white precipitate. The precipitate was collected by carefully removing the supernatant. The precipitate was then redissolved in THF and reprecipitated into another vial of cold, rapidly stirring hexanes. Decanting the supernatant and drying the resulting precipitate *in vacuo* resulted in the isolation of polyphosphinoborane, **5.4a**, with characterization data given below. For reactions involving **5.1b**, the obtained phosphinoborane dimer material **5.4b** was not isolated, and instead %conversion values are given.

**$[PhPH–BH_2]_n$ (5.4a)**: Using **5.3b**, 100% conversion was obtained after 24 h by NMR spectroscopy, and there was an isolated yield of 61% (76 mg). Using **3c**, 91% conversion was obtained after 24 h by NMR spectroscopy and there was an isolated yield of 54% (67 mg).

$^1H$ NMR (500 MHz, 298 K, $CDCl_3$): δ = 6.85 – 7.52 ppm (5 H, br m, Ar-H), 4.29 ppm (1 H, br d, $^1J_{HP}$ = 349 Hz, PH), 1.53 ppm (2 H, br, $BH_2$). $^{11}B\{^1H\}$ NMR (160 MHz, 298 K, $CDCl_3$):

δ = −34.7 ppm (br); $^{31}$P NMR (200 MHz, 298 K, $CDCl_3$): δ = −48.9 ppm (d, $^1J_{PH}$ = 349 Hz). GPC: $M_n$ = 10 280, $Đ$ = 1.84.

**$Ph_2PH•BH_2$–$Ph_2P•BH_3$ (5.4b)**: Using **5.3b,** 44% conversion was obtained after 24 h by NMR spectroscopy. Using **5.3c**, 71% conversion was obtained after 24 h by NMR spectroscopy.

$^{11}$B NMR ($CDCl_3$, 295 K, 161 MHz): −33.2 (br, $\underline{B}H_2$), –37.3 (br, $\underline{B}H_3$); $^{31}$P{$^1$H} NMR ($CDCl_3$, 298 K, 202 MHz): −3.3 ppm (br, $Ph_2PH$), −17.7 (br, $Ph_2P$).

**Reaction Procedure for Relative Rate Estimation**

To a 1-dram vial charged with a stirring bar was added phosphine-borane adduct (0.13 mmol; **5.1a** 16 mg, **5.1a-*d*$_5$** 17 mg, or **5.1b** 26 mg), amine-triflimidoborane adduct (0.13 mmol, **5.3b**: 48 mg, **5.3c**: 44 mg) and 750 µL of $C_6D_6$. The solution was allowed to stir for a few moments to ensure homogeneity and then transferred to a J-Young NMR tube. Then, to this tube was added *i*$Pr_2$EtN (0.13 mmol, 23 µL). The tube was then sealed, and removed from the glovebox. Just before inserting the tube into the NMR probe, the tube was inverted twice to ensure homogeneity of the reaction mixture. The first spectra was obtained within 5 minutes of the reaction starting and the reactions were then monitored over the next hour by $^{11}$B{$^1$H} spectroscopy. Data from the reactions between **1a** or **1b** with **2b** or **2c** are shown in **Figure 5.3** and the comparison of the reactions between **1a** or **1a-*d*$_5$** are shown in **Figure 5.6**. Stacked NMR spectra of the reactions are available in **Figures 5.7** to **Figure 5.11**.

**Reaction Procedure for Catalytic Transfer Dehydrocoupling of Phosphine-Borane Adducts**

To a 1-dram vial charged with a stirring bar was added phosphine-borane (1 mmol, **5.1a**: 124 mg, **5.1b**: 200 mg) and amine-borane adduct (1 mmol, **5.2b-H$_2$**: 86 mg, **5.2c-H$_2$**: 58 mg). To each vial was added 500 µL of $C_6D_6$. In a separate vial, a 0.1 M dark blue solution of Cp*TiMe (**5.5**) in $C_6D_6$ was prepared. To each rapidly stirring reaction 250 µL of the solution of **5.5** (0.025 mmol, 8 mg) was added, for a final volume of 750 µL, resulting in a change from a deep blue colour to green. This solution was then stirred over 24 hours and subsequently monitored by $^{31}P$ and $^{31}P\{^1H\}$ NMR spectroscopy. In a control reaction, no reactivity between **5.1b** and **5.5** was observed without **5.2c-H$_2$** present.

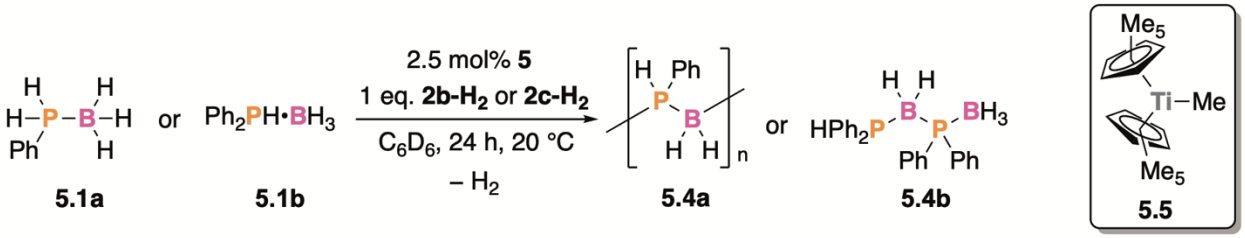


**Scheme 5.6:** Reactions attempted for the ambient condition catalytic dehydrocoupling of phosphine-borane adducts.

**Computational Details**

All the computations were performed using the Gaussian16.C01 program suite.[58] In each case, the PBE0 hybrid functional[59] was used with the def2-TZVP basis set,[60] and Grimme's empirical dispersion with Becke-Johnson dampening (D3)[61] was used.

Stationary points were confirmed as local minima by the lack of imaginary frequencies, while transition states were confirmed by the presence of one imaginary frequency.

**NMR Spectra**

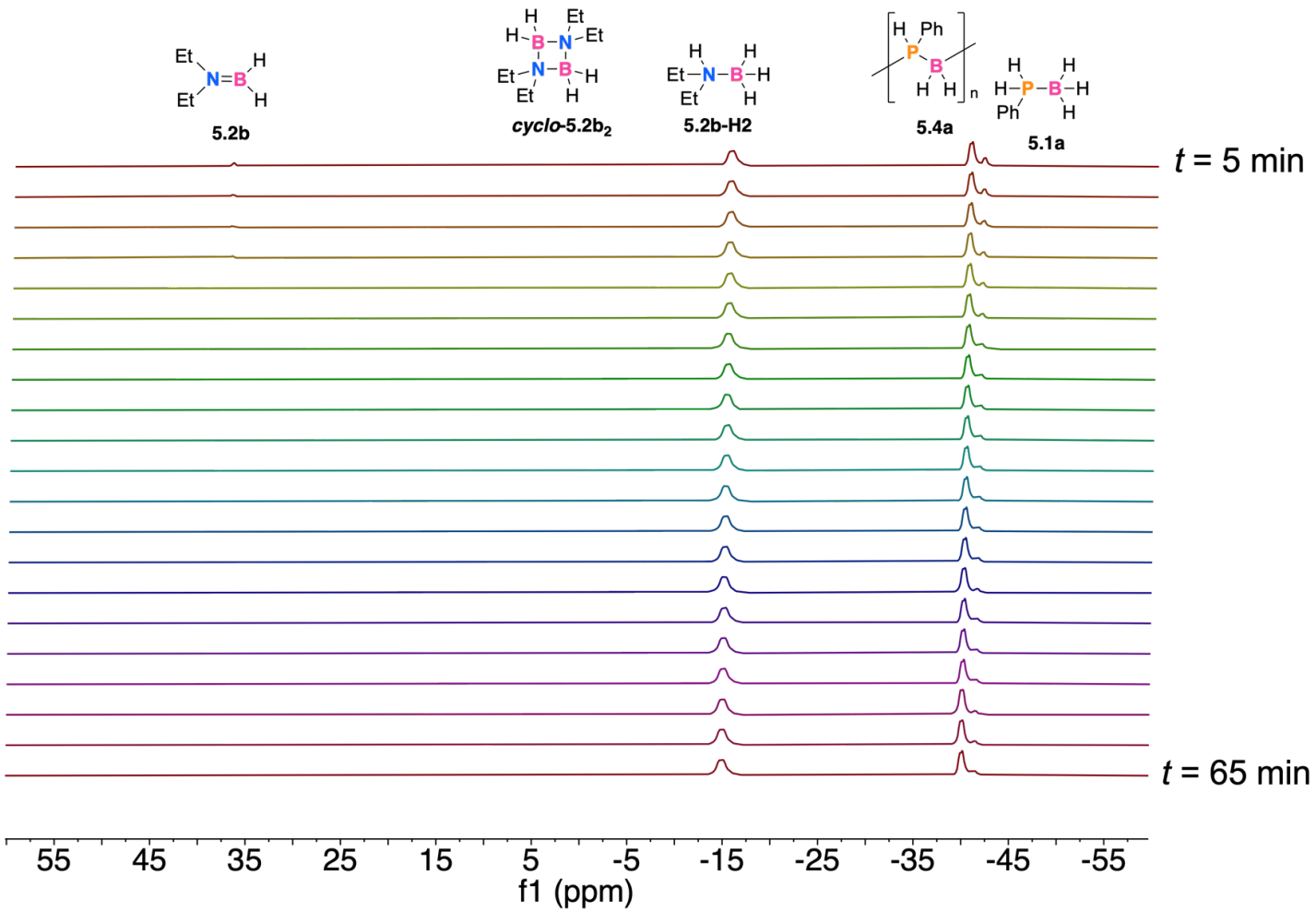


**Figure 5.7**: $^{11}$B NMR spectra taken over 60 min (160 MHz, 298 K, $C_6D_6$) of a reaction mixture containing **5.2b**, ***cyclo*-5.2b$_2$**, **5.2b-H$_2$**, **5.4a** and **5.1b**.

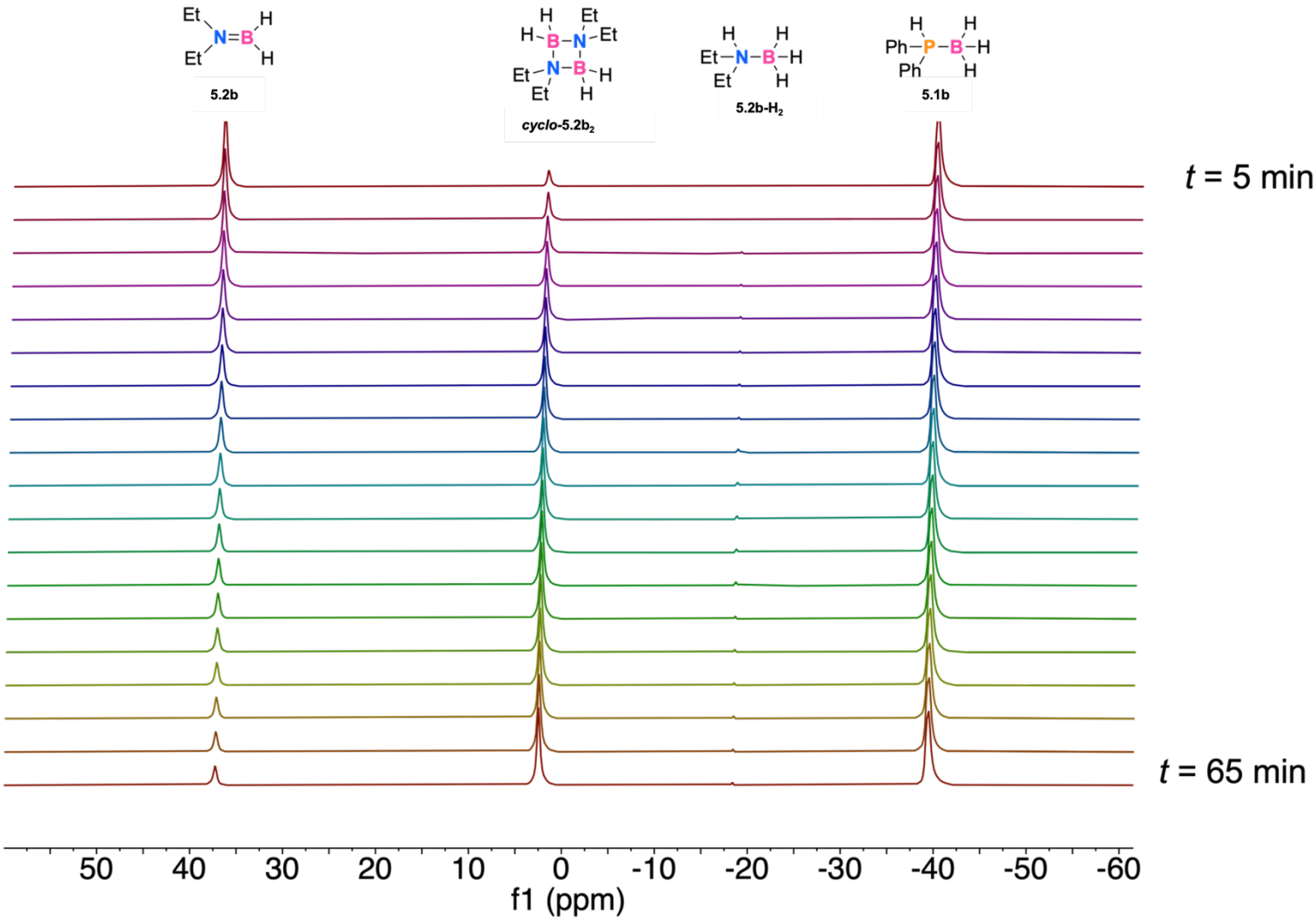


**Figure 5.8:** $^{11}$B NMR spectra taken over 60 min (160 MHz, 298 K, $C_6D_6$) of a reaction mixture containing **5.2b**, ***cyclo*-5.2b$_2$**, **5.2b-H$_2$**, and **5.1b**.

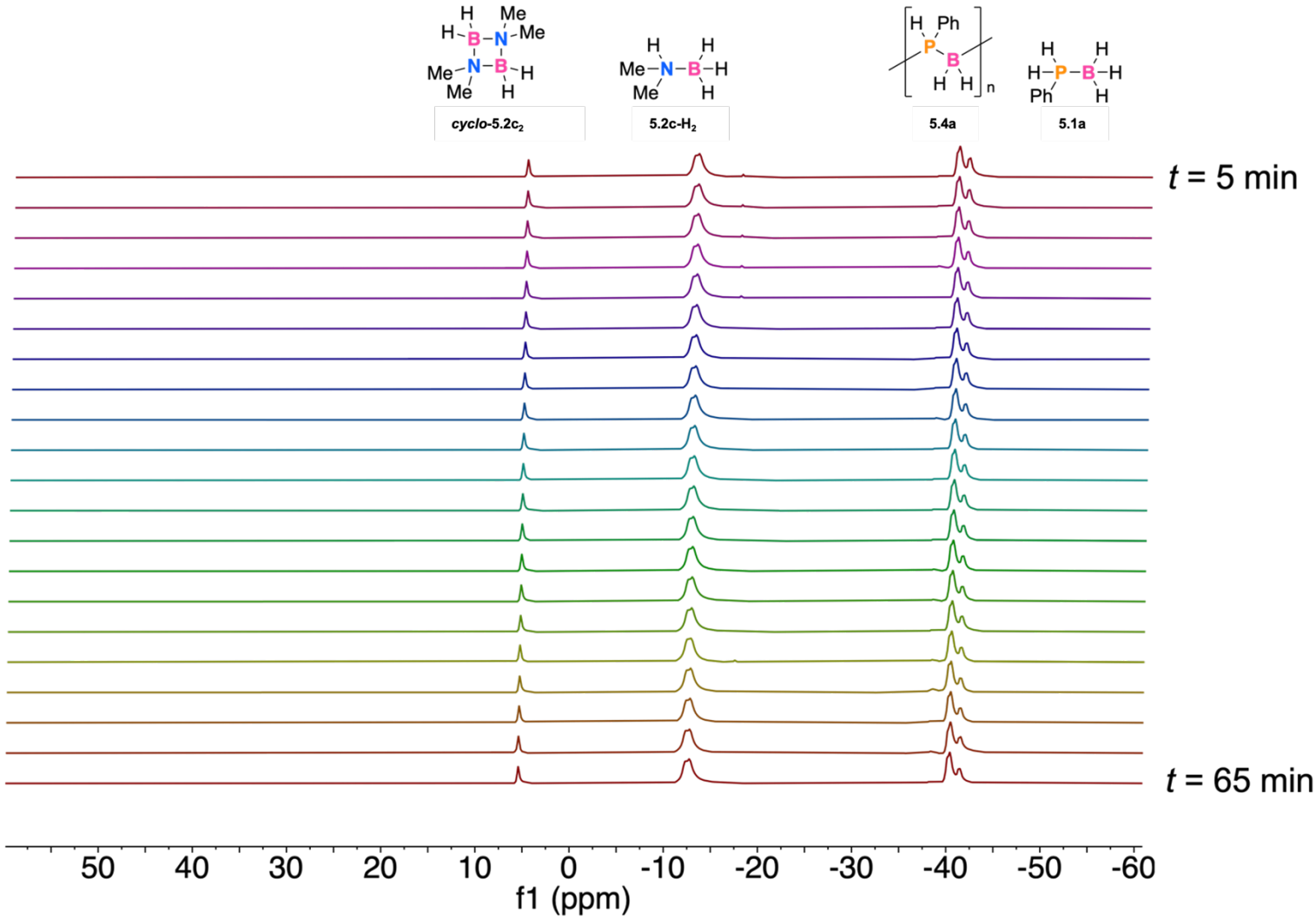


**Figure 5.9: :** $^{11}$B NMR spectra taken over 60 min (160 MHz, 298 K, $C_6D_6$) of a reaction mixture containing ***cyclo*-5.2c$_2$**, **5.2c-H$_2$**, **5.4a** and **5.1a.**

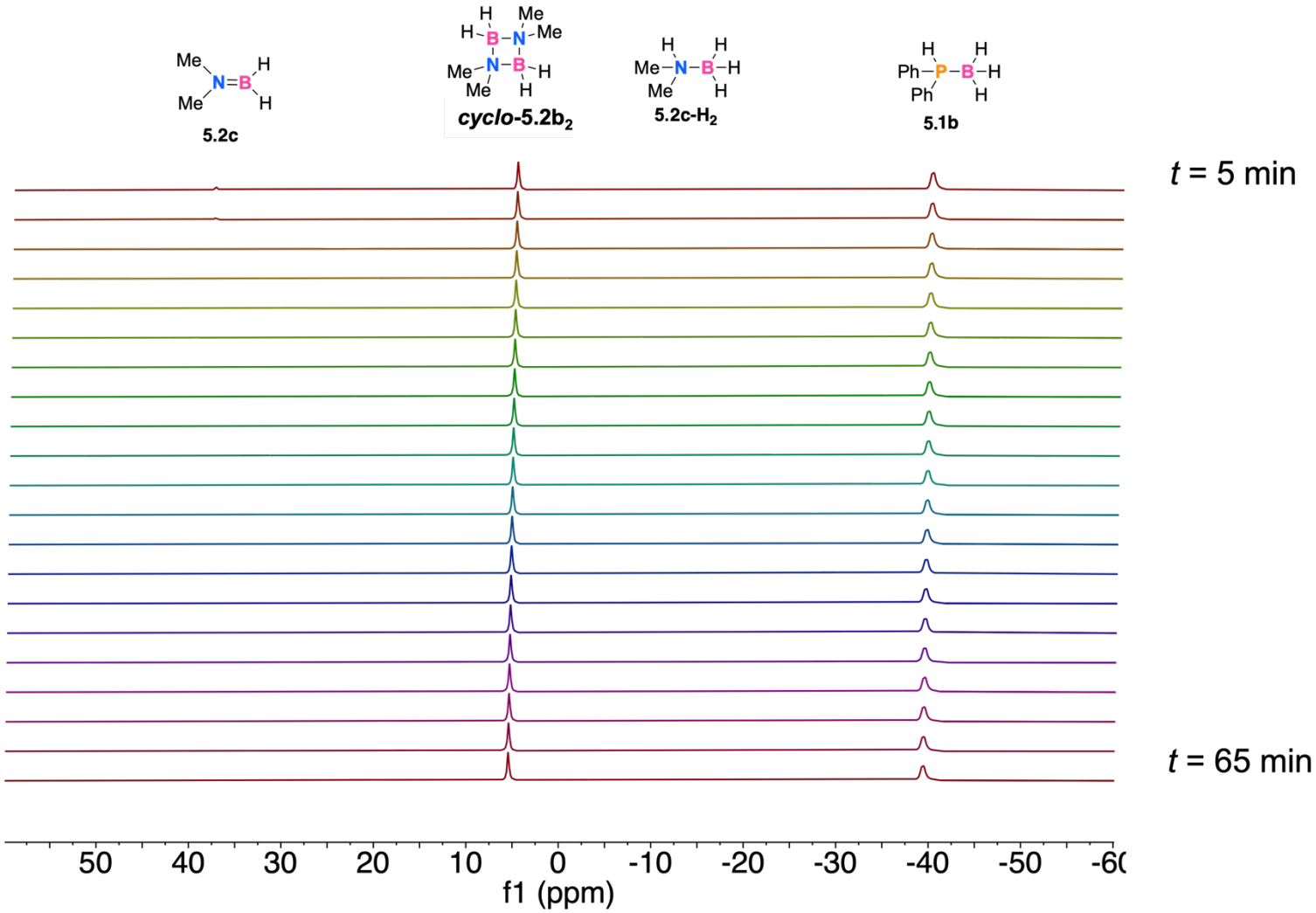


**Figure 5.10**: $^{11}$B NMR spectra taken over 60 min (160 MHz, 298 K, $C_6D_6$) of a reaction mixture containing **5.2c**, ***cyclo*-5.2c$_2$**, **2c-H$_2$**, and **5.1b**.

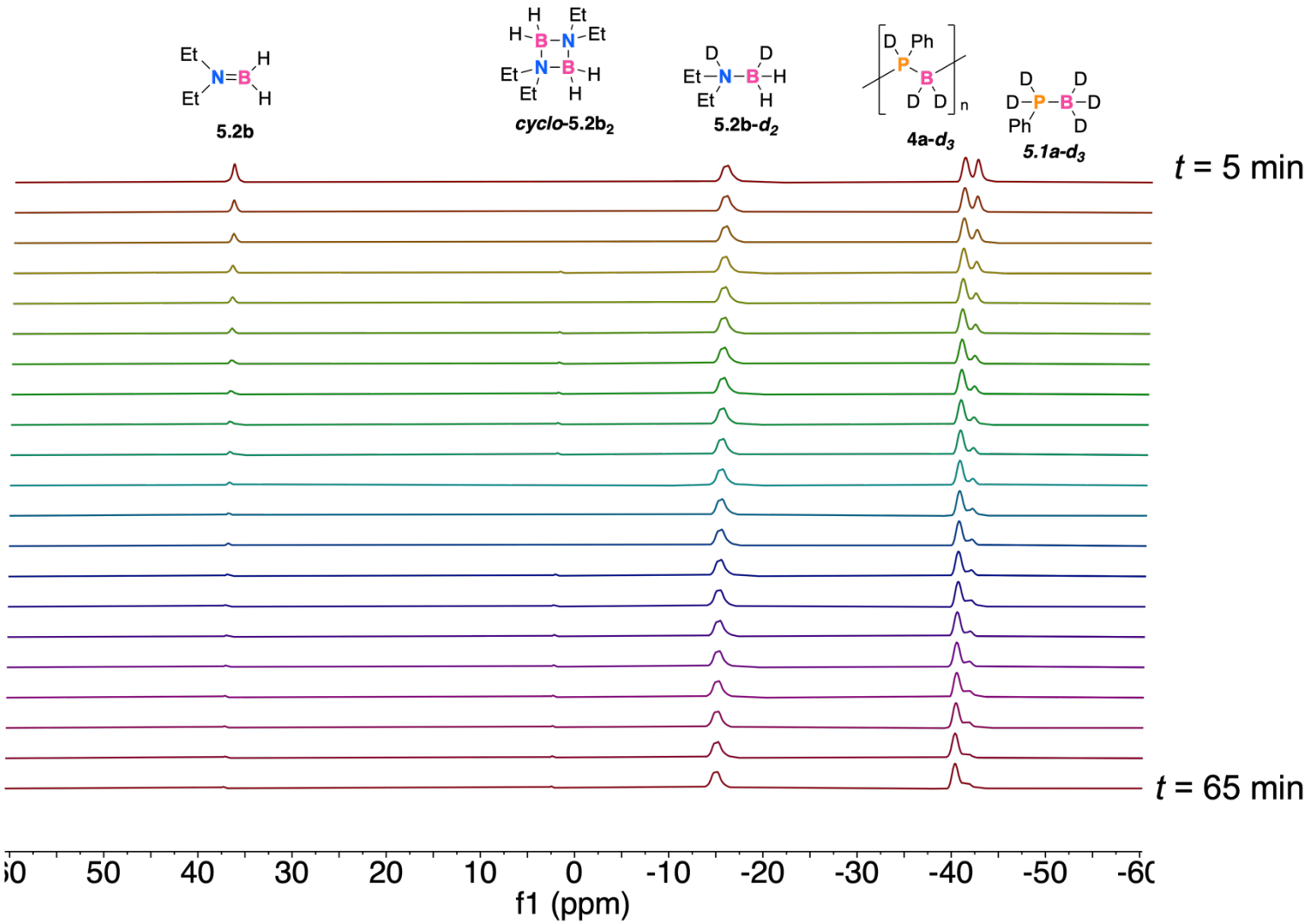


**Figure 5.11:** $^{11}$B NMR spectra taken over 60 min (160 MHz, 298 K, $C_6D_6$) of a reaction mixture containing **5.2b**, ***cyclo*-5.2b$_2$**, **2b-*d*$_2$**, **5.4a-*d*$_3$ and 5.1a-*d*$_5$**.

## 5.6 References


(1) Chivers, T.; Manners, I. *Inorganic Rings and Polymers of the P-Block Elements*; RSC Publishing, 2009.

(2) Staubitz, A.; Robertson, A. P. M.; Sloan, M. E.; Manners, I. Amine− and Phosphine−Borane Adducts: New Interest in Old Molecules. *Chemical Reviews* **2010**, *110* (7), 4023–4078. https://doi.org/10.1021/cr100105a.

(3) Leitao, E. M.; Jurca, T.; Manners, I. Catalysis in Service of Main Group Chemistry Offers a Versatile Approach to P-Block Molecules and Materials. *Nature Chemistry* **2013**, *5* (10), 817–829. https://doi.org/10.1038/nchem.1749.

(4) Han, D.; Anke, F.; Trose, M.; Beweries, T. Recent Advances in Transition Metal Catalysed Dehydropolymerisation of Amine Boranes and Phosphine Boranes. *Coordination Chemistry Reviews* **2019**, *380*, 260–286. https://doi.org/10.1016/j.ccr.2018.09.016.

(5) Vidal, F.; Jäkle, F. Functional Polymeric Materials Based on Main-Group Elements. *Angewandte Chemie International Edition* **2019**, *58* (18), 5846–5870. https://doi.org/10.1002/anie.201810611.

(6) Baumgartner, T.; Jaekle, F. *Main Group Strategies Towards Functional Hybrid Materials*; John Wiley & Sons, Incorporated: Newark, 2018.

(7) Dück, K.; Gates, D. P. Main-Chain, Phosphorus-Based Polymers. In *Main Group Strategies towards Functional Hybrid Materials*; John Wiley & Sons, Ltd, 2018; pp 329–355. https://doi.org/10.1002/9781119235941.ch13.

(8) Knights, A. W.; Chitnis, S. S.; Manners, I. Photolytic, Radical-Mediated Hydrophosphination: A Convenient Post-Polymerisation Modification Route to P-

Di(Organosubstituted) Polyphosphinoboranes $[RR'PBH_2]_n$. *Chemistry Science* **2019**, *10*, 7281–7289. https://doi.org/10.1039/C9SC01428D.

(9) Peret, J. L. Preparation and Properties of the Boron Phosphides. *Journal of the American Ceramic Society* **1964**, *47* (1), 44–46. https://doi.org/10.1111/j.1151-2916.1964.tb14639.x.

(10) Rothemund, S.; Teasdale, I. Preparation of Polyphosphazenes: A Tutorial Review. *Chemical Society Reviews* **2016**, *45* (19), 5200–5215. https://doi.org/10.1039/c6cs00340k.

(11) Wilfert, S.; Henke, H.; Schoefberger, W.; Brueggemann, O.; Teasdale, I. Chain-End-Functionalized Polyphosphazenes *via* a One-Pot Phosphine-Mediated Living Polymerization. *Macromolecular Rapid Communications* **2014**, *35* (12), 1135–1141. https://doi.org/10.1002/marc.201400114.

(12) Allcock, H. R. Polyphosphazene Elastomers, Gels, and Other Soft Materials. *Soft Matter* **2012**, *8* (29), 7521–7532. https://doi.org/10.1039/c2sm26011e.

(13) Mark, J. E. Some Interesting Things about Polysiloxanes. *Accounts of Chemical Research* **2004**, *37* (12), 946–953. https://doi.org/10.1021/ar030279z.

(14) Brook, M. A. *Silicon in Organic, Organometallic, and Polymer Chemistry*; J. Wiley: New York, 2000.

(15) Knights, A. W.; Nascimento, M. A.; Manners, I. An Investigation of Polyphosphinoboranes as Flame-Retardant Materials. *Polymer* **2022**, *247*, 124795. https://doi.org/10.1016/j.polymer.2022.124795.

(16) Clark, T. L.; Rodezno, J. M.; Clendenning, S. B.; Aouba, S.; Brodersen, P. M.; Lough, A. J.; Ruda, H. E.; Manners, I. Rhodium-Catalyzed Dehydrocoupling of

Fluorinated Phosphine-Borane Adducts: Synthesis, Characterization, and Properties of Cyclic and Polymeric Phosphinoboranes with Electron-Withdrawing Substituents at Phosphorus. *Chemistry – A European Journal* **2005**, *11* (15), 4526–4534. https://doi.org/10.1002/chem.200401296.

(17) Woo, K.; Lee, K.; Kovnir, K. BP: Synthesis and Properties of Boron Phosphide. *Material Research Express* **2016**, *3* (7), 074003. https://doi.org/10.1088/2053-1591/3/7/074003.

(18) Burg, A. B. Phosphinoborine Polymer Rings and Chains from Tetramethylbiphosphine. *Journal of Inorganic and Nuclear Chemistry* **1959**, *11* (3), 258. https://doi.org/10.1016/0022-1902(59)80257-8.

(19) Burg, A. B.; Wagner, R. I. Chemistry of P–B Bonding — the Phosphinoborines and Their Polymers. *Journal of the American Chemical Society* **1953**, *75* (16), 3872–3877. https://doi.org/10.1021/ja01112a002.

(20) Burg, A. B.; Slota, P. J. New Approaches to the Phosphinoborine Polymers [1]. *J. Am. Chem. Soc.* **1960**, *82* (9), 2145–2148. https://doi.org/10.1021/ja01494a014.

(21) Dorn, H.; Singh, R. A.; Massey, J. A.; Lough, A. J.; Manners, I. Rhodium-Catalyzed Formation of Phosphorus–Boron Bonds: Synthesis of the First High Molecular Weight Poly(Phosphinoborane). *Angewandte Chemie International Edition* **1999**, *38* (22), 3321–3323. https://doi.org/10.1002/(SICI)1521-3773(19991115)38:22<3321::AID-ANIE3321>3.0.CO;2-0.

(22) Dorn, H.; Singh, R. A.; Massey, J. A.; Nelson, J. M.; Jaska, C. A.; Lough, A. J.; Manners, I. Transition Metal-Catalyzed Formation of Phosphorus−Boron Bonds: A New Route to Phosphinoborane Rings, Chains, and Macromolecules. *Journal of*

*the American Chemical Society* **2000**, *122* (28), 6669–6678. https://doi.org/10.1021/ja000732r.

(23) Schäfer, A.; Jurca, T.; Turner, J.; Vance, J. R.; Lee, K.; Du, V. A.; Haddow, M. F.; Whittell, G. R.; Manners, I. Iron-Catalyzed Dehydropolymerization: A Convenient Route to Poly(Phosphinoboranes) with Molecular-Weight Control. *Angewandte Chemie International Edition* **2015**, *54* (16), 4836–4841. https://doi.org/10.1002/anie.201411957.

(24) Hooper, T. N.; Weller, A. S.; Beattie, N. A.; Macgregor, S. A. Dehydrocoupling of Phosphine-Boranes Using the [RhCp*Me($PMe_3$)($CH_2Cl_2$)][$BAr^F{}_4$] Precatalyst: Stoichiometric and Catalytic Studies. *Chemical Science* **2016**, *7* (3), 2414–2426. https://doi.org/10.1039/c5sc04150c.

(25) Hooper, T. N.; Huertos, M. A.; Jurca, T.; Pike, S. D.; Weller, A. S.; Manners, I. Effect of the Phosphine Steric and Electronic Profile on the Rh-Promoted Dehydrocoupling of Phosphine–Boranes. *Inorganic Chemistry* **2014**, *53* (7), 3716–3729. https://doi.org/10.1021/ic500032f.

(26) Hooper, T. N.; Weller, A. S.; Beattie, N. A.; Macgregor, S. A. Dehydrocoupling of Phosphine-Boranes Using the [RhCp*Me($PMe_3$)($CH_2Cl_2$)][$BAr^F{}_4$] Precatalyst: Stoichiometric and Catalytic Studies. *Chemical Science* **2016**, *7* (3), 2414–2426. https://doi.org/10.1039/c5sc04150c.

(27) Huertos, M. A.; Weller, A. S. Revealing the P-B Coupling Event in the Rhodium Catalysed Dehydrocoupling of Phosphine-Boranes $H_3B{\bullet}PR_2H$ (R = Bu-t, Ph). *Chemical Science* **2013**, *4* (4), 1881–1888. https://doi.org/10.1039/c3sc50122a.

(28) Huertos, M. A.; Weller, A. S. Intermediates in the Rh-Catalysed Dehydrocoupling of Phosphine-Borane. *Chemical Communications* **2012**, *48* (57), 7185–7187. https://doi.org/10.1039/C2CC32696E.

(29) Race, J. J.; Heyam, A.; Wiebe, M. A.; Diego-Garcia Hernandez, J.; Ellis, C. E.; Lei, S.; Manners, I.; Weller, A. S. Polyphosphinoborane Block Copolymer Synthesis Using Catalytic Reversible Chain-Transfer Dehydropolymerization. *Angewandte Chemie International Edition* **2023**, *62* (3), e202216106. https://doi.org/10.1002/anie.202216106.

(30) D. Paul, U. S.; Braunschweig, H.; Radius, U. Iridium-Catalysed Dehydrocoupling of Aryl Phosphine–Borane Adducts: Synthesis and Characterisation of High Molecular Weight Poly(Phosphinoboranes). *Chemical Communications* **2016**, *52* (55), 8573–8576. https://doi.org/10.1039/C6CC04363A.

(31) Coles, N. T.; Webster, R. L. Iron Catalyzed Dehydrocoupling of Amine- and Phosphine-Boranes. *Israel Journal of Chemistry* **2017**, *57* (12), 1070–1081. https://doi.org/10.1002/ijch.201700018.

(32) Coles, N. T.; Mahon, M. F.; Webster, R. L. Phosphine- and Amine-Borane Dehydrocoupling Using a Three-Coordinate Iron(II) β-Diketiminate Precatalyst. *Organometallics* **2017**, *36* (11), 2262–2268. https://doi.org/10.1021/acs.organomet.7b00326.

(33) Schön, F.; Sigmund, L. M.; Schneider, F.; Hartmann, D.; Wiebe, M. A.; Manners, I.; Greb, L. Calix[4]Pyrrolato Aluminate Catalyzes the Dehydrocoupling of Phenylphosphine Borane to High Molar Weight Polymers. *Angewandte Chemie*

*International Edition* **2022**, *61* (22), e202202176. https://doi.org/10.1002/anie.202202176.

(34) Jaska, C. A.; Manners, I. Catalytic Dehydrocoupling of Amine-Borane and Phosphine-Borane Adducts: The Mechanism Is Heterogeneous in One Case and Homogeneous in the Other. *Journal of the American Chemical Society* **2004**, *126* (5), 1334–1335. https://doi.org/10.1021/ja039162w.

(35) Marquardt, C.; Jurca, T.; Schwan, K. C.; Stauber, A.; Virovets, A. V.; Whittell, G. R.; Manners, I.; Scheer, M. Metal-Free Addition/Head-to-Tail Polymerization of Transient Phosphinoboranes, RPH-$BH_2$: A Route to Poly(Alkylphosphinoboranes). *Angewandte Chemie International Edition* **2015**, *54* (46), 13782–13786. https://doi.org/10.1002/anie.201507084.

(36) Stauber, A.; Jurca, T.; Marquardt, C.; Fleischmann, M.; Seidl, M.; Whittell, G. R.; Manners, I.; Scheer, M. A Convenient Route to Monoalkyl-Substituted Phosphanylboranes (HRP–$BH_2$–$NMe_3$): Prospective Precursors to Poly[(Alkylphosphino)Boranes]. *European Journal of Inorganic Chemistry* **2016**, *2016* (17), 2684–2687. https://doi.org/10.1002/ejic.201600226.

(37) Oldroyd, N. L.; Chitnis, S. S.; Annibale, V. T.; Arz, M. I.; Sparkes, H. A.; Manners, I. Metal-Free Dehydropolymerisation of Phosphine-Boranes Using Cyclic (Alkyl)(Amino)Carbenes as Hydrogen Acceptors. *Nature Communications* **2019**, *10* (1), 1–9. https://doi.org/10.1038/s41467-019-08967-8.

(38) Wiebe, M. A.; Kundu, S.; LaPierre, E. A.; Patrick, B. O.; Manners, I. Transition-Metal-Free Dehydropolymerization of Phosphine–Boranes at Ambient

Temperature. *Chemistry – A European Journal* **2023**, *29* (2). https://doi.org/10.1002/chem.202202897.

(39) Colebatch, A. L.; Weller, A. S. Amine-Borane Dehydropolymerization: Challenges and Opportunities. *Chemistry – A European Journal* **2019**, *25* (6), 1379–1390. https://doi.org/10.1002/chem.201804592.

(40) Robertson, A. P. M.; Leitao, E. M.; Manners, I. Catalytic Redistribution and Polymerization of Diborazanes: Unexpected Observation of Metal-Free Hydrogen Transfer between Aminoboranes and Amine-Boranes. *Journal of the American Chemical Society* **2011**, *133* (48), 19322–19325. https://doi.org/10.1021/ja208752w.

(41) Leitao, E. M.; Stubbs, N. E.; Robertson, A. P. M.; Helten, H.; Cox, R. J.; Lloyd-Jones, G. C.; Manners, I. Mechanism of Metal-Free Hydrogen Transfer between Amine–Boranes and Aminoboranes. *Journal of the American Chemical Society* **2012**, *134* (40), 16805–16816. https://doi.org/10.1021/ja307247g.

(42) Pasumansky, L.; Haddenham, D.; Clary, J. W.; Fisher, G. B.; Goralski, C. T.; Singaram, B. Lithium Aminoborohydrides 16. Synthesis and Reactions of Monomeric and Dimeric Aminoboranes. *The Journal of Organic Chemistry* **2008**, *73* (5), 1898–1905. https://doi.org/10.1021/jo702271c.

(43) Robertson, A. P. M.; Suter, R.; Chabanne, L.; Whittell, G. R.; Manners, I. Heterogeneous Dehydrocoupling of Amine–Borane Adducts by Skeletal Nickel Catalysts. *Inorganic Chemistry* **2011**, *50* (24), 12680–12691. https://doi.org/10.1021/ic201809g.

(44) Clark, T. J.; Russell, C. A.; Manners, I. Homogeneous, Titanocene-Catalyzed Dehydrocoupling of Amine-Borane Adducts. *Journal of the American Chemical Society* **2006**, *128* (30), 9582–9583. https://doi.org/10.1021/ja062217k.

(45) Vance, J. R.; Robertson, A. P. M.; Lee, K.; Manners, I. Photoactivated, Iron-Catalyzed Dehydrocoupling of Amine–Borane Adducts: Formation of Boron–Nitrogen Oligomers and Polymers. *Chemistry – A European Journal* **2011**, *17* (15), 4099–4103. https://doi.org/10.1002/chem.201003397.

(46) Leitao, E. M.; Manners, I. Rehydrogenation of Aminoboranes to Amine–Boranes Using H2O: Reaction Scope and Mechanism. *European Journal of Inorganic Chemistry* **2015**, *2015* (13), 2199–2205. https://doi.org/10.1002/ejic.201500117.

(47) Metters, O. J.; Chapman, A. M.; Robertson, A. P. M.; Woodall, C. H.; Gates, P. J.; Wass, D. F.; Manners, I. Generation of Aminoborane Monomers RR′$NBH_2$ from Amine–Boronium Cations [RR′$NH–BH_2L]^+$: Metal Catalyst-Free Formation of Polyaminoboranes at Ambient Temperature. *Chemical Communications* **2014**, *50* (81), 12146–12149. https://doi.org/10.1039/C4CC05145A.

(48) Power, P. P. Boron-Phosphorus Compounds and Multiple Bonding. *Angewandte Chemie International Edition in English* **1990**, *29* (5), 449–460. https://doi.org/10.1002/anie.199004491.

(49) Power, P. P. π-Bonding and the Lone Pair Effect in Multiple Bonds between Heavier Main Group Elements. *Chemical Reviews* **1999**, *99* (12), 3463–3504. https://doi.org/10.1021/cr9408989.

(50) Wigner, E. On the Quantum Correction For Thermodynamic Equilibrium. *Physical Review* **1932**, *40* (5), 749–759. https://doi.org/10.1103/PhysRev.40.749.

(51) LaPierre, E. A.; Patrick, B. O.; Manners, I. Trivalent Titanocene Alkyls and Hydrides as Well-Defined, Highly Active, and Broad Scope Precatalysts for Dehydropolymerization of Amine-Boranes. *Journal of the American Chemical Society* **2019**, *141* (51), 20009–20015. https://doi.org/10.1021/jacs.9b11112.

(52) Helten, H.; Dutta, B.; Vance, J. R.; Sloan, M. E.; Haddow, M. F.; Sproules, S.; Collison, D.; Whittell, G. R.; Lloyd-Jones, G. C.; Manners, I. Paramagnetic Titanium(III) and Zirconium(III) Metallocene Complexes as Precatalysts for the Dehydrocoupling/Dehydrogenation of Amine–Boranes. *Angewandte Chemie International Edition* **2013**, *52* (1), 437–440. https://doi.org/10.1002/anie.201207903.

(53) Pangborn, A. B.; Giardello, M. A.; Grubbs, R. H.; Rosen, R. K.; Timmers, F. J. Safe and Convenient Procedure for Solvent Purification. *Organometallics* **1996**, *15* (5), 1518–1520. https://doi.org/10.1021/om9503712.

(54) Jaska, C. A.; Temple, K.; Lough, A. J.; Manners, I. Transition Metal-Catalyzed Formation of Boron−Nitrogen Bonds: Catalytic Dehydrocoupling of Amine-Borane Adducts to Form Aminoboranes and Borazines. *Journal of the American Chemical Society* **2003**, *125* (31), 9424–9434. https://doi.org/10.1021/ja030160l.

(55) Sloan, M. E.; Staubitz, A.; Clark, T. J.; Russell, C. A.; Lloyd-Jones, G. C.; Manners, I. Homogeneous Catalytic Dehydrocoupling/Dehydrogenation of Amine−Borane Adducts by Early Transition Metal, Group 4 Metallocene Complexes. *Journal of the American Chemical Society* **2010**, *132* (11), 3831–3841. https://doi.org/10.1021/ja909535a.

(56) Johnson, H. C.; Robertson, A. P. M.; Chaplin, A. B.; Sewell, L. J.; Thompson, A. L.; Haddow, M. F.; Manners, I.; Weller, A. S. Catching the First Oligomerization Event in the Catalytic Formation of Polyaminoboranes: $H_3B{\bullet}NMeHBH_2NMeH_2$ Bound to Iridium. *Journal of the American Chemical Society* **2011**, *133* (29), 11076–11079. https://doi.org/10.1021/ja2040738.

(57) Dorn, H.; Rodezno, J. M.; Brunnhofer, B.; Rivard, E.; Massey, J. A.; Manners, I. Synthesis, Characterization, and Properties of the Polyphosphinoboranes $[RPH{-}BH_2]_n$ (R=Ph, iBu, p-n$BuC_6H_4$, p-dodecyl$C_6H_4$): Inorganic Polymers with a Phosphorus-Boron Backbone. *Macromolecules* **2003**, *36* (2), 291–297. https://doi.org/10.1021/ma021447q.

(58) Gaussian 16, Revision C.01, Frisch, M. J.; Trucks, G. W.; Schlegel, H. B.; Scuseria, G. E.; Robb, M. A.; Cheeseman, J. R.; Scalmani, G.; Barone, V.; Petersson, G. A.; Nakatsuji, H.; Li, X.; Caricato, M.; Marenich, A. V.; Bloino, J.; Janesko, B. G.; Gomperts, R.; Mennucci, B.; Hratchian, H. P.; Ortiz, J. V.; Izmaylov, A. F.; Sonnenberg, J. L.; Williams-Young, D.; Ding, F.; Lipparini, F.; Egidi, F.; Goings, J.; Peng, B.; Petrone, A.; Henderson, T.; Ranasinghe, D.; Zakrzewski, V. G.; Gao, J.; Rega, N.; Zheng, G.; Liang, W.; Hada, M.; Ehara, M.; Toyota, K.; Fukuda, R.; Hasegawa, J.; Ishida, M.; Nakajima, T.; Honda, Y.; Kitao, O.; Nakai, H.; Vreven, T.; Throssell, K.; Montgomery, J. A., Jr.; Peralta, J. E.; Ogliaro, F.; Bearpark, M. J.; Heyd, J. J.; Brothers, E. N.; Kudin, K. N.; Staroverov, V. N.; Keith, T. A.; Kobayashi, R.; Normand, J.; Raghavachari, K.; Rendell, A. P.; Burant, J. C.; Iyengar, S. S.; Tomasi, J.; Cossi, M.; Millam, J. M.; Klene, M.; Adamo, C.; Cammi, R.; Ochterski,

J. W.; Martin, R. L.; Morokuma, K.; Farkas, O.; Foresman, J. B.; Fox, D. J. Gaussian, Inc., Wallingford CT, 2016.

(59) Adamo, C.; Barone, V. Toward Reliable Density Functional Methods without Adjustable Parameters: The PBE0 Model. *The Journal of Chemical Physics* **1999**, *110* (13), 6158–6170. https://doi.org/10.1063/1.478522.

(60) Weigend, F.; Ahlrichs, R. Balanced Basis Sets of Split Valence, Triple Zeta Valence and Quadruple Zeta Valence Quality for H to Rn: Design and Assessment of Accuracy. *Physical Chemistry Chemical Physics* **2005**, *7* (18), 3297–3305. https://doi.org/10.1039/B508541A.

(61) Grimme, S.; Ehrlich, S.; Goerigk, L. Effect of the Damping Function in Dispersion Corrected Density Functional Theory. *Journal of Computational Chemistry* **2011**, *32* (7), 1456–1465. https://doi.org/10.1002/jcc.21759.

## Chapter 6

# Conclusions, Future Directions, and Outlook

## 6.1 Summary of Conclusions from Research Chapters

The work within this thesis expands upon the generation and reactivity of transient aminoboranes and phosphinoboranes. In Chapter 2, transient phosphinoboranes are generated *via* the deprotonation of phosphine-(triflimido)borane adducts. These transient species readily undergo addition polymerization to access polyphosphinoboranes, including polymeric materials that have two organic phosphorus substituents. End-group analysis of the polymeric materials obtained in Chapter 2 revealed residual unreacted base as end groups, implicating the base had a role in both deprotonation and chain propagation steps. In Chapter 3, transient aminoboranes are generated *via* deprotonation of amine-(triflimido)borane adducts. Here, maintaining temperatures at or below –60 °C allowed for the direct observation of transient primary aminoboranes as the sole species *in situ*. Further, the reactivity of primary aminoboranes as the sole species *in situ* was explored for the first time. Chapter 4 explored the ability of Lewis acid and base pairs to catalyze the dehydropolymerization of phosphine-borane adducts to access high molar mass, low dispersity polymers. Here it was revealed that simple salts such as lithium triflate or reagents such as borane dimethylsulfide could access high molar mass materials. It is hypothesized that these materials assist in the stabilization of the growing polymer chain, competing with chain termination reactions such as cyclization,

protonation or hydride transfer. Lastly, Chapter 5 explored the dehydrocoupling of phosphine-borane adducts under ambient conditions using aminoboranes as hydrogen acceptors. Here a remarkable transformation was explored, where aminoboranes accept hydrogen from phosphine-borane *via* a 6-membered transition state in which P-to-N and B-to-B hydrogen transfer yields amine-borane and transient phosphinoboranes. Unlike thermal catalytic dehydropolymerizations,[1] which occur at temperatures at or above 100 °C, typically over the course of 16 or more hours, the reaction between aminoboranes and phosphine-borane adducts occurs under ambient conditions nearly spontaneously.

## 6.2 Future Directions

From the findings within this thesis, I believe the logical next steps for research within phosphine- and amine-borane dehydrocoupling chemistry are to access *P*-disubstituted polyphosphinoboranes in a more atom economical manner, to gain greater control over the addition polymerization of aminoboranes formed *in situ*, and to further explore ambient condition catalytic dehydropolymerization of phosphine-borane adducts. My thoughts on how to achieve these goals are presented below.

### 6.2.1 Accessing *P*-Disubstituted Polyphosphinoboranes

*P*-Disubstituted polyphosphinoboranes are predicted to be less reactive than *P*-monosubstituted polyphosphinoboranes as they lack a P–H bond, making them attractive polymers for practical applications. *P*-disubstituted polymers can be accessed as the longer P–B bonds can accommodate a second substituent. However, most attempts to dehydropolymerize $Ph_2PH{\bullet}BH_3$ to $[Ph_2P–BH_2]_n$ produce $Ph_2PH{\bullet}BH_2–Ph_2P{\bullet}BH_3$ instead.[2–9] In 2019, the Manners group reported the CAAC-mediated dehydropolymerization of $PhRPH{\bullet}BH_3$ (R = Ph, Et) to access high molecular weight $[PhRP–BH_2]_n$, albeit in low yield

(*ca.* 10%).[10] End-group analysis of these materials found CAAC end groups, implicating their involvement beyond dehydrogenation.

In Chapter 2, it was determined that the choice of base influenced the reaction outcome in the addition polymerization of P-disubstituted phosphinoboranes generated *via* deprotonation of phosphine-(triflimido)boranes. When a simple amine base, *i*$Pr_2$EtN, is used, a product that is hypothesized to be PhRPH•$BH_2$–$Ph_2$P•$BH_2$($NTf_2$) (R = Ph, Et) is obtained. However, when an N-heterocyclic carbene (NHC) such as IPr (IPr = *N,N*-(2,6-diisopropylphenyl)imidazole-2-ylidene) is used, high molar mass [PhRP–$BH_2$]$_n$ is obtained in moderate to good yields (50% – 70%). End-group analysis of these polymeric materials revealed NHC end groups, thus NHCs have a role beyond deprotonation in this transformation. In Chapter 3, it was shown that in the high temperature catalytic phosphine-borane dehydropolymerizations, chain stabilization of growing polymer chains is key in accessing polymeric materials. Further, in the dehydrocoupling of $Ph_2$PH•$BH_3$ using aminoboranes, as described in Chapter 5, $Ph_2$PH•$BH_2$–$Ph_2$P•$BH_3$ is obtained, highlighting the need for an initiator in the addition polymerization of $Ph_2$P–$BH_2$ generated *in situ* to access polymeric material.

Thus, I believe that attempts to access [PhRP•$BH_2$]$_n$ from PhRPH•$BH_3$ (R ≠ H) have resulted in PhRPH•$BH_2$–PhRP•$BH_3$ as PhRP–$BH_2$ inserts into PhRPH•$BH_3$, generating a stable species that does not undergo further polymerization (**Scheme 6.1**). However, in the presence of either NHC or CAAC, a reaction occurs to form PhRP–$BH_2$(L) (L = NHC or CAAC), preventing insertion into unreacted PhRPH•$BH_2$, and initiating the addition polymerization of phosphinoboranes. Further, a recent computational study on [$PH_2$–$BH_2$]$_{10}$ revealed that coordination of an NHC to the B-terminus can prevent

cyclization of the decamer.[11] This may also be the case for polymerizations performed in the presence of residual NHC/CAAC. Accordingly, to access *P*-disubstituted polymers I believe it is necessary to both rapidly dehydrogenate the precursor phosphine-borane adduct to avoid the formation of stable dimeric species and to get a high concentration of phosphinoborane *in situ* and to have an initiator present that allows for polymerization to occur (**Scheme 6.1**).

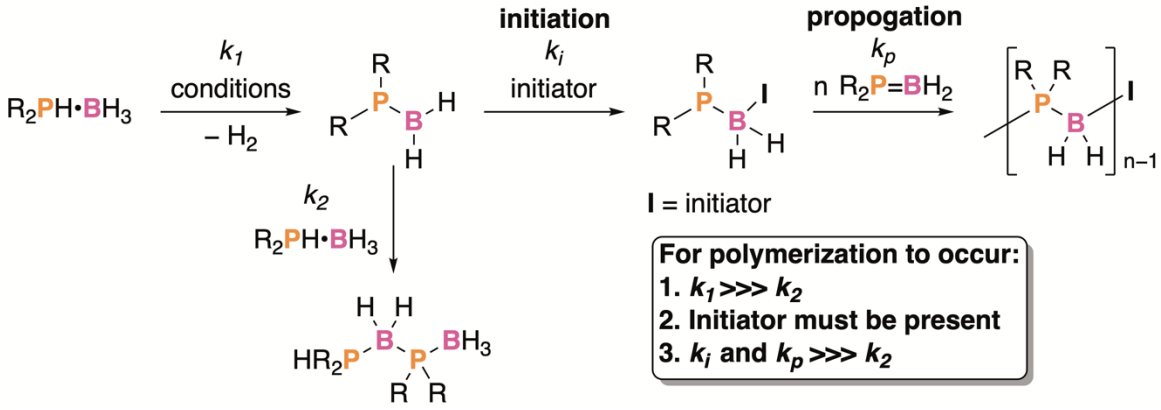


**Scheme 6.1:** Necessary conditions to access *P*-disubstituted polymeric material from phosphinoboranes formed *in situ*.

To access high concentrations of phosphinoboranes *in situ* I have shown that aminoboranes can accept hydrogen from phosphine-borane adducts rapidly under ambient conditions. But, for the polymerization to occur, initiation needs to happen. Accordingly, performing the dehydrogenation of $PhRPH{\cdot}BH_3$ in the presence of an initiator can potentially result in the formation of polymer with two phosphorus substituents (**Scheme 6.2**). If this initiator was something like an NHC or a CAAC, a significant portion would likely react with the precursor phosphine-borane or the amine-borane product.[10,12] However, addition of NHC-stabilized aminoboranes or phosphinoboranes, such as those synthesized in Chapters 2 and 3, to these *P*-disubstituted phosphine-borane

dehydrocoupling reactions may act as the initiated phosphinoborane unit and allow for access to these coveted polymers without the need for stoichiometric amounts of either NHC or CAAC. Further, molecular weight control over the polymers may be gained based on the amount of initiator added and may allow for the living polymerization of phosphine-borane adducts.

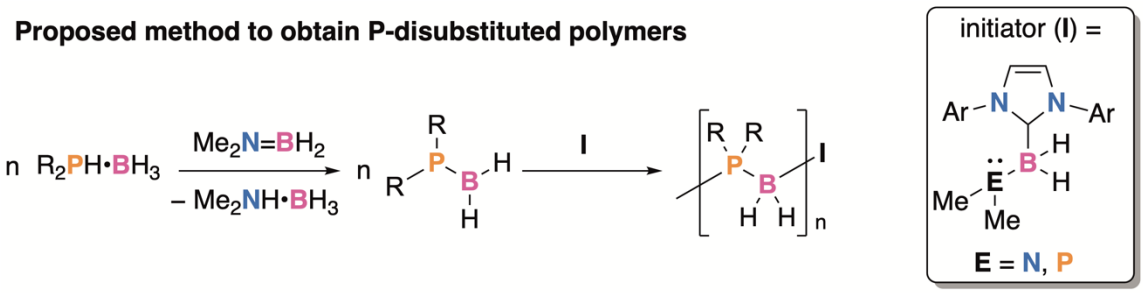


**Scheme 6.2:** Proposed method for accessing *P*-disubstituted polymeric materials from the dehydrocoupling of phosphine-borane adducts without the need for a stoichiometric (to phosphine-borane) amount of NHC or CAAC.

### 6.2.2 Obtaining Greater Control Over Aminoborane Addition Polymerization

Amine-borane dehydropolymerization has relied largely on catalysts that focus on the dehydrogenation of amine-borane adducts, and the subsequent polymerization is an off-metal phenomenon (**Scheme 6.3**).[1,13] Currently, control over the polymerization step has relied mostly on the addition of chain-transfer agents that interfere with chain-propagation and yield lower molecular weight polymers.[14]

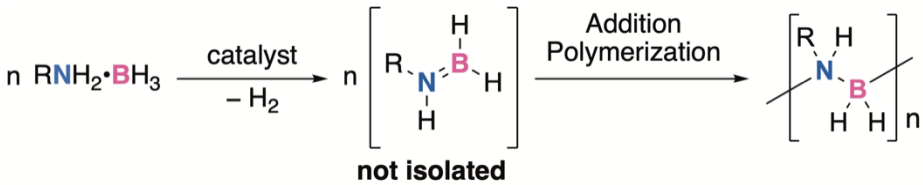


**Scheme 6.3:** General scheme for the catalytic dehydropolymerization of amine-borane adducts.

In Chapter 3, I described the synthesis of reactive primary aminoboranes as the sole species *in situ* for their subsequent reactivity studies. While these studies focussed on the synthesis of small molecules, these findings also will allow for the study of polymerization of transient primary aminoboranes and may allow for the development of aminoborane addition polymerization in a way analogous to that of olefin polymerization. For example, olefins can be polymerized *via* anionic, cationic, radical, or coordination-insertion mechanisms allowing for control such as living or stereoselective polymerizations (**Scheme 6.4** a).[15] These individual polymerization mechanisms have not yet been discovered for amine-borane adducts. Thus, addition of Lewis bases, such as NHC, or Lewis Acids such as $B(C_6F_5)_3$, or radical initiators to solutions of $RNH–BH_2$ (R = alkyl chain, allyl, benzyl) may allow for the controlled addition polymerization of aminoboranes (**Scheme 6.4** b). Further, the work described in Chapter 3 unlocks the potential to explore the role of the metal in the polymerization step and may allow for a catalyst that does operate *via* a coordination-insertion mechanism, opening the door for stereospecific polymerization of aminoboranes (**Scheme 6.4** b). Moreover, the synthesis of aminoborane block-copolymers can be explored from the addition polymerization of aminoboranes produced as the sole species *in situ*. The ability to subsequently form nanoscopic structures from a block copolymer consisting of two distinct polyaminoborane blocks may allow for the subsequent study of the ability to make well-defined nanostructures that could be converted to ceramic nanoparticles, a potentially very exciting material in nanotechnology (**Scheme 6.4** c).[16–21]

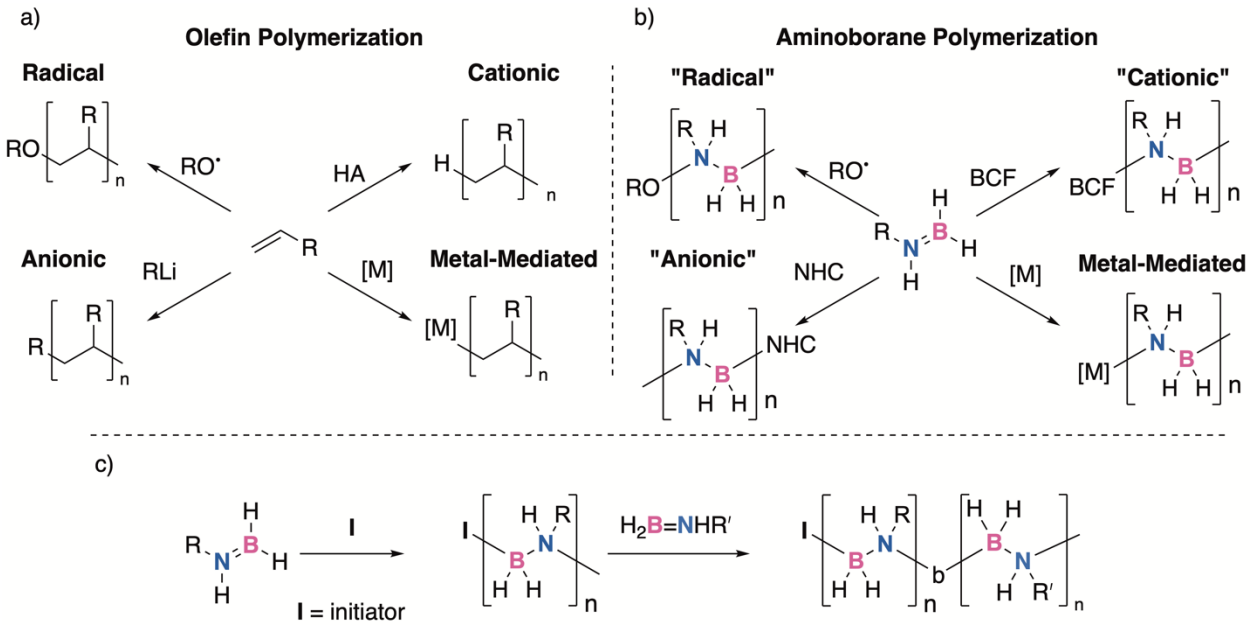


**Scheme 6.4:** Different mechanisms for the polymerization of olefins (a), potential routes for the polymerization of aminoboranes (b), and the proposed synthesis of aminoborane block copolymers consisting of two distinct polyaminoborane blocks (c).

### 6.2.3 Ambient Condition Catalytic Dehydropolymerization of Phosphine-Borane Adducts

Unlike amine-borane adducts, which readily undergo dehydropolymerization in the presence of several different metal catalysts, phosphine-boranes are currently only known to undergo catalytic dehydropolymerization at elevated temperatures over the course of 24 or more hours (**Scheme 6.5**).[22,23,8] The need for these high reaction

temperatures complicates reactivity studies and the elevated temperatures allows for different reactivity to occur than what might occur under ambient conditions.

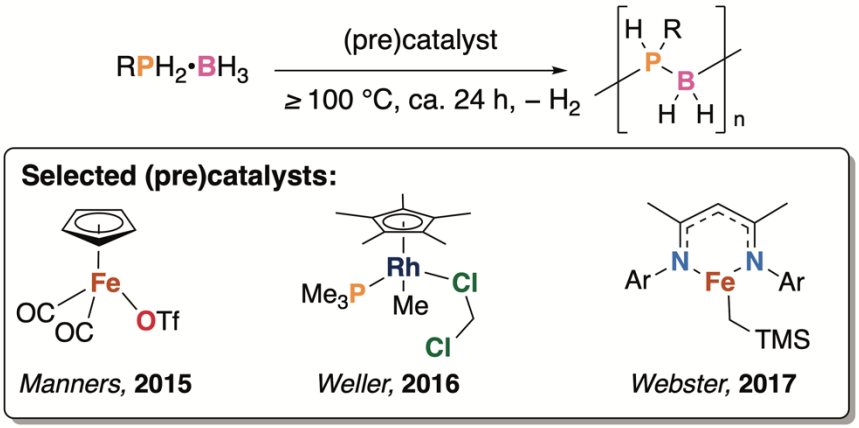


**Scheme 6.5:** Typical conditions for the catalytic dehydropolymerization of phosphine-boranes.

From the work in Chapter 2, it is known that transient phosphinoboranes will readily undergo addition polymerization under ambient conditions. Thus, the high temperatures in catalytic phosphine-borane dehydropolymerization are likely required primarily to assist in the challenging dehydrogenation of phosphine-borane adducts.[24] This was shown in Chapter 4, where additives as simple as LiOTf and $BH_3$•$SMe_2$ performed just as well in the dehydropolymerization of $PhPH_2$•$BH_3$ as $CpFe(CO)_2OTf$, the current state-of-the-art catalyst. It is believed that these additives assist in the stabilization of the growing chain, as found with the striking relationship between $BH_3$•$SMe_2$ loading and polymer molecular weight. Further, in Chapter 5, I discovered that aminoboranes can accept hydrogen from phosphine-borane adducts, opening the door for ambient condition phosphine-borane dehydrocoupling. Therefore, to obtain ambient condition catalytic dehydropolymerization of phosphine-borane adducts I envision two routes: first, the catalytic transfer

dehydrogenation of phosphine-borane adducts using aminoboranes as hydrogen acceptors, and second, the design of catalysts with aminoborane motifs included into the ligand framework.

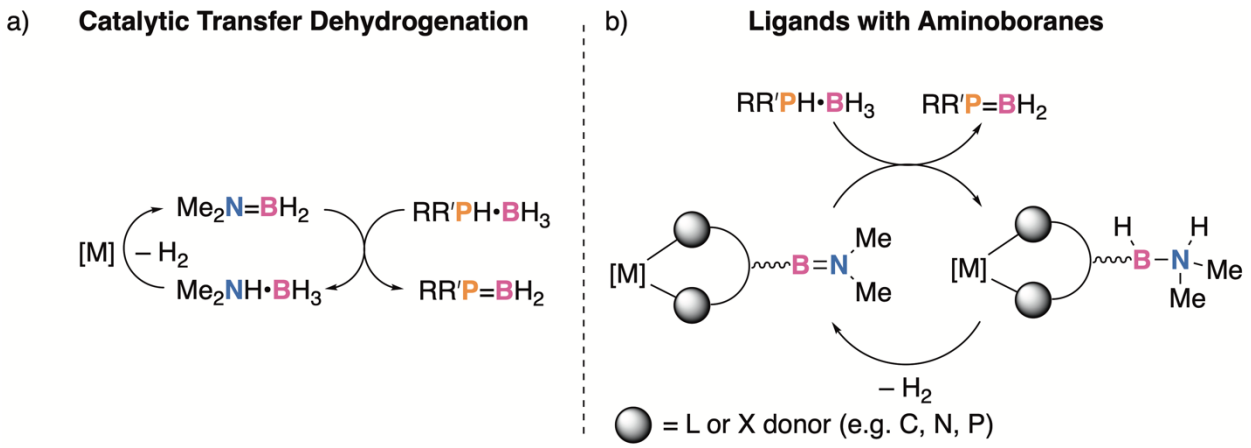


**Scheme 6.6:** Proposed routes to access ambient condition catalytic dehydrocoupling of phosphine-boranes.

The ambient condition catalytic transfer dehydrogenation of phosphine-boranes using aminoboranes as hydrogen acceptors should work as amine-borane adducts are readily dehydrogenated.[1,13,24] Further, as presented in Chapter 5, aminoboranes produced *in situ* readily accept hydrogen from phosphine-borane adducts. However, for this transformation to occur, a catalyst that does not react with, or is not significantly inhibited by phosphine-borane adducts must be identified. In a series of exploratory reactions, the single-site titanium catalyst, $Cp_2TiMe$, known for its high active in amine-borane dehydrogenation,[25] was tested for its ability to dehydrocouple $PhRPH•BH_3$ (R = H, Ph) in the presence of amine-borane adducts (**Scheme 6.7**, a). These reactions yielded only a 20% conversion of $Ph_2PH•BH_3$ to $Ph_2PH•BH_2–Ph_2P•BH_3$, with $Me_2N=BH_2$

as the hydrogen acceptor. No conversion of $PhPH_2{\bullet}BH_3$ to polymer was observed. However, it is likely that the catalyst is undergoing some sort of reaction with phosphine-borane *in situ*, producing an inactive species.[26] Alternatively, a single-site catalyst, based on a late-transition metal, such as (POCOP)$IrH_2$[27] may have a better chance of achieving ambient condition transfer dehydrogenation of phosphine-borane using aminoboranes as hydrogen acceptors (**Scheme 6.7**, b).

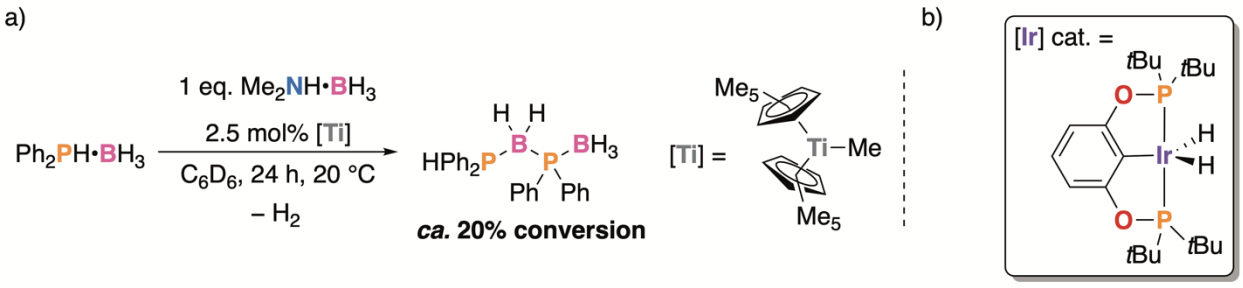


**Scheme 6.7:** Catalytic transfer dehydrogenation of *P,P*-diphenylphosphine borane adduct (a), and anticipated catalyst for improved performance (b).

Alternatively, the incorporation of aminoborane motifs into ligand frameworks may allow for the ambient condition catalytic dehydrocoupling of phosphine-boranes. I am inspired by the work on a phosphine-tethered aminoborane bound to a metal recently reported by the Moret group (**Scheme 6.8**, a).[28] I think this ligand framework has great potential in dehydropolymerization catalyst design, however, I imagine the *i*Pr groups on the nitrogen centre, and the phenyl linkers between the boron centre and phosphine ligands will be too sterically encumbering and prevent the dehydrogenation of phosphine-borane adducts to occur. While their search was largely for the observation of the side-on binding of an aminoborane to a metal centre, I believe that if an alkyl group between the borane and the phenyl substituents could be added, and the *N*-substituents could be

replaced with methyl groups, they could have a species that could readily accept hydrogen from a phosphine-borane adducts. Subsequent folding of the amine-borane back to the metal centre may result in the entropically favoured dehydrogenation, allowing for the regeneration of the reactive aminoborane. Similarly, I am inspired by the work of the Drover lab (**Scheme 6.8**, b). Their work has studied on the synthesis of ligands that have pendant boranes for the tethering of substrates to increase catalyst activity and unlock useful transformations.[29–35] If instead of just boranes, pendant aminoboranes could be accessed, I believe that with the right overall ligand framework and metal centre, potent single-site phosphine-borane dehydrocoupling catalysts could be designed. Here, the metal centres would ideally have a vacant coordination site that could participate in amine-borane dehydrogenation, and upon release of the aminoborane tendril, dehydrogenation of phosphine-boranes to transient phosphinoboranes could occur.

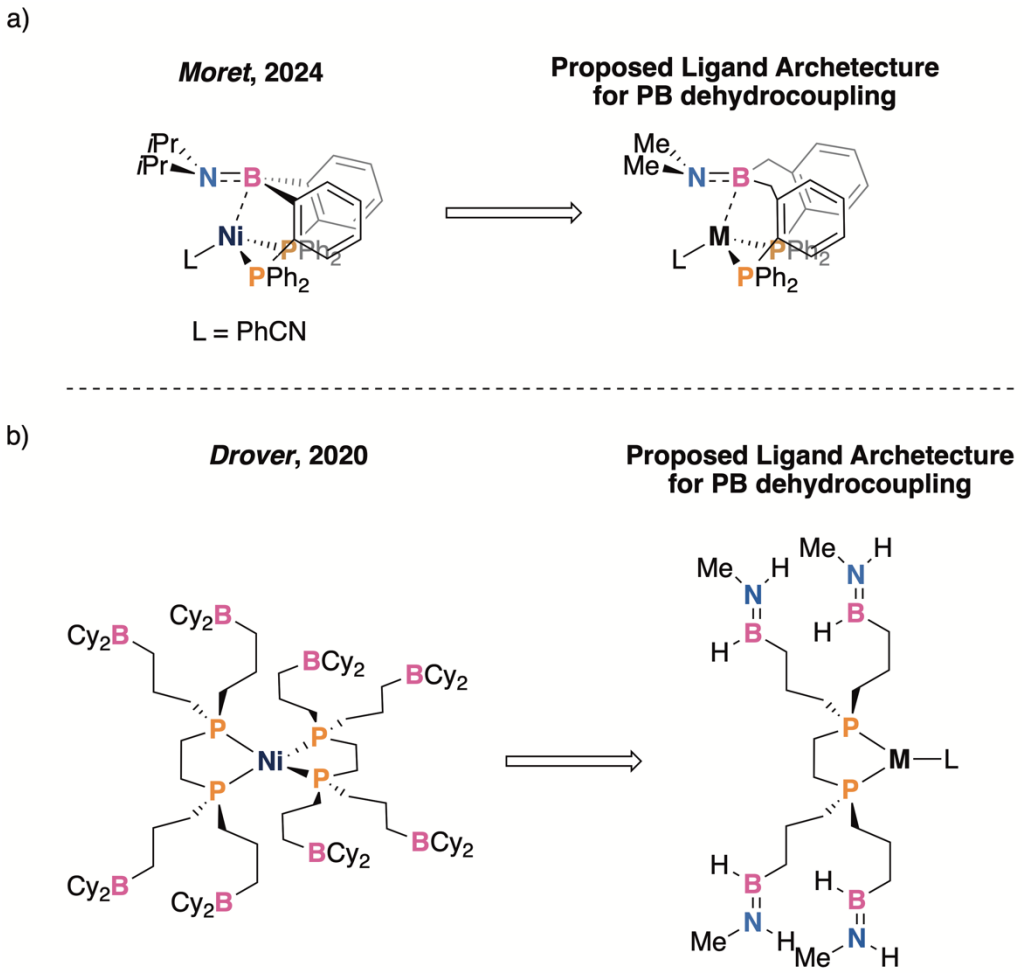


**Scheme 6.8:** Known catalysts (left) and proposed catalysts (right) for ambient condition catalytic phosphine-borane dehydrocoupling inspired by recent work by Moret *et. al*. (a) and Drover *et. al.* (b).

## 6.3 Outlook

This work has shown that phosphine-borane dehydropolymerization, a transformation once thought to require high temperatures and lengthy reaction times, can occur nearly spontaneously under ambient conditions with the right reagents, opening the door to more

efficient and sustainable syntheses with potentially greater control. Further, it has shown that primary aminoboranes, a class of molecule that has a reputation for ephemerality, can be trapped, observed, and subsequently transformed. The potential of polyphosphinoboranes and polyaminoboranes is just beginning to be tapped, and the research performed herein has deep implications for both practical synthesis and fundamental understanding of the polymerization of transient phosphinoboranes and aminoboranes. As we continue to explore these reactions, the possibilities for innovation are vast, paving the way for breakthroughs that could transform industries and expand our toolkit in main group element bond formation reactions.

## 6.4 References


(1) Han, D.; Anke, F.; Trose, M.; Beweries, T. Recent Advances in Transition Metal Catalysed Dehydropolymerisation of Amine Boranes and Phosphine Boranes. *Coordination Chemistry Reviews* **2019**, *380*, 260–286. https://doi.org/10.1016/j.ccr.2018.09.016.

(2) Dorn, H.; Singh, R. A.; Massey, J. A.; Lough, A. J.; Manners, I. Rhodium-Catalyzed Formation of Phosphorus–Boron Bonds: Synthesis of the First High Molecular Weight Poly(Phosphinoborane). *Angewandte Chemie International Edition* **1999**, *38* (22), 3321–3323. https://doi.org/10.1002/(SICI)1521-3773(19991115)38:22<3321::AID-ANIE3321>3.0.CO;2-0.

(3) Dorn, H.; Singh, R. A.; Massey, J. A.; Nelson, J. M.; Jaska, C. A.; Lough, A. J.; Manners, I. Transition Metal-Catalyzed Formation of Phosphorus−Boron Bonds: A New Route to Phosphinoborane Rings, Chains, and Macromolecules. *Journal of*

*the American Chemical Society.* **2000**, *122* (28), 6669–6678. https://doi.org/10.1021/ja000732r.

(4) Dorn, H.; Manners, I. Transition Metal-Catalyzed Formation of Phosphorus-Boron Bonds: A New Route to Phosphinoborane Rings, Chains and the First High Polymers. *Phosphorus, Sulfur and Silicon and the Related Elements* **2001**, *168–169*, 185–190. https://doi.org/10.1080/10426500108546552.

(5) Jaska, C. A.; Manners, I. Catalytic Dehydrocoupling of Amine-Borane and Phosphine-Borane Adducts: The Mechanism Is Heterogeneous in One Case and Homogeneous in the Other. *Journal of the American Chemical Society* **2004**, *126* (5), 1334–1335. https://doi.org/10.1021/ja039162w.

(6) Jaska, C. A.; Manners, I. Heterogeneous or Homogeneous Catalysis? Mechanistic Studies of the Rhodium-Catalyzed Dehydrocoupling of Amine-Borane and Phosphine-Borane Adducts. *Journal of the American Chemical Society* **2004**, *126* (31), 9776–9785. https://doi.org/10.1021/ja0478431.

(7) Lee, K.; Clark, T. J.; Lough, A. J.; Manners, I. Synthesis and Dehydrocoupling Reactivity of Iron and Ruthenium Phosphine-Borane Complexes. *Dalton Transactions* **2008**, No. 20, 2732–2740. https://doi.org/10.1039/b718918d.

(8) Coles, N. T.; Mahon, M. F.; Webster, R. L. Phosphine- and Amine-Borane Dehydrocoupling Using a Three-Coordinate Iron(II) β-Diketiminate Precatalyst. *Organometallics* **2017**, *36* (11), 2262–2268. https://doi.org/10.1021/acs.organomet.7b00326.

(9) Resendiz-Lara, D. A.; Annibale, V. T.; Knights, A. W.; Chitnis, S. S.; Manners, I. High Molar Mass Poly(Alkylphosphinoboranes) *via* Iron-Catalyzed

Dehydropolymerization. *Macromolecules* **2021**, *54* (1), 71–82. https://doi.org/10.1021/acs.macromol.0c02082.

(10) Oldroyd, N. L.; Chitnis, S. S.; Annibale, V. T.; Arz, M. I.; Sparkes, H. A.; Manners, I. Metal-Free Dehydropolymerisation of Phosphine-Boranes Using Cyclic (Alkyl)(Amino)Carbenes as Hydrogen Acceptors. *Nature Communications* **2019**, *10* (1), 1–9. https://doi.org/10.1038/s41467-019-08967-8.

(11) Pomogaeva, A. V.; Timoshkin, A. Y. Stability and Electronic Structure of Donor–Acceptor Stabilized Group 13/15 Oligomers. *The Journal of Physical Chemistry A.* **2021**, *125* (16), 3415–3424. https://doi.org/10.1021/acs.jpca.1c02258.

(12) Sabourin, K. J.; Malcolm, A. C.; McDonald, R.; Ferguson, M. J.; Rivard, E. Metal-Free Dehydrogenation of Amine–Boranes by an N-Heterocyclic Carbene. *Dalton Transactions* **2013**, *42* (13), 4625. https://doi.org/10.1039/c3dt32988g.

(13) Colebatch, A. L.; Weller, A. S. Amine-Borane Dehydropolymerization: Challenges and Opportunities. *Chemistry – A European Journal* **2019**, *25* (6), 1379–1390. https://doi.org/10.1002/chem.201804592.

(14) Brodie, C. N.; Boyd, T. M.; Sotorríos, L.; Ryan, D. E.; Magee, E.; Huband, S.; Town, J. S.; Lloyd-Jones, G. C.; Haddleton, D. M.; Macgregor, S. A.; Weller, A. S. Controlled Synthesis of Well-Defined Polyaminoboranes on Scale Using a Robust and Efficient Catalyst. *Journal of the American Chemical Society* **2021**, *143* (49), 21010–21023. https://doi.org/10.1021/jacs.1c10888.

(15) Odian, G. *Principles of Polymerization*, Fourth.; John Wiley & Sons, Inc.: Hoboken, New Jersey, 2004.

(16) Kim, D. P.; Moon, K. T.; Kho, J. G.; Economy, J.; Gervais, C.; Babonneau, F. Synthesis and Characterization of Poly-(Aminoborane) as a New Boron Nitride Precursor. *Polymers for Advanced Technologies* **1999**, *10* (12), 702–712. https://doi.org/10.1002/(sici)1099-1581(199912)10:12<702::aid-pat931>3.0.co;2-q.

(17) Nakhmanson, S. M.; Calzolari, A.; Meunier, V.; Bernholc, J.; Nardelli, M. B. Spontaneous Polarization and Piezoelectricity in Boron Nitride Nanotubes. *Physical Review B* **2003**, *67* (23). https://doi.org/10.1103/PhysRevB.67.235406.

(18) Terrones, M.; Romo-Herrera, J. M.; Cruz-Silva, E.; López-Urías, F.; Muñoz-Sandoval, E.; Velázquez-Salazar, J. J.; Terrones, H.; Bando, Y.; Golberg, D. Pure and Doped Boron Nitride Nanotubes. *Materials Today* **2007**, *10* (5), 30–38. https://doi.org/10.1016/S1369-7021(07)70077-9.

(19) Wang, X.; N. Hooper, T.; Kumar, A.; K. Priest, I.; Sheng, Y.; M. Samuels, T. O.; Wang, S.; W. Robertson, A.; Pacios, M.; Bhaskaran, H.; S. Weller, A.; H. Warner, J. Oligomeric Aminoborane Precursors for the Chemical Vapour Deposition Growth of Few-Layer Hexagonal Boron Nitride. *CrystEngComm* **2017**, *19* (2), 285–294. https://doi.org/10.1039/C6CE02006B.

(20) Caldwell, J. D.; Aharonovich, I.; Cassabois, G.; Edgar, J. H.; Gil, B.; Basov, D. N. Photonics with Hexagonal Boron Nitride. *Nature Reviews Materials* **2019**, *4* (8), 552–567. https://doi.org/10.1038/s41578-019-0124-1.

(21) Moon, S.; Kim, J.; Park, J.; Im, S.; Kim, J.; Hwang, I.; Kim, J. K. Hexagonal Boron Nitride for Next-Generation Photonics and Electronics. *Advanced Materials* **2023**, *35* (4), 2204161. https://doi.org/10.1002/adma.202204161.

(22) Schäfer, A.; Jurca, T.; Turner, J.; Vance, J. R.; Lee, K.; Du, V. A.; Haddow, M. F.; Whittell, G. R.; Manners, I. Iron-Catalyzed Dehydropolymerization: A Convenient Route to Poly(Phosphinoboranes) with Molecular-Weight Control. *Angewandte Chemie International Edition* **2015**, *54* (16), 4836–4841. https://doi.org/10.1002/anie.201411957.

(23) Hooper, T. N.; Weller, A. S.; Beattie, N. A.; Macgregor, S. A. Dehydrocoupling of Phosphine-Boranes Using the [RhCp*Me($PMe_3$)($CH_2Cl_2$)][$BAr^F4$] Precatalyst: Stoichiometric and Catalytic Studies. *Chemical Science* **2016**, *7* (3), 2414–2426. https://doi.org/10.1039/c5sc04150c.

(24) Leitao, E. M.; Jurca, T.; Manners, I. Catalysis in Service of Main Group Chemistry Offers a Versatile Approach to P-Block Molecules and Materials. *Nature Chemistry* **2013**, *5* (10), 817–829. https://doi.org/10.1038/nchem.1749.

(25) LaPierre, E. A.; Patrick, B. O.; Manners, I. Trivalent Titanocene Alkyls and Hydrides as Well-Defined, Highly Active, and Broad Scope Precatalysts for Dehydropolymerization of Amine-Boranes. *Journal of the American Chemical Society* **2019**, *141* (51), 20009–20015. https://doi.org/10.1021/jacs.9b11112.

(26) Helten, H.; Dutta, B.; Vance, J. R.; Sloan, M. E.; Haddow, M. F.; Sproules, S.; Collison, D.; Whittell, G. R.; Lloyd-Jones, G. C.; Manners, I. Paramagnetic Titanium(III) and Zirconium(III) Metallocene Complexes as Precatalysts for the Dehydrocoupling/Dehydrogenation of Amine–Boranes. *Angewandte Chemie International Edition* **2013**, *52* (1), 437–440. https://doi.org/10.1002/anie.201207903.

(27) Staubitz, A.; Presa Soto, A.; Manners, I. Iridium-Catalyzed Dehydrocoupling of Primary Amine–Borane Adducts: A Route to High Molecular Weight Polyaminoboranes, Boron–Nitrogen Analogues of Polyolefins. *Angewandte Chemie* **2008**, *120* (33), 6308–6311. https://doi.org/10.1002/ange.200801197.

(28) Tiddens, M. R.; Kappé, B. T.; Smak, T. J.; Lutz, M.; Moret, M.-E. Coordination of a Phosphine-Tethered Aminoborane to Group 10 Metals. *Chemistry – A European Journal* **2024**, *30* (32), e202400666. https://doi.org/10.1002/chem.202400666.

(29) Drover, M. W.; Dufour, M. C.; Lesperance-Nantau, L. A.; Noriega, R. P.; Levin, K.; Schurko, R. W. Octaboraneyl Complexes of Nickel: Monomers for Redox-Active Coordination Polymers. *Chemistry – A European Journal* **2020**, *26* (49), 11180–11186. https://doi.org/10.1002/chem.202001218.

(30) Drover, M. W. A Guide to Secondary Coordination Sphere Editing. *Chem. Soc. Rev.* **2022**, *51* (6), 1861–1880. https://doi.org/10.1039/D2CS00022A.

(31) Clapson, M. L.; Sharma, H.; Zurakowski, J. A.; Drover, M. W. Cooperative Nitrile Coordination Using Nickel and a Boron-Containing Secondary Coordination Sphere. *Chemistry – A European Journal* **2023**, *29* (17), e202203763. https://doi.org/10.1002/chem.202203763.

(32) Demchuk, M. J.; Zurakowski, J. A.; Drover, M. W. Iridium Diphosphine Complexes Featuring Pendant Lewis Acids: Efforts toward Selective Heteroarene Borylation. *European Journal of Inorganic Chemistry* **2023**, *26* (8), e202200731. https://doi.org/10.1002/ejic.202200731.

(33) Zurakowski, J. A.; Austen, B. J. H.; Drover, M. W. Exterior Decorating: Lewis Acid Secondary Coordination Spheres for Cooperative Reactivity. *Trends Chem.* **2022**, *4* (4), 331–346. https://doi.org/10.1016/j.trechm.2022.01.007.

(34) Zurakowski, J. A.; Austen, B. J. H.; Drover, M. W. Wrapping Rhodium in a Borane Canopy: Implications for Hydride Formation and Transfer. *Organometallics* **2021**, *40* (15), 2450–2457. https://doi.org/10.1021/acs.organomet.1c00194.

(35) Zurakowski, J. A.; Austen, B. J. H.; Dufour, M. C.; Bhattacharyya, M.; Spasyuk, D. M.; Drover, M. W. Preparation of a Borane-Appended Co(III) Hydride: Evidence for Metal–Ligand Cooperativity in O–H Bond Activation. *Dalton Transactions* **2021**, *50* (36), 12440–12447. https://doi.org/10.1039/D1DT02331D.

## Appendix – NMR Spectra of New Compounds

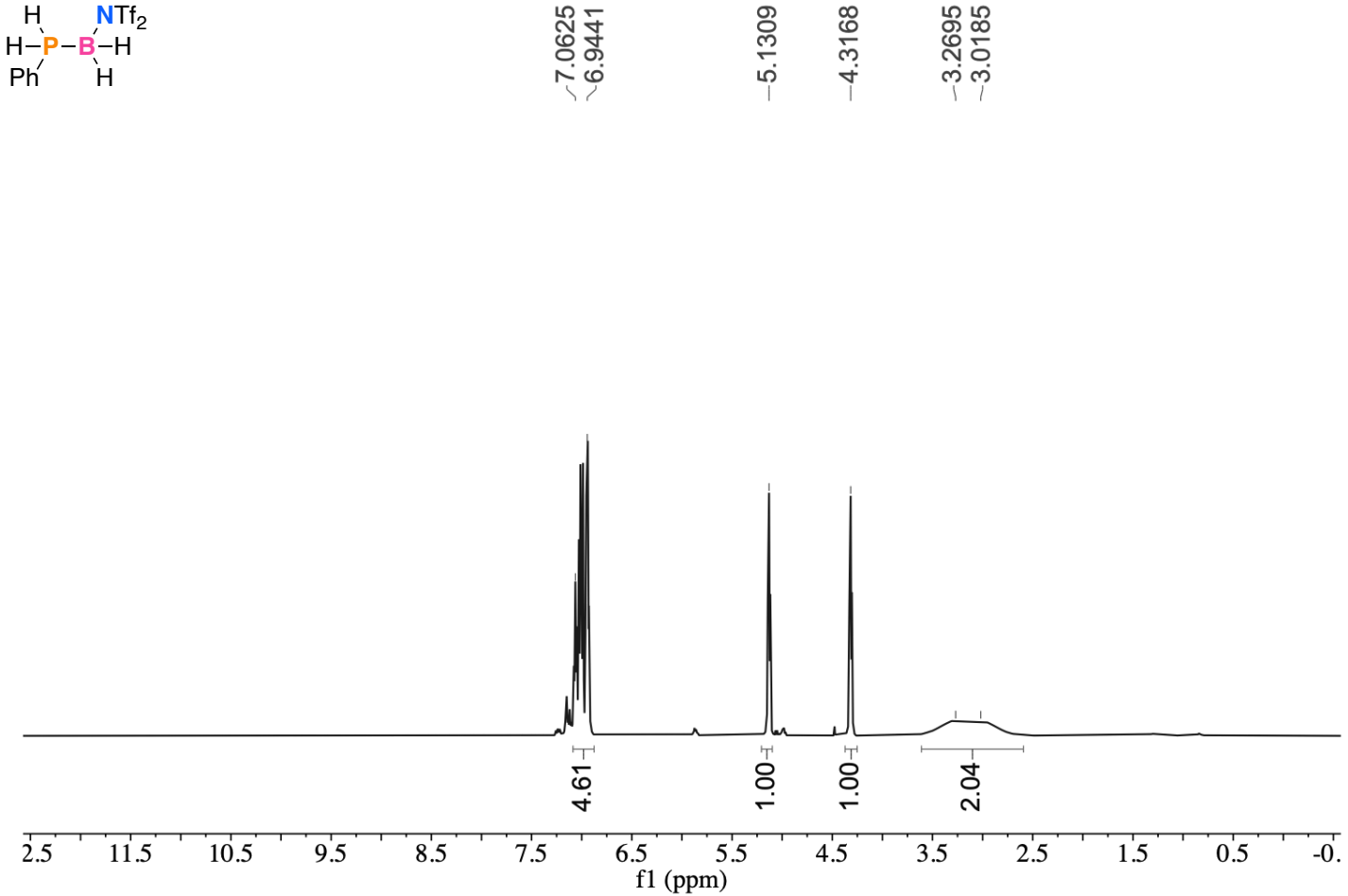


**Figure A.1**: $^{1}H$ NMR ($C_6D_6$, 500 MHz, 298 K) of **2.2a.**

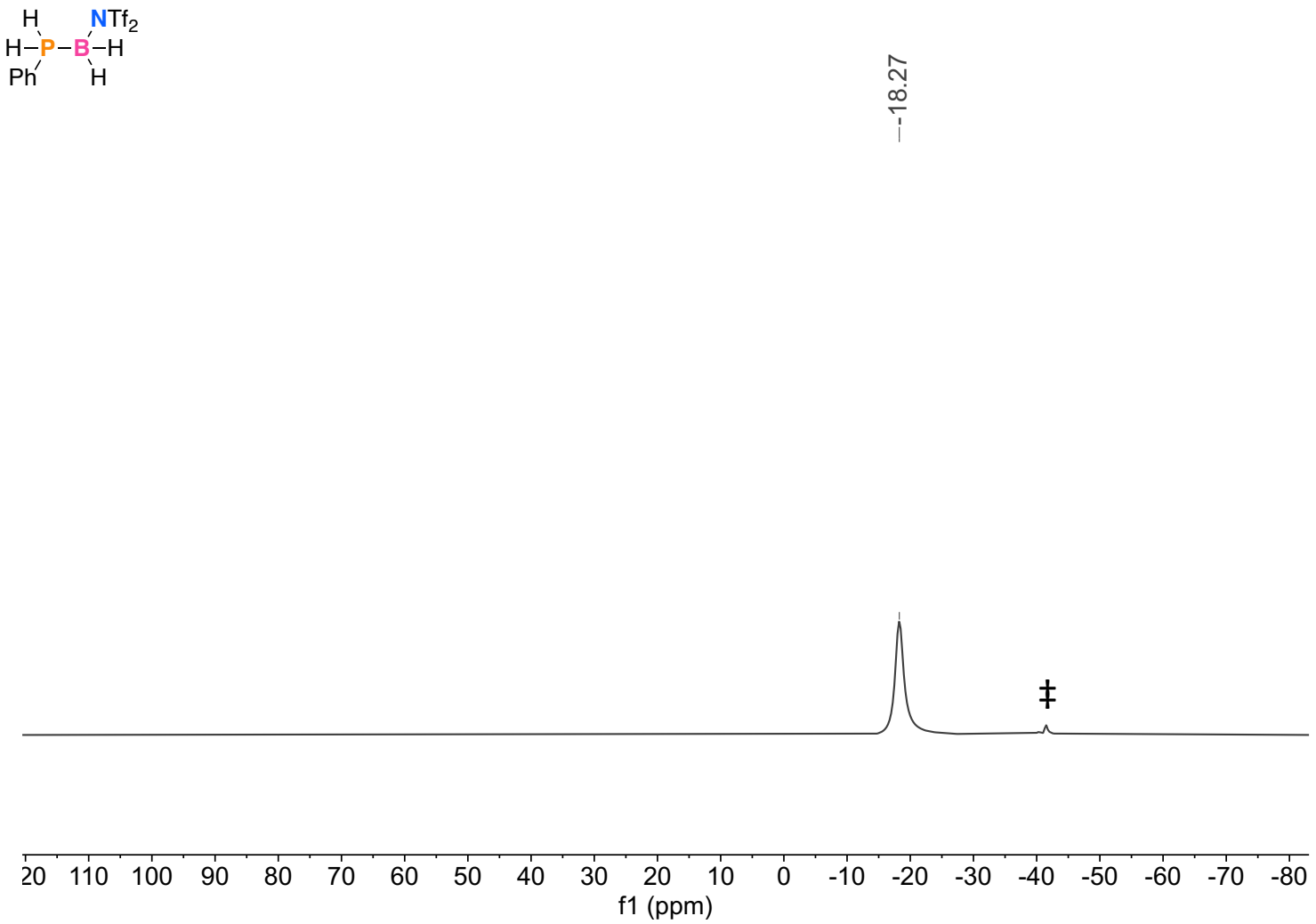


**Figure A.2**: $^{11}B\{^{1}H\}$ NMR ($C_6D_6$, 160 MHz, 298 K) of **2.2a**. ‡ Residual unreacted phosphine-borane adduct, **2.1a**.

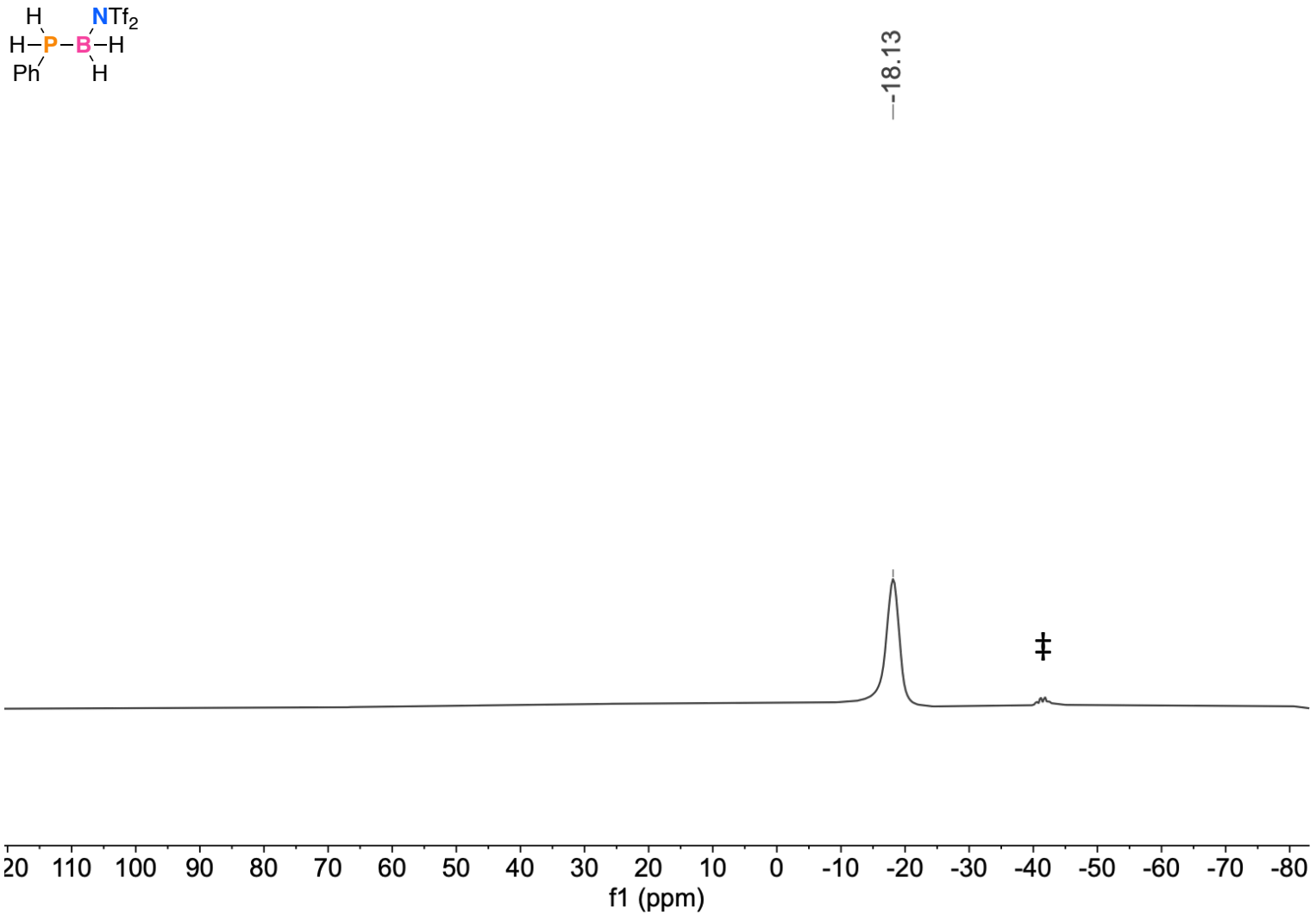


**Figure A.3:** $^{11}$B NMR ($C_6D_6$, 160 MHz, 298 K) of **2.2a**. ‡ Residual unreacted phosphine-borane adduct, **2.1a**.

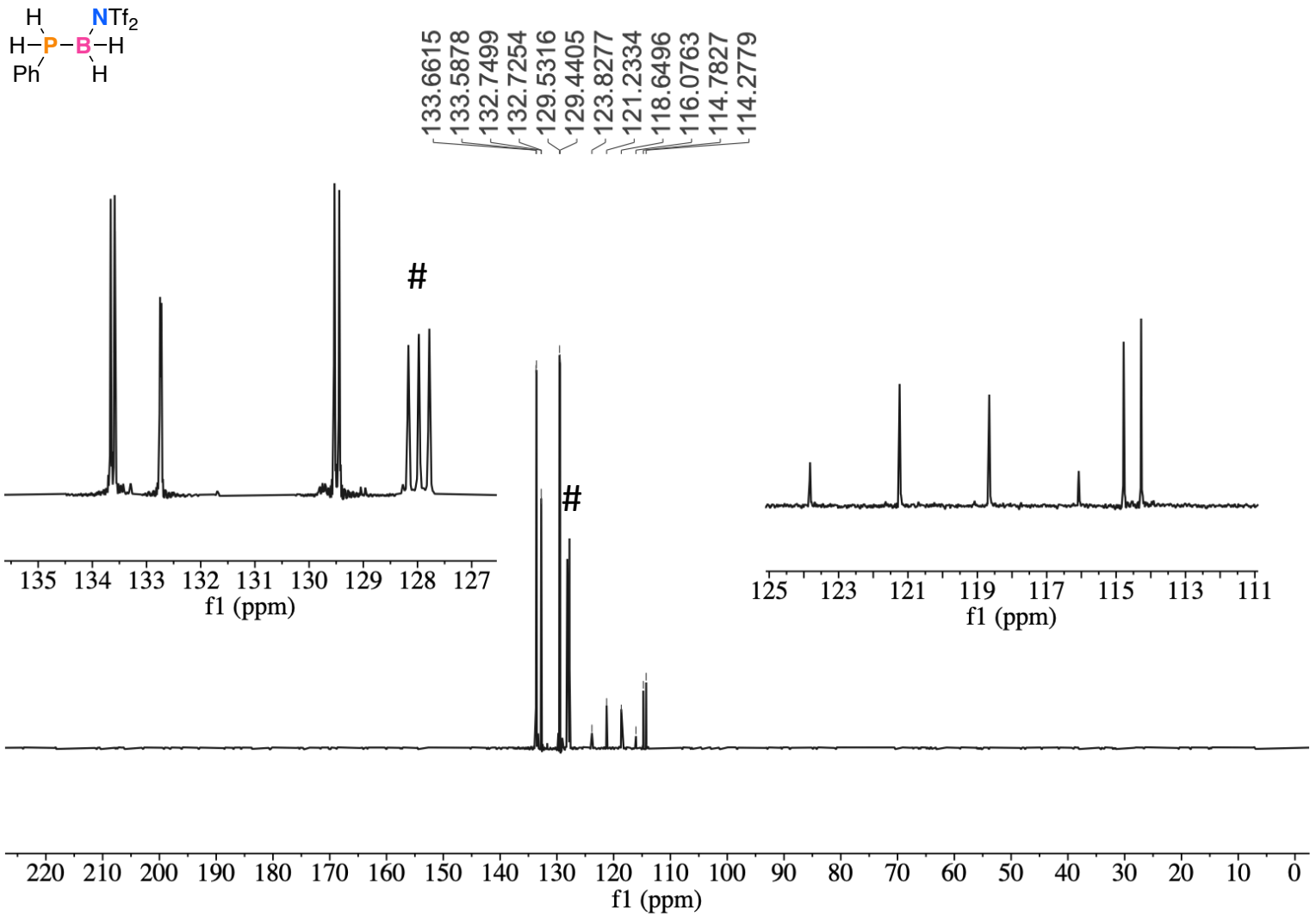


**Figure A.4**:[13]C NMR ($C_6D_6$, 126 MHz, 298 K) of **2.2a**. Inserted spectra are expanded portions of the full spectrum. # solvent peak for $C_6D_6$.

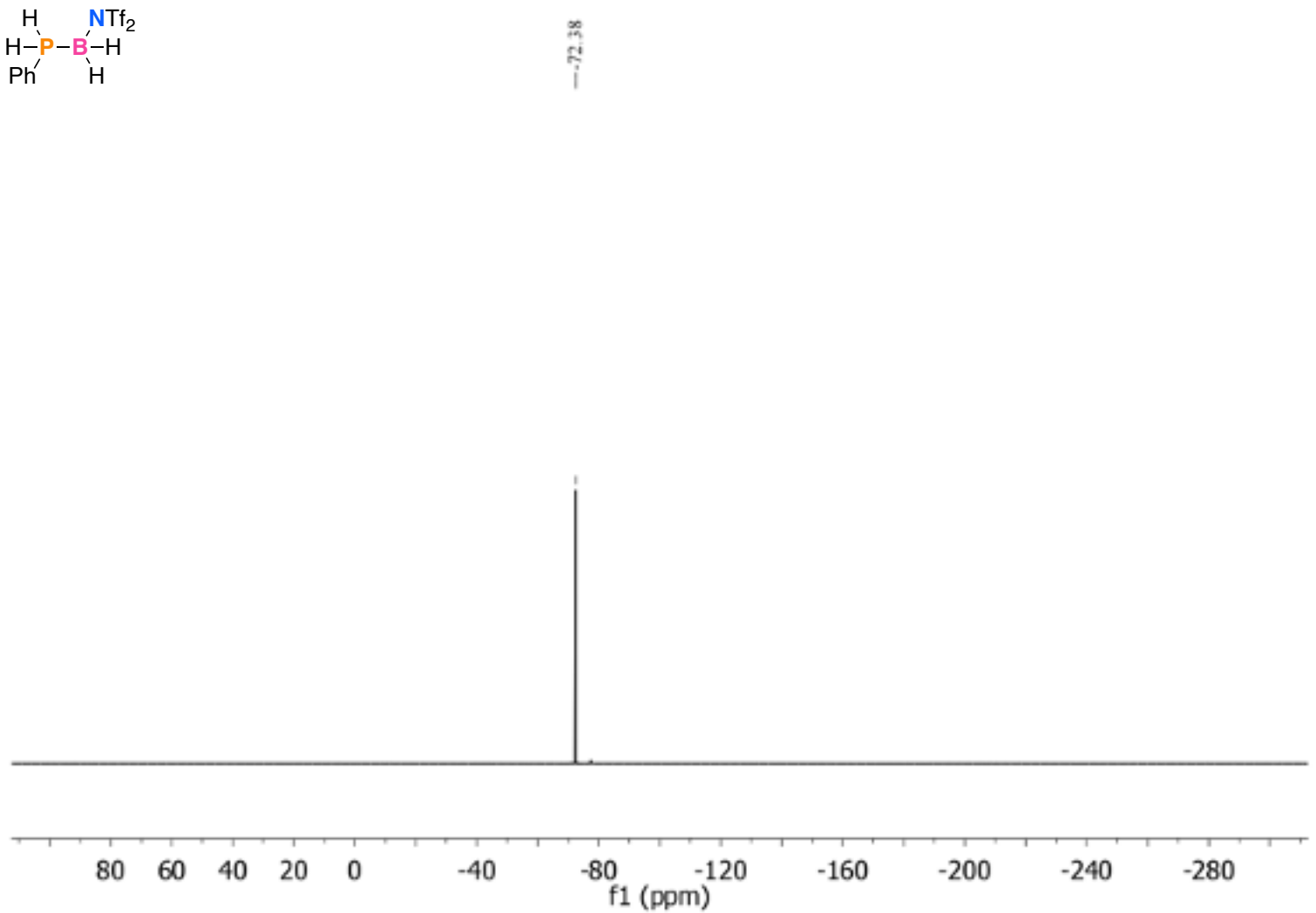


**Figure A.5**: $^{19}F$ NMR ($C_6D_6$, 471 MHz, 298 K) of **2.2a.**

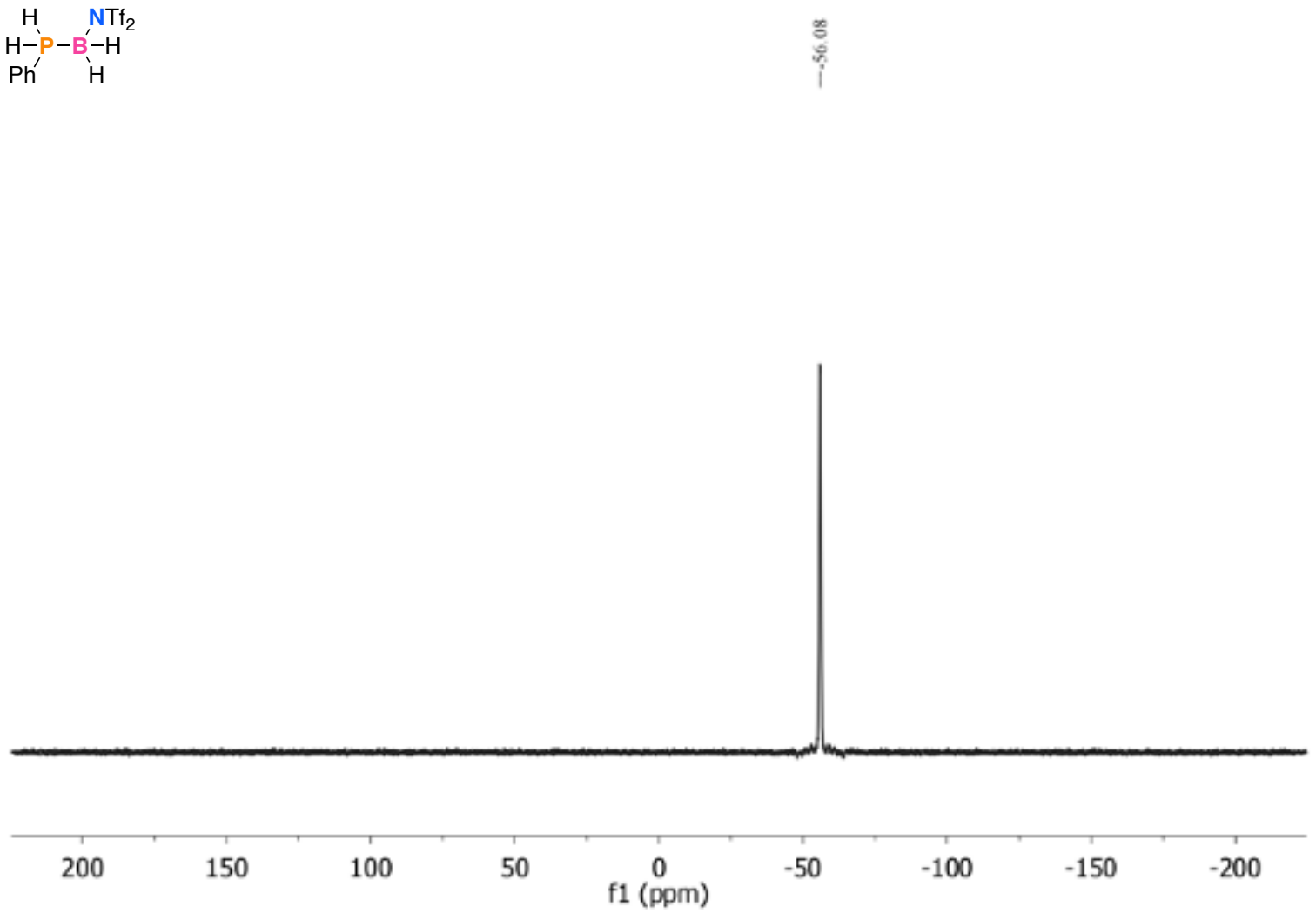


**Figure A.6**: $^{31}P\{^{1}H\}$ NMR ($C_6D_6$, 202 MHz, 298 K) of **2.2a.**

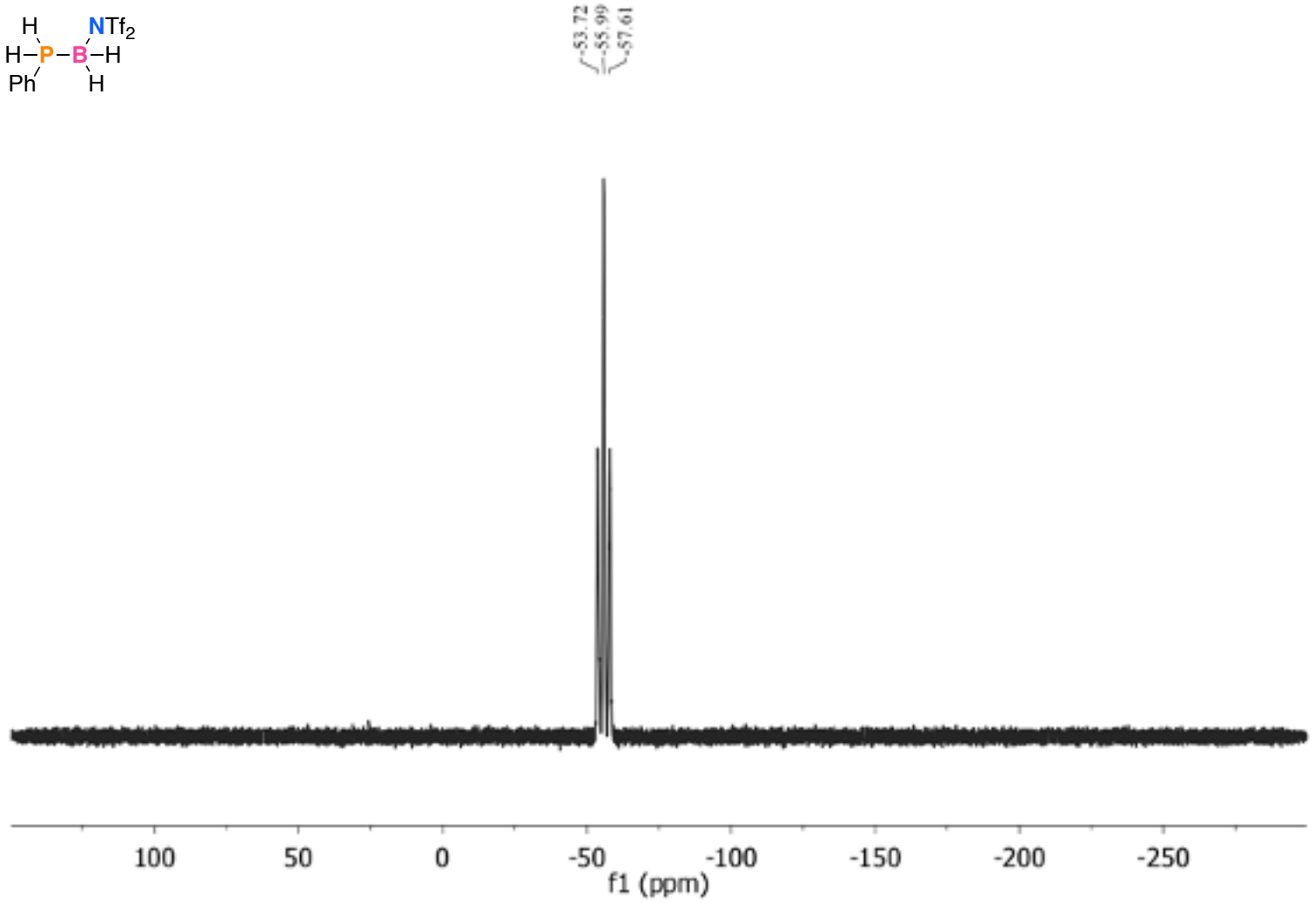


**Figure A.7**: $^{31}P$ NMR ($C_6D_6$, 202 MHz, 298 K) of **2.2a.**

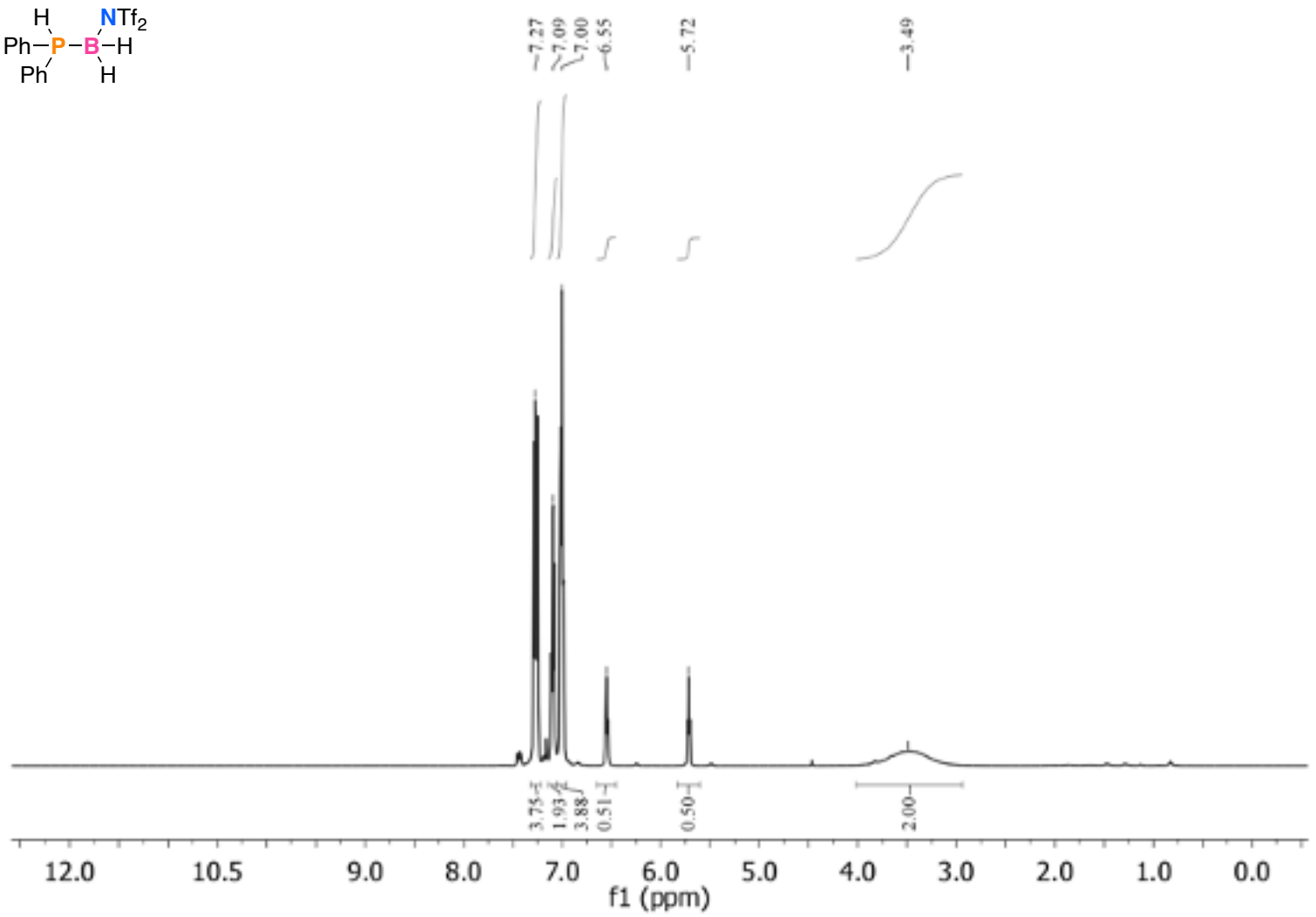


**Figure A.8**: **:** $^{1}$H NMR ($C_6D_6$, 500 MHz, 298 K) of **2.2b.**

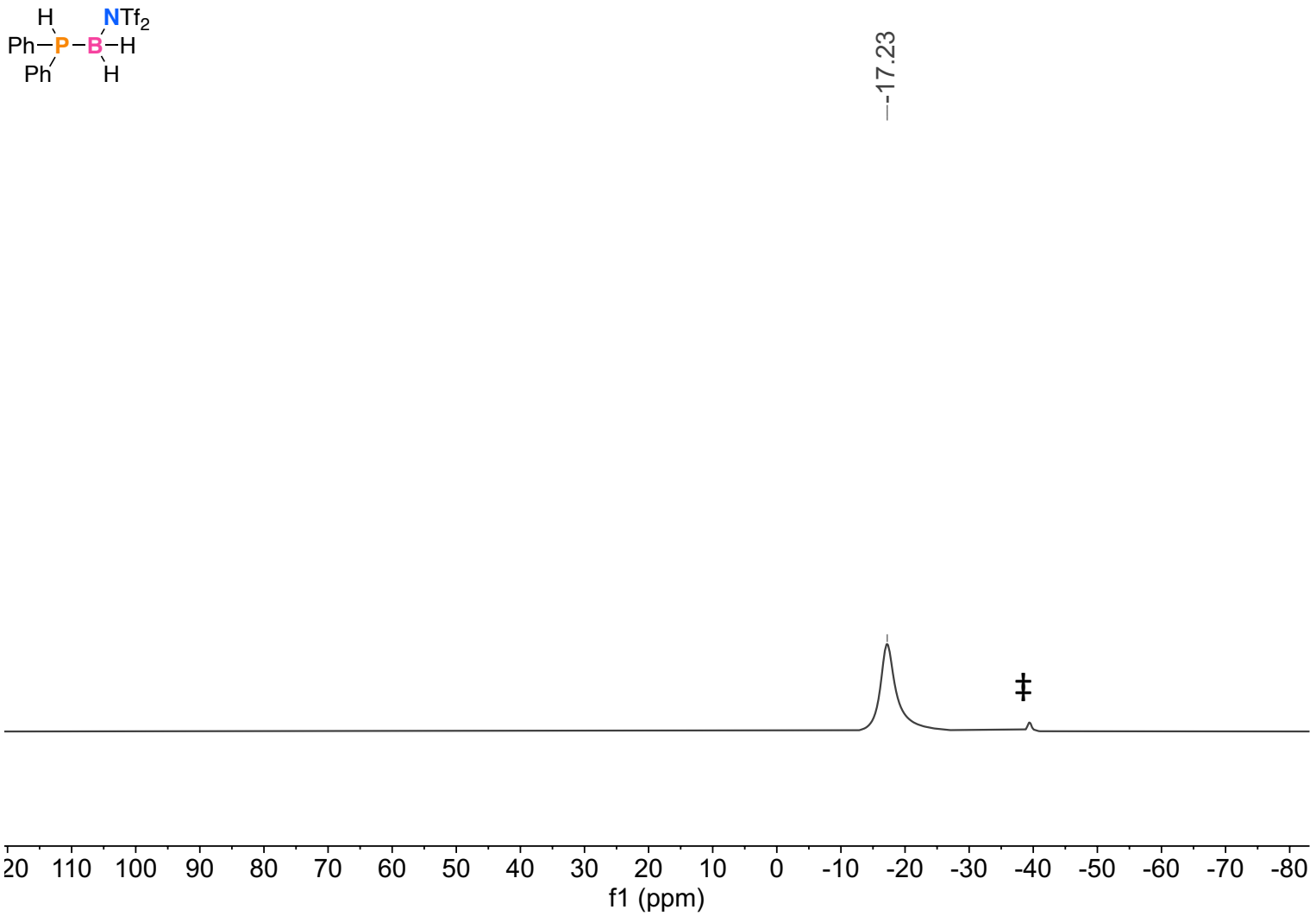


**Figure A.9:** $^{11}B\{^{1}H\}$ NMR ($C_6D_6$, 160 MHz, 298 K) of **2.2b.** ‡ Residual unreacted phosphine-borane adduct, **2.1b.**

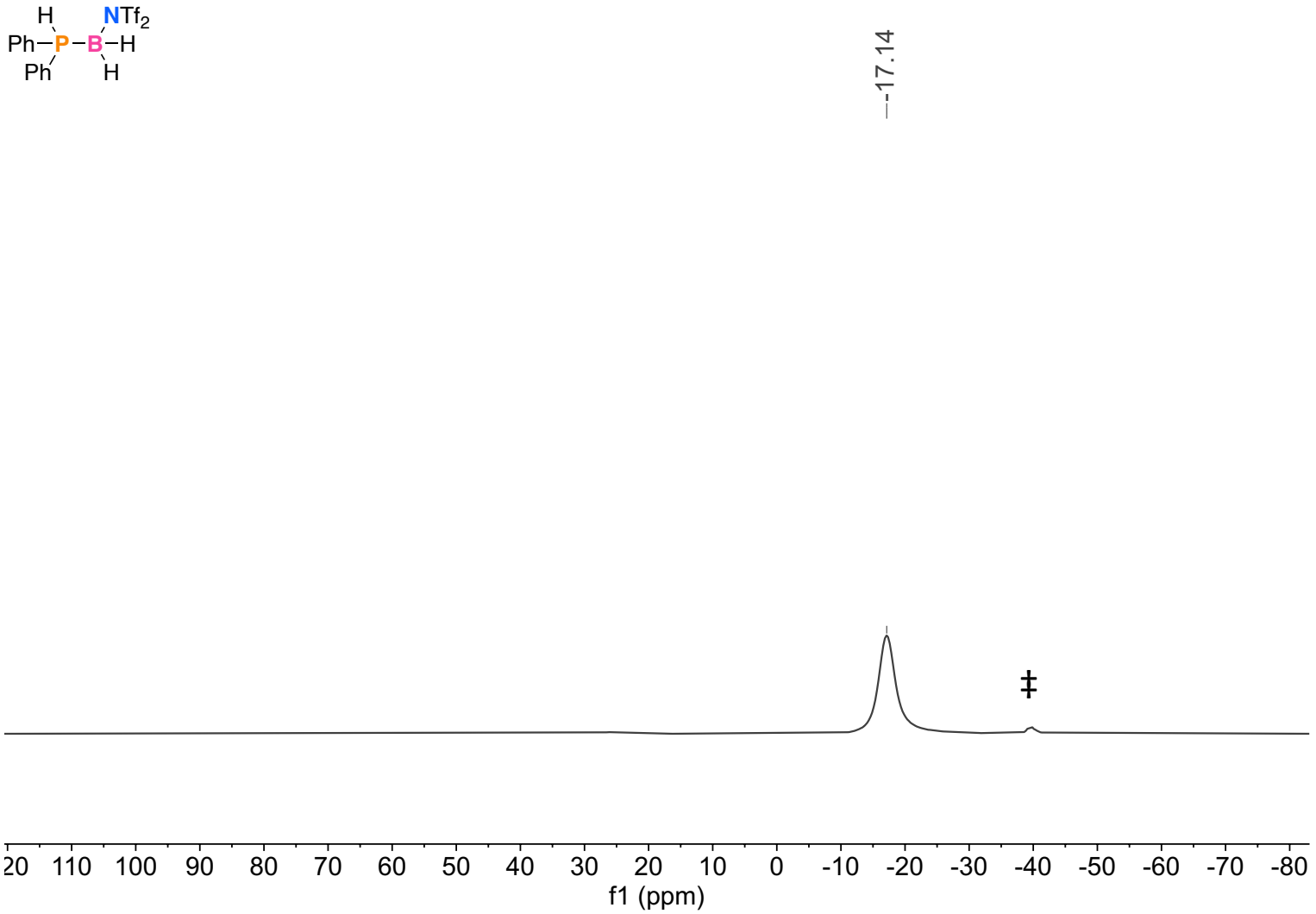


**Figure A.10**: $^{11}B\{^{1}H\}$ NMR ($C_6D_6$, 160 MHz, 298 K) of **2.2b**. ‡ Residual unreacted phosphine-borane adduct, **2.1b**.

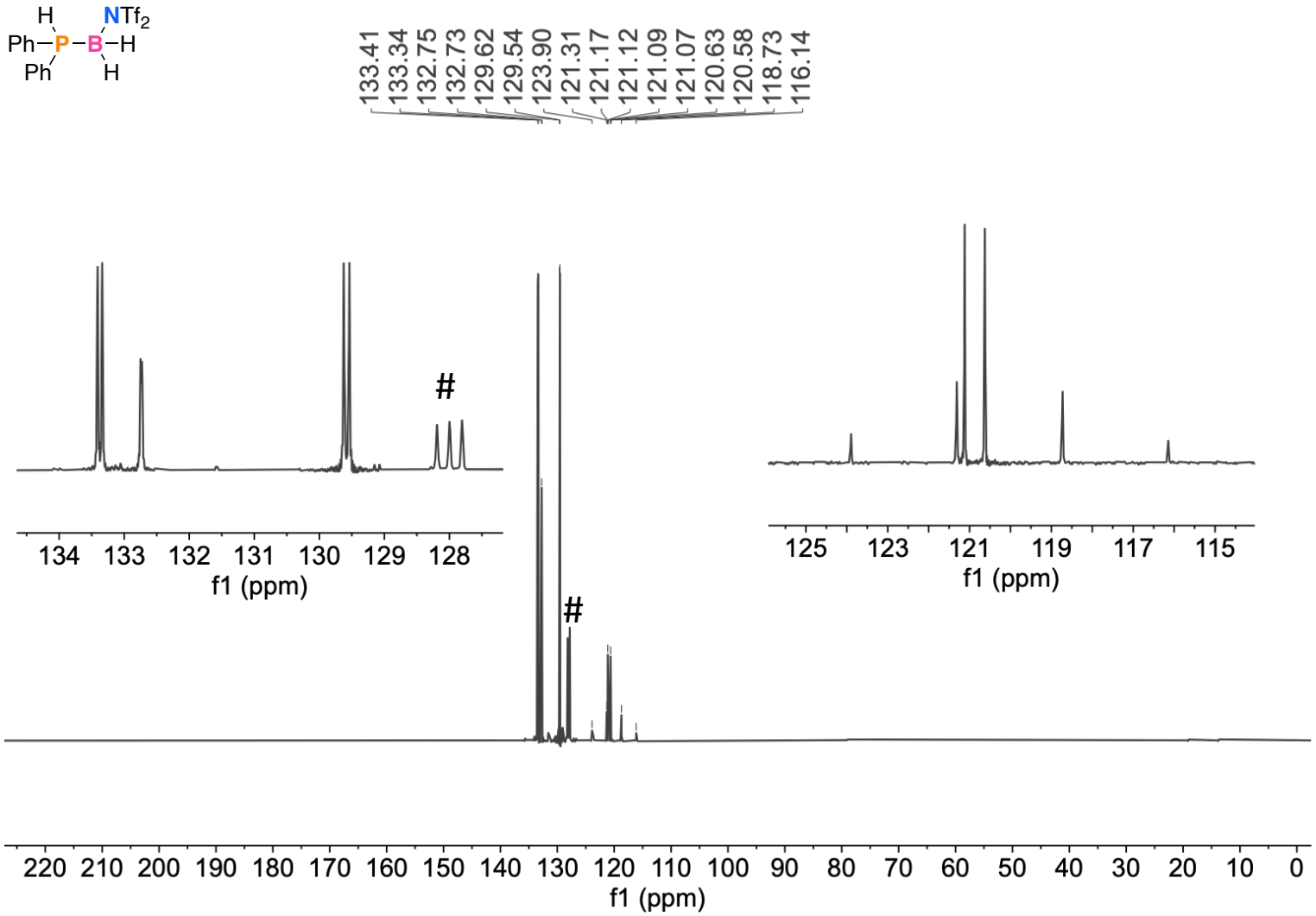


**Figure A.11**: $^{13}C\{^{1}H\}$ NMR ($C_6D_6$, 126 MHz, 298 K) of **2.2b**. Inserted spectra are expanded portions of the full spectrum. # Solvent peak for $C_6D_6$.

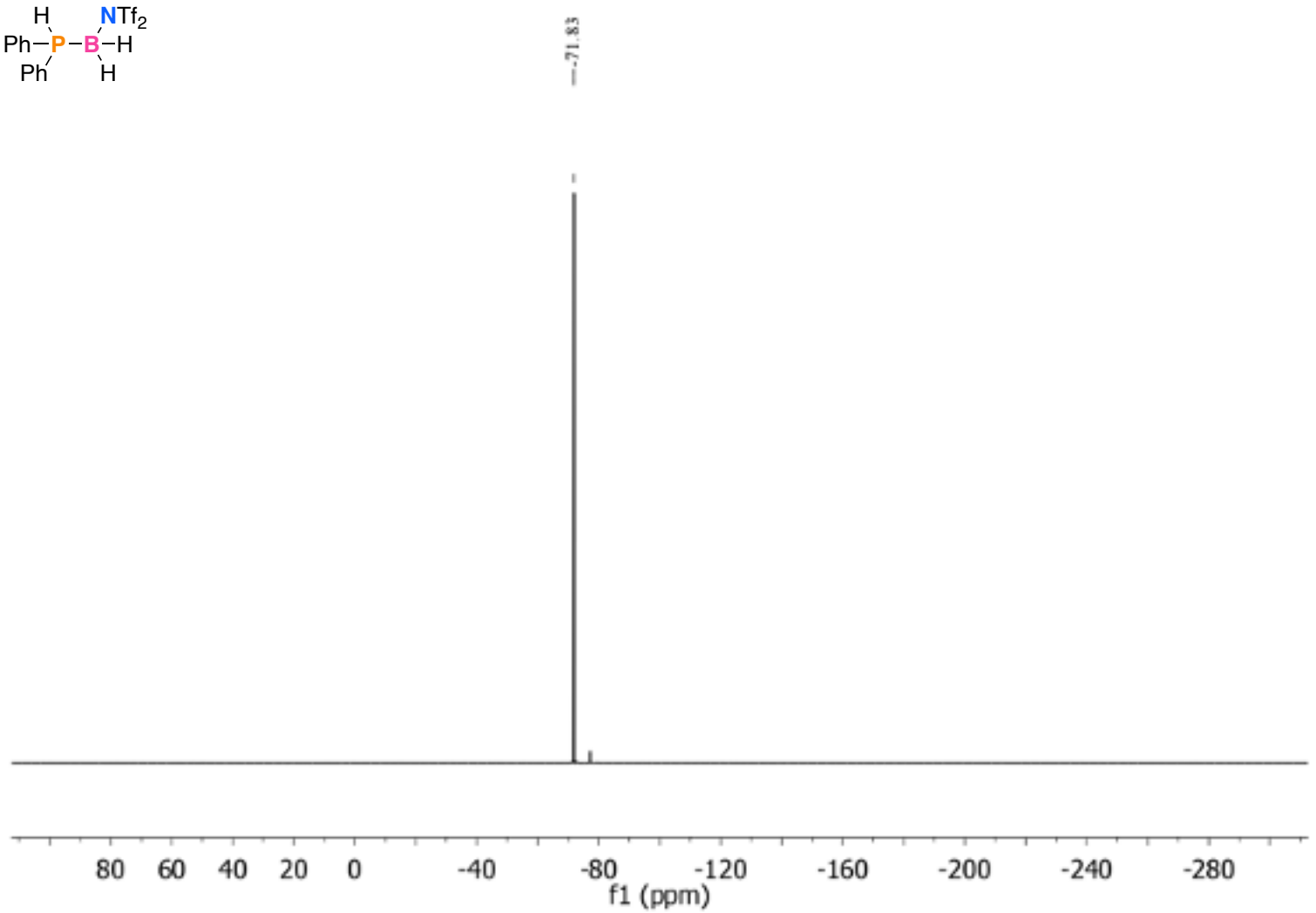


Figure A.12**:** $^{19}$F NMR ($C_6D_6$, 471 MHz, 298 K) of **2**.**2b**

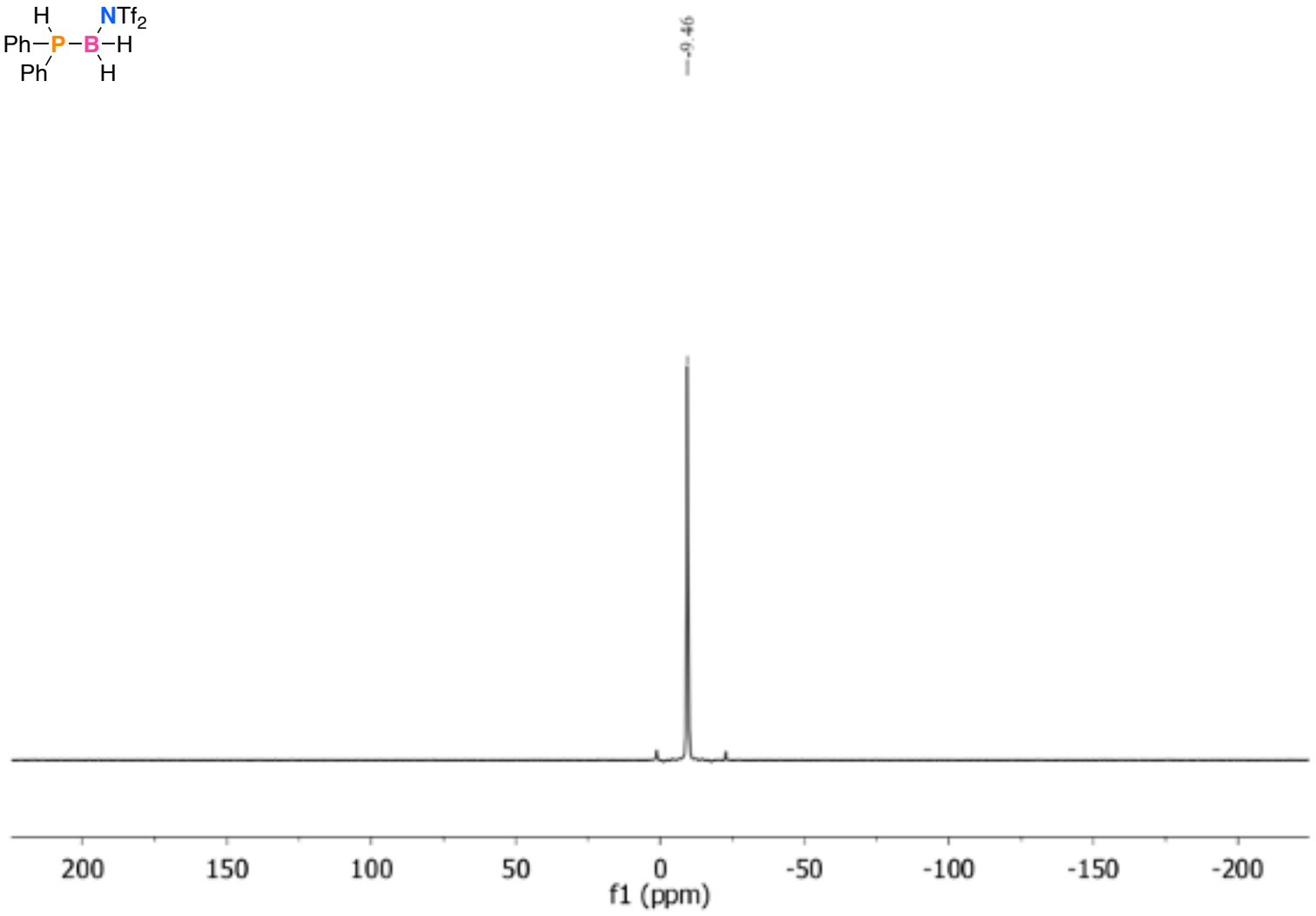


**Figure A.13**: $^{31}P\{^{1}H\}$ NMR ($C_6D_6$, 202 MHz, 298 K) of **2.2b.**

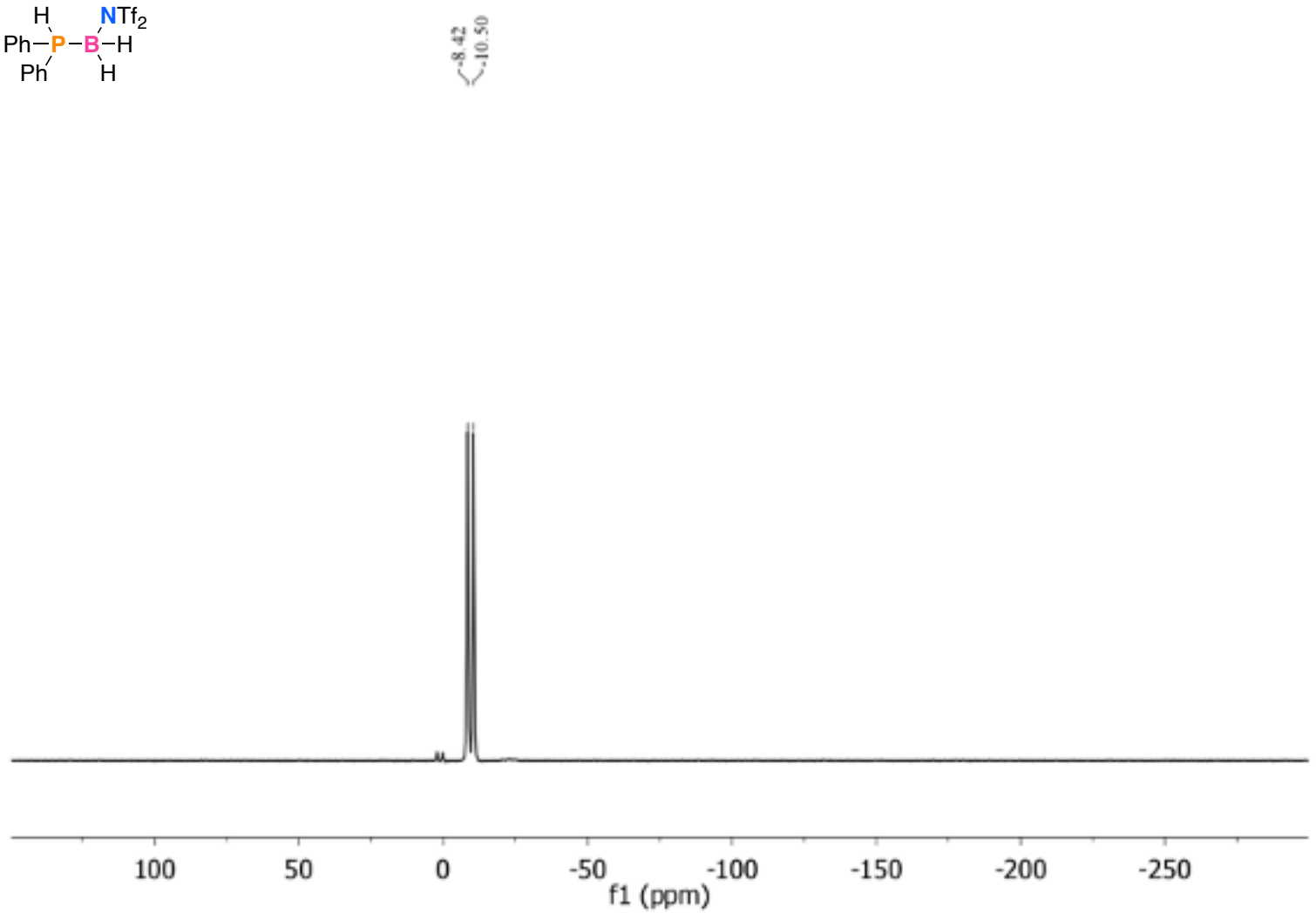


**Figure A.14**: $^{31}P$ NMR ($C_6D_6$, 202 MHz, 298 K) of **2.2b.**

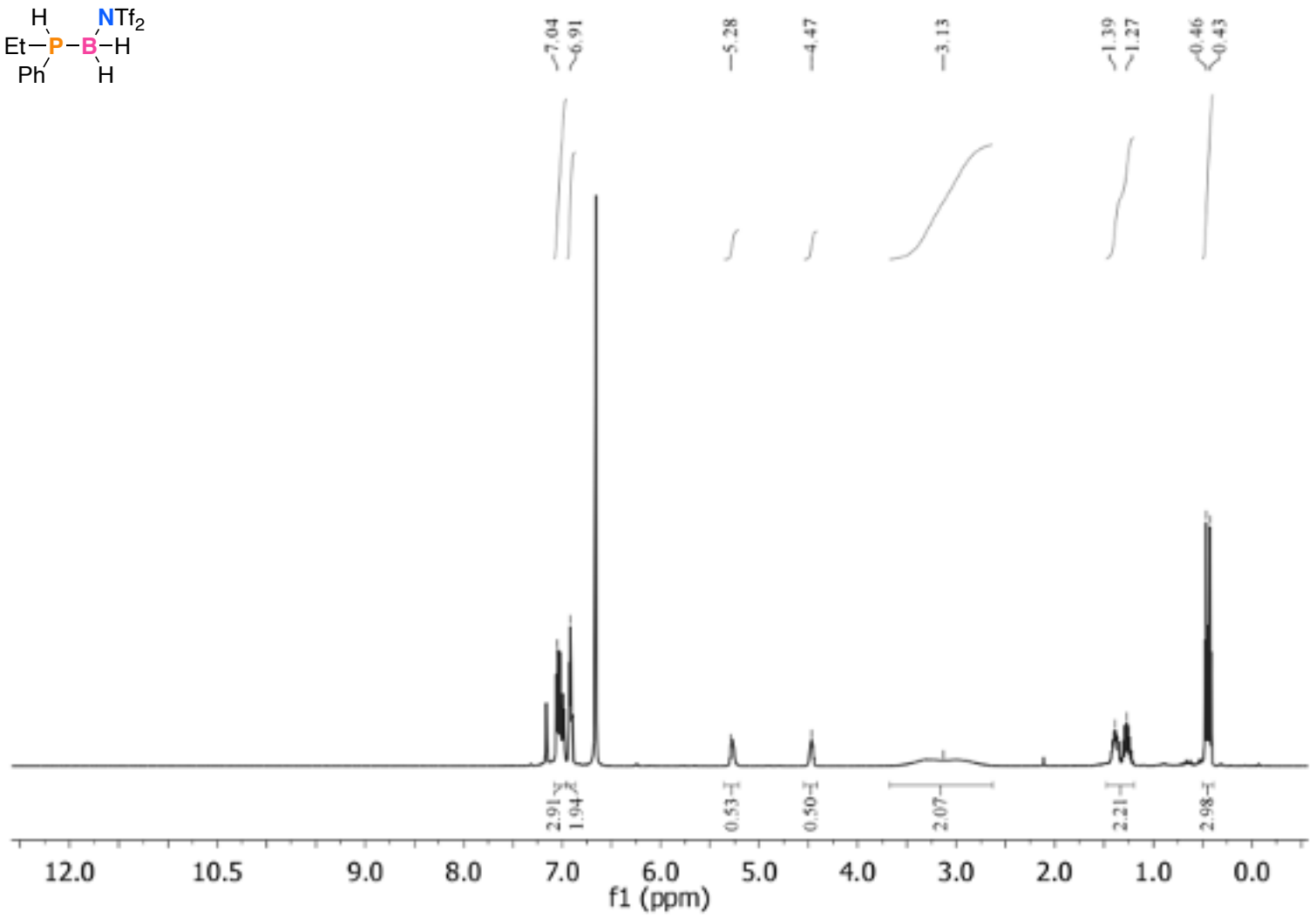


**Figure A.15**: $^{1}H$ NMR ($C_6D_6$, 500 MHz, 298 K) of **2.2c.**

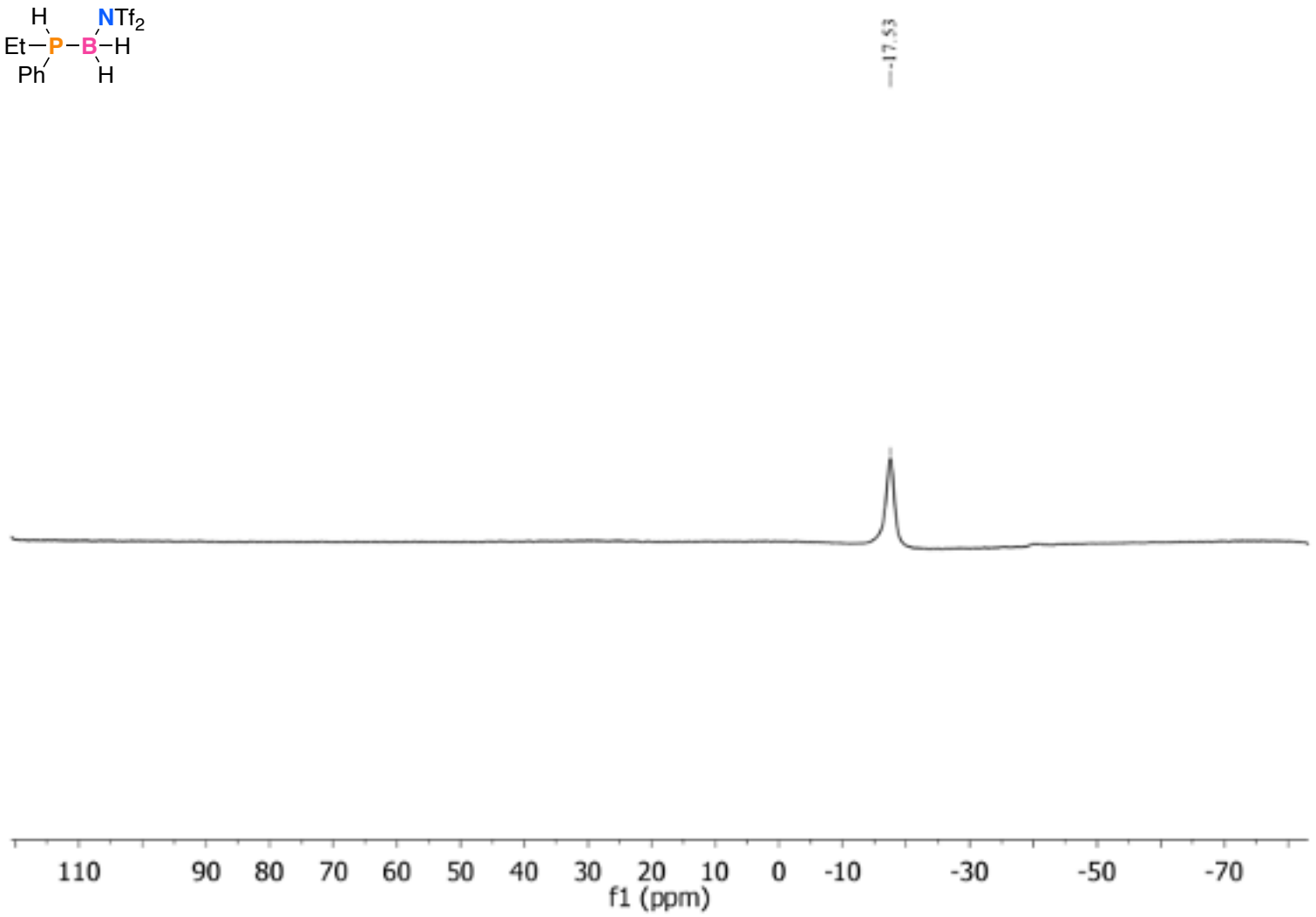


**Figure A.16:** $^{11}B\{^{1}H\}$ NMR ($C_6D_6$, 160 MHz, 298 K) of **2.2c.**

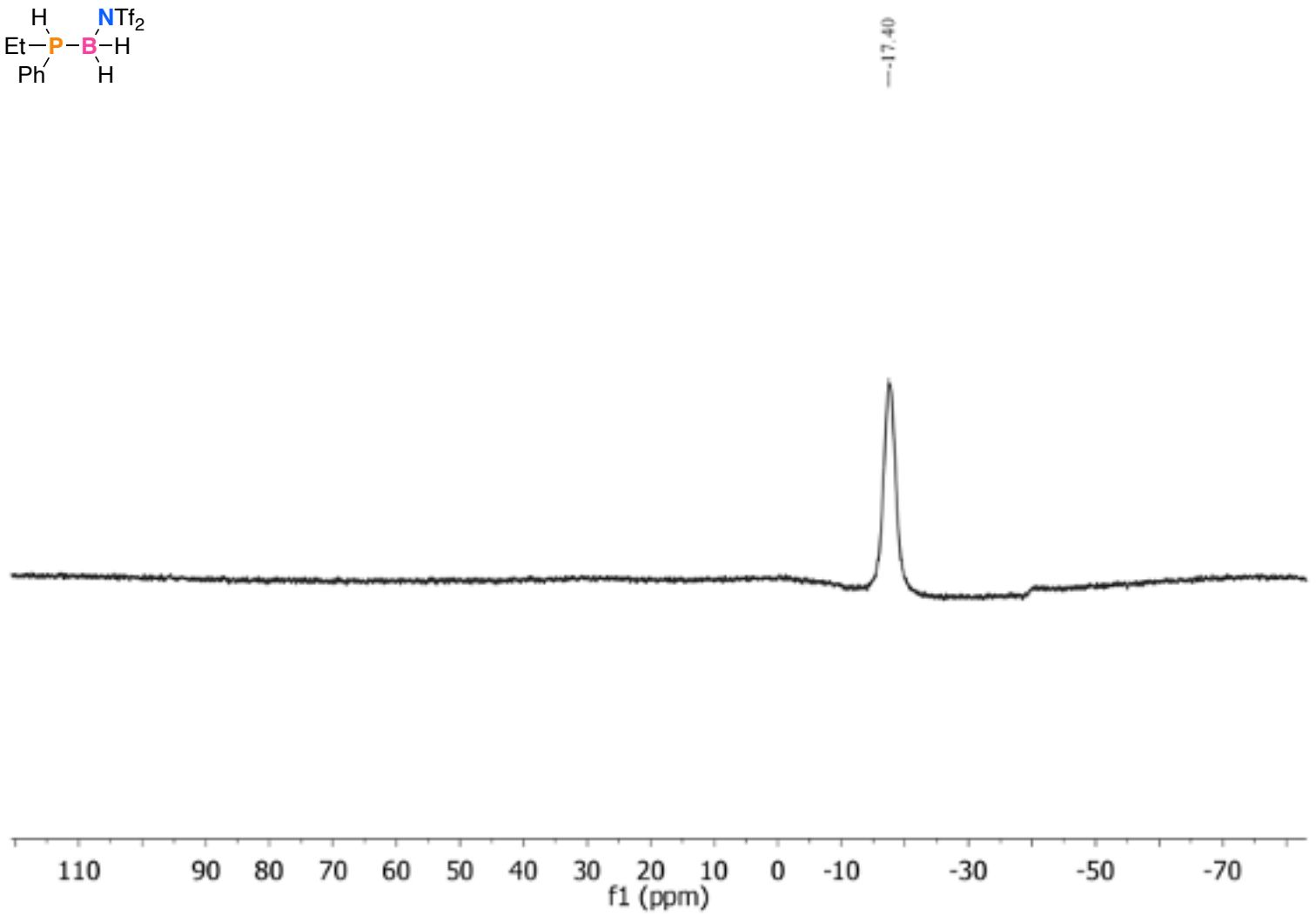


**Figure A.17:** $^{11}B\{^{1}H\}$ NMR ($C_6D_6$, 160 MHz, 298 K) of **2.2c**.

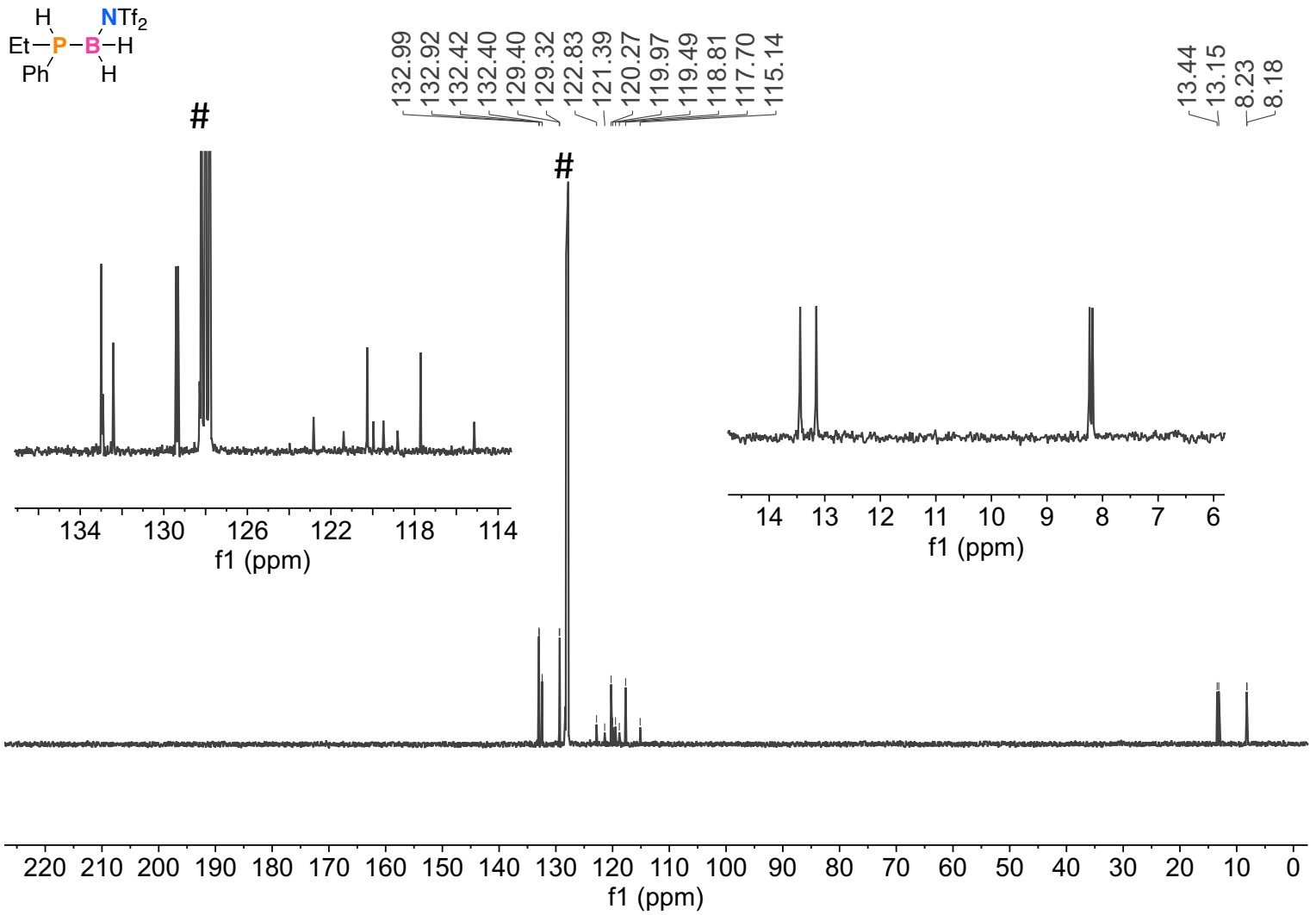


**Figure A.18:** $^{13}C\{^{1}H\}$ NMR ($C_6D_6$, 126 MHz, 298 K) of **2.2c**. Inserted spectra are portions of the full spectrum. # solvent peak for $C_6D_6$

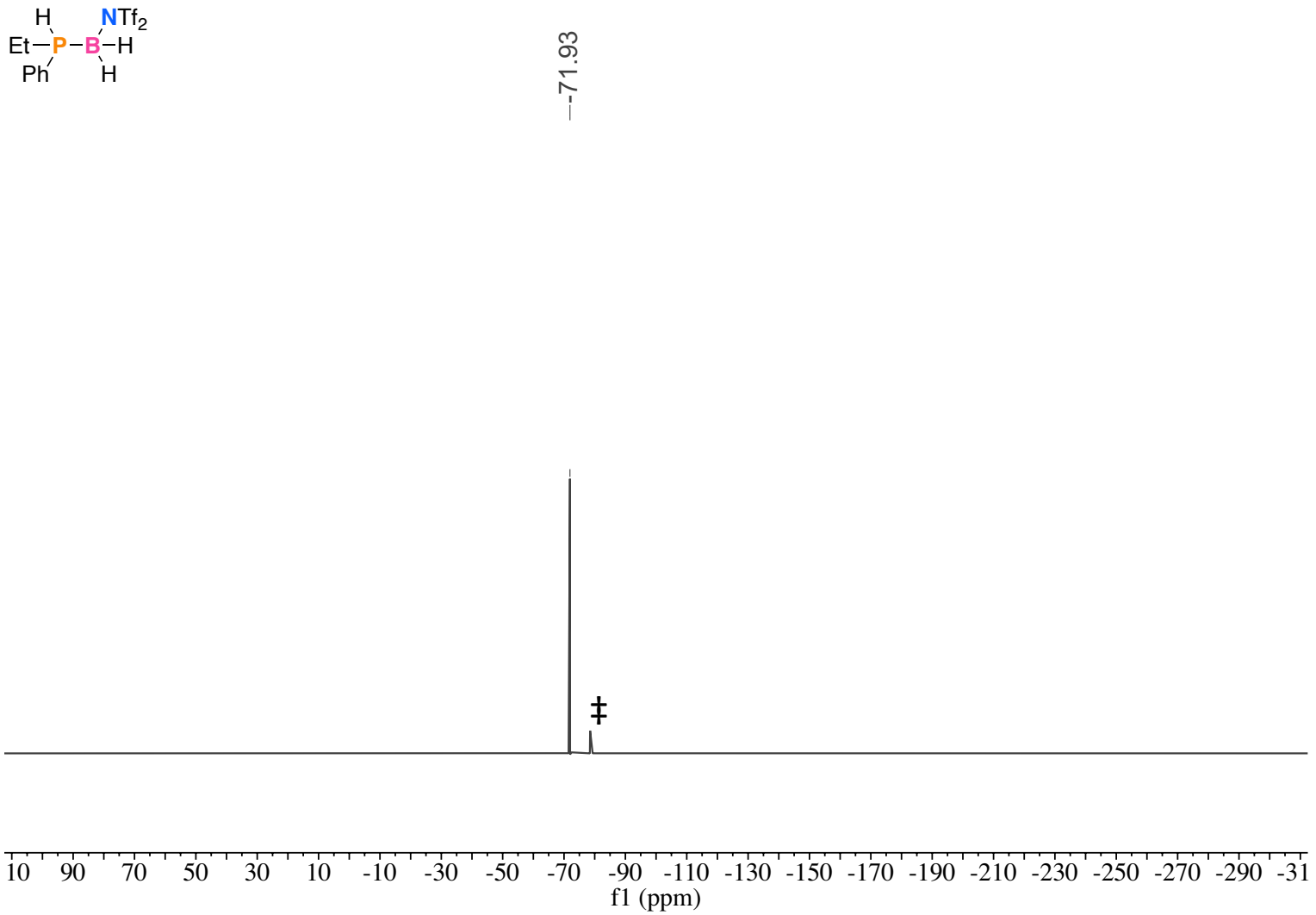


**Figure A.19**: $^{19}F$ NMR ($C_6D_6$, 471 MHz, 298 K) of **2.2c**. ‡ Uncharacterized residual impurity.

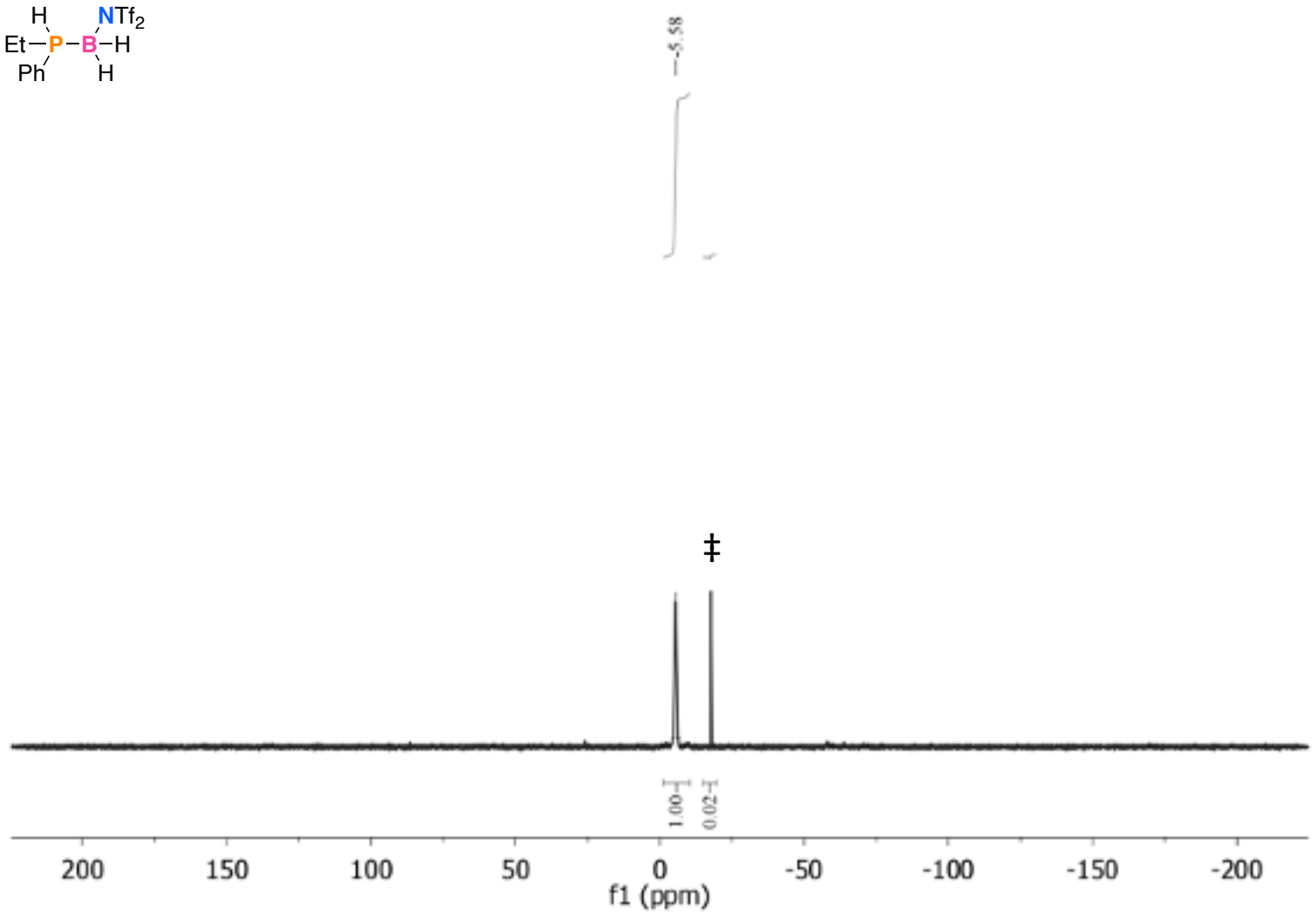


**Figure A.20:** $^{31}P\{^{1}H\}$ NMR ($C_6D_6$, 202 MHz, 298 K) of **2.2c**. ‡ Uncharacterized residual impurity (*ca*. 2% by integration).

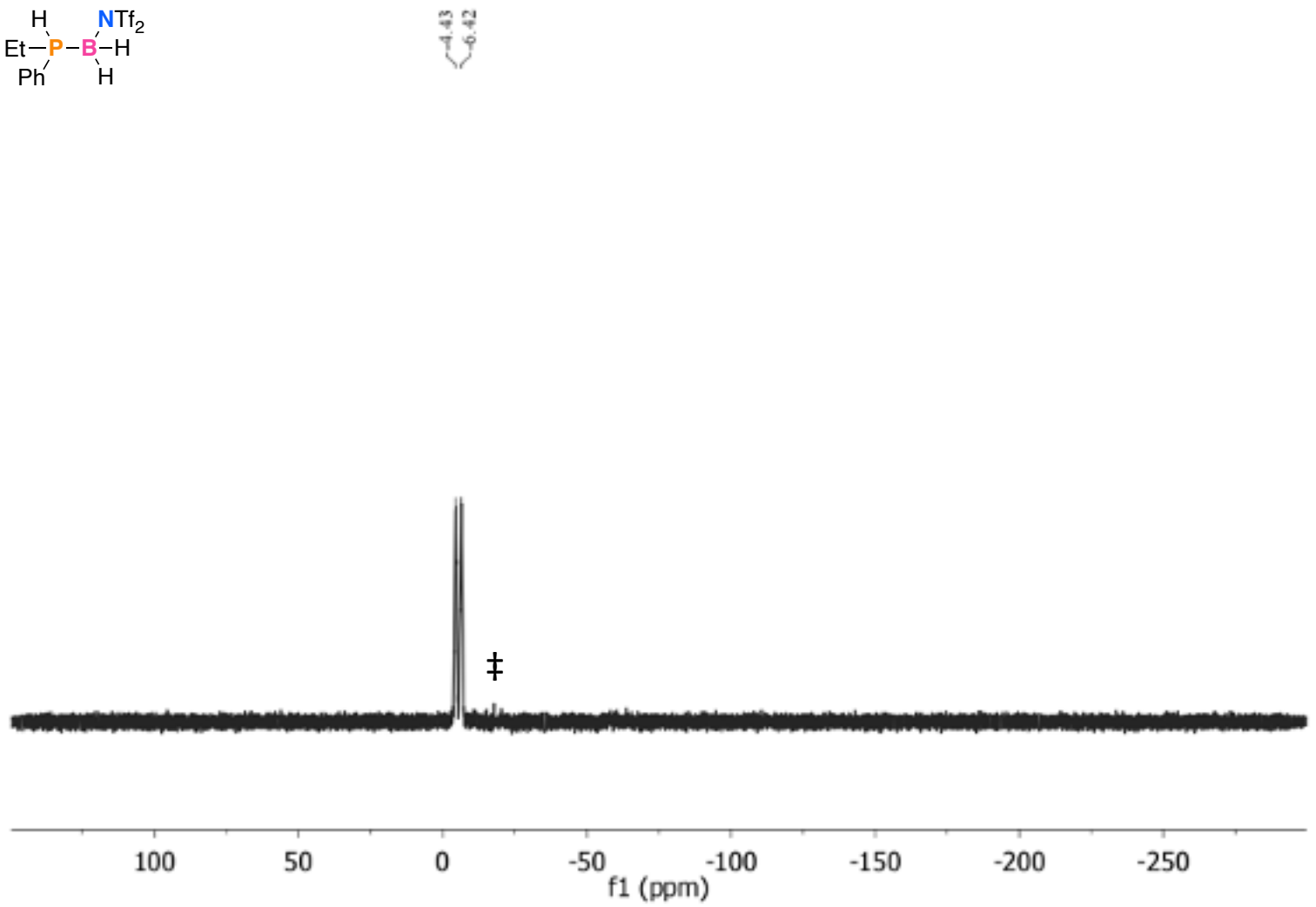


**Figure A.21**: $^{31}$P NMR ($C_6D_6$, 202 MHz, 298 K) of **2.2c**. ‡ Uncharacterized residual impurity.

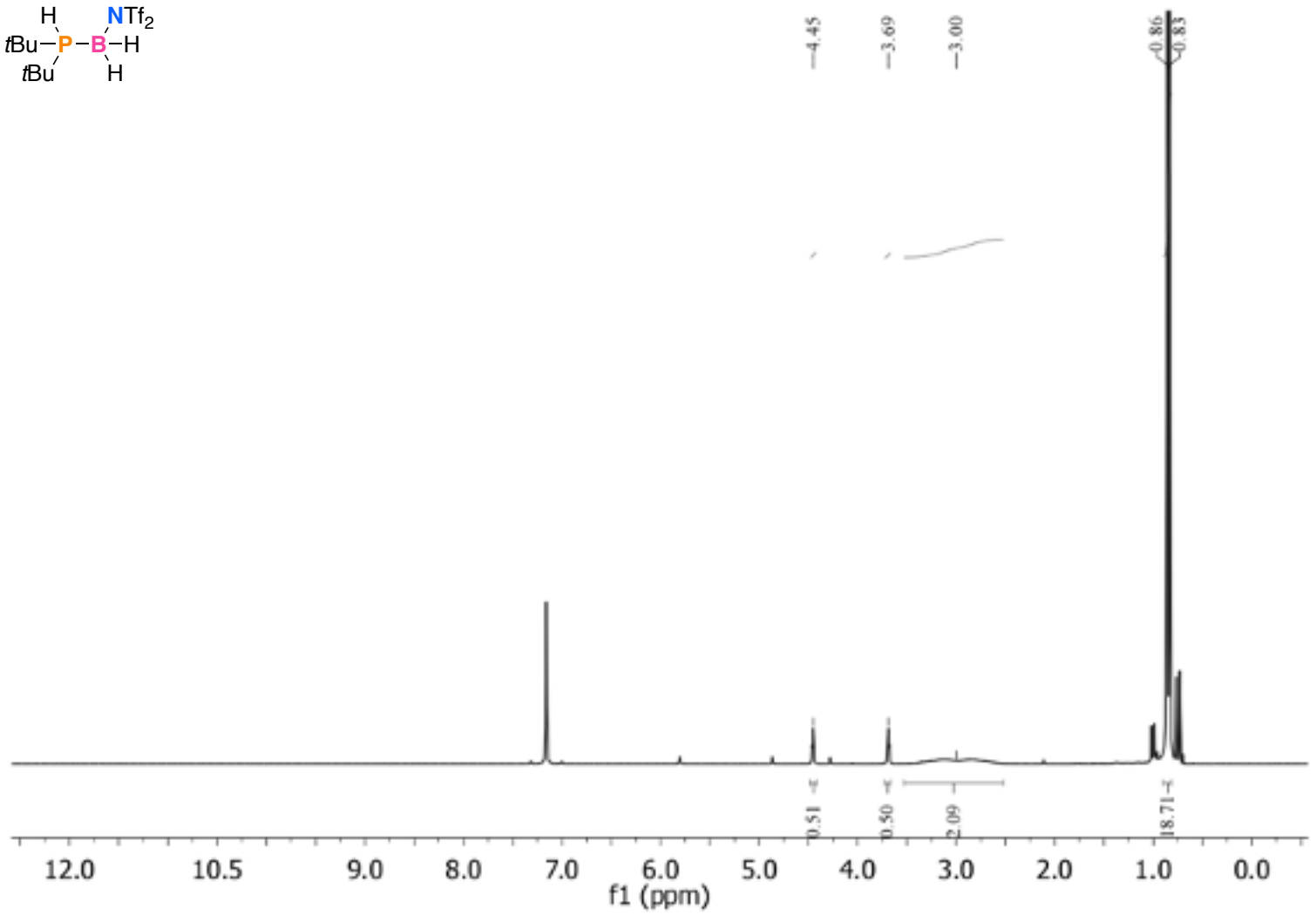


**Figure A.22**: $^{1}H$ NMR ($C_6D_6$, 500 MHz, 298 K) of **2.2d.**

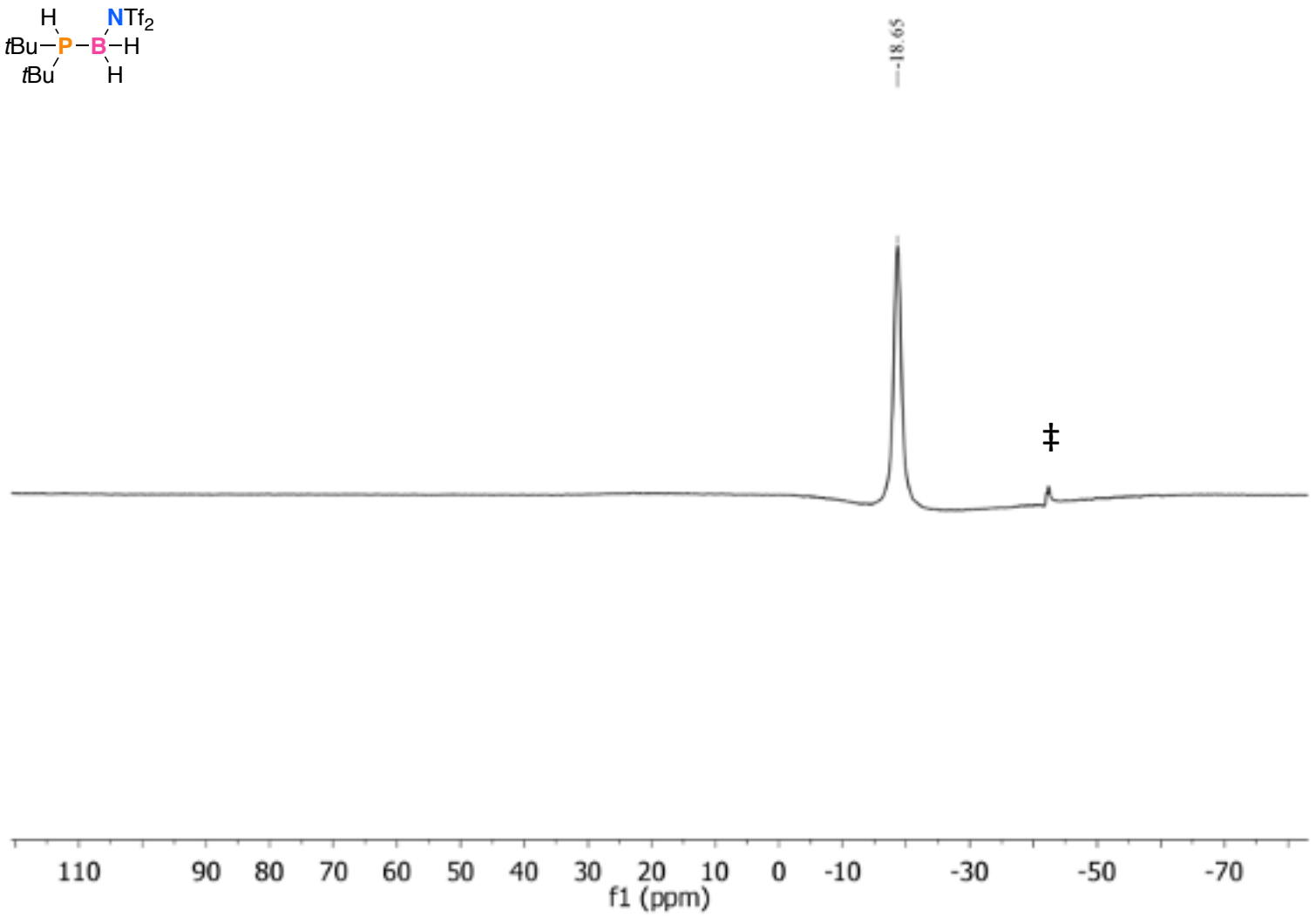


**Figure A.23**: $^{11}B\{^{1}H\}$ NMR ($C_6D_6$, 160 MHz, 298 K) of **2.2d**. ‡ Residual unreacted phosphine-borane adduct, **2.1d.**

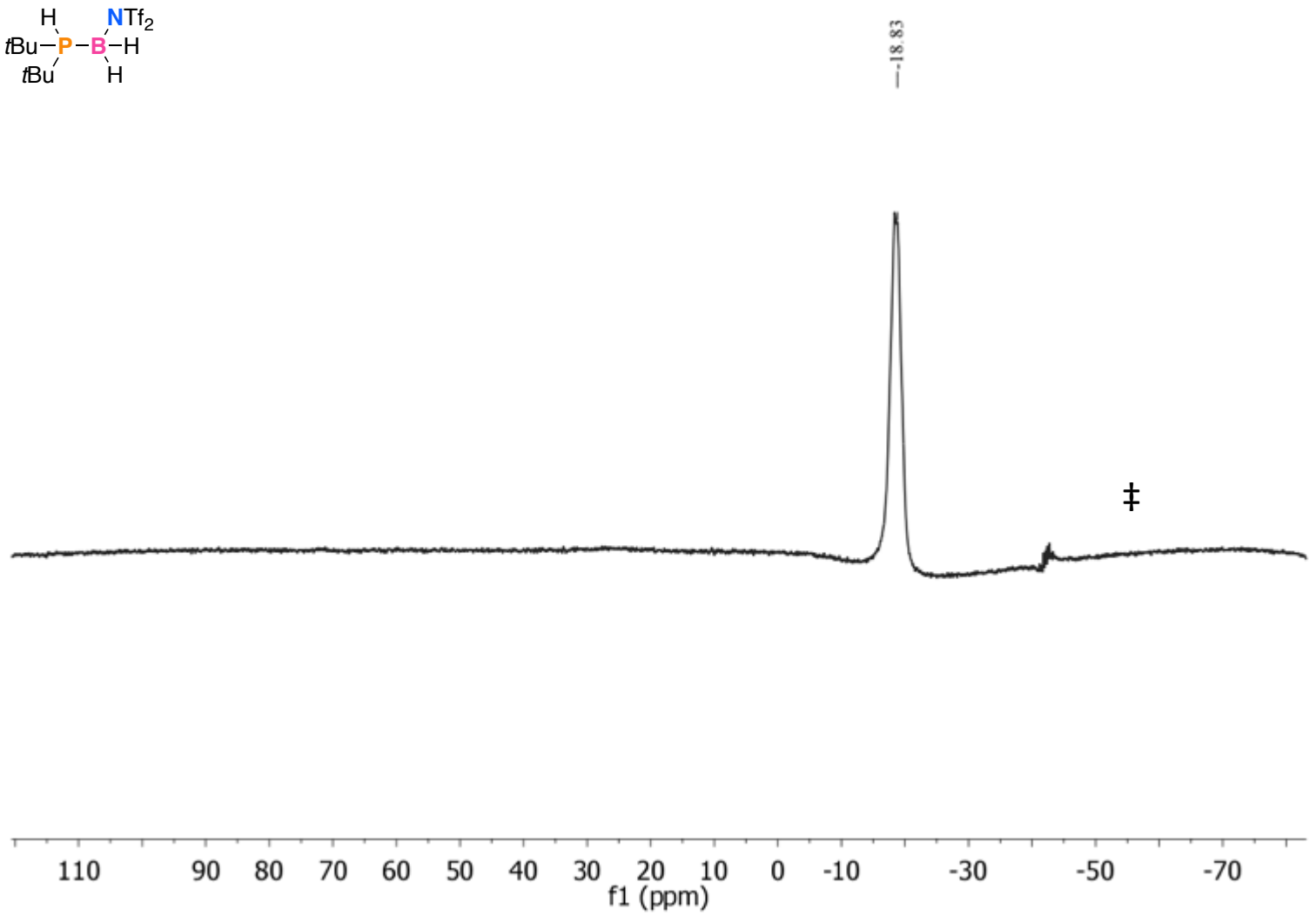


**Figure A.24**: $^{11}B$ NMR ($C_6D_6$, 160 MHz, 298 K) of **2.2d**. ‡ Residual unreacted phosphine-borane adduct, **2.1d.**

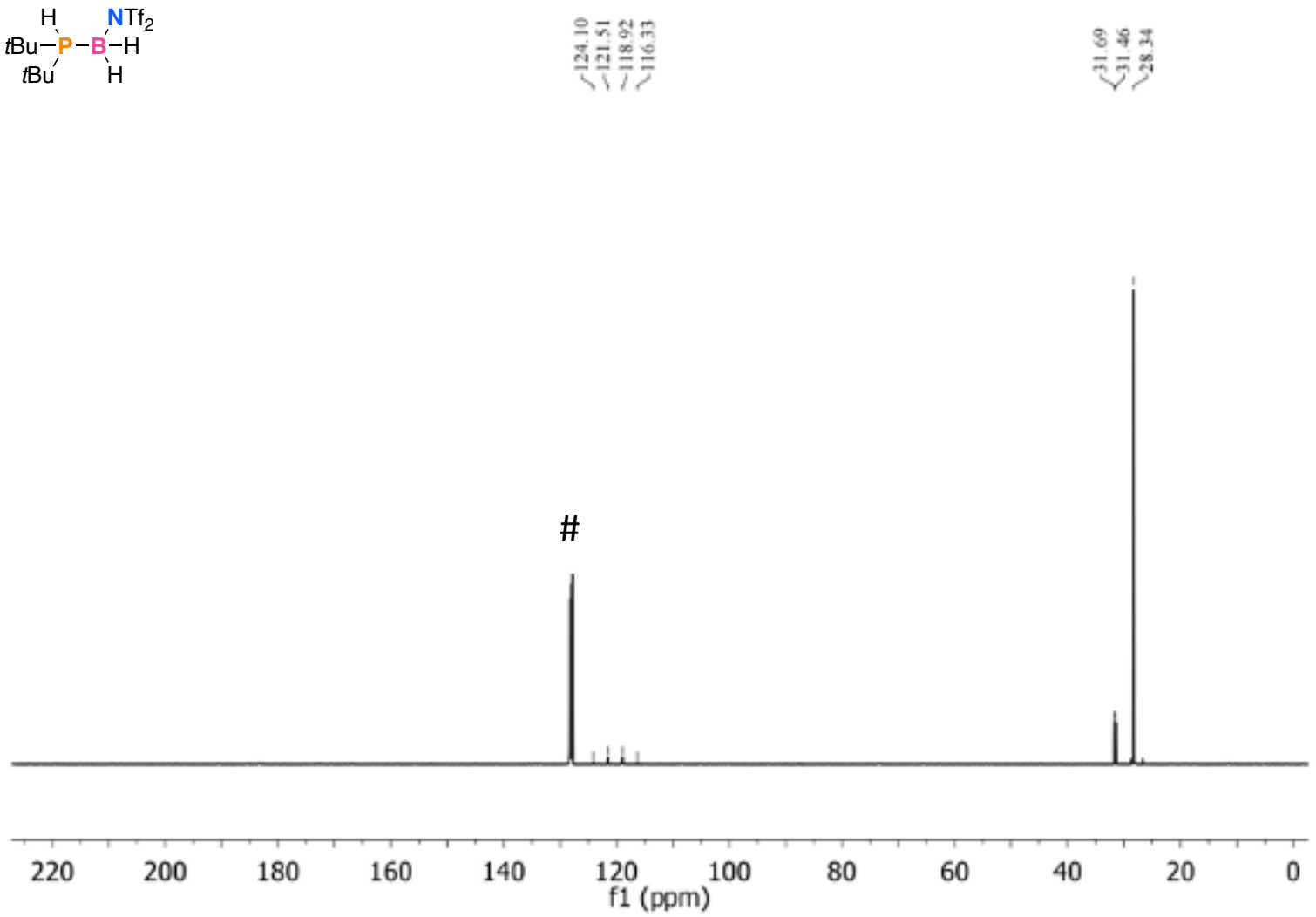


**Figure A.25:** $^{13}C$ NMR ($C_6D_6$, 126 MHz, 298 K) of **2.2d**. # Solvent peak for $C_6D_6$.

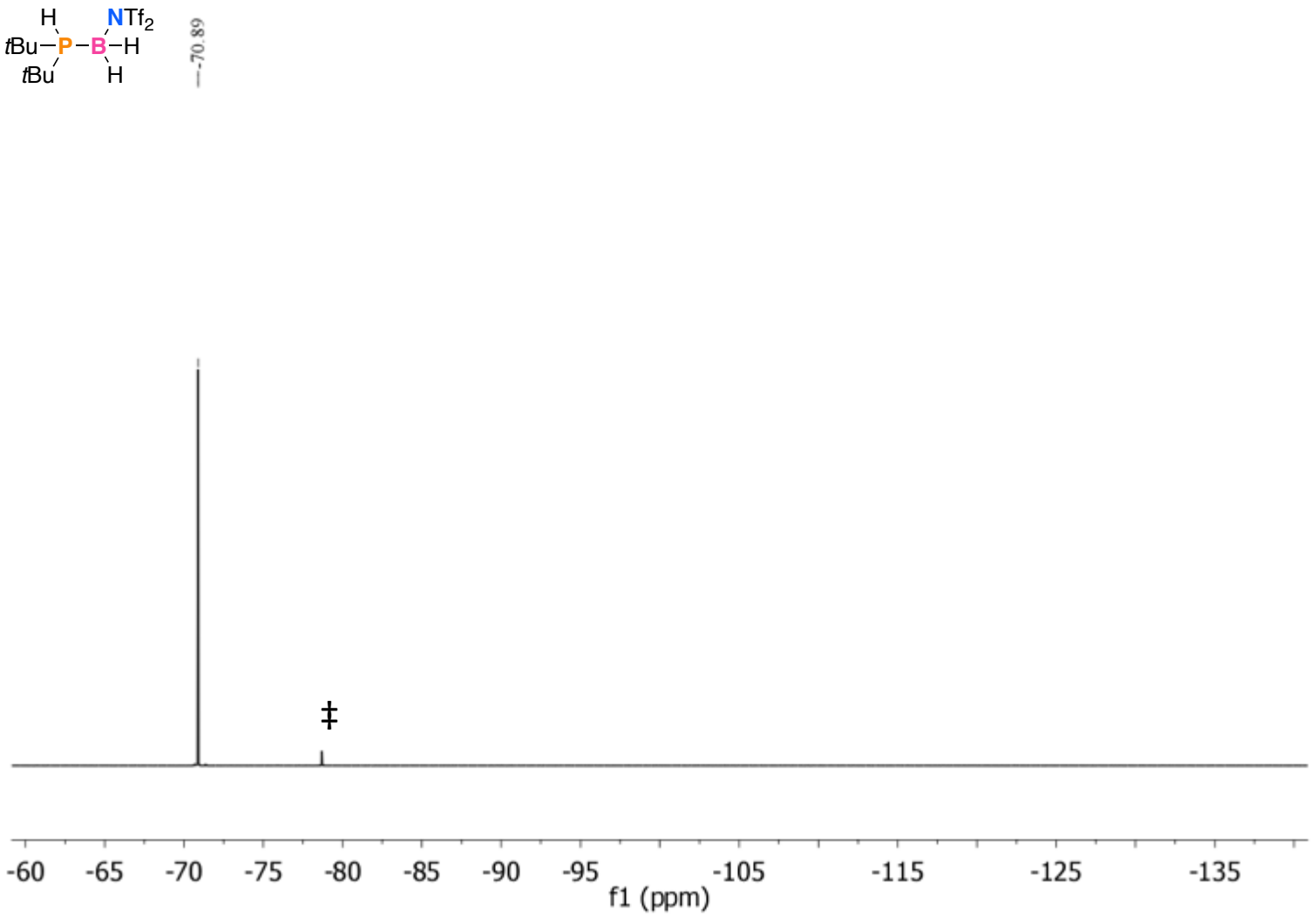


**Figure A.26**: $^{19}F$ NMR ($C_6D_6$, 471 MHz, 298 K) of **2.2d**. ‡ Uncharacterized residual impurity.

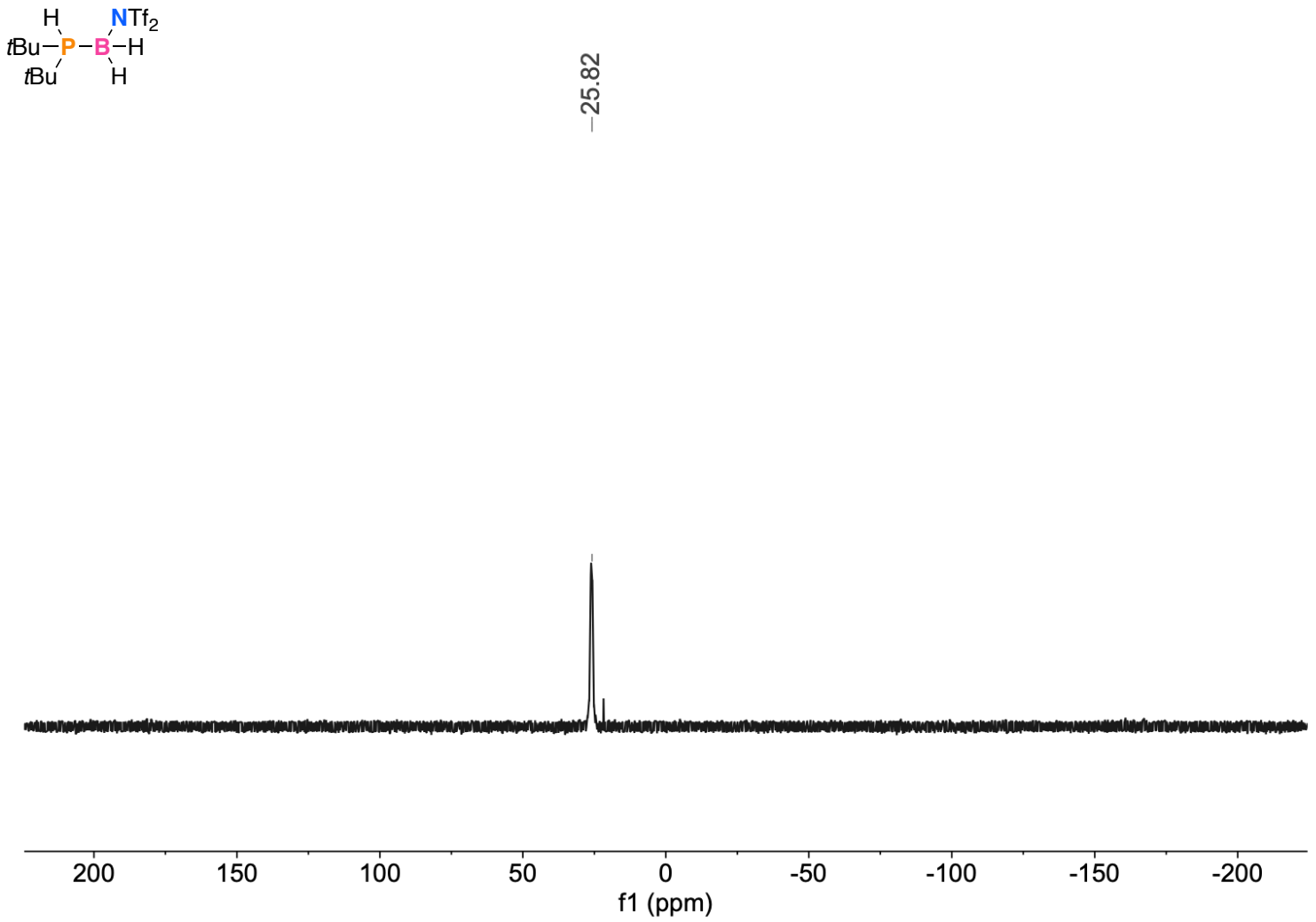


**Figure A.27**: $^{31}P\{^{1}H\}$ NMR ($C_6D_6$, 202 MHz, 298 K) of **2.2d.**

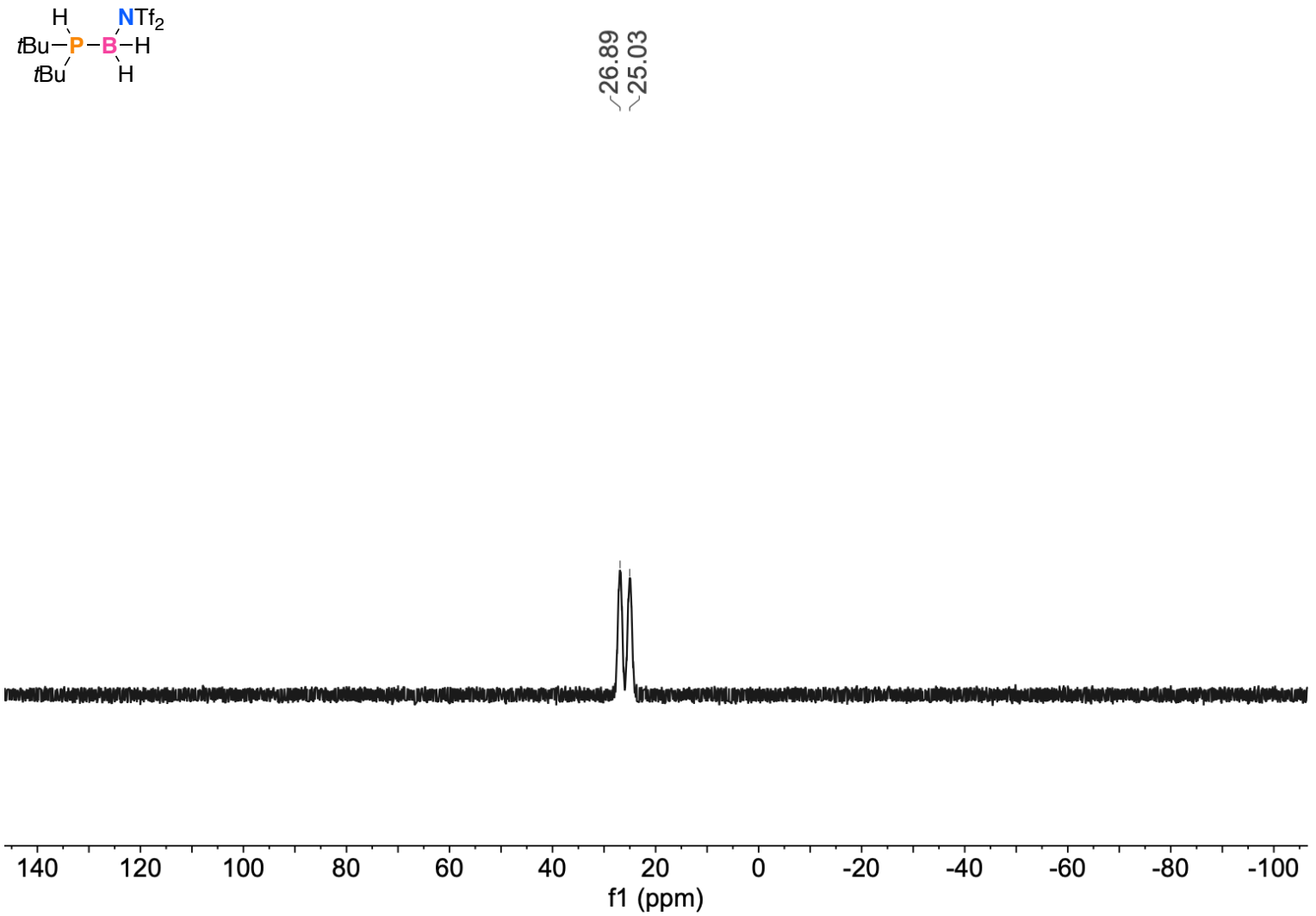


**Figure A.28**: $^{31}$P NMR ($C_6D_6$, 202 MHz, 298 K) of **2.2d.**

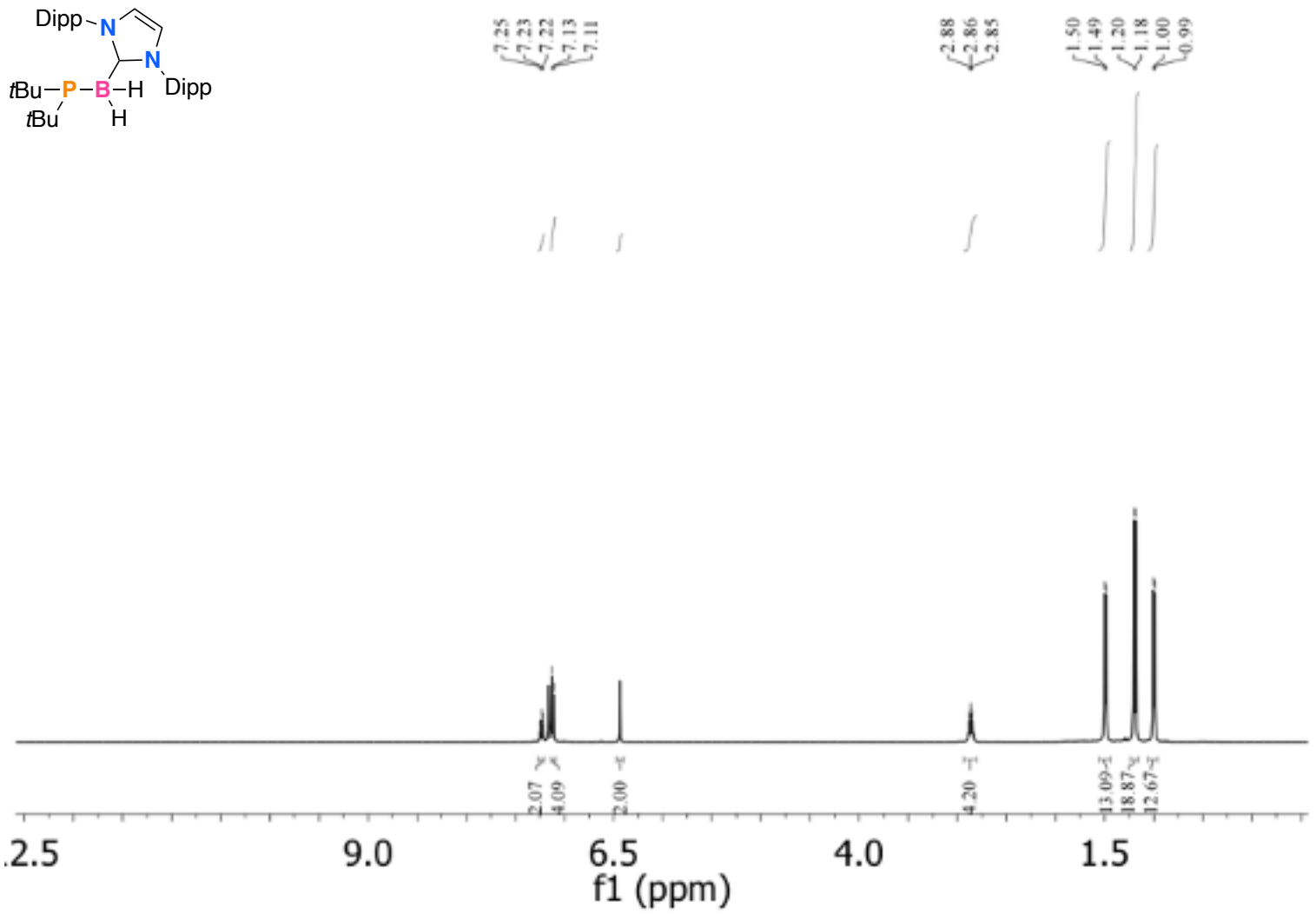


**Figure A.29**: $^{1}H$ NMR (500 MHz, $C_6D_6$, 298 K) of **2.5.**

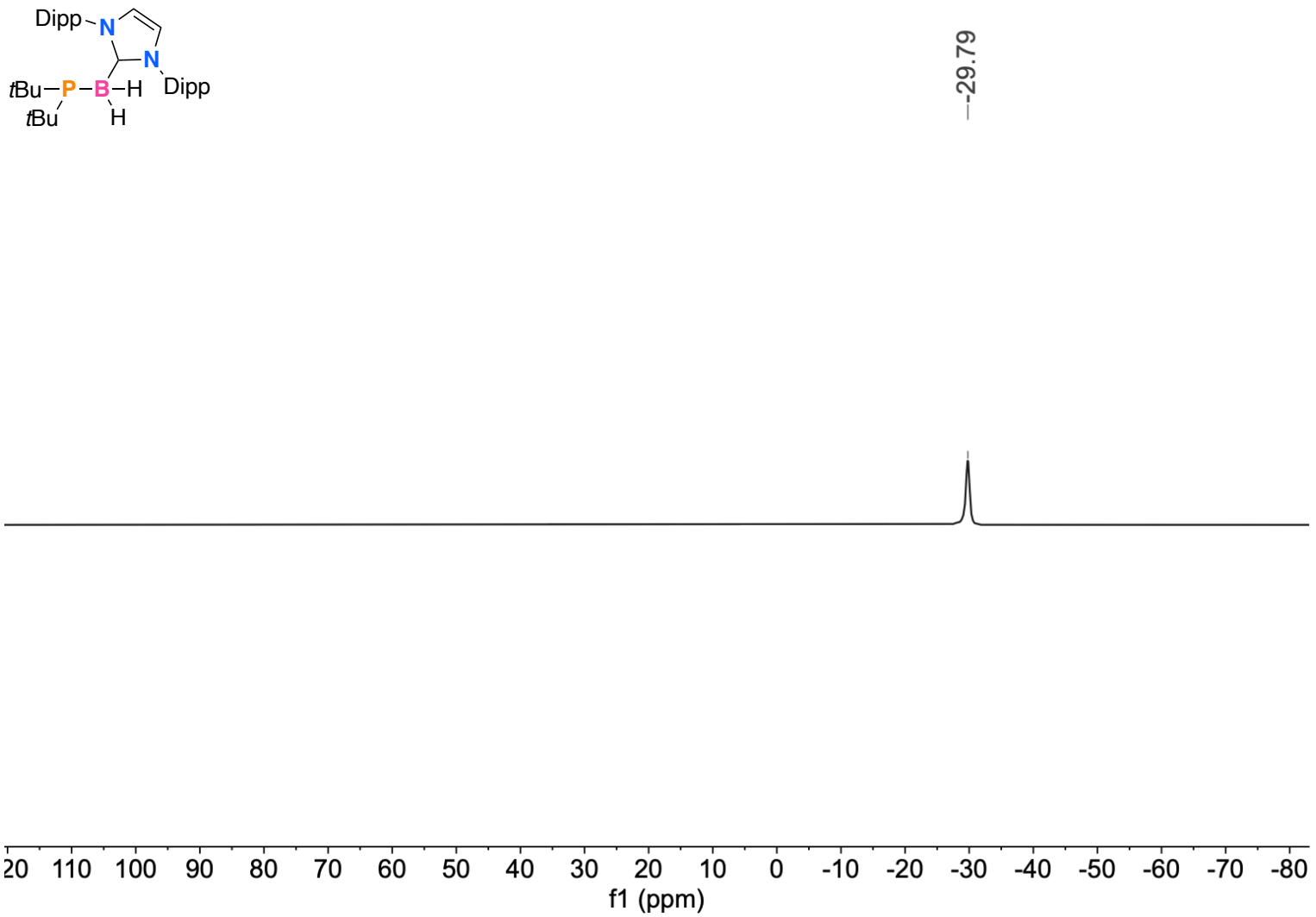


**Figure A.30**: $^{11}B\{^{1}H\}$ NMR (160 MHz, $C_6D_6$, 298 K) of **2.5.**

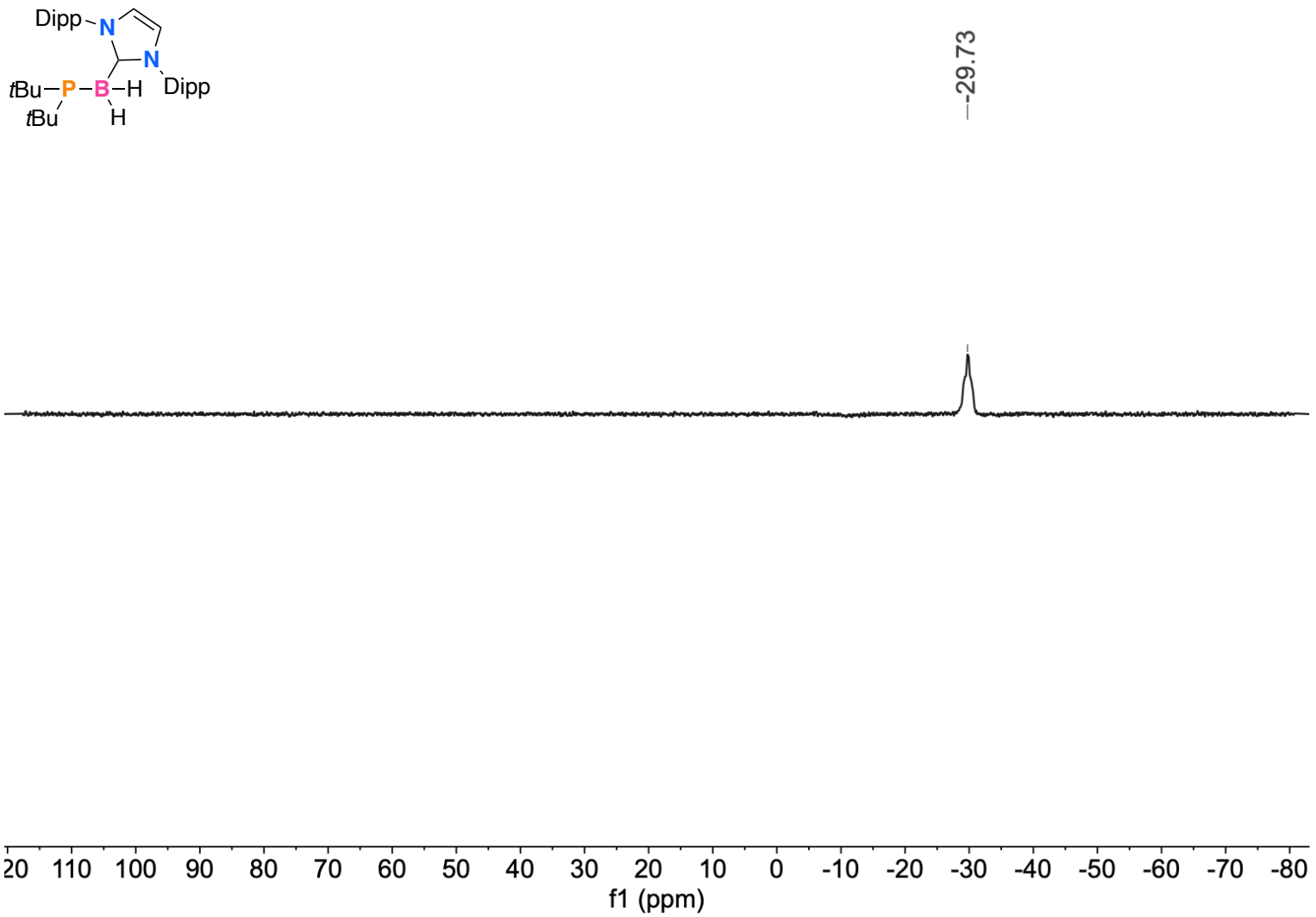


**Figure A.31**: $^{11}B$ NMR (160 MHz, $C_6D_6$, 298 K) of **2.5.**

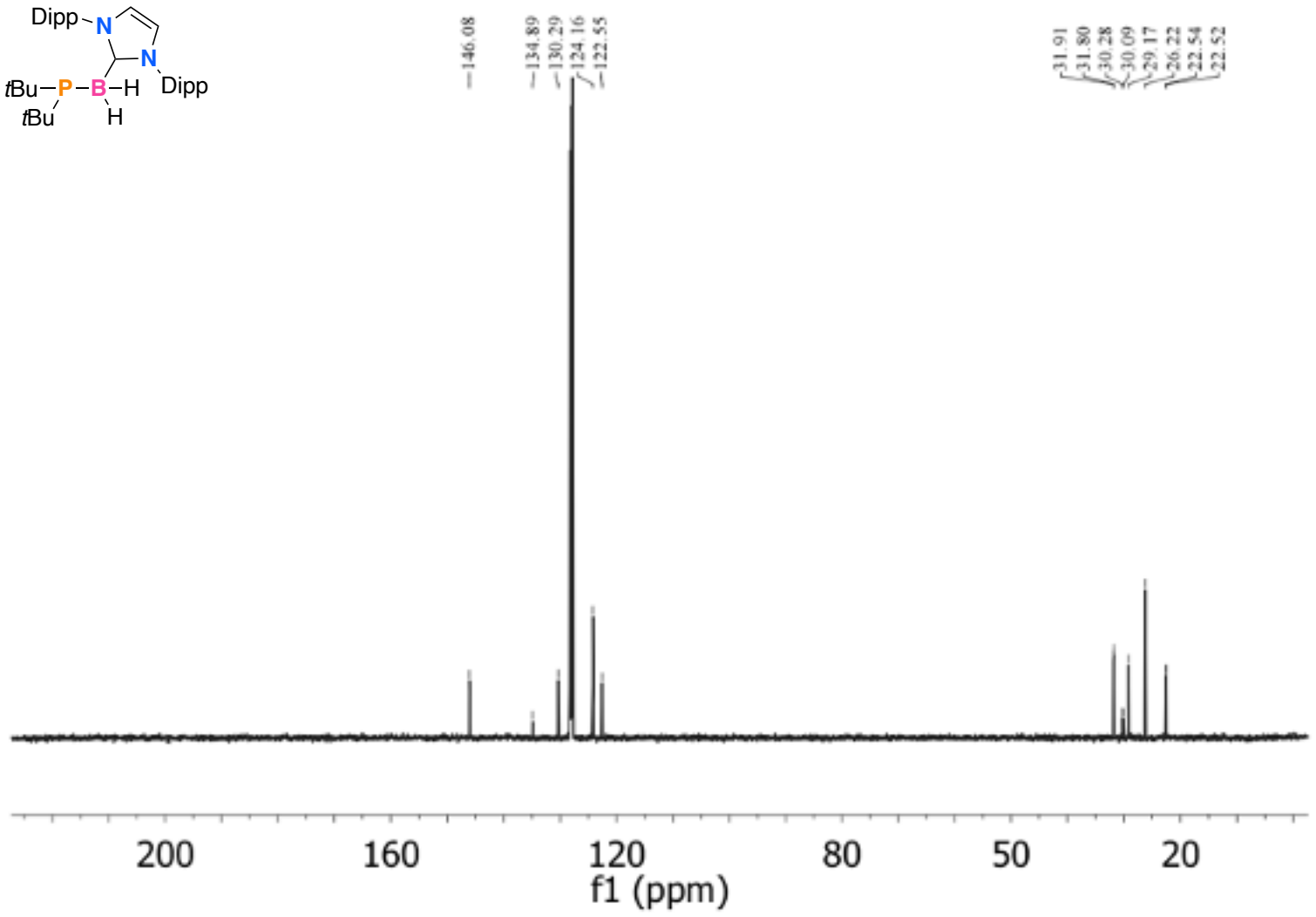


**Figure A.32:** $^{11}B$ NMR (160 MHz, $C_6D_6$, 298 K) of **2.5.**

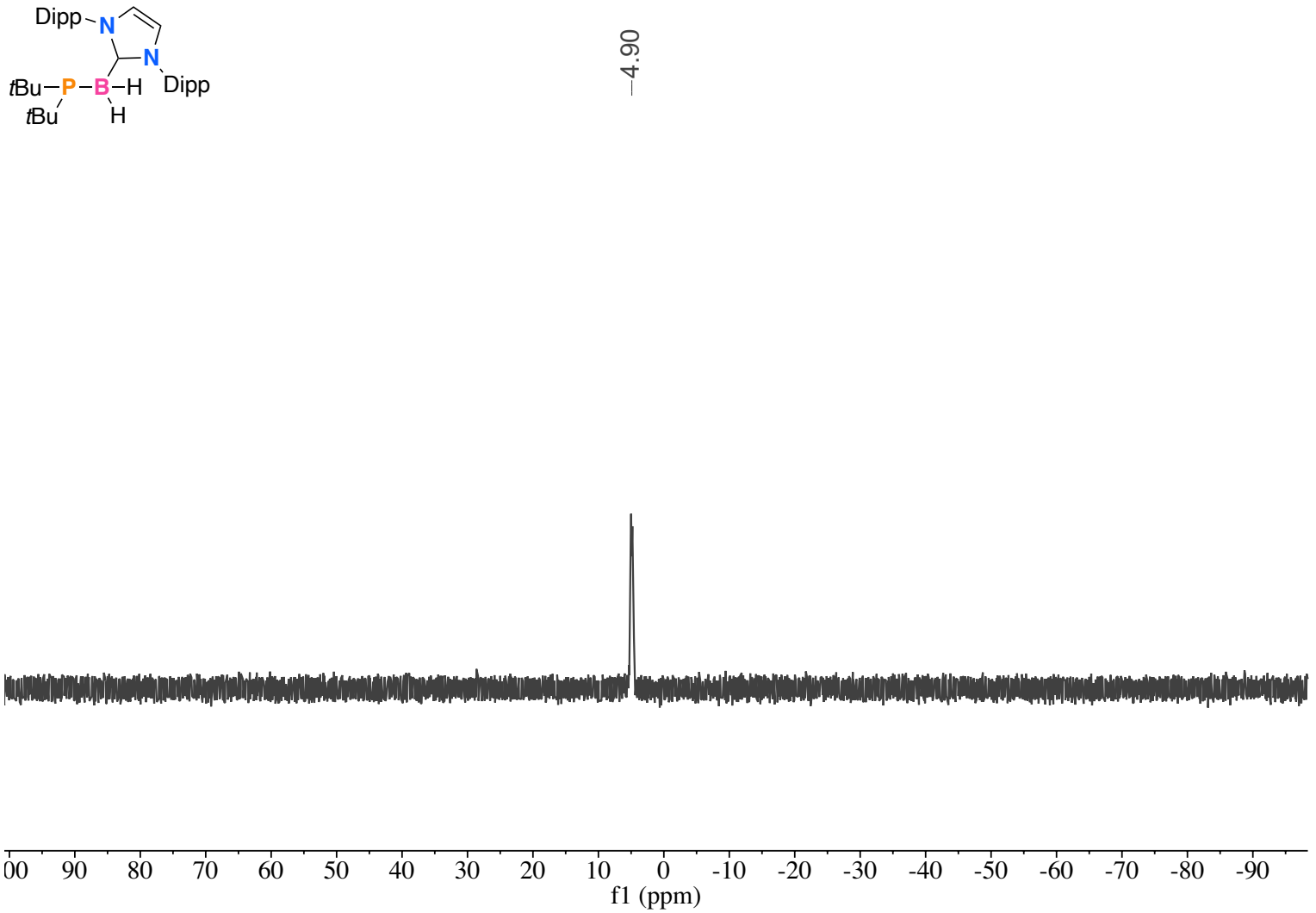


**Figure A.33:** $^{11}$B NMR (160 MHz, $C_6D_6$, 298 K) of **2.5.**

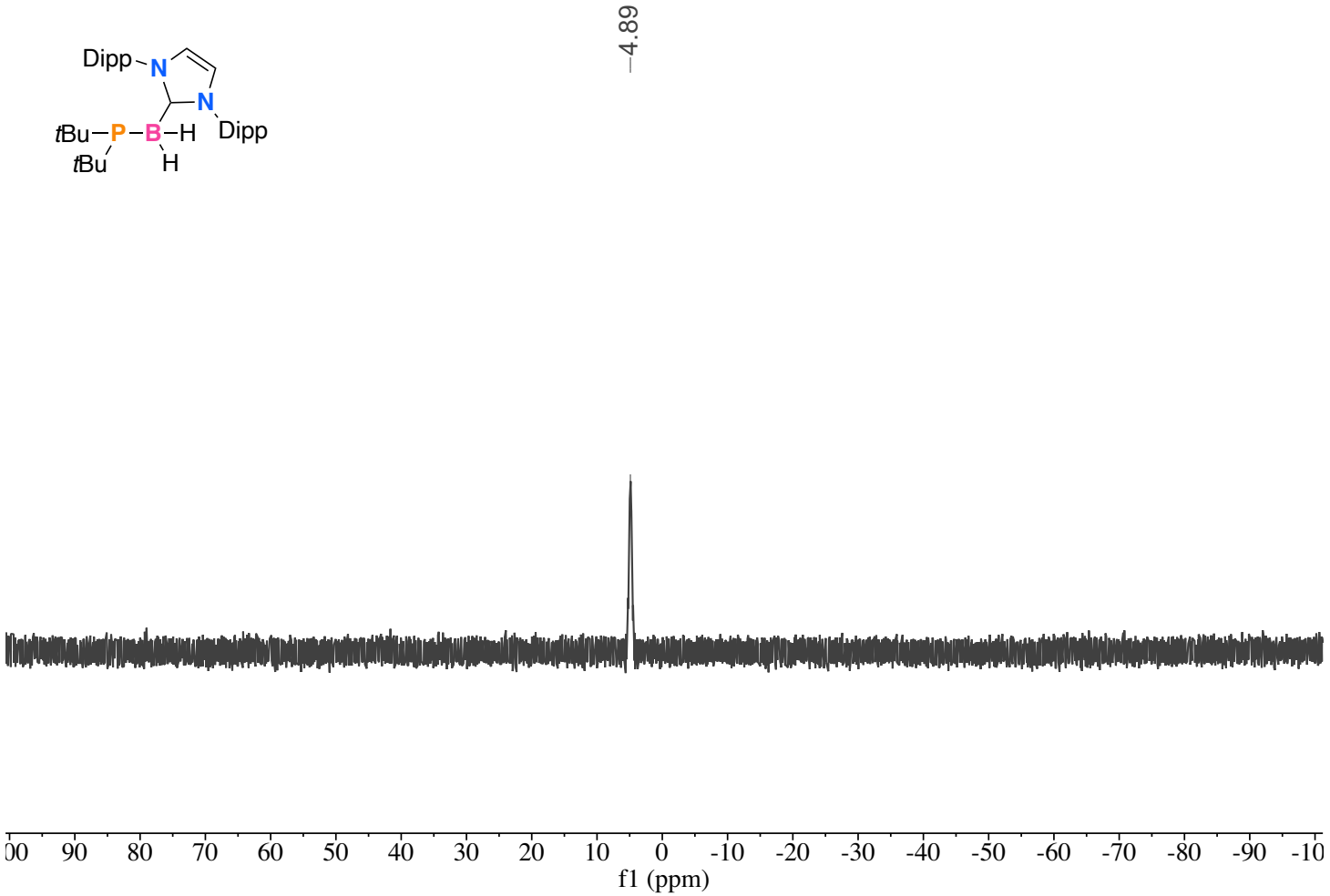


**Figure A.34:** $^{31}$P NMR (202 MHz, $C_6D_6$, 298 K) of **2.5.**

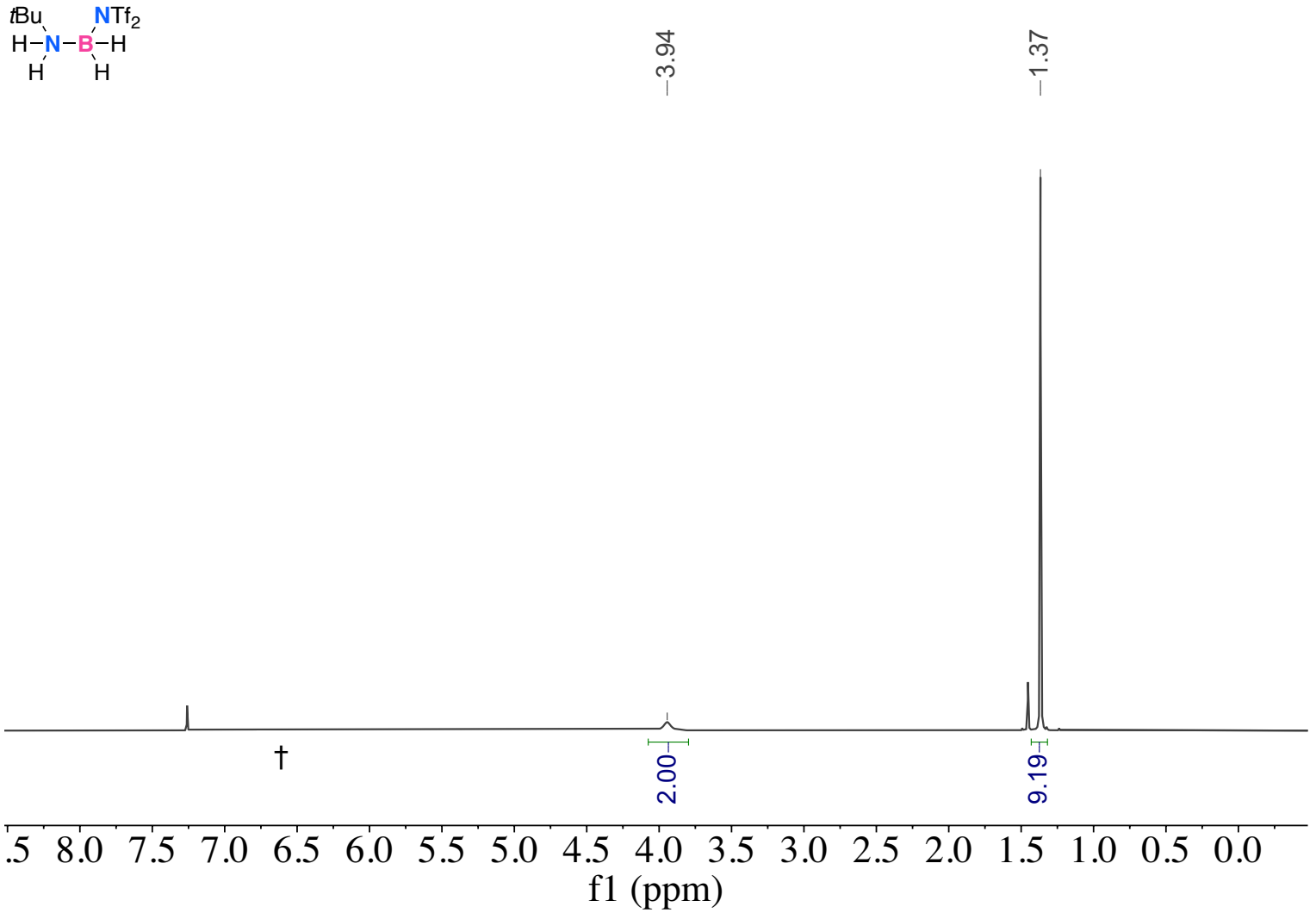


**Figure A.35:** $^{1}$H NMR ($CDCl_3$, 500 MHz, 298 K) spectrum of **3.2$_a$.** † Residual $CHCl_3$.

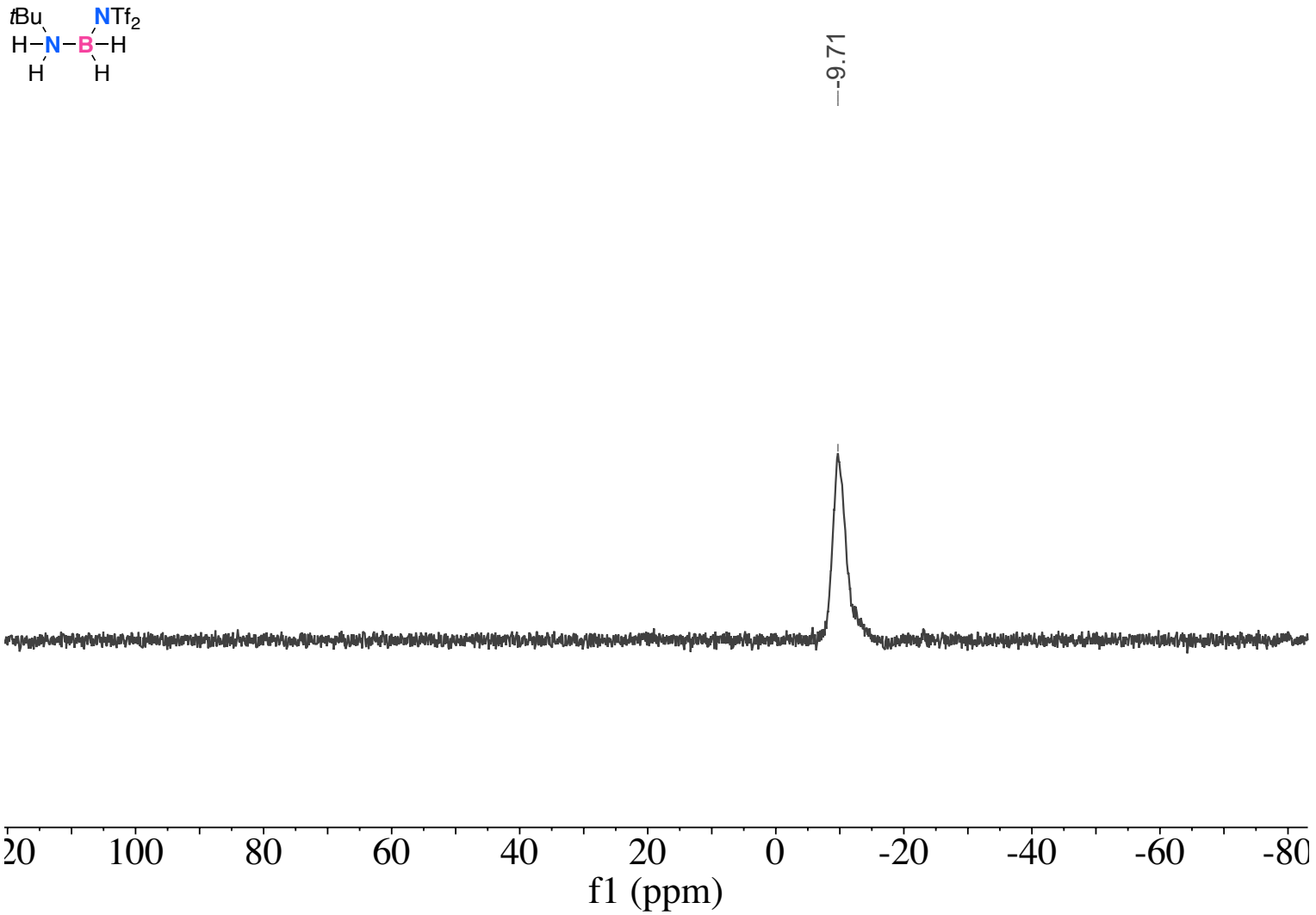


**Figure A.36:** $^{11}$B NMR spectrum ($CDCl_3$, 160 MHz, 298 K) of **3.2$_a$**.

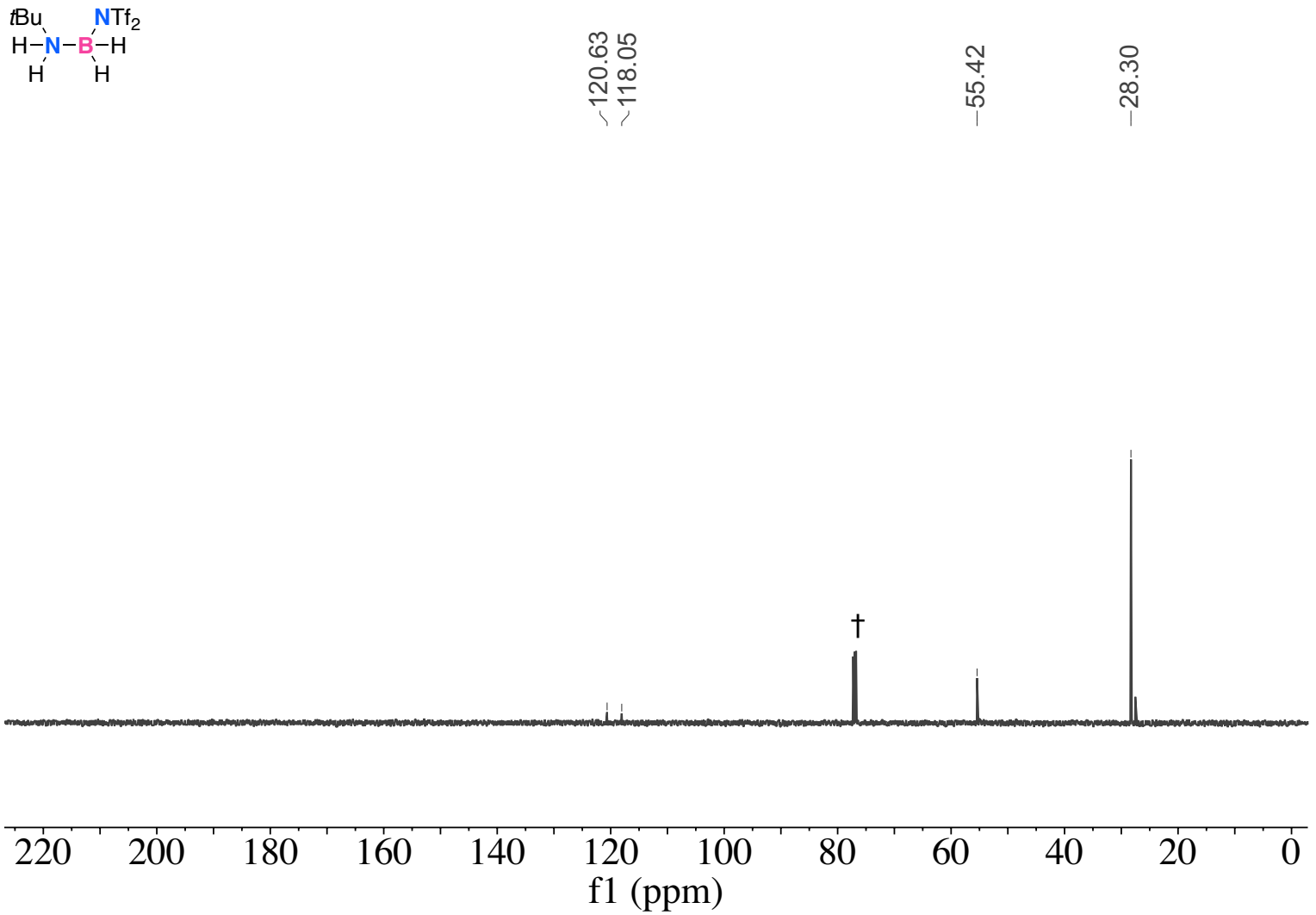


**Figure A.37:** $^{13}C\{^{1}H\}$ NMR spectrum ($CDCl_3$, 126 MHz, 298 K) of **3.2$_a$.** † $CDCl_3$ peak.

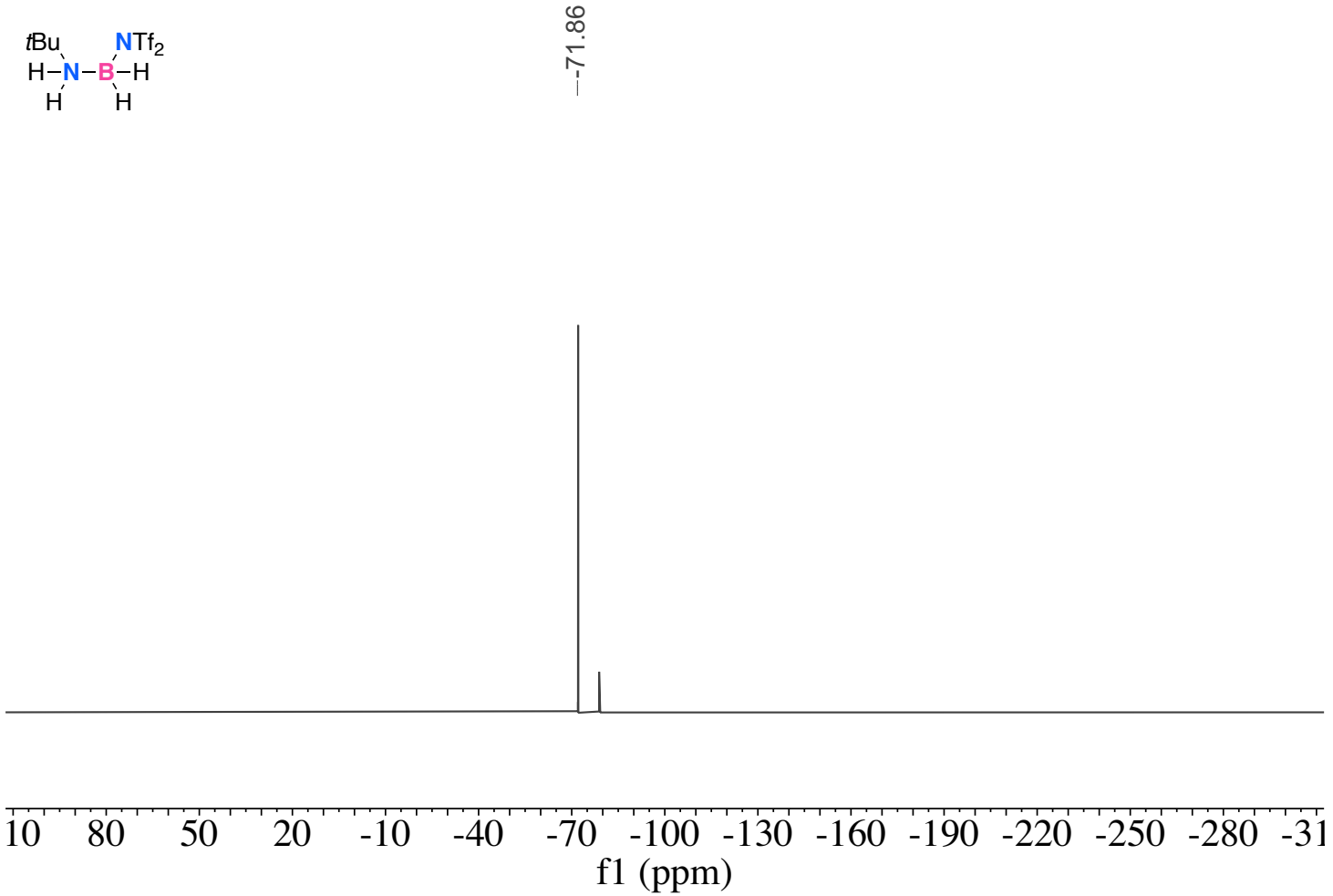


**Figure A.38:** $^{19}$**F** NMR spectrum ($CDCl_3$, 471 MHz, 298 K) of **3.2$_a$**. Unknown residual impurity.

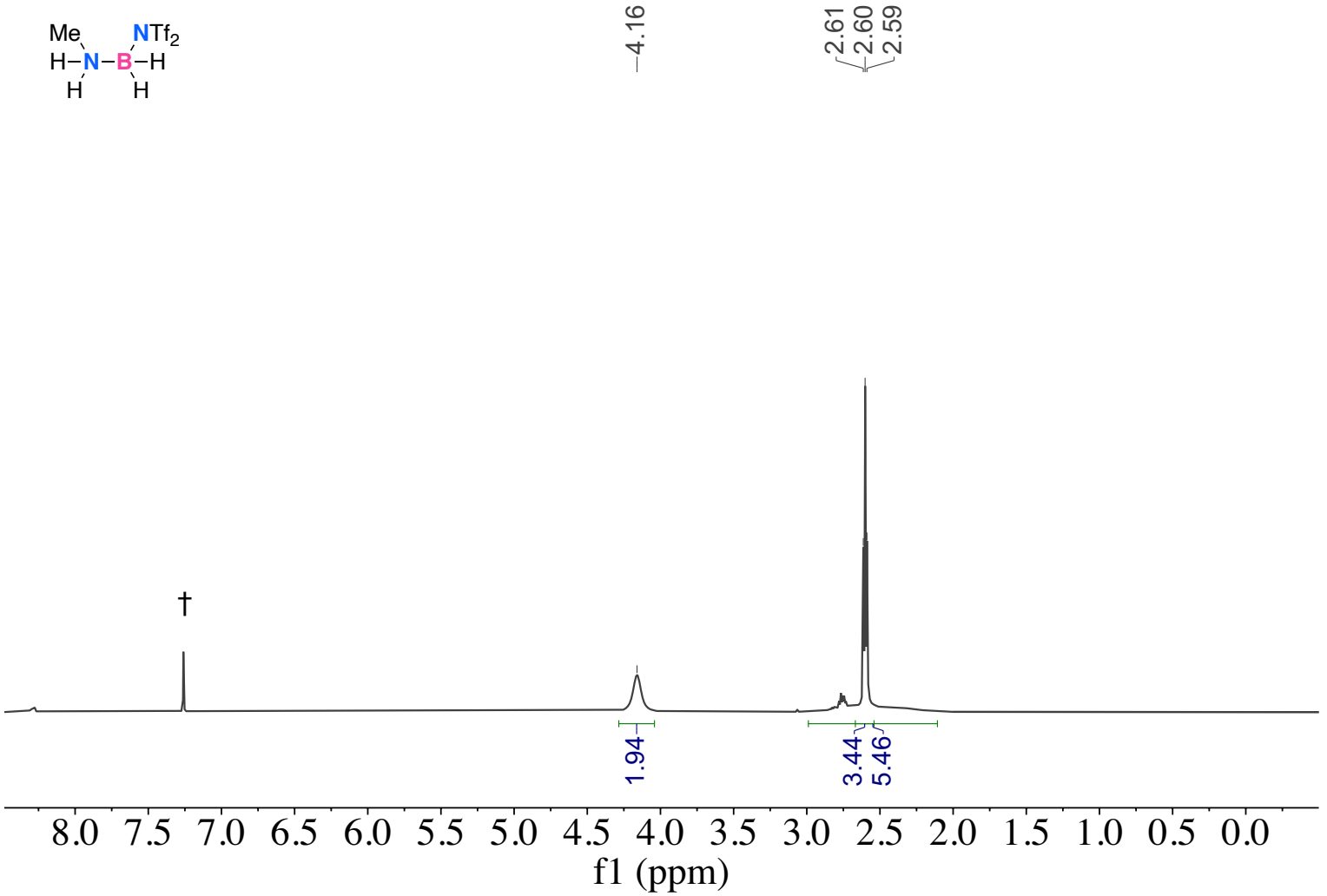


**Figure A.39:** $^{1}$H NMR spectrum ($CDCl_3$, 500 MHz, 298 K) of **3.2$_b$**. † Residual $CHCl_3$.

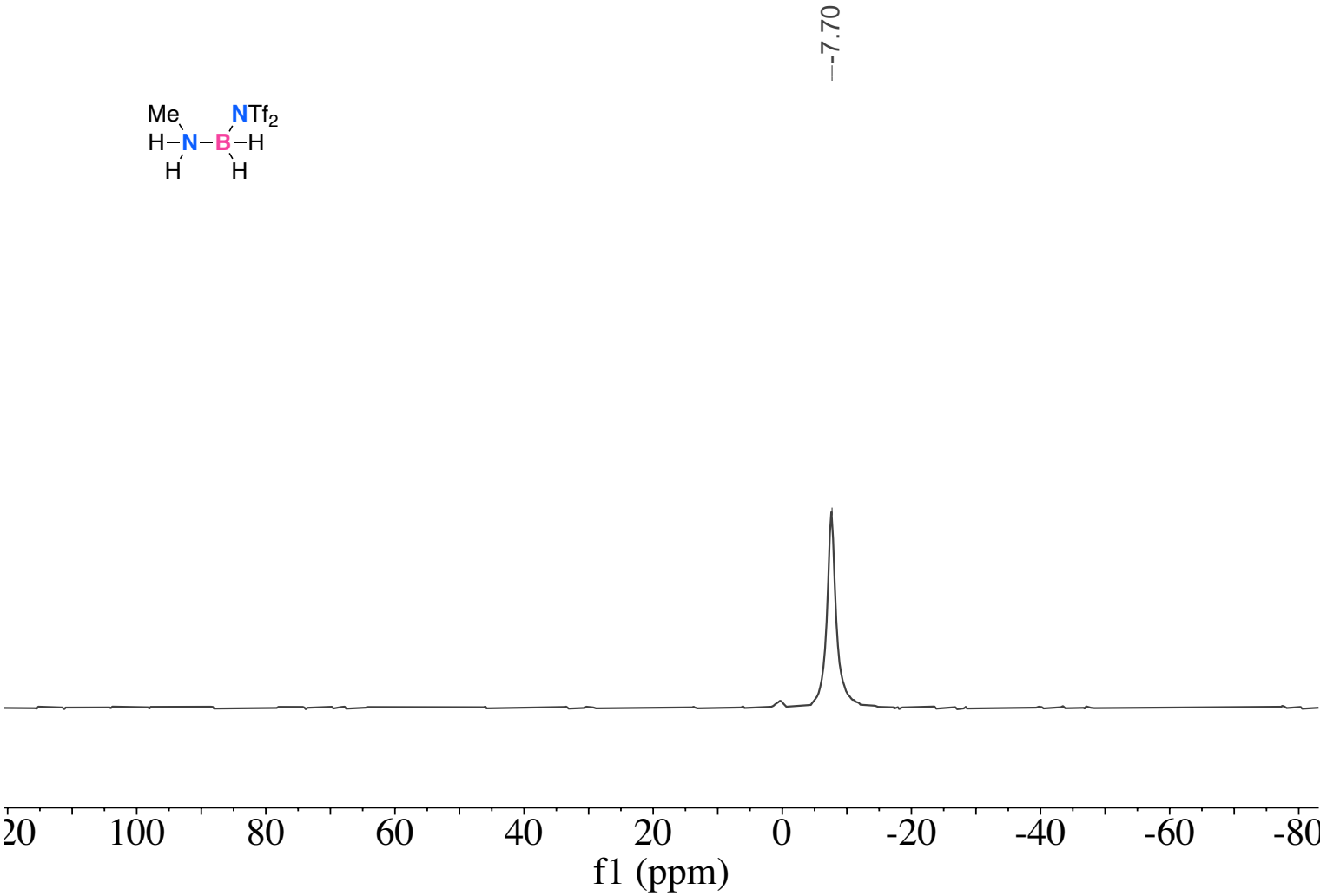


**Figure A.40:** $^{11}B$ NMR spectrum ($CDCl_3$, 160 MHz, 298 K) of **3.2$_b$**.

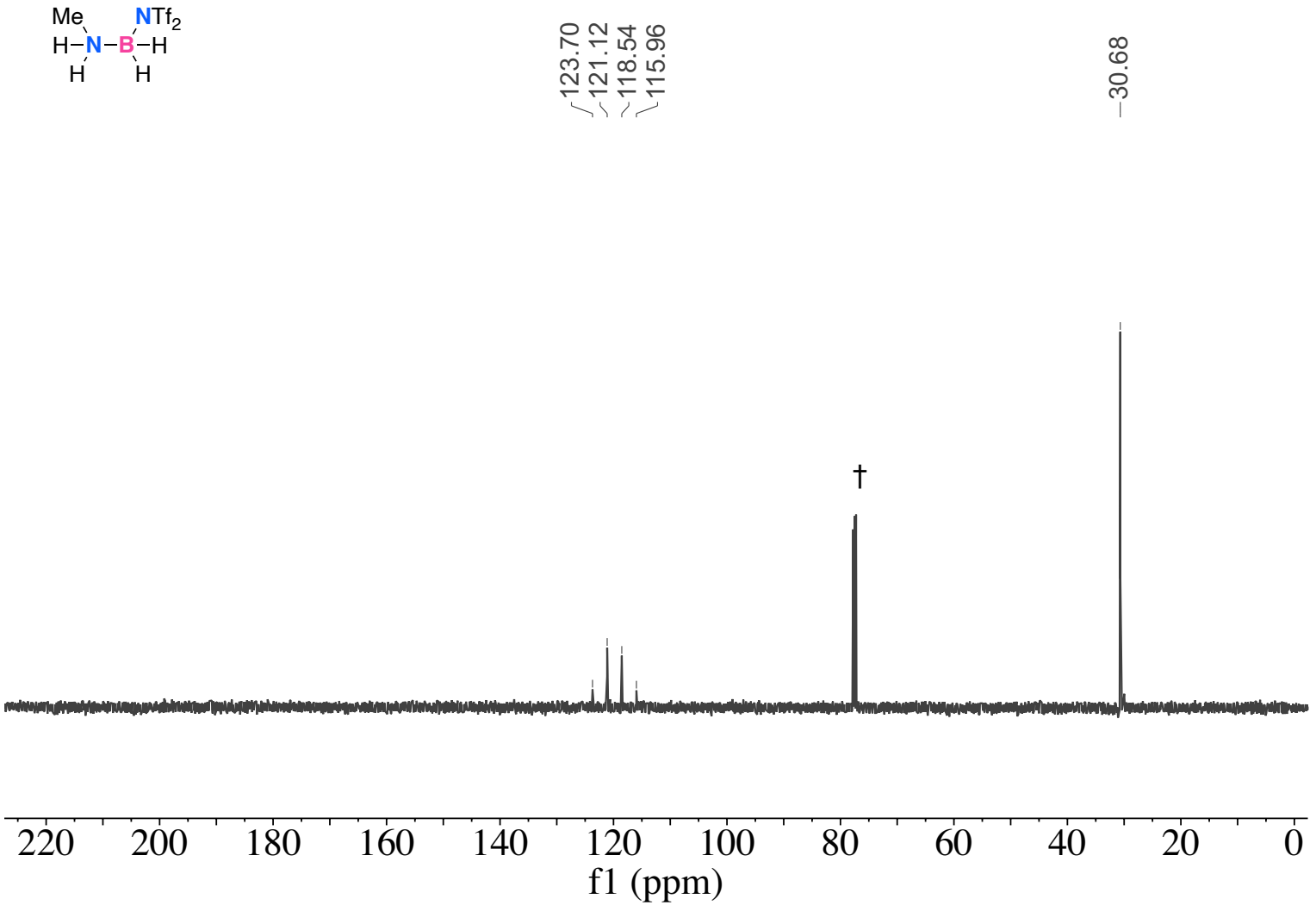


**Figure A.41:** $^{13}C$ NMR spectrum ($CDCl_3$, 126 MHz, 298 K) of **3.2$_b$**. † $CDCl_3$ peak.

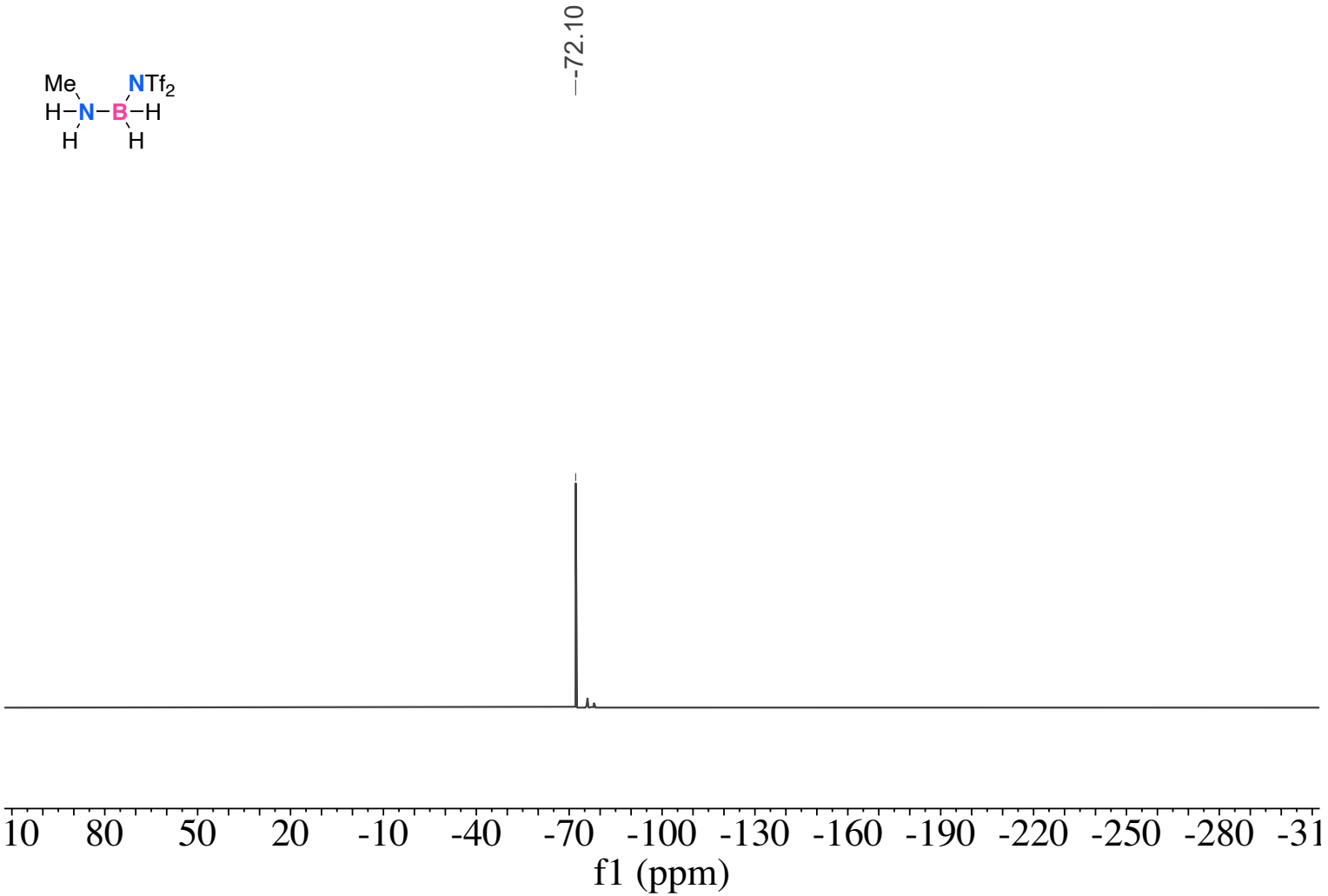


**Figure A.42: :** $^{19}F$ NMR spectrum ($CDCl_3$, 471 MHz, 298 K) of **$3.2_b$.**

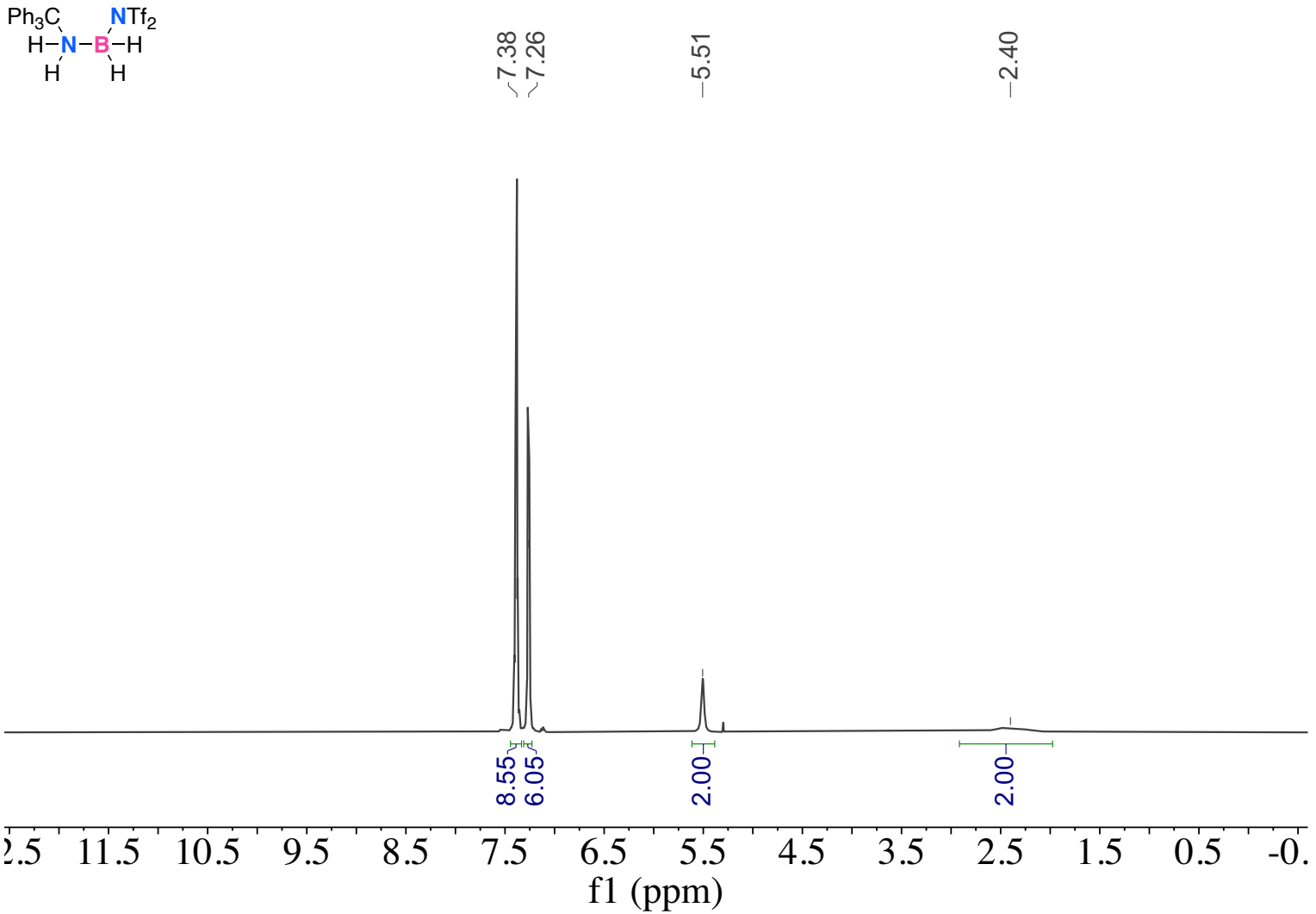


**Figure A.43:** $^{1}$H NMR spectrum ($CDCl_3$, 500 MHz, 298 K) of **3.2$_c$**. Residual $CHCl_3$ peak obscured by **3.2$_c$**.

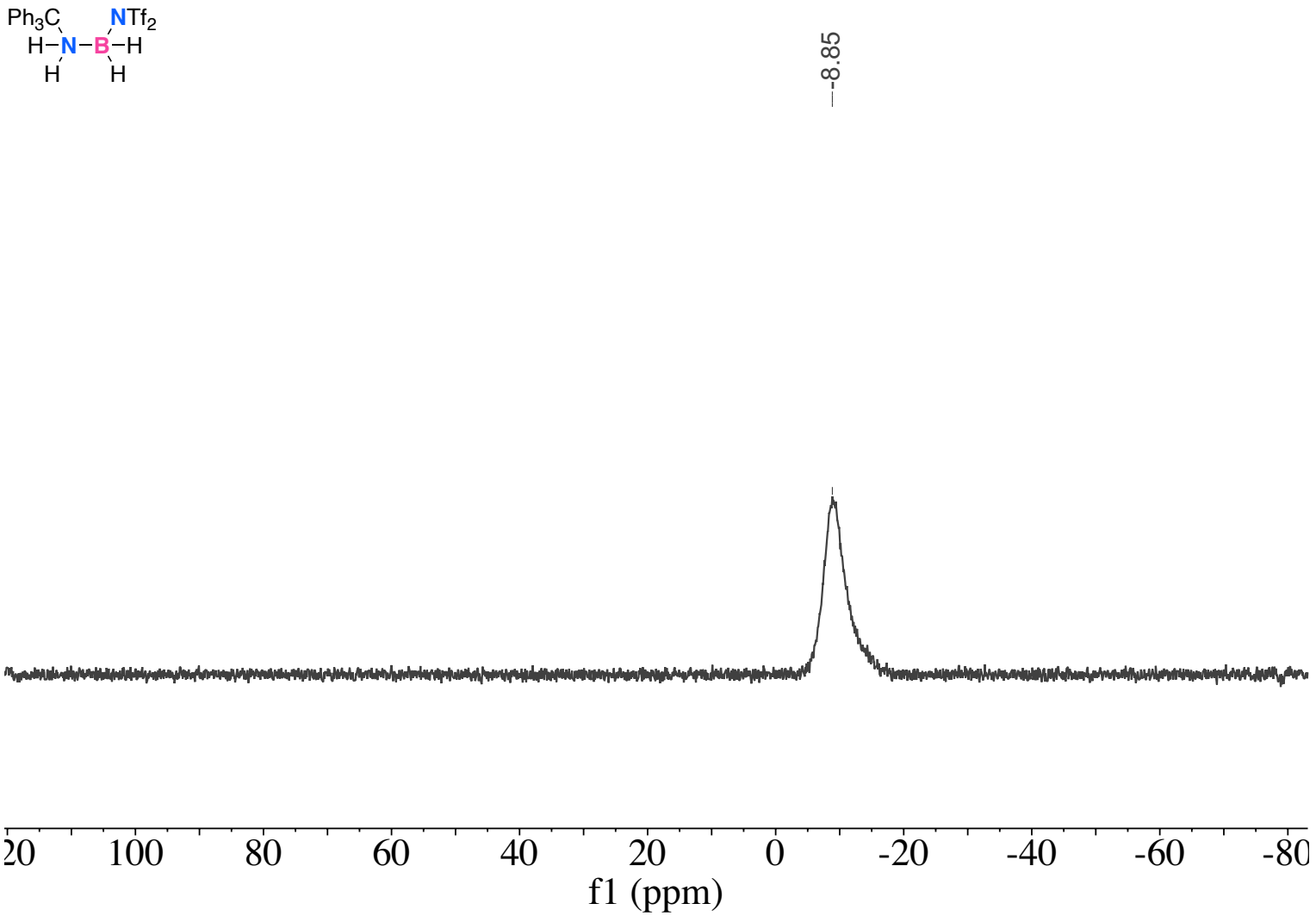


**Figure A.44:** $^{11}$B NMR spectrum ($CDCl_3$, 160 MHz, 298 K) of **3.2$_c$.**

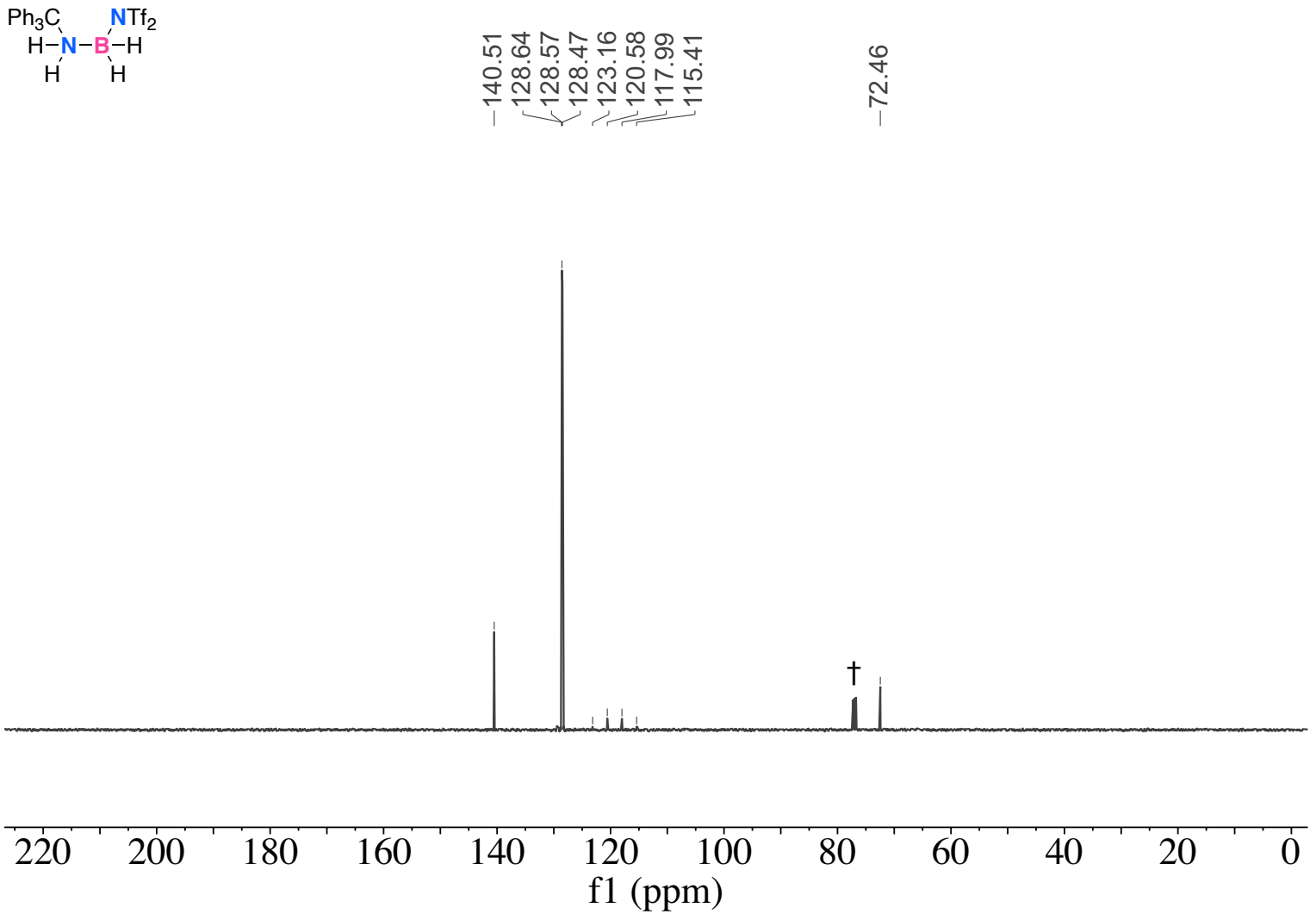


**Figure A.45:** $^{13}C$ NMR spectrum ($CDCl_3$, 126 MHz, 298 K) of **3.2c**. † $CDCl_3$ peak.

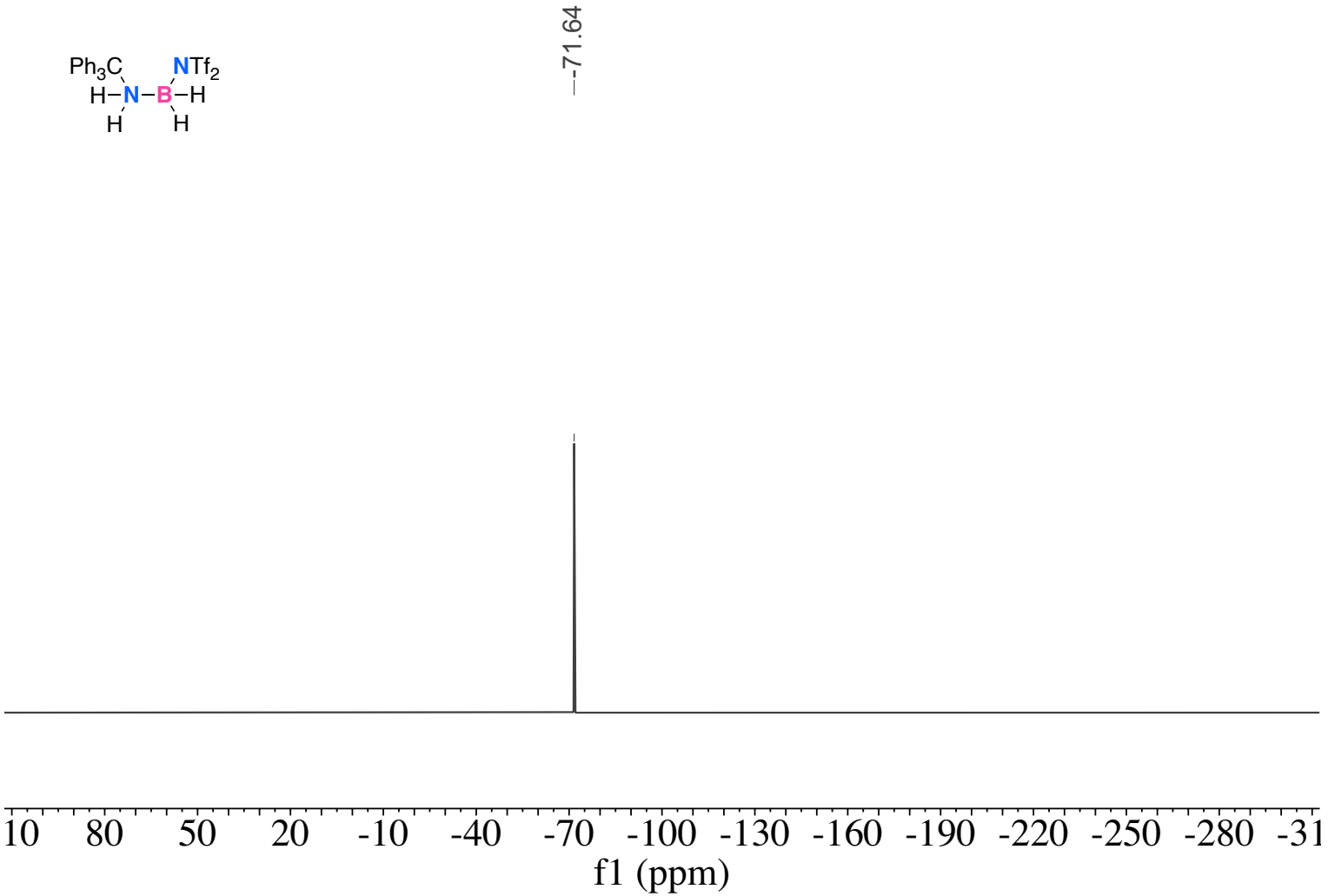


**Figure A.46: :** $^{19}F$ NMR spectrum ($CDCl_3$, 471 MHz, 298 K) of **3.2c**.

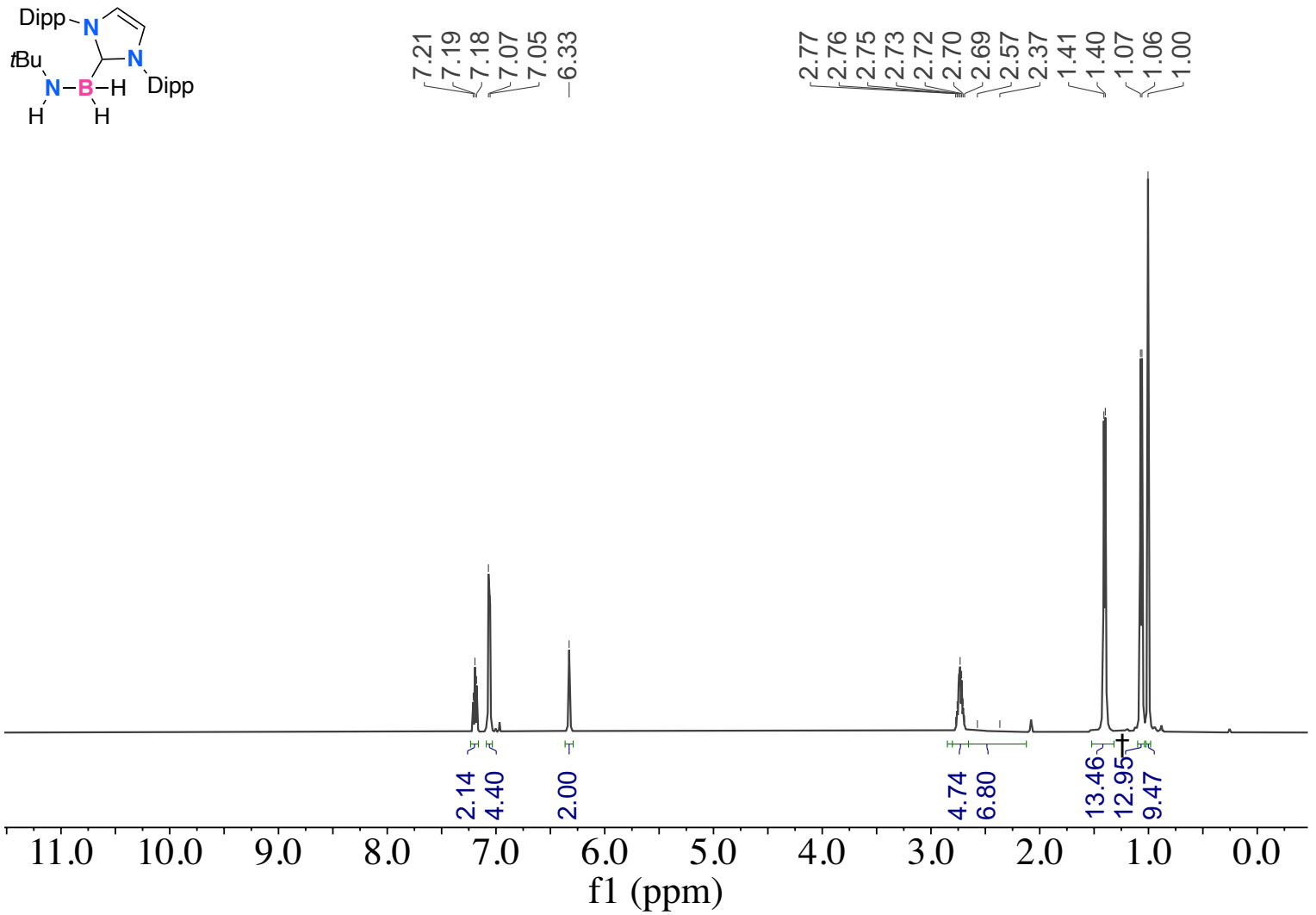


**Figure A.47:** $^{1}$H NMR spectrum (Toluene-d8, 500 MHz, 298 K) of **3.4**. † Residual proteo-toluene solvent.

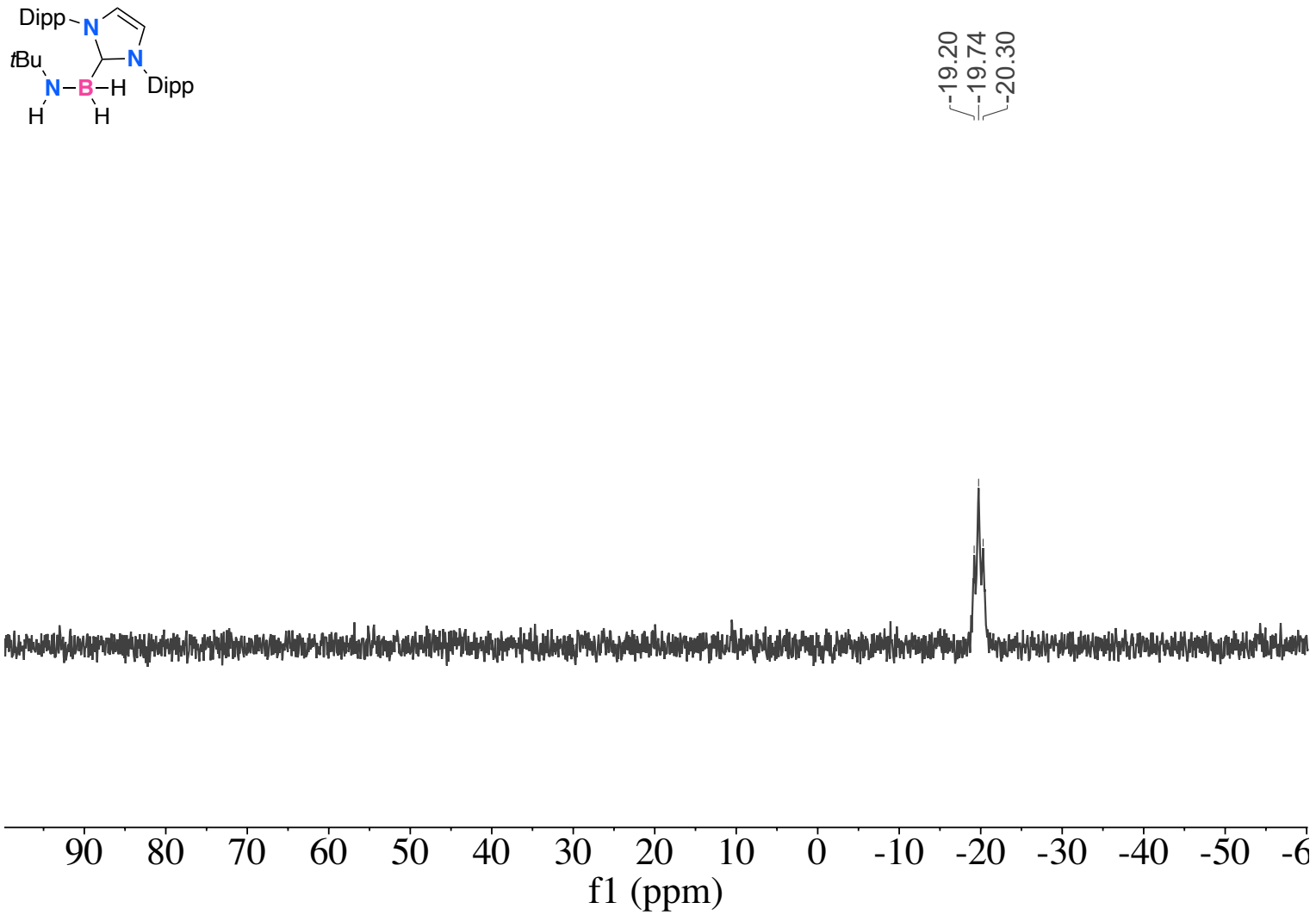


**Figure A.48:** $^{11}$B NMR spectrum (Toluene-d8, 160 MHz, 298 K) of **3.4.**

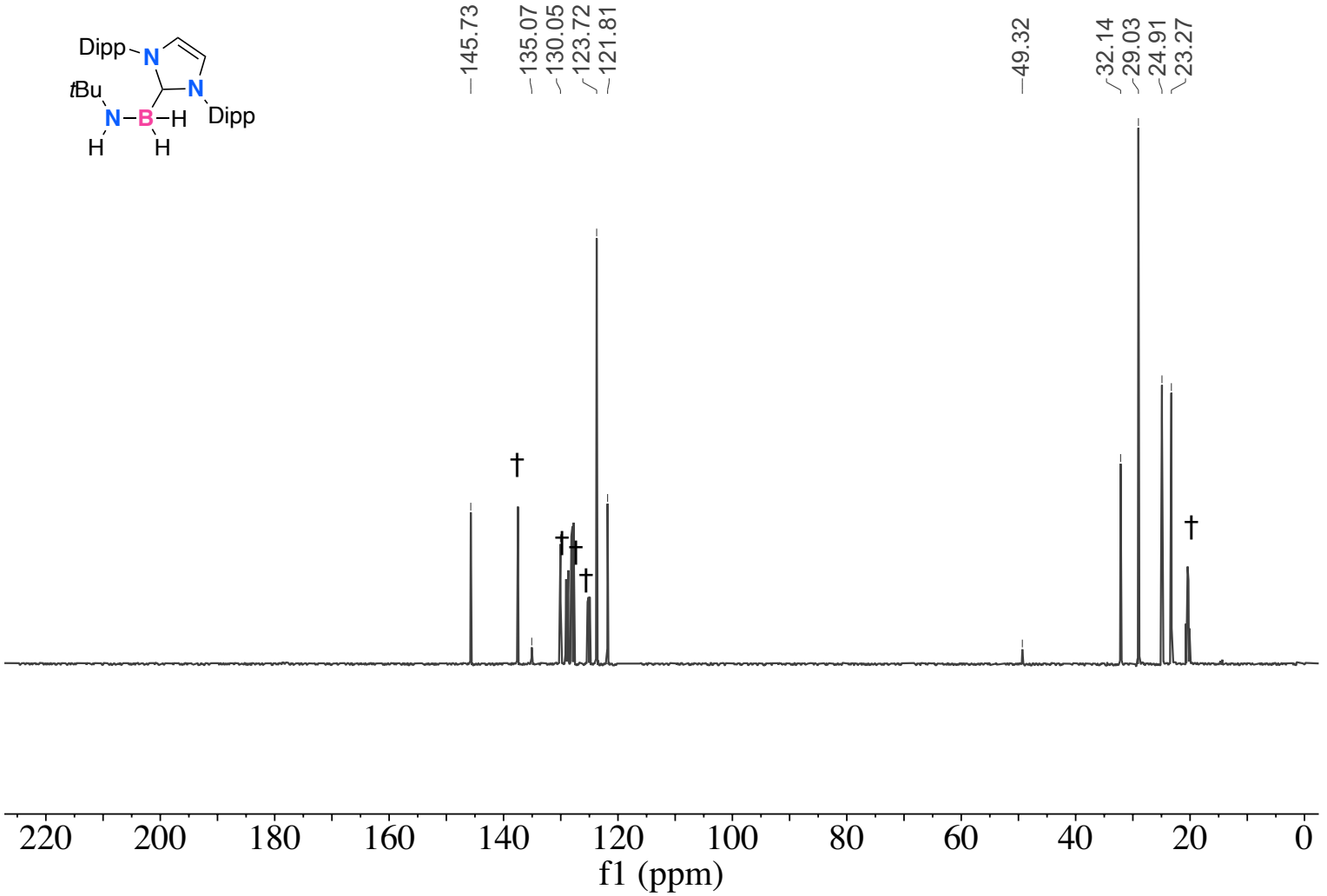


**Figure A.49:** $^{13}C\{^{1}H\}$ UDEFT NMR spectrum ($CDCl_3$, 126 MHz, 298 K) of **3.4**. † Toluene-d8 peaks.

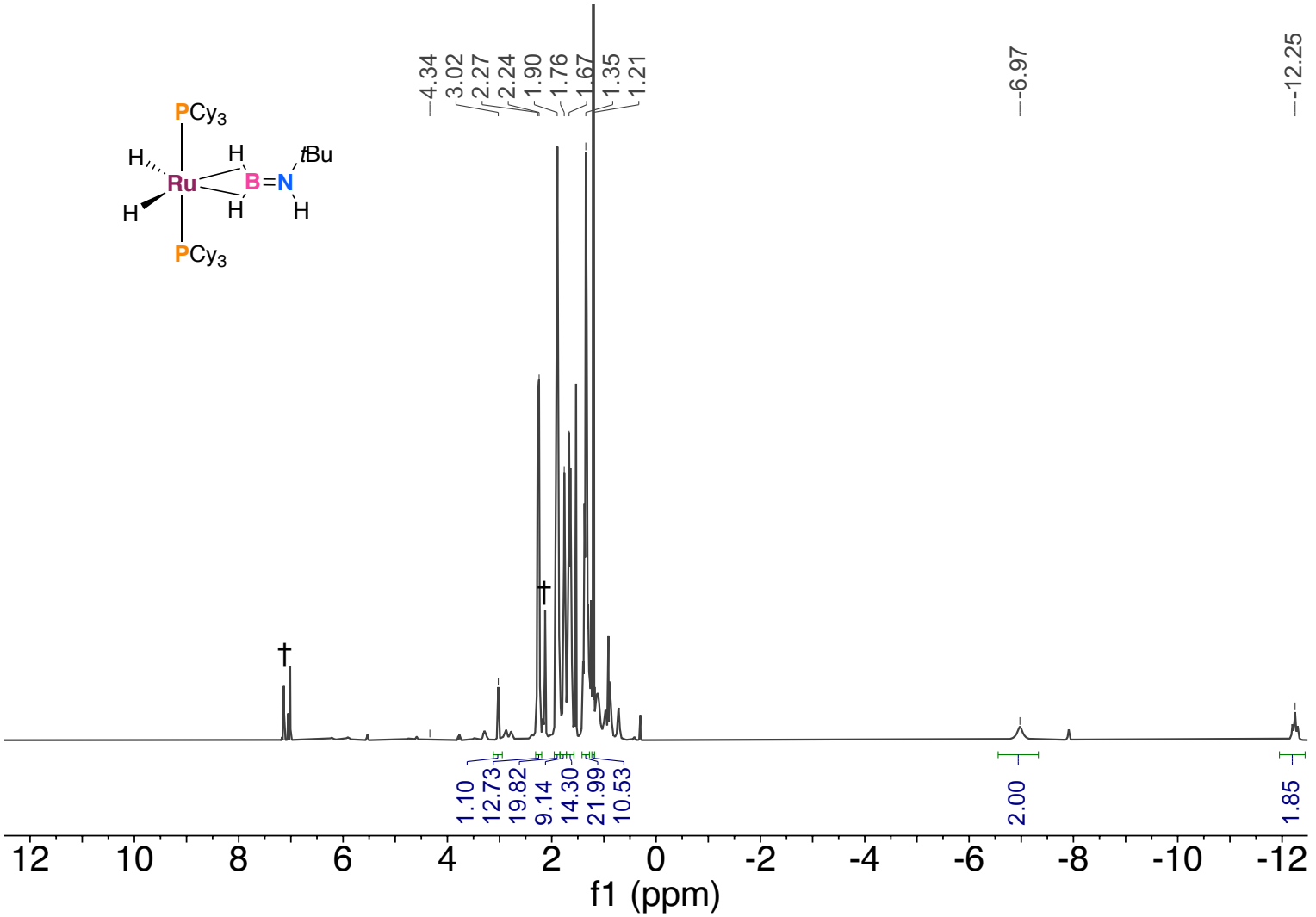


**Figure A.50:** $^{1}$H NMR spectrum (Toluene-d8, 500 MHz, 298 K) of **3.5**. † Residual proteo-toluene solvent.

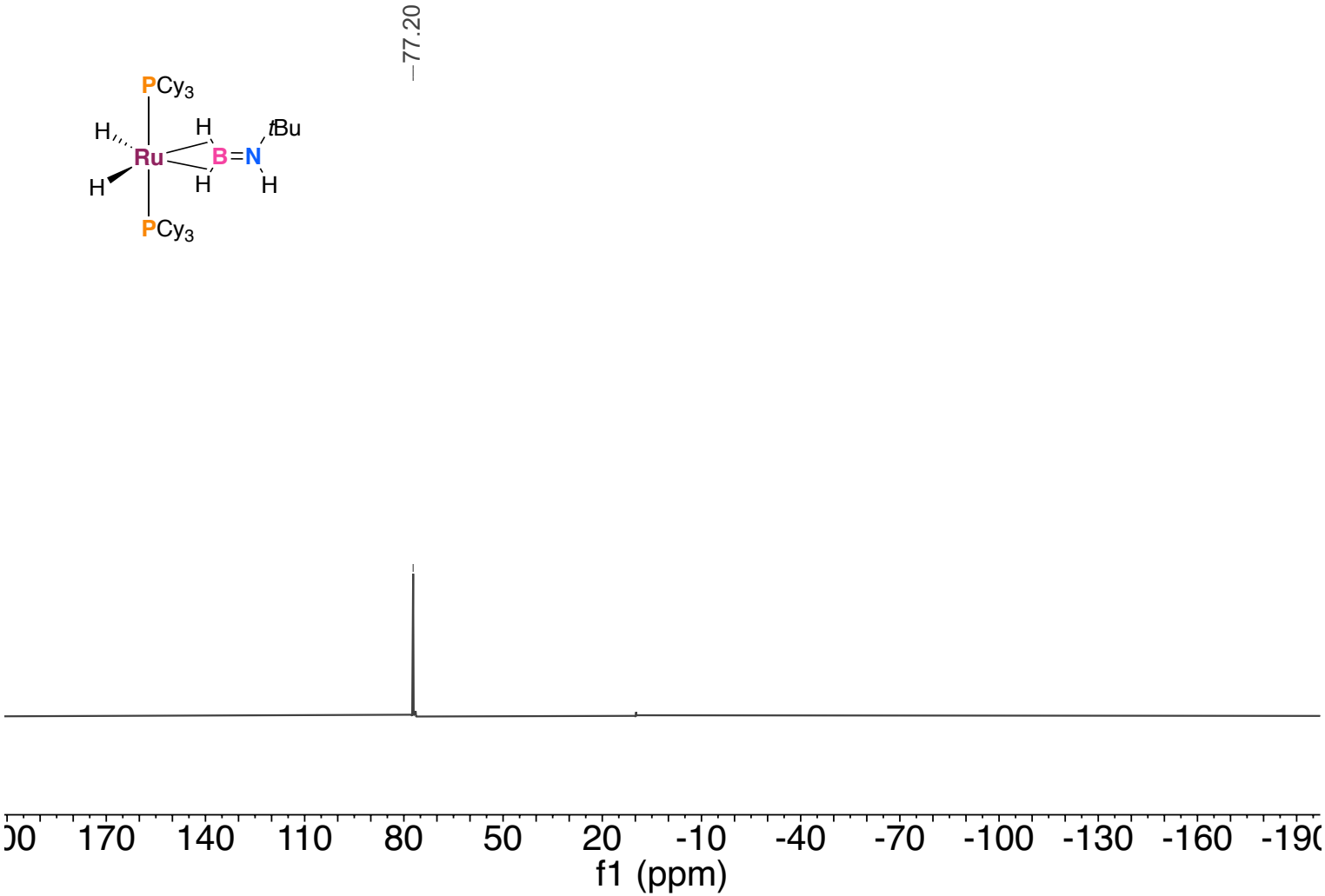


**Figure A.51:** $^{31}P\{^{1}H\}$ NMR (toluene-$d_8$, 202 MHz, 298 K) of **3.5.**

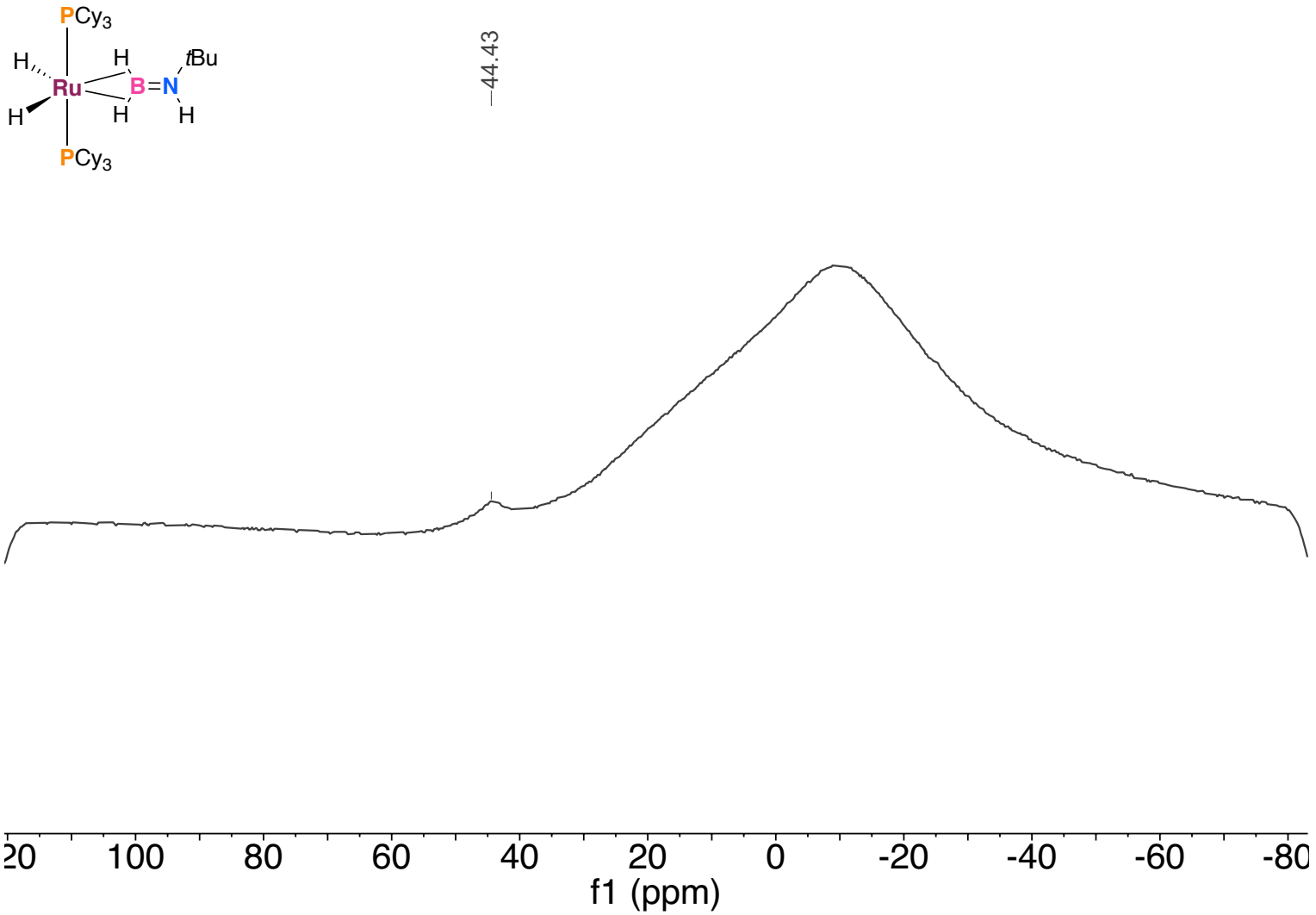


**Figure A.52:** $^{11}$B NMR spectrum (Toluene-d8, 160 MHz, 298 K) of **3.5.**

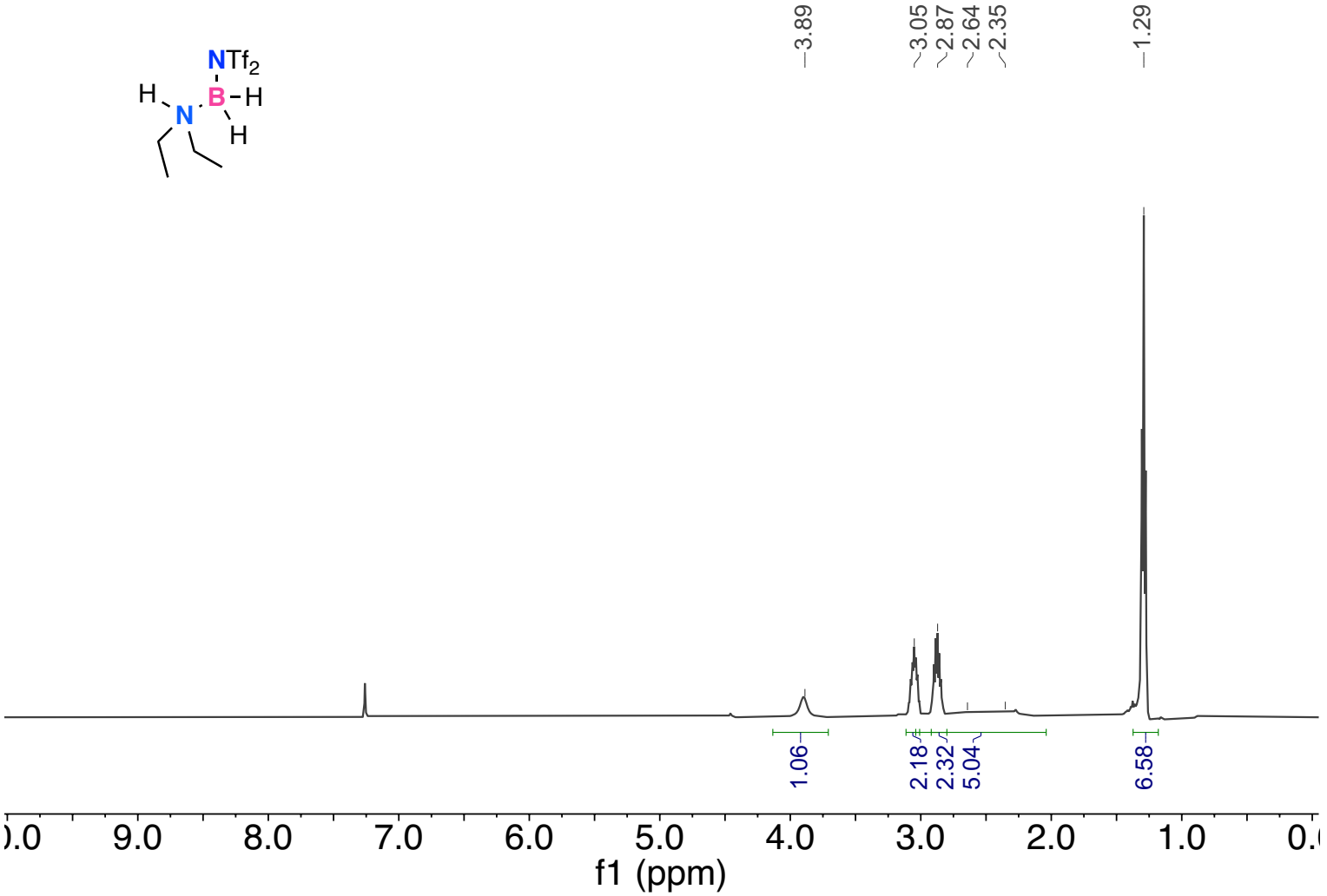


**Figure A.53:** $^{1}$H NMR spectrum (500 MHz, 298 K, $CDCl_3$) of **5.3b**.

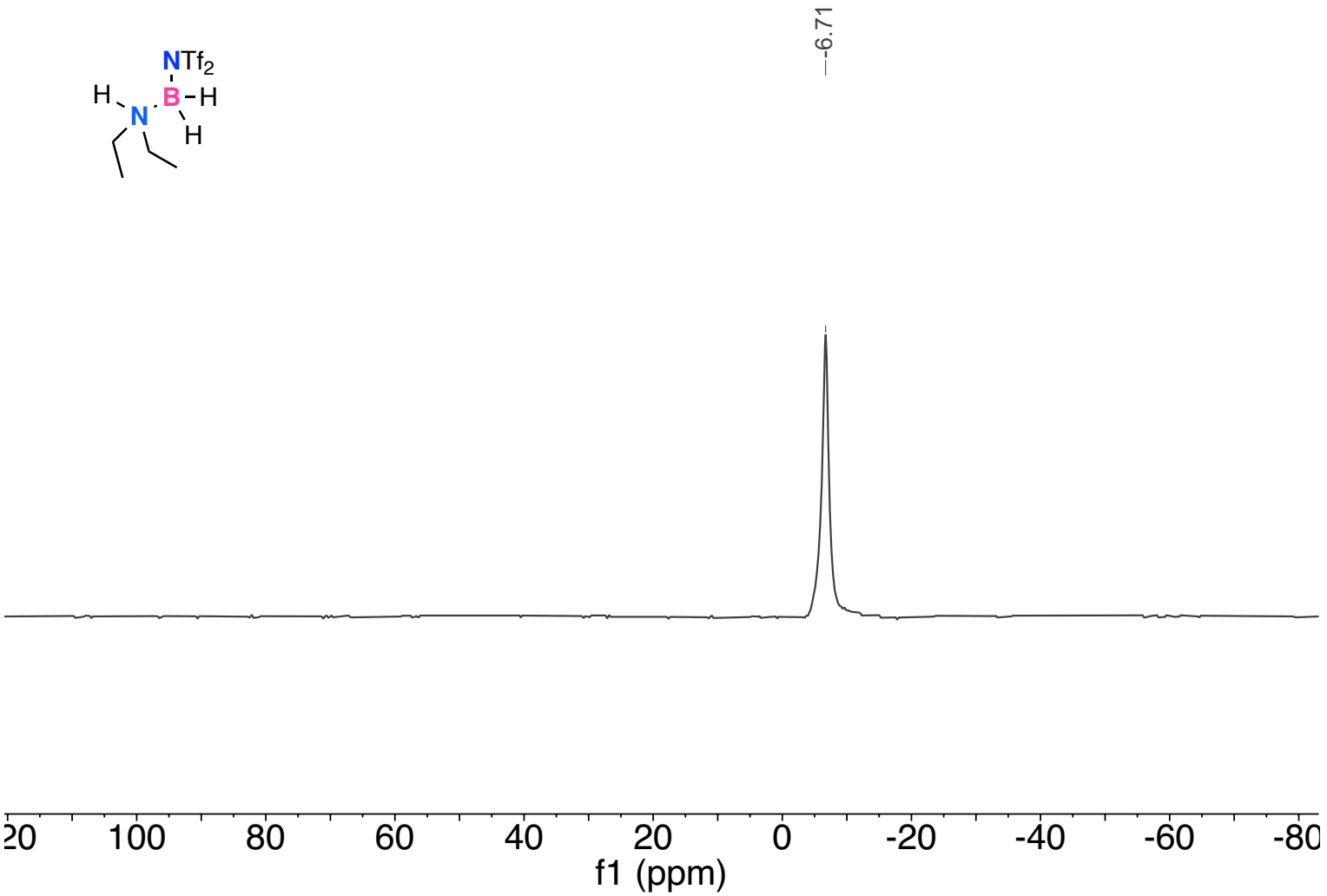


**Figure A.54:** $^{11}B\{^{1}H\}$ NMR spectrum (160 MHz, 298 K, $CDCl_3$) of **5.3b**.

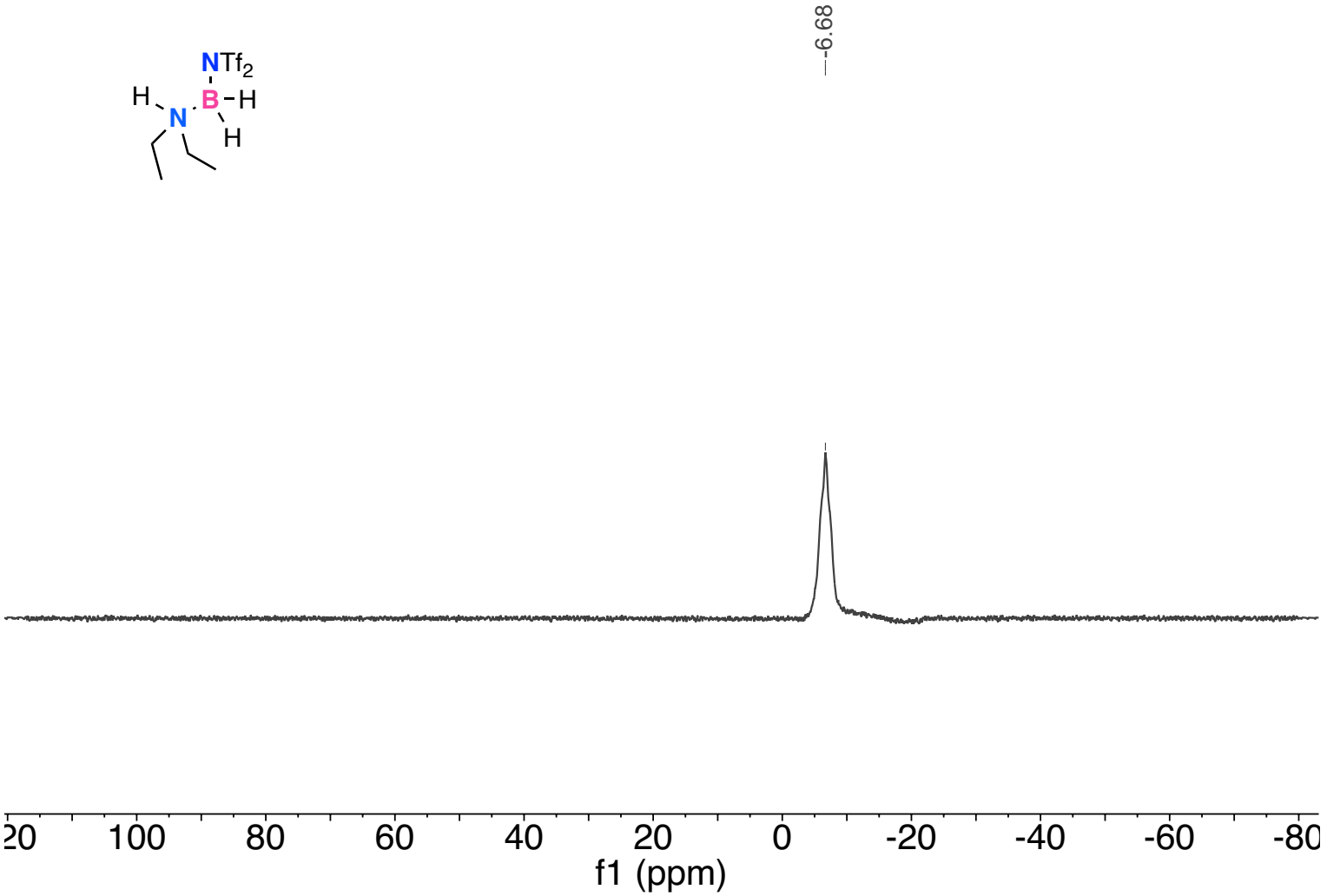


**Figure A.55: :** $^{11}$B NMR spectrum (160 MHz, 298 K, $CDCl_3$) of **5.3b**.

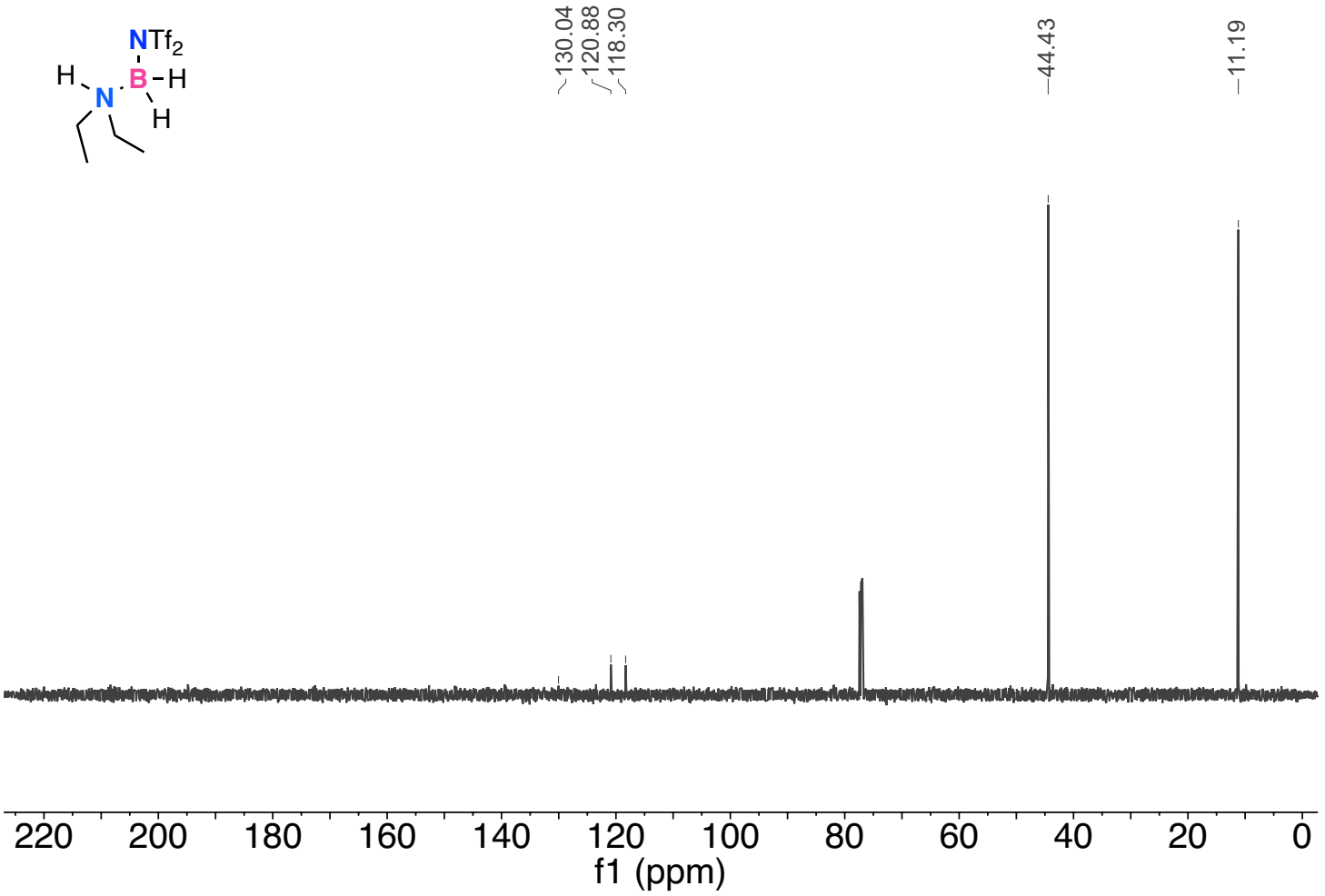


**Figure A.56: :** $^{13}C\{^{1}H\}$ NMR spectrum (125 MHz, 298 K, $CDCl_3$) of **5.3b.**

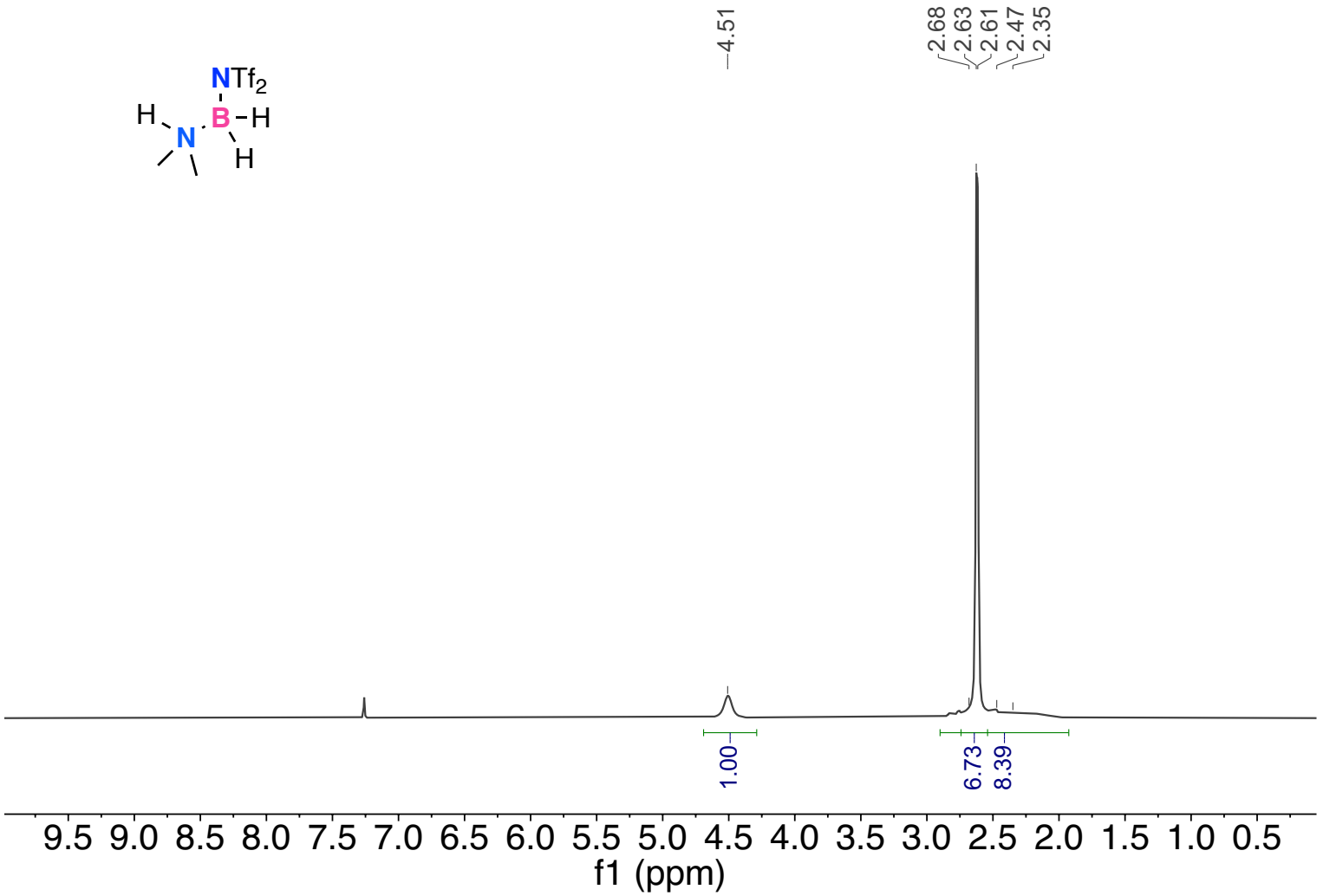


**Figure A.57:** $^{1}$H NMR spectrum (500 MHz, 298 K, $CDCl_3$) of **5.3c.**

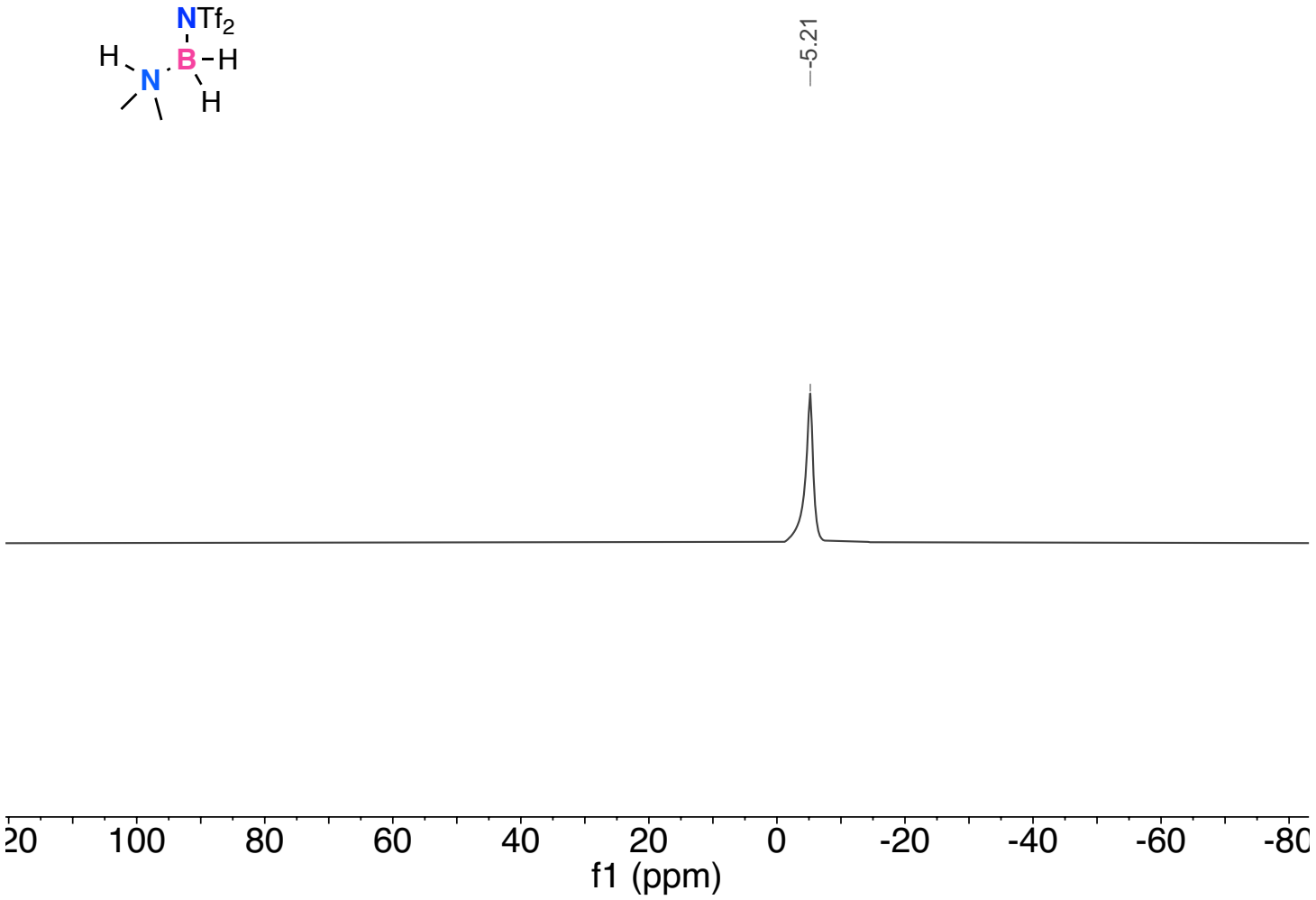


**Figure A.58: :** $^{11}B\{^{1}H\}$ NMR spectrum (160 MHz, 298 K, $CDCl_3$) of **5.3c**.

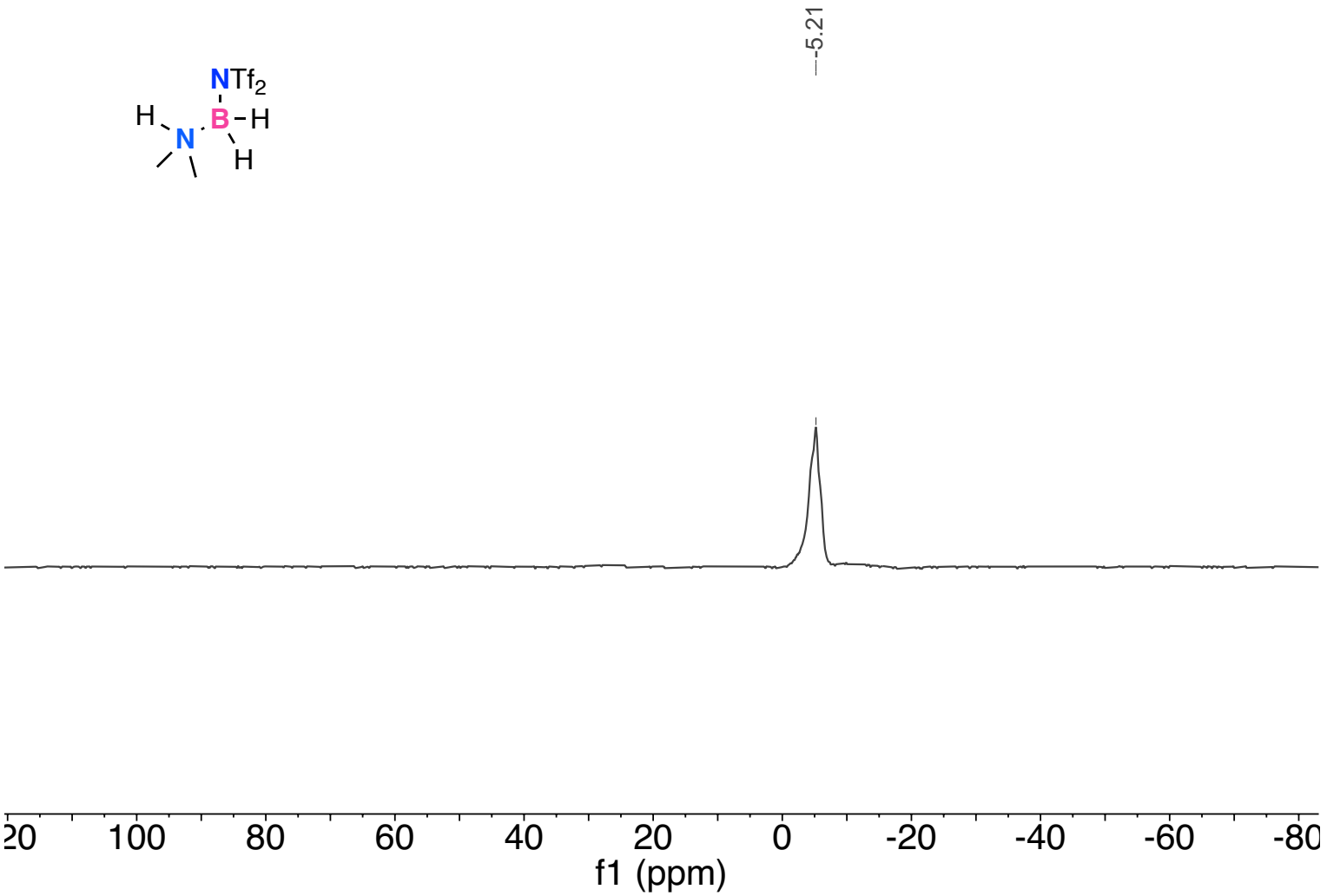


**Figure A.59:** $^{11}B$ NMR spectrum (160 MHz, 298 K, $CDCl_3$) of **5.3c**.

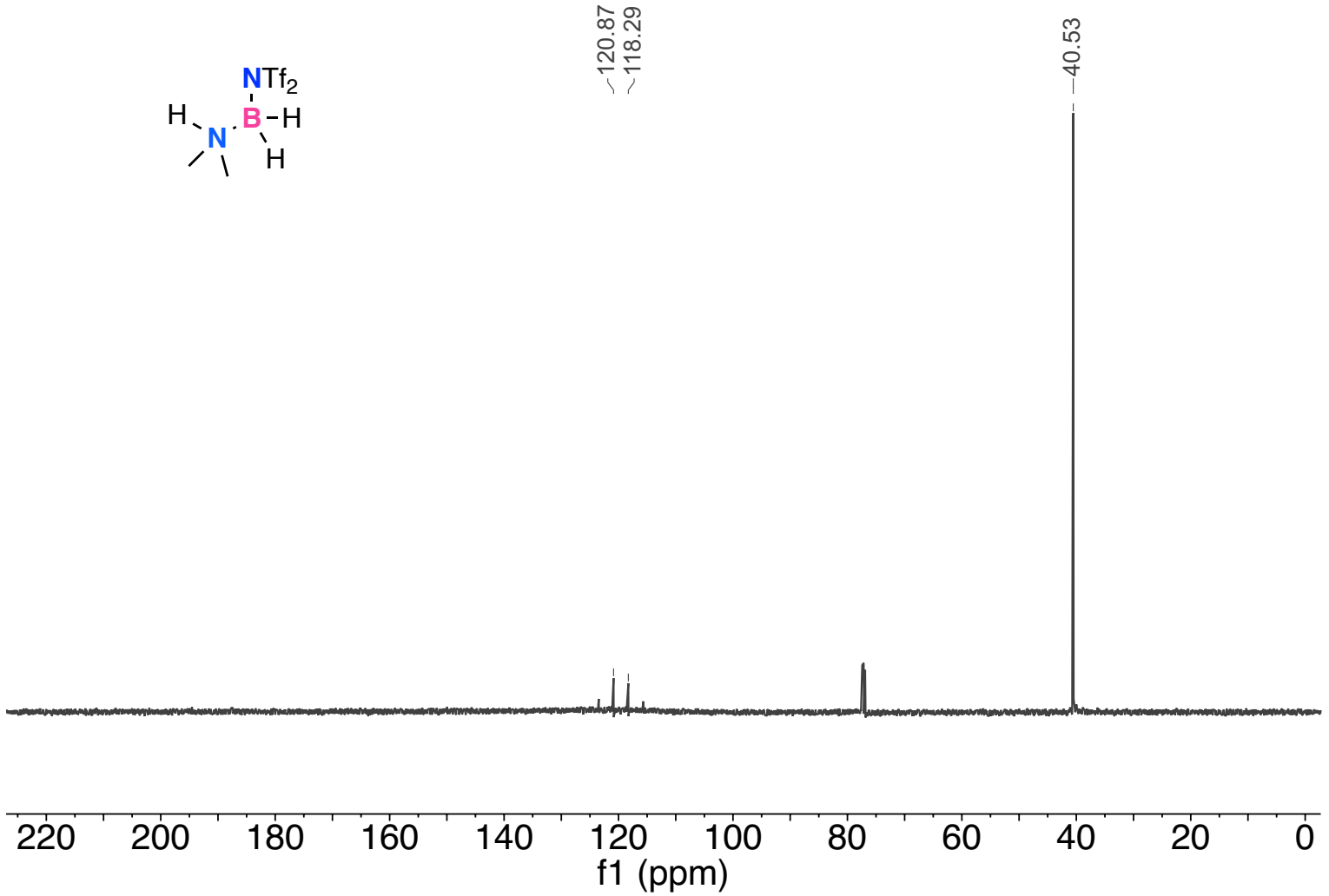


**Figure A.60:** $^{13}C\{^{1}H\}$ NMR spectrum (125 MHz, 298 K, $CDCl_3$) of **5.3c**